Lecture Notes in Electrical Engineering 249

Tong-Cun Zhang
Pingkai Ouyang
Samuel Kaplan
Bill Skarnes *Editors*

Proceedings of the 2012 International Conference on Applied Biotechnology (ICAB 2012)

Volume 1

Springer

Lecture Notes in Electrical Engineering

Volume 249

For further volumes:
http://www.springer.com/series/7818

Tong-Cun Zhang · Pingkai Ouyang
Samuel Kaplan · Bill Skarnes
Editors

Proceedings of the 2012 International Conference on Applied Biotechnology (ICAB 2012)

Volume 1

Springer

Editors
Tong-Cun Zhang
College of Bioengineering
Tianjin University of Science
and Technology
Tianjin
People's Republic of China

Pingkai Ouyang
Nanjing University of Technology
Nanjing
People's Republic of China

Samuel Kaplan
Department of Microbiology, Houston
Medical School
University of Texas
Texas, TX
USA

Bill Skarnes
Wellcome Trust Sanger Institute
Cambridge
UK

ISSN 1876-1100 ISSN 1876-1119 (electronic)
ISBN 978-3-642-37915-4 ISBN 978-3-642-37916-1 (eBook)
DOI 10.1007/978-3-642-37916-1
Springer Heidelberg New York Dordrecht London

Library of Congress Control Number: 2013945796

© Springer-Verlag Berlin Heidelberg 2014
This work is subject to copyright. All rights are reserved by the Publisher, whether the whole or part of the material is concerned, specifically the rights of translation, reprinting, reuse of illustrations, recitation, broadcasting, reproduction on microfilms or in any other physical way, and transmission or information storage and retrieval, electronic adaptation, computer software, or by similar or dissimilar methodology now known or hereafter developed. Exempted from this legal reservation are brief excerpts in connection with reviews or scholarly analysis or material supplied specifically for the purpose of being entered and executed on a computer system, for exclusive use by the purchaser of the work. Duplication of this publication or parts thereof is permitted only under the provisions of the Copyright Law of the Publisher's location, in its current version, and permission for use must always be obtained from Springer. Permissions for use may be obtained through RightsLink at the Copyright Clearance Center. Violations are liable to prosecution under the respective Copyright Law.
The use of general descriptive names, registered names, trademarks, service marks, etc. in this publication does not imply, even in the absence of a specific statement, that such names are exempt from the relevant protective laws and regulations and therefore free for general use.
While the advice and information in this book are believed to be true and accurate at the date of publication, neither the authors nor the editors nor the publisher can accept any legal responsibility for any errors or omissions that may be made. The publisher makes no warranty, express or implied, with respect to the material contained herein.

Printed on acid-free paper

Springer is part of Springer Science+Business Media (www.springer.com)

Preface

2012 International Conference on Applied Biotechnology (ICAB2012) was organized by Tianjin University of Science and Technology, Tianjin Institute of Industrial Biotechnology, Chinese Academy of Sciences was held from October 18–19, 2012 in Tianjin, China.

The conference served as a forum for exchange and dissemination of ideas and the latest findings among all parties involved in any aspects of applied biotechnology. The following distinguished professors gave keynote speeches: Hassan Ashktorab (Howard University, USA), William Carl Skarnes (The Wellcome Trust Sanger Institute, UK), Hiroyuki Takenaka (Kyushu Kyoritsu University, Japan) and Xueli Zhang (Tianjin Institute of Industrial Biotechnology, Chinese Academy of Sciences, China). The conference was complemented by talks given by other 51 professors and investigates.

More than 200 authors from 44 different universities, institutes and companies submitted conference papers. A lot of fields have been covered, ranging from fermentation engineering, cell engineering, genetic engineering, enzyme engineering and protein engineering.

Special thanks are given to Academic Committee, Organizing Committee and Secretary Staff of the conference for the commitment to the conference organization. We would like also to thank all the authors who contributed with their papers to the success of the conference.

This Book gathers a selection of the papers presented at the conference; it contains contributions from both academic and industrial researchers providing a unique perspective on the research and development of applied biotechnology from all over the world. The scientific value of the papers also helps the researchers in this field to get more valuable results.

Tianjin, China

Tong-Cun Zhang
Pingkai Ouyang
Samuel Kaplan
Bill Skarnes

Committees

Sponsor

Chinese Society of Biotechnology

Organizers

Tianjin University of Science and Technology
Key Lab of Industrial Fermentation Microbiology, Ministry of Education
Tianjin Institute of Industrial Biotechnology, Chinese Academy of Sciences

Co-Organizers

Tianjin Society for Microbiology
Tianjin International Joint Academy of Biotechnology and Medicine
College of Biotechnology and Pharmaceutical Engineering, Nanjing University of Technology
College of Life Science, Nankai University
School of Biotechnology, Jiangnan University
College of Life Science and Technology, Beijing University of Chemical Technology
School of Bioscience and Bioengineering, South China University of Technology
College of Biotechnology, Chongqing University
State Key Laboratory of Bioreactor Engineering, East China University of Science and Technology
School of Biological Engineering, Dalian Polytechnic University
School of Food and Bioengineering, Shandong Polytechnic University

Academic Committee

Chairman

Pingkai Ouyang, Academician, Nanjing University of Technology, China

Executive Chairman

Zixin Deng, Academician, Shanghai Jiao Tong University, China
Baoguo Sun, Academician, Beijing Technology and Business University, China
Tianwei Tan, Academician, Beijing University of Chemical Technology, China
Prof. George Fu Gao, Institute of Microbiology of Chinese Academy of Sciences, China
Prof. Xiaohong Cao, Tianjin University of Science and Technology, China
Prof. Jian Chen, Jiangnan University, China
Prof. Yanhe Ma, Tianjin Institute of Industrial Biotechnology, Chinese Academy of Sciences, China

Members

Prof. Baishan Fang, Xiamen University, China
Prof. Cheng Yang, Tianjin International Joint Academy of Biotechnology and Medicine, China
Prof. Cunjiang Song, Nankai University (Tianjin Society for Microbiology), China
Prof. Danqun Huo, Chongqing University, China
Prof. Fang Liu, Nankai University, China
Prof. Fuping Lu, Tianjin University of Science and Technology, China
Prof. Guocheng Du, Jiangnan University, China
Prof. He Huang, Nanjing University of Technology, China
Prof. Hongzhang Chen, Institute of Process Engineering, Chinese Academy of Sciences, China
Prof. Jianhe Xu, East China University of Science and Technology, China
Prof. Jianjiang Zhong, Shanghai Jiao Tong University, China
Prof. Jianjun Liu, Shandong Academy of Food and Fermentation Industries, China
Prof. Jibin Sun, Tianjin Institute of Industrial Biotechnology, Chinese Academy of Sciences, China
Prof. Lirong Yang, Zhejiang University, China
Prof. Longjiang Yu, Huazhong University of Science and Technology, China
Prof. Min Wang, Tianjin University of Science and Technology, China
Prof. Muyi Cai, China National Research Institute of Food and Fermentation Industries, China

Prof. Ning Chen, Tianjin University of Science and Technology, China
Prof. Qipeng Yuan, Beijing University of Chemical Technology, China
Prof. Ruiming Wang, Shandong Polytechnic University, China
Prof. Shiru Jia, Tianjin University of Science and Technology, China
Prof. Shuyi Qiu, Guizhou University, China
Prof. Shuangjiang Liu, Institute of Microbiology of Chinese Academy of Sciences, China
Prof. Youshu Xia, Sichuan Academy of Food and Fermentation Industries, China
Prof. Siliang Zhang, East China University of Science and Technology, China
Prof. Tong-Cun Zhang, Tianjin University of Science and Technology, China
Prof. Xianzhen Li, Dalian University of Technology, China
Prof. Xiaolei Wu, Beijing University, China
Prof. Xinhui Xing, Tsinghua University, China
Prof. Xueming Zhao, Tianjin University, China
Prof. Yin Li, Institute of Microbiology of Chinese Academy of Sciences, China
Prof. Yinbo Qu, Shandong University, China
Prof. Ying Lin, South China University of Technology, China

Organizing Committee

Chairman

Prof. George Fu Gao, Vice Dean, Beijing Institutes of Life Science, Chinese Academy of Sciences, China

Executive Chairman

Prof. Shuheng Ma, Vice Dean, Tianjin Institute of Industrial Biotechnology, Chinese Academy of Sciences, China
Prof. Dongguang Xiao, Dean, Tianjin University of Science and Technology, China

Members

Yinhua Wan, Deputy Secretary General, Chinese Society of Biotechnology, China
Lei Ma, Director, President's Office, Tianjin University of Science and Technology, China
Feng Wen, Secretary of the Party Committee, College of Bioengineering, Tianjin University of Science and Technology, China

Dingcheng Liu, Vice Dean, Division of Science and Technology, Tianjin University of Science and Technology, China
Cunjiang Song, Secretary General, Tianjin Society of Microbiology, China
Cheng Yang, Vice Dean, Tianjin International Joint Academy of Biotechnology and Medicine, China

Secretariat

Secretary General

Prof. Shuheng Ma, Vice Dean, Tianjin Institute of Industrial Biotechnology, Chinese Academy of Sciences, China

Deputy Secretary General

Prof. He Huang, Dean, Division of Science and Technology, Nanjing University of Technology, China
Prof. Cunjiang Song, Secretary General, Tianjin Society of Microbiology, China
Prof. Tong-Cun Zhang, Director, Key Laboratory of Industrial Fermentation Microbiology (Tianjin University of Science and Technology), Ministry of Education, China

Members

Yue Wang, Juke Wang, Hongling Wang, Jiaming Wang, Yanbing Shen, Yihan Liu, Jian Zhang, Chaozheng Zhang, Kui Lu, Hao Zhou, Xuegang Luo, Cheng Zhong, Qingyang Xu, Bin Jia,Xuewu Guo, Zhilei Tan

Contents

Part I
Industrial Microbial Technology

Chapter 1
Application of Kinetic Models and Neural Networks to Predict the Embedding Rate During Storage of Fingered Citron Essential Oil Microcapsules

Hanglin Xu, Jiang Wu, Keren Du, Hongjing Zhou and Gang Deng

Abstract The aim of this work was to develop kinetic models of the embedding rate during storage of fingered citron essential oil microcapsules and evaluate the performance of artificial neural network to predict the kinetic parameters. Release kinetics of microencapsulated (by β-cyclodextrin) fingered citron essential oil was investigated under a series of temperature levels (10, 25, 40, 55, 70, 85, and 100 °C). In addition, the model was trained using a back-propagation algorithm and one hidden layer artificial neural network (ANN) was employed. The results indicated that the optimal ANN model was developed when the optimal number of neurons in the hidden layer was 19. Additionally, the correlation coefficients between predicted k, $t_{1/2}$, or D-value and experimental values were greater than 0.9971 in all case. Thus, the overall results showed that ANN could be a potential tool for quick and accurate prediction of the kinetic parameters.

Keywords ANN · Essential oil · Fingered citron · Microcapsules · Kinetic

H. Xu · J. Wu · K. Du · H. Zhou · G. Deng (✉)
College of Chemistry and Life Science, Zhejiang Normal University, Jinhua 321004, People's Republic of China
e-mail: denggang@zjnu.cn

T.-C. Zhang et al. (eds.), *Proceedings of the 2012 International Conference on Applied Biotechnology (ICAB 2012)*, Lecture Notes in Electrical Engineering 249,
DOI: 10.1007/978-3-642-37916-1_1, © Springer-Verlag Berlin Heidelberg 2014

Fig. 1.1 The fresh fingered citron cultured in Jinhua, Zhejiang Province, China (29°07′ N, 119°35′ E, altitude 40 m)

1.1 Introduction

Fingered citron (*Citrus medica* L. var. Sarcodactylis Swingle) is a variation of *Citrus medica* L. belongs to Rutaceae, which is mainly distributed in southeastern China and Japan [1]. For its unique appearance and pleasant aroma (Fig. 1.1), fingered citron has highly valued as a decorative plant [2]. In addition, as a common used Traditional Chinese Medicine, fingered citron had the function of soothing the liver and regulating the stomach for alleviating pain [3]. Lu et al. reported citrus species have been cultivated in China for at least 1700 years, although human studies about fingered citron are rather limited [4].

Nowadays, consumers and research focuses on the versatile bioactivities of citrus species extracts such as flavonoids and essential oil. The essential oil is one of the quite well-investigated extracts, within past 20 years, and the antimicrobial activity of essential oil is well recognized [5, 6]. Thus, the essential oil composition had been already widely extensive used in the treatment of human diseases in the prevention of cancer, cardiovascular, antioxidant, and other biological activity area [7]. Such as Deans and Ritchie reported essential oils of thyme, cinnamon, bay, and clove have antimicrobial activity [8]. A number of studies had indicated that essential oil derived from various plants can induce apoptosis in cancer cells [9–12]. More worth mentioning is that Ma et al. studied effect of fingered citron essential oil on proliferation of MDA-MB-435 cells in vitro [13]. Because of the safe and nutritious supply, not only unceasingly speeds up in the medicine domain, the essential oils and their constituents also have been used extensively as flavoring ingredients in a wide variety of food, beverage, and confectionery products [14].

Intense interest and high consumption by consumers in essential oil, and wide availability from inexpensive raw materials in industry in from of peel, juice, and concentrate. However, like other essential oil, fingered citron essential oil is very

sensitive to temperature and is readily oxidized in the air. The functional components are unstable under nature conditions [15]. Thus, to enhance and improve stability of fingered citron essential oil is crucial issue for the maximum utilization rate. Luckily, microcapsule techniques can make essential oil stability and prevent temperature adverse in nature environment, but also help to build up the further processing industry and promote the essential oil with economic benefit [16]. Thus, it is advisable to keep essential oil away from external environment by the wall (usually β-cyclodextrin) after microencapsulation. We can get core materials (essential oil) by damaging capsule in high temperature and pressing it. In the food industry, core materials controlled release system is an important index, especially the release characteristics of core materials from powders, which play an important role in analyzing storage characteristics. Ideally, some authors have studied that the kinetics of core materials degradation in capsule during storage and stated that it follows a first-order kinetic model [17, 18]. However, to our knowledge no previous research has been reported as the release kinetics of microencapsulated (by β-cyclodextrin) fingered citron essential oil under different temperature conditions.

An artificial neural network (ANN) is a biologically inspired form of distributed computation which is composed of connection nodes. Neuron is the primary element of neural network that can be thought of as weighted transfer function [18]. In recent years, interest in using ANN with back-propagation algorithm as a modeling tool in supervised techniques is increasing, especially in food technology [19]. ANN has been successfully applied in several areas like microbial predictions, material identifications, and food rheology [20, 21]. Therefore, the aim of this work was to: (1) evaluate the kinetics of core materials degradation (embedding rate) during storage of fingered citron essential oil microcapsules and (2) assess the performance of ANN to predict the kinetic parameters.

1.2 Materials and Methods

1.2.1 Raw Materials Preparation

The fresh fruits used in this study were collected from fingered citron base in Jinhua, Zhejiang Province, China (29°07′ N, 119°35′ E, altitude 40 m). The peel was separated from endocarp with a hand knife and cut into pieces. The pieces were smashed by pulverizer (Wenling Aoli Mediciner Machinery co. LTD) and immersed in distilled water (The ratio of powder to water (w) is 1:3, kg). The essential oil from fingered citron was extracted by self-made vapor distillation device for 3 h with multi batches. Each batch oil yield is about 0.8 % (w/w), density is 0.78 g/ml. The extract was dried over anhydrous sodium sulfate and stored for subsequent use.

1.2.2 Fingered Citron Essential Oil Microcapsules Preparation

150 gram of β-cyclodextrin was dissolved in 1500 ml deionized water, and then 20 ml fingered citron essential oil was added. The kneading was continued for 2 h at 70 °C. Then the mixture was not placed into fridge under 5 °C and set for 24 h until the solution has cooled to room temperature. These samples were at final dried in a vacuum over at 50 °C till constant weight. The microcapsules products for subsequent use were prepared with multi batches.

1.2.3 Storage Treatments

To develop release kinetic model of the degradation of embedding rate in fingered citron essential oil microcapsules storage as a function of storage time and temperature, samples were placed in closed Petri dishes and stored in a temperature-controlled (10, 25, 40, 55, 70, 85, and 100 °C) storage locker for 15 days. The embedding rate was analyzed every 3 days (0, 3, 6, 9, 12, and 15) during storage. All treatments were conducted in five replications.

1.2.4 Determination of Embedding Rate

The embedding rate of fingered citron essential oil microcapsules was calculated as given below:

$$\text{Embedding rate} = \frac{\text{Sample weight after period of storage time}}{\text{Initial sample weight}} \times 100\,\% \quad (1.1)$$

The standard equation for a first-order reaction was used to calculate the loss of embedding rate in microcapsules as follows:

$$\ln E = \ln E_0 - kt, \quad (1.2)$$

Here t, the storage time (day); E, the embedding rate at time t; E_0, the embedding rate at time zero; k, the first-order rate constant.

Arrhenius equation

The most acceptable expression to explain the influence of temperature on the kinetic rate constants in food systems, Arrhenius equation, has been widely used. The Arrhenius relationship for temperature dependence for the rate constant k was given as follows:

$$k = A \exp(-E_a/RT) \quad (1.3)$$

Here, A is the pre-exponential constant, E_a is the activation energy of the reaction, R is gas constant, and T is the absolute temperature.

The kinetic parameters including $t_{1/2}$ and D-value mean the half destruction time and the time required for degradation of 90 % embedding rate, respectively:

$$t_{1/2} = \ln 2/k, \tag{1.4}$$

$$D = 1/k, \tag{1.5}$$

Here, k is the first-order rate constant.

1.2.5 Artificial Neural Network Analysis

Feed forward back-propagation neural network is the most common used one in recent years, (Fig. 1.2) shows a network structure with input, hidden, and output layers used in this study. The input layer had one neuron representing the temperature and the output layer consisted of three neurons which corresponded to k, $t_{1/2}$, and D-value. One hidden layer was used in this work. The number of neurons within each of these layers varies between from 3 to 20 and was empirically determined by trade-off between mean square error (MSE) and training time. The transfer function in the hidden layer and output layer was a hyperbolic tangent sigmoid and Levenberg–Marquardt (LM) algorithm was applied to accomplish the minimization of error. The input data used were normalized to interval [0, 1] before training as follows:

$$X_n \to f(X_n) = \frac{(X_n - X_{\min})}{(X_{\max} - X_{\min})} \tag{1.6}$$

Here, Xn, Xmin, and Xmax correspond to the normalized values, minimum, and maximum of the data sample, respectively. Training was based on a supervised

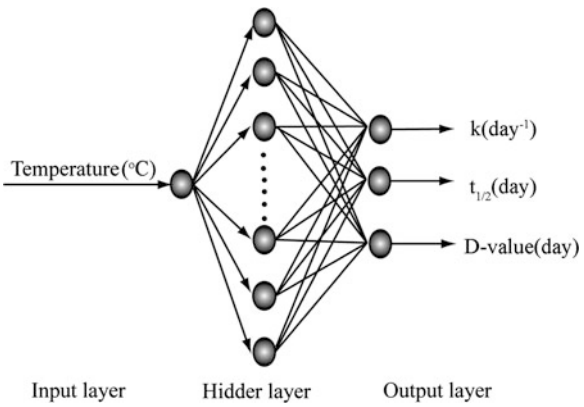

Fig. 1.2 ANN architecture for k, $t_{1/2}$, and D-value prediction

method and was finished when MSE converged or less than 0.0001. Training was completed after 3,000 epochs if the MSE did not go below 0.0001. The BP-ANN modeling program was realized using MATLAB software (The Mathworks, Inc., Natick, MA, USA, version 7.9 R2009b).

1.3 Results and Discussion

1.3.1 Degradation of Average Embedding Rate During Storage

Originally, the average embedding rate in various temperature treatments was 100 %. The average embedding rate was plotted as a function of storage time at different temperatures (Fig. 1.3). It was observed that the embedding rate decreased with the increasing of storage time temperature. Table 1.1 showed the kinetic parameters of embedding rate degradation at different temperatures and the R^2 values of fitted exponential curves ranged from 0.9487 to 0.9993. The Arrhenius plots of embedding rate degradation in fingered citron essential oil microcapsules storage was showed in (Fig. 1.4).

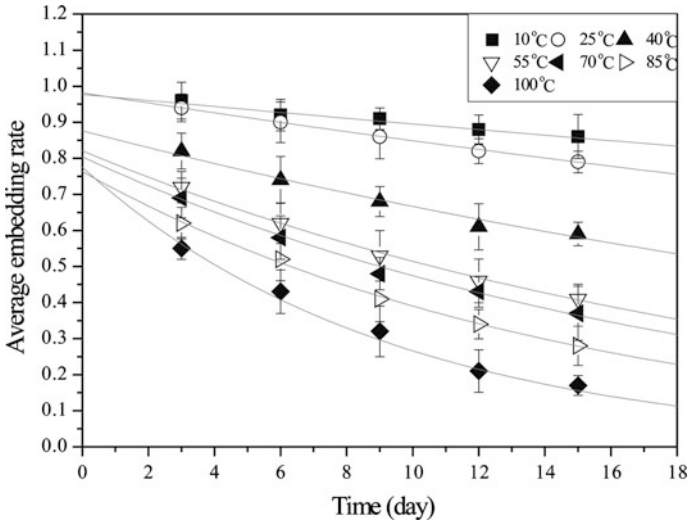

Fig. 1.3 The average embedding rate during storage of fingered citron essential oil microcapsules at different temperatures

Table 1.1 Kinetic parameters for the thermal degradation of embedding rate in fingered citron essential oil microcapsules during storage at different temperatures

Temperature (°C)	Variation kinetics	k (day^{-1})	$t_{1/2}$ (day)	D-value (day)	R^2
10	y = 0.9774exp(−0.0088x)	0.0088	78.77	113.64	0.9487
25	y = 0.9816exp(−0.0145x)	0.0145	47.80	68.97	0.9993
40	y = 0.8765exp(−0.0274x)	0.0274	25.30	36.50	0.9756
55	y = 0.8207exp(−0.0467x)	0.0467	14.84	21.41	0.9980
70	y = 0.8040exp(−0.0527x)	0.0527	13.15	18.98	0.9944
85	y = 0.7633exp(−0.0671x)	0.0671	10.33	14.90	0.9972
100	y = 0.7751exp(−0.1070x)	0.1070	6.48	9.35	0.9842

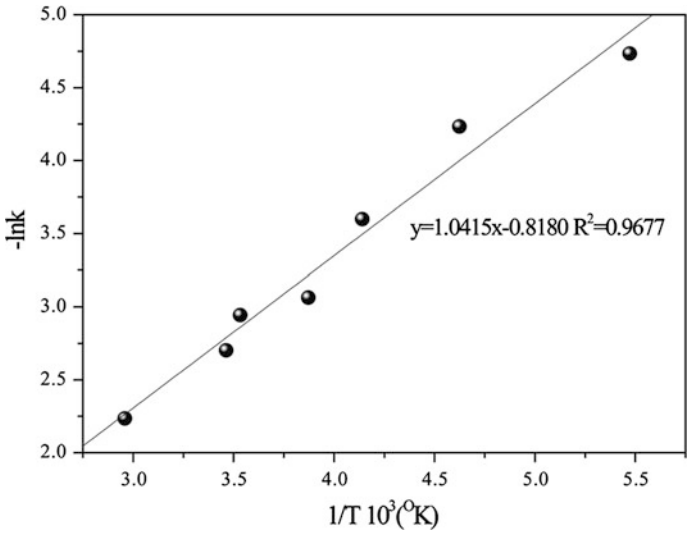

Fig. 1.4 Arrheninus plots of embedding rate degradation in fingered citron essential oil microcapsules

1.3.2 Optimal Artificial Neural Network Configuration for Kinetic Parameters Prediction

Training speed and MSE were used to compare the performance of various ANN model. Our results showed that the optimal number of nodes in the hidden layer used for training ANN model is 19 (Fig. 1.5). Therefore, a 1-19-3 back-propagation network was constructed. The development of the ANN model usually involves two basic steps including training and test phases. Table 1.2 showed the training data set and test data set used in this work. Figure 1.6 presented the plots of the correlations coefficients (R^2) between experimentally determined k, $t_{1/2}$ and D-value and ANN predicted values. In the training step, $R^2 = 0.9999$, 0.9999, and

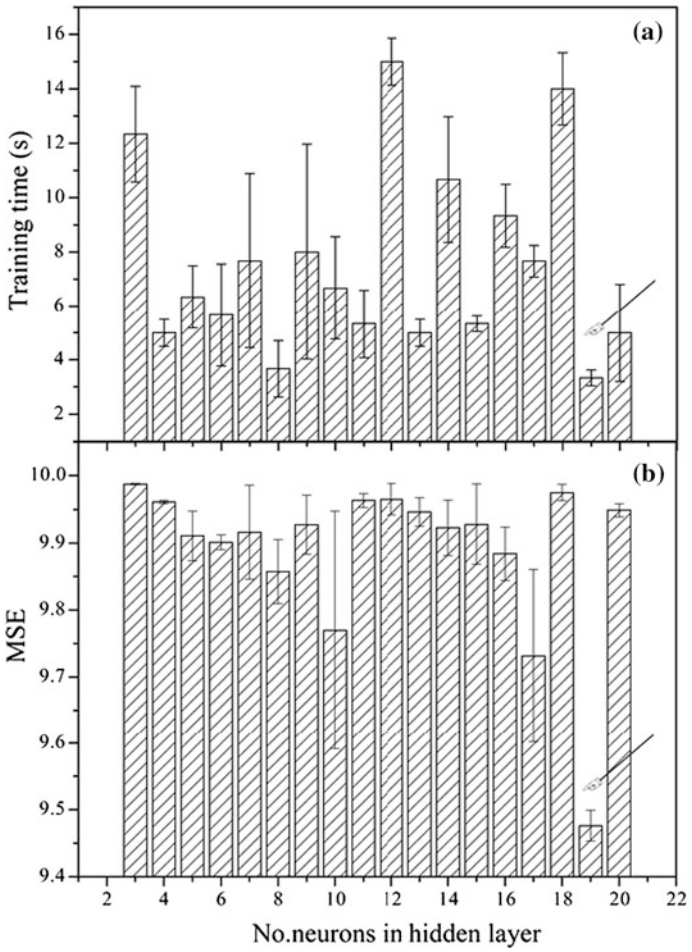

Fig. 1.5 Mean squared error (MSE) and training time in the prediction of kinetic parameters with different number of neurons in the hidden layer

Table 1.2 Training data set and test data set used in the development of ANN

	Temperature (°C)	k (day^{-1})	$t_{1/2}$ (day)	D-value (day)
Training data set				
	10	0.0088	78.77	113.64
	40	0.0274	25.30	36.50
	70	0.0527	13.15	18.98
	100	0.1070	6.48	9.35
Training data set				
	25	0.0145	47.80	68.97
	55	0.0467	14.84	21.41
	85	0.0671	10.33	14.90

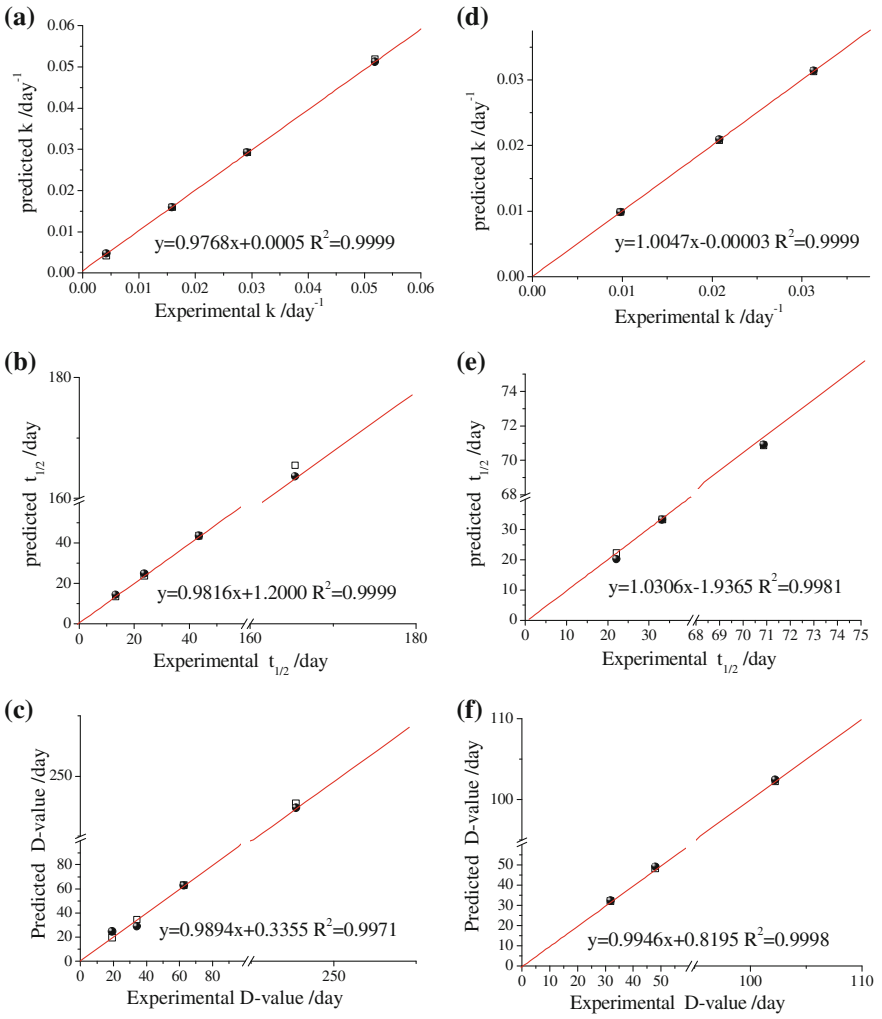

Fig. 1.6 Correlation of experimental and predicted kinetic parameters with training data sets (**a**–**c**), and test data set (**e**–**g**) for fingered citron essential oil microcapsules during thermal treatments using the optimal ANN

0.9971 for k, $t_{1/2}$ and D-value, respectively. In the test step, $R^2 = 0.9999$, 0.9981, and 0.9998 for k, $t_{1/2}$ and D-value, respectively.

Unlike in parts of the citrus family species such as the orange, lemon, mandarin, and lime, where fingered citron is an uncommon group [2]. The unprocessed fresh fruit is unsuitable to eat and has no seeds. Because of the lemon-like aroma and unique fingers of appearance, the fingered citron is usually used as an ornamental. However, the fruit ripens seasonal and not resistant to cold, which lead to only cultivation in subtropical areas. In addition, potting of fingered citron has not been

extensively used because the fruits' of irregular profile are easily squashed in transit, the fruits seem to fall off quite easily. This makes people in other unplanted regions do not know this fantasy species. Thus, its potential application and economic values are not developed abundantly.

More importantly, the volatile oil-related knowledge of fingered citron is seldom studied, though, are some reports of the flavones and coumarins in this fruit [2, 22, 23]. In this study, we evaluated the kinetics of core materials degradation (embedding rate) during storage of fingered citron essential oil microcapsules. Figure 1.3 showed the embedding rate decreased with the increasing of storage time temperature, the higher the temperature, the embedding rate declined more, which indicated that the temperature plays an important role in core materials degradation. The result correlates well with the findings of Slater and Johnson and Sharma and Stipanovic, who reported that the grease oxidation speed up when temperature increases [24, 25]. In addition, the temperature affects the core materials' Brown movement and microcapsules structure. As the temperature increases, the Brown movement becomes greater and the aperture of wall (β-cyclodextrin) becomes larger simultaneously, which help quicken the oil release process. What's more, our results show that fingered citron essential oil microcapsules have good temperature-resistance before 40 °C, while the embedding rate falls dramatically when the temperature is higher than 55 °C. Thus, the fingered citron essential oil microcapsules should also try to avoid high temperature environment during storage.

In fact, the first-order kinetic model has been used by numerous researchers in various areas [26–28]. However, no author proposes mathematical models and computer simulations to predict core materials degradation during storage of essential oil microcapsules. As a set of mathematical tool for prediction of nonlinearities, (ANN) attempt to mimic the functioning of human owing to their excellent pattern recognition capability for approximating any underlying relationship between the dependent and independent variables, without requiring a prior knowledge of the relationships of nodes, but learning from examples through iteration [18, 29]. In this study, we developed a release kinetic model of fingered citron essential oil microcapsules during storage based on ANN using a back-propagation algorithm. A standard network with one hidden layer including 19 nodes with additional direct connections from one input neuron (temperature) to three output neurons (k, $t_{1/2}$, and D-value) was constructed (Figs. 1.2, 1.5). ANN could have more than a single hidden layer, however, a large amount of works had shown that one hidden layer is sufficient to solve any complex nonlinear function [19, 30–32]. In addition, the optimal ANN provided encouraging results that the correlation coefficients between predicted k, $t_{1/2}$, or D-value and experimental values were greater than 0.99 in all case (Fig. 1.6). Therefore, our results could provide release kinetics with an alternative way for kinetic parameters determination.

1.4 Conclusion

In summary, the kinetic models of the embedding rate during storage of fingered citron essential oil microcapsules were constructed. The ANNs could predict the kinetic parameters of embedding rate degradation at different temperatures and the R^2 values of fitted exponential curves ranged from 0.9487 to 0.9993. The overall results indicated that ANN could be a potential tool for quick and accurate prediction of the kinetic parameters.

Acknowledgments The project is supported by the National Natural Science Foundation (21006098).

References

1. Guo WD, Zheng JS, Zhang ZZ et al (2009) Effects of short term chilling stress on the photosynthetic physiology of fingered citrons (*Citrus medica* L. var. Sarcodactylis Swingle). Acta Ecologica Sinica (in Chinese) 29(5):2286–2293
2. Shiota H (1990) Volatile components in the peel oil from fingered citron (*Citrus medica* L. var. Sarcodactylis Swingle). Flavour Frag J 5(1):33–37
3. He HY, Ling LQ (1985) Chemical studies of a Chinese traditional drug fingered citron (Citrus medica L. var sarcodactylis (Noot.) Swingle). Acta pharmaceutica Sinica (in Chinese) 20(6):433–435
4. Lu YH, Zhang CW, Bucheli P et al (2006) Citrus flavonoids in fruit and traditional Chinese medicinal food ingredients in china. Plant Food Hum Nutr 61(2):57–65
5. Farag RS, Daw ZY, Hewedi FM et al (1985) Antimicrobial activity of some Egyptian spice essential oils. J Food Protec 52(9):665–667
6. Raal A, Orav A, Pussa T et al (2012) Content of essential oil, terpenoids and polyphenols in commercial chamomile (*Chamomilla recutita* L. Rauschert) teas from different countries. Food Chem 131(2):632–638
7. Edris AE (2007) Pharmaceutical and therapeutic potentials of essential oils and their individual volatile constituents: a review. Phytother Res 21(4):308–323
8. Deans SG, Ritchie G (1987) Antibacterial properties of plant essential oils. Int J Food Mircrobiol 5(2):165–180
9. Buhagiar JA, Podesta MT, Wilson AP et al (1999) The induction of apoptosis in human melanoma, breast and ovarian cancer cell lines using an essential oil extract from the conifer *Tetraclinis articulate*. Anticancer Res 19(6B):5435–5443
10. Cavalieri E, Mariotto S, Fabrizi C et al (2004) α-Bisabolol, a nontoxic natural compound, strongly induces apoptosis in glioma cells. Biochem Bioph Res Co 315(3):589–594
11. Sharma PR, Mondhe DM, Muthiah S et al (2008) Anticancer activity of an essential oil from *Cymbopogon flexuosus*. Chemi-Biol Interact 179(2):160–168
12. Cha JD, Jeong MR, Kim HY et al (2009) MAPK activation is necessary to the apoptotic death of KB cells induced by the essential oil isolated from *Artemisia iwayomogi*. J Ethnopharmacol 123(2):308–314
13. Ma YF, Shao LX, Zhang JP et al (2010) Effects of fingered citron essential oil on proliferation of MDA-MB-435 cells in vitro. Chin. Pharm. J. (in Chinese) 45(22):1737–1741
14. Kim J, Marshall MR, Wei C (1995) Antibacterial activity of some essential oil components against five foodborne pathogens. J Agr Food Chem 43(11):2839–2845

15. Lnouye S, Takizawa T, Yamaguchi H (2001) Antibacterial activity of essential oils and their major constituents against respiratory tract pathogens by gaseous contact. J Antimicrob Chemoth 47(5):565–573
16. Moretti MDL, Sanna-Passino G, Demontis S et al (2002) Essential oil formulations useful as a new too for insect pest control. AAPS Pharmscitech 3(2):64–74
17. Burdurlu HS, Koca N, Karadeniz F (2006) Degradation of vitamin C in citrus juice concentrates during storage. J Food Eng 74(2):211–216
18. Zheng H, Fang SS, Lou HQ et al (2011) Neural network prediction of ascorbic acid degradation in green asparagus during thermal treatments. Expert Syst Appl 38(5):5591–5602
19. Lu HF, Zheng H, Lou HQ et al (2010) Using neural networks to estimate the losses of ascorbic acid, total phenols, flavonoid, and antioxidant activity in asparagus during thermal treatments. J Agr Food Chem 58(5):2995–3001
20. Ruan R, Almaer S, Zhang J (1995) Prediction of dough rheological properties using neural networks. Cereal Chem 72(2):308–311
21. Geeraerd AH, Herremans CH, Cenens C et al (1998) Application of artificial neural networks as a non-linear modular modeling technique to describe bacterial growth in chilled food products. Int J Food Microbiol 44(1):49–68
22. Kawaii S, Tomono Y, Katase E et al (1999) Quantitation of flavonoid constituents in citrus fruits. J Agr Food Chem 47(9):3565–3571
23. Mandalari G, Bennett RN, Bisignano G et al (2007) Antimicrobial activity of flavonoids extracted from bergamot (*Citrus bergamia* Risso) peel, a byproduct of the essential oil industry. J Appl Microbiol 103(6):2056–2064
24. Slater RAC, Johnson W (1967) The effects of temperature, speed and strain-rate on the force and energy required in blanking. Int J Mech Sci 9(5):271–276
25. Sharma BK, Stipanovic AJ (2002) Development of a new oxidation stability test method for lubricating oils using high-pressure differential scanning calorimetry. Thermochim Acta 402(1):1–18
26. Johnson JR, Braddock RJ, Chen CS (1995) Kinetics of ascorbic acid loss and nonenzymatic browning in orange juice serum: experimental rate constants. J Food Sci 60(3):502–505
27. Frias JM, Oliveira JC, Cunha LM et al (1998) Application of Doptimal design for determination of the influence of water content on the thermal degradation kinetics of ascorbic acid at low water contents. J Food Eng 38(1):69–85
28. Uddin MS, Hawlader MNA, Ding L et al (2002) Degradation of ascorbic acid in dried guava during storage. J Food Eng 51(1):21–26
29. Li ZX, Yang XM (2008) Damage identification for beams using ANN based on statistical property of structural responses. Comput Struct 86(1):64–71
30. Cybenco G (1989) Approximation by superposition of a sigmoidal function. Math Control Signal 2(4):303–314
31. Hornik K, Stinchcombe M, White H (1989) Multilayer feed forward networks are universal approximators. Neural Networ 2(5):359–366
32. Hagan MT, Menhaj MB (1994) Training feedforward networks with the Marquardt algorithm. IEEE T Neural Networ 5(6):989–993

Chapter 2
Effects of Medium Components and Fermentation Conditions on Cytidine Production by Recombinant *Escherichia coli* CYT20

Haitian Fang, Xixian Xie, Qingyang Xu, Chenglin Zhang and Ning Chen

Abstract Recently, cytidine is gaining more attention as a precursor for antiviral drugs. Cytidine is produced by some microorganisms fermentation. Cytidine producing strain *Escherichia coli* CYT20 was bred in our previous study. Glucose, $(NH_4)_2SO_4$, and temperature were selected as variables for optimization of fermentation medium and conditions for cytidine production. Among ingredients, different concentrations of initial glucose and $(NH_4)_2SO_4$ had positive effects on cytidine production, and pH 7.0 and temperature 36 °C were favoured fermentation conditions for cytidine production by *E. coli* CYT20. After shake flask batch fermentation, production of cytidine was measured by high performance liquid chromatography. The results showed that it was 1,866 mg/l under optimized condition and it was 1,115 mg/l under un-optimized condition, cytidine production was increased by 67.4 %.

Keywords Culture conditions · Cytidine · *Escherichia coli* · Fermentation · Optimization

2.1 Introduction

Cytidine is a nucleoside molecule that is formed when cytosine is attached to a ribose or deoxyribose ring. Cytidine is used as a precursor of a number of commonly used antiviral drugs. The production of cytidine depends on direct fermentation of carbohydrates by auxotrophic and regulatory mutant of *Escherichia coli* and *Bacillus*

H. Fang · X. Xie · Q. Xu · C. Zhang · N. Chen (✉)
College of Biotechnology, Tianjin University of Science and Technology, Tianjin 300457, People's Republic China
e-mail: ningch@tust.edu.cn

H. Fang
College of Agriculture, Ningxia University, Yinchuan 750021, People's Republic China

T.-C. Zhang et al. (eds.), *Proceedings of the 2012 International Conference on Applied Biotechnology (ICAB 2012)*, Lecture Notes in Electrical Engineering 249,
DOI: 10.1007/978-3-642-37916-1_2, © Springer-Verlag Berlin Heidelberg 2014

subtilis [1, 2]. Among these species, *E. coli* stains have been developed by mutagenesis or genetic manipulation for its high growth rate and well-known physiological characteristics [3]. A mutant of *E. coli* CYT20, which was released from the repression and inhibition of two key enzymes by end-products was isolated, and the concentration of glucose as a carbon source and $(NH_4)_2SO_4$ as a nitrogen source for the production of cytidine by this stain was optimized [4].

It is important to maintain the optimal fermentation conditions throughout the production process, including temperature, pH and carbon source content, and nitrogen source content [5–7]. A variable temperature control strategy is an efficient technique to control the organism's growth rate and achieves high yields of biomass and metabolites. The above-mentioned approach has been successfully applied in the productions of cytidine. In this study, the effects of the nitrogen source, the initial concentration of carbon source, temperature, and pH during the fermentation were examined to establish the optimum conditions for the improvement of cytidine production.

2.2 Materials and Methods

2.2.1 Bacterial Strain and Media

E. coli CYT20 (2-TU^r + 5-FU^r + 5-FC^r + 6-AU^r) (*ΔcddΔthrAΔhisG*) used in this study, carrying plasmid pYR115 containing two fragments of aspartate carbamoyltransferase and carbamyl phosphate synthase, and plasmid pGPZ15 containing three fragments of glucose 6-phosphate dehydrogenase, phosphoribosyl pyrophosphate kinase, and gluconate 6-phosphate dehydrogenase, was derived by repeated compound mutagenesis (DES plus NTG) from *Escherichia coli* K-12. The medium used for cell growth and cytidine production contained the following components (g/l): anhydrous glucose, 100; KH_2PO_4, 2; $(NH_4)_2SO_4$, 10; $MgSO_4$, 1; $FeSO_4{\cdot}7H_2O$ 0.01, $MnSO_4{\cdot}4H_2O$ 0.01. The carbon source was autoclaved separately for 15 min at 115 °C and added to the medium under aseptic condition.

2.2.2 Culture Conditions

A single colony of *E. coli* was inoculated to a 500-ml-baffled flask containing 25 ml growth medium and was cultivated at 37 °C, 220 rpm for 11 h, and then transferred into a fermentation baffled flask.

Fermentation experiments were performed with 500-ml baffled flask containing 30 ml production medium. The temperature and pH were controlled at 36 °C and 7.0, respectively. Culture time was 40 h in the medium containing 100 g/l glucose. Agitation speed was adjusted in the range of 220–240 rpm for the 40 h cultivation in order to maintain the higher dissolved oxygen concentration.

2.2.3 Analytical Methods

All experiments were conducted in triplicates and data were averaged and presented as mean ± standard deviation (SD). One-way analysis of variance (ANOVA) followed by Dunnett's multiple comparison test were used to determine significant differences. Statistical significance was defined as $p < 0.05$. The turbidity of cells in the fermentation broth was measured using a spectrophotometer at 600 nm. Dry cell weight (DCW) was gravimetrically determined using the pellet fraction from 30 ml samples, after centrifugation at 12,000 rpm for 10 min and washing twice with distilled water. This was poured into preweighed aluminium cups and placed overnight in an oven at 80 °C until constant weights were obtained. Cytidine concentration was analyzed by HPLC [8, 9] (Aglient 1200, Aglient, U.S.A.).

2.3 Results and Discussion

2.3.1 Effect of Initial Glucose Concentration on Cytidine Production

In order to determine the optimal initial glucose concentration, five medium with different concentrations of glucose (40, 60, 80, 100, 120 g/l) were used. The cytidine produced from different concentrations of glucose was determined after 40 h of cultivation in baffled flasks (Fig. 2.1).

Glucose consumption by *E. coli* CYT20 at different initial glucose concentrations are shown in Fig. 2.1. When the initial glucose concentration was high, glucose was uptaken slowly in the lag phase of cultivation and quickly after 10 h of cultivation. When initial concentrations of glucose were 40 and 60 g/l, the glucose was almost used up at 9 and 11 h, respectively. When initial concentration of glucose was 80 g/l, glucose was depleted after 14 h of cultivation. When the initial concentration of glucose was 100 g/l, glucose was depleted at 18 h. When the initial concentration of glucose was 120 g/l, glucose was depleted at 24 h.

Dry cell yield of *E. coli* at different initial glucose concentrations is shown in Fig. 2.2. The strain grew faster in the early phase of cultivation when initial concentrations of glucose were 40 and 60 g/l than when they were 80, 100 g/L, and the higher the initial glucose concentrations were 120 g/l, the slower the strain grew at the beginning. There were enough carbon sources in the medium for cell growth, so the DCW increased during the whole period of cultivation, faster in the early phase and slower in the late phase. Although the *E. coli* grew faster at low initial glucose concentrations, higher dry cell weights were achieved when the initial concentrations of glucose were 100 and 120 g/L, respectively (Fig. 2.3).

Time courses of cytidine production at different initial glucose concentrations are presented in Fig. 2.4. When initial concentration of glucose was 40 g/l, the

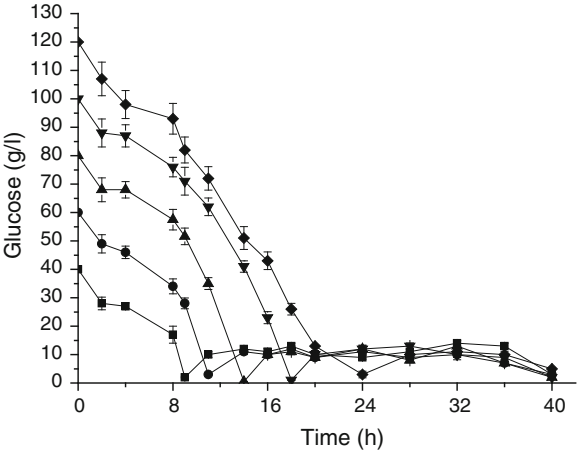

Fig. 2.1 Time courses of glucose consumption by *E. coli* at different initial glucose concentrations. After the glucose was depleted, a solution containing 800 g/l glucose was fed into the baffled flasks until the total glucose in the medium reached 10 g/l. The initial glucose concentrations were: (■) 40 g/l, (●) 60 g/l, (▲) 80 g/l, (▼) 100 g/l, (◆) 120 g/l

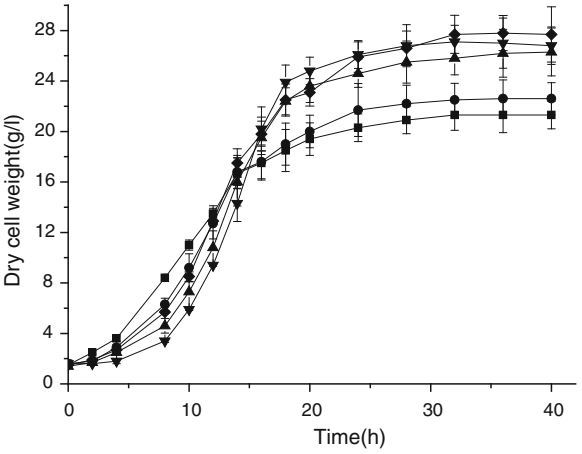

Fig. 2.2 Time courses of DCW of *E. coli* CYT20 at different initial glucose concentrations. The initial glucose concentrations were: (■) 40 g/l, (●) 60 g/l, (▲) 80 g/l, (▼) 100 g/l, (◆) 120 g/l

cytidine production reached its maximum concentration (650 mg/l) at 36 h, which was obviously lower than that from medium with other glucose concentrations. It was indicated that the yield of cytidine was determined by the cell growth rate and the final dry cell weight. When initial concentrations of glucose were 100 and 120 g/l, cytidine increased during the whole period of cultivation. The highest production and highest productivity of cytidine were obtained when the initial glucose concentration was 120 g/l, and the highest yield and productivity of cytidine were achieved at an initial glucose concentration of 120 g/l. It is probably due to the fact that in the early phase of cultivation, the growth of *E. coli* CYT20 was inhibited by the higher osmotic pressure of the media containing 100 and 120 g/l glucose. When the cultivation was proceeding, the consumption of glucose led to a decrease in the osmotic pressure and resulted in the accumulation of certain biomass. Within a certain range of osmotic pressures, a higher glucose

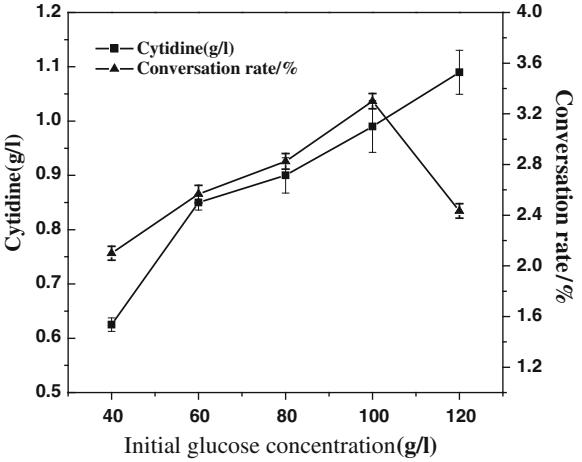

Fig. 2.3 Time courses of cytidine production of *E. coli* at different initial glucose concentrations. After the glucose was depleted, a solution containing 800 g/l glucose was fed into the baffled flasks until the total glucose in the medium reached 10 g/l. The initial glucose concentrations were: (■) Cytidine production, (▲) Conversation rate/%

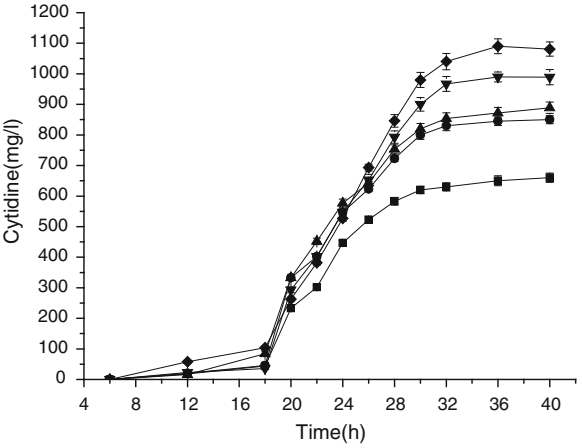

Fig. 2.4 Plots of the cytidine productions by *E. coli* at different initial concentrations. The initial glucose concentrations were: (■) 40 g/l, (●) 60 g/l, (▲) 80 g/l, (▼) 100 g/l, (◆) 120 g/l

concentration promoted the growth of the *E. coli* strains, which is influential to cytidine production.

Though maximum cytidine production was obtained after 40 h of cultivation when glucose concentration was 120 g/l according to above results, the strain grew slowly at the metaphase of cultivation and DCW was low at the end of fermentation. Therefore, the optimal initial glucose concentration is 100 g/l.

2.3.2 Effects of Temperature on Cytidine Production

In order to obtain higher yields of cytidine, four temperature control strategies were evaluated in a 500 ml baffled flask. The cell dry weight and cytidine

Table 2.1 Effect of temperature on cytidine production

Temperature (°C)	34	36	37	38
DCW (g/l)	24.3	27.2	26.7	27.3
Cytidine (mg/L)	687	1,188	1,034	971
Fermentation (h)	40	40	40	40

production were determined every 6 h throughout the whole cultivation process (Table 2.1). The four temperature control strategies were designed as follows: temperature of fermentation at 34, 36, 37, and 38 °C for 40 h. The different temperature control strategy was performed during the fermentation process because the optimal cell growth temperature was not necessarily the same as the temperature of product manufacture, especially since the product is not coupled with cell growth [10, 11]. Therefore, the fermentation temperature control of cytidine production was of great significance.

2.3.3 Effect of $(NH_4)_2SO_4$ on Cytidine Production

$(NH_4)_2SO_4$ is an important nitrogen source for the increase of cell growth and the concentration of desired products at the end of fermentation. The fed-batch fermentations were performed in 500 ml baffled flask with mediums containing different levels of $(NH_4)_2SO_4$ to investigate the effect of the $(NH_4)_2SO_4$ on cytidine fermentation (Fig. 2.5). The $(NH_4)_2SO_4$ concentration was adjusted to 20–150 mmol/L. The optimal concentration of $(NH_4)_2SO_4$ was found to be 110 mmol/L. A final cytidine production of 1,115 mg/l was obtained after 40 h of cultivation.

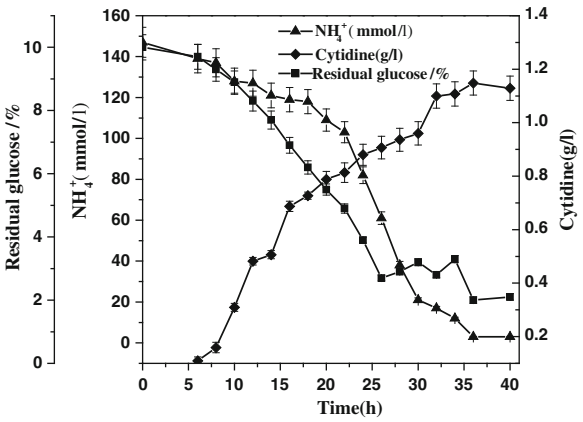

Fig. 2.5 Fermentation process curve of controlling concentration of glucose

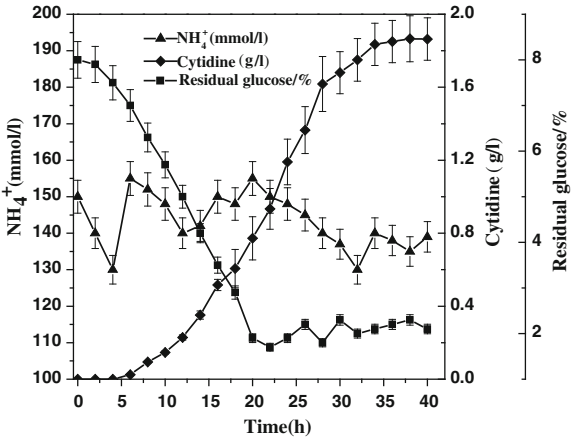

Fig. 2.6 Fermentation process curve of controlling concentration of glucose and $(NH_4)_2SO_4$

2.3.4 Verification of Cytidine Production by Baffled Flask

Using the optimized culture conditions, cytidine was produced by *E. coli* CYT20 in 500-ml baffled flask for 40 h (Fig. 2.6). As shown in Fig. 2.6, a final cytidine concentration of 1,866 mg/L was obtained after 40 h, which was 67.4 % higher than that from control.

In this study, an engineering bacteria, *E. coli* CYT20, has been successfully constructed, and the optimized fermentation conditions were determined, which indicate that the initial glucose concentration is 100 g/l, the $(NH_4)_2SO_4$ concentration is 110 mmol/l, and the temperature control is 36 °C at 40 h. Under the optimized conditions, the production of cytidine reached 1,866 mg/l, which was increased by 67.4 %. These results suggested that the strain improvement using genetic strategies and the fermentation conditions including the concentration of glucose, temperature, and $(NH_4)_2SO_4$ were important factors that affected cytidine production. The optimization of the fermentation process enhanced the cytidine productivity of *E. coli* dramatically and consequently lowered the production costs.

2.4 Conclusion

For cytidine production by microorganisms, an effective culture condition is very important [12–14]. The purpose of this study was to develop an optimal culture condition for the production of cytidine by *E. coli* CYT20. From a series of experiments, we determined that the concentration of glucose and $(NH_4)_2SO_4$ of the medium and temperature are the significant factors that affect the cytidine production. The optimum concentration of initial glucose and $(NH_4)_2SO_4$ were

100 g/l and 110–150 mmol/l, respectively. Fermentation temperature was 36 °C. Our results proved that controlling the culture conditions and modifying the medium can dramatically enhance the production of the cytidine of *E. coli* CYT20.

Acknowledgments We thank colleagues for critical reading of the manuscript and providing valuable suggestions. This work was supported by the Research Program of Tianjin University of Science and Technology (20100211), by Program for Changjiang Scholars and Innovative Research Team in University (IRT 1166), and by the Research Program of University in Ningxia (2012).

References

1. Asahi S, Tsunem Y (1994) Cytidine production by mutants of *Bacillus subtilis*. Biosci Biotech Biochem 58(8):1399–1402
2. Headrick JP, Ely SW, Matherne GP (1993) Methods for cytidine determination. Am J Physiol 264(1):31
3. Switzer RL (2009) Discoveries in bacterial nucleotide metabolism. J Biol Chem 284(11):6585–6594
4. Zhu J, Thakker C, San K-Y, Bennett G (2011) Effect of culture operating conditions on succinate production in a multiphase fed-batch bioreactor using an engineered *Escherichia coli* strain. Appl Microbiol Biotechnol 92(3):499–508
5. Wang J, Zhu J, Bennett GN, San K-Y (2011) Succinate production from different carbon sources under anaerobic conditions by metabolic engineered *Escherichia coli* strains. Metab Eng 13(3):328–335
6. Lin HY, Neubaur P (2000) Influence of controlled glucose oscillations on a fed-batch process of recombinant *Escherichia coli*. Biotechnology 79:27–37
7. Rahmen N, Kunze M, Büchs J (2011) Influence of recombinant protein production on respiration activity of *E. coli* shake flask cultures in auto induction media. Osaka Mini Symposium, Osaka University
8. Tramper J, Asahi S (1989) Methods for production of cytidine and deoxycytidine. Patent 4839285
9. Tyge G, Thomas A (2003) High-temperature liquid chromatography. J Chromtogr A 1000(12):743–755
10. Park KH, RubinL EG (1992) Research on determination of cytidine by reversed phase chromatography. Cric Lation Res 71(4):992
11. Carneiro S, Villas-Bôas SG, Eugénio C, Ferreira EC, Rocha I (2011) Metabolic footprint analysis of recombinant *Escherichia coli* strains during fed-batch fermentations. Mol BioSyst 7:899–910
12. Xiufu H, Daidi F, Yane L (2006) Kinetics of high cell density fed-batch culture of recombinant *Escherichia coli* producing human-like collagen. Chin J Chem Eng 14:242–247
13. Lennox B, Montague GA, Hiden HG, Kornfeld G, Goulding PR (2001) Process monitoring of an industrial fed-batch fermentation. Biotechnol Bioeng 74(2):125–135
14. Bakonyi P, Nemestóthy N, Lövitusz É, Bélafi-Bakó K (2011) Application of Plackett-Burman experimental design to optimize biohydrogen fermentation by *E. coli* (XL1-BLUE). Int J Hydrogen Energy 36(21):13949–13954

Chapter 3
Application of the *Cre-loxP* Recombination System for Two *ILV*2 Alleles Disruption in an Industrial Brewer's Yeast Strain

Jun Lu, Yefu Chen, Deguang Wu and Dongguang Xiao

Abstract Diacetyl has long been considered an unpleasant off-flavor component in beer. A recombinant industrial brewer's yeast strain in which two alleles of α-acetohydroxyacid synthase (AHAS) gene (*ILV*2) were disrupted using the *Cre-loxP* recombination system was constructed to produce the lower content of diacetyl. The results showed that the diacetyl production of recombinant yeast strain S-CSL5 is always lower than that of the parental strain S-6 at all stages of beer fermentation. The total process time (from the beginning of fermentation to the diacetyl reduction is finished) of beer fermented by the recombinant strain S-CSL5 could therefore be reduced to 12 days, in contrast to 15 days required for the parental strain. The AHAS activity of S-CSL5 was lowered by 58 % compared with that of the parental strain. In addition, the real-time PCR results revealed a low expression level of *ILV*2 as a potential molecular determinant for low diacetyl formation.

Keywords Diacetyl · *Cre-loxP* recombination system · *ILV*2 · Industrial brewer's yeast

3.1 Introduction

Diacetyl (2,3-butanedione) imparts an unpleasant "butterscotch-like" flavor to beer. It has long been considered a serious off-flavor component in beer. Diacetyl is a vicinal diketone and formed via a nonenzymatic decarboxylation from α-acetolactate outside the yeast cell during the main fermentation and removed by maturation process [1, 2]. It is particularly undesirable in lager beers and the

J. Lu · Y. Chen · D. Wu · D. Xiao (✉)
College of Biotechnology, Tianjin University of Science and Technology,
Tianjin 300457, People's Republic of China
e-mail: xdg@tust.edu.cn

T.-C. Zhang et al. (eds.), *Proceedings of the 2012 International Conference on Applied Biotechnology (ICAB 2012)*, Lecture Notes in Electrical Engineering 249,
DOI: 10.1007/978-3-642-37916-1_3, © Springer-Verlag Berlin Heidelberg 2014

threshold for diacetyl is 0.15 ppm or even lowers [3]. Its removal is the rate-limiting step in the maturation of beer. Diacetyl is a side product of the isoleucine-valine pathways. And the enzyme acetohydroxyacid synthase (Ilv2p) is of central importance for diacetyl formation. Concerning the metabolic pathway, an enhanced conversion of its precursor α-acetolactate to valine can reduce diacetyl formation. To this end, disruption of *ILV*2 encoding AHAS has a significant influence on the diacetyl production. Previous studies showed that disruption of the *ILV*2 gene can decrease of diacetyl production by 50–70 % compared to the control strain and significantly shorten the maturation period during beer production [4–6].

Previous studies in lager strains of yeast indicated that their genomes are hybrid and polyploid in nature and the copy number of certain genes in various strains of lager yeasts may range from haploid to tetraploid [7, 8]. The *Cre-loxP* system is a very versatile tool that allows for gene marker rescue and repeated use of the KanMX marker gene and will be of great advantage for the functional analysis of gene families [9, 10].

In this study, *Cre-loxP* recombination system was applied in efficiently and consecutively deleting two copies of *ILV*2 gene in polyploid industrial yeast. A recombinant industrial brewer's yeast strain that produces the lower content of diacetyl was constructed. The enzyme activities of AHAS were determined and fermentation performances of the recombinant strain were examined under the industrial brewing conditions. We also explored correlations in the expression level of *ILV*2 and AHAS activity.

3.2 Materials and Methods

3.2.1 Microorganisms and Cultivation Conditions

The yeast strains and *Escherichia coli* DH5α used in this study are listed in Table 3.1. The industrial brewer's yeast S-6 was obtained from the Yeast Collection

Table 3.1 Strains used in the current study

Strais	Relevant characteristic	Reference or source
E.coli.DH5	supE44 ΔlacU169(φ 80lacZΔM15) hsdR17 recAl endAl gyrA96 thi-1 relA	Stratagene
S-6	Wild-type industrial brewer's yeast	Our lab
S-L5	*ILV*2/*ilv*2Δ::*loxP-KanMX-loxP*	This work
S-CL5	*ILV*2/*ilv*2Δ::*loxP*	This work
S-SL5	*ilv*2Δ::*loxP-KanMX-loxP*/*ilv*2Δ::*loxP*	This work
S-CSL5	*ilv*2Δ::*loxP*/*ilv*2Δ::*loxP*	This work

Center of the Tianjin Key Laboratory of Industrial Microbiology, Tianjin University of Science and Technology, China. S-6 was used as the control strain.

Yeast strain was grown at 28 °C in YEPD medium (1 % yeast extract, 2 % peptone, 2 % glucose). For selection of Geneticin (G418) resistance after yeast transformation, the YEPD plate was supplemented with G418 at a final concentration of 800 mg/L. For selection of Zeocin resistance, Zeocin (500 mg/L, Promega, Madison, United States) was added to the YEPD plates for yeast. And YEPG medium (1 % yeast extract, 2 % peptone, 2 % galactose) was used for *Cre* expression in yeast transformants. Escherichia coli strain was grown at 37 °C in Luria–Bertani broth (composed of 1 % NaCl, 1 % tryptone, and 0.5 %yeast extract) supplemented with ampicillin at a final concentration of 100 mg/L.

3.2.2 DNA Manipulation and Construction of Plasmids

Plasmid DNA was prepared from E. coli as described by Sambrook et al. [11].Genomic DNA of yeast was prepared from industrial Brewer's yeast S-6 as described by Bruke et al. [12]. The primers used for plasmids construction in this study are listed in Table 3.2.

Table 3.2 The primary primers used in the current study

Primer	Sequence (5′ → 3′)
Primers for plasmids construction and verification[a]	
ILV2-SF	AACTGCAGCTTGGCTTCAGTTGCTG
ILV2-SR	CGGGATCCCTCTTAGCTCAAAGGGT
ILV2-XF	CGGGATCCCGTACAGGCGGTAAGCAC
ILV2-XR	GGGGTACCCGAGGTCTCGGAATGG
K-U	CGGGATCCCAGCTGAAGCTTCGTACGC
K-D	CGGGATCCGCATAGGCCACTAGTGGATCTG
YZ-SFI	ACTTTACGAAAGTTTGAGGAGG
YZ-2A	ACAACCTATTAATTTCCCCTCG
YZ-AUP	TTTTGATGACGAGCGTAATGGC
YZ-XRI	CTTTCCAATTGACTCCGTATGTG
ILV2-SSF	AACTGCAGCGTTATTACAGTGCGTCTC
ILV2-SSR	CGGGATCCGGTTTAGTGCGTTTGATG
ILV2-SXF	CGGGATCCAAATGTGGGCTGCTCAAC
ILV2-SXR	GGGGTACCCTTAGCGTCCAATTCCTC
Primers for real time PCR	
ACT1-F	TGGATTCTGAGGTTGCTGCTTTGG
ACT1-R	ACCTTGGTGTCTTGGTCTACCG
ILV2-U	CACGGTTGTGCTACTGC
ILV2-D	TGCCCAGATTGGTCGT

[a] The restriction site introduced in each primer is indicated by an underline

The *ILV*2 gene, the sequences of which were used for homologous recombination, was amplified from S-6 genomic DNA using PCR with the primers showed in Table 3.1. The PCR product was subsequently subcloned into pUC19 to generate the plasmid pUC-LSX. The KanMX cassette was amplified via PCR using plasmid pUG6 as the template with primer pair K-U/K-D and inserted into plasmid pUC-LSX after the digestion with BamH I, producing the plasmid pUC-KLSX. Based on the aforementioned strategy, recombinant plasmid pUC-SKLSX was constructed for the second *ILV*2 allele disruption. Recombinant fragment was amplified using retractive primer as described by Hao et al. [13].

3.2.3 Yeast Transformation and Verification

Transformation was performed using the lithium acetate/PEG method [14]. Transformants were screened on YEPD plate containing 800 mg/L G418. The strategy employed for disruption of the first *ILV*2 allele is shown in Fig. 3.1. The strategy employed for disruption of the second *ILV*2 allele is shown in Fig. 3.2. PCR was applied to verify the recombinant strains with accurate site integration. Primer binding region for PCR confirmation of successful homologous recombination was shown in Fig. 3.3.

3.2.4 Gene Expression Levels via Real-Time PCR

Yeast strains were cultured in YEPD medium for 18 h and collected for RNA extraction. RT-PCR was performed by use of an RT-PCR kit (CWBIO) according to the manufacturer's instructions. The *ILV*2 gene was amplified using primer ILV2-U/ILV2-D. And the reference gene ACT1 was amplified using primer ACT1-F/ACT1-D. All primers were shown in Table 3.2.

3.2.5 Assay of AHAS Activity

Reaction conditions for enzyme assays in vitro were as follows: α-acetolactate synthase activity was measured according to [15]. One unit (1 U) of AHAS activity is defined as the amount of enzyme required to produce 10^{-8} mol of acetolactate in 30 min at 30 °C.

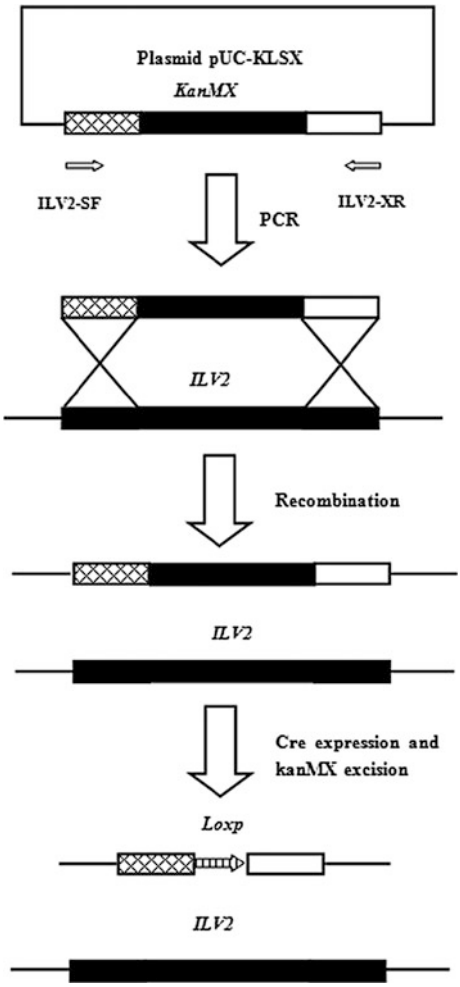

Fig. 3.1 Strategy employed for disruption of the first *ILV*2 allele and *kanMX* excision in yeast strains

3.2.6 Fermentation Test

After activation on YEPD slant, the yeast strain was inoculated to 5 mL of 10°P wort and cultivated at 28 °C (180 rpm) for 24 h, then all the suspension was inoculated into 50 ml of wort (11 °P) at 16 °C for 48 h. For the main fermentation, the preculture (50 ml) was transferred into 500 ml of 11 °P wort in conical flask with fermentation bung resulting in a cell density of $\sim 2 \times 107$ cells/ml. Main fermentations were carried out at 10 °C. Apparent extract and CO_2 reduction of wort was recorded every day. Diacetyl concentration of beer was assayed at different stage of fermentation.

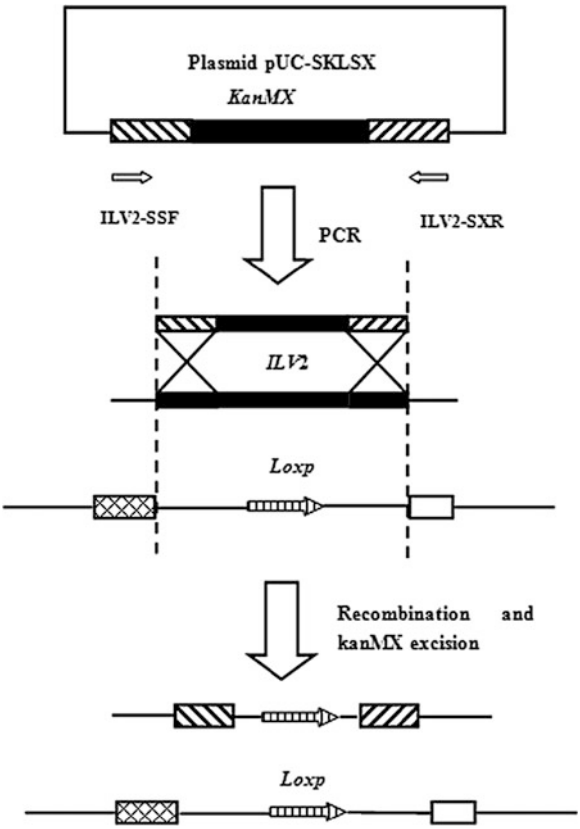

Fig. 3.2 Strategy employed for disruption of the second *ILV2* allele and *kanMX* excision in yeast strains

3.2.7 Measurement Diacetyl and Flavor Component

Before analysis, the samples were heated at 60 °C for 1 h to cause complete conversion of α-acetolactate into diacetyl. Headspace gas chromatography coupled with electron capture detection (GC-ECD) was used for the measurement of diacetyl content [16]. The esters and higher alcohols were measured using headspace gas chromatography coupled with flame ionization detection.

3.3 Results and Discussion

3.3.1 Construction and Verification of Recombinant Strains

The fragment for replacement was amplified by PCR using recombinant plasmid pUC-KLSX as the template with primer pairs of ILV2-SF/ILV2-XR (Tabel 3.1).

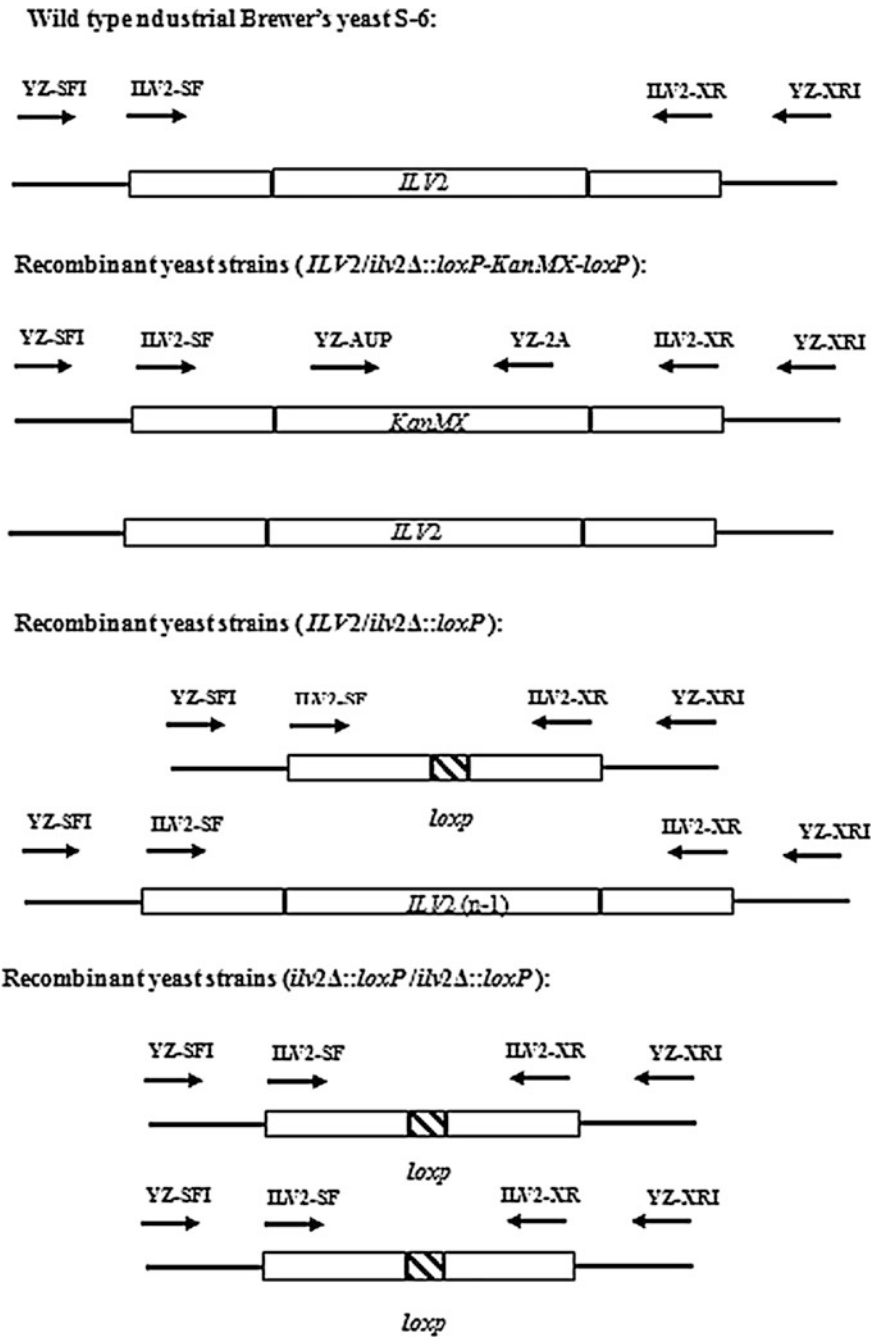

Fig. 3.3 Primer binding region for the confirmation of correct integration of the *KanMX* and *kanMX* excision in yeast strains

Then the fragment was transformed into the industrial brewer's yeast S-6. Therefore, one copy of *ILV*2 deletion strain was constructed via PCR-mediated homologous recombination, as shown in Fig. 3.1. To verify the correct integration of the KanMX cassette taking place on the target locus, the transformants were picked up, and then colony-PCR was carried out using primer pairs YZ-SFI/YZ-2A and YZ-AUP/YZ-XRI (Table 3.1). Amplified DNA fragments of 1859 bp and 1596 bp were obtained, respectively (Fig. 3.4, lane 1, 2). After the PCR verification, one transformant was selected and designated as S-L5. After the single *ILV*2 allele deletion strain S-L5 was successfully obtained, the plasmid of pSH-Zeocin (a *Cre* expression vector) was transformed into S-L5, so that the drug-resistance gene of KanMX was excised from the chromosome of the recombinant strain S-L5. The primer pairs ILV2-SF/ILV2-XR were used by colony-PCR for the confirmation of loss of KanMX gene, primer site was shown in Fig. 3.3. The KanMX removed strain was designated as S-CL5. When analyzing the transformants by diagnostic PCR with this set of primers, we also observed the presence of the wild type *ILV*2 allele in all transformants (Fig. 3.4, lane 3). These results indicated that more than one copy of the *ILV*2 gene might be present in the S-6 genome. In order to efficiently repeat deletion of *ILV*2 allelic genes, the retractive primer disruption strategy described by [13] was applied, as shown in Fig. 3.2. After the PCR verification, one verified transformant with the lowest diacetyl production was selected and was designated as S-SL5. After the two *ILV*2 allele deletion strain S-SL5 was obtained, the same method as described above was used to excise the KanMX of S-SL5. The resulting transformant was designated as S-CSL5. As diagnostic PCR of the *ILV*2 double deletion did not reveal any additional copy of this gene (Fig. 3.4 lane 7, 8), we concluded that strain S-6 was diploid for *ILV*2 gene. Therefore, S-CSL5 was an *ILV*2 completed deletion strain.

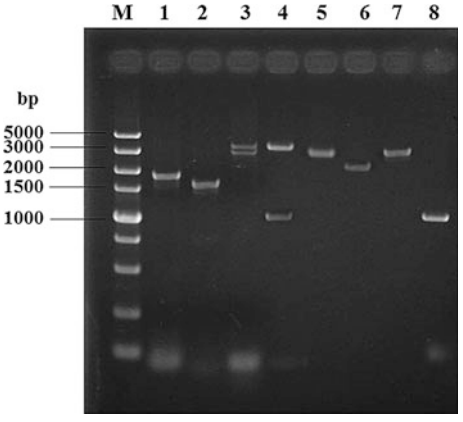

Fig. 3.4 PCR analysis of the yeast recombinant strains. DNA templates: S-L5 (lane 1, 2, 3); S-CL5 (lane 4); S-SL5 (lane 5, 6, 7); S-CSL5 (lane 8). Primers: YZ-SFI/YZ-2A (lane 1, 5); YZ-AUP/YZ-XRI (lane 2, 6); ILV2-SF/ILV2-XR (lane 3, 4); ILV2-SSF/ILV2-SXR (lane 7, 8)

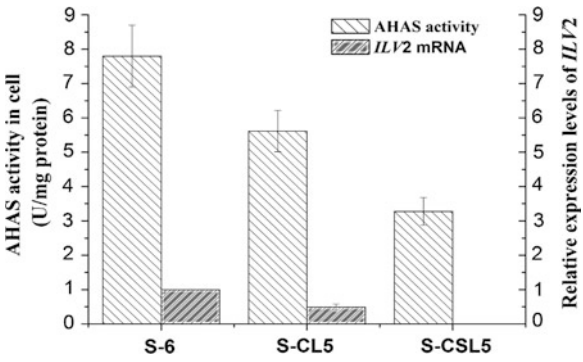

Fig. 3.5 Determination of expression levels of *ILV*2 gene in recombinant strains S-CL5 and S-CSL5 by real time PCR and measurement of AHAS activity of recombinant strains S-CL5, S-CSL5 and the parental strain S-6

3.3.2 AHAS Activity and ILV*2 Expression Levels*

The AHAS activity of recombinant strains S-CL5 and S-CSL5 cultivated in YEPD medium were measured. The enzyme activity in recombinant strain cells was lower than that of their host. The AHAS activity of S-CL5 and S-CSL5 decreased respectively by 28 and 58 % compared with their parental strain S-6 (Fig. 3.5). In addition, the expression levels of *ILV*2 gene were determined by qRT-PCR. The cDNAs of *ILV*2 single deletion strain S-CL5 decreased to 49 % that of its parental strain S-6 (Fig. 3.5). By contrast, no signal was detected in *ILV*2 double deletion strain S-CSL5. These results further proved that two copies of *ILV*2 gene existed in S-6 genome. It was noted that when deleting all allele of *ILV*2 gene, there was still AHAS activity detected. Based on this result, it has been assumed that there might be another isoenzyme of AHAS in this industrial brewer's yeast. However, further study is needed.

3.3.3 Diacetyl Content Assay During Beer Fermentation

The diacetyl content of the *ILV*2 single deletion strain S-CL5 and the *ILV*2 double deletion strain S-CSL5 were measured when wort reached an apparent extract of 8 % (day 3), 6 % (day 7), and 4 % (day 11). In order to compare the time consumption (from the beginning of fermentation to the diacetyl reduction is finished) for brewing with different strains, diacetyl concentration was also measured every day (days 12–15) after wort apparent extract reached 4 %. The results showed that the diacetyl production of recombinant yeast strain S-CL5 and S-CSL5 were always lower than that of the parental strain S-6 at all stages of beer fermentation (Fig. 3.6).

The time needed for diacetyl reducing to the taste threshold were 13 days and 12 days, respectively, when brewing using S-CL5 and S-CSL5, in contrast to 15 days required of parental strain S-6. The diacetyl level of the *ILV*2 double

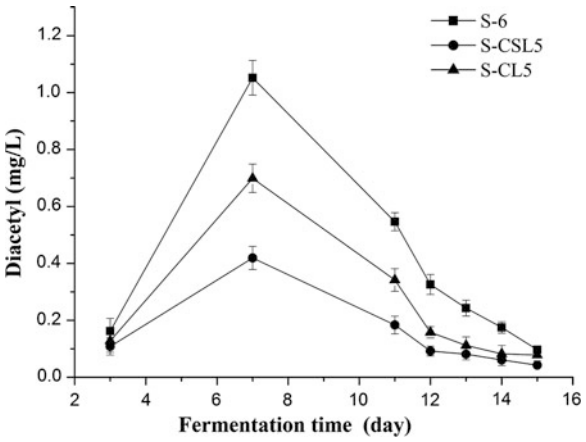

Fig. 3.6 Diacetyl contents of recombinant strains and the parental strain during the fermentation test

deletion strain S-CSL5 was lowered more significantly compared with that of *ILV*2 single deletion strain S-CL5, as was shown in Fig. 3.6. The results revealed that lowering the copy number of *ILV*2 gene was an effective way to decrease the diacetyl production of brewers' yeast strain. Previous studies are mostly deleting one copy of *ILV*2 gene to reduce diacetyl production [17–20]. This study report that the *ILV*2 complete deleted strain produce even lower content of diacetyl.

3.3.4 The Main Beer Performance Indices

To investigate the impact of the *ILV*2 gene single deletion or double deletion on the fermentation performance, real attenuation, real extract, ethanol, pH, esters, and higher alcohols were measured after the primary beer fermentation (days 15), as shown in Table 3.3. Compared to the reference beer (S-6 was used in brewing), a slight increase in production of isobutyl alcohol and ethyl acetate was observed,

Table 3.3 Parameters of fermented liquor

Parameter	S-6	S-CL5	S-CSL5
Real attenuation (%)	72.05 ± 0.21	71.25 ± 0.18	71.48 ± 0.22
Real extract (%)	4.38 ± 0.05	4.26 ± 0.08	4.18 ± 0.06
Ethanol (g l^{-1})	40.5 ± 0.42	40.2 ± 0.35	39.38 ± 0.25
pH	4.3 ± 0.1	4.4 ± 0.1	4.4 ± 0.2
Acetaldehyde (mg l^{-1})	6.83 ± 0.14	658 ± 0.24	6.96 ± 0.09
Ethyl acetate (mg l^{-1})	15.86 ± 0.3	15.67 ± 0.2	18.71 ± 0.4
Propyl alcohol (mg l^{-1})	15.92 ± 0.2	15.18 ± 0.3	15.58 ± 0.1
Isobutyl alcohol (mg l^{-1})	10.15 ± 0.5	10.41 ± 0.2	12.95 ± 0.4
Isoamyl acetate (mg l^{-1})	1.39 ± 0.15	1.43 ± 0.14	1.34 ± 0.25
Isoamyl alcohol (mg l^{-1})	54.96 ± 2.2	53.86 ± 3.1	47.98 ± 3.8

when brewing using *ILV*2 double deletion strain S-CSL5. Moreover, a slight decrease in production of isoamyl alcohol was also observed. There was no significant difference in fermentation performance between *ILV*2 gene single deletion S-CL5 and S-6.

All the results shown are mean values of three independent experiments including standard deviations. The parameters were measured after the primary beer fermentation.

3.4 Conclusion

A recombinant industrial brewer's yeast strain that produces the lower content of diacetyl was constructed in this study, in which two alleles of AHAS gene (*ILV*2) was disrupted using the *Cre-loxP* recombination system. The results showed that the diacetyl production of recombinant yeast strain S-CSL5 is always lower than that of the parental strain S-6 at all stages of beer fermentation. The time needed for diacetyl reducing to the taste threshold was reduced from 15 to 12 days. The AHAS activity of S-CSL5 was lower compared with that of parental strain. In addition, the real-time PCR results revealed a lower expression level of *ILV*2 in recombinant strain compared with that of control. There were no significant differences in the appearance and mouth-feel between recombinant strain and the parental strain.

Acknowledgments The current study was financially supported by the National Natural Science Foundation of China (No. 31271916), the Cheung Kong Scholars and Innovative Research Team Program in University of Ministry of Education, China (Grant No. IRT1166).

References

1. Haukeli A, Lie S (1978) Conversion of alpha-acetolatate and removal of diacetyl a kinatic study. J Inst Brew 84:85–89
2. Duong CT, Strack L, Futschik M et al (2011) Identification of Sc-type *ILV*6 as a target to reduce diacetyl formation in lager brewers' yeast. Metab Eng 13(6):638–647
3. Saison D, De Schutter DP, Uyttenhove B et al (2009) Contribution of staling compounds to the aged flavour of lager beer by studying their flavour thresholds. Food Chem 114(4):1206–1215
4. Wang ZY, He XP, Liu N et al (2008) Construction of self-cloning industrial brewing yeast with high-glutathione and low-diacetyl production. Int J Food Sci Tech 43(6):989–994
5. Gjermansen C, Nilsson-Tillgren T, Petersen JGL et al (1988) Towards diacetyl-less brewers' yeast. Influence of ilv2 and ilv5 mutations. J Basic Microbiol 28(3):175–183
6. Liu Z, Zhang G, Li J et al (2008) Integrative expression of glucoamylase gene in a brewer's yeast *Saccharomyces pastorianus* strain. Food Technol 46(1):32–37
7. Bond U, Neal C, Donnelly D et al (2004) Aneuploidy and copy number breakpoints in the genome of lager yeasts mapped by microarray hybridisation. Curr Genet 45(6):360–370

8. Dunn B, Sherlock G (2008) Reconstruction of the genome origins and evolution of the hybrid lager yeast *Saccharomyces pastorianus*. Genome Res 18(10):1610–1623
9. Ribeiro O, Gombert AK, Teixeira JA (2007) Application of the *Cre-loxP* system for multiple gene disruption in the yeast *Kluyveromyces marxianus*. J Biotechnol 131(1):20–26
10. Güldener U, Heck S, Fiedler T et al (1996) A new efficient gene disruption cassette for repeated use in budding yeast. Nucleic Acids Res 24(13):2519–2524
11. Sambrook J, Fritsch EF, Maniatis T (1989) Molecular cloning: a laboratory manual, 2nd ed., vol. I. Cold Spring Harbor Laboratory Press, Cold Spring Harbor, NY
12. Burke D, Dawson DS, Stearns T (2000) Methods in yeast genetics: A Cold Spring Harbor laboratory course manual. CSHL, Press, USA
13. Hao J, Dong J, Speers RA et al (2008) Construction of a single *PEP* 4 allele deletion in *Saccharomyces carlsbergensis* and a preliminary evaluation of its brewing performance. J Inst Brew 114(4):322–328
14. Daniel Gietz R, Woods RA (2002) Transformation of yeast by lithium acetate/single-stranded carrier DNA/polyethylene glycol method. Methods Enzymol 350:87–96
15. Zhang Y, Wang ZY, He XP et al (2008) New industrial brewing yeast strains with *ILV*2 disruption and *LSD*1 expression. Int J Food Microbiol 123(1−2):18–24
16. Saerens SMG, Verbelen P, Vanbeneden N et al (2008) Monitoring the influence of high-gravity brewing and fermentation temperature on flavour formation by analysis of gene expression levels in brewing yeast. Appl Microbiol Biotechnol 80(6):1039–1051
17. Wang JJ, Xiu PH, He XP et al (2010) Construction of amylolytic industrial brewing yeast strain with high glutathione content for manufacturing beer with improved anti-staling capability and flavor. J Microbiol Biotechnol 20(11):1539–1545
18. Wang D, Wang Z, Liu N et al (2008) Genetic modification of industrial yeast strains to obtain controllable NewFlo flocculation property and lower diacetyl production. Biotechnol Lett 30(11):2013–2018
19. Liu ZR, Zhang GY, Li J et al (2007) Stable expression of glucoamylase gene in industrial strain of *Saccharomyces pastorianus* with less diacetyl produced. Ann Microbiol 57(2):233–237
20. Liu ZR, Zhang GY, Liu SG (2004) Constructing an amylolytic brewing yeast *Saccharomyces pastorianus* suitable for accelerated brewing. J Biosci Bioeng 98(6):414–419

Chapter 4
Clone and Expression of High Yield Recombinant Trehalose Synthase in *Bacillus subtilis*

Jing Su, Chunling Ma, Tengfei Wang, Piwu Li and Ruiming Wang

Abstract Trehalose synthase is one kind of intermolecular transglucosylation enzyme, which catalyzes the conversion of maltose to trehalose. In this study the trehalose synthase gene was amplified from *Pseudomonas putida* P06 genomic DNA, ligated with pMA5 vector, cloned into *Bacillus subtilis* WB800 and had good expression with the molecular weight of 77 KD. The recombinant trehalose synthase expression conditions were performed and enzyme reaction key parameters were investigated. The results showed the enzyme had optimal activity when it reacted for 2 h at 35 °C with pH value of 7.5 and the substrate concentration was 30 %. Trehalose content of samples was detected by HPLC and the enzyme activity reached to 318.12 U/ml in crude enzyme solution. This study is the first report about the expression of trehalose synthase in *Bacillus subtilis*, which lays the basis for trehalose large scale industrial production.

Keywords Trehalose synthase · *Pseudomonas putida* · Gene expression · *Bacillus subtilis* WB800

4.1 Introduction

Trehalose is a non-reducing disaccharide, which has two glucose molecules linked in α, α-1, 1-glycosidic linkage. It widely spreads in bacteria, archaea, yeast, fungi, insects and a number of invertebrates [1]. It has high stability against extreme environment conditions such as temperature, pH and desiccation. So it plays important roles, such as a carbon energy reserve [2], a compatible solute under stress conditions [3–5] and a structural component of the cell wall. On the other

J. Su · C. Ma · T. Wang · P. Li · R. Wang (✉)
School of Food and Bioengineering, Qilu University of Technology, Jinan 250300, China
e-mail: ruiming3k@163.com

T.-C. Zhang et al. (eds.), *Proceedings of the 2012 International Conference on Applied Biotechnology (ICAB 2012)*, Lecture Notes in Electrical Engineering 249,
DOI: 10.1007/978-3-642-37916-1_4, © Springer-Verlag Berlin Heidelberg 2014

hand trehalose not only protects biomolecules in vivo but also has the same protection effect in vitro. This feature of trehalose has opened a new field for its application in food industry and pharmaceutical manufacturing practice [6, 7].

So far it is generally reported that there are at least three metabolized pathways for the biosynthesis of trehalose in microorganism. The first pathway is catalyzed by the trehalose-6-phosphate synthase, in which trehalose is synthesized through the glucosyl moiety from UDP-glucose to glucose-6-phosphate to form trehalose-6-phosphate that further dephosphorylated to trehalose by trehalose-6-phosphate phosphatase [8, 9]. The second pathway involves the rearrangement of internal glycosidic linkage between the molecules of glucose polymer such as maltooligosaccharides produced from the hydrolysis of starch using α-amylase [10, 11], which can convert α-(1−4) linkage of the terminal residue of the maltooligosaccharides into α-(1–1) linkage. The third pathway is also a process of internal rearrangement of the glycosidic linkage between the molecules. But it can only use maltose as the substrate, and the enzyme responsible for this process is trehalose synthase [12–14].

Currently the third pathway has been interested for industry because its substrate is only simple disaccharide (maltose). Trehalose synthase is apt for trehalose large scale production. But the main problem for trehalose synthase industrial production depends on its activity improvement. So far there are many reports about cloning and expression of trehalose synthase in *E. coli* [15–18]. However, *E. coli* is pathogenic and is not safe for food industry production. Compared with *E. coli, Bacillus subtilis* is one kind of safe expression system. Since the discovery of the method of transforming *B. subtilis* with plasmid DNA, *B. subtilis* has become an efficient expression host for the expression of foreign genes. These features include the non-pathogenic nature, well-established safety record, ability to secret extracellular proteins directly to culture medium, easy genetic manipulation, non-biased coden usage and fast growth rate [19–22]. Up to now, there is no report about the expression of the trehalose synthase gene in *B. subtilis* recombinant system. In this study the trehalose synthase gene was amplified from *Pseudomonas putida* P06 genomic DNA and was expression in *B. subtilis* under the control of the promoter of *HpaII*. The recombinant enzyme efficiently secreted into the culture. Trehalose content of samples was detected by HPLC and the enzyme activity reached to 318.12 U/ml in crude enzyme solution.

4.2 Materials and Methods

4.2.1 Bacterial Strains, Plasmids, Chemicals, Media and Culture Conditions

Bacillus subtilis WB800 was used as the expression host, which is an eight protease deficient strain. For protein studies, cell was cultivated in super-rich medium [23] containing appropriate antibiotics at 37 °C. *Pseudomonas putida* P06-2 was

obtained from screening and had been deposited in our laboratory. Expression plasmid pMA5 was obtained from Tianjin University of Science and Technology. Bacterial Genomic DNA Mini-Preps Kit, LATaq, restriction enzymes, and ligase were all purchased from Takara. All chemical products used in the experiment were purchased from Sigma Chemical Co. (St Louis, MO, USA).

4.2.2 Tres *Gene Cloning and Expression Vector Construction*

Tres gene was amplified from *Pseudomonas putida* P06-2 genomic DNA, which was purified with bacteria genome DNA extracting kit and used as a template for PCR amplification with the forward primer: 5′-CGGAATTCATGACCCAGC CCGACC-3, and the reverse primer: 5′-CCCAAGCTTTCAAACATGCCCGC TGC-3′. PCR amplification conditions were: 95 °C for 5 min followed by 30 cycles of 95 °C for 30 s, 54 °C for 30 s, 72 °C for 2 min. The PCR products were digested with *EcoRI* and *Hind*III restriction cutting sites, and then ligated into pMA5 expression vector, which had been treated with the same restriction enzymes. All the clones were confirmed by DNA sequencing. The constructed recombinant vector containing *tres* gene was named pMA5–*tres*, and used to transform *B. subtilis* WB800.

4.2.3 Tre *Gene Expression in* Bacillus Subtilis *WB800*

The pMA5–*tres* cells and empty vector control were cultured in the LB medium at 37 °C for 24 h. At the end of the culture period, cells were harvested by centrifugation at 14,000 × g for 45 min to give the culture supernatant and the cell pellet. The supernatant was dissolved into 2 × SDS-PAGE loading buffer and boiled for 10 min, centrifuged at 10,000 rpm for 2 min, and 5 μl supernatant was analyzed on SDS-PAGE followed by Coomassie blue staining.

4.2.4 *Assay of Trehalose Synthase Activity*

The activity of trehalose synthase was assayed by measuring the amount of trehalose produced from maltose. The quantity of sugars after each enzymatic reaction was measured by High-performance liquid chromatography (HPLC).

The effects of pH on trehalose synthase activity were performed at various pH 5.0–9.0 phosphate buffers. The effects of temperature on the enzyme activity were determined by setting the reaction temperature from 20 °C to 45 °C. The effects of reaction time on the enzyme activity were performed at 1, 2, 4, 6, 8, 20 h.

The effects of the substrate concentration were determined by 5, 10, 20, 30, 40 % maltose solution. The HPLC system of Shimadzu with NH_2-column and acetonitrile phosphate buffer (27:73 v/v, pH 7.0) as the mobile phase was used. The presence of trehalose as products of the enzyme reaction was identified using reference standard (Trehalose purity was above 99.5 %) obtained from Sigma.

4.3 Results and Discussion

4.3.1 Tres *Gene Cloning and pMA5–*Tres *Vector Construction*

(Fig. 4.1)

4.3.2 Expression Analysis of SDS-PAGE

Bacillus subtilis WB800 was used as pMA5–*tres* expression host to express the *tres* gene corresponded with about the molecular weight of 77 KD was seen on the SDS-PAGE (Fig. 4.2).

4.3.3 Trehalose Synthase Activity Measurement

The effects of pH on trehalose synthase were depicted in (Fig. 4.3a). The optimum pH for the enzyme activity was 7.5, when pH below 6.5 and above 8.0 the enzyme activity decreased sharply. The effects of temperature on the enzyme were depicted in (Fig. 4.3b). The optimum temperature was 35 °C, which was close to room temperature. So the energy consumption in temperature control could be

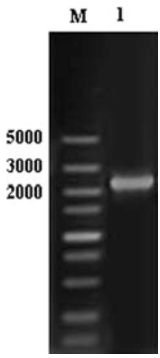

Fig. 4.1 Agarose electrophoresis of *tres* gene cloned from *Pseudomonas putida* P06 genomic DNA by PCR

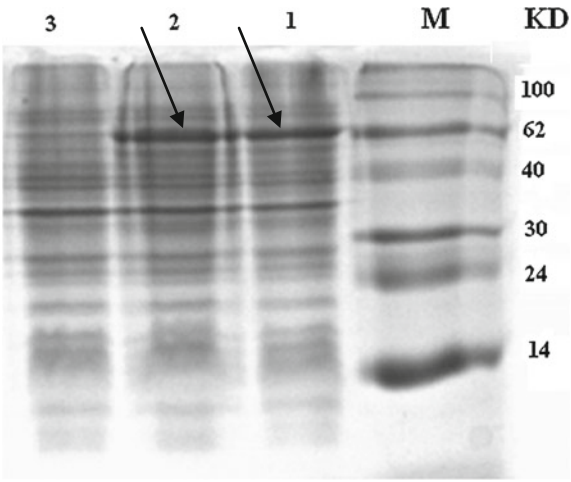

Fig. 4.2 Expression of trehalose synthase in *B. subtilis* WB800. The first and the second were transformed with pMA5–*tres* plasmid. The third was empty vector control. The arrows showed the positions of the target protein which corresponds to the molecular weight

decreased. The effects of reaction time on the enzyme were depicted in (Fig. 4.3c). The optimum reaction time on the enzyme was 2 h. The reaction time of this recombinant enzyme decreased more than previous reports. The effects of substrate concentration on the enzyme were depicted in (Fig. 4.3d). When maltose

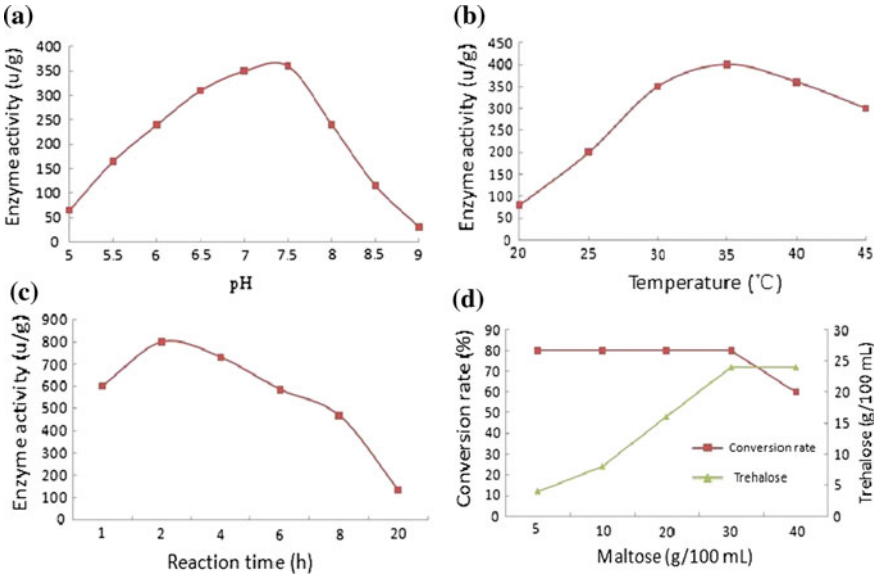

Fig. 4.3 **a** Optimum pH for the enzyme was investigated by phosphate buffer with pH in range of 5.0–9.0 **b** Optimum temperature was investigated between 20 °C and 45 °C **c** Optimum reaction time of the enzyme was investigated from 1 h to 20 h **d** Optimum substrate concentration for the conversion rate and trehalose synthase concentration

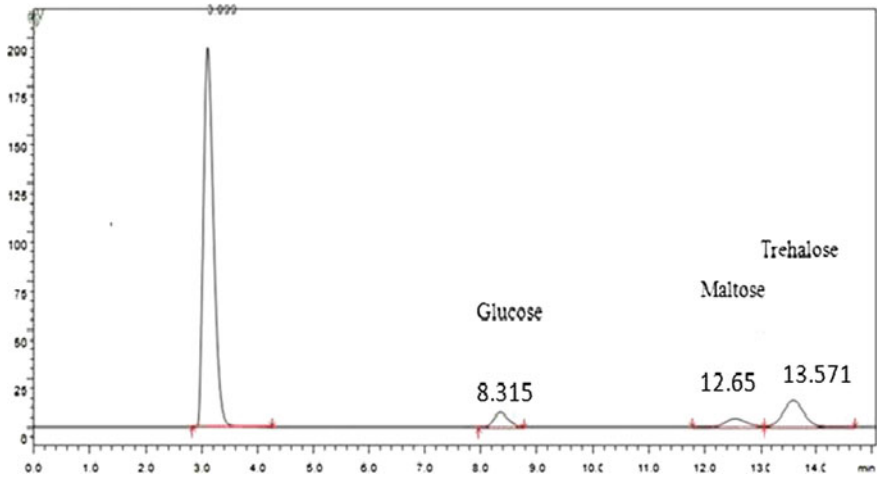

Fig. 4.4 HPLC analysis of the enzyme reaction with 30 % maltose as substrate for 2 h at 35 °C

concentration increased from 5 % to 30 %, the yield of trehalose increased at the same time. At last the enzyme reaction key parameters were investigated as follows: the optimum pH was 7.5, reaction temperature was 35 °C, reaction time was 2 h, and the substrate concentration was 30 %. After 2 h reaction, the supernatant was inspected for the presence of trehalose using HPLC (Fig. 4.4). From the chromatography it could be seen that the enzyme activity reached to 318.12 U/ml in crude enzyme solution.

4.4 Conclusions

Trehalose synthase catalyzes the conversion of maltose to trehalose, and several *TreS* have been cloned from various bacteria in *E. coli.* In our study, a *TreS* was cloned from *Pseudomonas putida* P06 used Plasmid pMA5 as vector and expression in *B. subtilis* W800. *B. subtilis* as expression host has some advantages compared with *E. coli*, such as no toxicity, solubility, secretory expression and so on. These features make *B. subtilis* apt for food and pharmaceutical industry. The recombinant trehalose synthase in our study had good expression in *B. subtilis*. The optimum reaction time for the recombinant enzyme was only 2 h, which decreased the reaction time than previous reports. On the other hand its optimum temperature was 35 °C, which is close to room temperature. So the energy consumption in temperature control could be decreased. These characteristics make it apt for large scale production of trehalose.

References

1. Elbein AD, Pan YT, Pastuazak I, Carroll D (2003) New insights on trehalose: a multifunctional molecule. Glycobiology 13:17–27
2. Thevelein JM (1984) Regulation of trehalose mobilization in fungi. Microbiol Rev 48:42–59
3. Giaver HM, Styrvold OB, Kaasen I, Stram AR (1988) Biochemical and genetic characterization of osmoregulatory trehalose synthesis in *Escherichia coli*. J Bacteriol 170:2841–2849
4. Reinders A, Bu rckert N, Hohmamm S, Thevelein JM, Boller T, Wiemken A, de Virgilio C (1997) Structural analysis of the subunits of the trehalose-6-phosphate synthase/phosphatase complex in Saccharomyces cerevisiae and their function during heat shock. Mol Microbiol 24:687–695
5. Silva Z, Alarico S, Nobre A, Horlacher R, Marrugg J, Boos W, Mingote AI, da Costa MS (2003) Osmotic adaptation of Thermus thermophilus RQ-1: a lesson from a mutant deficient in the synthesis of trehalose. J Bacteriol 185:5943–5952
6. Schiraldi C, Lernia ID, Rosa MD (2002) Trehalose production: exploiting novel approaches. Trends Biotechnol 20:420–425
7. Higashiyama T (2002) Novel functions and applications of trehalose. Pure Appl Chem 74:1263–1269
8. de Smet KAL, Weston A, Brown IN, Young DB, Robertson BD (2000) Three pathway for trehalose biosynthesis in *Mycobacteria*. Microbiology 146:199–208
9. Padilla L, Kramer R, Stephanopoulos G, Agosin E (2004) Overproduction of trehalose: Heterologous expression of *Escherichia coli* trehalose-6-phosphate synthase and trehalose-6-phosphate phosphatase in *Corynebacterium glutamicum*. Appl Environ Microbiol 70:370–376
10. Maruta K, Nakada T, Kubota M, Chaen H, Sugimoto T, Kurimoto M, Tsujisaka Y (1995) Formation of trehalose from maltooligosaccharides by a novel enzymatic system. Biosci Biotechnol Biochem 59:1829–1834
11. Nakada T, Ikegami S, Chaen H, Kubota M, Fukuda S, Sugimoto T, Kurimoto M (1996) Purification and characterization of thermostable maltooligosyl trehalose synthase from the thermoacidophilic archaebacterium Sulfolobus acidocaldarius. Biosci Biotechnol Biochem 60:263–266
12. Koh S, Kim J, Shin HJ, Lee DH, Bae J, Kim D, Lee DS (2003) Mechanistic study of the intramolecular conversion of maltose to trehalose by *Thermus caldophilus* GK24 trehalose synthase. Carbohydr Res 338:1339–1343
13. Nishimoto T, Nakano M, Nakada T, Chaen H, Fukuda S, Sugimoto T, Kurimoto M et al (1996) Purification and properties of a novel enzyme, trehalose synthase, from *Pimelobacter sp.* R48. Biosci Biotechnol Biochem 60:640–644
14. Tsusaki K, Nishimoto T, Nakada T, Kubota M, Chaen H, Fukuda S, Sugimoto T et al (1997) Cloning and sequencing of trehalose synthase gene from *Thermus aquaticus* ATCC 33923. Biochim Biophys Acta 1334:28–32
15. Tsusaki K, Nishimoto T, Nakada T, Kubota M, Chaen H, Sugimoto T, Kurimoto M (1996) Cloning and sequencing of trehalose synthase gene from *Pimelobacter* sp. R48. Biochim Biophys Acta 1290:1–3
16. Lee JH, Lee KH, Kim CG, Lee SY, Kim GJ, Park YH, Chung SO (2005) Cloning and expression of a trehalose synthase from Pseudomonas stutzeri CJ38 in *Escherichia coli* for the production of trehalose. Appl Microbiol Biotechnol 68:213–219
17. Chen YS, Lee GC, Shaw JF (2006) Gene cloning, expression, and biochemical characterization of a recombinant trehalose synthase from *Picrophilus torridus* in *Escherichia coli*. J Agric Food Chem 54:7098–8104
18. Wei YT, Zhu QX, Luo ZF, Lu FS, Chen FZ, Wang QY, Huang K, Meng JZ, Wang R, Huang RB (2004) Cloning, expression and identification of a new trehalose synthase gene from *Thermobifida fusca* genome. Acta Biochim Biophys Sin 36:477–484

19. Behnke D (1992) Protein export and the development of secretion vectors. In: Doi RH., McGloughlin, M. (eds), Biology of Bacilli: Applications to industry. MA: Butterworth-Heinemann, Biotechnology, pp. 143–188
20. Harwood CR (1992) *Bacillus subtilis* and its relatives: molecular biological and industrial workhorses. Trends Biotech 10:247–256
21. Nagarajan V (1993) Protein secretion. In: Sonenshein AL, Hoch JA, Losick R (eds) *Bacillus subtilis* and other gram-positive bacteria. Washington, D.C, American Society for Microbiology, pp 713–726
22. Sarvas M (1995) Gene expression in recombinant Bacillus. Bioprocess. Technol 22:53–120
23. Halling SM, Sanchez-Anzaldo FJ, Fukuda R, Doi RH, Meares CF (1997) Zinc is associated with the beta subunit of DNA dependent RNA polymerase of Bacillus subtilis. Biochemistry 16:2880–2884

Chapter 5
Expression of the Gene *Lg-ATF1* Encoding Alcohol Acetyltransferases from Brewery Lager Yeast in Chinese Rice Wine Yeast

Jianwei Zhang, Cuiying Zhang, Jianxun Wang, Longhai Dai and Dongguang Xiao

Abstract Brewery lager yeast has a homologous gene of *ATF1* called *Lg-ATF1* which encodes alcohol acetyltransferase, the most important enzyme for acetate esters synthesis. But only *ATF1* gene exists in Chinese rice wine yeast. In this study, the *Lg-ATF1* gene was cloned from brewery lager yeast S-6, and successfully expressed in the *IAH1* site of Chinese rice wine yeast genome, under the regulation of the yeast phosphoglycerate kinase I gene promoter ($PGK1_P$) and terminator ($PGK1_T$). Subsequently, the esters formation of the recombinant and control strain was monitored by gas chromatography. The results indicated that the expression of the *Lg-ATF1* gene could improve the level of ethyl acetate and isoamyl acetate in Chinese rice wine yeast. The concentration of ethyl acetate and isoamyl acetate produced by the recombinant increased to 70.91 and 8.66 mg L^{-1}, respectively. The observations can lead to the development of new strains of Chinese rice wine.

Keywords Acetate ester · Alcohol acetyltransferase · Chinese rice wine yeast · Ethyl acetate · Isoamyl acetate · *Lg-ATF1*

5.1 Introduction

During fermentation the yeast produces two main categories of volatile esters, which are responsible for the highly desired fruity, candy, and perfume-like aroma character of liquor such as beer and Chinese yellow rice wine, including the acetate esters and the medium-chain fatty acid ethyl esters [1–9].

J. Zhang · C. Zhang · J. Wang · L. Dai · D. Xiao (✉)
Tianjin Key Laboratory of Industrial Fermentation Microbiology, Ministry of Education, College of Biotechnology, Tianjin University of Science and Technology, Tianjin 300457, People's Republic of China
e-mail: xdg@tust.edu.cn

T.-C. Zhang et al. (eds.), *Proceedings of the 2012 International Conference on Applied Biotechnology (ICAB 2012)*, Lecture Notes in Electrical Engineering 249,
DOI: 10.1007/978-3-642-37916-1_5, © Springer-Verlag Berlin Heidelberg 2014

The acetate esters, such as ethyl acetate (solvent-like aroma) and isoamyl acetate (banana flavor) [10–12] are major and important determinant of Chinese yellow rice wine flavor. These esters are assumed to be simultaneously synthesized from an alcohol and an acetyl CoA by alcohol acetyltransferase (AATFase) [13–15]. There are two main AATase in Chinese rice wine yeast, AATase I and AATase II, which are respectively encoded by *ATF1* and *ATF2*. However, brewery lager yeast has a homologous gene of *ATF1* gene called *Lg-ATF1*, which encodes another AATase, Lg-AATase I [16–22].

In this study, the *Lg-ATF1* gene was cloned from brewery lager yeast S-6, and successfully expressed in the *IAH1* site of Chinese rice wine yeast genome, under the regulation of the yeast phosphoglycerate kinase I gene promoter ($PGK1_P$) and terminator ($PGK1_T$). The acetate esters concentrations of yellow rice wines prepared with recombinant and control strain were detected. The results showed that the *Lg-ATF1* expression can improve the acetate esters content of yellow rice wine. The observations can lead to the development of new production strategies and new yeast strains of Chinese yellow rice wine, allowing further optimization of Chinese yellow rice wine flavor profiles in order to satisfy the different sensory preferences of consumers, as well as to a better understanding of the physiological role of acetate esters synthesis.

5.2 Materials and Methods

5.2.1 Strains, Plasmids, and Culturing Conditions

Saccharomyces cerevisiae RY1 was obtained from Angel Yeast of China. *S. cerevisiae* RY1-a1 and RY1-α3 were haploid yeast strain obtained from RY1. *S. cerevisiae* EY3 was a recombinant strain, in which the gene *Lg-ATF1* has successfully expressed. *Escherichia coli* DH5α (F' *endA1hsdR17* (rk − mk +) *supE44thi-1recA1gyrA* (Nalr) *relA1* (*laclZYA-argF*) *U169deoR* [F80d*lac* DE (*lacZ*) M15]) was used as a host for plasmid amplification. Plasmid pUG6 (Kan^r, containing *loxP-kanMX-loxP* gene disruption cassette) was provided by Prof. Hegemann J. H. (Heinrich Heine University, Düsseldorf). Plasmid pUC-PGK1 (Ap^r, containing the $PGK1_p$-$PGK1_t$ expression cassette, cloning vector) and pUC-PILgK (Ap^r, Kan^r, recombinant plasmid with partial *IAH1* gene, and containing $PGK1_P$-*Lg-ATF1*-$PGK1_T$ gene expression cassette) were constructed by our lab.

Yeast cultures were routinely cultured at 28 °C in a yeast extract peptone dextrose (YEPD) medium (2 % glucose, 2 % peptone, and 1 % yeast extract) for growth, in YEPD with adding 100 $mgmL^{-1}$ G418 to a final concentration of 0.24 $mg{\cdot}mL^{-1}$ for selection of yeast integrated transformants, and in wort medium (prepared by treating freshly smashed malt with water at 65 °C for 30 min and adjusting the sugar content of wort to 12 °Bx) for fermentation. *E. coli* was grown at 37 °C in a Luria–Bertani (LB) medium containing 1 % Bacto tryptone,

1 % NaCl, and 0.5 % yeast extract. For selection of *E. coli* transformants, ampicillin was added into the LB media at a final concentration of 100 $\mu g \cdot mL^{-1}$. All solid media used in this study contained 2 % agar.

5.2.2 DNA Manipulations and Plasmid Constructions

Standard procedures for the isolation and manipulation of DNA were used [23]. Restriction enzymes, T4 DNA ligase, LA Taq DNA polymerase, and Expand highfidelity DNA polymerase (TaKaRa Biotechnol, Dalian, China) were used for enzymatic DNA manipulations as recommended by the supplier. The following primers were synthesized to amplify the coding regions of the different genes by means of the polymerase chain reaction (PCR) technique: the *Xho*I-*Lg-ATF1*-ORF-F (CCGCTCGAGGACATGGAAACAGAAGAAAGCC; the *Xho*I restriction site is underlined) and the *Xho*I-*Lg-ATF1*-ORF-R (CCGCTCGAGTCAGGGATTTAA AAGCAGAGCC; the *Xho*I restriction site is underlined); the *BamH*I-*IAH*-ORF-F (CGCGGATCCTCTTGGAGCCGCATTAGTCAACGAA; the *BamH*I restriction site is underlined) and the *BamH*I-*IAH*-ORF- R (CGCGGATCCCACCTTCCTG TTGAAACGCCTTATT; the *BamH*I site is underlined); the *Kpn*I-*Kan*-ORF-F (CGGGGTACC CAGCTGAAGCTTCGTACGC; the *Kpn*I restriction site is underlined) and the *Kpn*I-*Kan*-OR F-R (CGGGGTACCGCATAGGCCACTA GTGGATCTG; the *Kpn*I restriction site is underlined). Genomic DNA from the brewery lager yeast S6 was used as template to amplify the coding sequence of the *Lg-ATF1* gene, and the genome of commercial rice wine yeast strain RY1, was used as template to amplify the homologous sequence of the *IAH1* gene, while plasmid pUG6 was used to amplify the selection marker, *kan* gene.

The vector pUC19-PGK1, containing the promoter ($PGK1_P$) and terminator ($PGK1_T$) sequences of the yeast phosphoglycerate kinase I gene (*PGK1*), was used for subcloning the respective full-length open reading frames (ORFs). PCR-generated *Lg-ATF1*, *IAH*, and *Kan* fragments were digested with *XhoI*, *BamH*I, and *Kpn*I, respectively, and subcloned into pUC19-PGK1, thereby generating plasmid pUC-PILgK. To identify possible cloning artifacts, all inserts were sequenced.

5.2.3 Expression and Verification of Lg-ATF1 in Chinese Yellow Rice Wine

Standard procedures for the isolation and manipulation of DNA were using Plasmid pUC-PILgK was linearized by *Bpu1102*I, and integrated into the genomic of the haploids (a- and α-type) of yellow rice wine yeast strain RY1. Yeast transformation was carried out by the lithium acetate procedure described

previously [24]. The recombinant diploid was obtained after the fusion of the purified a- and α-type haploid recombinants.

Two steps were used to verify the correct integration of the *Lg-ATF1* cassette into the target locus. Firstly, the recombinants were verified via PCR using the primer pair *ILgK1*'F (TAGTCTGTTTGAGCAGTCCTACCCT) and *ILgK1*'R (GAACCTCAGTGGCAAATCCTAACCT), and the primer pair *ILgK2*'F (GGAGGAG ACCGAACAC AAGTATC) and *ILgK2*'R (TGGTTTGGAGGAGAAGATAACGACG). Then, the changes in gene expression were assessed by Real-time PCR (RT-PCR), when the *GAPDH* (*GPD1*) gene was selected as the internal control gene, using the following primers: TTGCCCCGTATCTGTAGC (*GPD1* forward), AGCACCAACTTCAAAACCC (*GPD1* reverse), CAACCTGAGCACAATGCC CTAA (*Lg-ATF1* forward), GGAGACAAATCAACCGCCAAGT (*Lg-ATF1* reverse). Yeast strains were cultured in YEPD medium for 16 h and collected for RNA extraction. RNA isolation was carried out using the Yeast RNA Kit (OMEGA, Norcross, GA, America) as recommended by the manufacturer. cDNA was soon synthesized from the isolated RNA using the Ultra SYBR Two Step qRT-PCR kit (with ROX) (CWBIO China, Beijing, China) as recommended by the manufacturer. The synthesized cDNA can be stored at −20 °C.

5.2.4 Simulated Rice Wine Fermentation Test

Yeast cells were pre-cultured in 5 mL wort medium at 28 °C for 12 h. 1 mL yeast pre-preculture was transferred into 25 mL fresh wort medium and incubated until 24 h. A 100 g rice was dipped in the water for 72 h at 28 °C, washed, cooked 25 min, and then put into 500 mL flask at last. A 10 g mature wheat Koji, 105 mL water (including 60 mL clean water and 45 mL serofluid), and 25 ml second-preculture of yellow rice wine yeast were added.

The mixture was were separately subjected to pre-fermentation at 28 °C for 5 days, then the temperature of rice wine broth was set to 16 °C and post-fermentation was continued for 30 days. The weight loss, alcohol, and glucose content of each tested strain were determinated separately after the two fermentation periods (the pre-fermentation that includes 5 days and the total fermentation that includes 5 days pre-fermentation and 30 days post-fermentation). All fermentations were performed in triplicate.

5.2.5 Analysis of Acetate Esters

Gas chromatography (GC) was used for the measurement of ethyl acetate and isoamyl acetate. The samples were filtered and distilled for GC analysis after fermentation. The analysis was performed on an Agilent 7890C GC. Amyl acetate was used as the internal standard. The column used was a HP-INNOWax

polyethylene glycol (higher limit temperature 260 °C; LabAlliance), which is an organic coated fused silica capillary column with 30 m × 320 μm i.d. and a 0.5 μm coating thickness. Nitrogen was used as the carrier gas and the temperature of the flame ionization detector (FID) was adjusted to 250 °C. The injector temperature was 230 °C, the split ratio was 25:1, and the injection volume was 1.0 μL. The oven temperature program was as follows: 52 to 70 °C at 2 °C min^{-1}, 70 to 90 °C at 4 °C min^{-1}, and 90 to 200 °C at 10 °C min^{-1}.

5.3 Results and Discussion

5.3.1 Constructions and Identifications of Recombinant Yeast Strains

Plasmid pUC-PILgK was linearized and transformed into the haploids (RY1-a1 and RY1-α3) of Chinese yellow rice wine yeast RY1. The resulting recombinants were verified using the methods described in the Materials and Methods section. The results (Figs. 5.1 and 5.2) suggested that the *Lg-ATF1* gene was successfully integrated into the genome of Chinese yellow rice wine yeast and expressed. The *Lg-ATF1*-expressing mutant EY3 (pUC-PILgK) was obtained after the fusion of the a- and α-type integrated haploid recombinants (EY3-a1 (pUC-PILgK) and EY3-α1 (pUC-PILgK)) and also identified (Data not shown, just like the results of the haploid strains).

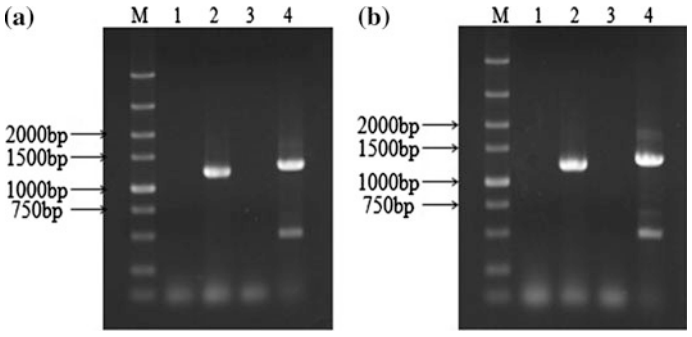

Fig. 5.1 The PCR verification results of genetic engineering haploids. **a** the verification results of a-type haploid recombinant; **b** the verification results of α-type haploid recombinant. M, 5000 bp DNA Ladder Marker, lane 1 was PCR amplification result from the haploid receptors (a/α) genome by using the forward primer (*ILgK1*'F) and reverse primer (*ILgK1*'R), lane 2 was PCR amplification result from the haploid recombinants (a/α) genome by using the forward primer (*ILgK1*'F) and reverse primer (*ILgK1*'R), lane 3 was PCR amplification result from the haploid receptors (a/α) genome by using the forward primer (*ILgK2*'F) and reverse primer (*ILgK2*'R), lane 4 was PCR amplification result from the haploid recombinants (a/α) genome by using the forward primer (*ILgK2*'F) and reverse primer (*ILgK2*'R)

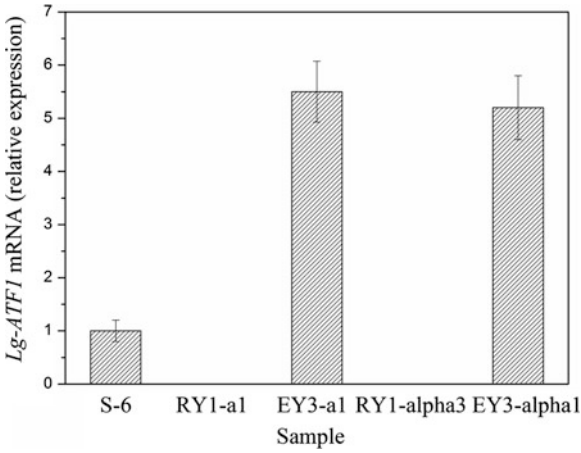

Fig. 5.2 The qRT-PCR results of genetic engineering haploids. *Lg-ATF1* mRNA levels were analyzed by qRT-PCR. The *GAPDH* (*GPD1*) gene was used as the internal control genes. *Error bars* indicate as the mean ± S.E. from the experiments performed in duplicate, and the experiments were repeated three times

5.3.2 *Effects of* Lg-ATF1 *Expression on Fermentation Performance of Rice Wine Yeast*

The yellow rice wine yeast strains, RY1 and EY3 (pUC-PILgK), were separately subjected to the simulated rice wine fermentation (as described in the Materials and Methods section). The fermentation performance results (Table 5.1) showed that there was no obvious distinctions could be obtained among the fermentation characteristics of the tested strains.

Table 5.1 Fermentation performance of test strains[a]

Parameters	After 5 days pre-fermentation	
	RY1	EY3(pUC-PILgK)
Weight loss (g)	28.5 ± 0.35	28.0 ± 0.22
Glucose (%)	0.81 ± 0.01	0.84 ± 0.01
Ethanol (%, v/v, 20 °C)	14.2 ± 0.07	14.1 ± 0.14
Parameters	After 5 days pre-fermentation and 30 days' post-fermentation	
	RY1	EY3(pUC-PILgK)
Weight loss (g)	34.38 ± 0.32	34.27 ± 0.33
Glucose (%)	0.32 ± 0.01	0.34 ± 0.01
Ethanol (%, v/v, 20 °C)	18.0 ± 0.07	17.0 ± 0.21

[a] Results are averages from three parallel independent experiments. Values are means ± standard deviations from three different tests

5.3.3 GC Analysis of Acetate Esters in Chinese Yellow Rice Wines

In order to evaluate the acetate esters production ability of the *Lg-ATF1* expressing mutant, the concentrations of acetate esters were determined for the distillates of Chinese yellow rice wines by GC analysis (Table 5.2). The GC analysis results confirmed high levels of AATase activity. Specifically, 2.5-fold increase in the production of ethyl acetate was observed for the yellow rice wine fermented with EY3 (pUC-PILgK) compared to the wine fermented with RY1, while the isoamyl acetate increased to 8.66 mg L^{-1} after 5 days of pre-fermentation.

In China, the fermentation period of yellow rice wine consists of two phases, named, pre-fermentation and post-fermentation. During pre-fermentation, yeast grows and produces a large amount of alcohol and a small amount of esters and higher alcohols. At this stage, a normal temperature of 28 °C is required. However, the concentrations of esters and higher alcohols after pre-fermentation are not sufficient. A long post-fermentation period (generally 1 to 3 months) at low temperature (16 °C), known as the "aging period," is required to promote the association between alcohol molecules and that between alcohol and water molecules, as well as the esterification between the alcohols and acid after pre-brewing. This aging period allows the production of softer, tastier, and more perfumed yellow rice wine.

To determine the effect of bottle-aging on the ester concentrations, Chinese yellow rice wines were bottle-aged continuously for 30 days at 16 °C and then filtered, distilled and also subjected to GC analysis (Table 5.2). After 5 days pre-fermentation and 30 days post-fermentation, the concentration of ethyl acetate in the yellow rice wines fermented with the control strain (RY1) drastically increased to 39.25 mg L^{-1}, during this storage period. But the difference in the concentration of ethyl acetate produced by the recombinant strain, EY3 (pUC-PILgK), between the pre-fermentation period with the post-fermentation period was not significant.

Table 5.2 GC measurement of acetate esters produced by each strain[a]

Esters	After 5 days pre-fermentation	
	RY1	EY3(pUC-PILgK)
Ethyl acetate (mg L^{-1})	28.30 ± 0.28	70.91 ± 0.71
Isoamyl acetate (mg L^{-1})	–	8.66 ± 0.44
Esters	After 5 days pre-fermentation and 30 days post-fermentation	
	RY1	EY3(pUC-PILgK)
Ethyl acetate (mg L^{-1})	39.25 ± 0.34	68.64 ± 0.73
Isoamyl acetate (mg L^{-1})	–	–

[a] Results are averages from three parallel independent experiments. Values are means ± standard deviations from three different tests. "–" represents no detected. GC results were statistically evaluated by a two-tailed test. The results indicated that the values obtained for all the yellow rice wines for ethyl acetate, isoamyl acetate differed significantly ($P \leq 0.05$)

However, the ethyl acetate concentration still remained 1.7-fold higher in the yellow rice wines fermented with the recombinant strain than in the control yellow rice wine. However, the isoamyl acetate content decreased more obviously compared with pre-fermentation period.

Not only does the recombinant strain keep excellent fermentation characteristics as the wild yellow rice wine yeast, but also has good production ability of esters. Our study lays foundation for screening yellow rice wine yeast strains and improving the flavor of yellow rice wine in the future.

5.4 Conclusion

In this study, $PGK1_P$ and $PGK1_T$ were used as the promoter and the terminator to express the *Lg-ATF1*-encoded alcohol acetyltransferase, which can only be cloned from brewery lager yeast, in Chinese yellow rice wine yeast. The results show that the acetate esters contents were increased through expression of the gene *Lg-ATF1*.

The observations of current study can lead to the development of new yeast strains, allowing further optimization of rice wine flavor profiles, as well as to a better understanding of the physiological role of ester synthesis.

Acknowledgments This work was financially supported by the program of National High Technology Research and Development Program of China (863 Program) (Grant No. SS2012AA023408) and the Cheung Kong Scholars and Innovative Research Team Program in University of Ministry of Education, China (Grant No. IRT1166).

References

1. Suomalainen H (1981) Yeast esterases and aroma esters in alcoholic beverages. J Inst Brew 87:296–300
2. Nykanen L (1986) Formation and occurence of flavor compounds in wine and distilled beverages. Am J Enol Vitic 37:84–96
3. Malcorps P, Dufour JP (1987) Ester synthesis by *Saccharomyces cerevisiae*—localization of the acetyl-CoA isoamyl alcohol acetyltransferase. J Inst Brew 93:160
4. Peddie HAB (1990) Ester formation in brewery fermentations. J Inst Brew 96:327–331
5. Meilgaard MC (1991) The flavor of beer. MBAA Techn Quart 28:132–141
6. Debourg A (2000) Yeast flavour metabolites. Eur Brew Conv Monogr 28:60–73
7. Cristiani G, Monnet V (2001) Food micro-organisms and aromatic ester synthesis. Sci Aliments 21:211–230
8. Pisarnitskii AF (2001) Formation of wine aroma: tones and imperfections caused by minor components (review). Appl Biochem Microbiol 37:552–560
9. Aritomi K, Hirosawa I, Hoshida H et al (2004) Self-cloning yeast strains containing novel FAS2 mutations produce a higher amount of ethyl caproate in Japanese sake. Biosci Biotechnol Biochem 68:206–214
10. Meilgaard MC (1975) Flavor chemistry of beer flavor and threshold of 239 aroma volatiles. MBAA Techn Quart 12:151–168

11. Meilgaard MC (1975) Flavor chemistry of beer flavor interaction between principal volatiles. MBAA Techn Quart 12:107–117
12. Meilgaard MC (2001) Effects on flavour of innovations in brewery equipment and processing: a review. J Inst Brew 107:271–286
13. Nordström K (1962) Formation of ethyl acetate in fermentation with brewer's yeast III: participation of coenzyme A. J Inst Brew 68:398–407
14. Nordström K (1963) Formation of ethyl acetate in fermentation with brewer's yeast IV: metabolism of acetyl coenzyme A. J Inst Brew 69:142–153
15. Nordström K (1964) Formation of esters from alcohols by brewer's yeast. J Inst Brew 70:328–336
16. Yoshioka K, Hashimoto N (1981) Ester formation by alcohol acetyltransferase from brewers yeast. Agr Biol Chem 45:2183–2190
17. Malcorps P, Dufour JP (1992) Short-chain and medium-chain aliphatic ester synthesis in *Saccharomyces cerevisiae*. Eur J Biochem 210:1015–1022
18. Fujii T, Nagasawa N, Iwamatsu A et al (1994) Molecular cloning, sequence analysis and expression of the yeast alcohol acetyltransferase gene. Appl Environ Microbiol 60:2786–2792
19. Fujii T, Yoshimoto H, Nagasawa N et al (1996) Nucleotide sequence of alcohol acetyltransferase genes from lager brewing yeast, *Saccharomyces carlsbergensis*. Yeast 12:593–598
20. Nagasawa N, Bogaki T, Iwamatsu A et al (1998) Cloning and nucleotide sequence of the alcohol acetyltransferase II gene (*ATF2*) from *Saccharomyces cerevisiae* Kyokai No. 7. Biosci Biotechnol Biochem 62:1852–1857
21. Yoshimoto H, Momma T, Fujiwara D et al (1998) Characterization of the *ATF1* and Lg-*ATF1* genes encoding alcohol acetyltransferases in the bottom fermenting yeast *Saccharomyces pastorianus*. J Ferment Bioeng 86:15–20
22. Yoshimoto H, Fujiwara D, Momma T et al (1999) Isolation and characterization of the *ATF2* gene encoding alcohol acetyl transferase II in the bottom fermenting yeast *Saccharomyces pastorianus*. Yeast 15:409–417
23. Ausubel FM, Brent R, Kingston RE et al (eds) (1994) Current protocols in molecular biology. Wiley, New York
24. Gietz RD, Schiestl RH (1995) Transforming yeast with DNA Methods. Mol Cell Biol 5:255–269

Chapter 6
Improving the Production of Epothilones by Precursors Addition Based on Metabolic Pathway Analysis

Lin Zhao, Hai-yan Gao, Ya-Wei Li, Zhen Lu, Xin Sun, Song Zhang and Xin-li Liu

Abstract Epothilones are a kind of poliketide macrolide with antifungal and anticancer bioactivity which are attracting more and more attention. However, despite a growing interest of epothilones, their practical use and research are very limited owing to the high production cost. Several studies have already demonstrated that yield of product can be affected by the addition of various precursors. In this paper, seven precursors of the biosynthesis of epothilones were analyzed by single-factor test and an L_9 3^4 orthogonal test. Finally, optimal condition led 1.55-fold of epothilone A and 1.46-fold of B increased in yields over that with the initial condition. The highest yields of epothilones were obtained in fermented culture with adding sodium acetate (80 mg/mL), sodium propionate (10 mg/mL), cysteine (20 mg/mL), and serine (60 mg/mL). The production profile under the optimized condition revealed that the serine, which could transform into cysteine and methylmalonyl-CoA, was the most significant precursor on the yields of both epothilones A and B. The result implied that the transformation of serine might be one of the key rate-limiting steps in the biosynthesis of epothilones.

Keywords Epothilone · Precursor · Inducing effect · *Sorangium cellulosum*

6.1 Introduction

Epothilones are a type of polyketide macrolide which are produced by *Sorangium cellulosum* (Fig. 6.1) [1]. They were reported having strong stabilizing activities on polymerized microtubules which mimicked the mechanism by which taxol

L. Zhao · H. Gao · Y.-W. Li · Z. Lu · X. Sun · S. Zhang · X. Liu (✉)
Shandong Provincial Key Laboratory of Microbial Engineering,
Qilu University of Technology, Jinan 250353,
People's Republic of China
e-mail: vip.lxl@163.com

T.-C. Zhang et al. (eds.), *Proceedings of the 2012 International Conference on Applied Biotechnology (ICAB 2012)*, Lecture Notes in Electrical Engineering 249,
DOI: 10.1007/978-3-642-37916-1_6, © Springer-Verlag Berlin Heidelberg 2014

affects tumor cells [2, 3]. This discovery leads to following extensive studies on epothilones in various aspects [4–6]. A range of synthetic and semi-synthetic epothilones analogues have been produced to further improve the adverse effect profile and to maximize the antitumor properties [7–9]. Several epothilones showed activity against many tumor types in preclinical studies and some of them have been or being evaluated in clinical trials [10, 11].

According to the epothilones biosynthesis pathway, they are assembled by a NRPS/PKS hybrid gene cluster in a stepwise polymerization sequence mainly from carboxylic acid and amino acid precursors such as sodium acetate, sodium propionate, cysteine, and methionine [12, 13]. Furthermore, sodium pyruvate, serine, threonine which can be transformed into the compounds above in cells can also be regarded as pre-precursors of epothilones (Fig. 6.2). There are several studies already demonstrated that yield of production can be affected by the addition of various precursors [14–17].

In this paper, we investigated the inducing effect on epothilone synthesis of the seven precursors in an epothilones high-producing strain *Sorangium cellulosum* So2161 and build an optimal method through orthogonal experiment to improve the fermented yield of epothilones.

6.2 Materials and Methods

6.2.1 Microorganism and Culture Conditions

So2161 is a *Sorangium cellulosum* strain that was isolated from a soil sample in our laboratory which has been morphologically and phylogenetically classified using previously reported methods [18, 19]. It has been routinely cultivated on solid CNST agar plates and in liquid M26 medium at 30 °C. The pH value of the medium was adjusted to 7.2 with KOH before autoclaving.

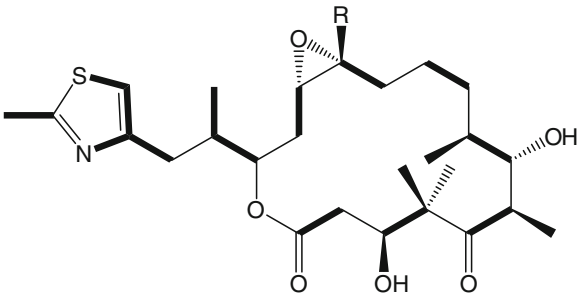

Fig. 6.1 Molecular structures of epothilones A and B (R = H, epothilone A; R = CH_3, epothilone B)

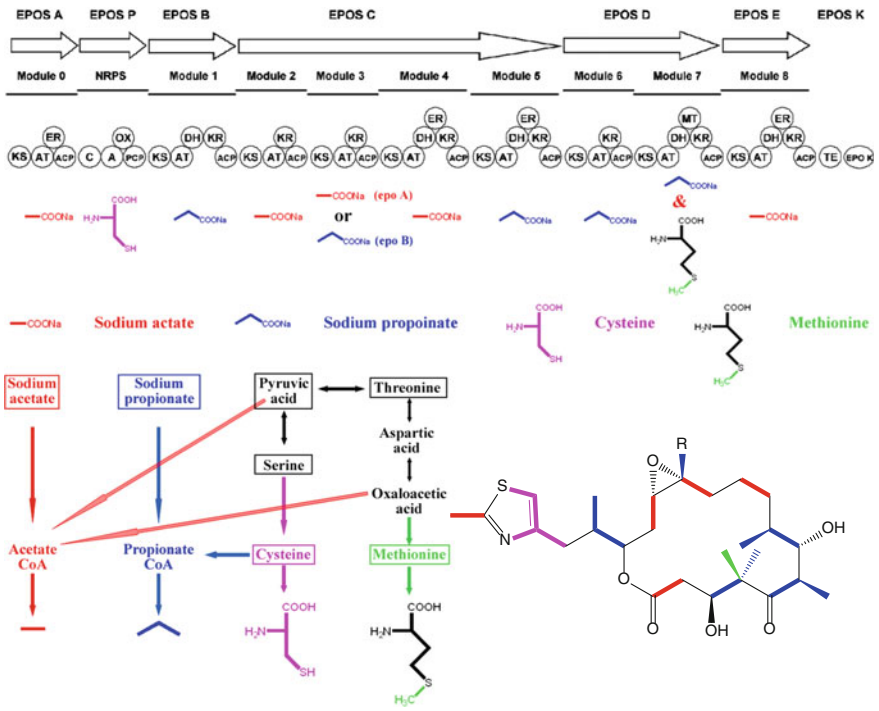

Fig. 6.2 Metabolite pathway and precursors for the biosynthesis of epothilones

Table 6.1 Design of the single-factor test in five levels of the seven precursors

Level (mg/L)	Sodium acetate	Sodium propionate	Sodium pyruvate	Serine (mg/L)	Cysteine (mg/L)	Methionine (mg/L)	Threonine (mg/L)
1	10	2.5	10	20	1	10	5
2	20	5	30	60	10	20	10
3	40	7.5	50	100	20	40	15
4	80	10	100	140	30	60	20
5	160	12.5	150	180	50	80	25

6.2.2 Fermentation

Strain So2161 was inoculated on the CNST agar plates and cultured for 3−4 days at 30 °C. Then it was evacuated to liquid M26 medium and shook for 4−5 days. Cells were collected and inoculated into EMP medium with each precursor for epothilone

Table 6.2 Design of the four factors and three levels orthogonal test

Trial	A	B	C	D
1	A 1	B 1	C 1	D 1
2	A 1	B 2	C 2	D 2
3	A 1	B 3	C 3	D 3
4	A 2	B 1	C 2	D 3
5	A 2	B 2	C 3	D 1
6	A 2	B 3	C 1	D 2
7	A 3	B 1	C 3	D 2
8	A 3	B 2	C 1	D 3
9	A 3	B 3	C 2	D 1

producing. The EMP medium contains potato starch 2.0 g; glucose 2.0 g; soy powder 2.0 g; skim milk powder 1.0 g; $MgSO_4$ 1.0 g; $CaCl_2$ 1.0 g, and trace element solution [20] 1.0 mL; VB_{12} 0.5 mg; distilled water 1,000 mL; pH 7.2. Sterilized XAD-16 resin was added (2 % v/v) into the medium for the products absorption. Following the addition of resin, cultures were incubated for 6 days for fermentation. Finally, the resin was collected and the metabolites absorbed in the resin including epothilones were extracted by methanol for HPLC analysis [21].

6.2.3 Single-Factor and Orthogonal Test

For the single-factor test (SFT) of the seven precursors, the So2161 cells were inoculated at the final concentration of 2×10^7 cell/mL in EMP medium with different precursors in a 250 mL Erlenmeyer flask. Each precursor at five concentration levels was added into the EMP medium to test the inducing effects on the production of epothilones (Table 6.1).

An orthogonal $L_9\ 3^4$ test design in the addition mode was used for optimizing the production of epothilones. In the single-factor test, four of the seven precursors that had better inducing effects on epothilone producing were selected and named A (Sodium acetate), B (Sodium propionate), C (Cysteine), and D (Serine), which would be used to perform the orthogonal test. Additional levels were chosen nearby the most proper amount of the single-factor test. Table 6.2 shows the four factors and three levels experimental conditions for the orthogonal test [22].

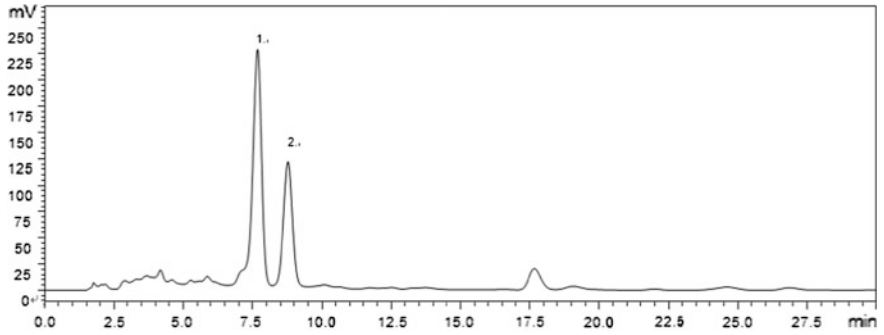

Fig. 6.3 HPLC analysis of epothilones A and B

6.2.4 Detection of Epothilone Production

The XAD-16 resin beads were collected from the cultures, washed with distilled water, air dried, and extracted with 1 mL methanol, shaking for 2 h at 40 °C. Extractions were centrifugation at 10,000 × g for 10 min, and then filtrated through 0.45 μm filter membrane.

Yields of epothilones were detected using HPLC chromatography with a 5 μm RP-C18 column (4.6 × 200 mm, Shimadzu, Japan). The methanol extract was eluted with methanol: water (70:30) at 1 mL/min. Epothilones were detected at 249 nm wavelength. Retention times of epothilone A and B were 7.72 min and 8.82 min (Fig. 6.3). The titers were quantified based on a standard curve generated from purified epothilones A and B.

6.3 Results and Discussion

6.3.1 Optimized Rapid Screening Method for Epothilone B High-Producing Mutants

Single-factor test was performed to analysis whether or not the precursors could affect on the biosynthesis of epothilones. Results showed that all of the precursors we chose induced the synthesis of epothilones in varied efficiencies (Fig. 6.4). From the perspective of epothilone B, which had better antitumor activity than epothilone A, sodium acetate (40 mg/mL), sodium propionate (5 mg/mL), serine (100 mg/mL), and cysteine (20 mg/mL) were more suitable, among which sodium propionate gave the highest yield, 35.95 % higher than the contrast. From the epothilone A, sodium pyruvate (30 mg/mL) had the best inducing effect which

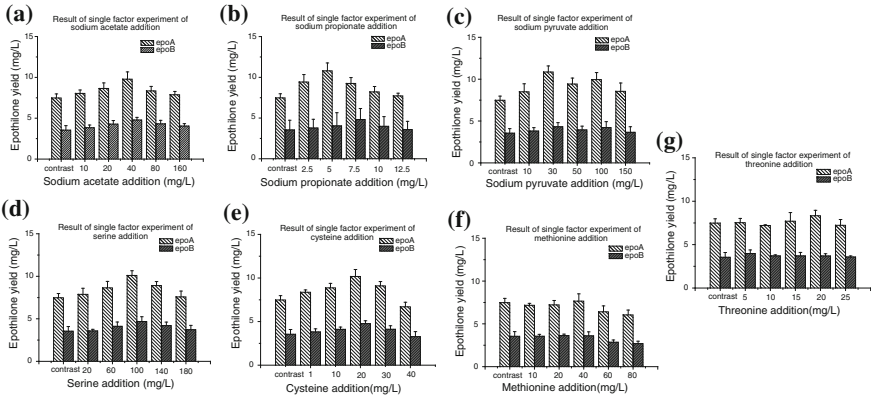

Fig. 6.4 Results of single-factor test. **a** addition of sodium acetate; **b** sodium propionate; **c** sodium pyruvate; **d** serine; **e** cysteine; **f** methionine; **g** threonine

increased 45.13 % than the contrast but with a relatively low yield increasing (21.96 %) in epothilone B. On the other hand, methionine and threonine did not show obviously inducing effect, which meant these precursors may not be the limiting, factor for the epothilone biosynthesis in fermentation medium.

6.3.2 Orthogonal Test

Orthogonal test with four factors and three levels ($L_9\ 3^4$) was performed to analyze the optimal parameters of epothilones yields. And the $L_9\ 3^4$ table was designed to detect the most suitable adding conditions of the four precursors we chose that with better inducing effect which were sodium acetate, sodium propionate, cysteine, and serine. According to the values of range RA (R value of epothilone A) and RB (R value of epothilone B) in Table 6.3, ratio of serine (factor D) showed the most significant effect on the yields of both epothilone A and B, and the order of importance that influenced yields of epothilones was found to be serine (D) >sodium propionate (B) >sodium acetate (A) >cysteine (C). The optimal combination parameters of the adding condition were $A_2B_3C_2D_1$ for epothilone A, and A3B3C2D1 for epothilone B, namely, sodium acetate (40 mg/mL), sodium propionate (10 mg/mL), cysteine (20 mg/mL), and serine (60 mg/mL) reached the maximum of epothilone A and sodium acetate (80 mg/mL), sodium propionate (10 mg/mL), cysteine (20 mg/mL), and serine (60 mg/mL) gave the highest yield of epothilone B.

Table 6.3 Result of the orthogonal test

Trial	A Sodium acetate (mg/L)	B Sodium propionate (mg/L)	C Cysteine (mg/L)	D Serine (mg/L)	Yield of epo A (mg/L)	Yield of epo B (mg/L)
1	1	1	1	1	9.59	6.13
2	1	2	2	2	9.13	5.71
3	1	3	3	3	9.36	5.70
4	2	1	2	3	9.44	5.82
5	2	2	3	1	10.28	6.02
6	2	3	1	2	10.04	6.45
7	3	1	3	2	9.29	5.80
8	3	2	1	3	8.55	5.76
9	3	3	2	1	10.36	6.93
$K1_A$	28.07	28.31	28.18	30.22		
$K2_A$	29.76	27.96	28.93	28.46		
$K3_A$	28.19	29.75	28.92	27.35		
$k1_A$	9.36	9.44	9.39	10.07		
$k2_A$	9.92	9.32	9.64	9.49		
$k3_A$	9.40	9.92	9.64	9.12		
R_A	0.563	0.597	0.249	0.959		
AF in epo A	3	2	4	1		
OP for epo A	A2	B3	C2	D1		
$K1_B$	17.54	17.75	18.337	19.08		
$K2_B$	18.29	17.48	18.46	17.96		
$K3_B$	18.49	19.08	17.53	17.28		
$k1_B$	5.85	5.92	6.11	6.36		
$k2_B$	6.10	5.83	6.15	5.99		
$k3_B$	6.16	6.36	5.84	5.76		
R_B	0.315	0.533	0.311	0.599		
AO in epo B	3	2	4	1		
OC for epo B	A3	B3	C2	D1		

6.3.3 Validation of the Optimal Condition

Then, the strain So2161 was inoculated into the fermentation medium with adding sodium acetate (80 mg/mL), sodium propionate (10 mg/mL), cysteine (20 mg/mL), and serine (60 mg/mL) to verify the conclusion of orthogonal test. Result showed that when we fermented the strain in optimal condition, the yields of epothilones A and B increased 55.23 and 45.95 % than the origin (Fig. 6.5).

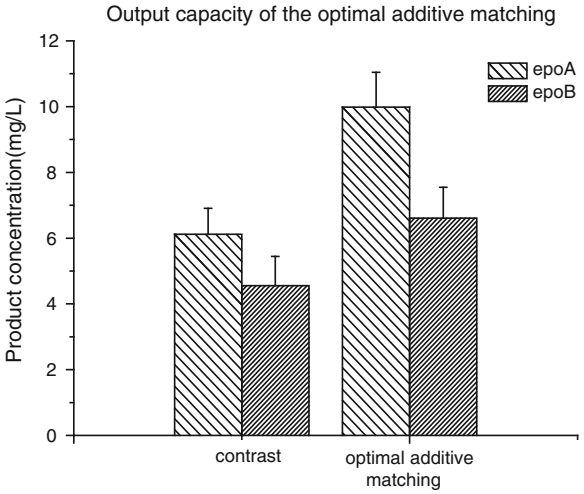

Fig. 6.5 Fermentation yields of epothilones under optimized precursor addition

6.4 Conclusions

Precursor is one of the most important factors affecting the yield of production. Many studies demonstrated the influence of the precursors on various products. In this paper, seven precursors of the biosynthesis of epothilones were analyzed by single-factor test and orthogonal test. Finally, optimal condition led 1.55-fold of epothilone A and 1.46-fold of B increased in yields over that with the initial condition. The highest yields of epothilones were obtained in fermented culture with adding sodium acetate (80 mg/mL), sodium propionate (10 mg/mL), cysteine (20 mg/mL), and serine (60 mg/mL). The production profile under the optimized condition revealed that the serine was the most significant factor on the yields of both epothilones A and B. According to the metabolite pathway, serine can transform into propionyl-CoA or cysteine, both of which were precursors of epothilones. In our laboratory, Expression of each modular in the epothilone biosynthesis gene cluster was analyzed by quantitative PCR (data not shown). Result showed that the expression of the NRPS modular which accept cysteine as precursor and some of the PKS modulars which accepted propionyl-CoA as precursor were all at a obvious low level. It might because the concentrations of cysteine and propionyl-CoA were much lower than acetyl-CoA in cells, so adding these precursors affected more to the yields of epothilones. In summary, as secondary metabolism, biosynthesis of epothilones is a branch metabolic pathway competing with others in the whole cell which consumes various precursors. Additional supplement of these precursors, especially the limiting factors, could significantly improve the yields of epothilones. Consequently, these findings can provide a basis for enhancing the industrial fermentation of epothilones.

Acknowledgments The work was financially supported by No. 2012GGA14017 of Province Science and Technology Development Project and grants ZR2011CQ006 of Shandong Provincial Natural Science Foundation.

References

1. Gerth K, Bedorf N, Höfle G et al (1996) Epothilons A and B: Antifungal and cytotoxic compounds from *Sorangium cellulosum* (Myxobacteria) -production, physico-chemical and biological properties. J Antibiot 49:560–564
2. Bollag DM, McQueney PA, Zhu J et al (1995) Epothilones, a new class of microtubule-stabilizing agents with a taxol-like mechanism of action. Cancer Res 55:2325–2333
3. Goodin S, Kane MP, Rubin EH (2004) Epothilones: mechanism of action and biologic activity. J Clin Oncol 2:2015–2025
4. Reichenbach H, Höfle G (2008) Discovery and development of the epothilones: a novel class of antineoplastic drugs. Drugs R D 9:1–10
5. Zhao L, Li PF, Lu CH et al (2010) Glycosylation and production characteristics of epothilones in alkalitolerant *Sorangium cellulosum* strain So0157-2. J Microbiol 48:438–444
6. Coderch C, Klett J, Morreale A et al (2012) Comparative binding energy (combine) analysis supports a proposal for the binding mode of epothilones to β-tubulin. Chem Med Chem 7:836–843
7. Altmann KH (2003) Epothilone B and its analogs - a new family of anticancer agents. Med Chem 3:149–158
8. Watkins EB, Chittiboyina AG, Jung JC (2005) The epothilones and related analogues-a review of their syntheses and anti-cancer activities. Curr Pharm Des 11:1615–1653
9. Fornier MN (2007) Ixabepilone, first in a new class of antineoplastic agents: the natural epothilones and their analogues. Clin. Breast Cancer 7:757–763
10. Dorff TB, Gross ME (2011) The epothilones: new therapeutic agents for castration-resistant prostate cancer. Oncologist 16:1349–1358
11. Araki K, Kitagawa K, Mukai H et al (2011) First clinical pharmacokinetic dose-escalation study of sagopilone, a novel, fully synthetic epothilone, in Japanese patients with refractory solid tumors. Invest New Drugs 29:1149–1458 (Epub ahead of print)
12. Julien B, Shah S, Ziermann R et al (2000) Isolation and characterization of the epothilone biosynthetic gene cluster from *Sorangium cellulosum*. Gene 249:153–160
13. Molnár I, Schupp T, Zirkle R et al (2000) The biosynthetic gene cluster for the microtubule-stabilizing agents epothilones A and B from *Sorangium cellulosum* So ce90. Chem Biol 7:97–109
14. Seo MJ, Kook MC, Kim SO (2012) Association of colony morphology with coenzyme Q(10) production and its enhancement from *Rhizobium radiobacter* T6102 W by addition of isopentenyl alcohol as a precursor. J Microbiol Biotechnol 22:230–233
15. Saudagar PS, Singhal RS (2007) A statistical approach using L_{25} orthogonal array method to study fermentative production of clavulanic acid by *Streptomyces clavuligerus* MTCC 1142. Appl Biochem Biotechnol 136:345–359
16. Dai WL, Tao WY (2008) Preliminary study on fermentation conditions of taxol-producing endophytic fungus. Chem Ind and Eng Progress 27:883–886
17. Nilüfer C (2002) Stimulation of the gibberellic acid synthesis by *Aspergillus niger* in submerged culture using a precursor. World J Microbiol Biotechnol 18:727–729
18. Jiang DM, Zhao L, Zhang CY et al (2008) Taxonomic analysis of *Sorangium* species based on HSP60 and 16S rRNA gene sequences and morphology. Int J Syst Evol Microbiol 58:2654–2659
19. Yan ZC, Wang B, Li YZ et al (2003) Morphologies and phylogenetic classification of cellulolytic myxobacteria. Syst Appl Microbiol 26:104–109

20. Reichenbach H and Dworkin M (1992) The myxobacteria. In: Balows A, Truper HG, Dworkin M, Harder W and Schleifer KH, (eds)The prokaryotes, 2nd edn. ASM press, Herndon
21. Gong GL, Sun X, Liu XL et al (2007) Mutation and a high-throughput screening method for improving the production of Epothilones of *Sorangium*. J Ind Microbiol Biotechnol 34:615–623
22. Li FL, Li QW, Gao DW et al (2009) The optimal extraction parameters and anti-diabetic activity of flavonoids from *Ipomoea batatas* leaf. Afr J Tradit Complement Altern Med 6:195–202

Chapter 7
A Rapid and Specific Method to Screen Epothilone High-Producing Strain with Spectrometry and its Application

Lin Zhao, Xin Sun, Yawei Li, Haiyan Gao, Qiang Ren, Yongwei Hao, Song Zhang and Xinli Liu

Abstract Epothilones are a kind of poliketide macrolide with strong stabilizing activities on polymerized microtubules which mimicked taxol. Microbial fermentation of *Sorangium cellulosum* is still the main way to produce epothilones with strain continuously improving by mutation. In general, yields of epothilones were detected by HPLC or LC–MS, which were time-consuming and not suited for high-throughput screening. In this paper, we described an efficient high-throughput method for epothilones high-producing strains with 96-well micro titer plate spectrometry combined with CCl_4 extracting. In this method, the purity of epothilones was 22 times higher than methanol extract. So the OD_{249} was much less disturbed by the impurities. Stabilization experiment and SPSS analysis of the relationship between the yields of epothilones detected by HPLC and the OD_{249} of the CCl_4 extracts of 192 mutated strains showed that our method was practical, accurate, and much more efficient.

Keywords Epothilones · *Sorangium cellulosum* · Rapid screening · Spectrometry

7.1 Introduction

Epothilones are a kind of poliketide macrolide with strong stabilizing activities on polymerized microtubules which mimicked taxol [1, 2] (Fig. 7.1). They are biosynthesized by a NRPS/PKS hybrid gene cluster in a stepwise polymerization

Zhao Lin and Sun Xin contributed equally to this work.

L. Zhao · X. Sun · Y. Li · H. Gao · Q. Ren · Y. Hao · S. Zhang · X. Liu (✉)
Shandong Provincial Key Laboratory of Microbial Engineering,
Qilu University of Technology, Jinan 250353, People's Republic of China
e-mail: vip.lxl@163.com

T.-C. Zhang et al. (eds.), *Proceedings of the 2012 International Conference on Applied Biotechnology (ICAB 2012)*, Lecture Notes in Electrical Engineering 249,
DOI: 10.1007/978-3-642-37916-1_7, © Springer-Verlag Berlin Heidelberg 2014

sequence in the genome of *Sorangium cellulosum*. Until their anticancer bioactivity was reported, more and more following extensive studies on epothilones in various aspects were performed, and many synthetic and semi-synthetic epothilone analogues have been produced to further improve the adverse effect profile and to maximize the antitumor properties [3, 4]. Several epothilones and chemically modified derivatives of epothilones are being used in clinical anticancer trials [5–7], and ixabepilone (16-aza-epothilone B, developed by Bristol-Myers Squibb) was authorized for clinical use by the Food and Drug Administration of the United States in 2007 [8].

For lacking of efficient molecular techniques, genetic engineering is hardly performed in *Sorangium cellulosum*. Microbial fermentation is still the main way to produce epothilones with strain continuously improving by mutation. In general, yields of epothilone were detected by HPLC or LC–MS [9–11], which were time-consuming and not suited for high-throughput screening [12, 13].

In this paper, we described an efficient high-throughput method for screening of overproduction of epothilone B with spectrum. Characteristic absorption under 249 nm wavelength was used as the basis for this method.

7.2 Materials and Methods

7.2.1 Microorganism and Culture Conditions

So2161 is a *Sorangium cellulosum* strain that was isolated from a soil sample in our laboratory which has been morphologically and phylogenetically classified using previously reported methods. It could be cultivated on solid CNST agar plates with filter paper and in liquid M26 medium at 30 °C. Submerged (liquid state) fermentations have been carried out for the preparation of the inoculums in liquid M26 medium (pH 8.0).

7.2.2 Mutation with Ultraviolet Radiation

Sorangium cellulosum So2161 was mutagenized with UV irradiation. First, the strain was inoculated into 50 mL M26 medium, shaking in liquid M26 medium for 4−5 days at 30 °C. Cells were collected, washed with water, and gently scattered with sterilized glass beads. Before irradiation, the cells were suspended and adjusted to titers of 10^8 cells/mL. 1.5 mL of the diluted cells were placed in a 9 mm petri dish and under a 30 W UV lamp at a distance of 30 cm for 3 min with a kill rate of 95−98 %, vigorously shaking during exposure, and immediately removed after the appropriate dose. Then they were harvested and spread on solid VY/2 agar and cultured for 7 days at 30 °C.

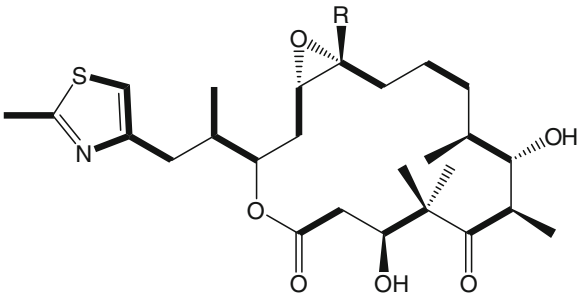

Fig. 7.1 Molecular structures of epothilones A and B (R = H, epothilone A; R = CH_3, epothilone B)

7.2.3 Optimized Rapid Screening Method for Epothilone B High-Producing Mutants

Two aseptic 96-well microtiter plates, named A and B, were chose to incubate the mutants. Each of them was filled with 0.2 mL sterile EMP medium containing 1.5 % agar. Clones of 191 Mutant strains and the wild strain So2161 that grew on solid VY/2 dish described above were transferred into corresponding wells of both the plates. After incubated at 30 °C for 4 days, sterilized XAD-16 resins were added into the wells of one of the plate (A) and go on culture for 6 days, while the other one (B) was stored at 4 °C for culture preservation. When the cultivation was ended, plate A was heated at 40 °C to dry the medium column and 250 μL CCl_4 was added into each well of the plate A and shaking for 8 h at 60 rpm to extract the epothilone B absorbed by the XAD-16 resins and let it sit for 10 min. 200 μL of each extracts were transferred into corresponding wells of a new aseptic 96-well microtiter plate. Then the plate was placed in a Sigma SPECTRAmax190 microplate spectrophotometer (St. Louis, MO, USA), and the absorption value under characteristic wavelength of epothilone B were read and recorded.

7.2.4 Relationship Between the Yield of Epothilone B and the OD_{249} of the Extract

To validate the high-throughput method, all the extracts including 191 mutant strains and the wild So2161 was analyzed by HPLC. Yields of epothilone B were detected using HPLC chromatography with a 5 μm RP-C18 column (4.6 × 200 mm, Shimadzu, Japan). The extract was eluted with methanol: water (70: 30) at 1 mL/min. Epothilone B was detected at 249 nm wavelength with a retention time at 8.82 min. The titers were quantified based on a standard curve generated from purified epothilones B.

Relationship between the yield of epothilone B and the OD_{249} of the extract was analyzed using regression analysis with SPSS statistical software.

7.2.5 Stabilization of the Extract

To observe the time base stability of epothilone during extracting, we chose 0, 5, 10, 15, 20, 25 h six point to analyze the degradation of epothilone B in 25 °C by HPLC and OD_{249} described above.

7.2.6 Shake Flask Cultures

Mutant strains screened by the high-throughput method was fermented carrying out in 250 mL shake flask filled with 50 mL liquid EMP medium with 2 % XAD-16 resin at 30 °C for 7 days. After fermentation, the XAD-16 resin beads were collected from the cultures, washed with distilled water, air dried, and extracted with 1 mL methanol, shaking for 2 h at 40°. Extractions were centrifuged at 10,000 g for 10 min, and then filtrated through 0.45 μm filter membrane for HPLC analysis.

7.3 Results and Discussion

7.3.1 Optimized Rapid Screening Method for Epothilone B High-Producing Mutants

Whole wavelength scan from 200−800 nm results showed that the epothilones had a maximum adsorption at 249 nm, which was chosen for the characteristic wavelength (Fig. 7.2).

After 3 cycles UV irradiation, 191 mutated strains were selected to analyze the relationship between the yield of epothilone B and the OD_{249}. In the optimized rapid screening method (Fig. 7.3a), we chose CCl_4 for the extract solvent, whose recovery rate and purity were much more than methanol (Fig. 7.3b). In this method, the purity of epothilones was 22 times higher than methanol extract. So the OD_{249} was much less disturbed by the impurities which showed more dependency with the concentration of epothilones.

7.3.2 Relationship Between the Yield of Epothilone B and the OD_{249} of the Extract

All the 191 mutated strains and the wild So2161 strain were fermented on solid EMP medium in 96-well microtiter plates and the CCl_4 extracts were detected by HPLC and microplate spectrophotometer at 249 nm wavelength. SPSS statistical

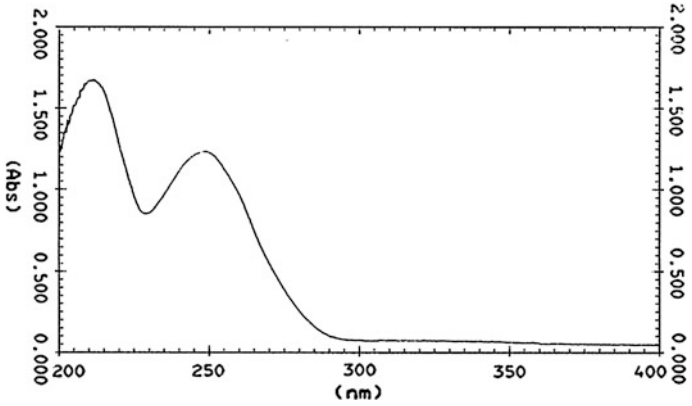

Fig. 7.2 Wavelength scan from 200–800 nm of epothilone B

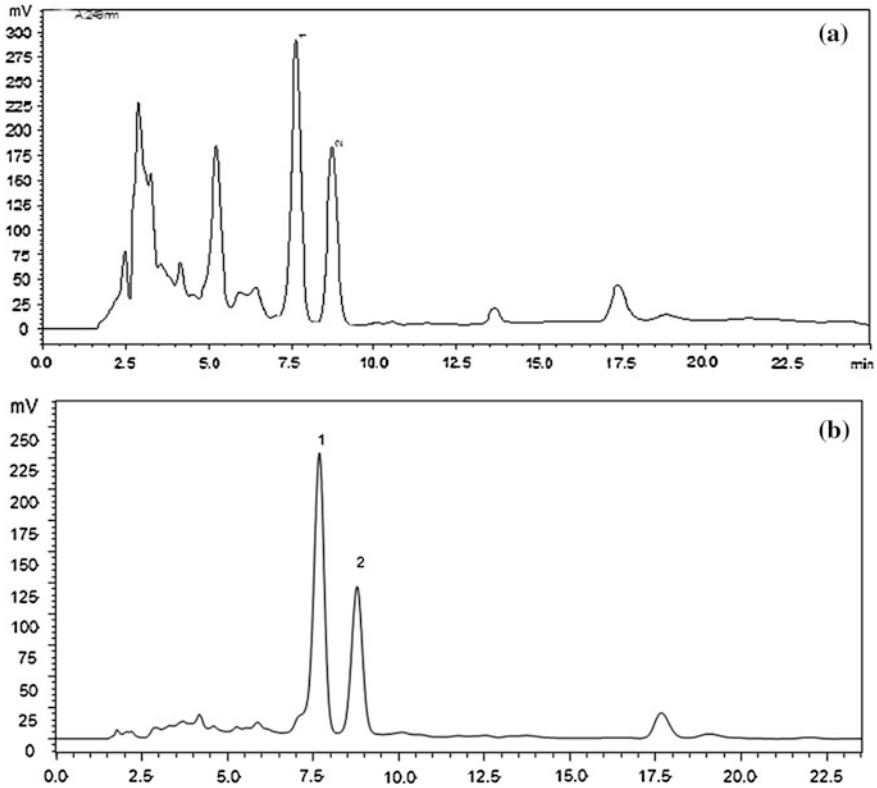

Fig. 7.3 HPLC analysis of the extracts ((**a**) extracted with methanol; (**b**) extracted with CCl_4)

analysis of all the 192 strains showed that the OD_{249} and yield of epothilone B were closely related (Fig. 7.4). Regression equation was generated as follows:

$$\begin{aligned} Y &= 0.088X + 0.074; \\ R^2 &= 0.558; \end{aligned} \tag{7.1}$$

Y:OD_{249} detected by microplate spectrophotometer; X:yield of epothilone B detected by HPLC.

Results showed that when the epothilone B concentration was lower than 10 mg/mL, the top 20 % samples with high OD_{249} also contained more epothilone B, which gave us a new efficient screening method for epothilone B high-producing strains.

7.3.3 Stabilization of the Extract

In order to visit the stabilization of epothilone B in the CCl_4 extract, we analyzed the degradation time of epothilone B in this method. Results showed that epothilone B had a good stability. In 36 h, there were only 7.7 % epothilone B

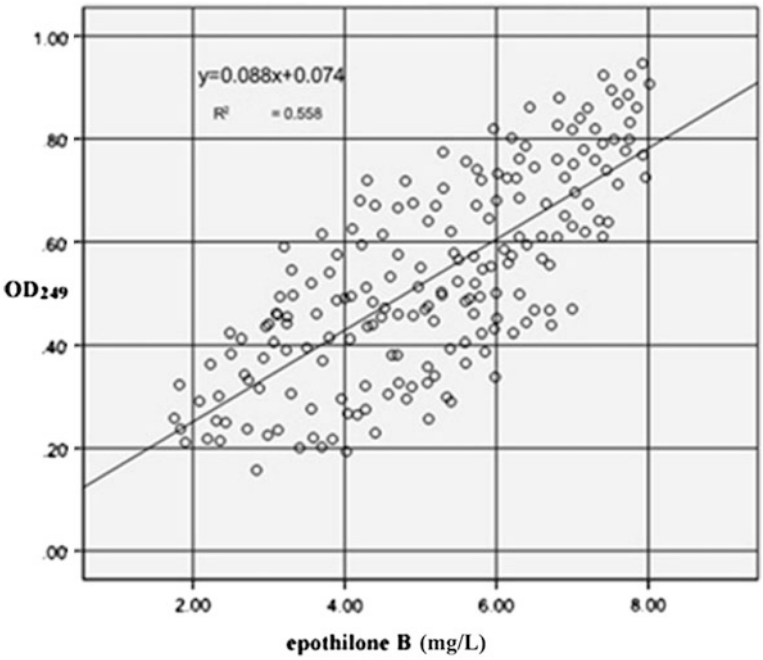

Fig. 7.4 Relationship between the yield of epothilone B and the OD_{249} of the extract

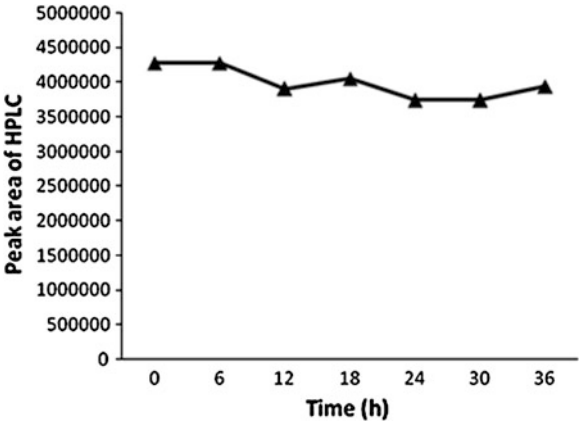

Fig. 7.5 Stability of epothilone B

degraded, which could barely affect on the result of the rapid screening method (Fig. 7.5).

7.4 Conclusions

Epothilones are a kind of poliketide macrolide with strong stabilizing activities on polymerized microtubules which mimicked taxol. Strain improved by mutation was still an important way to increasing the yields of production. However, high-throughput screen method for the over-producing strain was always time-consuming. In this paper, we described an efficient high-throughput method for epothilones high-producing strains with 96-well microtiterplate spectrometry combined with CCl_4 extracting. In this method, the purity of epothilones was 22 times higher than methanol extract. So the OD_{249} was much less disturbed by the impurities. SPSS analysis showed that the OD_{249} and the yield of epothilone B of the 192 strains were closely related. This new method was practical, accurate, and much more efficient.

Acknowledgments The work was financially supported by No. 2012GGA14017 of Province Science and Technology Development Project and grants ZR2011CQ006 of Shandong Provincial Natural Science Foundation.

References

1. Gerth K, Bedorf N, Höfle G et al (1996) Epothilons A and B: Antifungal and cytotoxic compounds from *Sorangium cellulosum* (Myxobacteria) -production, physico-chemical and biological properties. J. Antibiot 49:560–564
2. Shahabi S, Ping C, Huang Y et al (2010) Epothilone B enhances surface EpCAM expression in ovarian cancer Hey cells. Gynecol Oncol 119:345–350

3. Bollag DM, McQueney PA, Zhu J et al (1995) Epothilones, a new class of microtubule-stabilizing agents with a taxol-like mechanism of action. Cancer Res 55:2325–2333
4. Goodin S, Kane MP, Rubin EH (2004) Epothilones: mechanism of action and biologic activity. J Clin Oncol 2:2015–2025
5. Reichenbach H, Höfle G (2008) Discovery and development of the epothilones: a novel class of antineoplastic drugs. Drugs R D 9:1–10
6. Zhao L, Li PF, Lu CH et al (2010) Glycosylation and production characteristics of epothilones in alkalitolerant *Sorangium cellulosum* strain So0157-2. J Microbiol 48:438–444
7. Coderch C, Klett J, Morreale A et al (2012) Comparative binding energy (combine) analysis supports a proposal for the binding mode of epothilones to β-tubulin. Chem Med Chem 7:836–843
8. Puhalla S, Brufsky A (2008) Ixabepilone: a new hemotherapeutic option for refractory metastatic breast cancer. Biologics: Targets & Therapy 2:505–515
9. Hicks LM, O'Connor SE, Mazur MT et al (2004) Mass spectrometric interrogation of thioester-bound intermediates in the initial stages of epothilonethilone biosynthesis. Chem Biol 11:327–335
10. Cömezoğlu SN, Ly VT, Zhang D et al (2009) Biotransformation profiling of ^{14}C ixabepilone in human plasma, urine and feces samples using accelerator mass spectrometry (AMS). Drug Metab Pharmacok 24:511–522
11. Sun ZY, Zhang YG, Liao WQ et al (2010) LC–MS for in Vitro Determination of a Novel Epothilone D Derivative (Epothilone D 7-HD) in Human Plasma. Chromatographia 71:923–926
12. Furlan RL, Garrido LM, Brumatti G et al (2002) A rapid and sensitive method for the screening of DNA intercalating antibiotics. Biotechnol Lett 24:1807–1813
13. Xu ZN, Shen WH, Chen XY et al (2005) A highthroughput method for screening of rapamycin-producing strains of *Streptomyces hygroscopicus* by cultivation in 96-well microtiter plates. Biotechnol Lett 27:1135–1140

Chapter 8
Cloning of Glucoamylase Gene from *Aspergillus niger* and its Expression in *Saccharomyces cerevisiae* W303-1B

Ming Li, Liying Zhou, Xin Sun, Shuya Wang, Hongxin Wang, Dongxia Li and Fuping Lu

Abstract To further research the heterologous expression of glucoamylase gene, *Saccharomyces cerevisiae* W303-1B as host strain to express the glucoamylase gene from *Aspergillus niger* was studied. Glucoamylase gene GAL was cloned from *A. niger* and analyzed. The results showed the GAL had an open reading frame of 1923 bp that encoded a protein of 640 amino acids. The glucoamylase-producing engineering strain W303-1B/pYPGE15-GAL was constructed by cloning the GAL gene into *S. cerevisiae* expression vector pYPGE15 and transforming it into *S. cerevisiae* W303-1B. The results reveal that the recombinant glucoamylase is expressed and secreted correctly in engineering strain W303-1B/pYPGE15-GAL, and its enzyme activity in the medium reaches 212.9 U/ml.

Keywords Glucoamylase · Clone · Heterologous expression · *Saccharomyces cerevisiae*

8.1 Introduction

Glucoamylases (EC 3.2.1.3), also known as amyloglucosidases, glucamylases, maltases, saccharogenic amylases, and γ-amylases, are starch-degrading extracellular enzymes that are synthesized and secreted by some microorganisms [1]. It may hydrolyze α-1, 4 glycosidic bond from the non-reducing end of starch, dextrin, and glycogen, resulting in the production of glucose. Meanwhile, it also has the ability to digest α-1, 6 and α-1, 3 glycosidic bond, which makes it to have the same effect on the hydrolysis of amylopectin [2–4]. Generally, glucoamylase can hydrolyze all starch into glucose [5, 6]. Therefore, glucoamylase is the most important enzyme widely used in the industrial production related to starch,

M. Li · L. Zhou · X. Sun · S. Wang · H. Wang · DongxiaLi · F. Lu (✉)
Tianjin University of Science and Technology College of Biotechnology, Tianjin 300457, China
e-mail: liming09@tust.edu.cn

T.-C. Zhang et al. (eds.), *Proceedings of the 2012 International Conference on Applied Biotechnology (ICAB 2012)*, Lecture Notes in Electrical Engineering 249,
DOI: 10.1007/978-3-642-37916-1_8, © Springer-Verlag Berlin Heidelberg 2014

especially in the fermentation of *Saccharomyces cerevisiae* when using starch as raw material [7–11], where starch saccharification is an essential process because *S. cerevisiae* do not contain the glucoamylase gene [7], which requires to have to add a large number of enzymes into fermentation broth to catalyze starch into available glucose, resulting in the increased costs.

With the identification of glucoamylase molecular structure, it is possible to construct the engineering strain glucoamylase-producing by transforming the gene of glucoamylase into *S. cerevisiae* to express high-level glucoamylase. Moreover, *S. cerevisiae* as a eukaryotic engineering host has many advantages such as well studied genetic background, high fermentation rate, and easiness to manipulate [12, 13], which are in favor of the manipulation and expression for the gene of glucoamylase in *S. cerevisiae*, further improving the glucoamylase production. All these lay a foundation for the directed evolution and industrial application of glucoamylase.

The glucoamylase gene usually exist in many filamentous fungi and certain strains of yeast [14–16]. In recent years, there has been a keen interest in the production of heterologous glucoamylase by the introduction of the gene of glucoamylase into the *S. cerevisiae* that do not contain the glucoamylase gene. In Long's study [17], *Aspergillus awamori* glucoamylase gene was integrated into the genome of *S. cerevisiae* and the gene was successfully expressed in the *S. cerevisiae.* Yang et al. [7] had been reported that an isolated *R. arrhizus* glucoamylase gene was introduced into *S. cerevisiae* to construct amylolytic yeast strains, which were able to grow on raw starch and to secret glucoamylase enzyme in the culture supernatant. In Sakai's [18] study, the *Saccharomyces pastorianus* STA1 gene was introduced into *S. cerevisiae*, and the resulted transformants successfully expressed glucoamylase enzyme, which led to the amount of dextrin in the medium decrease by 22 %.

However, the vector pYPGE15 from yeast and *S. cerevisiae* W303-1B chosen as the vector and host strain for expression of the glucoamylase gene from *A. niger* has been not reported so far. In this paper, the gene GAL encoding glucoamylase obtained by RT-PCR technology from *A. niger* was cloned into the pYPGE15 vector containing a constitutive promoter PKG, which could make the producing strain synthesize and secret glucoamylase without addition of inducer, to construct the expression vector pYPGE15-GAL. The pYPGE15-GAL was then transformed into *S. cerevisiae* W303-1B to obtain the engineering strain W303-1B/pYPGE15-GAL, which could express and secret correctly glucoamylase in the medium with enzyme activity 212.9 U/ml.

8.2 Materials and Methods

8.2.1 Strains, Plasmids, and Media

Aspergillus niger TCCC 41,056 was used as honor of glucoamylase gene and cultivated in PDA medium. *Escherichia coli* DH5α was used as a host for recombinant DNA manipulation and *S. cerevisiae* W303-1B was used as a host

strain for expression of the glucoamylase gene, which was grown in LB medium and YPD medium, respectively.

The pUCm-T vector was purchased from TaKaRa (Dalian) and YPGE15 vector was provided by East China Normal University. SC-U plate containing 0.67 % YNB, 0.115 % the mixture of essential amino acid and adenine without uracil, 2 % glucose and 2 % agar were used for selecting recombination yeast clones. YWSX (SC-U without glucose, 0.5 % soluble starch, 0.05 % trypan blue) plate was used for testing the expression of transformants.

8.2.2 Method

8.2.2.1 Extraction of Total RNA from *A. niger* and Clone of Glucoamylase Gene

A. niger was cultivated in 50 ml PDB medium at 28 °C for 3 days. Total RNA from *A. niger* was extracted by Trizol method using TRIquick reagent, DEPC and phenol/chloroform. Agarose gel electrophoresis was then conducted to verify the extracted RNA. The cDNA was obtained by reverse transcription using RNase Inhibitor, dNTP, M-MLV with the primers, ANF (5′-ATGTCGTTCCGA TCTCTACTCGCC-3′) and ANR (5′-TCACAGTGTACATACCAGAGCGGG-3′), which was designed and synthesized according to the mRNA sequence of glucoamylase gene from *A. niger* in NCBI database (GenBank Accession No.HQ537427.1).

The glucoamylase gene GAL was synthesized by PCR using obtained cDNA as a template. The amplification was carried out under the following condition: the first step was initiated at 95 °C for 5 min, followed by 30 cycles of 95 °C for 45 s, 57 °C for 45 s, and 72 °C for 100 s, and the final extension was carried out at 72 °C for 10 min. A 1.9 kb PCR product was recovered from the agarose gel, which was then ligated to pUCm-T by T4 DNA Ligase at 16 °C for 10 h to obtain the recombinant Vector pUCm-T-GAL, which was transformed into *E. coli* DH5α by $CaCl_2$ transformation. The transformants were picked up by the Blue spot method and then sequenced by Shenggong Biotech Company (Shanghai).

8.2.2.2 Construction of pYPGE15-GAL and Sequencing

The GAL was amplified by PCR using the plasmid pUCm-T-GAL as a template, ANWF (5′-CGGAATTCATGTCGTTCCGATCTCTACTCGCC-3′) as forward primer and ANWR (5′-CCGCTCGAGTCACAGTGACATACCAGAGCGGG-3′) as reverse primer with restriction site *Eco*R I and *Xho* I (*the underlined*), respectively. PCR product (GAL gene) of 1.9 kb was digested with *Eco*R I and *Xho* I and was ligated into pYPGE15 digested by the same enzymes to construct the recombinant vectors pYPGE15-GAL, followed by transforming into *E. coli*

DH5α. The transformants were selected by PCR and pYPGE15-GAL was identified by digestion of *Eco*R I and *Xho* I and sequencing by Shenggong Biotech Company (Shanghai).

8.2.2.3 The Construction of Engineering Strain W303-1B/pYPGE15-GAL

The engineering strain W303-1B/pYPGE15-GAL was constructed by transforming pYPGE15-GAL with electroporation method into the *S. cerevisiae* W303-1B. W303-1B/pYPGE15-GAL was screened by culturing the transformants on the SC-U medium for 3–5 days and was identified by extracting the expression vectors pYPGE15-GAL in them.

8.2.2.4 Expression and Assays of Glucoamylase

The engineering strains W303-1B/pYPGE15-GAL were cultured on YWSX plate for 60 h at 30 °C and hydrolysis circles on YWSX plate were examined for the analysis of enzyme activity. In order to determine enzyme activity of glucoamylase, the engineering strains with bigger hydrolysis circle on YWSX plate were picked up and inoculated in SC-U medium and cultivated for 90 h at 30 °C. Assays of glucoamylase were conducted according to Sakai's method [18].

8.3 Results

8.3.1 Extraction of Total RNA from A. niger

The appropriate amount of spores of *A. niger* was inoculated into fermentation medium and cultivated for 3 days at 28 °C, 180 r/min. The mycelium of *A. niger* accumulated in the fermentation broth was collected by filtration and washed. The total RNA of *A. niger* was extracted from the collected mycelium by TRIZOL reagent method. The results (Fig. 8.1) showed that the bands of 28S rRNA and 18S rRNA from total RNA were bright and clear and the band of 28S rRNA was

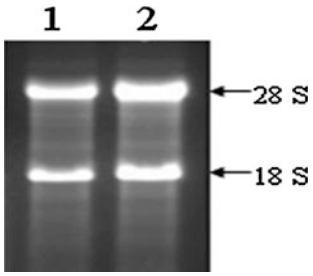

Fig. 8.1 The extraction results of total RNA of *A. niger*

almost twice as bright as that of 18S rRNA, which indicated RNA was successfully extracted from the donor strain.

Moreover, the quantitative analysis of RNA samples on purity (OD_{260}/OD_{280} between 1.9 and 2.0) also showed that the sample had a higher purity, and was not degraded by ribonuclease and not contaminated by DNA and proteins, indicating that it could meet the next requirement of experiments.

8.3.2 Cloning of Glucoamylase Gene GAL

The cDNA was amplified by reverse transcription using the total RNA from *A.niger* as a template. The GAL was cloned using template cDNA and primers ANF and ANR (Fig. 8.2a), then ligated to pUCm-T and transformed into *E. coli* DH5α. The recombinant plasmid pUCm-T-GAL was identified by digestion with restriction enzymes *Nco* I and *Hin*d III (Fig. 8.2b) and GAL was sequenced. The results of sequencing showed that the cloned GAL was 1923 bp, which was the same as the mRNA of *A.niger*'s glucoamylase reported (GenBank Accession No.HQ537427.1), and encoded a protein of 640 amino acids. These results demonstrated that GAL was cloned correctly.

8.3.3 Construction of the Express Vector pYPGE15-GAL

The GAL was amplified from plasmid pUCm-T-GAL using primers ANWF and ANWR, and then digested by *Eco*R I and *Xho* I and ligated into plasmid pYPGE15

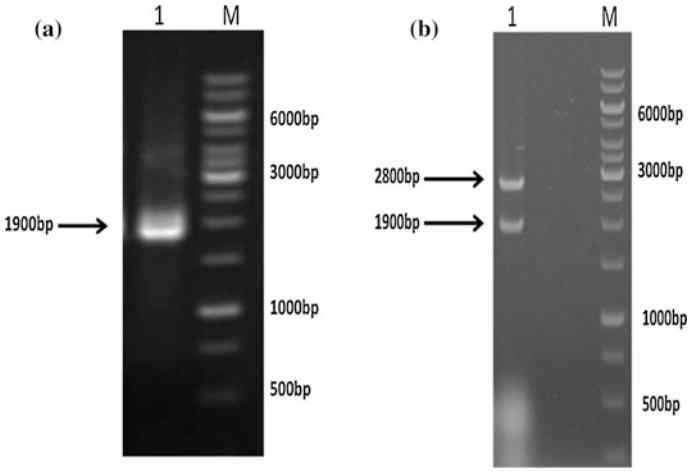

Fig. 8.2 Identification of the vector pUCm-T-GAL. **a** The results of PCR (*M*:10 kb DNA ladder, *1* The PCR results of the plasmid pUCm-T-GAL), **b** The results of enzyme digestion (*M*:10 kb DNA ladder, *1* The products of the pUCm-T-GAL digested with *Nco* I and *Hin*d III)

to construct expression vector pYPGE15-GAL. The ligation products were transformed into *E. coli* DH5α and identified by digestion with *Eco*R I and *Xho* I and sequenced. A 1.9 kb and a 6.4 kb fragments were produced by the digestion, which matched our expect (Fig. 8.3). The sequencing results showed that the GAL sequence and open reading frame were right, confirming that the expression vector pYPGE15-GAL was constructed rightly (Fig. 8.4).

8.3.4 Construction of the Engineering Strain W303-1B/pYPGE15-GAL

The express vector pYPGE15-GAL was introduced into W303-1B by electro-transformation to construct the engineering strain W303-1B/pYPGE15-GAL. The transformants were cultured on SC-U plates without uracil and were screened

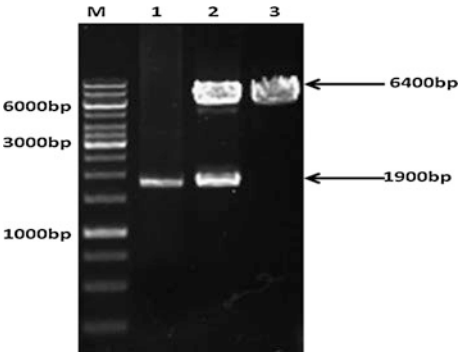

Fig. 8.3 Identification of the vector pYPGE15-GAL. *M*: 10 kb DNA ladder; *1* The PCR results of the plasmid pYPGE15-GAL; *2* The product of pYPGE15-GAL digested with *Eco*R I and *Xho* I; *3* The product of pYPGE15 digested with *Eco*R I

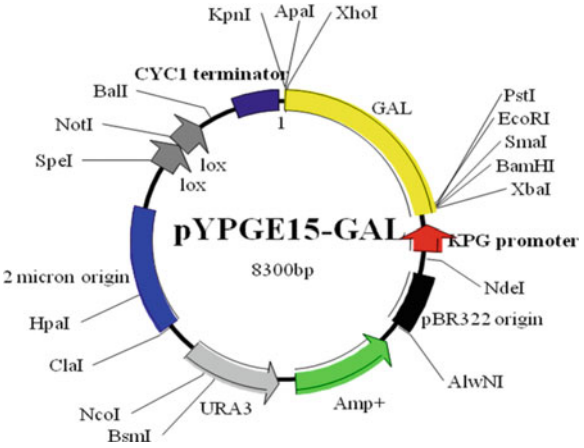

Fig. 8.4 Physical map of recombinant plasmid pYPGE15-GAL

(Fig. 8.5). The plasmids were extracted from the transformants and identified by digestion with *Eco*R I and *Xho* I (Fig. 8.6). The results showed that pYPGE15-GAL has been introduced into W303-1B, confirming that W303-1B/pYPGE15-GAL was generated.

8.3.5 Screen of the Engineering Strain W303-1B/pYPGE15-GAL Producing-Glucoamylase and Assays of Glucoamylase

The W303-1B/pYPGE15-GAL was inoculated on YWSX plates containing trypan blue and starch (without glucose) plates, respectively, and cultured for 3d at 30 °C. Transparent hydrolysis circles were observed on the YWSX plates (Fig. 8.7) and the starch-iodine starch plates (when iodine was added) (Fig. 8.8), while there was no hydrolysis circle on the plates (control) where the strain W303-1B containing plasmids pYPGE15 were inoculated. These results showed that the engineering strains W303-1B/pYPGE15-GAL could express and secret glucoamylase.

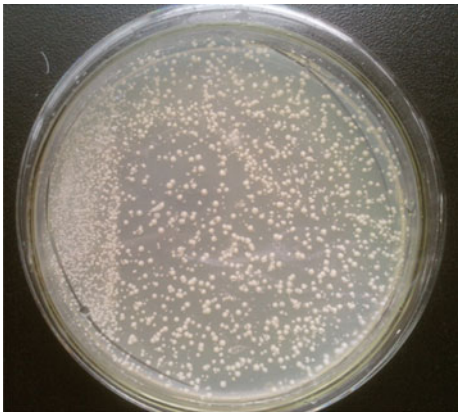

Fig. 8.5 Transformed plate of *S.cerevisiae* W303-1B/pYPGE15-GAL

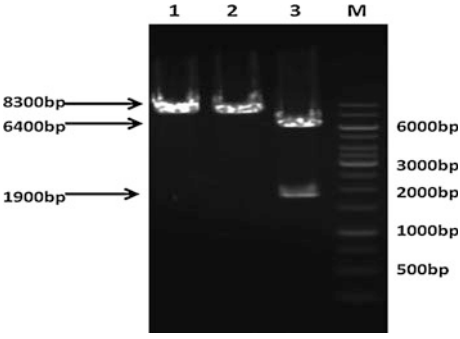

Fig. 8.6 Identification of the vector pYPGE15-GAL. *M*: 10 kb DNA ladder; *1* The result of the plasmid pYPGE15-GAL digested with *Eco*R I; *2* The result of the plasmid pYPGE15-GAL digested with *Xho* I; *3* The result of the plasmid pYPGE15-GAL digested with *Eco*R I and *Xho* I

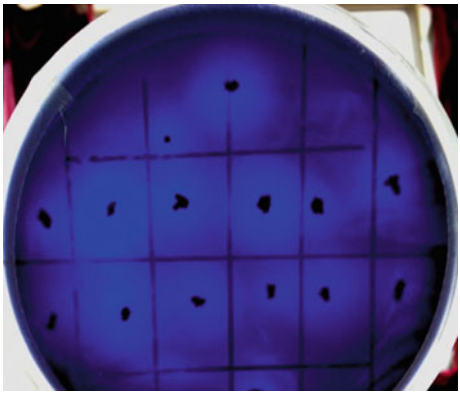

Fig. 8.7 The result of the transformants W303-1B/pYPGE15-GAL on the plate containing *Trypan-blue*

Fig. 8.8 The result of the transformants W303-1B/pYPGE15-GAL on the plate containing starch and iodine

In order to determine expression level of glucoamylase in W303-1B/pYPGE15-GAL, the enzyme activity of glucoamylase was measured. The bigger the ratio of hydrolysis circle diameter to colony diameter was, the higher the expression level of glucoamylase in W303-1B/pYPGE15-GAL was. The engineering strains producing high-level glucoamylase were picked up, inoculated in SC-U medium and cultivated for 90 h at 30 °C. The enzyme activity of glucoamylase was then determined. The results showed that its enzyme activity in the medium reached 212.9 U/ml.

8.3.6 Stability Analysis of the Engineering Strain W303-1B/pYPGE15-GAL

In order to analysis the stability of the engineering strains W303-1B/pYPGE15-GAL, they were inoculated and cultured for 20 generations continuously in YPD

medium, and enzyme activity of glucoamylase was then determined according to the above method. The results showed that the enzyme activity in the medium almost had no change, confirming that the engineering strain W303-1B/pYPGE15-GAL was stability.

8.4 Discussion

In this study, the total RNA was extracted from *A. niger* and the glucoamylase gene GAL obtained after the reverse transcription was cloned into the vector pYPGE15 to achieve pYPGE15-GAL, where the PKG promoter is a constitutive promoter, which can express the glucoamylase in W303-1B/pYPGE15-GAL without addition of inducer compared with the inducible promoter. Moreover, the pYPGE15-GAL in *S. cerevisiae* was free plasmid with a higher copy, which contributed to improve the expression of interested genes. In this study, enzyme activity of glucoamylase in the medium reached 212.9 U/ml, and the engineering strains W303-1B/pYPGE15-GAL kept stability when inoculated and cultured for 20 generations continuously. The transformants might be screened easily using the trypan blue method and the screened transformants could be picked up for the subsequent experience while not using the starch-iodine plate method. Therefore, the trypan blue method was easier and faster for the screening than the starch-iodine plate method.

To improve catalysis ability of glucoamylase, directed revolution was a major genetic engineering method. This paper laid a foundation for screening interested glucoamylase gene by directed revolution.

Acknowledgments This work was supported by Tianjin Research Program of Application Foundation and Advanced Technology (No. 11JCYBJC 09,600), Chinese National Program for High Technology Research and Development (‘863’ Plan) (No. 2013AA102106), National Natural Science Foundation of China (No. 21176190) and Key Technology Research and Development Program of Tianjin, China (No. 11ZCKFSY00900).

References

1. Gupta R, Gigras P, Mohapatra H et al (2003) Microbial α-amylases: a biotechnological perspective. Process Biochem 38:1599–1616
2. James JA, Lee BH (1997) Glucoamylases: microbial sources, industrial applications and molecular biology—a review. J Food Biochem 21:1–52
3. Pandey A, Nigam P, Soccol C et al (2000) Advances in microbial amylases. Biotechnol Appl Biochem 31:135–152
4. Kaur P, Satyanarayana T (2004) Production and starch saccharification by a thermostable and neutral glucoamylase of a thermophilic mould Thermomucor indicae-seudaticae. World J Microbiol Biotechnol 20:419–425

5. Horvathova V, Janecek S, Sturdik E (2001) Amylolytic enzymes: molecular aspects of their properties. Gen Physiol Biophys 20:7–32
6. Pavezzi FC, Carneiro AAJ, Bocchini-Martins DA et al (2011) Influence of different substrates on the production of a mutant thermostable glucoamylase in submerged fermentation. Appl Biochem Biotechnol 163:14–24
7. Yang S, Jia N, Li M et al (2011) Heterologous expression and efficient ethanol production of a Rhizopus glucoamylase gene in *Saccharomyces cerevisiae*. Mol Biol Rep 38:59–64
8. Janse B, Pretorius I (1995) One-step enzymatic hydrolysis of starch using a recombinant strain of *Saccharomyces cerevisiae* producing α-amylase, glucoamylase and pullulanase. Appl Microbiol Biotechnol 42:878–883
9. Murai T, Ueda M, Yamamura M et al (1997) Construction of a starch-utilizing yeast by cell surface engineering. Appl Environ Microbiol 63:1362–1366
10. Öner ET, Oliver SG, Kırdar B (2005) Production of ethanol from starch by respiration-deficient recombinant *Saccharomyces cerevisiae*. Appl Environ Microbiol 71:6443–6445
11. Kumagai MH, Sverlow GG, della-Cioppa G et al (1993) Conversion of starch to ethanol in a recombinant *Saccharomyces cerevisiae* strain expressing rice α-amylase from a novel Pichia pastoris alcohol oxidase promoter. Nat Biotechnol 11:606–610
12. Kolaříková K, Galuszka P, Sedlářová I et al (2009) Functional expression of amine oxidase from Aspergillus niger (AO-I) in *Saccharomyces cerevisiae*. Mol Biol Rep 36:13–20
13. Winzeler EA, Shoemaker DD, Astromoff A et al (1999) Functional characterization of the *S. cerevisiae* genome by gene deletion and parallel analysis. Science 285:901–906
14. Jørgensen AD, Nøhr J, Kastrup JS et al (2008) Small angle X-ray studies reveal that *Aspergillus niger* glucoamylase has a defined extended conformation and can form dimers in solution. J Biol Chem 283:14772–14780
15. Pazur J, Liu B, Miskiel F (1990) Comparison of the properties of glucoamylases from *Rhizopus niveus* and *Aspergillus niger*. Biotechnol Appl Biochem 12:63–78
16. Liu ZR, Zhang GY, Li J et al (2007) Stable expression of glucoamylase gene in industrial strain of *Saccharomyces pastorianus* with less diacetyl produced. Ann Microbiol 57:233–237
17. Lin LL, Ma YJ, Chien HR et al (1998) Construction of an amylolytic yeast by multiple integration of the *Aspergillus awamori* glucoamylase gene into a *Saccharomyces cerevisiae* chromosome. Enzyme Microb Technol 23:360–365
18. Sakai K, Fukui S, Yabuuchi S et al (1989) Expression of the Saccharomyces diastaticus STA1 gene in brewing yeasts. J Am Soc Brew Chem 47:87–91

Chapter 9
Effects of Environmental Conditions on Synthesis of the Mycosporine-Like Amino Acid in *Nostoc flagelliforme* Cells

Rong Liu, Haifeng Yu and Yuxia Sa

Abstract *Nostoc flagelliforme* is a terrestrial cyanobacterium distributed in arid or semiarid area, which has the capability of nitrogen-fixing and photosynthesis. The multifunction of MAAs is of great significance for *N. flagelliforme* to adapt to abiotic stresses. The changes of mycosporine-like amino acids in *N. flagelliforme* cells with UV-B radiation and salt stress were studied. The results showed that MAAs concentrations reached 32.26 mg/g after 12 h under UV-B radiation (5 W/m^2). After 2 days cultivation, MAAs synthesis was up to the maximum with the BG11 medium containing 50 mM NaCl and 50 mM NH_4Cl, and their concentrations were 45.09 and 35.14 mg/g respectively. HPLC analysis revealed the control sample contained nine MAAs. Ten MAAs were observed after UV-B treatment, and two new MAA compounds were found but one MAA disappeared. With the treatment of NaCl and NH_4Cl for 2 days, only seven MAAs were discovered and no new MAAs appeared.

Keywords Environmental conditions · Mycosporine-like amino acid · *Nostoc flagelliforme* · Synthesis

9.1 Introduction

Solar radiation plays an important role in life activity, especially for photosynthetic organisms. Nowadays with the depletion of stratospheric ozone concentration over the polar region, the intensity of UV-B radiation reaching the biosphere increases, which presents potential negative impacts on organisms [1]. Some

R. Liu · H. Yu (✉) · Y. Sa
Shandong provincial key laboratory of Microbial Engineeringy,
Qilu University of Technology, 250353 Jinan,
People's Republic of China
e-mail: yhfdzz@126.com

T.-C. Zhang et al. (eds.), *Proceedings of the 2012 International Conference on Applied Biotechnology (ICAB 2012)*, Lecture Notes in Electrical Engineering 249,
DOI: 10.1007/978-3-642-37916-1_9, © Springer-Verlag Berlin Heidelberg 2014

physiological and biochemical processes, such as photosynthesis, respiration, growth, and reproduction, will be inhibited or ended [2]. Therefore, the synthesis of UV-absorbing compounds is a vital adaptive mechanism for organisms surviving under the high intensity of UV-B.

Mycosporine-like amino acids (MAAs) are small, colorless, water-soluble substances. They are characterized by a cyclohexenone or cyclohexenimine chromophore conjugated with the nitrogen substituent [3]. MAAs can be synthesized in fungi, marine heterotrophic bacterium, cyanobacterium, and eukaryotic algae. So far, more than 30 MAAs have been elucidated [4]. MAAs considered as UV-absorbing compounds were first detected in the 1960s [5]. Numerous evidences indicate that MAAs could provide protection for radiation-sensitive organisms in biosphere [6]. They have absorption maxima ranging from 310 to 360 nm and high solar extinction coefficients ($e = 28{,}100–50{,}000\ M^{-1}cm^{-1}$). And most of MAAs compounds have their max absorption in the UV-B region [7]. In addition, MAAs can effectively absorb the high energy photons and dissipate the radiation as heat energy instead of producing reactive oxygen species [8].

In addition to UV radiation, the synthesis of MAAs may be affected by salt stress [9]. In order to keep the osmotic balance, organisms will accumulate some osmo-regulation substance characterized by uncharged organic molecules. In saline environments, cyanobacteria often contain high concentrations of MAAs [10]. Like other osmotic compounds, they must be contributed to a certain intracellular osmotic pressure.

Nostoc flagelliforme is a terrestrial filamentous cyanobacterium, which distributes in the northern and northwestern of China, thrives in arid or semiarid area characterized by high altitude, salinity environment, and intense solar radiation. It is reported that the UV-B level is about from 0.77 to 5.33 W/m^2 in Yinchuan, Ningxia, China [11, 12]. Because of rain shortage, the climate of Yinchuan is arid and the salt concentration is high. In recent years, the factors and functions of MAAs accumulation have been known in many cyanobacteria. However, there is a lack of study on the correlation between the content and components of MAAs and impact factors in liquid suspension cultured *N. flagelliforme* cells. Therefore, the effects of UV-B and salt stress on synthesis of the MAAs in *N. flagelliforme* cells were investigated.

9.2 Materials and Methods

9.2.1 Algal Material

The *N. flagelliforme* was collected in the east of the Helan Mountain in Yinchuan, Ningxia, China, and was stored in dry conditions at room temperature for 36 months before being used in experiments. The dissociated cells were obtained according to the methods previously reported [13]. Axenic cells were screened and cultured in $BG11_0$ (free of nitrogen) medium. They were cultured in BG11

medium in 500 mL shake-flask containing 200 mL medium at 25 °C under continuous illumination of 60 μmol photon $m^{-2}s^{-1}$.

9.2.2 UV Treatment and NaCl Treatment

A total of 50 mL culture of *N. flagelliforme* from their exponential growth phase was irradiated under UV-B lamps (313 nm), using UV light meters to insure the intensity of UV-B were 1 and 5 W/m^2. The culture suspension was placed in open glass Petri dishes of 90 mm diameter and irradiated for 3, 6, 12, 24, 36, 48 h, respectively. Cultures maintained under continuous illumination of 60 μmol photon $m^{-2}s^{-1}$ were treated as control. Deionized water was added in order to avoid volume changes due to evaporation.

NaCl or NH_4Cl solution was added to the BG11 medium with a concentration of 25, 50, 100, 200, 400, or 600 mM and exposed to continuous illumination of 60 μmol photon $m^{-2}s^{-1}$ for 2 days, respectively. The control culture of *N. flagelliforme* without NaCl or NH_4Cl was cultured under the same conditions.

9.2.3 Extraction and Estimation of MAAs

Cells were collected by centrifugation and extracted for 30 min in 5 mL of 30 % methanol (v/v) at 50 °C water bath in darkness. Extracts were clarified by centrifugation at 3000 rpm for 5 min. MAAs in supernatant were estimated at 338 nm in a UV-VIS spectrophotometer [14].

9.2.4 HPLC Analysis of MAAs

The methanol extract was further purified and analyzed by HPLC equipped with a Venusil XBP-C18 (5 μm; 250 × 4 mm I.D.). The extract was evaporated to dryness in a vacuum evaporator at 45 °C and re-dissolved in 2.5 mL double distilled water. A total of 7.5 mL chloroform was added to this solution and the supernatant was taken out carefully after centrifugation. The supernatants were evaporated to dryness and re-dissolved in 0.2 % acetic acid (v/v). The samples were filtered through 0.45 μm membrane filter for partial purification and 20 μL was used in this experiment. The mobile phase, consisting of 90 % aqueous methanol and 0.2 % acetic acid (v/v), run at a flow rate of 1 mL min^{-1}, and the MAAs were detected at 338 nm at a column oven temperature of 25 °C [15, 16].

9.2.5 Statistical Analysis

Statistical analysis was made by two-way analysis of variance (ANOVA): SPSS 18.0 and Origin 8.0. The data were carried out in triplicates and results were presented as mean ± standard deviation (SD).

9.3 Results and Discussion

9.3.1 Effect of UV-B Radiation and Salt Stress

Effect of UV-B radiation on the synthesis of MAAs content in *N. flagelliforme* cells was shown in Fig. 9.1. The production of MAAs increased slowly and reached the maximum after 12 h with 31.32 and 32.26 mg/g under UV-B exposure at 1 and 5 W/m^2. After 24 h, MAAs content decreased. This result suggested that the UV-B could induce the synthesis of MAAs in a very short period of time (less than 12 h). The high intensity of UV-B had a greater effect on the synthesis of MAAs content than the lower level.

Under the treatment of NaCl and NH_4Cl, changes of MAAs content showed the same trend (Fig. 9.2). They increased significantly with the lower concentrations of NaCl and NH_4Cl, respectively. After 2 days, MAAs content increased to the maximum treated by 50 mM NaCl and NH_4Cl, and the results were 45.09 and 35.14 mg/g, respectively. After that, MAAs content began to decrease with the salt concentrations increased. The above results indicated that the synthesis of MAAs could be induced by suitable concentrations of salt and ammonium, but inhibited by high salt and ammonium concentrations.

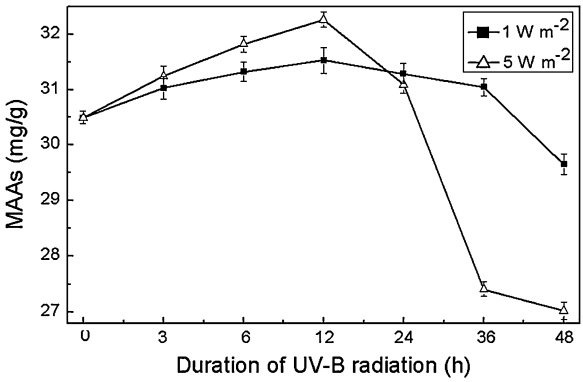

Fig. 9.1 MAAs content changes in *N. flagelliforme* cells under different UV-B levels and radiation times

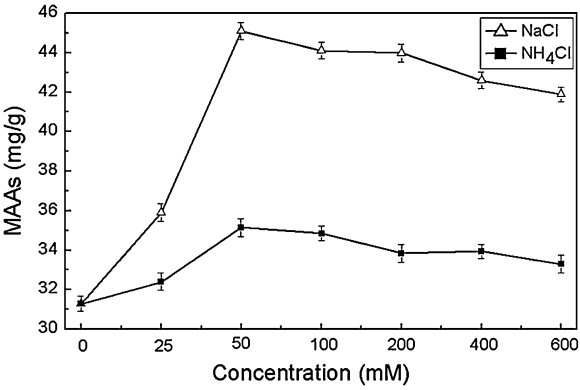

Fig. 9.2 MAAs content changes in *N. flagelliforme* cells under different concentrations of NaCl and NH_4Cl for 2 days, respectively

9.3.2 HPLC Analysis

Figure 9.3 demonstrated the components of MAAs produced by *N. flagelliforme*. There were nine MAAs in control *N. flagelliforme* cells in HPLC profiles. After 12 h of UV-B exposure at 1 W/m^2, seven MAAs increased and little change was observed in the first and third ones. In addition, two new MAAs appeared, but the sixth and seventh disappeared. The components of MAAs had the same changes expect for the sixth MAAs at the exposure level with 5 W/m^2. But the contents of MAAs were different in samples treated with different intensity of UV-B. The second, tenth, and eleventh MAAs in treatment of 5 W/m^2 were higher than the lower level. On the contrary, the fifth and eighth MAAs were lower. The above

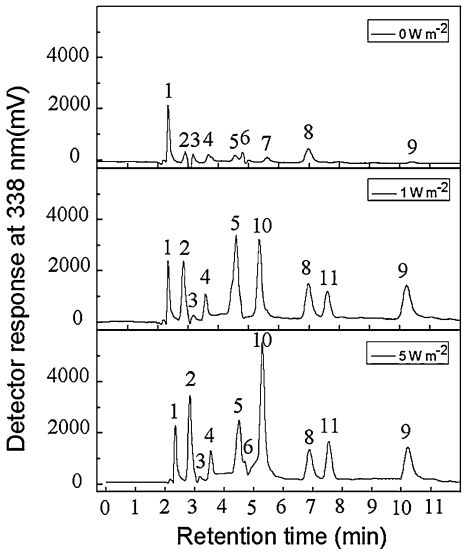

Fig. 9.3 HPLC chromatograms of 100 % methanol extract of *N. flagelliforme* cells treated with different intensity of UV-B for 12 h

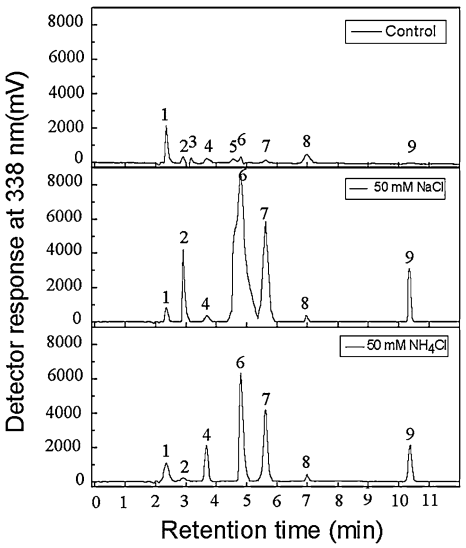

Fig. 9.4 HPLC chromatograms of 100 % methanol extract of *N. flagelliforme* cells treated with 50 mM NaCl and NH_4Cl for 2 days, respectively

result indicated that 5 W/m^2 had more significant effect on the synthesis of MAAs compared to the result in the lower level after 12 h.

The obtained results (Fig. 9.4) revealed that the content and components of MAAs were influenced by salt stress. Contrary to the control experiment, the third and fifth MAAs disappeared in both treatments, but the total MAAs content was higher. The second, sixth, seventh, and ninth MAAs increased under the treatment with 50 mM NaCl for 2 days. However, the other MAAs decreased. Four different MAAs appeared a rise trend in NH_4Cl media, which were the fourth, sixth, seventh, and ninth one. At the same time, the other MAAs showed lower than the control in HPLC chromatograms.

MAAs exist in *N. flagelliforme* cells under natural habits. MAAs content changed obviously under UV-B treatment and its production could be effectively responded by the UV-B dose. It was supposed that MAAs could serve as absorbing/screening compounds to avoid lethal doses of UV-B. The analysis of HPLC showed that some MAAs were increased or appeared. It is evident that MAAs had a photoprotective role. MAAs as sunscreen compounds could be found in many organisms exposed to high light intensities. In addition, the correlation between MAAs and UV-B has been observed in a wide variety of organisms. Study about light intensity could induce MAAs synthesis had been carried out in the cyanobacteria *Anabaena sp.*, *N. commune*, and *Scytonema sp* [17]. However, after a long time of UV-B exposure, some MAAs content decreased or disappeared. It may be because DNA and some physiological and metabolic processes were damaged by UV-B [18].

In addition to the photoprotective role of MAAs, many studies have shown that they are also considered as osmotic regulation compounds [19]. In our study, the synthesis of MAAs was also influenced by osmotic stress (either salt or ammonium

solutes). It is reported that MAA-producing cyanobacteria are abundant in hypersaline environments [20]. But it is opposite to this phenomenon in our work, and this might be because high concentration salt solutes destroy the balance in *N. flagelliforme* cells and change some metabolic activities. Although significant, it is still far from the concentrations required to balance the salinity, so that additional osmotic solutes, such as glucosylglycine [21], cerol trehalose, and glycine betaine [22], must be present in cells.

The obtained results imply that the two factors could cause the response of MAAs biosynthetic pathway, but the synthesis of particular metabolites is different, leading to different changes. In this study, UV-B could affect the production of MAAs, whereas osmotic stress would also induce the synthesis of MAAs.

9.4 Conclusions

As a terrestrial cyanobacterium, *N. flagelliforme* survived in arid or semiarid environment, exposed to intense solar radiation and salt environment. In the evolution of environmental conditions, MAAs play an important role in adaptive mechanism of *N. flagelliforme* for series of abiotic stresses. In this study, the results detected by spectrophotometry and HPLC show the content and compositions of MAAs have significant changes under the treatment of UV-B in the first 12 h, and the high-intensity (5 W/m^2) UV-B is more effective in inducing the synthesis of MAAs. Obvious changes also appear in *N. flagelliforme* cells treated with NaCl and NH_4Cl. The effects of 50 mM NaCl and NH_4Cl on MAAs production are significant than other concentrations. In addition, UV-B radiation and salt have different effects on the synthesis of MAAs in *N. flagelliforme* cells.

Acknowledgments This work was supported by the National Natural Science Foundation of China (No. 20806047; 20776112), China Postdoctoral Science Foundation (No. 20090450116) and Excellent Middle Aged and Young Scientist Award Foundation of Shandong Province (No. BS2011SW029).

References

1. Roleda MY, Lütz-Meindl U, Wiencke C et al (2010) Physiological, biochemical, and ultrastructural responses of the green macroalga *Urospora penicilliformis* from Arctic Spitsbergen to UV radiation. Protoplasma 243:105–116
2. Roleda MY, Wiencke C, Hanelt D et al (2007) Sensitivity of the early life stages of macroalgae from the Northern Hemisphere to ultraviolet radiation. Photochem Photobiol 83:851–862
3. Sinha RP, Hader DP (2008) UV-protectants in cyanobacteria. Plant Sci 174:278–289
4. Bandaranayake WM (1998) Mycosporines: are they nature's sunscreens? Nat Prod Rep 15:159–171

5. Rezanka T, Temina M, Tolsikov AG et al (2004) Natural microbial UV radiation filters – mycosporine-like amino acids. Folia Microbiol 49:339–352
6. Cockell CS (1998) Biological effects of high ultraviolet radiation on early Earth—a theoretical evaluation. J Theor Biol 193:717–731
7. Whitehead K, Hedges JI (2005) Photodegradation and photosensitization of mycosporine-like amino acids. J Photoch Photobio B 80:115–121
8. Conde FR, Churio MS, Previtali CM (2000) The photoprotector mechanism of mycosporine-like amino acids. Excited-state properties and photostability of porphyra-334 in aqueous solution. J Photoch Photobio B 56:139–144
9. Dunlap WC, Shick JM (1998) Ultraviolet radiation-absorbing mycosporine-like amino acids in coral reef organisms: a biochemical and environmental perspective. J Phycol 34:418–430
10. Oren A (1997) Mycosporine-like amino acids as osmotic solutes in a community of halophilic cyanobacteria. Geomicrobiol J 14:231–240
11. Pu AP, Song QR, Wang L (2005) A preliminary study of ultraviolet b radiation in the plain region of Ningxia. J Ningxia Medical College 27:297–299 (in Chinese)
12. Wang FX, Song QR (2007) Monitoring on the intensity of UVB radiation on different underlying grounds in Yinchuan. Mod Prev Med 34:4207–4208 (in Chinese)
13. Su J, Jia S, Chen X, Yu H (2008) Morphology, cell growth, and polysaccharide production of *Nostoc flagelliforme* in liquid suspension culture at different agitation rates. J Appl Phycol 20:213–217
14. Böhm GA, Pfleiderer W, Boger P et al (1995) Structure of a novel oligosaccharide-mycosporine-amino acid ultraviolet A/B sunscreen pigment from the terrestrial cyanobacterium *Nostoc commune*. J Biol Chem 270:8536–8539
15. Anne P, Ferran GP (1999) Ultraviolet and osmotic stresses induce and regulate the synthesis of mycosporines in the cyanobacterium *Chlorogloeopsis* PCC 6912. Arch Microbiol 172:187–192
16. Singh SP, Klisch M, Sinha RP et al (2010) Sulfur deficiency changes mycosporine-like amino acid (maa) composition of *Anabaena variabilis* PCC 7937: A possible role of sulfur in MAA bioconversion. Photochem Photobiol 86:862–870
17. Sinha RP, Klisch M, Helbling EW et al (2001) Induction of mycosporine-like amino acids (MAAs) in cyanobacteria by solar ultraviolet-B radiation. J Photoch Photobio B 60:129–135
18. Holzinger A, Karsten U, Lütz C et al (2006) Ultrastructure and photosynthesis in the supralittoral green macroalga *Prasiola crispa* from Spitsbergen (Norway) under UV exposure. Phycologia 45:168–177
19. Aharon O, Nina GC (2007) Mycosporines and mycosporine-like amino acids: UV protectants or multipurpose secondary metabolites? FEMS Microbiol Lett 269:1–10
20. Garcia-Pichel F, Nubel U, Muyzer G (1998) The phylogeny of unicellular, extremely halotolerant cyanobacteria. Arch Microbiol 169:469–482
21. Zavarzin GA, Gerasimenko LM, Zhilina TN (1993) Cyanobacterial communities in hypersaline lagoons of Lake Sivash. Microbio 62:645–652
22. Reed RH, Richardson DL, Warr SRC et al (1984) Carbohydrate accumulation and osmotic stress in cyanobacteria. Microbio 130:1–4

Chapter 10
Study on the Fermentation Conditions and the Application in Feather Degradation of Keratinase Produced by *Bacillus licheniformis*

Yu Li, Shuai Fan, Sheng Chen, Hao Er, Jianjie Du and Fuping Lu

Abstract The submerged fermentation medium was optimized in order to improve the keratinase activity produced by *Bacillus licheniformis* TCCC 11593. The keratinase showed maximum activity 98.0 U/mL after 48 h fermentation in 50 °C when adding 1 g/L maltose and 1.5 g/L NH_4Cl as the supplement of carbon and nitrogen sources. The optimal feather quantity was 20 g/L in fermentation. Ca^{2+} and Mn^{2+} inhibited the keratinase activity in fermentation medium, while keratinase activity was improved by adding 0.3 g/L Mg^{2+} to fermentation medium. At the same time, it was found that the complement of alkaline protease and neutral protease further improved the feather degradation in fermentation process. The total amino acid yield can reach 167.43 mg/g.

Keywords *Bacillus licheniformis* · Keratinase · Submerged fermentation · Feather degradation

10.1 Introduction

Chicken feather as the waste byproduct of commercial poultry processing plants and chicken slaughter industries is accumulating at a higher rate [1]. The accumulation of feathers can eventually lead to environmental pollution and can also be considered as a waste of feather protein [2]. Traditional ways to degrade feathers such as alkali hydrolysis and steam pressure cooking to produce feather meal may destroy amino acids and they also consume large amounts of energy [3]. Microbial keratinases mainly target the hydrolysis of highly rigid, strongly cross-linked

Y. Li · S. Fan · S. Chen · H. Er · J. Du · F. Lu (✉)
Key Laboratory of Industrial Fermentation Microbiology, Ministry of Education, National Engineering Laboratory for Industrial Enzymes, The College of Biotechnology, Tianjin University of Science and Technology, Tianjin 300457, People's Republic of China
e-mail: lfp@tust.edu.cn

T.-C. Zhang et al. (eds.), *Proceedings of the 2012 International Conference on Applied Biotechnology (ICAB 2012)*, Lecture Notes in Electrical Engineering 249,
DOI: 10.1007/978-3-642-37916-1_10, © Springer-Verlag Berlin Heidelberg 2014

structural polypeptide keratins, which are insoluble proteins, extremely resistant to degradation by common proteolytic enzymes [4]. Keratinases were found in bacteria, actinomycetes, and fungi, while keratinases from Bacillus sp., particularly *Bacillus licheniformis* (*B. licheniformis*) [5] and *Bacillus subtilis* (*B. subtilis*) [6] have been extensively studied due to their effectiveness in terms of feather degradation [7].

In our previous study, a feather degraded bacteria from chicken feces had been isolated and was identified as B. licheniformis by amplification of 16S rDNA. The bacteria was very effective in degradation of chicken feather and this appeared to be related to activity of the extracellular keratinase and disulfide reductase enzymes [8]. The keratinase showed maximum activity 24.0 U/mL after 48 h fermentation in 50 °C without optimizing the constitution of submerged fermentation medium.

So the constitution of submerged fermentation medium optimizated may improve enzyme activity of keratinase produced by *B. licheniformis* TCCC 11593. Feather keratin contains a large number disulfide bond which is hydrolyzed difficultly by general enzymes. In the study of Shohei Yamamura, the disulfide reductase has been research as disulfide bond-reducing enzyme [14]. As a consequence, alkaline protease and neutral protease were blended with fermented supernatant fluid in feather degrading process in order to investigate the potential role of disulfide reductase deeply and improve the efficiency of the feather degradation.

10.2 Materials and Methods

10.2.1 Microorganism and Inoculum

B. licheniformis TCCC 11593 used throughout this work, was isolated from chicken feces at hennery. The strain was maintained on the medium containing (g/L) yeast extract 5, peptone 10, NaCl 10, agar 20, pH 7.5.

10.2.2 Submerged Fermentation

The basal medium was prepared with the composition of (grams per liter) NaCl 0.4, K_2HPO_4 1.0 KH_2PO_4 0.4, and chicken feather 20.0 for submerged fermentation at pH 7.0. The fermentation was carried out in 250 mL Erlenmeyer flasks with addition of 2 % inoculum (10^9 CFU/mL) at 50 °C and 130 rpm for 48 h. After fermentation, the fermented broth was centrifuged at 7000 rpm for 10 min, and the supernatant was analyzed for keratinase activity.

10.2.3 Keratinase Assay

The keratinase activity was assayed with keratin (keratin powder) as a substrate with slight modification of the method previously used [9]. Keratin powder as substrate mixed with 2 mL of 50 mM Tris-HCl, pH 8.0, and 1 mL of enzyme solution (diluted 2-fold by buffer solutions) were incubated for 60 min at 50 °C with constant agitation at 130 rpm in a water bath. The reaction was terminated with 2 mL 10 % trichloroacetic acid and incubated at 4 °C for 10 min. Then, the reaction mixture was centrifuged at 12000 rpm for 10 min, and the supernatant was used to measure the absorbance at 280 nm using spectrophotometer. One unit(U/mL) of keratinolytic activity was defined as an increase of corrected absorbance of 280 nm (A280) [10] with the control for 0.01 per hour under the conditions described above.

10.2.4 Feather Degradation

To improve the proteolytic efficiency of feather meal by *B. licheniformis* TCCC 11593, feather degradation was carried out as follow: 250 mL erlenmeyer flask, containing 1 g feather meal was moistened with 9 mL of culture fluid (showed in 2.2). Each erlenmeyer flask was inoculated with *B. licheniformis* TCCC 11593 inocula or *B. licheniformis* TCCC 11593 cell-free culture filtrate. They were then incubated in relative humidity of 87 %, at 37 °C for 12 h, complemented with alkaline protease and neutral protease accordance with the mode of Fig. 10.8. Feather hydrolysis rate was determined after 48 h by the method of 2.5.

10.2.5 Free Amino Acid Determination

The free amino acid concentration was measured as described by Moore [11]. Samples (fermented product dissolved in 100 mL sterile water) 100 μL were added to 2 mL 0.1 mol/mL phosphate buffer pH 7.2, then 500 μL of these samples were mixed with 500 μL of 50 mg/mL ninhydrin. The mixture was incubated at 100 °C for 15 min followed by an ice bath to reach room temperature. Then, 5 mL of 40 % (v/v) ethanol was added to the tubes. The analysis was performed in triplicate and the absorbance at 570 nm was measured in spectrophotometer. The control was prepared simultaneously using distilled water (100 μL) instead of the sample. The standard curve was prepared with glycine.

10.2.6 Effect of Culture Condition on Keratinase Activity

Keratinase activity of *B.icheniformis* TCCC 11593 in the submerged medium containing different additional carbon sources (glucose, maltose, dextrin, bran, corn starch and sweet potato starch) at 1 g/L was investigated, and the optimal carbon source was added to the levels of 0.5–3 (g/L). The different additional nitrogen sources (yeast extract, tryptone, NH_4Cl, urea, KNO_3) were added separately to the medium at a concentration of 1 g/L, and the optimal nitrogen source was added in the range of 0.5–3 (g/L). The effect of different chicken feather concentrations 0.5–3 (g/100 mL) on the keratinase activity was also investigated. Additional minerals ($MnSO_4$, $CaCl_2$, $MgSO_4$, $FeSO_4$), each was added separately to the submerged medium at a final concentration of 0.1–0.5 M.

10.3 Results and Discussion

10.3.1 Effect of Feather Concentration on Keratinase Activity

The effect of different feather concentration on keratinase activity was shown in Fig. 10.1. The keratinase activity reached 28.8 U/mL, while the optimal feather concentration was 2 %, after fermentation for 48 h. When the feather concentration was added higher than 2 %, keratinase activity decreased. This high concentration of feather may cause substrate inhibition or repression of keratinase activity [12].

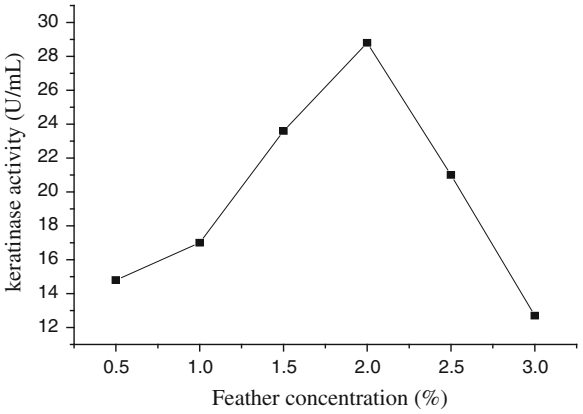

Fig. 10.1 Effect of feather concentration (%) on keratinase activity

10.3.2 Effect of Different Carbon and Nitrogen Sources on Keratinase Activity

The affection of extracellular keratinase activity by different carbon and nitrogen supplementations has been researched. After 48 h incubation, maltose as the supplemented carbon sources showed a promoting effect on keratinase activity (80.2 U/mL) (Fig. 10.2). The yield of keratinase increased up to 4.5-fold with the addition of 1.0 % maltose in the fermentation media (Fig. 10.3). Addition of simple carbohydrates like glucose partially inhibited keratinase activity by *B.licheniformis* TCCC 11593. The keratinases produced by strain *Aspergillus fumigatus fresenius* [13], *Thermoactinomyces candidus* [14], and *Stenotrophomonas*

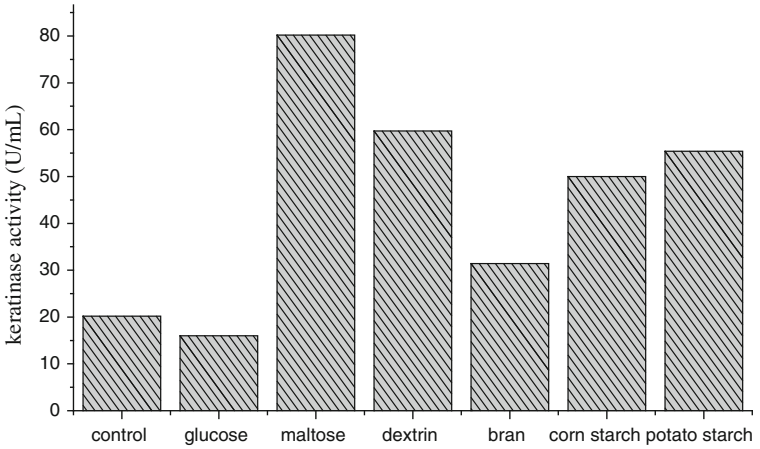

Fig. 10.2 Effect of different carbon source (1 g/L, supplement with 1 % chicken feather) on keratinase activity

Fig. 10.3 Effect of different carbon concentration on keratinase activity

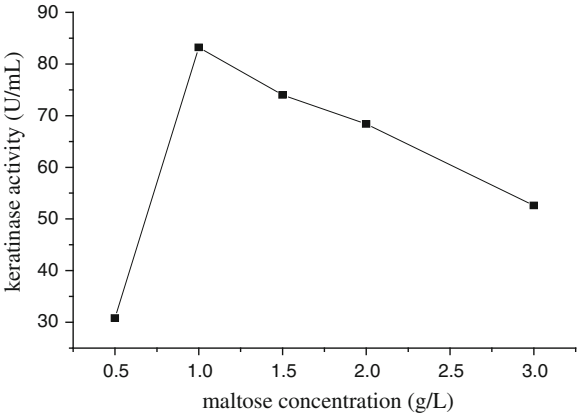

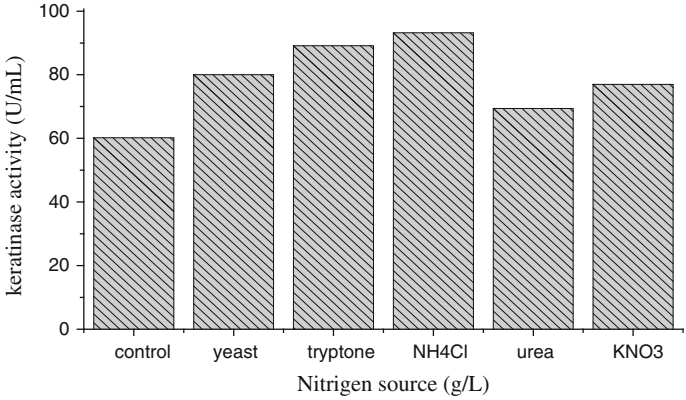

Fig. 10.4 Effect of different nitrogen source (1.5 g/L, supplement with 1 % chicken feather) on keratinase activity

Fig. 10.5 Effect of different nitrogen concentration on keratinase activity

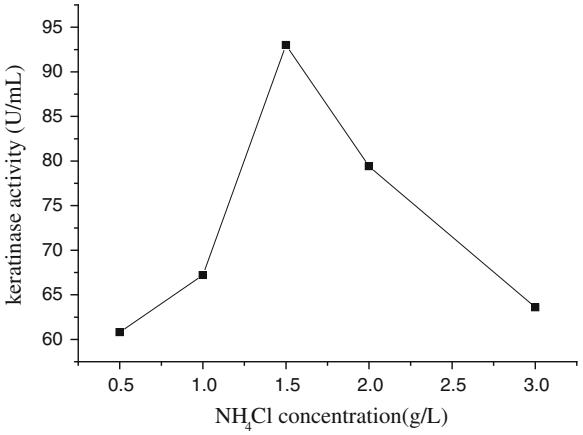

sp.D-1 [15] were also partially inhibited by glucose. The results indicated that glucose had negative effects on microbial protease activity, which may be due to catabolic repression on the enzyme activity [16].

The effects of nitrogen sources on keratinase activity varied. Among the different organic and inorganic nitrogen sources, the supplementation of NH_4Cl (1.5 %) resulted in maximal keratinase activity (93.0 U/mL) (Figs. 10.4, 10.5). This pattern was explained by Abdel-Fattah et al. [17], who suggested that the nitrogen limiting conditions might lead to an overall drop in the energy pool of the cell due to the consumption of intercellular ATP and/or GTP via the purine salvage and/or degradation pathways.

10.3.3 Effect of the Mg^{2+}, Ca^{2+}, Mn^{2+}, Fe^{2+}on Keratinase Activity

The results in Figs. 10.6 and 10.7 showed the effect of different salts on the keratinase activity. The addition of Mg^{2+} led to a marked increase in enzyme activity (98.0 ± 0.7 U/mL), while the addition of Fe^{2+}, Mn^{2+}, and Ca^{2+} brought definite inhibitions to the keratinase activity.

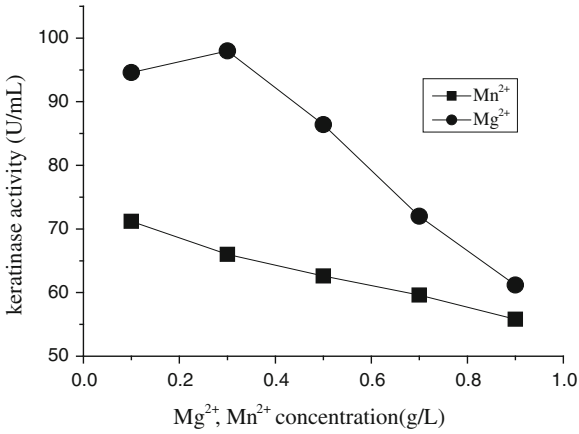

Fig. 10.6 Effect of the Mn^{2+} and Mg^{2+} concentration on keratinase activity

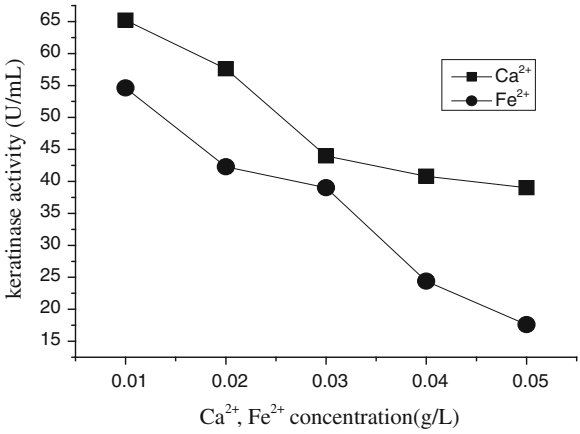

Fig. 10.7 Effect of the Ca^{2+} and Fe^{2+} concentration on keratinase activity

10.3.4 Feather Degradation in Fermentation Process

Cell-free culture filtrate did not completely degrade feather even after prolonged incubation [18]. It was verified that complete feather degradation occurred only when *B. licheniformis* TCCC 11593 cells existed in the improved medium. So it was very important to verify whether the keratinolytic enzymes could accomplish keratin degradation alone or *B. licheniformis* TCCC 11593 cells contribute to keratinolysis. The production of amino acids indicated a synergistic increase of nearly 2-fold when *B. licheniformis* TCCC 11593 inocula was inoculated in the medium (74.04 mg/g) compared with the cell-free culture filtrate alone (36.85 mg/g). The result suggested that bacterial cells played a important role in the feather degradation. The bacteria cell is superior to the cell-free culture filtrate in feather degradation because of the existence of intracellular disulfide reductase. Disulfide reductase is a cell-bound enzyme in prokaryotes [19]. Cell adherence will be important for complete feather degradation. The important role of the reduction of disulfide bonds on keratin degradation was further supported by the fact that keratin degradation by purified keratinases in vitro was only accomplished by the addition of reducing agents that help in sulfitolysis [4].

The result of Fig. 10.8 indicated that other protease lead to further degradation of keratin when the disulfide bond has been broken by disulfide reductase. Other

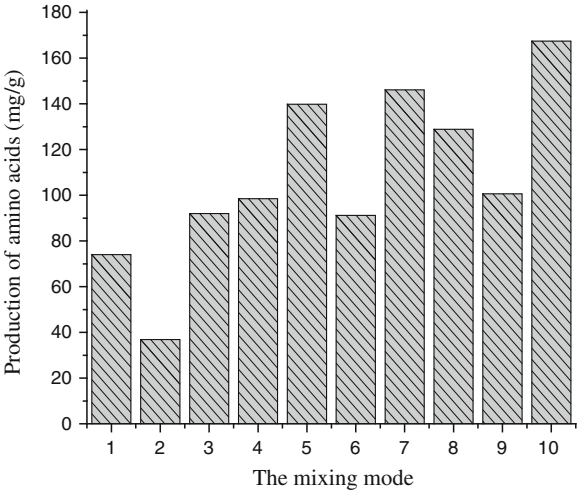

Fig. 10.8 Effect of the mixing mode on production of amino acids *1 B. licheniformis* TCCC 11593 inocula, *2 B. licheniformis* TCCC 11593 cell-free culture filtrate, *3* Alkali protease (1000 U/mL), *4* Neutral protease (1000 U/mL) *5* Inocula + Alkali protease (1000 U/mL, *6* Cell-free culture filtrate + Alkali protease (1000 U/mL), *7* Inocula + Neutral protease (1000 U/mL), *8* Cell-free culture filtrate + Neutral protease (1000 U/mL), *9* Alkali protease (1000 U/mL) + Neutral protease (1000 U/mL), *10* Inocula + Alkali protease (1000 U/mL) + Neutral protease (1000 U/mL)

researches also suggested that the keratinolytic production of the protease D-1, proteinase K, subtilisin, and trypsin were increased 50-fold, 2-fold, 17-fold, and 6-fold, respectively compared with the lack of disulfide reductase, when the disulfide reductase-like protein was added [14]. In our study, alkali protease and neutral protease combination proved a strong ability of the degradation of feather (100.66 mg/g production of amino acids,the mode 9), even higher than *B. licheniformis* TCCC 11593 alone (Fig. 10.8). So alkali protease and neutral protease were mixed with *B. licheniformis* TCCC 11593 in the process of feather fermented. It was found that the production of amino acids reached 167.43 mg/g, 2-fold more than for *B. licheniformis* TCCC 11593 alone fermentation after 60 h. In this fermentation process, the important role of *B. licheniformis* TCCC 11593 was to release disulfide reductase to break the disulfide bond of keratin. Then denatured keratin was transformed into amino acids through the further hydrolysis by alkali protease and neutral protease, which showed a strong capacity in feather degradation.

10.4 Conclusion

The *B. licheniformis* TCCC 11593 may be considered as microorganism which has a large prospect of application for overproduction of keratinase in statistically optimized medium. The feather degradation result suggested that future application of mixing alkaline protease and neutral protease in *B. licheniformis* TCCC 11593 fermentation process is very promising. The hydrolyzed feather can be used as a low cost ingredient in animal feed formulation, and can also be developed as an organic fertilizer as an eco-friendly alternative to chemical fertilizer.

Acknowledgments The authors gratefully acknowledge the support of Tianjin Municipal Science and Technology Committee (10ZCKFNC01700) and the National High Technology Research and Development Program ('863' Plan) (2013AA102106 and 2012AA021502).

References

1. Sahoo DK, Das A, Thatoi H (2012) Keratinase production and biodegradation of whole chicken feather keratin by a newly isolated bacterium under submerged fermentation. Appl Biochem Biotechnol 167(5):1040–1051
2. Onifade AA, Babatunde GM (1998) Comparison of the utilisation of palm kernel meal, brewers' dried grains and maize offal by broiler chicks. Br Poult Sci 39(2):245–250
3. Cai CG, Chen JS, Qi JJ (2008) Purification and characterization of keratinase from a new *Bacillus subtilis* strain. J Zhejiang Univ Sci B 9(9):713–720
4. Gupta R, Ramnani P (2006) Microbial keratinases and their prospective applications: an overview. Appl Microbiol Biotechnol 70(1):21–33
5. Lin X, Lee SW, Bae HD (2001) Comparison of two feather-degrading *Bacillus licheniformis* strains. Asian- austral J Anim 14(12):1769–1774

6. Macedo AJ, da Silva WOB, Gava R (2005) Novel keratinase from *Bacillus subtilis* S14 exhibiting remarkable dehairing capabilities. Appl Environ Microbiol 71(1):594–596
7. Thys RC, Lucas FS, Riffel A (2004) Characterization of a protease of a feather-degrading Microbacterium species. Lett Appl Microbiol 39(2):181–186
8. Prakash P, Jayalakshmi SK, Sreeramulu K (2010) Purification and characterization of extreme alkaline, thermostable keratinase, and keratin disulfide reductase produced by *Bacillus halodurans* PPKS-2. Appl Microbiol Biotechnol 87(2):625–633
9. Son HJ, Park HC, Kim HS (2008) Nutritional regulation of keratinolytic activity in *Bacillus pumilis*. Biotechnol Lett 30(3):461–465
10. Gradisar H, Friedrich J, Krizaj I (2005) Similarities and specificities of fungal keratinolytic proteases: comparison of keratinases of Paecilomyces marquandii and Doratomyces microsporus to some known proteases. Appl Environ Microbiol 71(7):3420–3426
11. Moore S (1968) Amino acid analysis: aqueous dimethyl sulfoxide as solvent for the ninhydrin reaction. J Biol Chem 243(23):6281–6283
12. Cortezi M, Monti R, Contiero J (2005) Temperature effect on dextransucrase production by *Leuconostoc mesenteroides* FT 045 B isolated from Alcohol and Sugar Mill Plant. Afr J Biotechnol 4(3):279–285
13. Santos RMDB, Firmino AA, de Sa CM (1996) Keratinolytic activity of *Aspergillus fumigatus* fresenius. Curr Microbiol 33(6):364–370
14. Yamamura S, Morita Y, Hasan Q (2002) Keratin degradation: a cooperative action of two enzymes from *Stenotrophomonas* sp. Biochem Biophys Res Commun 294(5):1138–1143
15. Ignatova Z, Gousterova A, Spassov G (1999) Isolation and partial characterisation of extracellular keratinase from a wool degrading thermophilic actinomycete strain *Thermoactinomyces candidus*. Can J Microbiol 45(3):217–222
16. Vidyasagar M, Prakash S, Jayalakshmi SK (2007) Optimization of culture conditions for the production of halothermophilic protease from halophilic bacterium Chromohalobacter sp TVSP101. World J Microbiol Biotechnol 23(5):655–662
17. Abdel-Fattah YR, Saeed HM, Gohar YM (2005) Improved production of *Pseudomonas aeruginosa* uricase by optimization of process parameters through statistical experimental designs. Process Biochem 40(5):1707–1714
18. Riffel A, Lucas F, Heeb P (2003) Characterization of a new keratinolytic bacterium that completely degrades native feather keratin. Arch Microbiol 179(4):258–265
19. Bockle B, Muller R (1997) Reduction of Disulfide Bonds by *Streptomyces pactum* during Growth on Chicken Feathers. Appl Environ Microbiol 63(2):790–792

Chapter 11
Hydroponic Culture of *Chamaedorea elegans*

Wuyuan Deng

Abstract Solution culture experiments were carried out to study effect of naphthylacetic acid (NAA) on formation of aquatic root system of *Chamaedorea elegans*. The influences of various nutrient solutions and different venting modes of plant root on growth and development of this hydroponic plant were also researched. The results showed that 2 mg/L NAA could increase number of roots, 0.1 mg/L NAA could speed up root formation and promote growth of root. Nutrient solution D was the most favorable culture solution for growth of *Chamaedorea elegans*, and this plant grew well when its venting mode of roots was full root length soaked in culture solution.

Keywords *Chamaedorea elegans* · Hydroponic culture · NAA · Nutrient solution · Venting mode

11.1 Introduction

Hydroponic culture of flowers is a innovative cultural model, which has changed the traditional mode of pot culture into water-cultivated model to achieve more artistic effects [1, 2]. The advantages of this method are simple, clean, and manageable [3]. *Chamaedorea elegans* was often grown as a houseplant because of its graceful shape and characteristic of being shade tolerant [4, 5]. In this paper, to provide scientific basis for water culture of *C. elegans*, we explored the hydroponics technology of *C. elegans*.

W. Deng (✉)
Experiment and Teaching Resources Management Center, Yibin University, Yibin 644007, People's Republic of China
e-mail: dengwuyuan78@163.com

T.-C. Zhang et al. (eds.), *Proceedings of the 2012 International Conference on Applied Biotechnology (ICAB 2012)*, Lecture Notes in Electrical Engineering 249,
DOI: 10.1007/978-3-642-37916-1_11, © Springer-Verlag Berlin Heidelberg 2014

11.2 Materials and Methods

11.2.1 Experiment Materials

C. elegans and special glass containers used for water culture were purchased from a local flower market in Yibin city of China.

11.2.2 Root Induction Test of Hydroponic Chamaedorea elegans

The tested trees of *C. elegans*, all of which were robust, equal in size and had graceful shape, no insect pests and plant diseases, were taken from soil and rinsed with water. Then sterilized in 1 % potassium permanganate, and all roots of them were removed. The experiment plants of above were put into some special glass containers containing aqueous solution with different naphthylacetic acid (NAA) concentrations and were fixed by a special-purpose plastics basket with mesh holes. In this experiment, five different concentrations of NAA were tested that were 0.1, 0.5, 1, 2, and 15 mg/L, respectively. Clean water (0 mg/L NAA) was used as control. There were three replicates per treatment and two sample trees of *C. elegans* per replicate (the following experiments were the same). Test temperature was 20–25 °C, the relative humidity of the atmosphere was 70–80 %. Throughout the test period, aqueous solutions of NAA were changed every 3 days before the new root appeared and every 7 days after the plants had taken new root. The experiments were halted after 63 days. The state of root system formation in the duration of experiments, including time of root formation, quantity of new roots per plant, length of roots, etc., were recorded. All experimental datas were analyzed by the statistical methods and every final value was three times repetitive average (the following experiment data processing was the same).

11.2.3 Screening Test of Nutrient Solutions

The tested trees of *C. elegans*, which were equal in size, were cleaned with water. The damage of their roots should be minimized in the operating process. These plants mentioned above were cultured in clean water for a week after sterilization to allow their roots to adapt to water training environment. Then put into the following nutrient solutions to conduct solution culture experiments. Four kinds of nutritional solution A [6], B [7], C [8], D [7] are selected in this experiment and clean water was used as control. Culture solution was stirred twice a day, morning and night, to maintain the dissolved oxygen content in the culture solution. Moisture on leaf surface was kept by sprinkling water over the plant. The

experiments were halted after 43 days and the culture solutions must be replaced weekly (Table 11.1).

11.2.4 The Effects of Different Venting Modes of Roots on Growth of Hydroponic Chamaedorea elegans

In this experiment, the nutritional solution used was nutrient solution D, three kinds of venting mode were respectively full length, 1/2 length and 1/3 length of root of *C. elegans* soaked in culture solution. The growth of plants was recorded, including the quantity of the new roots, rotten roots, new leaves, and yellow leaves. The experiments were halted after 21 days.

11.3 Results and Discussion

11.3.1 Root Induction Test

As we can know from Table 11.2, All *C. elegans* trees could take new roots when concentration range of NAA was 0–5 mg/L, the rooting rate was 100 %. However, the influences of NAA in different concentrations on formation of aquatic root system of *C. elegans* were extremely different ($F > F_{0.01}$). The mean number of new roots per plant was the most when concentration of NAA was 2 mg/L and the

Table 11.1 Formulas of different nutritional solutions (mg/L)

Composition of nutrient solution	Kinds of nutrient solutions			
	A	B	C	D
KH_2PO_4	156	200		136
$FeSO_4 \cdot 7H_2O$	27.8			
H_3BO_4	5.8			1.24
$Ca(NO_3)_2 \cdot 4H_2O$	800	1,150	945	
$MgSO_4 \cdot 7H_2O$	246	200	493	246
$(NH_4)_2SO_4$	187			
KNO_3		200	809	505
$NH_4H_2PO_4$			153	
NH_4NO_3				80
$MnSO_4 \cdot 4H_2O$				2.23
$ZnSO_4 \cdot 7H_2O$				0.864
$CaCl_2$				333
$Na_2FeEDTA$				24
$CuSO_4 \cdot 5H_2O$				0.125
$H_2MoO_4 \cdot 4H_2O$				0.117

Table 11.2 The influences of NAA in different concentrations on formation of aquatic root system of *Chamaedorea elegans*

Concentration of NAA (mg/L)	Rooting rate (%)	Number of new roots per plant (piece)	The longest root length (cm)	Mean length of roots (cm)	Time of root formation[a] (day)
0 (CK)	100	11	3.2	2.1	25
0.1	100	21	5.1	3.6	18
0.5	100	16	0.8	0.4	22
1	100	15	0.9	0.5	23
2	100	25	0.3	0.2	32
5	100	8	0.2	0.1	60

[a] The time was the duration of new roots sticking out cortex tissue

new roots were 25 pieces per tree. Both the longest root length and the mean root length were the longest and the duration of root formation was the shortest when concentration of NAA was 0.1 mg/L, they were 5.1, 3.6 cm, and 18 days, respectively. With NAA concentration increased, growth speed of root system of *C. elegans* presented downtrend basically. In a certain range of concentration, NAA could promote formation or growth of the roots, which agree with the other experiments [9], if the concentration is too big, it could inhibit the development of root system.

11.3.2 Screening Test of Nutrient Solutions

Table 11.3 shows growth of *C. elegans* was obviously better in various nutrient solutions than in clean water (CK), especially nutrient solution D could markedly promote growth or development of *C. elegans* and increases in total root length, total fresh weight and plant height were the largest. This demonstrated that various nutrient solutions of the above could promote growth or development of *C. elegans* at the different levels, this was the same as other hydroponics experiment of *Doritis pulcherrima* [10], *Cattleya hybrida* [11], and *Phalaenopsis* [12]. This could be accounted for the fact that nutrient solutions contain enough nutrient content that help plants grow [13, 14]. Moreover, there were significant difference in growth and development between different groups of nutrient solutions ($F > F_{0.01}$). This may be that the components and concentration of nutrient solution directly affected nutrient absorption and growth of plant [15], so the growth of plant cultivated in different nutrient solutions would be different [16, 17].

Table 11.3 The growth of *Chamaedorea elegans* cultivated in various nutrient solutions

Nutrient solutions	Increase in total length per plant of root system (cm)	Increase in total fresh weight per plant (g)	Increase in plant height per plant (cm)
A	29.4	1.9	1.4
B	30.6	2.1	1.8
C	32.7	3.3	2.3
D	45.9	4.2	3.2
Clean water (CK)	26.1	1.2	0.8

Table 11.4 The growth of hydroponic *Chamaedorea elegans* in different venting modes of root

Venting modes (root length soaked in culture solution)	Number of new roots per plant (piece)	Number of rotten roots per plant (piece)	Number of new leaves per plant (piece)	Number of yellow leaves per plant (piece)
Full root length	12	3	3	0
1/3 root length	6	1	1	3
1/2 root length	5	0	0	5

11.3.3 The Effects of Different Venting Modes of Roots on Growth of Hydroponic Chamaedorea elegans

It can be seen from Table 11.4, *C. elegans* in different venting modes of root differ markedly in its growth ($F > F0.05$, $F > F0.01$). The mean numbers of new roots, rotten roots ,and new leaves per plant were the largest when venting mode was full root length soaked in culture solution. *C. elegans* had the most yellow leaves under venting condition that its 1/2 root length was soaked in culture solution. This was perhaps because the deeper the roots was soaked in culture solution, the more nutrient content they absorbed, so the growth of plants was also better [18]. At the same time, the oxygen content in the deep part of culture solution is lower than in shallows and air [19], moreover; the culture solution was accessible to microbe [20], so it would cause more rotten roots when root length soaked in culture solution was longer. However, on the whole the optimum venting mode for hydroponic *C. elegans* was full root length soaked in culture solution.

11.4 Conclusion

NAA of definite concentration could promote root formation or growth of *C. elegans*, If NAA was used beyond suitable concentrations, it was shown to inhibit the root growth. *C. elegans* grew better in nutrient solution than in clean water, especially in nutrient solution D. Moreover, the optimum venting mode of roots for hydroponic *C. elegans* was full root length soaked in culture solution.

Acknowledgments The research was supported by the Science and Technology Plan Project of Sichuan Provincial Education Department (12ZB344). The author expresses her great thanks to the cell engineering lab of Yibin University for providing the experiment field.

References

1. Yin H (2002) Hydroponic technology of indoor flowers. Chin J Trop Agric 22(3):35–40 (Chinese)
2. Sun ZC, Du SY, Sun YJ et al (2011) Cultivation technique of hydroponics flowers. Jilin Agric 11:183 (Chinese)
3. Chen YH, Wu XF, Zhang DL et al (2007) Effects of different nutrition concentrations and formulas on the ornamental plants in water culture. J Cent South Univ Tech 27(6):34–37 (Chinese)
4. Li WQ, Fan L (2010) Study of hydroponic culture on *Chamaedorea elegans*. J Zhengzhou Coll An Husb Eng 30(3):10–11 (Chinese)
5. Lan WG (2010) The pathogen and control of brown-spot of *Chamaedorea elegan*. Hunan Agric Sci 13:96–98 (Chinese)
6. Bao MZ (2003) Flower cultivation science. Forestry Publishing House of China, Beijing, pp 80–81 (Chinese)
7. Wang CY, Shen J, Zhu LG et al (2007) Study on hydroponic techniques of *Aglaonema modestum* and Scindapsus aureus. Northern Hortic 5:143–144 (Chinese)
8. Zhang LG (2002) Hydroponic flower. Shanghai Scientific and Technical Publishing House, Shanghai, pp 65–66 (Chinese)
9. Wang DR, Liu XR, Chen M et al (2011) Development of aquatic-like roots of three foliage plants in hydroculture and effects of α-naphthaleneacetic acid (NAA) on rooting. Chin J Trop Crops 32(4):702–707 (Chinese)
10. Wu CH, Huang CY, Jiang BY et al (2011) Effect of nutrient solutions on the development of *Doritis pulcherrima* in water culture. J Guangdong Agric Sci 24:33–35 (Chinese)
11. Zhang YP, Qiu J, Chen JH (2009) A study of hydroponic culture on cattleya hybrida. Chin Agric Sci Bull 25(16):190–193 (Chinese)
12. Yang SH, Ji J, Wang G (2008) Effect of nutrient formulation on growth of water culture of *Phalaenopsis*. J Agric Univ Hebei 31(6):30–33 (Chinese)
13. Zhang ZX, Fang Z, Li YL (2007) Effects of different nutrient solutions on the growth and development of mimosa pudica in hydroponics. Acta Hortic Sin 34(4):1037–1040 (Chinese)
14. Luo J, Wang Y, Lin DJ et al (2007) Studies on rapid culture techniques and root adaptability of *Echinocactus grusonii* in hydroponics. Acta Hortic Sin 34(3):711–716 (Chinese)
15. Cheng YS, Shi GS, Xiang S et al (2011) Studies on nutrient solution of hydroponic hydrangea macrophylla. Acta Agric Jiangxi 23(1):74–76 (Chinese)
16. Chen YH, Wu XF, Zhang DL et al (2007) Comparative study on effects of indoor foliage plants under differ nutrition in water culture. Res Agric Modern 28(6):767–769 (Chinese)
17. Lin DJ, Luo J, Liu SZ et al (2004) A primary study on the growth of ball cactus in hydroponics. J South China Agric Univ (Nat Sci) 25(2):13–16 (Chinese)
18. Wang FL, Huang ZF, Zhou HG et al (2008) Effects of different treatments on the growth of woody flowers with water culture. J Anhui Agric Sci 36(26):11316–11318 (Chinese)
19. Li SL, Wang JH, Sun ZQ et al (2007) Effects of different depth nutrient solution on growth of lettuce. Chin Agric Sci Bull 23(8):343–345 (Chinese)
20. Chen GL, Gao XR et al (2002) Effect of partial replacement of nitrate by amino acid and urea on nitrate content of nonheading chinese cabbage and lettuce in hydroponics. Sci Agric Sin 35(2):187–191 (Chinese)

Chapter 12
Optimization of Diosgenin Production by Mixed Culture Using Response Surface Methodology

Jinxia Xie, Xing Xu and Songtao Bie

Abstract Optimization of four process parameters was attempted using Box-Behnken design for production of diosgenin by a mixed culture with *Aspergillus oryzae*, *Phanerochaete chrysosporium*, and *Aspergillus niger*. Maximum diosgenin yield of 42.89 ± 0.53 mg/g was obtained after optimization of culture conditions such as *Dioscorea zingiberensis* C.H.Wright (DZW) concentration 42.98 g/l, inoculum size 1.73 ml of spore suspension (1: 2: 3 ratio of *A. oryzae*, *P. chrysosporium*, and *A. niger*), initial pH 5.0, and cultivation time 5.27 days (127 h) and incubated at 30 °C on a rotary shaker set at 180 r/min as mixed culture.

Keywords Response surface optimization · Diosgenin · Mixed culture · *Aspergillus oryzae* · *Phanerochaete chrysosporium* · *Aspergillus niger*

12.1 Introduction

Diosgenin (CAS number 512-04-9) is an important steroidal precursor in pharmaceutical industry [1, 2] and used for the synthesis of adrenal cortex hormone, sex hormone, progestational hormone, and anabolic steroid [3, 4]. The tubers of some species of Dioscorea are important sources of diosgenin, early investigation showed that *Dioscorea zingiberensis* C.H.Wright (DZW) was one of the species containing high concentration of diosgenin [5]. DZW tubers contain 1–2 % diosgenin, 30–40 % starch, 10–15 % lignin, and 40–50 % cellulose [6, 7]. Saponin

J. Xie (✉) · X. Xu · S. Bie
Key Laboratory of Industrial Microbiology, Ministry of Education, National Engineering Laboratory for Industrial Enzymes, Tianjin Key Laboratory of Industrial Microbiology, College of Biotechnology, Tianjin University of Science and Technology, Tianjin 300457, People's Republic of China
e-mail: xiejinxia1233@163.com

T.-C. Zhang et al. (eds.), *Proceedings of the 2012 International Conference on Applied Biotechnology (ICAB 2012)*, Lecture Notes in Electrical Engineering 249,
DOI: 10.1007/978-3-642-37916-1_12, © Springer-Verlag Berlin Heidelberg 2014

is diosgenin and attachment of glucose or rhamnose to aglycone by C–O glucosidic bonds, which in plant cells are wrapped by the starch, cellulose, hemicellulose, and lignin [8]. So extraction of diosgenin needs separation of starch and others from Saponin and destroying C–O glucosidic bonds.

The conventional extraction of diosgenin from DZW tubers predominantly uses hydrochloric or sulfuric acid directly for acidic hydrolysis to decompose saponins and starch and so on [9]. As reported by the previous studies [10], the conventional acid approach could produce about 1.20 % diosgenin with high concentration of COD (about 120 g/L) in wastewater and acidic hydrolysis could generate a byproduct 25-spirosta-3, 5-dienes [11]. In addition, many cellulose and starch of DZW were conversed into sugar and discarded together with wastewater, resulting in wasting of resources. Several clean and new technological processes were reported to solve the problem about wastewater and lower yield. For instance, Qiu et al. [12] used ultrasound-assisted extraction for diosgenin. Although this technology for diosgenin production yield could achieve 2.30 %, the process was complex that included ultrasound extraction of the crude material fermented by yeast and then acidic hydrolysis, which is hardly applied in diosgenin industry.

Biotransformation approach is a well-known environmentally friendly technology due to their high selectivity and mild reaction conditions [13]. Zhang [14] applied polyethylene glycol (PEG) to modify cellulase, α-amylase and β-glycosidase were used to hydrolyze the DZW and Liu [15] screening kinds of enzymes draw a conclusion that the cellulase showed the highest efficiency of diosgenin yield. It is reported that the glucosyl residue at C-3 sugar chain of steroidal saponins hardly be hydrolyzed by some enzymes preparations such as β-glucosidase, amylase, and cellulase [16–18]. So acid hydrolysis was still used after enzyme hydrolysis to further improve diosgenin yield. In other hand, the cost of enzyme is expensive.

Microbial hydrolysis was an economic alternative [19, 20], nevertheless, the lower diosgenin yield limited its industrial development. So far, there were few references regarding an approach of microorganism, where mixed culture was used for hydrolyzing starch, lignin, and cellulose of the DZW and used for transforming saponin to diosgenin. Complex mixed cultures are widely used in biotechnology for many processes, e.g., for the production of antibiotics, enzymes, fermented food, composting, dairy fermentation, bioconversion of apple distillery, and domestic wastewater sludge [21]. Application of mixed fermentation to natural product drug discovery seems an obvious extension, but lack of reproducibility [22].

In this work, three fungi *Aspergillus oryzae*, *Phanerochaete chrysosporium*, and *Aspergillus niger* were used by mixed culture to degrade starch, lignin, and cellulose of DZW, biotransformation of saponins to diosgenin, and optimization of process parameters for the production of diosgenin by a mixed culture with these three fungi was carried out using a response surface Box-Behnken design.

12.2 Materials and Methods

12.2.1 Microorganism

P. chrysosporium (TCCC41024) was preserved in Tianjin University of Science and Technology Microbiological Culture Collection Center. *A. niger* (CICC2475) and *A. oryzae* (CICC40353) were purchased from China Center of Industrial Culture Collection (Beijing, China). These strains were stored at 4 °C on potato dextrose agar slant and subcultured routinely every 2 weeks. To prepare the inocula, spores in a 7-day-old agar slant were, respectively, suspended in 0.01 % Tween 80 solution (10^7 spores/ml), then mixed spore suspension with 1:2:3 ratios of *A. oryzae*, *P. chrysosporium*, and *A. niger.*

12.2.2 Materials and Fermentation Condition

The dried DZW tubers were supplied by Kangsheng Company, Qingyang, Gansu, China. The materials were ground by a pulverator (DJ-048 Pulverator, Beijing Huanya Tianyuan Co. Ltd., Beijing, China) and the powder was screened through a 40-mesh stainless steel sieve (0.2 cm). All culture and biotransformation experiments were performed in 250 ml Erlenmeyer flasks. Fermentation medium consisted of the powder DZW and tap water, sterilized by autoclaving for 20 min at 121 °C, inoculated mixed spore suspension, and incubated at 30 °C on a rotary shaker set at 180 r/min for diosgenin production.

12.2.3 Optimization of Culture Conditions for DZW Concentration, Inoculum Size, Initial pH, and Culture Time

Effect of DZW concentration, inoculum size, initial pH, and culture time were studied, primarily, one variable at a time (date not shown). Based on these experiments, these four independent variables were chosen for the further optimization studies for maximum yield of diosgenin using a response surface methodology (RSM). Variables were coded as −1, 0, and +1 as presented in Table 12.1, which corresponded to the lower, middle, and higher values, respectively. The software Design-Expert (Version 8.0.4, Stat-Ease Inc., Minneapolis, USA) was used for experimental design, the treatment schedule for the model is given in Table 12.2. The response value (Y) in each trial was the average of duplicates.

Table 12.1 Experimental range and levels of the four independent variables used in RSM in terms of actual and coded factors Variables Levels

Variables	Levels		
	−1	0	+1
Concentration of DZW (g/l)	33.33	50.00	66.67
Inoculation size (ml)	1.5	2.0	2.5
pH	4.5	5.0	5.5
Culture time (day)	4	5	6

Table 12.2 Experimental design used in the RSM studies of four independent variables with three center points for diosgenin yield by mixture fermentation

runs	*A* Concentration of DZW (g/l)	*B* Inoculation size (ml)	*C* pH	*D* Cultrue time (day)	Diosgenin yield (mg/g)
1	−1	−1	0	0	38.15 ± 0.53
2	1	−1	0	0	17.88 ± 0.78
3	−1	1	0	0	20.57 ± 0.67
4	1	1	0	0	25.36 ± 0.04
5	0	0	−1	−1	12.51 ± 0.23
6	0	0	1	−1	11.39 ± 0.02
7	0	0	−1	1	20.07 ± 0.34
8	0	0	1	1	18.21 ± 0.34
9	−1	0	0	−1	21.17 ± 0.78
10	1	0	0	−1	15.97 ± 0.23
11	−1	0	0	1	25.91 ± 0.21
12	1	0	0	1	19.28 ± 0.16
13	0	−1	−1	0	21.34 ± 0.19
14	0	1	−1	0	34.73 ± 0.87
15	0	−1	1	0	33.22 ± 0.41
16	0	1	1	0	10.33 ± 0.17
17	−1	0	−1	0	34.48 ± 0.90
18	1	0	−1	0	14.06 ± 0.98
19	−1	0	1	0	17.03 ± 0.37
20	1	0	1	0	23.17 ± 0.23
21	0	−1	0	−1	11.81 ± 0.49
22	0	1	0	−1	23.78 ± 0.56
23	0	−1	0	1	34.58 ± 0.13
24	0	1	0	1	18.88 ± 0.23
25	0	0	0	0	40.79 ± 0.67
26	0	0	0	0	40.07 ± 0.48
27	0	0	0	0	40.32 ± 0.14

The general equation of the second degree polynomial is as follows (12.1):

$$Y = \beta_0 + \Sigma\beta_i x_i + \Sigma\beta_{ii} x_i^2 + \Sigma\beta_{ij} x_i x_j \tag{12.1}$$

where Y is the predicted response for diosgenin yield; β_0, β_i, β_{ii}, and β_{ij} are constant regression coefficient; and x_i and x_j ($i = 1, 3$; $j = 1, 3$, $i \neq j$) represent the independent variables in the form of coded values.

12.2.4 Extraction and Analysis Diosgenin

At the end of culture, the steroidal saponins extraction was according to zhu et al. [20], the fermentation sample was centrifuged, dried at 60 °C, extracted with chloroform, and ultrasonicated for 30 min (KQ3200B ultrasonicator); centrifuged and analyzed on Agilent 1100 Multi-solvent Delivery System equipped with a Phenomsil C_{18} column, 250 × 4.6 mm (5 μm), the injection volume for all samples was 20 μl. The mobile phase column temperature of 30 °C.

$$\text{Yield of Diosgenin (mg/g)} = \frac{\text{diosgenin content(mg)}}{\text{DZW (g)}}$$

12.3 Results and Discussion

Interactive effects of the factors, concentration of DZW, inoculation size, pH, and culture time, were examined by RSM using Box-Behnken design. The actual yield of diosgenin yield (response) obtained is presented in Table 12.2. The ANOVA analysis yielded the following regression Eq. (12.2) in terms of the levels of diosgenin yield (Y) as a function of concentration of DZW (A), inoculation size (B), pH (C), and culture time (D).

$$\begin{aligned}\text{Diosgenin yield (mg/g)} = &+ 41.06 - 3.47 * A - 1.94 * B - 1.99 * C + 3.36 * D \\ &+ 6.27 * A * B + 6.64 * A * C - 0.36 * A * D \\ &- 9.07 * B * C - 6.92 * B * D - 0.18 * C * D \\ &- 8.23 * A^2 - 6.03 * B^2 - 11.04 * C^2 - 13.16 * D^2\end{aligned} \tag{12.2}$$

The subsequent analysis of variance showed aptness of the model for diosgenin production. The computed F-value of 52.00 implies significance of the model. There is only a 0.01 % chance that a model F-value this large could occur due to noise. The lack-of-fit F-value is not significant, and there is only a 6.28 % chance that a lack-of-fit F-value this large could occur due to noise. The model was found to be highly significant and occur due to noise. The lack-of-fit F-value is not sufficient to represent the actual relationship between the response and the

significant variables as indicated by the small model P value (<0.0001), large lack-of-fit P-value (0.0628), suitable coefficient of determination ($R^2 = 0.9811$), and adjusted coefficient of determination (R^2adjusted = 0.9623) from ANOVA (Table 12.3). The predicted sum of squares (PRESS) of 314.23 indicated fit of each point in this design. Signifiance of seven model terms (A, B, C, D, A^2, B^2, C^2, and D^2) and an adequate precision of 20.624 indicated low signal-to-noise ratio (Table 12.4).

Response surface contour plots graphically represented regression equations and were generally used to demonstrate relationships between the response and experimental levels of each variable in case of diosgenin yield (Fig. 12.1a–d). The points on the corners and center of the figure represent experimental design points. The point with number five in the center contour plots indicates the highest predicted value of selected variable with other variables constant at centra level.

Our results showed that the DZW concentration in the medium was the most significant single parameter which influenced diosgenin yield followed by culture time, inoculum size, and initial pH (Table 12.2). The interactions between DZW concentration and inoculum size, DZW concentration and pH, inoculum size and culture time, and that between pH and inoculum size also had significant effects.

Table 12.3 Analysis of variance for the fitted second-order polynomial model and lack of fit for diosgenin yield as per Box-Behnken design

Source	Sum of squares	df	Mean sum of squares	F-value	Prob > F	Significance
Model	2992.31	14	213.74	52.00	<0.0001	Significant
Concentration of DZW (A)	144.14	1	144.14	35.07	<0.0001	
Inoculation size (B)	45.36	1	45.36	11.04	0.0050	
pH (C)	47.36	1	47.36	11.52	0.0044	
Cultrue time (D)	135.34	1	135.34	32.93	<0.0001	
AB	157.00	1	157.00	38.20	<0.0001	
AC	176.36	1	176.36	42.91	<0.0001	
AD	0.51	1	0.51	0.12	0.7296	
BC	329.06	1	329.06	80.06	<0.0001	
BD	191.41	1	191.41	46.57	<0.0001	
CD	0.14	1	0.14	0.033	0.8578	
A^2	439.30	1	439.30	106.88	<0.0001	
B^2	235.82	1	235.82	57.38	<0.0001	
C^2	790.70	1	790.70	192.38	<0.0001	
D^2	1123.94	1	1123.94	273.45	<0.0001	
Residual	57.54	14	4.11			
Lack of Fit	53.44	10	5.34	5.21	0.0628	Not significant
Pure Error	4.10	4	1.03			
Cor Total	3049.85	28				

Table 12.4 Analysis of variance (ANOVA) Table for response-surface quadratic model

Parameter	Value
Standard deviation	2.03
Mean	25.14
R^2	0.9811
Adjusted R^2	0.9623
Predicted R^2	0.8970
F-value	52.00
PRESS	314.23
Adequate precision	20.624

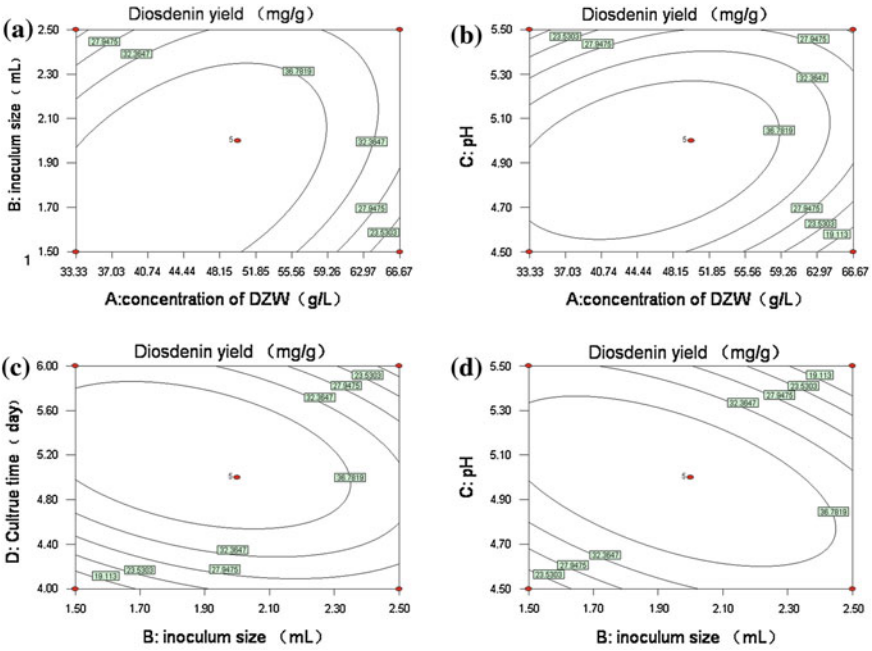

Fig. 12.1 **a** Response surface contour plots showing effect of concentration of DZW and inoculation size on diosgenin yield in mixed culture with other variables constant at centra level. **b** Response surface contour plots showing effect of concentration of DZW and pH on diosgenin yield in mixed culture with other variables constant at centra level. **c** Response surface contour plots showing effect of inoculum size and culture time on diosgenin yield in mixed culture with other variables constant at centra level. **d** Response surface contour plots showing effect of inoculum size and pH on diosgenin yield in mixed culture with other variables constant at centra level

The results presented in Fig. 12.1 indicated that the DZW concentration influenced diosgenin yield independent of the inoculum size. A 50 g/l concentration of DZW was selected as appropriate level since any further increase in concentration resulted in an undesirable increase of viscosity of the medium,

causing negative effect of the growth of fungi and decreasing diosgenin yield per gram of the DZW. Higher concentration of DZW always necessitated the requirement of a higher inoculum size, while at lower levels of DZW concentration, the yield increased initially with increase in inoculum size and then decreased. When there is lesser DZW in the medium, the addition of more inoculum probably result in a competition, with the result that growth and productivities might be affected which could be the reason for this observation [23]. The effect of pH and concentration of DZW on diosgenin yield, and the effect of pH and inoculum size on diosgenin yield were presented in Fig. 12.1b and d. Diosgenin yields increased with increasing pH up to a value of 5.0 pH influenced enzyme activity which play leading role for hydrolysis saponin. The appropriate pH of cellulase [24], glucoamylase [17], and β-glycosidase [25] is about 5. The yields of diosgenin were determined to be maximum at culture time of 5 days, no increase beyond culture time (Fig. 12.1c).

Analysis of response-surface curves and contour plots indicated optimum levels of the variables necessary to achieve better results. The results predicted by Box-Behnken design showed that a combination of concentration of DZW 42.98 g/l, inoculation size 1.73 ml, pH 5.0, and cultivation time 5.27 days (127 h), the diosgenin yield was 42.77 mg/g. A repeat fermentation of DZW for highest production of diosgenin by mixed culture under optimal conditions was carried out for verification of the optimization. Maximum diosgenin production was 42.89 ± 0.53 mg/g closely agree with the predicted value. The final diosgenin yield of optimization process increased by 61.18 % compared to the acid hydrolysis of DZW (26.61 ± 0.78 mg/g).

12.4 Conclusion

We report a study involving *A. oryzae*, *P. chrysosporium*, and *A. niger* for the production of diosgenin from DZW by mixed culture. Response-surface methodology was adopted to optimize the variables and to study their influence on diosgenin yield. The results predicted by Box-Behnken design showed that a combination of concentration of DZW 42.98 g/l, inoculation size 1.73 ml, pH 5.0, and cultivation time 5.27 days (127 h), which would yield a maximum yield of 42.77 mg/g diosgenin. Evaluation experiments carried out to verify the predictions revealed that three fungi yield 42.89 ± 0.53 mg/g closely agree with the predicted value.

Acknowledgments This work was financially supported by the Tianjin Science and Technology Support Plan Project (10ZCKFSH0060) and the Natural Science Foundation of China (No. 20906071).

References

1. Fernandes P, Cruz A, Angelova B et al (2003) Microbial conversion of steroids compounds: recent developments. Enzym Microb Technol 32:688–705
2. Saunders R, Cheetham PSJ, Hardman R (1986) Microbial transformation of crude fenugreek steroids. Enzym Microb Technol 8:549–555
3. Huang W, Zhao HZ, Ni JR et al (2008) The best utilization of *D. zingiberensis C.H. Wright* by an eco-friendly process. Bioresour Technol 99:7407–7411
4. Zhang CX, Wang YX, Yang ZH (2006) Chlorine emission and dechlorination in co-firing coal and the residue from hydrochloric acid hydrolysis of *Discorea zingiberensis*. Fuel 85:2034–2040
5. Ding Z, Zhou L, Wang Y et al (1981) Factors influencing diosgenin content of *Dioscorea zingiberensis*. Chin Tradit Herb Drugs 12:34–35
6. Li MX, Hu SB, Wang YJ et al (2010) Optimizated conditions of acid-microorganism-enzyme co-degradation to process residue of *Dioscorea zingiberensis* saponin production. Acta Agric Boreali-Occidentalis Sinica 19:196–201
7. Zhu YL, Ni JR, Huang W (2010) Process optimization for the production of diosgenin with *Trichoderma reesei*. Bioprocess Biosyst Eng 33:647–655
8. Adham NZ, Zaki RA, Naim N (2009) Microbial transformation of diosgenin and its precursor furostanol glycosides. World J Microbiol Biotechnol 25:481–487
9. Cheng P, Zhao HZ, Zhao B (2009) Pilot treatment of wastewater from *Dioscorea zingiberensis C.H. Wright* production by anaerobic digestion combined with a biological aerated filter. Bioresour Technol 100:2918–2925
10. He XJ, Liu B, Wang GH (2006) Microbial metabolism of methyl protodioscin by *Aspergillus niger* culture—a new androstenedione producing way from steroid. J Steroid Biochem Mole Biol 100:87–94
11. Peng Y, Yang ZH, Wang YX et al (2011) Pathways for the steroidal saponins conversion to diosgenin during acid hydrolysis of *Dioscorea zingiberensis C.H.Wright*. Chem Eng Res Des 89:2620–2625
12. Qi LL, Hai NB, Huang W (2011) Ultrasonic and fermented pretreatment technology for diosgenin production from *Diosorea zingiberensis C.H.Wright*. Chem Eng Res Des 89:239–247
13. Wendy AL (2000) Biotransformations in organic synthesis. Bioresour Technol 74:49–62
14. Yq Zhang, Tang L, An X et al (2009) Modification of cellulase and its application to extraction of diosgenin from *Dioscorea zingiberensis C.H. Wright*. Biochem Eng J 47:80–86
15. Liu W, Huang W, Sun WL et al (2006) Production of diosgenin from yellow ginger (*Dioscorea zingiberensis C.H.Wright*) saponins by commercial cellulase. World J Micro Biotechnol 26:1171–1180
16. Ma BP, Feng B, Huang HZ et al (2010) Biotransformation of Chinese herbs and their ingredients. TCM Materia Medica 12:150–154
17. Feng B, Hu W, Ma BP et al (2007) Purification, characterization, and substrate specificity of a glucoamylase with steroidal saponin-rhamnosidase activity from *Curvularia lunata*. Appl Microbiol Biotechnol 76:1329–1338
18. Feng B, Huang HZ, Zhou WB et al (2010) Substrate specificity, purification and identification of a novel pectinase with the specificity of hydrolyzing the α-1,4-glycosyl residue in steroidal saponin. Process Biochem 45:1383–1392
19. Dong YS, Teng H, Qi SS (2010) Pathways and kinetics analysis of biotransformation of *Dioscorea zingiberensis* by *Aspergillus oryzae*. Biochem Eng J 52:123–130
20. Liu L, Dong YS, Qi SS et al (2010) Biotransformation of steriodal saponins in *Dioscorea zingiberensis C. H. Wright* to diosgenin by Trichoderma harzianum. Appl Microbiol Biotechnol 85:933–940

21. Alam MZ, Fakhru'l-Razi SA, Abd-Aziz A (2001) Bioconversion of wastewater sludge by immobilized microbial treatment. In: Proceedings of the international water association (IWA) conference on water and waste water management for developing countries, Kauala Lampur, Malaysia, PP 344–353
22. Robin K, Pettit (2009) Mixed fermentation for natural product drug discovery. Appl Microbiol Biotechnol 83:19–25
23. Rojan P, Rajeev K, Sukumaran K et al (2007) Statistical optimization of simultaneous saccharification and l(+)-lactic acid fermentation from cassava bagasse using mixed culture of *lactobacilli* by response surface methodology. Biochem Eng J 36:262–267
24. Percival Zhang YH, Michael EH, Jonathan RM (2006) Outlook for cellulase improvement: screening and selection strategies. Biotechnol Adv 24:452–481
25. Lei J, Niu H, Li TH et al (2012) A novel β-glucosidase from *Aspergillus fumigates* releases diosgenin from spirostanosides of *Dioscorea zingiberensis C.H. Wright* (DZW). World J Microbiol Biotechnol 28:1309–1314

Chapter 13
Effect of *LEU*2 Gene Deletion on Higher Alcohols Production of High Adjunct Beer

Yanwen Liu, Jian Dong, Yefu Chen, Mingyue Wu, Xiaopei Peng and Dongguang Xiao

Abstract With the increase of the proportion of beer adjunct, the concentration of higher alcohols in the final product is high, resulting to a heavier beer flavor. In our previous work, we constructed a *LEU*2-deleted strain *S*6-2 to reduce the higher alcohol production. This study focuses to further reduce the production of higher alcohols, especially isoamyl alcohol, in high adjunct beer via disrupting a second copy of *LEU*2 gene in the host strain *S*6-2. We constructed a recombined plasmid vector pUC-LBKA, from which the LA-KanMX-LB cassette was cloned through PCR amplification. The cassette was subsequently transformed into *S*6-2, creating the mutant strain *S*6-3 with disruptions of two *LEU*2 gene copies. Finally, we examined the β-isopropylmalate dehydrogenase (β-IPM) activity and the production of higher alcohol. Our results indicate that *LEU*2 deletion can significantly reduce the β-IPM activity as well as the total higher alcohol production in high adjunct beer.

Keywords β-isopropylmalate dehydrogenase · Gene disruption · High adjunct beer · Higher alcohols · *LEU*2 gene

13.1 Introduction

With the rapid development of beer industry in recent years, competitions among beer enterprise in beer quality, price, and market were intense increasingly. Therefore, how to utilize the superiority of agricultural resources reasonably, increase the ratio of auxiliary raw materials, and reduce the dosage of malt have attracted more and more attention of researchers. Using rice as raw materials, not

Y. Liu · J. Dong · Y. Chen · M. Wu · X. Peng · D. Xiao (✉)
Key Laboratory of Industrial Fermentation Microbiology, Ministry of Education; Tianjin Industrial Microbiology Key Lab, College of Biotechnology, Tianjin University of Science and Technology, Tianjin 300457, People's Republic of China
e-mail: xdg@tust.edu.cn

T.-C. Zhang et al. (eds.), *Proceedings of the 2012 International Conference on Applied Biotechnology (ICAB 2012)*, Lecture Notes in Electrical Engineering 249,
DOI: 10.1007/978-3-642-37916-1_13, © Springer-Verlag Berlin Heidelberg 2014

only the brewed beer pale in color, pure in taste, a typical light flavor beer was obtained. However, the low amount of malt results in a series of problems, such as the shortage of nitrogen source, filter difficulties, high content of higher alcohols etc.

During beer fermentation, *Saccharomyces cerevisiae* produces a range of minor but sensorially important volatile metabolites that gives beer its vinous characters [1]. The primary volatile metabolites produced by yeast include esters, higher alcohols, and fatty acids [2]. In beer fermentation, the total content of higher alcohols, which are important compounds for beer flavor, is usually controlled in the range of 50–90 mg/L. Therefore, regulating the biosynthetic pathway of higher alcohols through genomic regulation of the related genes is an effective manner to control the higher alcohol production of beer.

The higher alcohols are formed via the Ehrlich pathway [3] or anabolically via the biosynthetic route from the carbon source [4]. In the Ehrlich pathway, the branched-chain amino acids are converted to their corresponding α-keto acids by transamination, and then processed into higher alcohols by decarboxylation and reduction [5]. In the third step of the biosynthesis of leucine, the enzyme *β*-isopropylmalate dehydrogenase, which is encoded by the *LEU*2 gene in yeasts [6], is responsible for dehydrogenation and decarboxylation of *β*-isopropylmalate leading to the formation of *a*-ketoisocaproate [7]. The *S. cerevisiae LEU2* gene has been widely used as a transformation marker and its regulation has been well studied [8, 9]. Such leucine synthesis capacity is one of the obstacles to decrease the productivity of higher alcohols especially isoamyl alcohol. Numerous recent researches have focused on how to block the synthesis of leucine. It is reported that deletion of *BAT*2 gene could greatly reduce the production of higher alcohols, especially the content of isoamyl alcohol [10]. However, there is still no research on the influence of the *LEU*2 gene on beer quality parameters especially higher alcohols.

In this study, we constructed a recombined plasmid vector pUC-LBKA to disrupt a second copy of *LEU*2 gene in the host strain *S*6-2, in which one copy of *LEU*2 was deleted from the host strain *S*6 in our previous work. We investigated the *β*-IPM activities and the higher alcohols production of strains *S*6, *S*6-2, *S*6-3. Our data proved a positive effect of *LEU*2 disruption in reducing the content of high alcohols.

13.2 Materials and Methods

13.2.1 Strains, Plasmids, Reagents, and Cultivation Conditions

The relevant genotypes of all strains and plasmids used in this study are listed in Table 13.1. The host industrial Brewer's yeast *S*6 was obtained from the Yeast Collection Center of the Tianjin Key Laboratory of Industrial Microbiology.

Table 13.1 Strains and plasmids used in this study

Strain or plasmid	Relevant characteristic	Reference or source
Strains		
Escherichia coli DH5a	supE44ΔlacU169(φ80lacZΔM15)hsdR17recAl endAl gyrA96 thi-1 relA	Stratagene
S6	Wild-type industrial brewer's yeast	This study
S6-2	*LEU2*(n−1)/*leu2*Δ::loxP	This study
S6-3	*LEU2*(n−2)/*leu2*Δ::loxP/*leu2*Δ::loxP-KanMX-loxP	This study
Plasmids		
pUC19	Ap^r, cloning vector	Invitrogen
pUG6	*E. coli*/*S. cerevisiae* shuttle vector, containing Amp+, loxP-kanMX-loxP disruption cassette	Güldner et al. 2002
pUC-BKA	Apr, Kan^r containing loxP-kanMX-loxP gene expression cassette	This study

Tianjin University of Science and Technology, China. Antibiotic G418 and ampicillin (Amp) were bought from Promega (Shanghai, China). dNTP, Taq polymerase, restriction enzymes, T4 DNA ligase were purchased from Takara Biotechnology Co., LTD (DaLian, China).

Escherichia coli strain was grown at 37 °C in Luria–Bertani brothand supplemented with 100 mg/L ampicillin. Yeast strain was grown at 28 °C in YEPD medium. 800 mg/L G418 was added in YEPD plate for the selection of Geneticin (G418) resistance after yeast transformation.

13.2.2 Recombinant DNA and Plasmids Construction

All the primers used for the construction were listed in Table 13.2. A 287 bp *LEU2* upstream fragment LA with restriction site *Eco*R I and *Bam*H I was amplified by PCR with LA-U and LA-D primers. Meanwhile, a 510 bp *LEU2* downstream fragment LB with restriction site *Bam*H I and Hind III was amplified with LB-U and LB-D primers. After the PCR products were obtained, LA and LB fragments were cloned into pUC19 successively to construct plasmid pUC-LBA. A 1631 bp KanMX fragment containing G418 resistance obtained from pUG6 plasmid with KU and KD primers was finally inserted into the *Bam*H I site of pUC-LBA to generate plasmid pUC-LBKA.

13.2.3 Yeast Transformation Strategy and PCR Identification

Generally, a majority of industrial brewer's yeast strains are polyploidy, at present the genetic background of host strain S6 was not clear. LA -KanMX -LB disruption cassettes were cloned from pUC-LBKA by PCR and transformed into

Table 13.2 Oligonucleotide primers used in PCR amplification

Primers	Sequence (5′ → 3′)	Restriction site
For plasmid construction		
LA-U	CCGGAATTCAATTGGTTGTTTGGCCGA	*Eco*R I
LA-D	CGCGGATCCATTTAGTCATGAACGCTT	*Bam*H I
LB-U	CGCGGATCCATAATAGAAACGACACGA	*Bam*H I
LB-D	CCCAAGCTTAAGGATGATGCATTAGCC	*Hin*d III
KU	CGCGGATCCCAGCTGAAGCTTCGTACGC	*Bam*H I
KD	CGCGGATCCGCATAGGCCACTAGTGGATCTG	*Bam*H I
For PCR verification		
L-A-S	TACAGAAGCAGAAATACACGCAGTC	–
L-K–S	AAGAAGAACCTCAGTGGCAAATCCT	–
L-K-X	ATGCGAGTGATTTTGATGACGAGC	–
L-B-X	TACGGTTGGGAAACAAATACTGCTG	–

S6-2 mutants by LiAC/SS Carrier DNA/PEG method [11]. Primers L-A-S and L-B-X used for transformation validation are outside the ORF of *LEU2* gene, L-K-S, and L-K-X are positioned in the TEF promoter for KanMX gene. The electrophoretic diagram for PCR identification was shown in Fig. 13.1. The method of Cha et al. [12] was adopted to research the genetic stability of the mutant strain.

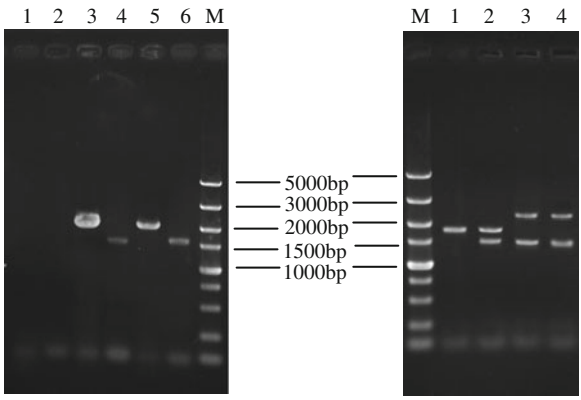

Fig. 13.1 PCR analysis of yeast recombinants and their hosts. **a** DNA templates: M, maker DL5000; lane *1*, lane *3*, and lane *5*, PCR product from host strain *S*6 and two transformations *S*6–3*a*, *S*6–3*b* with primer pair L-A-S and L-K-S; lane *2*, lane *4*, and lane *6*, PCR product from host strain *S*6 and two transformations *S*6–3*a*, *S*6–3*b* with primer pair L-K-X and L-B-X. **b** PCR verifications of deletion the second *LEU*2 allele: M, maker DL5000; lane *1*, lane *2*, lane *3* and lane *4*, PCR product from *S*6, *S*6–2, *S*6–3*a*, and *S*6–3*b* with primer pair LA-U and LB-D

13.2.4 β-isopropylmalate dehydrogenase Activity

Extraction of β-IPM was performed by high-pressure homogenization, and the activity of β-IPM used the assayed method described by Sarah et al. [13]. One unit of β-IPM activity was defined as the amount of enzyme that catalyzes the formation of 1 micromole of NADH per minute. Protein concentration was determined with a protein assay kit (Bio-Rad Laboratories).

13.2.5 Fermentation Test

The use of rice as an adjunct to barely malt was at a level of 60 %. The specific saccharification process was shown as below.

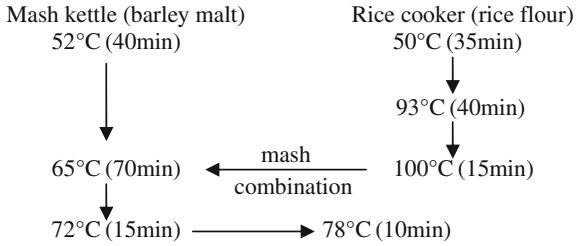

The pitching rate was 2×10^7 viable cells/mL, all fermentations were carried out in duplicate, in 300 mL coke bottle, containing 200 mL sterile 12°P wort. The fermentations were performed at 10 °C for 10 days. Higher alcohols and esters were determined by headspace gas chromatography.

13.3 Results and Discussion

13.3.1 Construction of Recombinant Plasmid Vector and LEU2 Gene Disruption

The LA-KanMX-LB deletion cassette with homologous regions for target gene was amplified by PCR form pUC-LBKA to delete the *LEU*2 gene encoding β-IPM enzyme, and transformed into *S*6-2 mutants in which one of the copies of *LEU*2 gene was disrupted using lithium acetate method. Transformants with G418 resistant were selected on YEPD plates with 800 μg/mL G418, according to the gene sequences which located at two ends of the FLP recognition target, two primer pairs L-A-S/L-K-S and L-K-X/L-B-X were designed to verify the correct integration of the cassette into *S.cerevisiae S6-2* by PCR diagnostic. As expected,

1700 bp and 2100 bp gene segments were amplified by primer pairs L-A-S/L-K-S and L-K-X/L-B-X, respectively (Fig. 13.1). The results showed that the LA-KanMX-LB deletion cassette had transformed into *S6-2* accurately, we named the mutants *S*6-3.

13.3.2 Determination of the Activity of β-IPM

In *S. cerevisiae*, leucine is biosynthesized by the actions of four enzymes, *β*-IPM encoded by *LEU*2 gene is active in the third step of the biosynthesis of leucine [14]. The purpose of this research was to study the effect of *LEU*2 gene disruption on the product of higher alcohols, the change of *β*-IPM activity indicate the synthesis ability of leucine. Chen [15] has shown that the Ehrlich pathway contributed 85 % to the formation of its corresponding higher alcohols in the case of leucine. Meanwhile, isoamyl alcohol is reported to be the most quantitatively significant flavor compound in the higher alcohol groups [16]. The purpose of this research was to study the effect of *LEU*2 gene disruption on the production of higher alcohols. Therefore, it is necessary to further study the effect of *LEU*2 gene disruption on the *β*-IPM activity.

The production of NADH at 340 nm was equivalent to the *β*-IPM activity [17]. We determined the activity of *β*-IPM crude extract as described in materials and methods. Fig 13.2 shows the activities of the tested strains *S*6, *S*6-2, and *S*6-3. It is clear that the curve of activity growth of *β*-IPM was flat in earlier stage. However, at the time of 10 min, the activity of *S*6 had a spike, the activity of *S*6-2 was distinctly increased, and the *β*-IPM activity of *S*6-3 was no significant variation. The results showed that the *β*-IPM activity of recombinant strain *S*6-3 with two copies of *LEU*2 gene disruption have a great degree reduction by 98 % than *S*6, and 70.7 % than *S*6-2 which only one copy of *LEU*2 gene was disrupted.

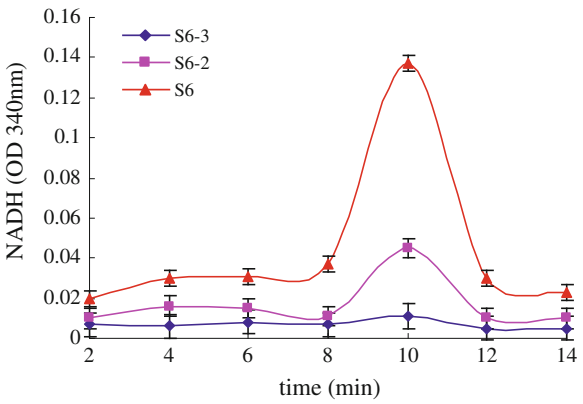

Fig. 13.2 The comparison of *β*-IPM activity between *S*6, *S*6-2 and *S*6-3

13.3.3 *Effect of* LEU2 *disruption on the characteristics of beer fermentation*

In order to study the effect of *LEU*2 disruption on the characteristics of beer fermentation, the growth curve of three strains *S*6-3, *S*6-2, and *S*6 were assessed and compared first. As expected, we did not obtain any significant distinctions between the *LEU*2-deleted strain and the host strains in the growth tendency, meaning that the disruption of *LEU*2 gene had no effect on yeast growth. Moreover, we also examined the fermentation rate. Similarly, our data did not display any obvious distinctions between the *LEU*2-deleted strain and the host strains. Sugar reduction tendency indicated that the metabolism of yeast strains was also normal and the fermentation rate almost the same during fermentation. At the end of main fermentation, the beer physiochemical indexes were detected. The results showed that indexes such as apparent degree of fermentation, alcohols, diacetyl, pH, total acid, etc. were normal (data not shown). Esters, play an important part in the beer flavor and aroma, are the most relevant family of compounds produced by yeast [18]. Headspace gas chromatography analysis of ethyl acetate and isoamyl acetate proved that the deletion of *LEU*2 had no affect on their production (data not shown).

13.3.4 *Determination of Higher Alcohols Production During Beer Fermentation*

Barley malt was normally used in traditional beer brewing, rice is widely used as raw materials in beer brewing and the addition generally more than 50 %, sometimes 30 % rice as adjunct was added [19]. In order to reduce the cost of brewing materials, 60 % rice was used in this study. Compared the wort physiochemical indexes with normal beer, a great majority of indexes are relatively similar except that the α-amino nitrogen and total nitrogen were lower, therefore protease and amylase were added. Furthermore, the brewed beer with 60 % rice as adjunct is not only pale in color, pure in taste, durable fine and smooth in foam, but also had a typical style of light beer.

Higher alcohols are the main byproducts in beer brewing, as well as the major industrial interest because of their contribution to the flavor and aroma of beer [20, 21]. An increase in higher alcohols concentration results in a dry and aroma less beer character [22]. In order to study the influence of *LEU*2 disruption on the production of higher alcohols especially isoamyl alcohol, the content of higher alcohols was determined by headspace gas chromatography. As the data shown in Table 13.3, both the n-propyl alcohol and isobutyl alcohol levels of *S6-3* after fermentation were similar to that of *S*6-2 and *S*6, indicating that *LEU*2 gene's disruption did not affect them. The isoamyl alcohol content of *S*6-3, *S*6-2, and *S*6 were 60.1, 81.0, 91.5 mg/L, respectively. Compared to *S*6-2 and *S*6, the content of

Table 13.3 Higher alcohols production of *S*6, *S*6-2 and *S*6-3

Yeast strains (mg/L)	*S*6	*S*6-2	*S*6-3
n-propyl alcohol	12.6 ± 0.1	11.7 ± 0.2	11.2 ± 0.2
Isobutyl alcohol	22.7 ± 0.4	23.8 ± 0.5	21.0 ± 0.3
Isoamyl alcohol	91.5 ± 1.9	81.0 ± 2.4	60.1 ± 3.2
Total higher alcohols	126.8 ± 2.4	116.5 ± 3.1	92.3 ± 3.7

isoamyl alcohol decreased 25.8 and 34.3 %, respectively. The total higher alcohols were 92.3, 116.5, 126.8 mg/L, respectively. Compared to *S*6-2 and *S*6, the content of total higher alcohols decreased 20.8 % and 27.2 %, respectively. The results showed that the disruption of the *LEU*2 gene leaded to the reduction in the concentration of higher alcohols especially isoamyl alcohol. Interesting that the total higher alcohols of *S*6-3 with two copies *LEU*2 disrupted significantly lower than *S*6-2 with one copy was disrupted.

13.4 Conclusion

The enzyme β-IPM, encoded by *LEU*2 gene, plays an important part in the third step of the biosynthesis of leucine, and then the amino acid was converted to isoamyl alcohol by transamination and decarboxylation. To study the effect of *LEU*2 gene disruption on the production of higher alcohols especial isoamyl alcohol, industrial brewer's yeast strain *S*6-3 was constructed in this study, in which two copies of *LEU*2 gene encoding the enzyme β-IPM were disrupted. Compared to *S*6-2, in which one copy of *LEU2* was disrupted, as well as the host strain *S*6, the β-IPM activity of *S*6-3 displays a significant reduction by 70.7 and 98 %, respectively. Total higher alcohols and isoamyl alcohol of *S*6-3 were decreased by 25.8 and 34.3 %, respectively compared to *S*6. Our data demonstrated that *LEU*2 gene disruption can effectively reduce the production of higher alcohols especial isoamyl alcohol in high materials beer brewing process.

Acknowledgments This work was financially supported by the program of National High Technology Research and Development Program of China (863 Program) (Grant No. SS2012AA023408), the Cheung Kong Scholars and Innovative Research Team Program in University of Ministry of Education, China (Grant No. IRT1166), and Application Base and Frontier Technology Project of Tianjin, China (Grant No. 09JCZDJC17900).

References

1. Swiegers JH, Bartowsky EJ, Henschke PA, Pretorius IS (2005) Yeast and bacterial modulation of wine aroma and flavour. Aust J Grape Wine Res 11:139–173
2. Lambrechts MG, Pretorius IS (2000) Yeast and its importance to wine aroma. S Afr J Enol Vitic 21:97–129

3. Ehrlich F (1904) Uber das natürliche isomere des leucins. Ber Dtsch Chem Ges 37:1809–1840
4. Hammond JRM (1993) Brewer's yeasts. The yeasts, vol 5. New York, 7–67
5. Derrick S, Large PJ (1993) Activities of the enzymes of the Ehrlich pathway and formation of branched-chain alcohols in *Saccharomyces cerevisiae* and *Candida utilis* grown in continuous culture on valine or ammonium as sole nitrogen source. J Gen Microbiol 139:2783–2792
6. Ronald JM, Bergkamp (1991) Cloning and disruption of the *LEU*2 gene of Kluyveromyces marxianus CBS 6556. Yeast 7:963–970
7. Hsu YP, Kohlhaw GB (1980) Leucine biosynthesis in *Saccharomyces cerevisiae*. Purification and characterization of β-isopropylmalate dehydrogenase. J Biol Chem 255:7255–7260
8. Hiep TT, Noskov VN, Pavlov YI (1993) Transformation in the methylotrophic yeast *Pichia methanolica* utilizing homologous *ADE1* and heterologous *ADE2* and *LEU2* genes as genetic markers. Yeast 9:1189–1197
9. Kimura H, Matamura S, Suzuki M et al (1995) Sequencing of the β-isopropylmalate dehydrogenase gene (*LEU2*) from *Acremonium chrysogenum* and its application to heterologous gene expression. J Ferment Bioeng 80:534–540
10. Yoshimoto H, Fukushige T, Yonezawa T et al (2002) Genetic and physiological analysis of branched-chain alcohols and isoamyl acetate production in *Saccharomyces cerevisiae*. Appl Microbiol Biotechnol 59:501–508
11. Daniel GR, Woods RA (2002) Transformation of yeast by lithium acetate/single-stranded carrier DNA/polyethylene glycol method. Methods Enzymol 350:87–96
12. Cha HJ, Chae HJ, Choi SS et al (2000) Production and secretion patterns of cloned glucoamylase in plasmid-harboring and chromosome-integrated recombinant yeasts employing an *SUC2* promoter. Appl Biochem Biotechnol 87:81–93
13. Sarah J, Parsons RO, Burns (1969) Purification and properties of β-isopropylmalate dehydrogenase. J Biol Chem 244:996–1003
14. Andreadis A, Hsu YP, Hermodson M et al (1984) Yeast *LEU2* Repression of mRNA levels by leucine and Primary structure of the gene Product. Biol Chem 259:8059–8062
15. Chen EC-H (1977) The relative contribution of Ehrlich and biosynthetic pathways to the formation of fusel alcohols. J Am Soc Brew Chem 36:39–43
16. Guymon JF, Ingraham JL (1961) The formation of n-propyl alcohol by *Saccharomyces cerevisiae*. Arch Biochem Biophys 95:163–168
17. Parsons SJ, Burns RO (1970) β-Isopropylmalate dehydrogenase. Methods Enzymol 17A:793–799
18. Lambrechts MG, Pretorius IS (2000) Yeast and its importance to wine aroma. S Afr J Enol Vitic 21:97–129
19. Ting-deng Chen, Ming-hua Ye (2002) Study on the technology of high ratio rice as adjunct in brewing. Food Sci Technol 11:51–54
20. Meilgaard M (1975) Flavor chemistry of beer: Part II: Flavor and threshold of 239 aroma volatiles. MBAA Tech Quart 12:151–168
21. Swiegers JH, Pretorius IS (2005) Yeast modulation of wine flavor. Adv Appl Microbiol 57:131–175
22. Annemüller G (2009) Gärung und Reifung des Bieres: Grundlagen-technologie-anlagentechnik. VLB, Berlin

Chapter 14
Using Digital Holographic Imaging Technology to Study the Flocculation of HAB Organisms (*Coscinodiscus sp.*) with Clay

Lujie Cao, Xinying Zhu, Ruofan Pan, Jiawei Chen, Jipeng Yin and Weihan Li

Abstract Flocculation of organisms with clay is an effective method of harmful algal blooms (HABs) removal. Exploring the mechanism in detail is necessary but very challenging. Based on a digital holographic imaging system with objective lens, we build up the technology for full flocs characterization within a 3D volume in situ. We recorded and reconstructed the field of fine particles and their aggregates. Furthermore, we directly measured the key parameters of flocculation procedure, such as flocs concentration, size spectrum, settling velocities, and their morphology structures. The technology and the algorithm are tested by an experimental study on the flocculation kinetic of *Coscinodiscus sp*. with clay. We optimized the algorithm in size measurement and fractal characterization for flocs with irregular shape. We confirmed the evolution of flocs in size, settling, and the fractal dimensions at non-equilibrium state of flocculation. From this experimental study to directly observe the morphological characteristics of flocs and their evolution, we pave the road to explore the mechanism of HABs removal.

Keywords Digital holography · Flocculation · Harmful algal blooms (HABs) removal · Clay · *Coscinodiscus sp*

14.1 Introduction

The control of Harmful Algal Blooms (HABs) is the intensive concern of public health and economics. Flocculation of organisms with clay has been proved to be an effective method of harmful algal blooms removal [1–4]. The underlying

L. Cao (✉) · X. Zhu · R. Pan · J. Chen · J. Yin · W. Li
Department of Mechanical Engineering, College of Engineering, Ocean University of China, Qingdao 266100, People's Republic of China
e-mail: lujiecao@ouc.edu.cn

T.-C. Zhang et al. (eds.), *Proceedings of the 2012 International Conference on Applied Biotechnology (ICAB 2012)*, Lecture Notes in Electrical Engineering 249,
DOI: 10.1007/978-3-642-37916-1_14, © Springer-Verlag Berlin Heidelberg 2014

mechanism is critical to be explored for new low-cost flocculants, dosage estimation, and more efficient applications [5–7].

Flocculation is an effective procedure that can be used to separate suspended solids from liquid. It involves the collision and adherence processes of small and destabilized particles to form larger and loosely packed particles [8, 9]. Such continuously growing, breaking up, and settling aggregates are called flocs. Those flocs have complex morphology and are expected to be shear resistant and sink rapidly for a fast separation procedure [8, 9]. It is now accepted that the key parameters to describe floc properties and the flocculation kinetics are size, concentration, settling velocities, and the morphology of aggregates [8–13]. Fractal dimension has been identified as a valid parameter to quantify the complexity of the aggregates [10–13].

Unfortunately, there are no general models that can predict the floc properties yet [8]. Experimental efforts are required to look in detail at both the flocculation kinetics and other environmental factors [11–13]. This is a challenging mission because it requires the in situ measurement with resolutions covering both macroscopic and microscopic scales.

Digital holography is the state-of-the-art technology with inherent capability of 3D measurement for particle field [14–21]. It developed rapidly during last 20 years. Now it is a family of technologies with different capabilities. Digital Holographic Imaging (DHI) is the most frequently used one. Digital Holographic Particle Imaging Velocimetry (DHPIV) is the technique that addresses on the measurement of velocity field from tracing particles [14, 15, 21]. Microscopic Digital holographic imaging (Micro-DHI) is an alternative technique on exploring characteristics of smaller particles when objective lenses have to be introduced [15–21]. Particular efforts were put on the measurement of particle size around tens micrometer, the accuracy was satisfied [20, 21].

In this paper, we designed an experimental study on the flocculation of *Coscinodiscus sp*. with clay using a microscopic in-line digital holographic imaging technology. The evolution of flocs in size, settling velocity, and the fractal dimensions were obtained and analyzed. Different behaviors of flocs were identified at the nonequilibrium state. We want to optimize the algorithms for full flocs characterization.

14.2 Materials and Methods

14.2.1 Digital Holographic Imaging Technology

Figure 14.1 provides a schematic of an in-line digital holographic imaging system. The flocculation volume is illuminated by a collimated and coherent laser beam. The scattered light from algal cells, from suspended clay particles or from flocs are called object wave (O) which will interfere with those original source light (R).

Fringe patterns are formed and recorded by digital camera located at the same axis. The information of particle size and position are kept by a hologram as intensity and phase. The decode procedure of these patterns is called reconstruction and can be done numerically. Details about the algorithm and accuracy evaluation can be found in references [15–21].

The collimated laser beam with diameter of 30 mm is formed by a beam expander (Edmund Optics, 15X); 10 mW diode laser at wavelength of 635 nm is used as light source (Edmund Optics). The digital recorder is a color CMOS camera (DLC 500, Patriot, Huaqi digital lab, Beijing) at full resolution of 2592 × 1944 pixel (2.2 μm/pixel), given a 2D recording area of 5.7 × 4.2 mm. A 10X flat field long working distance objective lens is attached in front of the camera. The final resolution is calibrated as 0.57 μm/pixel, thus the valid recording area is 1.51 × 1.13 mm. The limitation in the small cross section area of the test volume can be compensated by the extension in depth as to 10 mm, given the total test volume (V) of 3.42 ml.

Holograms are reconstructed by two algorithms for double checking, Holoprix [15, 18] and UU (the Cross-platform image-processing program, the Southeast University, China). Holoprix has already been applied successfully on the characteristics of variant particle fields [15, 18]. Its particle extraction algorithm, i.e., to locate the X, Y, and Z coordinates of each particle, is based on intensity (PEI) distribution of particles in space [18].

Counting the number of all particles (N) extracted within the fixed volume (V) will give the number density (n_a) as the parameter of particle concentration.

$$n_a = \frac{N}{V} \tag{14.1}$$

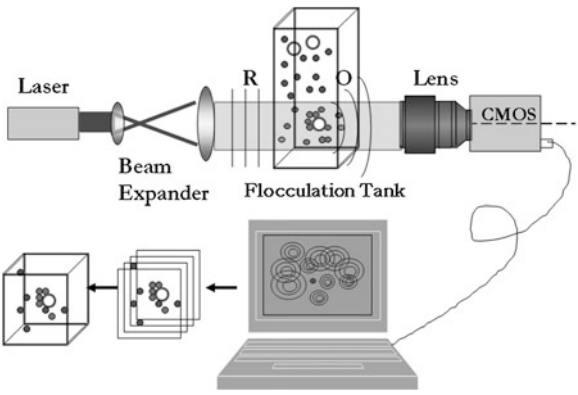

Fig. 14.1 Schematic of experimental apparatus

14.2.2 Aggregate Development Monitoring

For the same floc, there are two holograms recorded at two different moments with preset time interval (Δt). By subtracting one hologram from the other, we obtain a new hologram for the floc movement measurement as shown in Fig. 14.2a.The morphology of flocs can be obtained directly from the reconstructed in-focus image Fig. 14.2b. From which the maximum length l of a floc can be measured as the diameter of its minimum circumcircle. The floc displacement L is defined as the distance between the centers of these two circles. Different from traditional 2D imaging technique, L measured with holography is the function of X, Y, and Z.

Particular attentions are paid on particle size measurements using holography [19–21]. Calibration results are satisfied for sphere particles whose scattering can be characterized by Mie theory. However, the size measurement is hard to conduct for live cells which are half transparent, and for flocs which are irregular shaped. In this study, we developed a hybrid algorithm to solve this problem. First, using Holoprix and UU to reconstruct and locate the in-focus images of target cells, and then applying the commercial software μScope (PixelLINK^{TM} for microscopy, Edmund Optics) to measure the maximum length l in 2D image.

14.2.3 Aggregate Size Measurement

No matter how complex the aggregate is, its area (A_i) is obtained directly by accumulating all pixels belonging to the floc at its in-focus image. Thus the area-based diameter d_a can be calculated as

$$d_a = \left(\frac{4A_i}{\pi}\right)^{1/2} \tag{14.2}$$

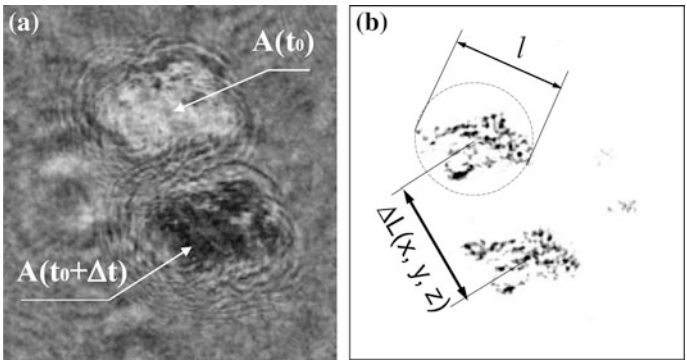

Fig. 14.2 Aggregates reconstruction and measurement. **a** Hologram of floc pairs **b** Reconstructed floc pairs

According to the Nyquist theory, at least 2 pixels are required for an accurate location of one particle. And at least 3 pixels are necessary for particle area measurement. When the physical resolution of the microscopic digital holographic system is set to be 0.57 μm/pixel, the minimum diameter of particle size estimated from (14.2) will be around 1 micrometer, accurate enough for clay particles characterization.

14.2.4 Aggregate Velocity Measurement

It is the settling velocity of flocs that we are mostly interested. The calculation is based on the measurement of the displacement of flocs during time interval Δt.

$$v_{\mathrm{i}} = \frac{\Delta L}{\Delta \mathrm{t}} = \frac{\sqrt{(\Delta X)^2 + (\Delta Y)^2 + (\Delta Z)^2}}{\Delta \mathrm{t}} \tag{14.3}$$

Δx, Δy, and Δz are the coordinate differences of the same floc from two holographic recordings.

14.2.5 Aggregate Fractal Dimension Measurement

It is widely accepted that the random flocs formed during flocculation are of fractal nature [8–15]. It is the quantification of whether the floc is loose or compact, thus it is related to the characteristics of shear resistance or drag force.

We calculate the 2D fractal dimension D_2 from the reconstructed in-focus image of aggregates.

$$D_2 = \frac{\ln(A_{\mathrm{i}})}{\ln(l)} \tag{14.4}$$

Where A_i is the area of floc and l is the maximum length scale.

14.2.6 Clay Sample and Cell Culture

The *Coscinodiscus sp*. was provided by the Institute of Oceanology, Chinese Academy of Sciences, (IOCAS). The cells were grown in batch culture using f/2 medium at 20° with a 12:12 h light:dark cycle. Flocculation experiments were performed using cultures in exponential growth. The culture was diluted to maintain the free floating condition of each cell.

The unmodified clay sample was also obtained from IOCAS. The main components are illite (25 %), montmorillonite (68 %), and kaolinite (5 %) [4, 7]. The clay was mixed with filtered sea water (<2 μm) and was settled over 24 h. Only the neutrally buoyant solution is taken for flocculation experiment. The number concentration of clay particle is calibrated to be 50 particles/ml by holographic system. We keep particles at low concentration to minimum the self-flocculation of clay.

14.2.7 Flocculation Experiment

Before conducting a flocculation test of *Coscinodiscus sp*. with clay suspension, the number concentration and size information for both cells and clay particles have been recorded and analyzed. Such information will be used as background of each test for the calibration and start point of the flocculation evolution.

In this experimental study, we choose to measure the behavior of *Coscinodiscus sp*. cells within the suspension of clay particles. We set the number densities of both cells and clay particles to be low, addressing the interaction between cells and clay particles, but not within each other. The ratio between the initial cell concentration and suspended clay particles is 1:90.

The cell of *Coscinodiscus sp*. has shape of cylinder. The front view of cell is circle, and half transparent at center region. The side face view of a cell is rectangular with the thickness of 10–20 μm, opaque, and uniform all over. Thus, the side face view will occupy smaller area on the in-focus image, compared to its front view results. It causes the deviation in the measurement of area based diameter. In data processing, we analyze cells separately according to their view angles to eliminate this bias.

Flocculation experiments were conducted in a specially designed tank made of polyglass. Two optical windows were used for less distortion to laser beam. The inner dimensions of the tank were 140 × 40 × 10 mm, given the enough growth distance for particle aggregates.

Drawing a line of 100 μl liquid of algal cells on a glass slide uniformly, and then putting it smoothly into the clay suspension, thus we released cells with minimum mechanical disturbs. Experiments will repeat more than three times depending on the total number of flocs recorded.

The holographic recording region is 120 mm below the top of flocculation tank, given an enough distance for the growth of flocs. Total recording time was set to be more than 10 min at rate of 3 frames/sec, covering the whole procedure of flocculation and flocs settlements. Holograms with interested morphology of flocs were extracted from the video at preset time interval (1 s) for the settling velocity calculation.

For each data group, the mean, median, maximum, minimum values, and standard deviation will be calculated for statistics analysis. The histogram is used for flocs size distribution and comparison.

14.3 Results and Discussions

14.3.1 Reconstruction of Aggregate Structure

Using image subtraction method, two holograms with the same floc recorded at different moments were processed and analyzed, resulting new holograms shown in Fig. 14.3 (left). The corresponding reconstructed in-focus images were listed at the right part. Based on morphology, we identify four different groups of flocs, which are (1) flocs of pure clay particles, (2) front view recording of single cell with clay, (3) side face view recording of single cell flocs, and (4) the developed

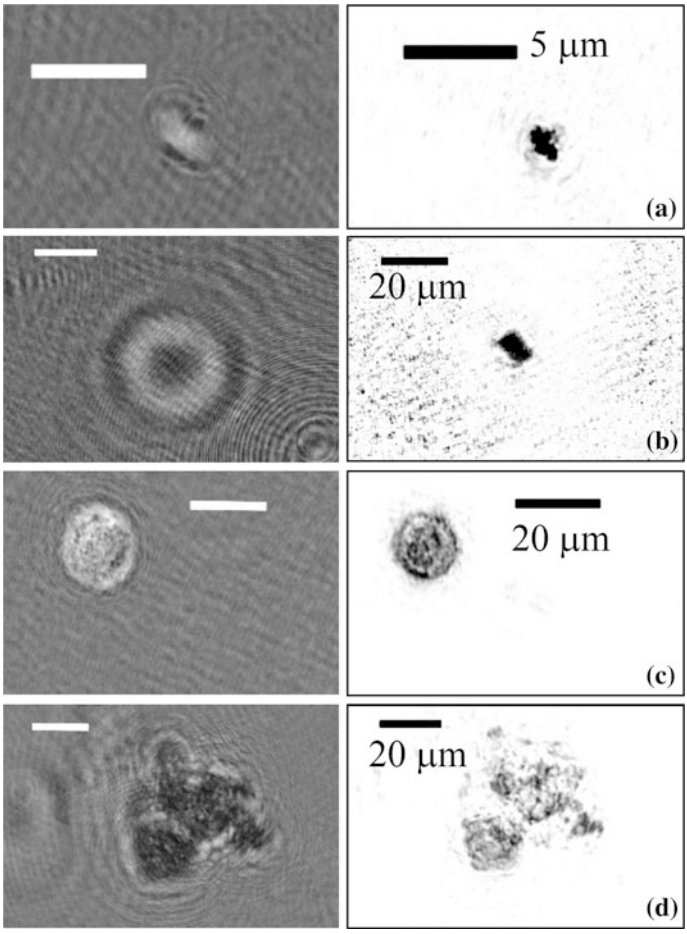

Fig. 14.3 Typical flocs morphology (*Left* holograms. *Right* Reconstructed in-focus images.) **a** Flocs of pure clay particles. **b** Single cell with clay (*side face view*). **c** Single cell with clay (*front view*). **d** Aggregates of multicells

aggregates of multicells with larger size and loose structures. Each group of flocs were identified and labeled, for area, size, fractal dimensions, and settling velocities measurement.

14.3.2 Primary Cell Size Distribution

The cell size of *Coscinodiscus sp*. was calibrated using microscope (4X, Phoenix Optics Ins.) and commercial software μScope. A total of 1065 samples from 20 images were measured. Given the mean diameter of 50.4 ± 4.6 μm, it ranged from 32.9 to 67.7 μm.

By digital holographic technique, we measured the size of clay particles to evaluate the effect of self-flocculation. More than 2000 particles were extracted from 40 holograms for each analysis. We measured the size of clay particles was 3.10 ± 0.85 μm at free and low suspension. This value changed to be 3.32 ± 1.75 μm at the suspension for flocculation test after a while. We conclude that the self-flocculation of clay particles will not disturb the flocculation of *Coscinodiscus sp.*

14.3.3 Evolution of Aggregate Size

Figure 14.4 plots the distribution of area-based diameter of particles before and after the flocculation. An obvious growth in size and in width exists. However, compared to the original cell size of 50.4 ± 4.6 μm, the area-based diameter of flocs was 25.7 ± 13.6 μm, which was unreasonable.

From Fig. 14.3 we learned that the cells have two views, their areas from in-focus images are different. For typical cell thick of 10–20 μm, the side face view will provide 48–74 % less value in area compared to its front view result.

To solve the problem, we further measured the maximum length of each cells from their in-focus images, this value should not change from any recording direction. The flocs size distributions from different parameters were plotted together in Fig. 14.5 for comparison. In this case, the value of flocs size obtained from the maximum length is from 20–184 μm, with the mean value of 59.96 μm. It also confirms that the growth of cell due to the flocculation is real.

14.3.4 Settling Velocity of Aggregate

As a preliminary experiment for algorithm development, we extract totally 135 aggregates of cells with clay for analysis. More data are under processing for further study.

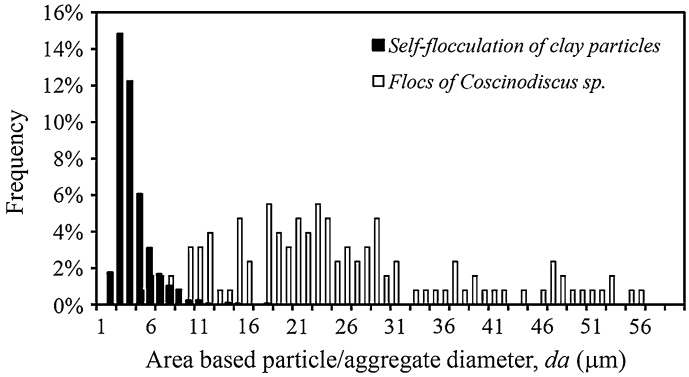

Fig. 14.4 Size evolution after flocculation

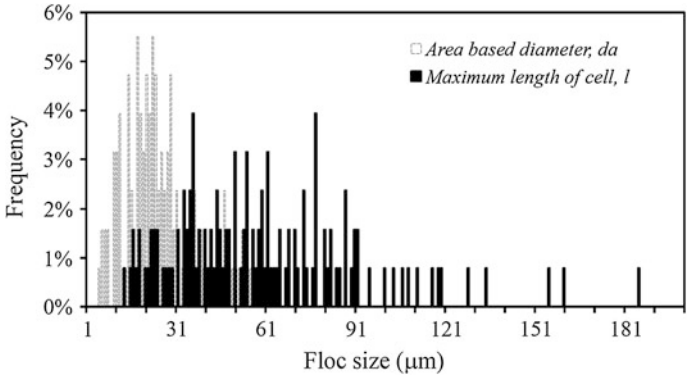

Fig. 14.5 Comparison on aggregates size distribution characterized by different parameters

Before the flocculation experiment, we have confirmed that the cells of *Coscinodiscus sp*. were neutrally buoyant and free floating in sea water. When flocculation starts, we can attribute the sink of cells to the aggregation with clay particles. The relationship of floc settling speed with its size and shape were studied with results shown in Fig. 14.6. We found that larger flocs tend to sink faster, implying the accumulation of more clay particles.

The morphology analysis confirmed that the flocs were made of single cell attached by clay particles. Flocs were grouped according to their view direction and were treated separately to identify the source of bias in size calculation.

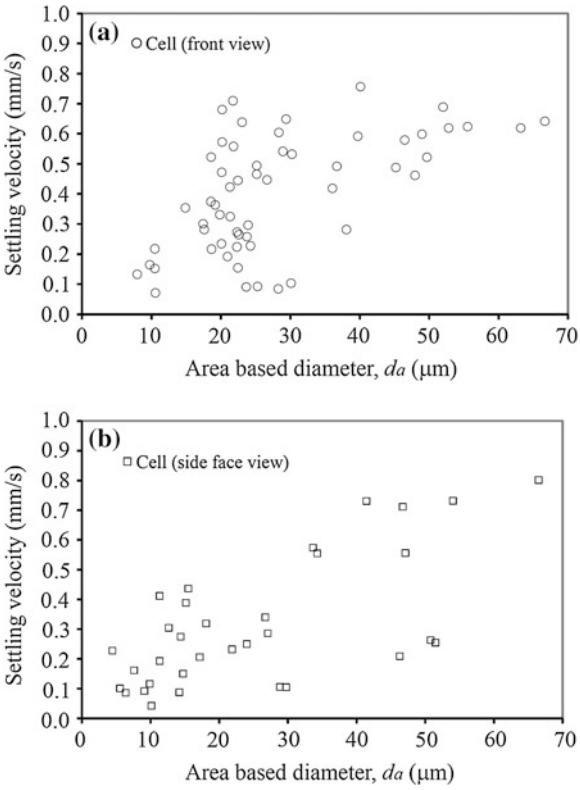

Fig. 14.6 Cells quickly settling due to aggregates with clay. **a** Front view recording of cells. **b** Side face view recording of cells

14.3.5 Fractal Dimensions of Aggregates

According to Eq. 14.4, there is a fractal relationship between the areas of flocs with their typical length scales. In Fig. 14.7 we plotted the values of area and maximum length for all floc groups in natural logarithm scale, either from single cell based or from large aggregates of multicells and clay. An obvious linear relationship exists. By linear interpolating data of multicell aggregates in Fig. 14.7, we get the slope value of 1.57 which is the value of 2D fractal dimension (D_2), confirming the fractal nature of the flocculating procedure. However, results from single cell based flocs show the scattered distributions around the slope indicating that this procedure does not reach the equilibrium state yet.

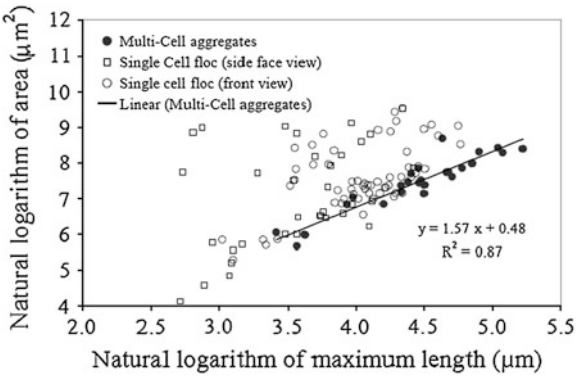

Fig. 14.7 2D fractal relationship between the flocs area and the typical length scale

14.4 Conclusions

In this experimental study on the flocculation of *Coscinodiscus sp*. with clay, we successfully applied the digital holographic imaging technology to directly measure key parameters that characterize the flocculation kinetics, particularly at the non-equilibrium state.

Based on the developed algorithm of small particle characterization from holography, we further build up a method to study larger and irregular shaped flocs in detail. Area-based diameter and the maximum length scale of each floc can be measured as the quantification of particle size. The correlation between floc settling velocity with its size confirms the accumulation of clay particles from background. The 2D fractal dimensions we obtained is 1.57, which is a smaller value than those from report [4] indicating that the floc is not fully developed yet, confirms that the flocculation is at non-equilibrium state.

We proved that the growth of flocs during the flocculating procedure both in value and in the width of size spectrum is real. We further identified differences of floc behavior in settling and in morphology at the non-equilibrium state. Such subtle differences are hard to find using traditional techniques. With digital holographic imaging technology, we are able to explore the flocculation procedure *in situ* and continuously with great details. It paves the road to further explore the underlying mechanism.

Acknowledgments This work is supported by the grant from Ocean University of China through "Outstanding Youth Plan" (No. 841012010), and National Natural Science Foundation of China No.51175485 and No. 51276174.

References

1. Pierce RH, Henry MS, Higham CJ et al (2004) Removal of harmful algal cells (*Karenia brevis*) and toxins from seawater culture by clay flocculation. Harmful Algae 3:141–148
2. Beaulieu SE, Sengco MR, Anderson DM (2005) Using clay to control harmful algal blooms: deposition and resuspension of clay/algal flocs. Harmful Algae 4:124–138
3. Vaezi GF, Sanders RS, Masliyah JH (2011) Flocculation kinetics and aggregate structure of kaolinite mixtures in laminar tube flow. JCIS 355:96–105
4. Wang HL, Yu ZM, Cao XH et al (2011) Fractal dimensions of flocs between clay particles and HAB organisms. Chin J Oceanol Limnol 29(3):656–663
5. Pan G, Zhang MM, Chen H et al (2006) Removal of cyanobacterial blooms in Taihu lake using local soils. I. equilibrium and kinetic screening on the flocculation of *Microcystis aeruginosa* using commercially available clays and minerals. Environ Pollut 141:195–200
6. Pan G, Chen J, Anderson DM (2011) Modified local sands for the mitigation of harmful algal blooms. Harmful Algae 10:381–387
7. Wang HL, Yu ZM, Song XX et al (2010) Removal of *Heterosigma akashiwo* by modified wheat straw. Environ Sci 31(2):296–300 (In Chinese)
8. Thomas DN, Judd SJ, Fawcett N (1999) Flocculation modelling: a review. Wat Res 33(7):1579–1592
9. Wang DS, Tang HX (2001) Application of fractal theory on coagulation: a critical review. Ind Water Treat 21(7):16–19 (in Chinese)
10. Wang XC, Tambo N (2000) A study on the morphology and density of flocus I. the fractal structure of flocs. Acta Sci Circumstantiae 20(3):257–262 (in Chinese)
11. Cuthbertson AJS, Dong P, Davies PA (2010) Non-equilibrium flocculation characteristics of fine-grained sediments in grid-generated turbulent flow. Coast Eng 57:447–460
12. Rasteiro MG, Gareia FAP, Ferreira P et al (2008) The use of LDS as a tool to evaluate flocculation mechanisms. Chem Eng Process 47:1323–1332
13. Uduman N, Qi Y, Danquah MK et al (2010) Marine microalgae flocculation and focused beam reflectance measurement. Chem Eng J 162:935–940
14. Mantovanelli A, Ridd PV (2006) Devices to measure settling velocities of cohesive sediment aggregates: A review of the in situ technology. J Sea Res 56:199–226
15. Cao L, Pan G, de Jong J et al (2008) Hybrid digital holographic imaging system for 3d dense particle field measurement. Appl Opt 47(25):4501–4508
16. Berg MJ, Videen G (2011) Digital holographic imaging of aerosol particles in flight. JQSRT 112(11):1776–1783
17. Khanam T, Rahman MN, Rajendran A et al (2011) Accurate size measurement of needle-shape particles using digital holography. Chem Eng Sci 66:2699–2706
18. Cao L, Zhu XY, Yin JP, et al (2012) Particle characterization for coal water slurry by digital holography. Int Conf Mater Renew Energy Environ (ICMREE 2012).May 18–20 Beijing China, pp.1372–1376
19. Jericho SK, Klages P, Nadeau J et al (2010) In-line digital holographic microscopy for terrestrial and exobiological research. Planet Space Sci 58:701–705
20. Wu XC, Pu XG, Pu SL et al (2009) Particle sizing for gas-solids flow with digital in-line holography. CIESC J 60(2):311–316 (In Chinese)
21. Lü QN, Ge BZ, Gao Y et al (2010) Simultaneous measurement of size and velocity of alcohol spray with digital holography. Acta Photonica Sinica 39(2):266–270 (In Chinese)

Chapter 15
Cloning of ATP-Citrate Lyase (*acl1*) from *Aspergillus niger* and its Expression in *Escherichia coli*

Fang Sun, Hong Chen, Xihong He and Hao Liu

Abstract *Aspergillus niger* is an important strain used for industrial fermentation of citrate. The production of citrate is closely related to the growth and metabolism of *A. niger*. ATP-citrate lyase (ACL) is responsible for catalyzing the conversion of citrate into oxaloacetate and acetyl-CoA, which is a bridge between glucose metabolism and fatty acid synthesis. In *A. niger*, tandem divergently transcribed genes (*acl1* and *acl2*) encode the subunits of ACL, whose physiological function is unclear. In this study, *acl1* was obtained from *A. niger* by RT-PCR. The sequencing result was consistent with the sequence of genome database. We constructed the expression vector pET28a^{+}-*acl1-his6* which was suitable for the efficient expression in *Escherichia coli* BL21. After purification with Ni^{2+} chelating chromatography column, SDS-PAGE analysis showed that the molecular mass of the ACL1 was 66 KDa. The result laid the foundation for further research about protease characteristics and physiological functions of ACL1 in *A. niger*.

Keywords *Aspergillus niger* · ATP-citrate lyase · Acetyl-CoA · Protein expression · RT-PCR

15.1 Introduction

Aspergillus niger is an important industrial workhorse with extensive application in the sectors of industrial enzymes, heterogeneous proteins, organic acids, and so on [1]. *A. niger* is economically important as a fermentation organism used for the

F. Sun · H. Chen · X. He · H. Liu (✉)
College of Biotechnology, Tianjin University of Science and Technology,
Tianjin 300457, People's Republic of China
e-mail: liuhao@tust.edu.cn

H. Liu
Tianjin University of Science and Technology, No. 29 13th Avenue, TEDA,
Tianjin 300457, People's Republic of China

T.-C. Zhang et al. (eds.), *Proceedings of the 2012 International Conference on Applied Biotechnology (ICAB 2012)*, Lecture Notes in Electrical Engineering 249,
DOI: 10.1007/978-3-642-37916-1_15, © Springer-Verlag Berlin Heidelberg 2014

production of citric acid. Industrial citric acid production by *A. niger* represents one of the most efficient, highest yield bioprocesses in use currently by industry. At present, the annual output of citric acid is more than 1.5 million tons in the world, of which 99 % citric acid is fermented from *A. niger*. The production of citric acid is closely related to the growth and metabolism of *A. niger* [2–4]. For a long time, researchers have focused on the genes related to the metabolism of *A. niger*. The researches have clarified the significant roles of the glycolytic pathway, the tricarboxylic acid cycle, and the glyoxylate cycle in the citric acid metabolism and revealed that pyruvate dehydrogenase, pyruvate carboxylase, and citrate synthase directly involved in the function of key enzyme encoding the genes in the citric acid metabolism [5, 6]. The disclosure of the genomic sequence to the public brought the study of *A. niger* into the post-genomic era [7, 8]. The genome of *A. niger* ATCC 1015, historic strain was used in research that resulted in the first patented citric acid process, that was accepted for sequencing through the US Department of Energy Microbial Genome Program. Acetyl coenzyme A (CoA) is an important intermediate involved in both intermediary carbon and energy metabolism as well as in biosynthetic pathways [9]. Acetyl-CoA generated through the degradation of lipids, carbohydrates, and amino acids is used for the synthesis of several cellular components, and nucleocytosolic acetyl-CoA is particularly important in the acetylation of histones [10]. Acetyl-CoA also serves as an important precursor for several metabolites, such as polyketides, terpenes and lipids [11]. ATP-citrate lyase is considered to be an essential cytoplasmic enzyme of the carbon dioxide-fixing reductive tricarboxylic acid cycle, since it catalyzes the formation of oxaloacetate and acetyl-CoA from the cleavage of citrate. A survey of a wide variety of oil-producing microorganisms has found a correlation between those that accumulate high levels of lipids and the presence of ACL activity. Another important function of the ACL is the regulation of gene expression. The study found that the ACL activity is required to link growth factor-induced increases nutrient metabolism to the regulation of histone acetylation and gene expression [12]. ACL is present in fungi, plants, animals, and some prokaryotes [10]. The ACL polypeptides of animal have a molecular mass of 110–120 kDa and are encoded by a single gene [13]. ACL of mammalian positively regulates the glycolytic pathway by regulating transcriptional activation through histone acetylation and by inhibiting glycolysis during hypoxic conditions [14]. In filamentous fungi, ACL is thought to consist of two different subunits of 70 and 55 kDa, respectively [15, 16]. It was reported that in filamentous fungi two different subunits of ACL are encoded by two separate genes adjacent on a chromosome, and this is in contrast to animals where ACL is encoded by a single gene. The 66 kDa ACL1 polypeptide of *A. niger* shows significant homology to the C-terminal parts of animal ACL polypeptides. *A. niger* has been shown to have two adjacent genes (*acl1* and *acl2*) for different subunits of ACL separated by 2.6 kb, and these are divergently transcribed. The catalytic center is conserved in both the rat ACL and the fungal ACL1 polypeptides [17]. Analysis of sequenced fungal genomes indicates that predicted ACL1 encoding genes are present widely in fungi and have high similarity (Fig. 15.1). The catalytic enter of *A. niger* ACL1

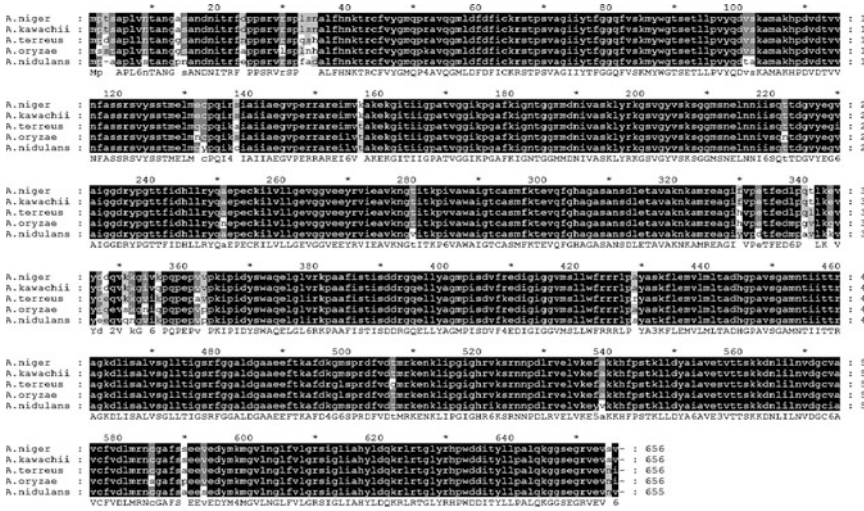

Fig. 15.1 Alignment of ACL1 polypeptide sequences from filamentous fungi. Amino acid residues conserved in all sequences are shown in *black*. The following sequences were used for comparison: *A. niger* (Accession no. xp_001394055); *A. kawachii* (Accession no. GAA84137); *A. terreus* (Accession no. xp_001211553); *A. oryzae* (Accession no. xp_001820781); *A. nidulans* (Accession no. xp_660040)

protein also has a conserved histidine. It is unknown whether autophosphorylation occurs in the catalytic process.

In this study, we reported cloning and sequence analysis of cDNA that encode the *A. niger* ACL1. Moreover, the recombinant fusion protein was expressed and purified using Ni^{2+} chelating chromatography column successfully. The result laid the foundation for further research of protease characteristics and physiological functions of ACL1 in *A. niger*.

15.2 Materials and Methods

15.2.1 Strains

The *Aspergillus niger* strain ATCC1015 used in this study was held in our laboratory collection and propagated on potato dextrose agar. The *E.coli* JM109 and BL21 used for cloning and protein expression were both held in our laboratory collection.

15.2.2 Chemicals and Reagents

KOD FX polymerase, all PCR reagents, enzymes for molecular cloning and PrimeScript RT reagent Kit were purchased from Takara. Gel Extraction Kit and the rapid plasmid DNA mini-prep kit were from Solaribio. Trizol were purchased from Invitrogen. His-select Ni-Chelating affinity gel column used for protein purification was purchased from Novagen.

15.2.3 RNA Isolation and cDNA Synthesis of acl1

Mycelia used for genomic DNA and RNA extraction were harvested from cultures grown in liquid potato dextrose medium at 30 °C for 2 days. Total RNA of *A. niger* was extracted using the Trizol method, and the initial mycelia amount was 500 mg [18]. DNA was removed from RNA by scavenger of DNA. Genomic DNA of *A. niger* was extracted using the CTAB protocol [19]. The extraction of total RNA was identified and isolated by agarose gel electrophoresis to check the integrity.

Fist strand cDNA synthesis was carried out with a PrimeScript RT reagent Kit Perfect Real Time using Oligo (dT) primers and total RNA as the template. Reaction condition was as follows: 65 °C 5 min, then chilling on ice 5 min, 37 °C 15 min, 42 °C 15 min, 50 °C 15 min, 85 °C 5 s. The PCR specific primers for *acl1* were designed according to *acl1* sequence of *A. niger* published in GenBank. The two specific primers used were as follow: *acl1*-F: ATGCC TAC-CTCTGCTCCCCTCGTC; *acl1*-R: TTAGACGCTGACCTCGACACGACCC. PCR amplification was performed in 20μL reaction mixture containing 1.6 μL of cDNA, 10 μL of 2 × PCR buffer, 2 μL of 2 mM dNTPs, 0.4 μL each of 10 μM forward and reverse primers, 0.4 μL of KOD FX. The temperature gradients (55–72 °C) were used to determine the optimum annealing temperature. The reaction conditions comprised an initial denaturation of 2 min at 94 °C, followed by 42 cycles of 98 °C for 10 s, 68 °C for 30 s, and 68 °C for 2 min, with a final extension at 68 °C for 10 min. After checking the product on an analytical 1 % agarose gel, the 1.9 kb band was then extracted from the gel by Gel Extraction Kit.

15.2.4 Cloning and Sequencing of the PCR Products

The purified PCR product was then ligated into vector pIJ2925 at 16 °C overnight and transformed. The pIJ2925-*acl1* vector was transformed into competent JM109 *E. coli* cells and plated on LB-ampicillin/IPTG/X-gal plates followed by incubation at 37 °C for about 20 h. (We prepared plates containing X-Gal and IPTG, 50 μL of 50 mg/mL X-Gal and 100 μL of 0.1 M IPTG onto previously prepared LB plates

containing ampicillin. Allow these components to absorb for at least 30 min at 37 °C prior to plating cells). The resulting colonies were screened by Colony PCR using the gene specific oligonucleotide primers. The plasmid DNA was purified from overnight culture using the rapid plasmid DNA mini-prep kit and the presence of insert was verified by *Eco*R I and *Pst* I, *Sac* I, *Xho* I, *Mun* I restriction digestion of purified recombinant plasmid, respectively. One clone was selected and sequenced. The sequence of cloned fragment was analyzed using public domain database of NCBI http://blast.ncbi.nlm.nih.gov/Blast.cgi.

15.2.5 Sub-cloning of acl1 *into Expression Vector pET28a*$^+$

The *A. niger acl1* gene was amplified from pIJ2925-*acl1* vector using the gene specific forward and reverse primers: *acl1-Nde* I: GGGAATTCCATATGCCTAC CTCTGCTCCCCTCG; *acl1-Eco*R I: CGGAATTCTTAGACGCTG ACCTCGA-CACGAC. The primers containing the restriction enzyme sites in order to generate the *Nde* I and *Eco*R I sites in the PCR product. The PCR amplified *acl1* gene and the pET28a$^+$ expression vector was restriction digested, gel purified, and the digested *acl1* gene product was ligated into the *Nde* I and *Eco*R I sites of pET28a$^+$ expression vector by incubation at 16 °C overnight and the transformation was carried out by mixing 10 μL of ligation mix to 100 μL of competent BL21 *E. coli* cells following the standard procedure. The transformed cells were plated on LB-agar plates containing 100 $\mu g \cdot mL^{-1}$ of kanamycin, and incubated at 37 °C for about 20 h. The positive clones were selected by Colony PCR and confirmed by restriction digestion.

15.2.6 Expression and Purification of ACL1 in E. coli

For analytical studies, induction was done at different IPTG concentrations (0.1, 0.4, 1 mM), different temperatures (20, 28, 37 °C), and different time intervals (4, 6, 8, 12 h). After optimizing the expression conditions, a starter culture was set up by inoculating 3 mL of LB broth containing 100 $\mu g \cdot mL^{-1}$ of kanamycin with single bacterial colony of pET28a$^+$-*acl1-his6* plasmid, and the culture was grown overnight in 37 °C orbital shaker at 200 rpm. The 4 mL of LB broth supplemented with kanamycin was inoculated with 5 % of the starter culture and allowed to grow at 37 °C with shaking at 200 rpm till OD_{600} reached 0.5–0.6, then induction was done with 0.1 mM IPTG at 20 °C for 12 h. The cultures were chilled on ice and the cell pellet harvested by centrifugation at 12000 rpm for 10 min at 4 °C, was suspended in 1 × bind buffer (50 mM NaH_2PO_4, 500 mM NaCl, pH 8.9). The cell suspension was sonicated (4 s each with 6 s cooling between successive bursts in 20 min). The resulting lysate was centrifuged at 12000 rpm for 20 min at 4 °C.

The supernatant and the pellet obtained from the uninduced and induced cells were analyzed on SDS-PAGE.

To purify the ACL1 protein, the large amount of pellet obtained as described above, was resuspended in 1 × Ni-NTA Buffer (50 mM NaH_2PO_4, 500 mM NaCl, 5 mM imidazole, 10 % glycerin, pH 8.9). The cell suspension was sonicated as described above. One milliliters of the supernatant was applied onto a column filled with His-select Ni-Chelating affinity gel preconditioned with 1 × Ni-NTA Buffer. The elution was performed with 5 mL of 1 × bind buffer containing 50 mM imidazole and then 5 mL of 1 × bind buffer containing 100 mM imidazole and then 5 mL of 1 × bind buffer containing 300 mM imidazole and then 5 mL of 1 × bind buffer containing 500 mM imidazole. The purity of recombinant ACL1 was analyzed on SDS-PAGE.

15.3 Results and Discussion

15.3.1 Isolation and Sequencing of acl1 *in* A. niger

It is important to obtain total RNA of high quality and integrity for the further PCR amplification. The total RNA of *A. niger* was pure without genome DNA pollution (Fig. 15.2). The full length of *acl1* cDNA was amplified from total RNA of *A. niger* by RT-PCR using gene specific primers corresponding to the *acl1* cDNA. The PCR amplification of gene coding for ACL1 using a temperature gradient from 55 to 72 °C showed maximum amplification of 1.9 kb PCR product at 68 °C. The amplified *acl1* cDNA showed an electrophoretic mobility on agarose gel corresponding to about of *acl1* cDNA fragment was smaller than the size of *acl1* DNA, which confirmed that the total RNA was not polluted by genome DNA (Fig. 15.3).

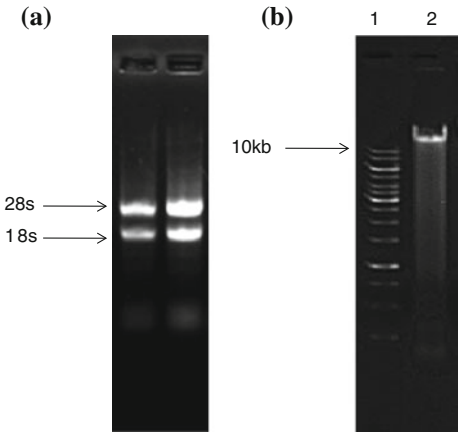

Fig. 15.2 Isolation of total RNA and genome DNA from *A. niger*, **a** total RNA of *A. niger*, **b** genome DNA of *A. niger*: Lane *1*: 1 kb DNA ladder, Lane *2*: Product of Genome DNA from *A. niger*

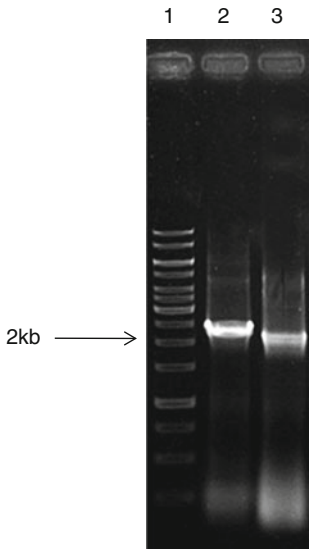

Fig. 15.3 RT-PCR amplification of *acl1* from *A. niger*. Lane *1*: 1 kb DNA ladder, Lane *2*: PCR product of *acl1* genome DNA generates fragment of 2139 bp, Lane *3*: RT-PCR product of *acl1* cDNA generates fragment of 1971 bp

The PCR product was cloned into pIJ2925 vector and its restriction digestion is shown in Fig. 15.4. The presence of *acl1* cDNA fragment was verified by *Eco*R I and *Pst* I restriction digestion. The pIJ2925-*acl1* vector has two *Sac* I restriction sites, one is in the *acl1*, and the other is in the multiple cloning site. So the direction of ligation was verified by *Sac* I restriction digestion. The full length of pIJ2925-*acl1* vector was verified by *Xho* I single restriction digestion. The *Mun* I restriction digestion confirmed *acl1* cDNA without genome DNA pollution.

The *acl1* cDNA inserted was then sequenced. Nucleotide sequence corresponding 1971 bp was then compared with the nucleotide sequences deposited in the GenBank database using the BLAST program on the NCBI Blast server. The isolated *acl1* showed that no mutations were found in the cDNA compared to the deposited *acl1* sequence from *A. niger*. The full length cDNA of *A. niger acl1* was deposited in GenBank under accession number XM_001394018. The open reading frame of *A. niger* ACL1 consisted of coding region of 1971 nucleotides and the deduced amino acid sequence represents 657 amino acid residues with a calculated molecular weight of 66 KDa.

15.3.2 Cloning of acl1 *into Expression Vector*

The isolated DNA was amplified with forward and reverse primers containing the restriction sites *Nde* I at 5′ and *Eco*R I at 3′ (see Materials and methods) for inserting it in the pET28a$^+$ vector which has been previously used for the expression of proteins [20]. The presence of *acl1* cDNA fragment was verified by *Nde* I and *Eco*R I restriction digestion (Fig. 15.5). The recombinant pET28a$^+$-*acl1*

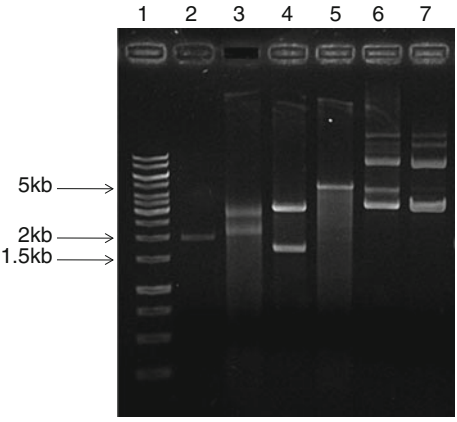

Fig. 15.4 Analysis of pIJ2925-*acl1* vector by restriction enzyme digestion. Lane *1*: 1 kb DNA ladder, Lane *2*: PCR amplification of *acl1* cDNA generates fragment of 1971 bp, Lane *3*: Digestion of pIJ2925-*acl1* with *Eco*R I and *Pst* I generates fragments of 1971 and 2706 bp, Lane *4*: Digestion of pIJ2925-*acl1* with *Sac* I generates fragments of 1597 and 3080 bp, Lane *5*: Digestion of pIJ2925-*acl1* with *Xho* I generates fragment of 4677 bp, Lane *6*: Digestion of pIJ2925-*acl1* with *Mun* I generates the same fragments as pIJ2925-*acl1* vector, Lane *7*: Undigested pIJ2925-*acl1* vector

Fig. 15.5 Analysis of pET28a^{+}-*acl1-his6* by double digestion. Lane *1*: 1 kb DNA ladder, Lane *2*: PCR amplification of *acl1* cDNA generates fragment of 1971 bp, Lane *3*: Digestion of pET28a^{+}-*acl1-his6* with *Nde* I and *Eco*R I generates fragments of 1971 and 5371 bp

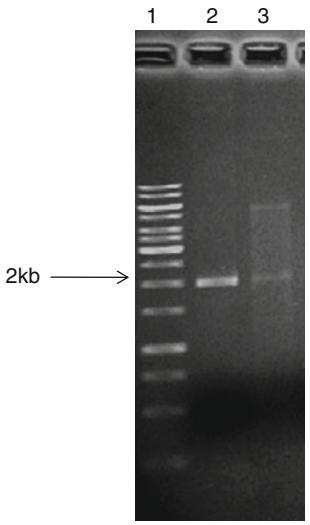

plasmid, encoding ACL1 fused with the 34 amino acid extra N-terminal sequence MGSSHHHH HHSSGLVPRGSHMASMTGGQQMGRGS, containing a *his6* tag, was used for heterologous expression and purification of the protein in the *E. coli* BL21 by Ni^{2+} chelate chromatograph column.

15.3.3 Expression and Purification of ACL1

To optimize the expression of ACL1, the time after induction by IPTG and growth temperature were varied. The cell lysates obtained under the different conditions were separated in the soluble and the insoluble fractions by centrifugation. The whole extracts, soluble and insoluble fractions of cell lysates were analyzed by SDS-PAGE. To optimize the expression of ACL1 in *E. coli* BL21 transfected with the pET28a^{+}-*acl1-his6* construct, the IPTG concentration was varied from 0.1 to 1 mM. The best level of expression was obtained at 0.1 mM of the inducer IPTG. As shown in Fig. 15.6, based on the molecular weight of ACL1 protein, the expression was notably visible on SDS-PAGE following IPTG induction and reached its maximum level after 12 h incubation at 20 °C. The apparent molecular mass was determined on the basis of the molecular mass of marker proteins (Fig. 15.6 lane 1). Its value was 66 KDa.

The purification of the recombinant *A. niger* ACL1 was achieved in a single chromatographic step on Ni^{2+} chelate chromatograph column with gradient elution of 100 mM imidazole, 300 mM imidazole and 500 mM imidazole. Fractions from the affinity column containing purified ACL1 were pooled together and analyzed by SDS-PAGE (Fig. 15.6).

SDS-PAGE analyses showed a single protein band of 66 kDa that represent the molecular weight of the *A. niger* ACL1 fused to vector specific fusion histidine tag peptide. The calculated ACL1 molecular weight was in agreement with the reported molecular weight value for *Aspergillus nidulans* [21].

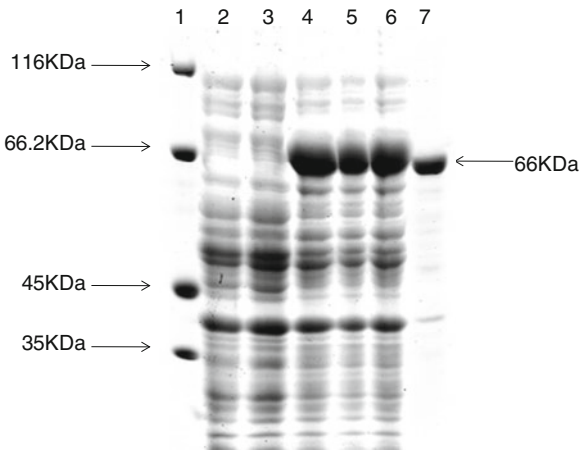

Fig. 15.6 Expression of recombinant pET28a^{+}-*acl1-his6* in *E. coli* BL21. Lane *1*: Protein molecular weight marker, Lane *2*: *E.coli* BL21 transformed with pET28a^{+}, Lane *3*: *E.coli* BL21 transformed with pET28a^{+}-*acl1-his6* without induction, Lane *4-6*: *E.coli* BL21 transformed with pET28a^{+}-*acl1-his6* whole extracts, soluble fractions and insoluble fractions, respectively, induced at 20 °C by 0.1 mM IPTG for 12 h, Lane *7*: The protein purified with Ni^{2+} chelating chromatography column generates fragments of 66 kDa

15.4 Conclusion

In the present study, we have amplified and cloned the *acl1* from total RNA of *A. niger* using the primer pairs based on the *acl1* cDNA sequence. The sequencing and characterization of pIJ2925-*acl1* vector confirmed the open reading frame of *acl1* gene was the same as the sequence in GenBank under accession number XM_001394018. We have cloned *acl1* cDNA into pET28a$^+$ expression vector to construct pET28a$^+$-*acl1-his6*. The ACL1 fusion protein was expressed and highly purified in *E. coli* with IPTG induction. The expression and purity of fusion protein was analyzed by SDS-PAGE and stained with Coomassie Brilliant Blue. The *acl1* gene of *A. niger* was homologous to the ACL gene of mammalian, suggesting that it has ACL activity. However, we need further experimental verification to confirm whether ACL1 protein has the ACL activity. This research has cloned and expressed *acl1* gene in E. coli to obtain the high purity ACL1 protein. The result laid the foundation for the activity of ACL1 protein analysis in vitro, to determine ACL and kinetic characteristics of ACL1 protein.

Acknowledgments The authors gratefully acknowledge the support of the seventh Singapore–China JRP (2011DFA31280) the National Nature Science Foundation of China (No. 31270125, 31170134), the National High Technology Research and Development Program of China (863 Program) (No. 2011AA02A213, 2012AA020403), and the Cheung Kong Scholars Programme of China (No. IRT1166).

References

1. Guo Y, Zheng P, Sun J (2010) *Aspergillus niger* as a potential cellular factory: prior knowledge and key technology. Chin J Biotechnol 26:1410–1418
2. Grimm LH, Kelly S, Krull S et al (2005) Morphology and productivity of filamentous fungi. Appl Microbiol Biotechnol 69:375–384
3. Gomez R, Schnabei I, Garrido J (1988) Pellet growth and citric acid yield of *Aspergillus niger* 110. Enzym Microbiol Technol 10:188–191
4. Paul GC, Priedeb MA, Thomas CR (1999) Relationship between morphology and citric acid production in submerged *Aspergillus niger* fermentations. Biochem Eng J 3:121–129
5. Karaffa L, Kubicek CP (2003) *Aspergillus niger* citric acid accumulation: do we understand this well working black box. Appl Microbiol Biotechnol 61:189–196
6. Torres NV (1994) Modeling approach to control of carbohydrate metabolism during citric acid accumulation by *Aspergillus niger*: I. Model definition and stability of the steady state. Biotechnol Bioeng 44:104–111
7. Cullen D (2007) The genome of an industrial workhorse. Nat Biotechnol 25:189–190
8. Backer SE (2006) *Aspergillus niger* genomics: past, present and into the future. Med Mycol 44:S17–S21
9. Hynes MJ, Murray SL (2010) ATP-citrate lyase is required for production of cytosolic acetyl coenzyme A and in *Aspergillus nidulans*. Eukaryot Cell 9:1039–1048
10. Fatland BL, Ke J, Anderson MD et al (2002) Molecular characterization of a heteromeric ATP-citrate lyase that generates cytosolic acetyl-coenzyme A in Arabidopsis. Plant Physiol 130:740–756

11. Guenther JC, Hallen-Adams HE, Bucking H et al (2009) Triacylglyceride metabolism by *Fusarium graminearum* during colonization and sexual development on wheat. Mol Plant Microbe Interact 22:1492–1503
12. Wellen KE, Hatzivassiliou G, Sachdeva UM et al (2009) ATP-citrate lyase links cellular metabolism to histone acetylation. Science 324:1076–1080
13. Elshourbagy NA, Near JC, Kmetz PJ et al (1990) Rat ATP citrate lyase. Molecular cloning and sequence analysis of a full-length cDNA and mRNA abundance as a function of diet, organ, and age. Biol Chem 265:1430–1435
14. Bauer DE, Hatzivassiliou G, Zhao F et al (2005) ATP citrate lyase is an important component of cell growth and transformation. Oncogene 24:6314–6322
15. Mahlen A (1973) Purification and some properties of ATP citrate lyase from *Penicillium spiculisporum*. Eur J Biochem 36:342–346
16. Adams IP, Dack S, Dichinson FM et al (1997) ATP citrate lyase from *Aspergillus nidulans*. Biochem Soc Trans 25:S670
17. Nowrousian M, Kuck U, Loser K et al (2000) The fungal *acl1* and *acl2* genes encode two polypeptides with homology to the N- and C-terminal parts of the animal ATP citrate lyase polypeptide. Curr Genet 37:189–193
18. Chomczyncki P, Machey K (1995) Short technical report. Modification of the TRIZOL reagent procedure for isolation of RNA from Polysaccharide-and proteoglycan-rich sources. Biotechniques 19:942–945
19. Xu JR, Hamer JE (1996) MAP kinase and cAMP signaling regulate infection structure formation and pathogenic growth in the rice blast fungus *Magnaporthe grisea*. Genes Dev 10:2696–2706
20. Lian J, Fang X, Cai J et al (2008) Efficient expression of membrane-bound water channel protein (Aquaporin Z) in *Escherichia coli*. Protein Pept Lett 15:687–691
21. Adams IP, Dack S, Dickinson FM et al (2002) The distinctiveness of ATP:citrate lyase from *Aspergillus nidulans*. Biochim Biophys Acta 1597:36–41

Chapter 16
Optimization of Conjugated Linoleic Acid Production by *Lactobacillus planetarum*

Fan Li, Xihong He and Hao Liu

Abstract Conjugated linoleic acid (CLA), a mixture of positional and geometric isomers of linoleic acid (LA)with conjugated double bonds, has been proved to have a series of physiological functions, including anticarcinogenic activity, antiatherogenic activity, reducing body fat, and modulating immune system. In this paper, we focused on the optimization of culture medium, which is used to convert linoleic acid into CLA by *Lactobacillus planetarum*. The results showed that the optimal medium was as follows: glucose 2 %, yeast extract 4, $MgSO_4 \cdot 7H_2O$ 0.05, $MnSO_4 \cdot H_2O$ 0.05 CH_3COONa 0.2, $K_2HPO_4 \cdot 3H_2O$ 0.1 %. In this medium, the yield of CLA has increased to 0.259 g/l, while the transformation rate is 26 %.

Keywords CLA · LA · *Lactobacillus planetarum* · Optimization

16.1 Introduction

Conjugated linoleic acid (CLA) is a mixture of positional and geometric isomers of linoleic acid (18: 2 n-6 or 9, 12-cis, cis-octadecadienoic acid, LA) with conjugated double bonds [1–3]. The double bonds occur at carbon atoms 7, 9; 8, 10; 9, 11; 10, 12; 11, 13 or 12; and 14 positions, with either cis (c) or trans (t) configuration [4, 5]. Although there are more than 20 different CLA isomers, c9, t11-C18:2, and t10, c12-C18:2 are the two major CLA isomers because of their biological activities [6].

F. Li · X. He
College of Biotechnology, Tianjin University of Science and Technology, Tianjin 300457, People's Republic of China

H. Liu (✉)
College of Biotechnology, Tianjin University of Science and Technology, No. 29 13th Avenue, TEDA, Tianjin 300457, People's Republic of China
e-mail: liuhao@tust.edu.cn

T.-C. Zhang et al. (eds.), *Proceedings of the 2012 International Conference on Applied Biotechnology (ICAB 2012)*, Lecture Notes in Electrical Engineering 249,
DOI: 10.1007/978-3-642-37916-1_16, © Springer-Verlag Berlin Heidelberg 2014

CLA exists widely in ruminant food products because of the process of the bacterial biohydrogenation of LA in the rumen [7]. CLA was first discovered accidentally from fried ground beef by Pariza and Hargraves in 1987 [8]. They isolated four isomeric derivatives of LA each containing a conjugated double-bond system (designated CLA), which exhibited anticarcinogenic property. In recent years, CLA has been recognized as one of the most important polyunsaturated fatty acids (FUFAs), because some of the isomers are believed to have a series of physiological functions, such as anticarcinogenic property [9, 10], antiatherogenic property [11–13], regulating blood glucose and blood fat, reducing body fat [14–16] and improving immune system [17, 18].

CLA can be prepared commercially through alkaline isomerization or by partial hydrogenation of LA [19], but complex mixtures of byproductions unexpected are produced, which do not have beneficial effects. Accordingly, a specific and safe process is required. Biological transformation is an effective way of CLA production. In this paper, we focused on the optimization of culture medium, which is used to convert LA into specific CLA (c9, t11-C18:2, and t10, c12-C18:2) by *Lactobacillus planetarum*. The results showed that the optimal medium was as follows: glucose 2 %, yeast extract 4, $MgSO_4 \cdot 7H_2O$ 0.05, $MnSO_4 \cdot H_2O$ 0.05, CH_3COONa 0.2, $K_2HPO_4 \cdot 3H_2O$ 0.1 %. In this medium, the yield of CLA has increased to 0.259 g/l, while the transformation rate is 26 %.

16.2 Materials and Methods

16.2.1 Materials

Standard samples of LA and CLA (c9, t11-C18:2 isomer/t10, c12-C18:2 isomer) were purchased from Sigma Chemical Co. Hexane was GC pure and all other solvents or chemicals used were of analytical grade.

16.2.2 Preparation of Linoleic Acid Emulsions

Five times volume of Tween-80 and appropriate amount of distilled water were added to LA to make the final concentration 10 mg/ml. Then the solutions were mixed well by sonicating under supersonic and sterilized by filtration.

16.2.3 Strains and Culture Conditions

Lactobacillus planetarum strain used throughout this study was reserved in our laboratory of biochemical engineering, College of Biotechnology, Tianjin University of Science and Technology. The strain was activating in De Manr-Rogosa-Sharpe medium (MRS) containing glucose 2 %, yeast extract 2, $MgSO_4 \cdot 7H_2O$ 0.02,

$MnSO_4 \cdot H_2O$ 0.02, CH_3COONa 0.5, $K_2HPO_4 \cdot 3H_2O$ 0.2 % at 42 °C for 24 h before the experiments. The initial pH was 6.5 and the liquid medium was autoclaved at 121 °C for 20 min. The experiment was divided into two stages, seed culture and flask culture. The seed culture was incubated statically twice in MRS medium at 42 °C for 12 h. After inoculating with 1 % (v/v) of the inoculums, the flask culture was incubated statically in 250-ml flasks containing 100 ml of the fermentation medium (0.1 % linoleic acid emulsions were added) at 42 °C for 36 h.

16.2.4 Extraction and Analysis of Lipids

After fermentation, samples of the bacterial suspensions were centrifuged at 4000 rpm for 15 min to discard the bacteria. Fermentation broth was mixed well with twice volume of chloroform/methanol (2:1) [20, 21]. Then the organic phase, which containing the lipid acid, was separated and then concentrated under vacuum at 30 °C. The sample was added 4 ml chloroform for dissolution again.

GC method was obtained to identity the component of the samples, therefore, formation of fatty acid methyl esters (FAMEs) was necessary. First, 4 ml sulphuric acid/methanol (2 % H_2SO_4 was dissolved in methanol) was mixed well with the lipid acid in the tube with screw cap. The mixture was heated in 75 °C aqueous bath for 60 min to make the reaction completely and cooled down to room temperature. Then, 4 ml n-hexane was transformed into the above tube and mixed well. Finally, the upper layer was collected and dehydrated thoroughly with anhydrous Na_2SO_4.

FAMEs were analyzed in a GC (Gas Chromatography) system (Agilent 7890A, USA). Nitrogen was used as a carrier gas through a fused silica capillary column (CP-Sil88, 50 m × 0.25 mm × 0.2 μm). Injection (1μl) was performed with an inlet temperature of 250 °C and the flow rate of gas was 1 ml/min with a split ratio of 50:1 [22, 23]. The initial temperature was 120 °C for 3 min, and the temperature was raised to 170 at 10 °C/min, and then the temperature was further raised to 230 at 5 °C/min. Detection was carried out by flame ionization at 260 °C. The compositions of the samples were identified by comparison with relative retention times of standard LA or CLA. The quantitative of the samples was showed by peak area.

16.3 Results and Discussion

16.3.1 Growth Curve *of* Lactobacillus planetarum

The biomass of *Lactobacillus planetarum* was measured the absorbance of the bacterial suspensions by UV spectrophotometry at 600 nm (OD_{600}). According to Fig. 16.1, the growth of *Lactobacillus planetarum* got into the logarithmic phase at

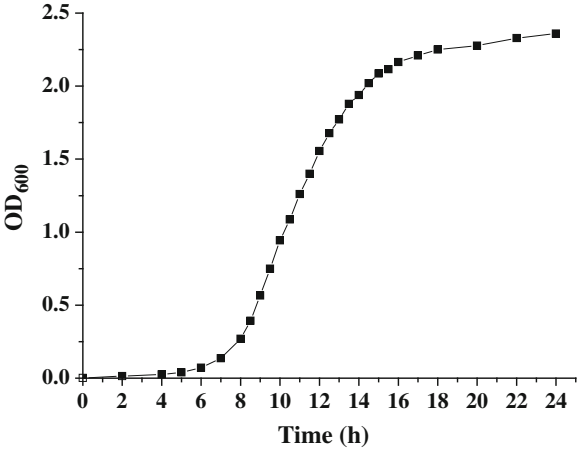

Fig. 16.1 Growth *curve* of *Lactobacillus planetarum.* The strain grew slowly at 0–6 h which was defined as the adjustment phase. 6–16 h was the logarithmic phase, while the concentration of the bacterial suspensions increased quickly. After 16 h, the growth of *Lactobacillus planetarum* reached stable phase

6 h and reached its maximum and remained stable at 16 h. The inoculation should be selected at 10 h, when the growth rate is the highest and the activity of the strain is the best.

16.3.2 Production Curve of CLA

The standard samples of LA Fig. 16.2a and CLA Fig. 16.2b were separated properly by the GC system. We analyzed the fatty acid compositions from the fermentation broth of *Lactobacillus planetarum* after the flask culture. There was clear production of CLA including two isomers Fig. 16.2c. As shown in Fig. 16.3, the lag phase was at 0–4 h, and the exponential phase is at 4–16 h with the highest growth rates. After 16 h, the growth of the strain reached the stationary phase because of the stable absorbance. There was a drastic decrease in reducing sugar, and the biomass increased after entering the exponential phase. CLA cannot be detected until 8 h, but the quantity of CLA production was little and the rate was lower relatively. There was a significant increase of CLA production at 12–24 h, and the maximum CLA concentrations were 0.0455 g/l at 24 h. After 24 h, the yield of CLA presented a trend of decline, because there is other metabolic pathway in *Lactobacillus planetarum*, which can convert LA to other metabolites.

16.3.3 Effect of Carbon Sources on CLA Production

Carbohydrates are an important kind of nutrients for the growth and development of bacteria, and a major component of the cytoskeleton. The functions of carbon sources on the metabolism of microorganism are mainly to provide carbon frame

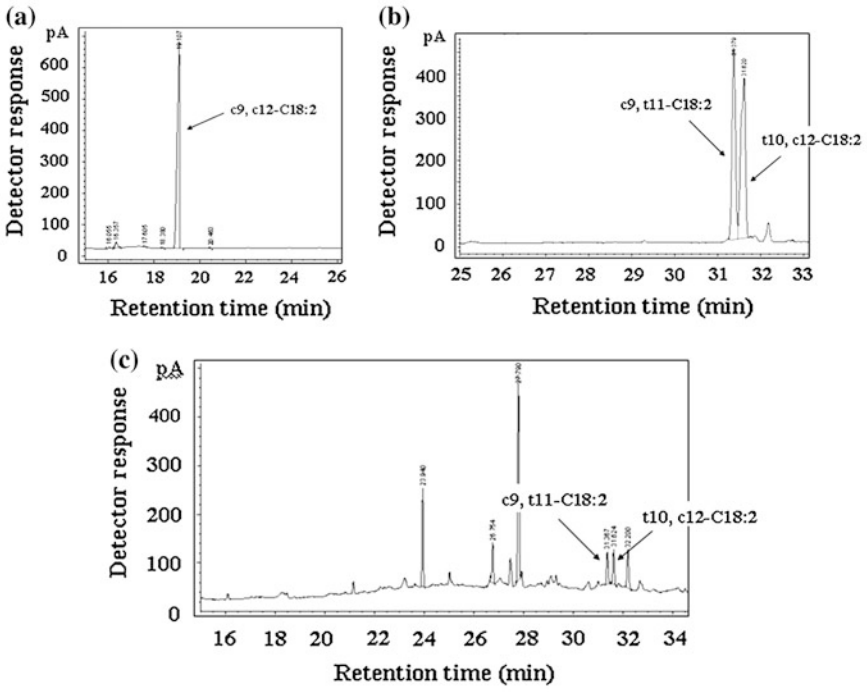

Fig. 16.2 Gas chromatographic analysis of fatty acid methyl esters (FAMEs). **a** Shows the chromatogram of the standard sample of LA: the retention time was 19.107 min. **b** Shows the chromatogram of the standard sample of CLA: c9, t11-C18:2 was at 31.379 and t10, c11-C18:2 was at 31.620 min. **c** The lipids were extracted from the fermentation broth of *Lactobacillus planetarum*, esterified fatty acids were transmethylated and analyzed by GC as described under materials and methods

to the cells and the metabolites, in addition to provide the energy to life activities of cells. In this study, glucose, fructose, sucrose, lactose, maltose, and starch were added, respectively, to the initial medium as the only carbon source with 2 % concentration. Figure 16.4 indicates that *Lactobacillus planetarum* can make use of glucose, sucrose, and lactose to convert LA into CLA. A highest production of CLA was obtained when glucose were selected as carbon source, the CLA concentration was 0.0639 g/l. In addition, with the advantages of simple component and low price, glucose was chosen as the carbon source.

16.3.4 Effect of Nitrogen Sources on CLA Production

Microbial growth and product synthesis need nitrogen source. Nitrogen sources are mainly used to consist of somatic cell material such as amino acids, proteins, and nucleic acids, and nitrogen metabolites synthesis. Tryptone (T), yeast extract (Y),

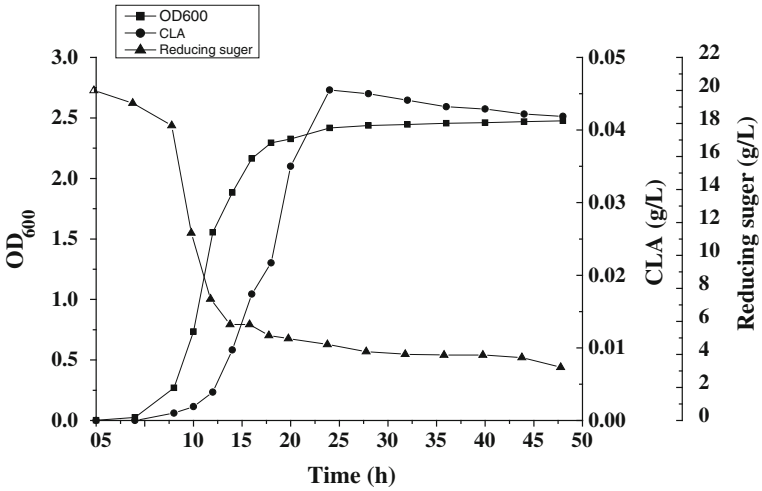

Fig. 16.3 Production of CLA in the fermentation broth of *Lactobacillus planetarum*. *Lactobacillus planetarum* was cultured statically in MRS medium in 250-ml flasks at 42 °C. (■) The UV absorbance of the bacterial suspensions at different times at 600 nm; (●) The concentrations of CLA; (▲) The concentrations of reducing sugar

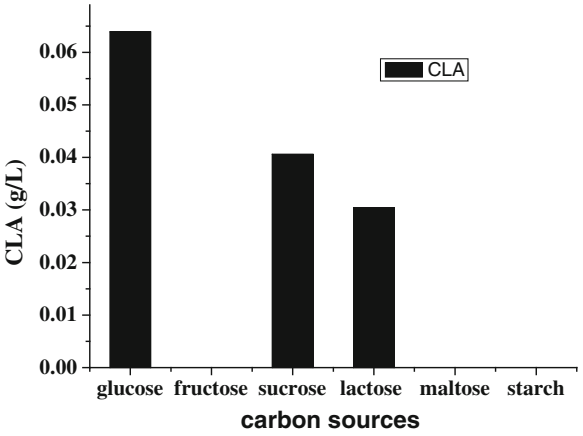

Fig. 16.4 Effect of carbon sources on CLA production. CLA in the fermentation broth was detected by GC method when the glucose, sucrose, or lactose was selected as the only carbon source. The highest concentration of CLA was 0.0639 g/l, when the carbon source was glucose

beef extract (B), corn steep liquor (C), diammonium citrate (D), and $(NH_4)_2SO_4$ (N) was added, respectively, to the initial medium as the only nitrogen source with 3 % concentration, while MRS medium with the compound nitrogen sources preformed as a comparison. Figure 16.5 shows that CLA can be produced in the medium containing whether organic nitrogen source or inorganic nitrogen source. There is a marked increase in CLA production (0.112 g/l) when yeast extract was applied as the only nitrogen source. As a result, yeast extract was selected as the nitrogen source.

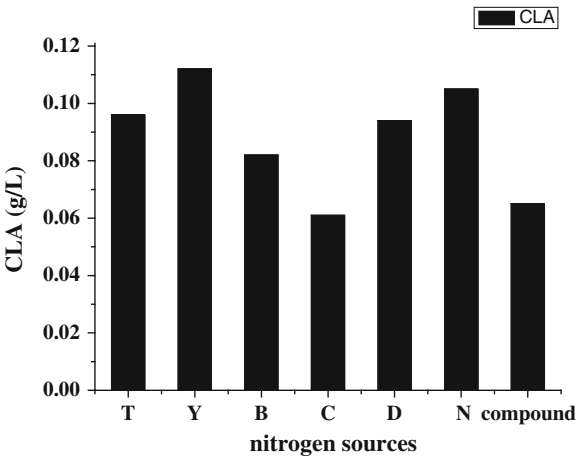

Fig. 16.5 Effect of nitrogen sources on CLA production. CLA can be detected in each medium and the productions were improved obviously. The concentration of CLA were almost the same (respectively was 0.112 and 0.105 g/l) when yeast or $(NH_4)_2SO_4$ was as the only nitrogen source

16.3.5 Effect of Carbon Nitrogen Ration on CLA Production

A number of researches found that the proper carbon nitrogen ration is beneficial to microbial fermentation. No matter too low or too high carbon nitrogen ration is not good for cell growth and exogenous protein expression and accumulation, because too low leads to autocatalysis early; too high make bacterial metabolism do not balance, eventually go against the accumulation of products. Based on the experiments above, glucose was as the carbon source, while yeast extract was as the nitrogen source. The results were investigated by setting different carbon nitrogen ration containing 1:1, 1:2, 1:3, 2:1, 2:3, 4:3. Figure 16.6 shows that when the carbon nitrogen ration is too low (1:3) or too high (2:1), the productions of CLA decreased correspondingly. The maximum CLA production was 0.1929 g/l, when the carbon nitrogen ration was 1:2 (glucose 2 % and yeast extract 4 %).

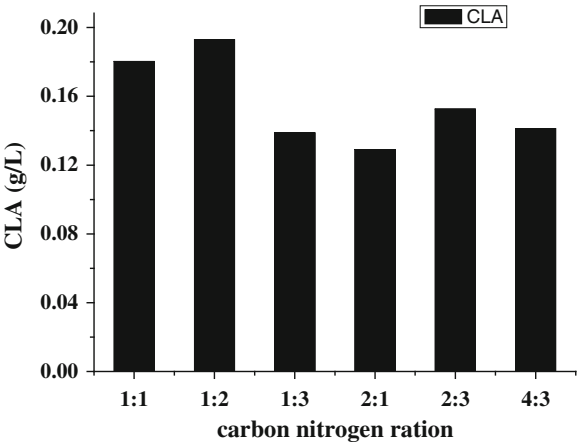

Fig. 16.6 Effect of carbon nitrogen ration on CLA production. When the carbon nitrogen ration was 1:2, the concentration of CLA reached the maximum

16.3.6 Effect of Inorganic Salts on CLA Production

As most other microorganisms, the participation of inorganic salts was needed in the process of the growth and metabolism. The orthogonal matrix [L16 (5^4)] was used to study the effect of these important growth factors on CLA production Table 16.1. A total of 16 experiments were necessary, with 3 parallel ones in each of them Table 16.2.

According to the experiment results shown in Table 16.3, inorganic salts can obviously affect the productions of CLA. The effect of factors on CLA concentration could be ordered as A > B > D > C, i.e. $MgSO_4$ > $MnSO_4$ > CH_3COONa > KH_2PO_4. The optimum composition obtained by range analysis was $A_3B_3C_1D_2$. Therefore, $MgSO_4$ concentration proved is the most important factor, the $MnSO_4$ is the second.

Table 16.1 Experimental factors and their levels for orthogonal projects

Experimental factors	$MgSO_4$ (%) A	$MnSO_4$ (%) B	KH_2PO_4 (%) C	CH_3COONa (%) D	Blank E
1	0.01	0.01	0.1	0.1	1
2	0.02	0.02	0.2	0.2	2
3	0.05	0.05	0.3	0.5	3
4	1.00	1.00	0.4	0.8	4

Table 16.2 Application of L 16 (5^4) orthogonal projects to the CLA production

Run	A	B	C	D	E	CLA (g/l)
1	0.1	0.1	1	1	1	0.138 ± 0.0026
2	0.1	0.2	2	2	2	0.072 ± 0.0017
3	0.1	0.5	3	5	3	0.053 ± 0.0029
4	0.1	1.0	4	8	4	0.058 ± 0.0021
5	0.2	0.1	2	5	4	0.041 ± 0.0005
6	0.2	0.2	1	8	3	0.065 ± 0.0017
7	0.2	0.5	4	1	2	0.061 ± 0.0024
8	0.2	1.0	3	2	1	0.134 ± 0.0019
9	0.5	0.1	3	8	2	0.132 ± 0.0005
10	0.5	0.2	4	5	1	0.205 ± 0.0017
11	0.5	0.5	1	2	4	0.259 ± 0.0021
12	0.5	1.0	2	1	3	0.151 ± 0.0040
13	1.0	0.1	4	2	3	0.157 ± 0.0005
14	1.0	0.2	3	1	4	0.092 ± 0.0017
15	1.0	0.5	2	8	1	0.257 ± 0.0012
16	1.0	1.0	1	5	2	0.128 ± 0.0037

Table 16.3 The range analysis of L 16 (5^4) orthogonal experiment of CLA production

	A	B	C	D	E
M1	0.080	0.117	0.148	0.110	0.183
M2	0.075	0.108	0.130	0.155	0.098
M3	0.187	0.158	0.103	0.107	0.107
M4	0.159	0.118	0.120	0.128	0.112
Rf	0.112	0.050	0.045	0.048	0.085
Optimal level	3	3	1	2	

16.4 Conclusions

Through the experiments, the optimum cultivation conditions for CLA production were determined as: glucose 2 %, yeast extract 4, $MgSO_4$ 0.05, $MnSO_4$ 0.05, CH_3COONa 0.2, KH_2PO_4 0.1 %. The seed culture was incubated statically twice in MRS medium at 42 °C for 10 h. The flask culture was incubated statically in 250-ml flasks containing 100 ml of the fermentation medium (0.1 % linoleic acid emulsions were added) 42 °C for 24 h after inoculating with 1 % (v/v) of the inoculums at. In this condition, the yield of CLA has increased to 0.259 g/l, while the transformation rate is 26 %. This paper is an attempt to study different mediums for CLA production of *Lactobacillus plantarum* through flask culture experiments. Of course, during the actual production, there are more factors to consider, such as the concentration of LA added to the medium. Besides, due to CLA with conjugated double bonds is not stable, so the protection of nitrogen gas is necessary in the process of extraction, which is one of issues in the large scale production.

Acknowledgments The authors gratefully acknowledge the support of the seventh Singapore–China JRP (2011DFA31280) the National Nature Science Foundation of China (No. 31201282), the National High Technology Research and Development Program of China (No. SS2012AA023408, 2012AA020403) and the Cheung Kong Scholars Programme of China (No. IRT1166).

References

1. Lp C, Chin SF, Scimeca JA et al (1991) Mammary cancer prevention by conjugated dienoic derivative of linoleic acid. Cancer Res 51:6118–6124
2. Chin SF, Liu W, Storkson JM et al (1992) Dietary sources of conjugated dienoic isomers of linoleic acid, a newly recognized class of anticarcinogens. J Food Compos Anal 5:185–197
3. Zhao HW, Lv JP, Li SR (2011) Production of conjugated linoleic acid by whole-cell of *Lactobacillus plantarum* A6-1F. Biotechnol Biotechnol Eq 25:2266–2272
4. Sieber R, Collomb M, Aeschlimann A et al (2004) Impact of microbial cultures on conjugated linoleic acid in dairy products. Int Dairy J 14:1–15
5. Bhattacharya A, Banu J, Rahman M et al (2006) Biological effects of conjugated linoleic acids in health and disease. J Nutr Biochem 17:789–810

6. Pariza MW, Park Y, Cook ME (2001) The biologically active isomers of conhugated lionleic acid. Prog Lipid Res 40:283–298
7. Alonso L, Cuesta EP, Gilliland SE (2003) Production of free conhugated linoleic acid by *Lactobacillus acidophilus* and *Lactobacillus casei* of human intestinal origin. J Dairy Sci 86:1941–1946
8. Ha YL, Grimm NK, Pariza MW (1987) Anticarcinogens from fried ground beef: heat-altered derivatives of linoleic acid. Carcinogenesis 8:1881–1887
9. Pariza MW, Hargraves WA (1984) A beef-derived mutagenesis modulator inhibits initiation of mouse epidermal tumors by 7,12-dimethylbenz [a] anthracene. Carcinogenesis 6:591–593
10. Parodi PW (1994) Conjugated linoleic acid-an anticarcinogenic fatty acid present in milk fat. Aust J Dairy Technol 47:93–97
11. Whigham LD, Cook ME, Atkinson RL (2004) Conjugated linoleic acid: implications for human health. Pharma Res 42:503–610
12. Lee KN, Kritchevsky D, Pariza MW (1994) Conjugated linoleic acid and atherosclerosis in rabbits. Atherosclerosis 108:19–25
13. Kritchevsky D, Tepper SA, Wright S et al (2000) Influence of conjugated linoleic acid (CLA) on establishment and progression of atherosclerosis in rabbits. J Am Col Nutr 19:472S–477S
14. Dugan MER, Aalhus JL, Jeremiah LE et al (1999) The effects of feeding conjugated linoleic acid on subsequent pork quality. Can J Anim Sci 79:45–51
15. Park Y, Albright KJ, Liu W et al (1997) Effect of conjugated linoleic acid on body composition in mice. Lipids 32:853–858
16. Smedman A, Vessby B (2001) Conjugated linoleic acid supplementation in humans-metabolic effects. Lipids 36:773–781
17. Chew BP, Wong TS, Shultz TD et al (1997) Effects of conjugated dienoic derivatives of linoleic acid and beta-carotene in modulating lymphocyte and macrophage function. Anticancer Res 17:1099–1106
18. Wong MW, Chew BP, Wong TS et al (1991) Effects of dietary conjugated linoleic acid on lymphocyte function and growth of mammary tumors in mice. Anticancer Res 17:987–993
19. Kepler CR, Hirons KP, McNeill JJ et al (1966) Intermediates and products of the biohydrogenation of linoleic acid by *Butyrivibrio fibrisolvens*. J Biol Chem 241:1350–1354
20. Wang LM, Lv JP, Chu ZQ et al (2007) Production of conjugated linoleic acid by *Propionibacterium freudenreichii*. Food Chem 103:313–318
21. Bligh EG, Dyer WJ (1959) A rapid method of total lipid extraction and purification. Can J Biochem Physiol 37:911–917
22. Kramer JKG, Fellner V, Dugan MER et al (1997) Evaluating acid and base catalysts in the methylation of milk and rumen fatty acids with special emphasis on conjugated dieners and total trans fatty acids. Lipids 32:1219–1228
23. Ogawa J, Matsumura K, Kishion S et al (2001) Conjugated linoleic acid accumulation via 10-hydtoxy-12-octadecaenoic acid during microaerobic transformation of linoleic acid by *Lactobacillus acidophilus*. Appl Environ Microbiol 67:1246–1252

Chapter 17
Characterization of a 2,3-Butanediol Producing Bacterial Strain and Optimization of Fermentation Medium

Songsong Gao, Hongjiang Yang and Xuying Qin

Abstract A bacterial strain G12 capable of producing high content of 2,3-butanediol (2,3-BD, BD) was isolated from raw milk samples. With the analysis of its 16S rRNA gene sequence, strain G12 was identified as *Serratia marcescens*. Carbon source evaluation experiments showed that with glycerol as carbon source, strain G12 produced relatively high amount of 2,3-BD and the lowest amount of byproduct acetoin among the tested carbon sources. Furthermore, the optimal fermentation medium was determined by single factor experiments and orthogonal experimental design, and it was composed of glycerin 130 g/L, peptone 16 g/L, yeast extract 5 g/L, K_2HPO_4 1 g/L, and $MnSO_4 \cdot 7H_2O$ 0.025 g/L. Confirmation experiments were also performed. The final yield of 2,3-BD in the shaking-flask was up to 37.400 g/L, and the substrate conversion rate was 79.62 % of the theoretical value.

Keywords 2,3-butanediol · *Serratia marcescens* · Glycerol · Optimization of fermentation medium

17.1 Introduction

Nowadays, due to the shortage of oil sources supplies and the rising of petroleum price, the bulk chemical products manufactured by microbial fermentation would be the ideal substitutes [1, 2]. In order to meet the future energy needs, it is necessary to develop the renewable energy sources especially bio-based chemical compounds such as ethanol, butanol, and butanediol (BD) [3, 4].

S. Gao · H. Yang (✉) · X. Qin
Key Laboratory of Industrial Microbiology, Ministry of Education, Tianjin Key Laboratory of Industrial Microbiology, College of Biotechnology, Tianjin University of Science and Technology, Tianjin 300457, China
e-mail: hongjiangyang@tust.edu.cn

T.-C. Zhang et al. (eds.), *Proceedings of the 2012 International Conference on Applied Biotechnology (ICAB 2012)*, Lecture Notes in Electrical Engineering 249,
DOI: 10.1007/978-3-642-37916-1_17, © Springer-Verlag Berlin Heidelberg 2014

BD could be used in the production of antifreeze agents [5], plastics, solvents [6], drug carriers [6]. Through dehydrogenation, BD could be converted to acetoin (AC) and diacetyl, which could be used as flavoring agents in the manufacture of margarine and cosmetics for daily life [7, 8].

Compared with ethanol and butanols, 2,3-butanediol showed relatively low toxicity to microbial cells during fermentation process [9]. BD was produced from the condensation of 2 pyruvate molecules. There were many bacterial species could convert carbon sources to BD, such as *Klebsiella pneumoniae* [10], *Klebsiella terrigena* [11], *Enterobacter aerogenes* [9], *Bacillus polymyxa* [12], *Bacillus licheniformis* [13], and *Serratia marcescens* [14]. Among these microbes, *S. marcescens* is a species of Gram-negative bacterium and ubiquitously present in the environment. It can grow in temperatures ranging from 5 to 40 °C and in pH values ranging from 5 to 9 [15]. In addition, *Serratia marcescens* has a wide range of substrates. *S. marcescens* strains were often chosen as fermenters for BD production studies [16]. In shake-flask fermentation, a *S. marcescens* strain produced 39.270 g/L BD with sucrose as carbon source [17], while *S. marcescens* H30 which selected from mutagenesis achieved a BD concentration of 44.790 g/L [18].

In this work, a *S. marcescens* strain was isolated from fresh raw milk samples and identified with 16S rRNA gene analysis. Furthermore, the isolate was quantitatively characterized with its ability of BD production under various conditions. The optimal fermentation medium was determined by single factor experiments and orthogonal experimental design.

17.2 Materials and Methods

17.2.1 Samples and Media

The raw milk samples were collected from Zhangjiakou, Hebei Province. The samples were stored at 4 °C before analyzing. LB medium was used for routinely culturing and it was composed of yeast extract 5 g/L, peptone 10 g/L, and NaCl 10 g/L. MR-VP medium is used to screen microbes secreting neutral compounds [19], it contained glucose 5 g/L, peptone 7 g/L, and K_2HPO_4 5 g/L. The seed medium was composed of glucose 40 g/L, yeast extract 10 g/L $(NH_4)_2SO_4$ 1 g/L, and K_2HPO_4 1 g/L. Fermentation medium was composed of glucose 100 g/L, yeast extract 5 g/L, corn steep liquor 20 g/L, $MnSO_4$ 0.025 g/L, and K_2HPO_4 1 g/L.

17.2.2 Isolation of Microbes Producing BD

Milk samples were subjected to 10-fold serial dilutions before spreading on L-agar plates. The plates were incubated at 35 °C for 24 h.

Colonies of different morphologies were picked out and inoculated in 5 mL MR-VP medium for cultivation at 35 °C for 24 h. After incubation, take out 2 mL fermentation broth and add 5 drops methyl red, the culture will show red or yellow color depending on what kind of chemicals synthesized by the tested strains. After recording the colors, add 0.6 mL α-naphthol and 0.2 mL 40 % KOH to the remaining fermentation broth and observe the color change after standing 20 min [19–22].

The strains selected from MR-VP test were continuously cultivated in 5 mL seed medium at 35 °C to prepare primary and secondary seeding cultures. The secondary seeding cultures were transferred into 30 mL fermentation medium at 5 % inoculum sizes. After cultivation at 35 °C for 72 h in 250 mL shake flasks, fermentation samples were centrifuged at 12,000 rpm for 10 min. The supernatants were subjected to GC analysis of BD and AC quantitatively.

17.2.3 Gas Chromatography Analysis

Agilent 7890A with column HP–INNOWAX 1909IN-213 (30 m * 0.32 mm * 0.25 μm) was used. Sample preparation includes centrifugation and filtering with 0.25 μm filter. Isoamyl alcohol was used as internal control standard. The main parameters were set up according to the manual with modifications [18]. Briefly, for analysis of BC and AC, the temperature of column oven was held at 95 °C for 1 min, and then programmed at 10 °C/min to 150 °C and held for 2 min, and then programmed at 2 °C/min to 160 °C and held for 2 min; the flow rates of nitrogen gas, hydrogen gas, and air were 2,30, and 300 mL/min, respectively. The injection port temperature was maintained at 250 °C and the dual hydrogen flame ionization detector temperature was 250 °C.

For glycerol analysis, the same column was used and the temperature of column oven was held at 100 °C for 1 min, and then programmed at 10 °C/min to 220 °C and held for 3 min; the flow rates of nitrogen gas, hydrogen gas, and air were 4, 30, and 300 mL/min, respectively. The injection port temperature was maintained at 300 °C and the dual hydrogen flame ionization detector temperature was 320 °C.

17.2.4 Identification of the Isolated Strains with 16S rRNA Analysis

Bacterial genomic DNA was extracted as described previously [23, 24]. Specific primers 27F and 1492R were used to amplify bacterial 16S rRNA gene fragment, and the primers sequences were as follows [25]: 27F: 5′-AGAGTTTGA TCCTGGCTCAG-3′ (corresponding to *Escherichia coli* positions 8 to 27) 1492R: 5′-GGTTACCTTGTTACGACTT-3′ (corresponding to *Escherichia coli* positions 1507 to 1492)

The PCR reaction system was 50 μL and the parameters include 1 cycle of denaturation at 94 °C for 5 min,; 33 cycles of denaturation at 94 °C for 40 S, annealing at 51 °C for 2 min, and extension at 72 °C for 3 min; 1 cycle of extension at 72 °C for 10 min.

PCR fragments were purified from gel and subjected to sequencing analysis with the same primers used in PCR. Sequence homology search was carried out with BLAST provided by NCBI to identify the isolates [26]. The isolates were grouped to genus level with Classifier program (Ribosomal Database Project II) [27].

17.2.5 Optimization of Fermentation Medium for the Isolate

For fermentations, the primary seed culture was prepared by cultivation at 35 °C for 16 h, and then 1 mL culture were transferred to 5 mL fresh seed medium for continuously cultivation for 8 h at 35 °C. The culture was used as secondary seed and was transferred to 30 mL fermentation medium at 5% inoculums size in 250 mL shake flask.

Single factor experiments were used to analyze the influences of the types and concentrations of carbon sources, nitrogen sources, and growth factor, respectively [28]. In brief, fermentation medium was used as the basic medium. To investigate the effects of carbon source on BD synthesis, glucose was replaced by maltose, sucrose, xylose, glycerin, fructose, or sodium citrate in fermentations. To investigate the effects of nitrogen source on BD synthesis, corn steep liquor was replaced by peptone, urea, ammonium sulfate, or ammonium chloride in fermentations. The effects of concentrations of the selected carbon or nitrogen source on BD yields were also analyzed.

Orthogonal experimental design was used to optimize the fermentation medium to produce the highest level of BD [28].

17.2.6 Other Methods

The biomass of fermentation broth was determined at different times by the optical density (OD_{600}) at 600 nm in a spectrophotometer (UV-722). The glucose concentration of fermentation broth at different times was determined by the SBA-40C biosensor.

17.3 Results and Analysis

17.3.1 Isolation of BD Producing Strains

Colonies with different morphologies were selected from L-agar plates for subsequent screenings. Since AC was the precursor of BD metabolite in most microorganisms [29], microorganisms synthesizing AC were the screening targets. Via MR-VP tests, 14 strains (G6, G7, G9, G10, G11, G12, G13, G16, G17, G19, G22, G23, G31, and G33) were selected. Their fermentation broths turned yellow when the methyl red was added, indicating only residual amount of acids produced [22]. With the addition of α-naphthol and KOH, the fermentation broths turned red, suggesting AC or diacetyl compounds likely produced by the tested strains (Fig. 17.1) [19–22].

To further confirm if the isolated strains synthesize the neutral compounds, their fermentation broths were analyzed with GC according to the descriptions in Materials and Methods. At the end of fermentation, strain G12 produced 26.730 g/L BD, the highest yield of the 14 strains and selected for subsequent fermentation processes.

17.3.2 Identification of Strain G12 by 16S rRNA gene Sequence Analysis

The amplified 16S rRNA gene fragment was purified and sequenced. As described in Materials and methods, the obtained sequence was analyzed with BLAST and Classifier, respectively. The analyses showed that G12 belonged to the genus of *Serratia* and was close to *S. marcescens* Db11 [18] with similarity of 98%. Previous studies have shown that *S. marcescens* was negative for the methyl red (MR) test due to their production of 2,3-butanediol and ethanol, but positive for Voges-Proskauer (VP) test indicating its ability to convert pyruvate to AC.

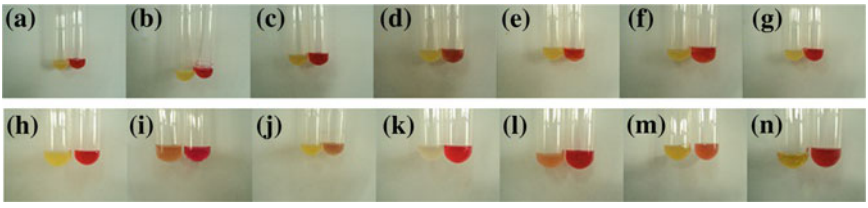

Fig. 17.1 MR-VP screening test of the isolated strains. Two panels through *A* to *N* representing the cultures of the strains G6, G7, G9, G10, G11, G12, G13, G16, G17, G19, G22, G23, G31, and G33. A drop of methyl red was added into the left test tubes, fermentation broth showing yellow color showing neutral chemicals synthesized; α-naphthol and KOH was added into the right test tubes, fermentation broth showing red color indicating the existence of acetoin or diacetyl

17.3.3 The Effect of Different Carbon Sources on the BD Production

Various carbon sources were tested in fermentation processes. BD yields in fermentation broths were analyzed. The results were shown in Fig. 17.2. When sucrose (100 g/L) was added as sole carbon source, the total amount of BD and AC reached the highest level 29.365 g/L. However, BD production was only 9.268 g/L, much lower than the yield 18.986 g/L using glycerin as sole carbon source. Glycerin was eventually chosen as suitable carbon source for further experiments.

Fermentation medium was modified with adjustment of glycerin to various final concentrations. The prepared media were used in fermentation processes to investigate the effects of glycerin concentrations on BD production. When glycerin concentration was 120 g/L, the yield of BD achieved the highest amount 35.208 g/L while the byproduct AC was only 2.172 g/L (Fig. 17.3). The substrate conversion rate was 71.82 % of the theoretical value. The acidity range of cultures was narrow in end of fermentations.

17.3.4 The Effect of Different Nitrogen Sources on BD Production

As described in Materials and methods, nitrogen sources effects on BD production were tested. The modified fermentation medium with 120 g/L glycerin was used

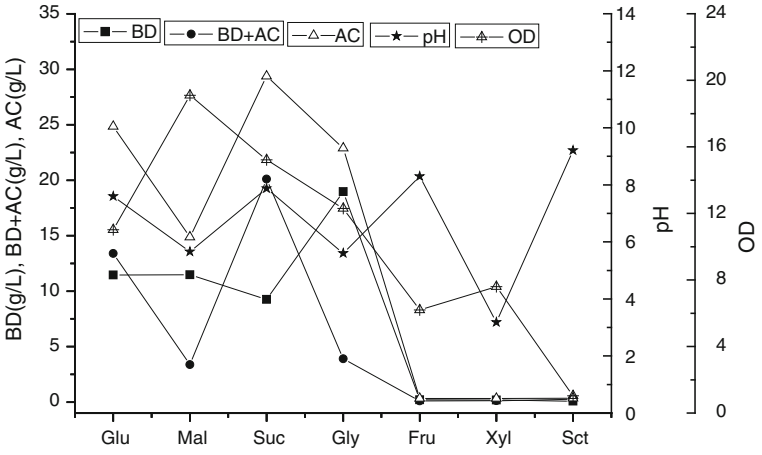

Fig. 17.2 The effect of different carbon sources on BD production. BD, 2,3-butanediol; AC, acetoin; BD+AC, the total amount of BD and AC; pH, the acidity of fermentation broth at the end of fermentation; OD_{600}, the cell density measured at the wave length 600 nm. Glu, glucose; Mal, maltose; Suc, sucrose; Gly, glycerin; Fru, fructose; Xyl, xylose; Sct, sodium citrate

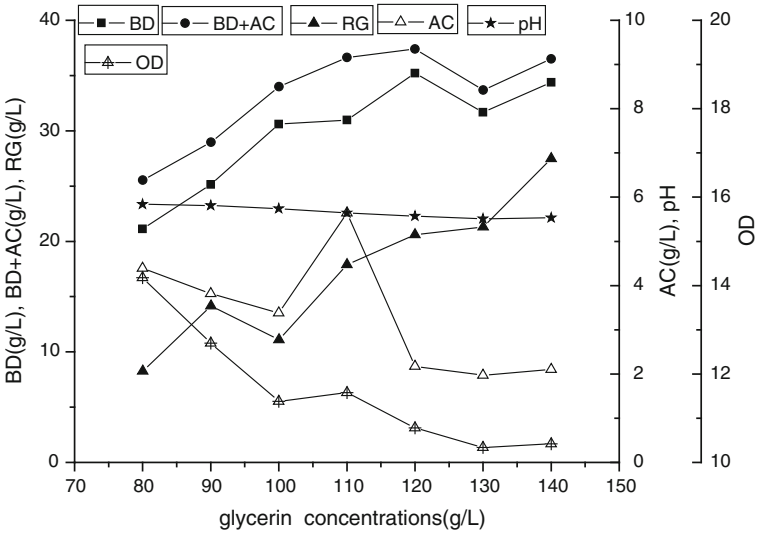

Fig. 17.3 The effects of glycerin concentrations on BD yields. BD, 2,3-butanediol; AC, acetoin; BD+AC, the total amount of BD and AC; RG, remaining glycerin in fermentation broth; pH, the acidity of fermentation broth at the end of fermentation; OD_{600}, the cell density measured at the wave length 600 nm

with various nitrogen sources (10 g/L). The experiment results showed that BD yield reached the highest level 36.529 g/L when peptone was used as nitrogen source (Fig. 17.4).

Various concentrations of peptone were used in fermentation processes to determine the best concentration for BD production. As shown in Fig. 17.5, BD yield reached the highest level 37.348 g/L when peptone was 14 g/L in the modified fermentation medium.

17.3.5 Optimization of Yeast Extract Concentration for BD Production

A series of concentrations of yeast extract were used in fermentation processes to determine the best concentration for BD production. The yield of BD was highest 37.961 g/L when yeast extract concentration was 7 g/L, however, the yield of BD was 37.371 g/L when yeast extract was 5 g/L (Fig. 17.6). Taking in account of the price of yeast extract, 5 g/L was chosen as the optimal yeast extract concentration.

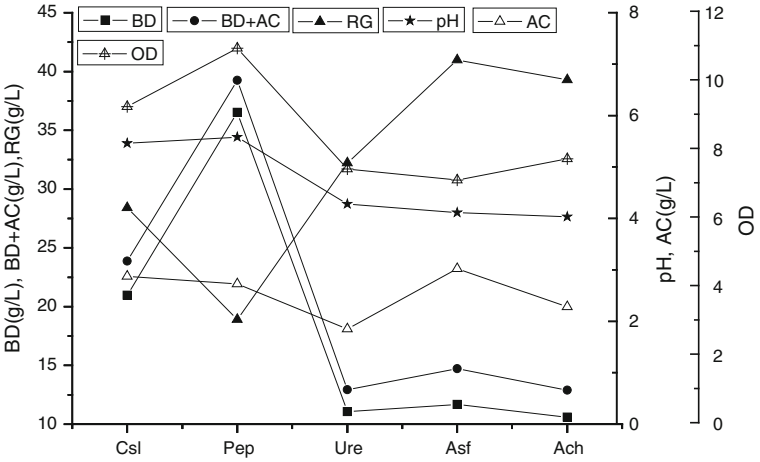

Fig. 17.4 The effect of different nitrogen sources on BD production. BD, 2,3-butanediol; AC, acetoin; BD+AC, the total amount of BD and AC; RG, remaining glycerin in fermentation broth; pH, the acidity of fermentation broth at the end of fermentation; OD_{600}, the cell density measured at the wave length 600 nm; Csl, corn steep liquor; Pep, peptone; Ura, urea; Asf, ammonium sulfate; Ach, ammonium chloride

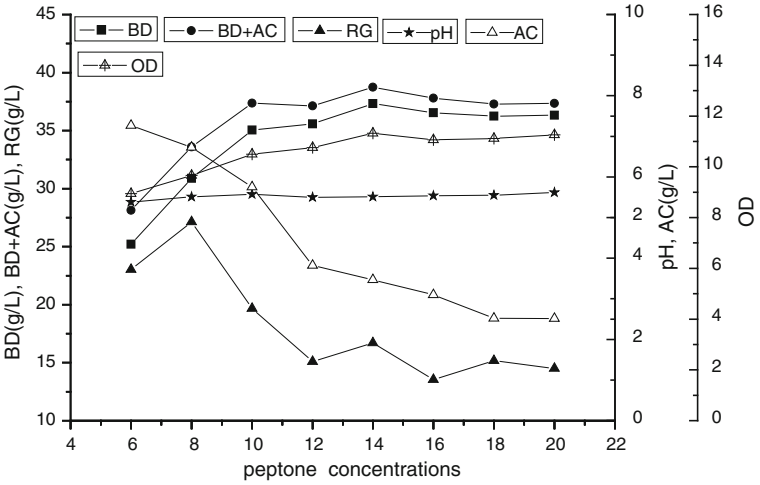

Fig. 17.5 The effects of peptone concentrations on BD production. BD, 2,3-butanediol; AC, acetoin; BD+AC, the total amount of BD and AC; RG, remaining glycerin in fermentation broth; pH, the acidity of fermentation broth at the end of fermentation; OD_{600}, the cell density measured at the wave length 600 nm

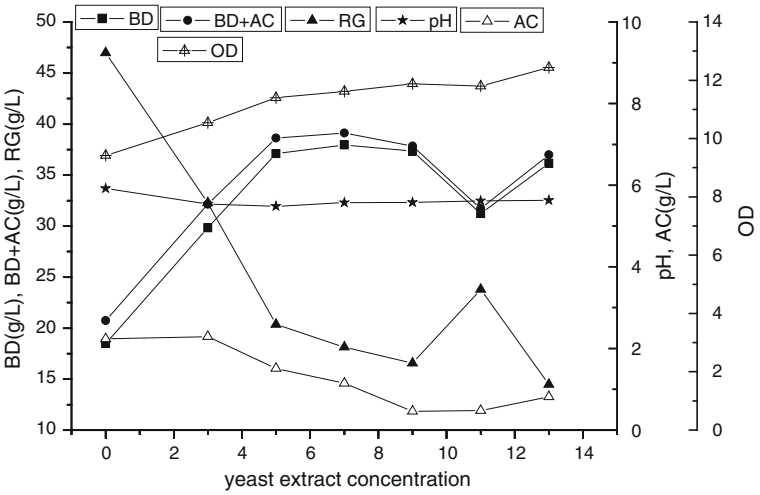

Fig. 17.6 The effect of yeast extract concentration on BD production. BD, 2,3-butanediol; AC, acetoin; BD+AC, the total amount of BD and AC; RG, remaining glycerin in fermentation broth; pH, the acidity of fermentation broth at the end of fermentation; OD_{600}, the cell density measured at the wave length 600 nm

17.3.6 Orthogonal Experimental Design on BD Production

Glycerin, peptone, and yeast extract were selected as three single factors for orthogonal experimental design, and three levels were taken into considerations (Table 17.1). The array was shown in Table 17.2.

With the analysis, the effects of the factors on BD synthesis were in a order of yeast extract> glycerol> peptone, and the best combination was A3B3C2. Namely, the optimal fermentation medium was composed of glycerol 130 g/L, peptone 16 g/L, yeast extract 5 g/L, $MnSO_4$ 0.025 g/L, and K_2HPO_4 1 g/L. Confirmation experiments were also performed. The final yield of BD in the shaking-flask was up to 37.400 g/L, and the substrate conversion rate was 79.62% of the theoretical value. The BD production level was similar to the results reported previously [17, 18]. In addition, glycerin was adopted as carbon source in this work, which might be replaced with the byproducts from biodiesel production [30]. This would decrease the cost for BD production and add value to biodiesel production process [31].

Table 17.1 Factors and levels for the orthogonal experimental design

Level	Factor A glycerol (g/L)	Factor B peptone (g/L)	Factor C yeast extract (g/L)
1	110	12	3
2	120	14	5
3	130	16	7

Table 17.2 Orthogonal experiment design for optimization of fermentation medium

Number	A	B	C	BD (g/L)
1	1	1	1	26.930
2	1	2	2	35.898
3	1	3	3	31.875
4	2	1	2	33.263
5	2	2	3	37.074
6	2	3	1	32.648
7	3	1	3	35.986
8	3	2	1	27.766
9	3	3	2	39.238
$T_1/3$	31.568	32.060	29.115	
$T_2/3$	34.328	33.579	36.133	
$T_3/3$	34.330	34.587	34.978	
R	2.762	2.527	7.018	

17.4 Conclusions

In this work, a *S. marcescens* strain G12 which produced BD was selected from raw milk samples. Fermentation medium optimization was carried out with single factors tests and orthogonal experiment design analysis. The final yield of BD in shaking-flask was up to 37.400 g/L, and the substrate conversion rate was 79.62 % of the theoretical value. The results suggested that strain G12 could be a good candidates for BD production. In future, glycerin waste from biodiesel production will be tested to investigate if it can replace pure glycerin as carbon source in BD production.

Acknowledgments This work was partly supported by The National Natural Science Foundation of China (Grant No. 30970114) and The National Key Technology R&D Program of China (Grant No. 2011BAC11B05).

References

1. Kaul RH, Törnvall U, Gustafsson L et al (2007) Industrial biotechnology for the production of bio-based chemicals-a cradle-to-grave perspective. Trends Biotechnol 25:119–124
2. Kamm B, Kamm M (2004) Principles of biorefineries. Appl Microbiol Biot 64:137–145
3. Shota A, Taizo H, James C (2008) Non-fermentative pathways for synthesis of branched-chain higher alcohols as biofuels. Nature 451:86–89
4. Fischer CR, Marcuschamer DK, Stephanopoulos G (2008) Selection and optimization of microbialhosts for biofuelsproduction. Metab Eng 10:295–304
5. Soltys KA, Batta AK, Koneru B (2001) Successful nonfreezing, subzero preservation of rat liver with 2,3-butanediol and typeI antifreeze protein Source. J Surg Res 96:30–34
6. Garg SK, Jain A (1995) Fermentative production of 2,3-butanediol: a review Source. Fuel Cells 36:275***–275
7. Xiu ZL, Zeng AP (2008) Present state and perspective of downstream processing of biologically produced 1,3-propanediol and 2,3-butanediol. Appl Microbiol Biot 78:917–926

8. Celińska E, Grajek W (2009) Biotechnological production of 2,3-butanediol current state and prospects. Biotechnol Adv 27:715–725
9. Zeng A, Biebl H, Deckwer WD (1990) Effect of pH and acetic acid on growth and 2,3-butanediol production of *Enterobacter aerogenes* in continuous culture. Appl Microbiol Biot 33:485–489
10. Yu EK, Saddler JN (1983) Fed-batch approach to production of 2,3-butanediol by *Klebsiella pneumoniae* grown on high substrate concentrations. Appl Eeviron Microb 46:630–635
11. Mayer D, Schlensog V, Boeck A (1995) Identification of the transcriptional activator controlling the butanediol fermentation pathway in *Klebsiella terrigena*. J Bacteriol 177:5261–5269
12. Mase DE, Jansen NB, Tsao GT (1988) Production of optically active 2,3-butanediol by *Bacillus polymyxa*. Biotechnol Bioeng 31:366–377
13. Perego P, Converti A, Borghi AD et al (2000) 2,3-Butanediol production by *Enterobacter aerogenes*: selection of the optimal conditions and application to food industry residues. Bioproc Biosyst Eng 23:613–620
14. Neish AC, Robertson FM, Blackwood AC et al (1947) Production and properties of 2,3-Butanediol. XVIII. dissimilation of glucose by *Serratia marcescens*. Can J Res 25:65–69
15. Grimont PA, Grimont F, Rosnay HL (1977) Taxonomy of the genus *Serratia*. Microbiology 98:39–66
16. Zhang LY, Yang YL, Sun JA et al (2010) Microbial production of 2,3-butanediol by a mutagenized strain of *Serratia marcescens* H30. Bioresource Technol 101:1961–1967
17. Fang LY, Xu Q, Cao X et al (2007) Optimization of fermentation medium for 2,3-butanediol production by *Serratia marcescens*. Ind Microbiol 37:24–28
18. Zhang LY (2010) Research on 2,3-butanediol Production by *Serratia Marcescens* H30 and Its Metabolic Regulation. East China University of Science and Technology, Shanghai
19. Xie L, Yang RC, Hu YY (2001) The common bacterial system identification manual. Science Press, Beijing
20. Werkman CH (1930) An improved technic for the voges-proskauer test. J Bacteriol 20:121–125
21. Westerfeld W (1945) A colorimetric determination of blood acetoin. J Biol Chem 161:495–502
22. Vaughn R, Mitchell NB, Levine M (1939) The Voges-Proskauer and methyl red reactions in the coli-*aerogenes* group. J AWWA 31:993–1001
23. Fitzgerald JR, Meaney WJ, Hartigani PJ (1997) Fine-structure molecular epidemiological analysis of *Staphylococcus aureus* recovered from cows. Epidemiol Infect 119:261–269
24. Shinefield HR (2006) Use of a conjugate polysaccharide vaccine in the prevention of invasive staphylococcal disease: Is an additional vaccine needed or possible. Vaccine 24:65–69
25. Amann RI, Ludwig W, Schleifer KH (1995) Phylogenetic identification and in situ detection of individual microbial cells without cultivation. Microbiol Mol Biol R 59:143–169
26. Zhang JH, Madden TL (1997) Power BLAST: a new network BLAST application for interactive or automated sequence analysis and annotation. Genome Res 7:649–656
27. Tiedje JM, Wang QG, Garrity M et al (2007) Naive bayesian classifier for rapid assignment of rRNA sequences into the new bacterial taxonomy. Appl Environ Microb 73:5261–5267
28. Mason RL, Gunst RF, Hess JL (2003) Statistical design and analysis of experiments with applications to engineering and science, 2nd edn. Hoboken, Wiley, pp 121–124
29. Houdt RV, Moons P, Buj MHC et al (2006) N-Acyl-L-Homoserine Lactone Quorum sensing controls Butanediol fermentation in Serratia plymuthica RVH1 and *Serratia marcescens MG*1. J Bacteriol 188:4570–4572
30. Dasari MA, Kiatsimkul PP, Sutterlin WR et al (2005) Low-pressure hydrogenolysis of glycerol to propylene glycerol. Appl Catalysis A: Gen 281:225–231
31. Abbad AS, Manginot DC, Raval G (1996) Carbon and electron f low in *Clostridium butyricum* grown in chemostat culture on glycerol and on glucose. Microbiology 142:1149–1158

Chapter 18
Effect of *GPD*1 and *GPD*2 Deletion on the Production of Glycerol and Ethanol in the Yeast *Saccharomyces cerevisiae*

Jingjing Yu, Jian Dong, Cuiying Zhang, Junxia Li and Dongguang Xiao

Abstract Glycerol is the main by-product in ethanol production during the very high gravity (VHG) fermentation process by *Saccharomyces cerevisiae*. This study investigates the effect of *GPD*1 or *GPD*2 (encoding 3-phosphate dehydrogenase) deletion on the production of glycerol and ethanol through the VHG fermentation. We observed that deletion of *GPD*1 resulted in 45.30 % reduction in glycerol production compared with the parent strain, and ethanol production reached the levels of 15.8 ± 0.03 (v/v), while we failed to observe such a significant decrease in glycerol production for the *GPD*2 deletion mutants whose ethanol production was 15.7 ± 0.03 (v/v). It can be concluded that deletion of either *GPD*1 or *GPD*2 can elevate ethanol production, and that *GPD*1 deletion can significantly reduce glycerol production, suggesting that *GPD*1 plays a dominant role in regulating glycerol synthesis during the process of VHG fermentation.

Keywords *GPD*1 · *GPD*2 · Ethanol · Glycerol · VHG fermentation · *Saccharomyces cerevisiae*

18.1 Introduction

Ethanol, as the high-value renewable energy, plays an important role for the future [1, 2]. It is produced by anaerobic fermentation of glucose in yeast cells [3, 4]. Under normal anaerobic fermentation of *Saccharomyces cerevisiae*, in addition to the biomass, ethanol, and carbon dioxide, a number of other by-products such as glycerol, organic acids, and amino acids compounds are produced [3, 5]. In these

J. Yu · J. Dong · C. Zhang · J. Li · D. Xiao (✉)
Key Laboratory of Industrial Fermentation Microbiology, Ministry of Education, Tianjin Industrial Microbiology Key Laboratory, College of Biotechnology, Tianjin University of Science and Technology, Tianjin 300457, People's Republic of China
e-mail: xdg@tust.edu.cn

T.-C. Zhang et al. (eds.), *Proceedings of the 2012 International Conference on Applied Biotechnology (ICAB 2012)*, Lecture Notes in Electrical Engineering 249,
DOI: 10.1007/978-3-642-37916-1_18, © Springer-Verlag Berlin Heidelberg 2014

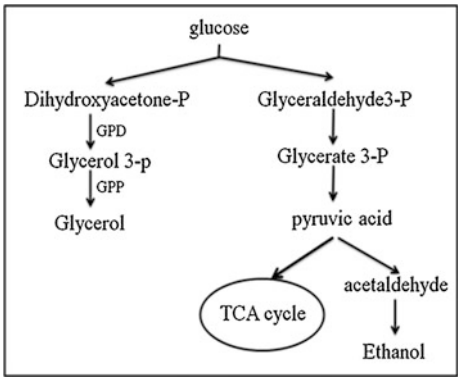

Fig. 18.1 Metabolic pathway of glycerol production in *S. cerevisiae*

by-products, glycerol is produced at up to 5 g/l, which is one of the main by-products, accounting for up to 5 % of the carbon source in industrial fermentations [6]. If the target fermentation product is ethanol, then the formation of glycerol is a kind of waste.

In *S. cerevisiae* cells, glycerol is synthesized from the reduction of dihydroxyacetone phosphate, which is a glycolytic intermediate in two sequential steps catalyzed by the rate-limiting NAD+-dependent glycerol-3-phosphate dehydrogenase (Fig. 18.1), and a secondary reaction catalyzed by glycerol-3-phosphatase. *GPD*1 and *GPD*2 encode two isoenzymes of glycerol-3-phosphate dehydrogenase [6–8]. The main role of glycerol is to balance the intracellular redox and adjust the osmotic stress within the cells [9, 10].

The purpose of this work was to study the effect of *GPD*1 and *GPD*2 deletion on the production of glycerol and ethanol. We constructed two recombinant plasmid vectors (pABK-G1 and pABK-G2), which were subsequently transformed into S. cerevisiae strains (A8ΔB, α5ΔB), generating two *GPD*1-deleted strains (A8ΔBΔG1, α5ΔBΔG1) and *GPD*2-deleted strains (A8ΔBΔG2, α5ΔBΔG2). The fermentation results revealed that *GPD*1 deletion could effectively reduce glycerol production and enhance ethanol production, while we did not observe such a significant effect for *GPD*2-deleted strains.

18.2 Materials and Methods

18.2.1 Strains, Plasmids, and Growth Conditions

The *S. cerevisiae* strains used in this study were all derived from a8ΔB and α5ΔB. The genetic properties of all strains and plasmids used in this study are listed in Table 18.1.

S. cerevisiae cells were routinely grown at 28 °C in a yeast extract peptone dextrose (YEPD) medium containing 2 % peptone [Difco] and 1 % yeast extract

Table 18.1 Characteristics of strains and plasmids used in this study

	Relevant features	Reference or source
Strains		
A8ΔB	MATa *bat2Δ*	This Lab
α5ΔB	MATα *bat2Δ*	This Lab
A8ΔBΔG1	MATa *bat2Δ gpd1::pABK*	This study
α5ΔBΔG1	MATα *bat2Δ gpd1::pABK*	This study
A8ΔBΔG2	MATa *bat2Δ gpd2::pABK*	This study
α5ΔBΔG2	MATα *bat2Δ gpd2::pABK*	This study
Plasmids		
pUC19	Apr, cloning vector	This Lab
pUG6	Kanr, containing loxP-kanMX-loxP gene disruption cassette	Hegemann JH, Heinrich-Heine-University Düsseldorf
pABK	A-Kan-B	This study

[Difco] supplemented with 2 % glucose [Merck]. Escherichia coli was grown at 37 °C in Luria-Bertani broth (10 g l^{-1} tryptone, 5 g l^{-1} yeast extract, 10 g l^{-1} NaCl) with 100 μg ml^{-1} ampicillin.

18.2.2 Plasmid and Strain Constructions

The primers used in this study are listed in Table 18.2. The pABK-G1 plasmid used for deletion of *GPD*1 was created by the following process: an *EcoRI* and *KpnI* upstream homologous fragment of the *GPD*1 gene, named G1A and amplified with G1A-U and G1A-D primers, was cloned into the pUC19 cloning vector, resulting in the pUC19-A-G1 plasmid. The *BamHI* and *SphI* downstream homologous fragment of *GPD1* named G1B, was also amplified by PCR using A8ΔB genomic DNA as templates with the G1B-U and G1B-D primers, and inserted into the *BamHI* and *SphI* sites of the pUC19-A-G1, resulting in a plasmid

Table 18.2 Primers used in this study (restriction sites are underlined)

Primer name	Sequence 5′-3′
G1A-U	CCGGAATTCCAAACGCAACACGAAACAAC
G1A-D	CGGGGTACCACGAAACTGCCAATACCAAG
Kan-U	CGGGGTACCCAGCTGAAGCTTCGTACGC
Kan-D	CGCGGATCCGCATAGGCCACTAGTGGATCTG
G1B-U	CGCGGATCCCTTTCCCCCACTTTTTTCG
G1B-D	ACATGCATGCATTTTCTTAGGACGCCGCA
G2A-U	CCGGAATTCCACCCGTTGATGACAGCA
G2A-D	CGGGGTACCTGATAAGGAAGGGGAGCG
G2B-U	CGCGGATCCCCAGCCACTGACATAAGAGC
G2B-D	ACATGCATGCTGGGCAAGAACAAGGGAG

named pUC19-AB-G1. The marker excised with primers Kan-U and Kan-D from pUG6 as a *Kan* fragment with the KpnI and BamHI sites, was inserted into the pUC19-AB-G1 to obtain a whole plasmid called pABK-G1.

To make the *GPD*2 gene disruption plasmid, three steps were sequentially constructed. The first step: pUC19-A-G2 was created by inserted a 588 bp of chromosomal DNA to pUC19. The 588 bp fragment was isolated from genomic DNA of the parent strain α5ΔB and amplified by PCR using primers G2A-U and G2A-D that contain *EcoRI* and *KpnI* sites, respectively. Then, the 304 bp fragment, which was also isolated from α5ΔB, was amplified through PCR utilizing primers G2B-U and G2B-D that include *BamHI* and *SphI* sites, respectively. The second step: pUC19-AB-G2 was built by cloning the 304 bp fragment into the cloning vector pUC19-A-G2. Finally, the *Kan* fragment, which used as a marker, was amplified from pUG6 through PCR with the primer *Kan*-U and *Kan*-D. Subsequently, digestion of the PCR product and pUC19-AB-G2 by *KpnI* and *BamHI* and ligation resulted in a final step of pABK-G2. Plasmids pABK-G1 and pABK-G2 were finally transformed into the starting strains of A8ΔB and α5ΔB, resulting in *GPD*1- and *GPD*2-deleted mutants (A8ΔBΔG1, α5ΔBΔG1, A8ΔBΔG2, and α5ΔBΔG2).

18.2.3 Fermentation Conditions

The first stage seed medium was prepared by adding 0.5 % yeast extract to 4 ml 8° Brix corn hydrolysates. Sterilization was performed with boiling water for 15 min. The strains were inoculated into tubes containing 4 ml sterilized first stage seed medium and stationarily cultivated at 30 °C for 24 h. The secondary stage seed medium containing 0.5 % yeast extract, 36 ml 12° Brix corn hydrolysates in a 150 ml beaker flask was sterilized by boiling water. Activation cells, which were cultivated in 4 ml first stage seed medium, were all decanted into 36 ml secondary stage seed medium and then stationarily cultured at 30 °C for 16 h.

VHG fermentation medium: 60 g cornmeal was decanted into a 250 ml beaker flask and 130 ml water of 60–70 °C added. After 20 min, 30 μl (10 U/g) thermostable α-amylase was added to the beaker flask and placed in the water bath (85–90 °C) for 1.5 h, followed by adding 90 μl (150 U/g) glucoamylase, and the reactions were allowed to proceed at 55–60 °C for 20 min. Subsequently, 1.2 ml acid protease (15 U/g) and 1 ml nutrient solution (150 g/l $MgSO_4$, 75 g/l KH_2PO_4, 81 g/l CON_2H_4) were added to the beaker flask, and maintained at 55–60 °C for another 20 min. Finally, 10 % (v/v) precultured secondary stage seed was transferred to the VHG fermentation medium and stationarily cultured at 30 °C.

18.2.4 Measurement of CO_2 Generation, Residual Reducing Sugar, Ethanol and Glycerol Production

In this study, CO_2 generation in VHG fermentation was examined every 12 h, and the ethanol production was determined through distillation. The samples were centrifuged at 12,000 r/min for 10 min at 4 °C, and the resulting supernatant was kept at −20 °C for residual reducing sugar and glycerol analysis. The concentration of glycerol was determined via high performance liquid chromatography (HPLC) analysis. HPX-87H carbohydrate column (Agilent) was used for determination of glycerol eluted with 0.02 mmol H_2SO_4 at 65 °C. Fehling's reagent was used to calculate the levels of residual reducing sugar.

18.3 Results and Discussions

18.3.1 Effect of GPD1 and GPD2 Disruptions on the CO_2 Generations

Given that *GPD*1 and *GPD*2 genes, which encode NAD^+-dependent glycerol 3-phosphate dehydrogenase, are involved in mediating the redox balance [11–14], we expected that disruption of *GPD*1 or *GPD*2 might have a negative effect on the respective mutant strains' fermentation properties. Construction of *GPD*1 or *GPD*2 deletion strains was performed as mentioned in the materials and methods section. Two A-type deletion mutant strains A8ΔBΔG1 and A8ΔBΔG2 were obtained. Moreover, we also constructed two α-type mutant strains α5ΔBΔG1 and α5ΔBΔG2. The ability of four mutants to produce CO_2 was determined. As shown in Fig. 18.2a, mutants A8ΔBΔG1 and α5ΔBΔG1 entered into the main fermentation stage after 12 h. After the main fermentation stage, the fermentation abilities of the two strains were weakened, and then A8ΔBΔG1 and α5ΔBΔG1 proceeded to the secondary fermentation stage. The strain A8ΔBΔG1 generated slightly lower levels of CO_2 compared with the parent strain A8ΔB at 12 h; when it entered the main fermentation stage, fermentation was slower and the fermentation period was longer than A8ΔBΔG2 and its parental strain A8ΔB. As shown in Fig. 18.2b, the amount of CO_2 produced by the α5ΔBΔG2 mutant was similar to that of the parental strain α5ΔB under microaerobic conditions. But α5ΔBΔG1 had a slower fermentation than the parent strain α5ΔB in terms of CO_2 generation. Thus, deletion of *GPD*1 gene had a significant negative effect on the CO_2 generation of *S. cerevisiae* in VHG fermentation.

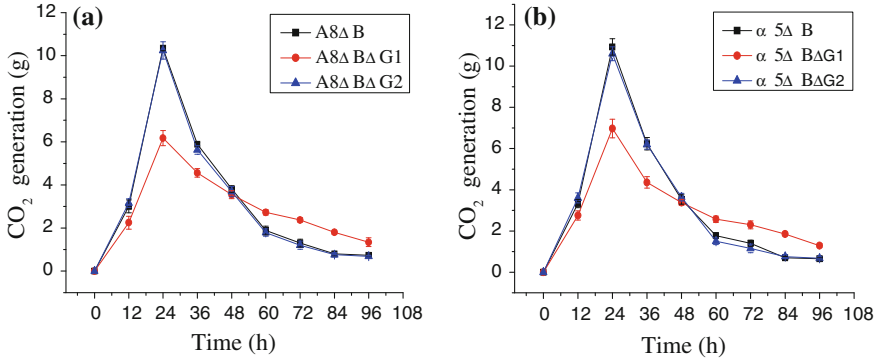

Fig. 18.2 CO_2 generation in VHG fermentation of different strains were shown in (**a**) and (**b**)

18.3.2 Effect of GPD*1 and* GPD*2 Disruptions on the Glycerol Production*

It has been reported that glycerol is the primary metabolite accumulated and is involved in the osmoregulation of *S. cerevisiae* [12, 13]. Glycerol also plays a role in maintaining the cytosolic redox balance. Therefore we expected that *GPD*1 or *GPD*2 deletion might play a positive role in yeast glycerol production. The fermentation properties of A8ΔB, A8ΔBΔG1, and A8ΔBΔG2; α5ΔB, α5ΔBΔG1, and α5ΔBΔG2 were studied under anaerobic conditions. During VHG fermentation, deletion of *GPD*1 resulted in a 45.3 % decline in glycerol formation in A8ΔBΔG1, in comparison to the parental strain A8ΔB. However, A8ΔBΔG2 deletion mutant did not show such a significant decrease in the glycerol production compared with the parent strain A8ΔB (Fig. 18.3a). There was a dramatic reduction in glycerol production in two mutants, α5ΔBΔG1 and α5ΔBΔG2, whose *GPD*1 or *GPD*2 was deleted, resulting in reduction of glycerol production by 48.2 and 7.58 %, respectively, compared to that of the parent strain α5ΔB (Fig. 18.3b). The results

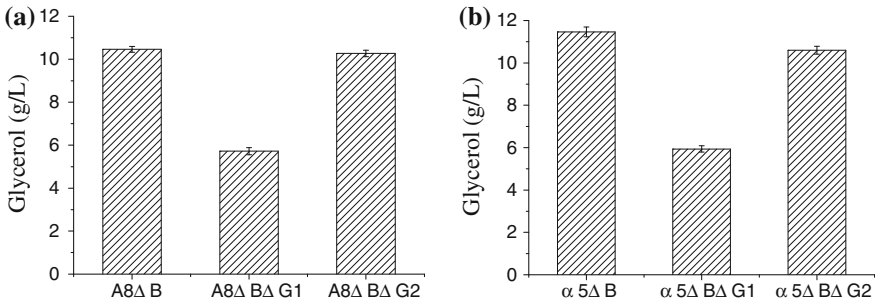

Fig. 18.3 Glycerol production of *S. cerevisiae* in VHG fermentation of different strains were shown in (**a**) and (**b**)

Table 18.3 Ethanol production and the residual level of reducing sugar in VHG fermentation

Strains	A8ΔB	A8ΔBΔG1	A8ΔBΔG2	α5ΔB	α5ΔBΔG1	α5ΔBΔG2
Ethanol (v/v)	15.5 ± 0.04	15.8 ± 0.03	15.7 ± 0.03	15.5 ± 0.02	15.4 ± 0.03	15.3 ± 0.02
The residual reducing sugar (g/100 ml)	0.19 ± 0.04	1.45 ± 0.02	1.65 ± 0.03	0.19 ± 0.02	0.19 ± 0.01	0.17 ± 0.01

from this study showed that deletion of *GPD*1 gene was obviously more effective than *GPD*2 deletion in improving glycerol production with VHG fermentation.

18.3.3 Effect of GPD*1 and* GPD*2 Deletion on the Ethanol Production and the Residual Level of Reducing Sugar*

For the purpose of increasing ethanol yield, glycerol formation pathway was blocked by deletion of either *GPD*1 or *GPD*2, which encode the glycerol 3-phosphate dehydrogenase [14, 15]. We expected that deletion of *GPD*1 or *GPD*2 (in strains A8ΔBΔG1, α5ΔBΔG1, A8ΔBΔG2, and α5ΔBΔG2) might have a positive effect on improving ethanol production. In order to determine the degree of fermentation, we examined the residual of reducing sugar. As shown in Table 18.3, ethanol production by A8ΔBΔG1 and A8ΔBΔG2 reached the levels of 15.8 ± 0.03 (v/v) and 15.7 ± 0.03 (v/v) respectively. But the residual levels of reducing sugar in A8ΔBΔG1 and A8ΔBΔG2 fermentation broth were much higher compared to that of the starting strain A8ΔB, indicating that the mutant strains A8ΔBΔG1 and A8ΔBΔG2 showed a declining fermentation capability. For strains α5ΔBΔG1 and α5ΔBΔG2, no significant increase in ethanol production was observed. However, in comparison to the parent strain α5ΔB, the residual levels of reducing sugar in the fermentation broth were similar. These results show that α-type strain was much better than a-type strain in degree of fermentation with VHG fermentation. In the yeast cells, the metabolic pathway from glucose to ethanol is redox neutral, but the formation of other metabolites leads to over-production of NADH. In order to adapt to the environmental changes, *S. cerevisiae* utilize other pathways for reoxidizing NADH to NAD^+ [16, 17].

18.4 Conclusion

It has been reported that deletion of *GPD*1 or *GPD*2 could result in an increase in ethanol and a decrease in glycerol production. This could be explained by the fact that part of the glycerol is rerouted to produce ethanol [18, 19]. In this study, we

separately disrupted *GPD*1 and *GPD*2 genes and investigated their effects on glycerol and ethanol production, and the fermentation performances of the four deletion mutants (A8ΔBΔG1, α5ΔBΔG1 and A8ΔBΔG2, α5ΔBΔG2). Our results show that deletion of *GPD*1 result in 45.30 % reduction in glycerol production compared with the parent strain, and the production of ethanol reached the levels of 15.8 ± 0.03 (v/v). However, we failed to obtain such a significant decrease in the glycerol production after *GPD*2 deletion and the production of ethanol reached 15.7 ± 0.03 (v/v). Moreover, *GPD*2 deletion mutants exhibited no significant effects on fermentation performances. Importantly, our results demonstrate that *GPD*1 plays a dominant role in regulating glycerol synthesis in the conditions of high osmotic stress during the VHG fermentation process.

Acknowledgments This work was financially supported by the program of National High Technology Research and Development Program of China (863 Program) (Grant No. SS2012AA023408), the Cheung Kong Scholars and Innovative Research Team Program in University of Ministry of Education, China (Grant No. IRT1166), and Tianjin Municipal High School Science and Technology Development Fund Program, China (No. 20110625).

References

1. Zhang AL, Kong QX, Cao LM et al (2006) Effect of *FPS1* deletation on the fermentation properties of *Saccharomyces cerevisiae*. Lett Appl Microbiol, ISSN 0266-8254
2. Cooper C (2001) A renewed boost for ethanol. Chem Eng 106:35
3. Nissen TL, Kielland-Brandt MC, Nielsen J (2000) Optimization of ethanol production in *Saccharomyces cerevisiae* by metabolic engineering of the ammonium assimilation. Metab Eng 2:69–77
4. Lin QY, Zhao CX, Jin FY (2003) Comparison of physiological properties between two osmophilic alcohol yeast strains. Liquor-making Sci Technol 30(2):27–30
5. Kong QX, Cao LM, Zhang AL et al (2007) Overexpressing *GLT1* in *gpd1*Δ mutant to improve the production of ethanol of *Saccharomyces cerevisiae*. Appl Microbiol Biotechnol 73:1382–1386
6. Norbeck J, Pahlman AK, Akhtar N et al (1996) Purification and characterization of two isoenzymes of DL-glycerol-3-phosphatase from *Saccharomyces cerevisiae*. J Biol Chem 271:13875–13881
7. Pahlman AK, Granath K, Ansell R et al (2001) The yeast glycerol 3-phosphatases Gpp 1p and Gpp2p are required for glycerol biosynthesis and differentially involved in the cellular responses to osmotic, anaerobic and oxidative stress. J Biol Chem 276:3555–3563
8. Remize F, Barnavon L, Dequin S (2001) Glycerol export and glycerol-3-phosphate dehydrogenase, but not glycerol phosphatase, are rate limiting for glycerol production in *Saccharomyces cerevisiae*. Metab Eng 3:301–312
9. Ausubel FM, Brent R, Kingston RE et al (1994) Current protocols in molecular biology. Wiley, New York
10. Jiang TX, Xiao DG, Gao Q (2008) Characterisation of maltose metabolism in lean dough by lagging and non-lagging baker's yeast strains. Ann Microbiol 58:655–660
11. Gietz RD, Schiestl RH (1995) Transforming yeast with DNA methods. Mol Cell Biol 5:255–269
12. Nissen TL, Schulze U, Nielsen J et al (1997) Flux distributions in anaerobic, glucose-limited continuous cultures of *Saccharomyces cerevisiae*. Microbiology 143:203–218

13. Torben L, Nissen TL, Morten C et al (2000) Optimization of ethanol production in *Saccharomyces cerevisiae* by metabolic engineering of the ammonium assimilation. Metab Eng 2:69–7
14. Kong QX, Zhang AL, Cao LM et al (2007) Over-expressing *GLT1* in a *gpd2*Δ mutant of *Saccharomyces cerevisiae* to improve ethanol production. Appl Microbiol Biotechnol 75:1361–1366
15. Kong QX, Gu JG, Cao LM et al (2006) Improved production of ethanol by deleting *FPS1* and over-expressing *GLT1* in *Saccharomyces cerevisiae*. Biotechnol Lett 28:2033–2038
16. Sun X, Zhang CY, Dong J et al (2012) Enhanced leavening properties of baker's yeast overexpressing *MAL62* with deletion of *MIG1* in lean dough. J Ind Microbiol Biotechnol 39:1–7
17. Cao LM, Kong QX, Zhang AL et al (2010) Overexpression of *SYM1* in a gpdDelta mutant of *Saccharomyces cerevisiae* with modified ammonium assimilation for optimization of ethanol production. J Taivan Inst Chem E 41:2–7
18. Cao LM, Zhang AL, Kong QX et al (2007) Overexprission of *GLT1* in *fps1*Δ*gpd*Δ mutant for optimum ethanol formation by *Saccharomyces cerevisiae*. Biomol Eng 24:638–642
19. Edgardo A, Carolina P, Manuel R et al (2007) Selection of thermotalerant yeast strains *Saccharomyces cerevisiae* for bioethanol Production. Appl Microbiol Biotechnol 75:1361

Chapter 19
Screening of the Best Strain for Naked Oat Fermentation Beverage and its Production Process Study

Jian Wang, Yuan Liu, Fengying Lan and Jing Wang

Abstract Saccharifying naked oat juice was chosen for fermentation by instant active dry yeast, lactic acid bacteria, and wine active dry yeast to produce fermentation beverage. Effects of the strains, inoculum size, fermentation time, and the addition of xylitol and pectin on physical and chemical indexes and sensory evaluation of the beverage were studied. On the basis of single factor test, orthogonal experiment of L_9 (3^4) was used to optimize the technical parameters. The results indicated that the optimal process conditions were: 4 % wine yeast, 20 h, 7 % xylitol, and 0.45 % pectin. Under these conditions, the obtained beverage was perfectly clear and cream-colored, with its well-distributed constitution and rich naked oat flavor. Its sensory score reached up to 95.2 and its precipitation rate 13.5 %. This study aims to provide the theory basis for the development of highly processed products of naked oat.

Keywords Fermentation beverage · Naked oat · Process parameters · Wine yeast

19.1 Introduction

The nutritional value of naked oat is ranked the first among the cereals. According to the analysis, it contains 15.53 % protein, 6.35 % fat, 42.44 % linoleic acid of unsaturated fatty acid [1, 2], and it has eight kinds of essential amino acid with

J. Wang · J. Wang (✉)
Institute of Quality Standards and Testing Technology for Agri-products of CAAS, Beijing 100081, People's Republic of China
e-mail: w_jing2001@126.com

J. Wang · J. Wang
Key Laboratory of Agrifood Safety and Quality, Ministry of Agriculture, Beijing 100081, People's Republic of China

J. Wang · Y. Liu · F. Lan
Department of Food Science, Hebei North University, Zhangjiakou 075000, People's Republic of China

T.-C. Zhang et al. (eds.), *Proceedings of the 2012 International Conference on Applied Biotechnology (ICAB 2012)*, Lecture Notes in Electrical Engineering 249,
DOI: 10.1007/978-3-642-37916-1_19, © Springer-Verlag Berlin Heidelberg 2014

their balanced ratio. Its carbohydrate content is the lowest among the cereals, its dietary fiber content relatively high, and its soluble dietary fiber content obviously higher than that of rice and wheat flour. It is rich in mineral elements which can meet the requirements of human body, especially the content of Fe, Zn, and other trace elements necessary for children's growth. Besides, naked oat is a good food source of vitamin [3]. Research shows that naked oat food contributes to people's health a lot, such as reducing blood lipid, lowering blood pressure, regulation of blood glucose, prevention of cardiovascular disease. Therefore, it is acknowledged as healthy food, especially for diabetic patients [4–7].

At present, the naked oat products in the domestic market generally belong to instant edible food, such as naked oat instant noodle, naked oat rice, naked oat pastry and so on [8, 9]. Therefore, the research focus in this field is how to further improve their nutritional value and economic value [10–12]. Fermented food can not only enhance the nutritional value of the original food, but also increase its added value. Thus, if the fermentation technology is used in their exploitation, it will promote the transformation of the naked oat industry to deep processing direction [13, 14].

In the research, saccharifying naked oat juice was chosen for fermentation by different strains with different treatments. According to the fermentation effect, the optimal strain was selected and one kind of naked oat fermentation beverage with good flavor was prepared. Then its stability and process were studied in order to provide the theory basis for the development of new naked oat products.

19.2 Materials and Methods

19.2.1 Test Strains

Instant active dry yeast (*Saccharomyces cerevisiae* CICC 1616), lactic acid bacteria (*Lactobacillus delbrueckii subsp.bulgaricus* CICC 6064 & *Streptococcus thermophilus* CICC 6063), and wine active dry yeast (*Saccharomyces logos* CICC 32888) in this study were purchased from China center of industrial culture collection (CICC).

19.2.2 Preparation of Saccharifying Naked Oat Juice

The naked oat flour as material was mixed with the self-made malt powder as enzyme preparation according to the proportion (naked oat flour: malt powder: water(g/g/mL) = (40: 3: 400). Then the saccharification of the mixture was carried out by constant temperature infusion mashing method [15]. Finally, the saccharifying naked oat juice was obtained and sterilized by high pressure steam (115–117 °C, 25 min) before use.

19.2.3 Activated Culture of Strains [16, 17]

19.2.3.1 Activation and Domestication of Lactic Acid Bacteria

Activation: at first, lactic acid bacteria were inoculated to the prepared medium, then filled into the tube sterilized by dry heat air, and cultured at 43 °C for 4–6 h until the milk became solidified.

Domestication: The activated lactic acid bacteria were inoculated to the mixture of gradually increasing naked oat juice and skim milk powder.

19.2.3.2 Activation of Instant Active Dry Yeast

In the superclean bench, dry yeast with accuracy of 0.001 g was inoculated to the sterile tube with 10 mL sterile distilled water. Then it was diluted according to the ratio of 10^{-1}, 10^{-2}, and 10^{-3}, and then 1 mL of each concentration was put into the potato medium to be cultured at 25 °C for 48 h. The well-growing ones were selected to spread evenly on the surface of potato slant culture, and cultured at 25 °C for 48 h, and then stored in the refrigerator.

Two or three of the above yeast colonies were inoculated to 100 mL conical flask with 20 mL sterile potato liquid medium, and cultured at 25 °C for 24 h; the above cultured yeast liquid was dumped into 500 mL conical flask with 100 mL sterile PDA liquid medium, and cultured at 25 °C for 24 h; then the above yeast liquid was imported into the conical flask with 120 mL sterile PDA liquid medium, and cultured at 25 °C for 24 h before use.

19.2.3.3 Activation of Wine Active Dry Yeast

Three-four grams of wine active dry yeast were put into 100 mL glucose medium of 5 % prepared under sterilized condition, then shaken up, filled into 5 large tube and sealed, cultured at 28 °C for 1–1.5 h, and stored at 2–8 °C after cooling.

19.2.4 Design for Screening the Optimal Strain

Three prepared strains were inoculated to saccharifying naked oat juice according to the proportion of 3, 4, and 5 %, respectively. And it was repeated three times altogether. The samples inoculated with lactic acid bacteria, instant active dry yeast, and wine active dry yeast were incubated respectively at 42–44 °C, 25 °C, and 28 °C. After fermentation, the products were estimated by sensory evaluation.

19.2.5 Design for Optimization of Fermentation Process Conditions

19.2.5.1 Effects of Inoculum Size on Fermentation Effects

Each group of prepared naked oat juice was inoculated by the selected strain according to five different ratios (1–5 %) respectively, and incubated at 28 °C for 36 h. Then they were estimated by sensory evaluation.

19.2.5.2 Effects of Fermentation Time on its Effects

Each group of the prepared naked oat juice was inoculated by the selected inoculum size and inoculated at 28 °C. Their sensory evaluation was conducted and their sugar degree and acidity were determined at 4, 8, 12, 16, 20, 24, 28 h, respectively. Sugar degree and acidity were respectively measured by hand-held saccharimeter mensuration and acid–base titration.

19.2.5.3 Effects of Addition of Xylitol on Fermentation Effects

Because the sour taste of fermented naked oat juice was relatively strong, some sweetener was essential to be added to conciliate it. On the basis of the principle of health care, xylitol was chosen as a sweetener in the research. It was added into the fermented naked oat juice according to six different ratios to season, and their sensory evaluation was conducted respectively.

19.2.5.4 Effects of Addition of Pectin on Fermentation Effects

Precipitation appears in naked oat fermentation beverage easily, so it is necessary to add stabilizer to improve the structural state. In the research, pectin was chosen as a stabilizer and added into the fermented naked oat juice according to six different ratios, and then the ratio was determined in term of the results of precipitation rate. It was measured by centrifugal sedimentation method [18].

19.2.6 Quality Analysis of Products

The degustation experiment was carried out among 20 healthy persons (half male and half female) selected randomly. Every one of them evaluated the quality of products by grading methods, and the standard of sensory evaluation was shown in Table 19.1 [19].

Table 19.1 Standard of sensory evaluation

Index	Standard	Score
Color (20)	Lucent and cream-colored	20–18
	Slightly gray	18–16
	Gray-yellow	16–14
	Light gray	<14
Bubble (20)	Abundant	20–15
	Many	15–10
	Very few	<10
Taste and flavor (40)	Naked oat flavor, moderate and soft taste	40–35
	Naked oat flavor, light and uncoordinated taste	35–30
	Too light taste, obviously peculiar smell	<30
Structural state (20)	Clear and transparent, uniform, with a little precipitate	20–18
	Slightly turbid, uniform, with a little precipitate	18–16
	Comparatively cloudy, with a little precipitate	16–14

19.3 Results and Discussion

19.3.1 Effects of Strains on Fermentation Effects

Different strains prepared were inoculated to the saccharifying naked oat juice for fermentation respectively, then the fermented naked oat juices were estimated by sensory evaluation, and the results were shown in Table 19.2.

From Table 19.2, the naked oat juice fermented by activated wine active dry yeast was 88.2 in sensory score, then the tamed lactic acid bacteria secondly; whether the instant active dry yeast was amplified and cultured or not, the naked oat juice by them were both poor in taste and flavor; the naked oat juice by tamed lactic acid bacteria was better than the juice by untamed one no matter in quality, or flavor and taste; while the naked oat juice by wine active dry yeast was superior to others in all the sensory index. Therefore, the activated wine active dry yeast was chosen for the study of fermentation process conditions.

Table 19.2 Sensory score of fermentation beverage with different strains

Strains	Structural state (30)	Color (20)	Taste (30)	Flavor (20)	Total score
Amplified and cultured instant active dry yeast	18.8	10.3	18.7	9.9	57.7
Activated instant active dry yeast	19.2	9.5	19.3	10.6	58.6
Activated wine active dry yeast	27.1	17.1	27.0	17.0	88.2
Tamed lactic acid bacteria	25.4	15.5	25.1	16.1	82.1
Untamed lactic acid bacteria	24.0	14.5	23.7	14.9	77.1

19.3.2 Determination of Inoculum Size

The activated strains were respectively inoculated to the saccharifying naked oat juice according to the ratios of 1, 2, 3, 4, and 5 %, and fermented for 26 h. Their sensory evaluation was implemented on the basis of the standard. As shown in Table 19.3, when the inoculum size was 4 %, the quality of the product was the best and the score was highest, so the optimal inoculum size was 4 %.

19.3.3 Determination of Fermentation Time

19.3.3.1 Effects of Fermentation Time on the Sensory Quality of Products

The saccharifying naked oat juice was inoculated according to the inoculum size determined, then evaluated respectively at 4, 8, 12, 16, 20, 24, 28 h by sensory evaluation, and the results were shown in Table 19.4. It indicated that when the fermentation time was at 20 h, the score was highest and the color, taste, structural state, and other sensory qualities were better than those at other fermentation times.

19.3.3.2 Effects of Fermentation Time on the Total Acidity and Total Sugar Content of Products

The saccharifying naked oat juice was inoculated according to the determined inoculum size, and the total acidity and total sugar content of the final products were determined respectively at 4, 8, 2, 16, 20, 24, 28 h, and the results were shown in Fig 19.1.

From Fig. 19.1, it can be found that the total acidity gradually increased with the prolongation of fermentation time. When the fermentation time was at 20 h, its acidity was up to 7.1 %, then went up sharply after 24 h. It suggested that the

Table 19.3 Sensory evaluation results of naked oat juice with different inoculation size

Inoculum size	Sensory evaluation	Total score
1 %	Lucent, a few bubbles, light taste, slightly cloudy, a little precipitate	77
2 %	Lucent, a few bubbles, slight taste, a little precipitate	76
3 %	Lucent, many bubbles, slight taste, a little precipitate	78
4 %	Lucent, abundant bubbles, common taste, a little precipitate	86
5 %	Slightly lucent, many bubbles, obviously peculiar smell, slightly cloudy, a little precipitate	65

Table 19.4 4 Sensory evaluation results of the beverage with different fermentation time

Fermention time (h)	Sensory evaluation	Total score
4	Cloudy and yellow, a few bubbles, the little taste of sour and alcohol, the little taste of yeast, strongly sweet	72.5
8	Slightly cloudy and yellow, a few bubbles, the little taste of sour and alcohol, the little taste of sweet and yeast	76.0
12	Relatively lucent, light yellow, many bubbles, the little taste of sour, alcohol and yeast, slightly sweet	80.5
16	Relatively lucent, light yellow, abundant bubbles, the little taste of sour, alcohol and yeast, slightly sweet	85.5
20	Clear and lucent, light yellow, abundant bubbles, sour and slightly sweet, slight yeast taste, strong alcoholic taste	93.5
24	Clear and lucent, light yellow, abundant bubbles, the strong taste of sour and yeast, slight alcoholic taste, slightly sweet	86.5
28	Clear and lucent, light gray, abundant bubbles, the strong taste of sour and yeast, slight alcoholic taste, almost hardly sweet	81.5

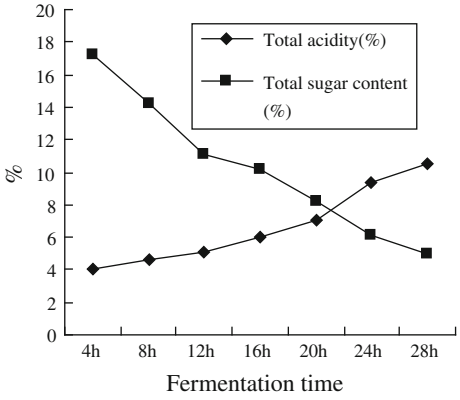

Fig. 19.1 Effects of fermentation time on the total acidity and total sugar content of products

strain selected had intense fermentability to naked oat juice at 20 h, because most of the strains were in the stage of ethanol fermentation, and only partial strains produced acid, and at that time its sour taste was favorable. If the time prolonged, most of the strains were in the stage of acid production, which can cause a strong sour taste [20, 21].

With the prolongation of fermentation time, the sugar consumption increased continuously, so the total sugar content gradually decreased, which showed that the strain selected had intense fermentability. At 20 h, the total sugar content was 8.24 %, and the product had a moderate sour and sweet. After 24 h, the total sugar content was so low that the sweet was too low and the taste was bad.

Table 19.5 Effects of addition of xylitol on taste of the beverage

Xylitol (%)	Sensory evaluation	Total score
3	Slightly sweet, strongly sour, a little taste of yeast	78.5
5	Rather slightly sweet, relatively strong sour	85.5
7	Moderately sour and sweet	93.5
9	Rather strongly sweet, rather slightly sour, no peculiar smell	87.5
11	Strongly sweet, nearly seldom sour	84
13	Rather strongly sweet, no other tastes but sweet	81.5

19.3.4 Determination of Addition of Xylitol

Xylitol was put into fermented naked oat juice according to six different ratios respectively, then the sensory evaluation was conducted in the final product (see Table 19.5). The results showed that when the addition of xylitol was at 7 %, the beverage had a mellow and moderate taste which was suitable to the public.

19.3.5 Determination of Addition of Pectin

Pectin was added into fermented naked oat juice according to six different ratios respectively, and the precipitation rate was determined (see Fig. 19.2).

The results showed that when the addition of pectin was 0.4 %, the precipitation rate was the lowest (0.76 %), and the beverage exhibited its strongest stability; when the addition was from 0.1 to 0.3 %, the beverage was layered significantly; when the addition was from 0.4 to 0.5 %, the beverage was very stable. But the beverage when the addition was from 0.1 to 0.3 % is better than that when it was from 0.4 to 0.5 %.

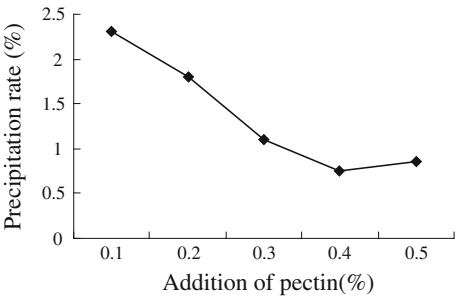

Fig. 19.2 Effects of the addition of pectin on precipitation rate

Table 19.6 The factors and levels of orthogonal experiment

Levels	A inoculum size (%)	B time (h)	C pectin (%)	D xylitol (%)
1	3.5	15	0.35	6
2	4	20	0.4	7
3	4.5	25	0.45	8

19.3.6 Determination of Optimizing Process Parameters

On the basis of the above single factor experiment, the process parameters were optimized by orthogonal experiment of L_9 (3^4). Inoculum size of wine active dry yeast, fermentation time and the addition of xylitol and pectin were used as contributing factors, and total sugar content, precipitation rate, and sensory score as indexes. The specific factors and levels are as follows (Table 19.6), and the results were shown in Table 19.7.

The results demonstrated that the sequence of effects of four factors on the indexes was B>D>C>A. The best optimal combination was A2 B2 C3 D2, that is, on the condition of inoculum size being 4.0 %, fermentation time 20 h, addition of pectin 0.45 %, addition of xylitol 7 %. On the basis, the verification experiment was conducted and repeated three times. The mean value of the precipitation rate

Table 19.7 L_9 (3^4) Orthogonal design and results

No.	Factors				(%)	Sensory score
	A	B	C	D	Precipitation rate	
1	1	1	1	1	19.45	51
2	1	2	2	2	21.27	92.5
3	1	3	3	3	22.30	83
4	2	1	2	3	14.70	61
5	2	2	3	1	13.60	95.5
6	2	3	1	2	15.63	88.5
7	3	1	3	2	16.69	68.75
8	3	2	1	3	14.76	81
9	3	3	2	1	14.92	75.5
K_1	226.5	180.75	220.5	222		
K_2	245	269	229	249.75		
K_3	225.25	247	247.25	225		
k_1	75.5	60.3	73.5	74		
k_2	81.7	89.7	76.3	83.3		
k_3	75.1	82.3	82.4	75		
R	6.6	29.4	8.9	9.3		
Optimization levels	A2	B2	C3	D2		

Note When the pectin is added, the temperature of sample solution should be up to 80 °C and the solution should be shaken at the same time

was 13.5 %, the sensory score was 138.9, which indicated that the results of the verification experiment were basically identical with them optimized by the orthogonal experiment.

19.4 Conclusion

(1) By comparing the effects of strains on the sensory score of the naked oat fermentation beverage, wine active dry yeast was chosen for fermentation.
(2) Through single factor experiment, inoculum size, fermentation time, and the addition of xylitol and pectin selected respectively were 4 %, 20 h, 7 % and 0.4 %. The final product under these conditions had the best fermentation effects.
(3) Four significant factors of inoculum size, fermentation time, and the addition of xylitol and pectin were optimized by orthogonal experiment. The better fermentation conditions were as follows: inoculum size being 4 %, fermentation time 20 h, the addition of xylitol and pectin 7 % and 0.45 %. Under these conditions, the product obtained had better sensory score which was up to 95.2 and its precipitation rate 13.5 %. In order to applied successfully fermentation technology to the deep processing of the naked oat, increased the number of the naked oat product categories, the production process should be further studied.

References

1. Hu BH, Liu SX, Xia YB et al (2011) Manufacture of oat corn alcoholic fermentation beverages. Crop Res 25:145–148
2. Yang C, Zhou HT, Li TL et al (2010) Nutrition comparison of naked oat and ordinary oat. Innovatl Edit Farm Prod Proc 2:53–54
3. Peterson DM, Wood DF (1997) Composition and structure of high-oil oat. J Cer Sci 26:11–128
4. Zhang JP (2006) Study on naked oats nutrition components and functions. Food Fermentat Indus 37:128–130
5. Zhang DS (2002) Medical and health function of naked oat. Chin Seed Indus 21:128–130
6. Zhang LP, Zhai AH (2004) Function feature and comprehesive processing utility of oats. Food Mac 20:55–57
7. Gruenwald J (2009) Novel botanical ingredients for beverages. Clin Dermatol 27:210–216
8. Yang C, Li TL, Yang XH et al (2008) The important status of industrialization production of oats in the agricultural economy development in Zhangjiakou city. J Hebei Agric Sci 12(139–140):142
9. Zhao MM, Ren JY, Xu DF (2009) Development of convenience food of cereal and prospect of combination with agricultural industrialization. Sci Technol Food Indus 31(355–358):363

10. Pan TT, Pang J, Liu FL (2010) Study on and manufacture of stirred oats yogurt. Chin Dairy Indus 38:6–58
11. Dong JL, Zheng JQ, Shen RL (2007) Application of oat β-glucan ice cream production. Food Res Dev 28:193–196
12. Zhang WG (2004) Fermentation food technology. Chin Light Indus Press, Beijing
13. Ma XF, Liu S (2005) Quality analysis of oat and its commercialization development. Trans Chin Soc Agric Eng 21:242–244
14. Hu XZ, Wei YM, Ren CZ (2009) Quality and process of oat. Sci press, Beijing
15. Zhang HJ, Chi YJ (2006) Research on 14° Bx aroma black rice beer. Food Indus 28:41–43
16. Shen P, Fan XR, Li GW (1999) Experiment in microbiology. Higher Educ Press, Beijing
17. Huang L, Lin QL, Wang ZL (2009) Preparation of fermented functional milk beverage from early long grain rice. J Chin Cereals Oils Assoc 24:116–119
18. Bai WD, Wang Q, Zhao WH (2006) Study on the stability of soybean-milk. Mod Food Sci Technol 22:5–7
19. Pu HY, Xie WY, Li YQ (2009) Study on processing technique of smallanthus Sonchifolius beverage. Food Indus 31:34–36
20. Blandino A, Al-Aseeri ME, Pandiella SS et al (2003) Cereal-based fermented foods and beverages. Food Res Int 36:527–543
21. Angelov A, Gotcheva V, Kuncheva R et al (2006) Development of a new oat-based probiotic drink. Int J Food Microbiol 112:75–80

Chapter 20
Optimization of Medium Constituents for Laccase Production by *Trametes Versicolor* As 5.48

Liang Huang, Yihan Liu, Yu Wang, Chuang Song, Xiaoyuan Xu and Fuping Lu

Abstract The present investigation provides a report on statistical optimization of medium components to improve Laccase production by *Trametes Versicolor* As 5.48. Glucose and starch were identified as significant components influencing the biomass and laccase production by *T. Versicolor* As 5.48 using orthogonal experiment design. The higher laccase production could be obtained when nitrogen source in the medium was at lower level compared with which was for the growth of *T. Versicolor* As 5.48. In accordance with three significant factors, orthogonal experiment was applied for further optimization to improve the laccase production by *T. Versicolor* As 5.48. Based on the further optimization results of statistical analyses, the concentrations of medium components for improved laccase production were as follows: Glucose 5.25 g/L, starch 5 g/L, ammonium chloride 67 mM, guaiacol 0.02 mM, potassium dihydrogen phosphate 1 g/L, trace elements 7 mL/L, Vitamin B_1 8 mg/L, Vitamin C 1.5 mM, and copper sulfate 0.05 mM. Under the optimized medium, the laccase activity of 17.46 U/mL was attained. From this study, it is evident that orthogonal experiment design can be used to determine the significant variables and the optimum conditions for laccase production, respectively. The optimization of the medium resulted not only in one-fold increase in laccase activity than in the primary optimized medium, but also in a reduction of the constituent number and constituents costs.

Keywords *Trametes versicolor* · Laccase · Medium optimization · Orthogonal experiment

L. Huang · Y. Liu · F. Lu (✉)
Key Laboratory of Industrial Fermentation Microbiology, Ministry of Education, The College of Biotechnology, Tianjin University of Science and Technology, Tianjin 300457, People's Republic of China
e-mail: lfp@tust.edu.cn

Y. Wang · C. Song · X. Xu
Department of Agronomy, Tianjin Agricultural University, Tianjin 300384, People's Republic of China

T.-C. Zhang et al. (eds.), *Proceedings of the 2012 International Conference on Applied Biotechnology (ICAB 2012)*, Lecture Notes in Electrical Engineering 249,
DOI: 10.1007/978-3-642-37916-1_20, © Springer-Verlag Berlin Heidelberg 2014

20.1 Introduction

Laccases (EC 1.10.3.2) are blue multicopper-containing enzymes that catalyze the oxidation of a variety of organic substances coupled to the reduction of molecular oxygen to water [1–3]. Because of their broad specificity for the reducing substrates, laccases from white-rot fungi are receiving increasing attention as potential industrial enzymes in various applications such as pulp delignification, wood fiber modification, dye or stain bleaching, chemical or medicinal synthesis, and contaminated water or soil remediation [4].

However, as constitutive extracellular laccases from basidiomycetes are produced only in small amounts, the use of laccases for industrial applications has been limited by low process productivities and, as a consequence, high enzyme costs [5, 6]. Enhancing laccase production through the use of inducers and different nutritional conditions has been reported [7–10].

Particularly, laccase production is influenced by carbon and nitrogen concentrations in culture media [11–14]. The use of enzyme inducers has also been investigated as they not only influence the type of isoenzymes produced but also increase volumetric activity. Much attention has been paid to the chemical induction of laccases by the addition of aromatic or phenolic compounds [15, 16], copper [17, 18], lignin [19], and ethanol [20], among others.

Laccase production and isoenzyme profile can be modified through medium composition and the use of inducers [21]. The objective of this work was to increase laccase production by *Trametes versicolor* through culture medium optimization and the use of copper as inducer. It has been shown here that a combination of $CuSO_4$ and trace elements stimulates the synthesis of laccase in *T. versicolor*; Different carbon source and nitrogen source may have effect on the laccase production; also the combination of the carbon and nitrogen concentrations in medium played an important role on the synthesis of laccase.

20.2 Materials and Methods

20.2.1 Materials

20.2.1.1 Strains

Trametes versicolor was from Chinese Academy of Sciences. The microorganism was maintained on 2 % (w/v) malt extract-agar slants at 4 °C.

20.2.1.2 Chemicals

ABTS (2,2′-azinobis [3-ethylbenzothiazoline-6-sulfonic acid]) was from Sigma. Other reagents used were Analytical reagents.

20.2.1.3 Medium

In the present investigations, *T. versicolor* was studied to produce laccase in submerged agitation culture in cotton-plugged 250 mL Erlenmeyer flasks containing 50 mL of production medium. *T. versicolor* young culture was grown for 6 days and the culture was used for biomass measurement and enzyme assay. The initial medium consisted of (/L of distilled water): 20 g glucose, 1 g corn powder, 12 mmol urea, 15 mmol ammonium chloride, 1 g potassium dihydrongen phosphate, 8 mg Vitamin B1, 1.5 mmol Vitamin C, 0.05 mmol copper sulfate and 7 mL of trace elements liquid. The trace elements liquid consisted of 3.2556 g potassium dihydrogen phosphate, 0.3931 g copper sulfate, 0.0671 g magnesium sulfate, 0.0043 g calcium chloride, 0.0033 g zinc sulfate; 0.5 g Vitamin C, 0.0038 g ferrous sulfate heptahydrate, 0.0024 g potassium aluminium sulfate, 0.0222 g sodium chloride, 0.0145 g Glycine, 0.0028 g ammonium molybdate and Vitamin B_1 30 mg dissolved in 100 mL of distilled water. The pH was adjusted to 5.0 using 3 M HCl prior to sterilization (15 min, 121 °C).

20.2.2 Biomass Measurement and Enzyme Assay

The biomass concentration was determined by dry weight method. The culture medium was filtered through 0.45 μm filter paper. Retained biomass was washed with distilled water and dried at a temperature of 80 °C for 24 h.

Assay of laccase activity culture aliquots (1 mL) were collected and cells were removed by centrifugation (10,000 g for 15 min). The laccase activity assay system contained 100 mM sodium acetate (pH 4.5), 0.5 mM ABTS (Sigma), and 100 μL culture supernatant appropriately diluted in a total volume of 1.0 mL. The reaction mixture was kept at 25 °C for 5 min, and then the change in absorbance at 420 nm was recorded with a spectrophotometer. One unit was defined as the amount of enzyme which oxidized 1 μmol ABTS per minute. The molar extinction coefficient for ABTS at 420 nm was taken to be 36,000 M^{-1} cm^{-1} [22].

20.2.3 Experimental Design and Statistical Analysis

In all experiments, orthogonal experimental design was applied, using three replicates per strain and substrate. Symbols, coded and actual level of variables of the

Table 20.1 Experimental conditions for the first screening study

Level of variables	Symbols					
	Guaiacol (A) mM	Glucose (B) g/L	Starch (C) g/L	Corn powder (D) g/L	Ammonium chloride (E) mM	Urea (F) mM
1	0.01	0	0	0	0	0
2	0.02	5	2	0.1	6	6
3		7.5	5	0.15	12	12
4		10	10	0.2	24	24

Table 20.2 Experimental conditions for the second screening study

Level	Glucose (A) (g/L)	Starch (B) (g/L)	Ammonium chloride (C) (mM)
1	5.25	2	61
2	7.75	5	67
3	10.25	10	79

screening study are shown in Tables 20.1 and 20.2. Variance analysis was performed by DPS 7.05 statistical package, using the least significant difference (LSD) test at 5 % level of probability to compare mean values of biomass production and laccase activities. Correlations were elaborated between the achieved values of these parameters and the constituents of the substrates.

20.3 Results and Discussion

20.3.1 The Optimization of the Initial Medium

20.3.1.1 Audio-Visual Analysis of the Orthogonal Experiment One

Orthogonal experimental design ($L_{32}(2^1 \times 4^5)$) was applied for the optimization of the initial medium, the results are showed in Table 20.3. Guaiacol, a substrate for laccase, can be used as an inducer to enhance the laccase production by *T. versicolor*. In this study, two guaiacol concentrations were adopted to play the role of guide. The other compositions in cultural medium served as carbon source or nitrogen source. To screening one or two of the five compositions of cultural medium for being replaced by other compositions, each composition were set at zero level in this orthogonal experiment to simply the composition of the medium.

Through mathematical analysis of the values of biomass, the results can be concluded as follows: first, the factor of starch shows the most notable influence, followed by glucose and urea. Second, the highest yield of biomass occurred using the medium consists of 0.02 mM guaiacol, 10 g/L glucose, 10 g/L starch, 0.2 g/L corn powder, 12 g/L ammonium chloride, and 0 g/L urea. Moreover, the average

Table 20.3 Experimental results of orthogonal experiment one of six factors

Variable code Run order	A mM	B g/L	C g/L	D g/L	E mM	F mM	Yield of biomass g/L	Laccase activity U/mL
1	1 (0.01)	1 (0)	1 (0)	1 (0)	1 (0)	1 (0)	6.34	0.1
2	1 (0.01)	1 (0)	2 (2)	2 (0.1)	2 (6)	2 (6)	7.64	1.14
3	1 (0.01)	1 (0)	3 (5)	3 (0.15)	3 (12)	3 (12)	8.26	1.45
4	1 (0.01)	1 (0)	4 (10)	4 (0.2)	4 (24)	4 (24)	9.3	1.49
5	1 (0.01)	2 (5)	1 (0)	1 (0)	2 (6)	2 (6)	7.8	0.88
6	1 (0.01)	2 (5)	2 (2)	2 (0.1)	1 (0)	1 (0)	10.9	0.92
7	1 (0.01)	2 (5)	3 (5)	3 (0.15)	4 (24)	4 (24)	13.82	4.55
8	1 (0.01)	2 (5)	4 (10)	4 (0.2)	3 (12)	3 (12)	23.96	2.71
9	1 (0.01)	3 (7.5)	1 (0)	2 (0.1)	3 (12)	4 (24)	7.66	1.53
10	1 (0.01)	3 (7.5)	2 (2)	1 (0)	4 (24)	3 (12)	9.8	1.94
11	1 (0.01)	3 (7.5)	3 (5)	4 (0.2)	1 (0)	2 (6)	14.44	1.83
12	1 (0.01)	3 (7.5)	4 (10)	3 (0.15)	2 (6)	1 (0)	22.56	1.52
13	1 (0.01)	4 (10)	1 (0)	2 (0.1)	4 (24)	3 (12)	10.78	2.00
14	1 (0.01)	4 (10)	2 (2)	1 (0)	3 (12)	4 (24)	14.12	1.05
15	1 (0.01)	4 (10)	3 (5)	4 (0.2)	2 (6)	1 (0)	12.72	0.94
16	1 (0.01)	4 (10)	4 (10)	3 (0.15)	1 (0)	2 (6)	19.48	4.01
17	2 (0.02)	1 (0)	1 (0)	4 (0.2)	1 (0)	4 (24)	4.34	0.80
18	2 (0.02)	1 (0)	2 (2)	3 (0.15)	2 (6)	3 (12)	7.62	1.46
19	2 (0.02)	1 (0)	3 (5)	2 (0.1)	3 (12)	2 (6)	12.72	1.69
20	2 (0.02)	1 (0)	4 (10)	1 (0)	4 (24)	1 (0)	15.5	0.33
21	2 (0.02)	2 (5)	1 (0)	4 (0.2)	2 (6)	3 (12)	7.68	0.41
22	2 (0.02)	2 (5)	2 (2)	3 (0.15)	1 (0)	4 (24)	4.5	2.25
23	2 (0.02)	2 (5)	3 (5)	2 (0.1)	4 (24)	1 (0)	15.72	1.82
24	2 (0.02)	2 (5)	4 (10)	1 (0)	3 (12)	2 (6)	18.16	1.97
25	2 (0.02)	3 (7.5)	1 (0)	3 (0.15)	3 (12)	1 (0)	8.46	0.90
26	2 (0.02)	3 (7.5)	2 (2)	4 (0.2)	4 (24)	2 (6)	16.08	2.49
27	2 (0.02)	3 (7.5)	3 (5)	1 (0)	1 (0)	3 (12)	11.92	2.85
28	2 (0.02)	3 (7.5)	4 (10)	2 (0.1)	2 (6)	4 (24)	18.16	1.24
29	2 (0.02)	4 (10)	1 (0)	3 (0.15)	4 (24)	2 (6)	13.38	3.29
30	2 (0.02)	4 (10)	2 (2)	4 (0.2)	3 (12)	1 (0)	17.68	1.20
31	2 (0.02)	4 (10)	3 (5)	1 (0)	2 (6)	4 (24)	9.22	3.54
32	2 (0.02)	4 (10)	4 (10)	2 (0.1)	1 (0)	3 (12)	21.98	3.99
I_{1j}	199.58	71.72	66.44	92.86	93.9	109.88	$T = 402.7$	
II_{2j}	203.12	102.54	88.34	105.56	93.4	109.7		
III_{3j}		109.08	98.82	98.08	111.02	102		
IV_{4j}		119.36	149.1	106.2	104.38	81.12		
R	0.2212	5.955	10.3325	1.6675	2.2025	3.595		
I_{1j}'	28.06	8.46	9.91	12.66	16.75	7.73		$T' = 58.29$
II_{2j}'	30.23	15.51	12.45	14.33	11.13	17.3		
III_{3j}'		14.3	18.67	19.43	12.5	16.81		
IV_{4j}'		20.02	17.26	11.87	17.91	16.45		
R′	0.1356	1.445	1.095	0.945	0.8475	1.1963		

yield of biomass reached 25.42 g/L under the optimized medium composition (data not shown).

The following results can also be concluded by analyzing the values of laccase activity. (1) Glucose which has the largest range R among six factors showed the greatest influence on enzyme activity, followed by urea and starch. Guaiacol has the smallest range R; (2) from the table, it is found that the combination of group seven with guaiacol concentration 0.01 mM, glucose concentration 5 g/L, the starch concentration 5 g/L, corn powder concentration 0.15 g/L, ammonium chloride concentration 24 g/L, and the urea concentration is 24 g/L, produced much more laccase than others. By comparing the magnitudes of I_{1j}', II_{2j}', III_{3j}' and IV_{4j}', the optimum combination is : the guaiacol concentration is 0.02 mM, the glucose concentration is 10 g/L, the starch concentration is 5 g/L, the corn powder concentration is 0.15 g/L, the ammonium chloride concentration is 24 g/L, and the urea concentration is 12 g/L. In conclusion, high guaiacol and glucose with lower urea concentration could promote the production of laccase. The laccase activity reached its maximum value of 8.21 U/mL under the optimized medium composition (data not shown).

20.3.1.2 Variance Analysis of the Orthogonal Experiment One

Variance analysis was performed according to the biomass of *T. versicolor* and laccase activity respectively. Results are showed in Tables 20.4 and 20.5. The *F*-value and the value of probability showed factors of glucose (B) and starch (C) were statistically significant at the 95 % confidence level; factor urea (F) was also significant at the 90 % confidence level. Other factors in the medium such as guaiacol, corn powder and ammonium chloride did not affect the yield of biomass significantly. The *F*-value of factors of guaiacol (A) and corn powder (D) were less than 1 due to the pure error of the DF. The fundamental way to confirm the significant of other factors in the medium is to increase the number of the

Table 20.4 ANOVA table for the orthogonal experiment one based on the biomass

Source	Sum of squares	df	Mean square	*F*-value	*p*-value
A	0.39	1	0.39	0.05	0.83
B	157.71	3	52.57	6.19	0.01**
C	459.08	3	153.03	18.01	0.00**
D	15.27	3	5.09	0.60	0.63
E	27.45	3	9.15	1.08	0.39
F	68.79	3	22.93	2.70	0.08*
Error	127.46	15	8.50		
Total	856.14				

* Statistically significant at the 90 % confidence level

** Statistically significant at the 95 % confidence level

A:$F_{0.05} = 4.54$, $F_{0.01} = 8.08$; B–F:$F_{0.05} = 3.29$, $F_{0.01} = 5.42$

Table 20.5 ANOVA table for the orthogonal experiment one based on the laccase activity

Source	Sum of squares	df	Mean square	*F*-value	*p*-value
A	0.15	1	0.15	0.30	0.59
B	8.50	3	2.83	5.75	0.01**
C	6.28	3	2.09	4.25	0.02**
D	4.33	3	1.44	2.93	0.07*
E	4.00	3	1.33	2.71	0.08*
F	7.85	3	2.62	5.31	0.01**
Error	7.39	15	0.49		
Total	38.50				

* Statistically significant at the 90 % confidence level
** Statistically significant at the 95 % confidence level
A:$F_{0.05} = 4.54$, $F_{0.01} = 8.08$; B–F:$F_{0.05} = 3.29$, $F_{0.01} = 5.42$

experiments. Another approach is to combine the SS and DF of factors which *F*-value was less than 1 with the SS and DF of error; As a result, the sensitivity of the hypothesis testing could be increased by increasing the DF of error as well as decreasing mean square of error. The data have been reprocessed. However, the results showed little changed (data not shown).

From the ANOVA analysis results (Table 20.5), it can be seen that the *F*-value and the value of probability showed factors of glucose (B), starch (C) and urea (F) were statistically significant at the 95 % confidence level; factors of corn powder (D) and ammonium chloride (E) were significant at the 90 % confidence level. In conclusion, glucose and starch could be the best mixed carbon source for the growth of *T. versicolor* and the laccase production. Meanwhile urea could be chosen as the nitrogen source in the medium.

20.3.2 Further Optimization of the Initial Medium

20.3.2.1 Audio-Visual Analysis of the Orthogonal Experiment Two

Table 20.5 shows that glucose and starch are the most significant factors ($p < 0.05$); they were selected as mixed carbon source for further optimization. Corn powder was water-insoluble; it's not so convenient in flask or fermentation tank culture. To simply the composition of the medium, the factor of corn powder playing the role of carbon source was not the most significant. The factor of corn powder was abandoned in the further optimization. On the target selection of the nitrogen source, taking into consideration the fact that urea contains carbon and nitrogen simultaneously, ammonium chloride was chosen as nitrogen source of the culture medium for further optimization. Nitrogen content in the urea was supplemented by improving the mass of ammonium chloride. Besides these three factors, the concentrations of other medium components were as follows: guaiacol 0.02 mM,

Table 20.6 Experimental results of orthogonal experiment two of three factors

Variable code Run Order	A g/L	B g/L	C g/L	Laccase activity U/mL
1	1	1	1	6.11
2	1	2	2	17.46
3	1	3	3	13.4
4	2	1	2	10.05
5	2	2	3	14.8
6	2	3	1	12.95
7	3	1	3	9.24
8	3	2	1	15.12
9	3	3	2	12.97
I_{1j}'	36.97	37.8	37.33	T'= 112.1
II_{2j}'	25.4	47.38	39.32	
III_{3j}'	34.18	40.48	37.44	
R′	0.28	7.33	2.10	

Table 20.7 ANOVA table for the orthogonal experiment two

Source	Sum of squares	df	Mean square	*F*-value	*p*-value
A	0.12	2	0.06	0.02	0.98
B	82.43	2	41.21	13.14	0.07
C	6.62	2	3.31	1.06	0.49
Error	6.27	2	3.14		
Total	95.43				

$F_{0.05} = 19$, $F_{0.01} = 99$

potassium dihydrogen phosphate 1 g/L, trace elements 7 mL/L,Vitamin B_1 8 mg/L, Vitamin C 1.5 mM and copper sulfate 0.05 mM. Orthogonal experimental design ($L_9(3 \times 3)$) was applied for the optimization of the primary optimized medium, the results are showed in Table 20.6. The orthogonal table L_9 (3^4) are used to arrange the experiments, three factors are evaluated each time and each factor take three levels.

Table 20.6 illustrates: (1) starch has the greatest influence on laccase activity, followed by ammonium chloride, and glucose has the least influence; (2) the optimized combination of three factors is $A_1B_2C_2$, where the glucose concentration is 5.25 g/L, the starch concentration is 5 g/L, the ammonium chloride concentration is 67 mM. Moreover, the average laccase activity value reached 17.46 U/mL under the optimized medium composition (group two) (Table 20.7).

20.3.2.2 Variance Analysis of the Orthogonal Experiment Two

Variance analysis was performed according to the laccase activity by *T. versicolor*. Three factors were not significant at the 95 % confidence level either; factors of

starch (B) were significant at the 90 % confidence level. The concentration of each factors appeared to reach the right level in present study, interaction of factors could be investigated in future research.

20.4 Conclusion

Based on above results, the performance of the medium optimization described in this work was satisfactory. The biomass and laccase activity were both investigated in the optimization experiment. Glucose followed by starch appeared to be the best carbon sources for the mycelia growth and laccase accumulation by *T. versicolor*. As nitrogen source, urea had the greater influence on the mycelia growth and laccase accumulation by *T. versicolor* than ammonium chloride. By future optimization, the optimum culture components were: glucose 5.25 g/L, starch 5 g/L, ammonium chloride 67 mM, guaiacol 0.02 mM, potassium dihydrogen phosphate 1 g/L, trace elements 7 mL/L,Vitamin B_1 8 mg/L,Vitamin C 1.5 mM and copper sulfate 0.05 mM. Under the optimized medium, the laccase activity of 17.46 U/mL was attained. The optimization of the medium resulted not only in one-fold increase in laccase activity than in the primary optimized medium, but also in a reduction of the constituent number and constituents costs.

Acknowledgments This work was supported by the National High Technology Research and Development Program ('863' Plan) (2013AA102106), and the Program for Changjiang Scholars and Innovative Research Team in University (IRT1166).

References

1. Reinhammar BRM (1984) Laccase. In: Lontie R (ed) Copper proteins and copper enzymes. Enzymes, CRC Press, FL, p 1–35, Chapter 1
2. Solomon EI, Sundaram UM, Machonkin TE (1996) Multicopper oxidases and oxygenases. Chem Rev 96:2563–2605
3. Alcalde M, Ferrer M, Plou FJ et al (2006) Environmental biocatalysis: from remediation with enzymes to novel green processes. Trends Biotechnol 24:281–287
4. Rodríguez Couto S, Toca Herrera JL (2006) Lacasses in the textile industry. Biotechnol Mol Biol Rev 1:115–120
5. Hou H, Zhou J, Wang J et al (2004) Enhancement of laccase production by *Pleurotus ostreatus* and its use for the decolorization of anthraquinone dye. Process Biochem 39:1415–1419
6. Minussi R, Pastore G, Dura′ n N (2007) Laccase induction in fungi and laccase/N-OH mediator systems applied in paper mill effluent. Bioresour Technol 98:158–164
7. Dekker R, Barbosa A, Giese E et al (2007) Influence of nutrients on enhancing laccase production by *Botryosphaeria rhodina* MAMB-05. Int Microbiol 10:177–185
8. Galhaup C, Wagner H, Hinterstoisser B et al (2002) Increased production of laccase by the wood-degrading basidio-mycete *Trametes pubescens*. Enzyme Microb Technol 30:529–536

9. Prasad K, Mohan V, Rao S et al (2005) Laccase production by *Pleurotus ostreatus* 1804: optimization of submerged culture conditions by Taguchi DOE methodology. Biochem Eng J 24:17–26
10. Vasconcelos AFD, Barbosa AM, Dekker RFH et al (2000) Optimization of laccase production by *Botriosphaeria sp.* in the presence of veratryl alcohol by the response-surface method. Process Biochem 35:1131–1138
11. Bettin F, Montanari Q, Calloni R et al (2009) Production of laccases in submerged process by *Pleurotus sajorcaju* PS-2001 in relation to carbon and organic nitrogen sources, antifoams and Tween 80. J Ind Microbiol Biot 36:1–9
12. Mikiashvili N, Elisashvili V, Wasser S et al (2005) Carbon and nitrogen sources influence the ligninolytic enzyme activity of *Trametes versicolor*. Biotechnol Lett 27:955–959
13. Mikiashvili N, Wasser S, Nevo E et al (2006) Effects of carbon and nitrogen sources on *Pleurotus ostreatus* ligninolytic enzyme activity. World J Microbiol Biotechnol 22:999–1002
14. Stajic M, Persky L, Friesem D et al (2006) Effect of different carbon and nitrogen sources on laccase and peroxidases production by selected *Pleurotus* species. Enzyme Microb Technol 38:65–73
15. Hou H, Zhou J, Wang J et al (2004) Enhancement of laccase production by *Pleurotus ostreatus* and its use for the decolorization of anthraquinone dye. Process Biochem 39:1415–1419
16. Marques de Souza CG, Tychanowicz GK, Farani de Souza D et al (2004) Production of laccase isoforms by *Pleurotus pulmonariusin* response to presence of phenolic and aromatic compounds. J Basic Microbiol 44:129–136
17. Klonowska A, Le Petit J, Tron T (2001) Enhancement of minor laccases production in the basidiomycete *Marasmius quercophilus* C30. FEMS Microbiol Lett 200:25–30
18. Palmieri G, Giardina P, Bianco C et al (2000) Copper induction of laccase isoenzymes in the ligninolytic fungus *Pleurotus ostreatus*. Appl Environ Microbiol 66:920–924
19. Dong J, Zhang Y, Zhang R et al (2005) Influence of culture conditions on laccase production and isozyme patterns in the white-rot fungus Trametes gallica. J Basic Microbiol 45:190–198
20. Lomascolo A, Record E, Herpoë l-Gimbert I et al (2003) Overproduction of laccase by a monokaryotic strain of *Pycnoporus cinnabarinus* using ethanol as inducer. J Appl Microbiol 94:618–624
21. Tinoco Raunel, AbisaíAcevedo Enrique Galindo et al (2011) Increasing *Pleurotus ostreatuslaccase* production by culture medium optimization and copper/lignin synergistic induction. J Ind Microbiol Biotechnol 38:531–540
22. Guo M, Lu FP, Pu J et al (2005) Molecular cloning of the cDNA encoding laccase from *Trametes versicolor* and heterologous expression in Pichia methanolica. Appl Microbiol Biotechnol 69(2):178–183

Chapter 21
The Preparation Methods and Scientific Development of Metal Nanoparticles by Microorganism

Pei Gong, Fang Wang and Jingran Liu

Abstract Metal nanoparticles (NPs) have been applied to different scientific fields. The synthesis of metal NPs is one of the most important research focuses. Metal NPs are synthesized by microorganism (such as bacteria, actinomyces, and fungi). It is well accepted that biosynthesis of inorganic NPs by microorganism is significant for both learning bio-mineralization mechanism and synthesis of advanced functional materials. The bottle-neck of current studies and the development orientation is pointed out by the recent processes.

Keywords Metal nanoparticles (NPs) · Microorganisms · Synthesis mechanism

21.1 Introduction

The field of nanotechnology is one of the most active areas of research in modern materials science. New applications of nanoparticles (NPs) and nanomaterials are emerging rapidly. There is tremendous current excitement in the study of nanoscales with respect to their fundamental properties, organization to form superstructures and applications. The unusual physicochemical and optoelectronic properties of NPs arise primarily due to confinement of electrons within particles of dimensions smaller than the bulk electron delocalization length, and this process is termed quantum confinement [1]. The exotic properties of NPs have been considered in applications such as optoelectronics [2], catalysis [3], reprography

P. Gong (✉) · J. Liu
College of Life Science, Inner Mongolia Agricultural University, Hohhot 010018, China
e-mail: gongpei022@yahoo.cn

F. Wang
TEDA School of Biological Science and Biotechnology, Nankai University, Tianjin 300457, China

T.-C. Zhang et al. (eds.), *Proceedings of the 2012 International Conference on Applied Biotechnology (ICAB 2012)*, Lecture Notes in Electrical Engineering 249,
DOI: 10.1007/978-3-642-37916-1_21, © Springer-Verlag Berlin Heidelberg 2014

[4], single-electron transistors and light emitters [5], nonlinear optical devices [6], and photoelectro-chemical applications [7].

The synthesis of NPs and their self-assembly is a cornerstone of nanotechnology. New methods to manufacture NPs are constantly being studied and developed. Various strategies are employed to synthesize semiconductor and transition metal NPs. Foremostly, among these chemical methods because of their inherent advantage in producing large quantities of NPs is relatively short periods of time with a fairly good control on the size distribution. Moreover, chemical synthesis of a variety of shapes of particles can be realized by adjusting the concentration of reacting chemicals and controlling the reaction environment [8]. Colloidal NPs so formed can be held apart by electrostatic interactions while in solution. However, upon extraction in powder form, the particles tend to grow and may lose their characteristic properties. Such a coalescence of the NPs can inhibited by passivating the particle surfaces either by adding organic/inorganic 'capping' molecules or by arresting their aggregation in a matrix of glass [9], zeolite [10], or organic polymers [11]. Chemically synthesized NPs can be directly deposited by spin or dip coating methods on suitable substrates. Composite bilayer or multilayer films of polymer/NPs can also be fabricated [12]. On the other hand, in physical synthesis of NPs [13], such as sputter deposition, laser ablation, or cluster beam deposition, thin films are directly grown. However, narrow size distribution of the particles or clusters is often difficult to achieve. Methods such as micelles or inverse micelles [14], Langmuir–Blodget films or self-assembled particles are other attractive possibilities to obtain a variety of NPs [15]. Desired assemblies of atoms can also be achieved using various scanning probe methods [16]. However, these methods are time consuming and still under development.

It has been known for a long time that a variety of nanomaterials are synthesized by biological processes in nature. The use of microorganisms in the synthesis of NPs is an eco-friendly and exciting approach. For example, the magnetotactic bacteria synthesize intracellular magnetite or greigite nanocrystallites [17]. Similarly, certain yeasts, when challenged with toxic metals such as cadmium, synthesize intracellular CdS nanocrystallites as a mechanism of detoxification [18].

In this chapter, we provide a brief overview of the research efforts worldwide on the use of microorganisms in the biosynthesis of inorganic NPs.

21.2 Recent Development of Biosynthesis NPs

21.2.1 Bacteria

Silver NPs were synthesized by a silver-tolerant strain *Pseudomonas stutzeri* AG259, which was incubated in the flasks at 30 °C and challenged with 50 mM soluble silver nitrate in dark for 48 h and this is the first report of mental NPs synthesized by bacteria [19]. Silver NPs were synthesized by a strain of

Lactobacillus sp. A09 and some characteristics of Ag biosorption and bioreduction by *Lactobacillus* sp. A09 were reported subsequently [20]. Single-crystalline gold nanoplates were produced by treating an aqueous solution of chloroauric acid with the extract of the unicellular green alga *Chlorella vulgaris* at room temperature [21]. The reduction of Pd(II) to Pd(0) was accelerated by using the sulfate-reducing bacterium *Desulfovibrio desulfuricans* NCIMB 8307 at the expense of formate or H2 as electron donors at pH 2–7, palladium (Pd) NPs were synthesized [22]. *Lactobacillus* strains, common in buttermilk, assist the growth of gold, silver, and gold–silver alloy crystals of submicron dimensions upon exposure to the precursor ions. Several well-defined crystal morphologies are observed. Crystal growth occurs by the coalescence of clusters, and tens of crystals are found within the bacterial contour [23]. *Pseudomonas aeruginosa* were used for extracellular biosynthesis of gold NPs (Au NPs). Consequently, Au NPs were formed due to reduction of gold ion by bacterial cell supernatant of *P. aeruginos* ATCC 90271, *P. aeruginos*, and *P. aeruginos* [24]. The bacteria *Rhodopseudomonas capsulata* was screened and found to successfully produce gold NPs of different sizes and shapes. The important parameter, which controls the size and shape of gold NPs, was pH value. It is continuing for the study of the biological mechanism of the NPs formation and the control of its shapes and sizes [25]. *Lactobacillus* sp. assisted to synthesize titanium (Ti) NPs at room temperature. Individual NPs as well as a number of aggregates almost spherical in shape having a size of 40–60 nm are found [26]. The silver NPs in size of 40−60 nm was synthesized by the supernatant of *Bacillus licheniformis* [27]. The exposure of culture supernatant of *Bacillus subtilus* and microwave irradiation to silver ion lead to the formation of silver NPs. The silver NPs were in the range of 5–60 nm in dimension and stable for several months [28]. *Bacillus megaterium* isolated from fluvial zone of North Bihar has been used for the extracellular synthesis of metal NPs via silver, lead, and cadmium and the synthesized NPs got accumulated on the surface of the cell wall of bacteria. *Bacillus megaterium* was grown aerobically and the cultures were challenged with the solutions of silver nitrate, lead nitrate, and cadmium nitrate in requisite ambience of laboratory [29]. The process of synthesis of well-dispersed NPs using a novel microorganism isolated from the gold enriched soil sample has been reported, leading to the development of an easy bioprocess for the synthesis of gold NPs. It is the first in which an extensive characterization of the indigenous bacterium isolated from the actual gold enriched soil was conducted. Promising mechanism for the biosynthesis of GNPs by the strain and their stabilization via charge capping is suggested, which involves an NADPH-dependent reductase enzyme that reduces Au^{3+} to Au^{0} through electron shuttle enzymatic metal reduction process [30]. The test strains *Klebsiella pneumoniae*, *Escherichia coli*, *Enterobacter cloacae* were cultivated in their special conventional conditions for 24 h. Silver nitrate at concentration of 10^{-3} M was separately added to the each reaction vessels that contained the supernatants, and the silver NPs were effectively produced and this is the first report on the production of silver NPs by enterobacteriaceae [31]. Devendra Jain experimented the mixed culture of various *Bacillus thuringiensis* to synthesis silver NPs, which were found to be highly toxic

against different multi drug resistant human pathogenic bacteria, also it is the first to synthesize NPs using mixed bacteria [32]. It was identified that extracellular biosynthesis of crystalline silver NPs is a unique biochemical character of all the members of genus *Morganella*, which was independent of environmental changes. Significantly, the inability of other closely related members of the family *Enterobacteriaceae* toward Ag-NPs synthesis strongly suggests that Ag-NPs synthesis in the presence of Ag^+ is a phenotypic character that is uniquely associated with genus *Morganella* [33].

21.2.2 Actinomycete

Thermomonospora sp. reduced the metal ions extracellularly when exposed to gold ions, yielding gold NPs with a much improved polydispersity [34]. The gold NPs of the dimension 5–15 nm were synthesized by an alkalotolerant actinomycete (*Rhodococcus* sp.) intracellularly. Electron microscopy analysis of thin sections of the gold actinomycete cells indicated that gold particles with good monodispersity were formed on the cell wall as well as on the cytoplasmic membrane. The particles are more concentrated on the cytoplasmic membrane than on the cell wall, possibly due to reduction of the metal ions by enzymes present in the cell wall and on the cytoplasmic membrane. The metal ions were not toxic to the cells and the cells continued to multiply after biosynthesis of the gold NPs [35]. The thermoalkalo-tolerant strain *Streptomyces* sp. and *Aspergillus fumigatus* were used for biosynthesis of silver NPs from $AgNO_3$ solutions in vitro. NPs formation was indicated by a change of the solution from colorless or light brown to dark brown after 24 h or more. The initial formation kinetics was faster with *Aspergillus*, but formation continued for a longer period with *Streptomyces*, resulting in higher concentrations after 48 h [36]. It is identified that the antibacterial activity of silver NPs can be synthesized by novel strain of *Streptomyces* sp., and this is the first report of synthesis from *Streptomyces* sp. The silver NPs exhibited a tremendous potential antibacterial activity against various gram positive and gram negative bacterial strains which are multi drug resistant [37].

21.2.3 Yeast

Silver NPs in the size of 2–5 nm were synthesized extracellularly by a silver-tolerant yeast strain MKY3, when challenged with 1 mM soluble silver in the log phase of growth. The NPs were separated from dilute suspension by devising a new method based on differential thawing of the sample. Extracellular synthesis of NPs could be highly advantageous from the point of synthesis in large quantities and easy downstream processing [38].

21.2.4 Fungi

When the fungus *Fusarium oxysporum was* exposed to aqueous $AuCl^{4-}$ ions, it reduced the metal ions and extracellularly produced the gold NPs [39]. The fungus *Verticillium* sp. reduced Ag^{+} and $AuCl^{4-}$ ions, leading to the accumulation of silver and gold NPs within the fungal biomass [34]. The gold NPs were synthesized by the geranium leaves (*Pelargonium graveolens*) and its endophytic fungus. Sterilized geranium leaves and an endophytic fungus (*Colletotrichum* sp.) growing in the leaves were separately exposed to aqueous chloroaurate ions. In both cases, rapid reduction of the metal ions was observed resulting in the formation of stable gold NPs of variable size. In the case of gold NPs synthesized using geranium leaves, the reducing and capping agents appear to be terpenoids while they are identified to be polypeptides/enzymes in the *Colletotrichum* sp. case. The biogenic gold NPs synthesized using the fungus were essentially spherical in shape while the particles using the leaves exhibited a variety of shapes that included rods, flat sheets, and triangles [40]. The silver NPs were synthesized by *Aspergillus fumigatus* in the extracellular. The synthesis process was so fast that the silver NPs were formed within minutes of silver ion coming in contact with the cell filtrate. The process of reduction being extracellular and fast may lead to the development of an easy bioprocess for synthesis of silver NPs [41]. The intracellular gold NPs were biosynthesized using three fungi including *Aureobasidiumv pullulans*, *Fusarium* sp., and *Fusarium oxysporum* after immersion the fungal cells in $AuCl^{4-}$ ions solution, active biomolecules of reducing sugar of *A. pullulans*, and proteins in *Fusarium* sp. and *F. oxysporum* were tested positive of providing the function of the reduction of $AuCl^{4-}$ ions and the formation of the gold crystals. The Au nano-fungal cells ultrathin sections of *Fusarium* sp. and *F. oxysporum* showed that the gold NPs mainly produced in intracellular vacuoles of fungal cells. The growth of gold NPs in three fungal cells indicated the reducing sugar lead to the gold NPs in spherical morphology and proteins benefited to the gold aggregates [42]. It is a report on photo-irradiated extracellular synthesis of silver NPs using the aqueous extract of edible oyster mushroom (*Pleurotus florida*) as a reducing agent. The biofunctionalized silver NPs thus produced have shown admirable antimicrobial effects, and the synthetic procedure involved is eco-friendly and simple, and hence high range production of the same can be considered for using them in many pharmaceutical applications [43]. The silver NPs were synthesized by the cell-free filtrate of *Aspergillus flavus* NJP08 when supplied with aqueous silver (Ag^{+}) ions. UV–Visible and Fourier transform infrared spectroscopy confirmed the presence of extracellular proteins. SDS-PAGE profiles of the extracellular proteins showed the presence of two intense bands of 32 and 35 kDa, responsible for the synthesis and stability of silver NPs, respectively. A probable mechanism behind the biosynthesis is discussed, which leads to the possibility of using the present protocol in future 'nano-factories' [44]. Silver NPs were synthesized extracellularly by a common fungus, *Alternaria alternata*. These NPs were evaluated for their part in increasing the antifungal activity. The antifungal

activity of fluconazole was enhanced in presence of silver NPs against the test fungi. Fluconazole in combination with Ag-NPs showed the maximum inhibition against *C. albicans*, followed by *P. glomerata* and *Trichoderma* sp. No significant enhancement of activity was found against *P. herbarum* and *F. semitectum* [45].

21.2.5 Virus

The central channel of the tobacco mosaic virus can be used as a template to synthesize nickel and cobalt nanowires only a few atoms in diameter, with lengths up to the micrometer range [46]. Various nanoarchitectures including NPs arrays, hetero-NPs architectures, and nanowires were assembled by utilizing highly engineered M13 bacteriophage as templates. The genome of M13 phage can be rationally engineered to produce viral particles with distinct substrate-specific peptides expressed on the filamentous capsid and the ends, providing a generic template for programmable assembly of complex nanostructures. Phage clones with gold-binding motifs on the capsid and streptavidin-binding motifs at one end are created and used to assemble Au and CdSe nanocrystals into ordered one-dimensional arrays and more complex geometries. These NPs arrays can be further used as templates to nucleate conductive nanowires that are important for addressing/interconnecting individual nanostructures [47].

21.3 Recent Development of NPs Synthesis Mechanism

Most metal ions are toxic and therefore, reduction of the ions or formation of water insoluble complexes is a defense mechanism developed by bacteria to overcome such toxicity. Microorganisms are often exposed to extreme environmental conditions, forcing them to resort to specific defense mechanisms to quell such stresses, including the solubility and toxicity of foreign metal ions. The toxicity of metal ions is reduced or eliminated by changing the redox state of the ions or precipitation of the metals intracellularly, thus forming the basis of many important applications of microorganisms such as bioleaching, bioremediation, microbial corrosion, as well as the synthesis of NPs.

It is identified that there are some adsorption groups of metal ions on the microbial surface, such as carboxyl, amino, phosphate group, sulfate, phenolic groups, and hydroxyl. Adsorption mechanism includes electrostatic adsorption, ion-exchange, complexation, sedimentation, and oxidation–reduction. The metal ions are adsorpted and reduced by enzymes presented in the cell wall leading to the formation of metal NPs, which subsequently grow by further reduction of metal ions and accumulation on these nuclei. The metal ions can be chelated by the amide group and carboxyl in the cell wall; the metal ions can be reduced to metal atoms by utilizing the electron donor that is from the aldehyde and ketone groups

of monosaccharides which is hydrolyzed by the polysaccharide compound of peptidoglycan layer; the protein, and sugars in the cell wall can also adsorb the metal ions.

The biological reduction mechanism includes enzyme-dependent catalytic mechanism and enzyme-independent reduction mechanism. Enzyme-dependent mechanism is considered that the metal ions were reduced by the microorganism's biological enzyme, the enzyme reduction sites may be in the cytoplasmic membrane, cytoplasm periplasmic, or extracellular, and different biological enzyme involved in different metal ion reduction mechanism. Enzyme-independent reduction mechanism considered that the metal ions were reduced by the functional groups on the cell wall surface without the biological enzyme. This process includes two steps: Adsorption to fixed and in situ reduction. Metal particles were restored as single quality when they were reduced, because the functional groups on the cell wall surface interfered the aggregation, and the metal particles were in the nanometre size.

The synthesis process of NPs intracellular includes two steps: metal ions were combined with the protein of cell wall surface and they were reduced to nanocluster by the secreted enzyme firstly; then the nanocluster diffuse through the cell wall and are reduced by enzymes present on the cytoplasmic membrane and within the cytoplasm.

In contrast, the study on the extracellular synthesis of NPs is more clear. It was identified that there are three related genes associated with the synthesis of silver NPs, *silE*, *silP*, and *silS*, encoding periplasmic binding protein, transport P-ATPase of positive ions, and bicomponent membrane Kinase, respectively. Silver NPs were synthesized when challenged with silver nitrate because of the three secreted protein.

We speculate that since the NPs are formed on the surface of the mycelia and not in solution, the first step involves trapping of the Ag^+ on the surface of the fungal cells possibly via electrostatic interaction between the Ag^+ and negatively charged carboxylate groups in enzymes present in the cell wall of the mycelia. Thereafter, the silver ions are reduced by enzymes present in the cell wall leading to the formation of silver nuclei, which subsequently grow by further reduction of Ag^+ and accumulation on these nuclei.

In short, a variety of biologically active molecules are used to synthesize metal NPs by microorganisms, such as reductase, naphthoquinone, anthraquinone, reducing sugars, reduced glutathione, and proteins. It is believed that the NADH and NADH-dependent nitrate reductase play an important role in the reduction reaction.

So far, the synthesis mechanism is not clear, but most speculation are similar.

21.4 Conclusions and Future Directions

In summary, a brief overview of the use of microorganisms, such as bacteria, actinomycetes, yeasts, and fungi in the biosynthesis of metal NPs has been described. The biosynthesis of metal NPs by bacteria and eukaryotes has been

matured, but actinomycetes are not. The actinomycetes have important feature of prokaryotes and eukaryotes, which are easy to culture and can secrete a lot of proteins, therefore, the biosynthesis of metal NPs by actinomycetes should become an important research direction.

We hope it has been made for the serious study of the synthesis of NPs by microorganisms as a possible viable alternative to the more popular inorganic methods. The use of microorganisms as sources of enzyme that can catalyze specific reactions leading to inorganic NPs is a new and rational strategy. Extracellular secretion of enzyme offer the advantage of obtaining large quantities in a relatively pure state, free from other cellular proteins associated with the organism and can be easily processed by filtering of the cells, and isolating the enzyme for NPs synthesis from cell-free filtrate. The use of specific enzymes secreted by microorganisms in the synthesis of NPs is exciting. Firstly, the process can be extended to the synthesis of NPs of different chemical compositions. Secondly, different shapes and sizes by suitable identification of enzymes can be secreted by microorganisms. Understanding the surface chemistry of the biogenic NPs would be equally important.

This would then lead to the possibility of genetically engineering microorganisms to over express specific reducing molecules and capping agents and thereby, control the size and shape of the biogenic NPs. The rational use of constrained environments within cells such as the periplasmic space and cytoplasmic vesicular compartments to modulate NPs size and shape is an exciting possibility yet to be seriously explored. The microorganisms-mediated green approach toward the synthesis of NPs has many advantages such as ease with which the process can be scaled up, economic viability, and possibility of easily covering large surface areas by suitable growth of the mycelia. The shift from inorganic methods to biosynthesis as a means of developing natural 'nano-factories' has the added advantage that downstream processing and handling of the biomass would be much simpler. Compared to inorganic methods, in which the process technology involves the use of sophisticated equipment for chemistry synthesis, microorganisms medium can be easily filtered by filter press of similar simple equipment, thus saving considerable investment costs for equipment. Fungi have been found to be extremely efficient secretors of soluble protein and under optimized conditions of fermentations, mutant strains secrete up to 30 g per liter of extracellular protein. In the strains selected for enzyme fermentations, the desired enzyme constitutes the only component or at least form the major ingredient of the secreted protein with high specific activities. It is this trait of high-level protein secretion, besides their eukaryotic nature, that has made fungi as favorite hosts for heterologous expression of high-value mammalian protein for manufacturing by fermentation. Further, compared to bacteria, fungi and actinomycetes are known to secrete much higher amounts of proteins, thereby significantly increasing the productivity of this biosynthetic approach.

Equally intriguing are questions related to the selection of microbial medium, the control of NPs shapes, the industrial production, the metal ion reduction process in cellular metabolism and whether the NPs formed as by-products of the

reduction process have any role to play in a cellular activity. They are expected to be solved and applied.

References

1. Fendler JH, Meldrum FC (1995) The colloid chemical approach to nanostructured materials. Adv Mater 7(7):607–632
2. Colvin VL, Schlamp MC, Alivisatos AP (1994) Light-emitting diodes made from cadmium selenide nanocrystals and a semiconducting polymer. Nature 370(4):354–357
3. Schmid G (1992) Large clusters and colloids, metals in the embryonic state. Chem Rev 92(8):1709–1727
4. Hamilton JF, Baetzold RC (1979) Catalysis by small metal clusters. Science 205:1213–1220
5. Klein DL, Roth R, Lim AKL et al (1997) A single-electron transistor made from a cadmium selenide nanocrystal. Nature 389:699–701
6. Wang Y (1991) Nonlinear optical properties of nanometer-sized semiconductor clusters. Acc Chem Res 24(5):133–139
7. Mansur HS, Grieser F, Marychurch MS et al (1995) Photoelectrochemical properties of 'Q-State' CdS particles in arachidic acid Langmuir-Blodgett films. J Chem Soc Faraday Trans 91:665–672
8. Murray CB, Kagan CR (2000) Synthesis and characterization of monodisperse nanocrystals and close-packed nanocrystal assemblies. Annu Rev Mater Sci 30:545–610
9. Shiang JJ, Risbud SH, Alivisatos AP (1993) Resonance Raman studies of the ground and lowest electronic excited state in CdS nanocrystals. J Chem Phys 98:8432–8440
10. Stucky GD, Dougall JEM (1990) Quantum confinement and host/guest chemistry, probing a new dimension. Science 247:669–678
11. Kane RS, Cohen RE, Silbey R (1996) Synthesis of PbS nanoclusters within block copolymer nanoreactors. Chem Mater 8(8):1919–1924
12. Gao MY, Richter B, Kirstein S (1998) Electroluminescence studies on selfassembled films of PPV and CdSe nanoparticles. J Phys Chem 102(21):4096–4103
13. Ayyub P, Chandra R, Taneja P et al (2001) Synthesis of nanocrystalline material by sputtering and laser ablation at low temperatures. Appl Phys A Mater Sci Process 73(1):67–73
14. Pileni MP (1997) Nanosized particles made in colloidal assemblies. Langmuir 13(13):3266–3276
15. Torimoto T, Tsumura N, Miyake M et al (1999) Preparation and photoelectrochemical properties of two-dimensionally organized CdS nanoparticle thin films. Langmuir 15(5):1853–1858
16. Eigler DM, Schweizer EK (1990) Positioning single atoms with a scanning tunnelling microscope. Nature 344:524–526
17. Frankel RB, Papaefthymiou GC, Blakemore RP (1983) Fe_3O_4 precipitation in magne-totactic bacteria. Biochim Biophys Acta Mol Cell Res 763(2):147–159
18. Dameron CT, Reese RN, Mehra RK et al (1989) Biosynthesis of cadmium sulphide quantum semiconductor crystallites. Nature 338:596–597
19. Klaus T, Olsson E, Granqvist CG et al (1999) Silver-based crystalline nanoparticles, microbially fabricated. Natl Acad Sci 24:13611–13614
20. Zho FJ (2000) Spectroscopic charcterization on the biosorption and bioreduction of Ag by *Lactobacillus* sp. A09. Acta Phys Chim Sin 6(9):779–782
21. Xie JP, Ting YP (2007) Identification of active biomolecules in the high-yield synthesis of single-crystalline gold nanoplates in algal solutions. Small 3(4):672–682

22. Yong P (2002) Bioreduction and biocrystallization of palladium by desulfovibrio desulfuricans NCIMB 8307. Biotechnol Bioeng 80(4):369–379
23. Nair B, Pradeep T (2002) Coalescence of nanoclusters and formation of submicron crystallites assisted by *Lactobacillus* strains. Crystal Growth Design 2:293–298
24. Husseiny MI, Badrc Y, Mahmoud MA et al (2007) Biosynthesis of gold nanoparticles using *Pseudomona saeruginosa*. Spectrochim Acta A Mol Biomol Spectrosc 67:1003–1006
25. He SY, Zhang Y, Zhang S et al (2007) Biosynthesis of gold nanoparticles using the bacteria *Rhodopseudomonas capsulata*. Mater Lett 61:3984–3987
26. Prasad K, Kulkarni AR (2007) *Lactobacillus* assisted synthesis of ttitanium nano-particles. Nanoscale Res Lett 2(5):248–250
27. Kalimuthu K, Bilal M, Gurunathan S et al (2008) Biosynthesis of silver nanocrystals by *Bacillus licheniformis*. Colloids Surf B Biointerfaces 65(1):150–153
28. Saifuddin N (2009) Rapid biosynthesis of silver nanoparticles using culture supernatant of bacteria with microwave irradiation. E J Chem 6(1):61–70
29. Prakash A, Ahmad N, Sinha P et al (2010) Bacteria mediated extracellular synthesis of metallic nanoparticles. Int Res J Biotechnol 1(5):71–79
30. Nangia Y (2009) A novel bacterial isolate stenotrophomonas maltophilia as living factory for synthesis of gold nanoparticles. Microb Cell Fact 8:39–40
31. Minaeian S (2008) Extracellular biosynthesis of silver nanoparticles by some bacteria. Indian J Biotechnol 117:1–4
32. Jain D, Jain R, Kothari SL et al (2010) Novel microlbial route to synthesize silver nanoparticles using spore crystal mixture of *Bacillus thuringiensis*. Indian J Exp Biol 48:1152–1156
33. Parikh R, Coloe P, Ramanathan R et al (2011) Genus-wide physicochemical evidence of extracellular crystalline silver nanoparticles biosynthesis by *Morganella* spp. PLoS One 6(6):1–7
34. Sastry M (2003) Biosynthesis of metal nanoparticles using fungi and actinomycete. Curr Sci 85:162–170
35. Ahmad A (2003) Intracellular synthesis of gold nanoparticles by a novel alkalotolerant Actinomycete, *Rhodococcus* species. Nanotechnology 14:286–294
36. Alani F,Anderson W (2012) Biosynthesis of silver nanoparticles by a new strain of *Streptomyces* sp. compared with *Aspergillus fumigatus*. World J Microbiol Biotechnol 28:1081–1086
37. Shirley A, Sreedhar B (2010) Antimicrobial activity of silver nanoparticles synthesized from novel *Streptomyces* species. Digest J Nanomater Bio-struct 5(2):447–451
38. Kowshik M, Kharrazi S (2003) Extracellular synthesis of silver nanoparticles by a silver-tolerant yeast strain MKY3. Nanotechnology 14:95–100
39. Mukherjee P, Ahmad A, Sastry M et al (2002) Extracellular synthesis of gold nanoparticles by the Fungus *Fusarium oxysporum*. ChemBioChem 3(5):461–463
40. Shankar SS (2003) Bioreduction of chloroaurate ions by geranium leaves and its endophytic Fungus yields gold nanoparticles of different shapes. J Mater Chem 13(7):1822–1828
41. Kuber C, Bhainsa S, Souza FD (2006) Extracellular biosynthesis of silver nano-particles using the fungus *Aspergillus fumigatus*. Colloids Surf B Biointerfaces 47(2):160–164
42. Zhang XR (2011) Different active biomolecules involved in biosynthesis of gold nanoparticles by three fungus species. Plant Resour Conserv Util Res 2(1):53–64
43. Bhat R (2011) Photo-irradiated biosynthesis of silver nanoparticles using edible mushroom pleurotus Florida and their antibacterial activity studies. Bioinorg Chem Appl 5:1–7
44. Jain N (2011) Extracellular biosynthesis and characterization of silver nanoparticles using *Aspergillus flavus* NJP08: a mechanism perspective. Nanoscale 3(2):635–639
45. Gajbhiye M (2009) Fungus-mediated synthesis of silver nanoparticles and their activity against pathogenic Fungi in combination with fluconazole. Nanomedicine 5(4):382–386
46. Knez M, Boes F (2003) Biotemplate synthesis of 3-nm nickel and cobalt nanowires. Nano Lett 3:1079–1082
47. Huang Y, Lee SK (2005) Programmable assembly of nanoarchitectures using genetically engineered viruses. Nano Lett 5:1429–1434

Chapter 22
Increasing Galactose Utilized Ability of *Saccharomyces cerevisiae* Through Gene Engineering

Tong Shen, Xuewu Guo, Jing Zou, Yueqiang Li, Jun Ma and Dongguang Xiao

Abstract *Saccharomyces cerevisiae* is capable of fermenting galactose into ethanol, but the productivity from galactose is much lower than those from glucose. An effective approach is undertaken to improve galactose utilized ability and ethanol productivity through gene engineering of the regulatory network controlling the expression of the *GAL* genes. The *GAL* gene regulatory network of *S. cerevisiae* is a tightly regulated system. *Gal6*, *Gal80*, and *Mig1* are three known negative regulators of the *GAL* system. In this paper, *Gal6*, *Gal80*, and *Mig1* were knockout by the way of homologous recombination. This led to a 76 % increase in specific galactose uptake rate compared with the wild-type strain. And the ethanol yield has advanced greatly. Further study showed that *GAL80* and *MIG1* played more important roles in galactose fermentation of *S. cerevisiae* than *GAL6* did.

Keywords Galactose · *MIG1* · *GAL80* · *GAL6* · *Saccharomyces cerevisiae*

22.1 Introduction

Because of increasing oil shortage, fuel ethanol fermentation from different renewable resource has attracted considerable attention. Galactose is widely present in the molasses and ethanol bio-fermentation raw materials. Unfortunately, ethanol yield and productivity from galactose are significantly lower than those from glucose [1].

An effective approach improved galactose utilized ability and ethanol productivity through engineering of the regulatory network controlling the expression of the *GAL* genes [2–4]. Previous studies reported that the *GAL* genes are tightly

T. Shen · X. Guo · J. Zou · Y. Li · J. Ma · D. Xiao (✉)
Key Laboratory of Industrial Fermentation Microbiology, Ministry of Education; Tianjin Industrial Microbiology Key Lab, College of Biotechnology, Tianjin University of Science and Technology, Tianjin, People's Republic of China
e-mail: xdg@tust.edu.cn

T.-C. Zhang et al. (eds.), *Proceedings of the 2012 International Conference on Applied Biotechnology (ICAB 2012)*, Lecture Notes in Electrical Engineering 249,
DOI: 10.1007/978-3-642-37916-1_22, © Springer-Verlag Berlin Heidelberg 2014

regulated [5, 6]. *GAL* gene expression requires the well-studied transcriptional activator protein Gal4, which binds to the *GAL* gene promoters. Gal4 function is inhibited by Gal80 [7, 8], which binds directly to Gal4, and by Mig1, which represses expression of *GAL1* and *GAL4* in the presence of glucose [9–11]. *GAL6*, which was recently devoted as member of the GAL regulon [12], also played a negative role in *GAL* gene expression. In this work, the galactose metabolic flux of saccharomyces cerevisiae was increased by deleting three negative regulatory genes (*GAL6*, *GAL80*, and *MIG1*), this led to a 76 % increase in specific galactose uptake rate compared with the wild-type strain, and the ethanol yield has advanced greatly. Further study showed that *GAL80* and *MIG1* played more important roles in galactose fermentation of *Saccharomyces cerevisiae* than *GAL6* did.

22.2 Materials and Methods

22.2.1 Plasmids and Strains

The recombinant plasmid pUC-MABK used for *MIG1* deletion provided by Zhang [13]. The recombinant plasmid pUC-G80ABK and pUC-G6ABK used for *GAL80* and *GAL6* deletion provided in this study. Yeast strain AY-5α and Escherichia coli strain DH5α used in this study were obtained from the Yeast Collection Center of TianJin industrial Microbiology Key Laboratory of Tianjin University of Science and Technology, P.R. China. The EY-501α, EY-502α, EY-503α, FY-501α, FY-502α, FY-503α, and GY-501α were generated from AY-5α, and the genotype of all the yeast strains was listed in Table 22.1.

Table 22.1 Yeast strains used in this study

Strains	Genotype	Source
AY-5α		X. Guo (5)
EY-501α	*mig1::KanMX*	This study
	gal80::KanMX	This study
EY-502α	*gal6::KanMX*	This study
	gal80::loxP::mig1::KanMX	This study
EY-503α	*gal80::loxP::gal6::KanMX*	This study
FY-501α	*gal6::loxP::mig1::KanMX*	This study
FY-502α		
FY-503α		
GY-501α	*gal80::loxP:: gal6::loxP::mig1::KanMX*	This study

22.2.2 Media and Cultivation Conditions

Escherichia coli strain DH5α was incubated in Luria–Bertani medium added ampicillin resistance for plasmid maintenance. Yeast strains were cultured in YEPD medium at 30 °C. The recombinant strains were screened on YEPD plates additionally added 1000 μg/mL G418. Galactose medium (galactose 6 %; $(NH_4)_2SO_4$ 0.5 %; KH_2PO_4 0.1 %; $MgSO_4{\cdot}7H_2O$ 0.05 %; 10 ml/L trace element solution; 1 mL/L vitamin solution), and mixture sugar media (glucose 3 %, galactose 3 %, $(NH_4)_2SO_4$ 0.5 %; KH_2PO_4 0.1 %; $MgSO_4{\cdot}7H_2O$ 0.05 %; 10 ml/L trace element solution; 1 mL/L vitamin solution) is used for the glucose repression assay [14].

22.2.3 Standard Solutions for the Media Used

The trace-element solution and vitamin solution contained the following compositions: Trace element solution: 3 g/L EDTA; 0.09 g/L $CaCl_2{\cdot}2H_2O$; 0.90 g/L $ZnSO_4{\cdot}7H_2O$; 0.60 g/L $FeSO_4{\cdot}7H_2O$; 200 mg/L H_3BO_3; 156 mg/L $MgCl_2{\cdot}2H_2O$; 80 mg/L $Na_2MoO_4{\cdot}2H_2O$; 60 mg/L $CoCl_2{\cdot}2H_2O$; 60 mg/L $CuSO_4{\cdot}5H_2O$; and 20 mg/L KI. The pH of the trace element solution was adjusted to 4.00 with NaOH, and autoclaved.

Vitamin solution: 50 mg/L d-biotin; 200 mg/L *para*-amino-benzoic acid; 1 g/L nicotinic acid; 1 g/L Capantothenate; 1 g/L pyridoxine·HCl; 1 g/L thiamine·HCl; and 25 g/L *m*-inositol. The pH was adjusted to 6.5 and stored at 4 °C after sterile filtration [15].

22.2.4 Analytical Methods

Glucose and galactose concentrations were determined by high-performance liquid chromatography [16]. Ethanol concentration was determined by gas chromatography.

22.3 Results and Discussion

22.3.1 Construction of Recombinant Strains

The recombinant cassette *MIG1A-Kan-MIG1B*, *GAL80A-Kan-GAL80B*, *and GAL6A-Kan-GAL6B* fragment was amplified by PCR from plasmid pUC-MABK, pUC-G80ABK, and pUC-G6ABK, respectively, and transformed into the parental

strains AY-5α by the lithium acetate method [17], resulting three single gene deletion mutant strains (EY-501α, EY-502α, and EY-503α). Then the plasmid pGAPza which expressed the Cre recombinase was transformed into the transformant in order to excise the drug resistance gene of *KanMX* from the chromosome of recombinant strains [18]. After that, by transforming a different recombinant cassette into the transformant we constructed by the same method, three successfully double genes deletion mutant strains (FY-501α, FY-502α, and FY-503α). Repeating the procedures above, the three genes deletion mutant strain (GY-501α) was constructed finally. In the procession of constructing the transformant mentioned, the *loxp-kan-loxp* resistant cassette amplified from plasmid pUG6 (a generous gift from professor Hegemann) was repeatedly used through transforming the plasmid pGAPza expressing the Cre recombinase [19].

22.3.2 Fermentation on Galactose of all the Strains

In the same culture condition, all the strains were cultured in galactose medium. The galactose utilized ability and ethanol productivity were compared (Tables 22.2 and 22.3). The maximum specific galactose uptake rate was shown in Table 22.4. The rates demonstrated that all the recombinant strains showed an

Table 22.2 Galactose concentration during the fermentation (g/100 ml)

Time(h)	AY-5α	EY-501α	EY-502α	EY-503α	FY-501α	FY-502α	FY-503α	GY-501α
0	5.71	5.71	5.71	5.71	5.71	5.71	5.71	5.71
12	5.44	5.08	5.05	5.27	4.82	5.09	5.06	4.83
24	4.57	3.94	3.87	4.32	3.57	3.91	3.89	3.51
36	3.56	2.75	2.64	3.34	2.32	2.53	2.73	2.29
48	2.78	1.93	1.77	2.44	1.13	1.45	1.89	1.22
60	1.97	1.02	0.88	1.54	0.22	0.44	1.01	0.31
72	1.15	0.31	0.13	0.62	0.00	0.00	0.29	0.00

Table 22.3 Ethanol yield (g/100 ml)

Time(h)	AY-5α	EY-501α	EY-502α	EY-503α	FY-501α	FY-502α	FY-503α	GY-501α
72	1.62	2.09	2.18	1.88	2.36	2.32	2.09	2.34

Table 22.4 The maximum specific galactose uptake rate[a] (g gal/g dry yeast/h)

AY-5α	EY-501α	EY-502α	EY-503α	FY-501α	FY-502α	FY-503α	GY-501α
1.24	1.57	1.71	1.35	2.11	1.73	1.57	2.18

[a] The maximum specific galactose uptake rate was calculated from the biomass yield and the maximum specific growth rate. The biomass yield was obtained as the slope of the linear curve when plotting the biomass or metabolite concentration versus the galactose concentration during exponential growth

obvious increase in flux through the galactose utilization pathway compared with the wild-type strain, so was the ethanol yield. Among all the strains, GY-501α showed a 76 % increase in specific galactose uptake rate [20] compared with the wild-type strain. The comparisons of the whole fermentation period of all the strains indicated that *GAL80* and *MIG1* played more important roles in galactose fermentation of *S. cerevisiae* than *GAL6* did.

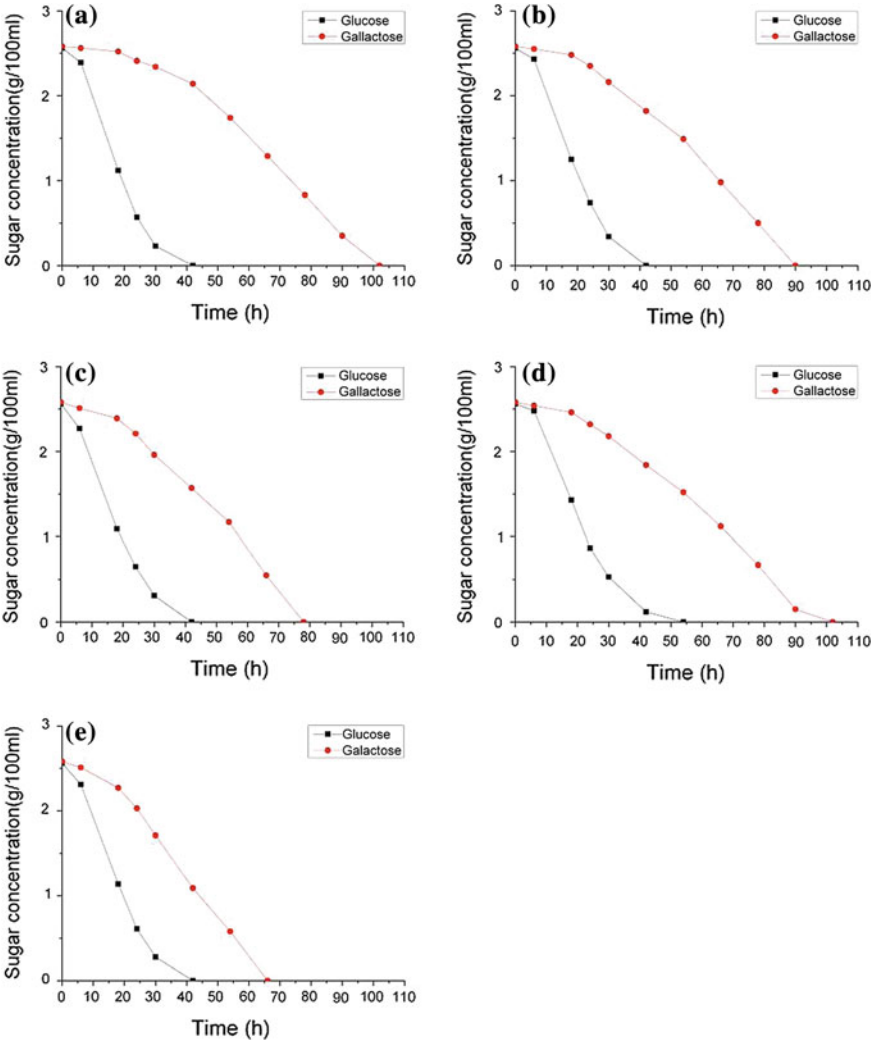

Fig. 22.1 The curves of sugar consumption of strains in the glucose-galactose mixture

22.3.3 The Curves of Sugar Consumption in Glucose–galactose Mixture Medium of Different Carbon Source

The glucose and galactose utilization in the two sugars mixture media of the five strains AY-5α, EY-501α, EY-502α, EY-503α, and FY-501α (listed in Fig. 22.1) were determined. There was glucose repression in all of the strains, the consumption order of glucose and galactose was obvious, but the curves of sugar consumption of each strains were significantly different. In wild type strain AY-5α (Fig. 22.1a), during the time of glucose completely consumpted, only a little of the galactose was consumed. In strain EY-503α (Fig. 22.1d), the phenomenon was little less than that in AY-5α. In strains EY-501α (Fig. 22.1b), EY-502α (Fig. 22.1c), and FY-501α (Fig. 22.1e), the consumption of glucose and galactose was simultaneous, while glucose still present in the media, galactose began to be consumpted, the fermentation time was much shorter than that of AY-5α.

22.4 Conclusion

To increase flux through the galactose utilization pathway of *S. cerevisiae*, we constructed mutant strains missing *GAL6* and/or *GAL80* and/or *MIG1*. Rates from the galactose fermentation were gratifying. The *ΔGAL6* mutants, *ΔGAL80* mutants, and *ΔMIG1* mutants showed a 9, 27, and 38 % increase in specific galactose uptake rate, respectively. The maximum increase in flux (76 %) was achieved by deletion of all three genes. In glucose–galactose mixture medium, galactose utilization was repressed by glucose. Deletion of *GAL8*0 gene or *MIG1* gene had partly relieved glucose repression of galactose metabolism. However, deletion of *GAL6* gene did not have a marked effect.

Acknowledgments This work was financially supported by the program of National High Technology Research and Development Program of China (863 Program) (Grant No. SS2012AA023408), the Cheung Kong Scholars, and Innovative Research Team Program in University of Ministry of Education, China (Grant No. IRT1166), and Application Base and Frontier Technology Project of Tianjin, China (Grant No. 09JCZDJC17900). The work is supported by the "2012–2013" Foundation of Laboratory of Tianjin University of Science and Technology, P.R. China (Grant No. 1204A209).

References

1. Lee KS, Hong ME, Jung SC et al (2011) Improved galactose fermentation of Saccharomyces cerevisiae through inverse metabolic engineering. Biotechnol Bioeng 108:621–631
2. Replogle K, Hovland L, Rivier DH (1999) Designer deletion and prototrophic strains derived from Saccharomyces cerevisiae strain W303-1a. Yeast 15:1141–1149

3. Ostergaard S, Olsson L, Nielsen J (2000) Metabolic engineering of Saccharomyces cerevisiae. Microbiol Mol Biol R 64:34–50
4. Golovleva L, Golovlev E (2000) Microbial cellular biology and current problems of metabolic engineering. J Mol Catal B-Enzym 10:5–21
5. Rubio TM (2005) A comparative analysis of the GAL genetic switch between not-so-distant cousins: Saccharomyces cerevisiae versus Kluyveromyces lactis. FEMS Yeast Res 5:1115–1128
6. Lohr D, Venkov P, Zlatanova J (1995) Transcriptional regulation in the yeast GAL gene family: a complex genetic network. FASEB J 9:777–787
7. Igarashi M, Segawa T, Nogi Y et al (1987) Autogenous regulation of the Saccharomyces cerevisiae regulatory gene GAL80. Mol Gen Genet 207:273–279
8. Gill G, Ptashne M (1988) Negative effect of the transcriptional activator GAL4. Nature 334:721–724
9. Nehlin JO, Carlberg M, Ronne H (1991) Control of yeast GAL genes by MIG1 repressor: a transcriptional cascade in the glucose response. EMBO J 10:3373–3377
10. Treitel MA, Carlson M (1995) Repression by SSN6-TUP1 is directed by MIG1, a repressor/activator protein. P Natl Acad Sci Usa 92:3132–3136
11. Keleher CA, Redd MJ, Schultz J et al (1992) Ssn6-Tup1 is a general repressor of transcription in yeast. Cell 68:709–719
12. Zheng W, Xu HE, Johnston SA (1997) The cysteine-peptidase bleomycin hydrolase is a member of the galactose regulon in yeast. J Biol Chem 272:30350–30355
13. Zhang Y, Xiao DG, Zhang CY (2011) Effect of MIG1 gene deletion on glucose repression in baker's yeast. Adv Mater Res 396–398:1531–1535, Advances in chemical engineering: ICCMME
14. van den Brink J, Akeroyd M, van der Hoeven R, et al (2009) Energetic limits to metabolic flexibility: responses of Saccharomyces cerevisiae to glucose–galactose transitions. Microbiology+ 155:1340–1350
15. Thomas TD, Turner KW, Crow VL (1980) Galactose fermentation by Streptococcus lactis and Streptococcus cremoris: pathways, products, and regulation. J Bacteriol 144:672–682
16. Chen SF, Mowery RA, Castleberry VA et al (2006) High-performance liquid chromatography method for simultaneous determination of aliphatic acid, aromatic acid and neutral degradation products in biomass pretreatment hydrolysates. J Chromatogr A 1104:54–61
17. Gietz RD, Schiestl RH (1995) Transforming yeast with DNA Methods. Mol Cell Biol 5:255–269
18. Ribeiro O, Gombert AK, Teixeira JA et al (2007) Application of the Cre-loxP system for multiple gene disruption in the yeast Kluyveromyces marxianus. J Biotechnol 131:20–26
19. Güldener U, Heck S, Fiedler T et al (1996) A new efficient gene disruption cassette for repeated use in budding yeast. Nucleic Acids Res 24:2519–2524
20. Ostergaard S, Olsson L, Johnston M et al (2000) Increasing galactose consumption by Saccharomyces cerevisiae through metabolic engineering of the GAL gene regulatory network. Nat Biotechnol 18:1283–1286

Chapter 23
Expression and Characterization of a Thermophilic Trehalose Synthase from *Meiothermus ruber* CBS-01 in *Pichia pastoris*

Yufan Wang, Wenwen Wang, Jun Zhang, Yueming Zhu, Yanchao Liu, Laijun Xing and Mingchun Li

Abstract Trehalose synthase (TreS) was proved to catalyze the reversible reaction of maltose into trehalose by intramolecular transglucosylation. In this work, a yeast expression system was constructed to express TreS from *Meiothermus ruber* CBS-01 in the eukaryotic *Pichia pastoris* expression system. The *TreS* gene with 6× His tag at the 3′ end was subcloned into the eukaryotic expression vector pPIC3.5K. Then the constructed vector was integrated into *Pichia pastoris* strain KM71. The recombinant was induced by sterile methanol and the bioactive TreS was expressed successfully intracellular. After optimizing culture conditions, we got approximately 150 mg/L recombinant protein. It was the first time to express TreS from *M. ruber* CBS-01 in eukaryotic expression system. The purified TreS was also characterized in details.

Keywords *Meiothermus ruber* CBS-01 · Optimal expression and characterization · *Pichia pastoris* · Trehalose synthase (TreS)

Y. Wang · W. Wang · Y. Zhu · Y. Liu · L. Xing · M. Li (✉)
Key Laboratory of Molecular Microbiology and Technology, Ministry of Education, Department of Microbiology, Nankai University, Tianjin 300071, People's Republic of China
e-mail: nklimingchun@yahoo.com.cn

J. Zhang
Tianjin Forestry and Pomology Institute, Tianjin 300192, People's Republic of China

Y. Wang
Tianjin Third Central Hospital, Tianjin 300170, China

Y. Zhu
Tianjin Institute of Industrial Biotechnology, Chinese Academy of Sciences, Tianjin 300308, China

T.-C. Zhang et al. (eds.), *Proceedings of the 2012 International Conference on Applied Biotechnology (ICAB 2012)*, Lecture Notes in Electrical Engineering 249,
DOI: 10.1007/978-3-642-37916-1_23, © Springer-Verlag Berlin Heidelberg 2014

23.1 Introduction

Trehalose is a non-reducing disaccharide widely found in various organisms [1]. It has been reported that this sugar is heat- and acid-stable, and can protect organisms or tissues against environmental stresses such as dryness, osmotic stress, heat or cold shock, and so on [2, 3]. Hence, trehalose has been widely used in cosmetic industry, food industry, and in medical industry [4, 5].

Up to now, there are five pathways involved in trehalose biosynthesis [6]. Among all of these, the trehalose synthase (TreS) can convert maltose into trehalose in only one-step reaction and the substrate of the enzyme is inexpensive. Therefore, the enzyme is suitable to produce trehalose in industry. Some *TreS* genes have been isolated and cloned from different organisms. Many of them had been purified and/or expressed in *Escherichia coli* [7–11]. However, TreSs reported so far processed a problem of low yield in the original organisms.

Up to the present, some thermophilic TreSs were discovered in some bacteria, such as *Thermus thermophilus* [12], *Thermus aquaticus* [13], and *Meiothermus ruber* [14]. They will be more suitable for industrial application because of the thermophilicity and stability. But there is not any report about the expression of thermophilic TreSs in eukaryotic expression systems.

The methylotrophic yeast *Pichia pastoris* is well known for being effective in producing recombinant proteins. As a eukaryote, *P. pastoris* can perform some co- and/or post-translational modifications of foreign proteins. The proteins expressed in *P. pastoris* were usually folded with the correct disulfide bonds [15]. Additionally, *P. pastoris* needs a low maintenance energy, which was fitted for high density fermentation.

In our previous research, a *TreS* gene was obtained from *Meiothermus ruber* strain CBS-01 [14]. In this work, a yeast expression system was constructed to express TreS of *M. ruber* CBS-01 in eukaryotic expression system. Under optimal culture conditions, the recombinant protein was expressed and purified. Furthermore, the properties of the enzyme were characterized in details.

23.2 Materials and Methods

23.2.1 Strains, Plasmids, and Regents

E. coli DH5α, *P. pastoris* KM71 (Darmstadt, German) were used for cloning and expression, respectively. Intracellular expression vector pPIC3.5K was purchased from Invitrogen (California, USA).

E. coli DH5α was cultured in LB broth (100 μg/mL ampicillin). The medium MD was used for selection of transformant, the medium YPD, BMGY, and BMMY were used for *P. pastoris* culture and induction, respectively. All the

media were prepared following the methods mentioned in the introduction of Pichia Expression Kit (Invitrogen, USA)

Binding buffer and elution buffer were used for protein purification by NTA-Ni column as described previously [16]. Washing buffer (10 mmol/L potassium phosphate buffer (pH 6.5)) was used for protein purification by Hi-trap Q column.

The restriction enzymes and Taq polymerases were obtained from Takara (Dalian, China). Columns for protein purification were purchased from GE (Tokyo, Japan). Glucose, maltose, and trehalose were got from Sigma (St.Louis, MO). The other chemicals and reagents were of analytical grade.

23.2.2 Construction of Expression Plasmid

The *TreS* gene of *M. ruber* CBS-01 was amplified from pET21a-TreS with primers pPICF (5′-CGGAATTCGCGAGTATGGGTGTGGATCCTCTTTGG, *Eco*R I restriction enzyme site underlined) and pPICR (AATGCGGCCGCCTA **GTGGTGGTGATGATGGTG**GCGGGCCCGTTCCTTCCACC, *Not* I restriction enzyme site underlined and a 6× His tag sequence in bold). The ORF is 2913 bp and encodes 970 amino acid residues. The amplified DNA was ligated into *Eco*R I-and *Not* I-digested pPIC3.5K to produce pPIC3.5K-TreS for intracellular expression.

23.2.3 **Pichia pastoris** *Transformation, Expression, and Activity Detection of TreS*

The purified vector pPIC3.5K-TreS was linearized by *Sal* I. The linearized DNAs were transformed into *P. pastoris* strain KM71 by electroporation following the guide of the Pichia expression kit (Invitrogen, USA). Then the positive transformants were selected on the MD plates. The recombinant strain KM71/pPIC3.5K-TreS was identified by PCR using primers 5′AOXI and 3′AOXI.

Identified transformants were cultured in 5 ml BMGY medium at 30 °C for 2 days. Cells were harvested by centrifugation at 3000 g for 10 min, and then were resuspended in 5 ml BMMY medium and grown for another 2 days. For inducing of the expression of TreS, sterile methanol was added into the BMMY medium to a final concentration of 0.5 % (v/v) every day. After intracellular expression, the culture was centrifuged at 3000 g for 5 min and the supernatant was decanted. The cell pellet was suspended in 1 ml washing buffer and cells were disrupted by shaking with glass beads for 5 times of 1 min shaking, with 1 min intermission on ice. After incubated at 60 °C for 1 h and centrifuged at 10000 g for 10 min, the supernatant was analyzed by SDS-PAGE. At the same time, a same volume of

50 mmol/L maltose solution in washing buffer was added and the mixture was incubated at 50 °C for 60 min to detect the activity of TreS.

The activity of TreS was analyzed by measuring the amount of trehalose produced from maltose. The production was assayed by high performance liquid chromatography (HPLC). HPLC was performed as follows: Hypersil-NH_2 column Ø 4.6 * 250 mm; 80 % acetonitrile- 20 % water eluent (v/v); flow rate 1.0 ml/min; column temperature 30 °C; evaporative light scattering detection.

23.2.4 Optimized Expression of TreS in Pichia pastoris

Each single clone of *P. pastoris* transformants was cultivated and induced as described above. To yield a highest level of TreS, the cultivations were carried out at different conditions including the final concentration of methanol, initial cell density for induction, the times to add methanol every day, and the induction time.

All data were obtained at least 3 times and were shown as mean ± SD.

23.2.5 Purification of TreS and Enzyme Characterization

A single clone of recombinant strain was inoculated in 5 ml BMGY medium, grown overnight at 3 °C with shaking. A 1 mL of culture was inoculated into 100 mL the same medium and grown at 30 °C for 24 h with 200 r/min. Cells were then harvested by centrifuging for 5 min at 3000 g. The cell pellets were resuspended in 50 mL of BMMY medium in a 500-mL shake flask and cultured under the optimum condition for TreS expression. At the end of incubation, the culture broth was centrifuged at 3000 g for 5 min and the supernatant decanted. The cells were grinded by liquid nitrogen, and then suspended in washing buffer. The supernatant was centrifuged at 10000 g for 10 min and then filtered through 0.22 μm filter. The crude enzyme was purified using NTA-Ni column chromatography as described previously [16]. The eluted solution was loaded on a Hi-trap Q ion-exchange column (200 * 10 mm) equilibrated with a washing buffer. The protein was eluted with a linear gradient of 0–1.0 mol/L NaCl in washing buffer. The active fractions were pooled, then concentrated and desalted by Amicon Ultra-4 centrifugal filter. The protein concentration was quantified using Bradford's method [17]. The purified enzymes were analyzed with 10 % SDS–PAGE. The kinetic parameters, effect of temperature, and pH on the activity and stability of TreS were measured by the methods described previously [16].

23.3 Results

23.3.1 *Expression and Activity Detection of TreS in* Pichia pastoris

After induction using methanol, the expression of TreS was analyzed by SDS-PAGE and the activity of enzyme was detected. In contrast with the negative control, a single protein band around 110 kDa was clearly visible by SDS-PAGE analysis of crude extract from cell pellet for KM71/pPIC3.5K-TreS.

The activity of TreS was determined by HPLC. After cell-free extracts of KM71/pPIC3.5K-TreS reacted with 2 % (w/v) maltose at 50 °C for 60 min, trehalose and a small amount of glucose were detected by HPLC (data not shown). All of the above results indicated that TreS was expressed successfully intracellular in *P. pastoris* KM71.

23.3.2 *Optimized Expression of TreS in* Pichia pastoris

23.3.2.1 The Optimal Harvest Time of TreS Expression in *Pichia pistoris*

To determine the optimal time for TreS production, a time-course analysis on the TreS accumulation was carried out within 168 h. At each time point, the expression samples were withdrawn to analyze the activity of TreS. The accumulation of TreS was proportional to its activity, so the activity of TreS was used to estimate its expression level. As shown in Fig. 23.1, the sample of 96 h after induction showed the highest activity. A plateau was reached beyond this time point, which indicated that 96 h is the best time to harvest the cells.

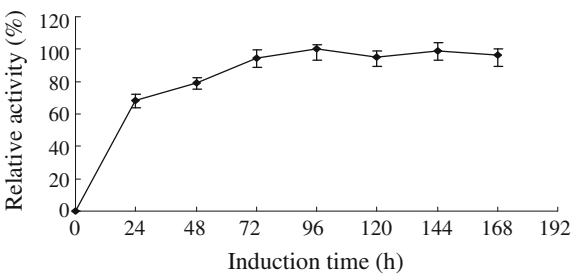

Fig. 23.1 The effect of induction time on the accumulation of TreS in *P. pastoris* KM71

23.3.2.2 Effect of Inoculum Concentration at Induction Phase on TreS Production

Generally, a high density of cells resulted in an increase of recombinant protein production. However, high cell densities mean that oxygen and nutrition will become limiting factors. The initial culture was adjusted to different OD_{600} before induction. We observed that when the density of biomass from BMGY culture reached about $OD_{600} = 12$ (as shown in Fig. 23.2), a culminating point could be achieved in the accumulation of TreS. And inoculum densities above $OD_{600} = 12$ did not result in obvious increase in TreS accumulation.

23.3.2.3 Effect of Methanol Addition on the Induction of TreS

During the expression of TreS, the addition of methanol into the media was performed once every 12 or 24 h to keep induction. The TreS production induced by different concentrations of methanol was compared to determine the optimal condition. When the concentration of methanol in the medium was below 0.75 % (v/v), there was no inhibition on the growth of yeast cells. The TreS accumulation was proportional to the concentration of methanol and peaked at 0.75 % (Fig. 23.3). When the concentration of methanol was too high (above 0.75 %), the production of TreS was suppressed, and the yield of the enzyme was reduced. Therefore, TreS expression reached the highest level by the addition of methanol to a final concentration of 0.75 % each 12 h.

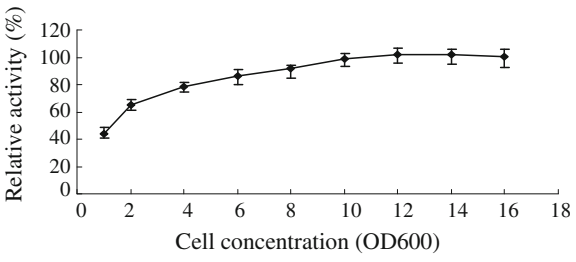

Fig. 23.2 The effect of cell density before induction on the accumulation of TreS in *P. pastoris* KM71

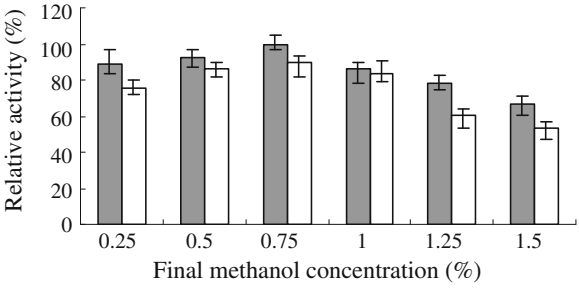

Fig. 23.3 The effect of methanol concentration and adding frequency on the accumulation of TreS in *P. pastoris* KM71. Methanol was added every 12 h (*solid bar*) or 24 h (*open bar*)

23.3.2.4 Optimal Expression and Purification of TreS

Under optimal culture conditions, the TreS expressed abundantly. The recombinant TreS was purified and analyzed by SDS-PAGE which revealed a single protein band around 110 kDa consisted with the deduced molecular weight of TreS (data not shown). The protein concentration was approximately 2 mg/mL. And the yield of the expression of TreS in *P. pastoris* was about 150 mg/L.

23.3.3 *Kinetics Analysis of TreS Expressed in* Pichia pastoris

The kinetic parameters of TreS expressed in *P. pastoris* were showed in Table 23.1. The K_m value using maltose as substrate was nearly to that using trehalose as substrate, implying that TreS from *M. ruber* CBS-01 expressed in *P. pastoris* had the same affinity to maltose and trehalose. However, the enzyme had approximately twofold conversion rate (k_{cat}) and catalytic efficiency (k_{cat}/K_m) using maltose as substrate to that using trehalose as substrate, which led the priority to produce trehalose.

23.3.4 *Effects of Temperature and pH on the Activity and Stability of TreS Expressed in* Pichia pastoris

The optimum temperature for TreS expressed in *P. pastoris* was about 50 °C. Besides, TreS showed outstanding thermo-tolerance, and it could maintain more than 90 % of its activity within a temperature range of 0–60 °C (Fig. 23.4a).

As shown in Fig. 23.4b, TreS expressed from *P. pastoris* showed the highest activity at pH 6.5. And between pH 5.0–8.0, the enzyme could highly maintain the original activity. This indicated that TreS has both good adaptability and survivability against pH.

The purified TreS from *P. pastoris* was thermostable and acid tolerant, which made it suitable to produce trehalose in industry.

And all the results above showed that TreS from *M. ruber* was successfully expressed in *P. pastoris*.

Table 23.1 Kinetic parameters of the recombinant TreS expressed in *Pichia pastoris* KM71

Substrate	K_m (mmol/L)	V_{max} (mmol/L·min)	k_{cat} (s^{-1})	k_{cat}/K_m (L/mol·s)
Maltose	97.2 ± 3.5	943.5 ± 28.6	174.7 ± 5.3	1798.2 ± 10.7
Trehalose	95.6 ± 6.9	424.9 ± 22.4	78.7 ± 4.1	823.9 ± 16.2

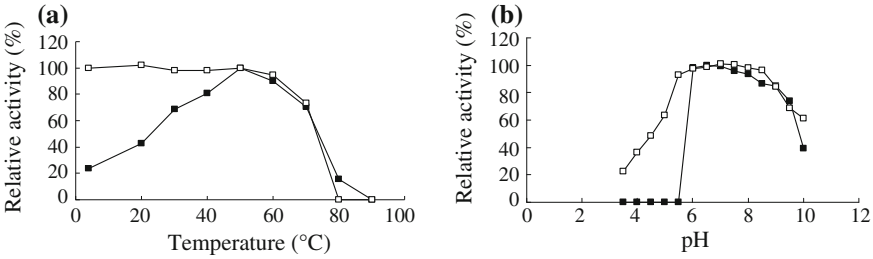

Fig. 23.4 Effects of temperatures (**a**) and pH (**b**) on the activity (*solid square*) and stability (*open square*) of TreS expressed in *P. pastoris* KM71, respectively

23.3.5 *Effects of Metal Ions on the Activity of TreS Expressed in* Pichia pastoris

Table 23.2 showed the effects of metal ions on the activity of purified TreS expressed in *P. pastoris*. The activity of the enzyme was inhibited strongly by 10 mmol/L divalent and trivalent cations in our experiment except Mg^{2+}. However, we did not find any metal ion which can increase the enzyme activity remarkably.

23.3.6 *The Stability of TreS Expressed in* Pichia pastoris *During Storage*

The hetero-expressed TreS was stored at 4 °C for some time and then the residual activities were examined. In was shown that TreS can reserve 98.2 % of its activities after 60 days of storage at 4 °C, indicating that the TreS expressed by *P. pastoris* was very stable during storage.

Table 23.2 Effects of metal ions on the activity of TreS expressed in *P. pastoris* KM71

Reagent concentration	Relative activity (%)										
	None	Na^+	K^+	Zn^{2+}	Fe^{2+}	Ca^{2+}	Cu^{2+}	Mg^{2+}	Mn^{2+}	Co^{2+}	Al^{3+}
1 mmol/L	100	99.1	98.6	75.3	102.2	68.5	61.3	103.7	81.6	92.8	94.2
2 mmol/L	100	102.5	101.3	86.4	97.6	53.1	65.4	101.3	70.4	79.2	0
10 mmol/L	100	103.7	104.0	0	0	8.8	0	95.1	0	0	0

23.4 Discussion

Due to the outstanding advantage of TreS in producing trehalose, there have been lots of TreS isolated from different organisms, and most of them were expressed successfully in *E. coli.* However, *E. coli* and other prokaryotic expression systems have several disadvantages. For example, in these expression systems, the foreign protein is prone to form inclusion body during fermentation, and the expression level is not very high. Moreover, the expression vector is easy to lose [15]. On the other hand, there is little reports to show that the TreS was expressed in eukaryotic expression systems.

In our precious work, a *TreS* gene was cloned from the thermophilic bacteria *M. ruber* CBS-01 and expressed in *E. coli*. However, the expression level in *E. coli* was low (about 5 mg/L), which greatly hindered it to be applied in industrial production. Considering the notable advantages of *P. pastoris* in expressing foreign proteins, we tried out the *P. pastoris* expression system to produce TreS to investigate the character of the enzyme in eukaryotic cells.

Using the intracellular eukaryotic expression system, we optimized the inducing condition of TreS in *P. pastoris*. Under the optimal condition, the KM71/pPIC3.5K-TreS produced approximately 150 mg/L recombinant TreS, which was almost 30 times of that in *E. coli* expression system. This provided an experimental basis for further industrial production of TreS.

One factor that affects expression of foreign proteins in *P. pastoris* is the Mut phenotype of the recombinant strain. KM71/pPIC3.5K-TreS constructed in this study was Mut^S. In principle, Mut^S recombinant is better for intracellular expression because the strain produces little alcohol oxidase, and the purification of foreign proteins will be easier [18]. For secreted expression, Mut^+ is a preferable choice. However, there is not a specific relationship between them, so both Mut^+ and Mut^S recombinants are useful as one phenotype may favor better expression of the foreign proteins than the other. Therefore, we will investigate and the expression of TreS in the Mut^+ recombinant of *P. pastoris* GS115 system in our further study. Besides, it was demonstrated that multiple copy integration of recombinant genes into the genome of *P. pastoris* could enhance the expression of foreign proteins [19]. So we will screen the recombinants of multiple inserts of *TreS* and test whether mutli-copy of *TreS* can increase expression at the same time.

We have investigated the expression of secreted TreS in both *E.coli* and *P. pastoris,* previously. Unfortunately, no activity of TreS was detected in the culture supernatant after induction. It is probable that the TreS is a naturally endocellular protein in *M. ruber*. However, the soluble fraction of protein extract after cell breaking showed TreS activity. It was indicated that the TreS was expressed endocellularly, but failed to be secreted to the medium. The amino acid sequence was predicted as a hydrophilicity protein by Expasy (http://www.expasy.ch/tools/protscale.html). There was no predicted transmembrane region in the protein which may inhibit the protein to secrete.

The TreS expressed in *P. pastoris* was a thermostable protein which was easy to be purified from non-thermophilic proteins expressed in *P. pastoris*. At same time, it could maintain 90 % of its activity after incubating at pH 5.5–pH 9.0. The storage of TreS expressed in *P. pastoris* was convenient. Hence, the TreS reported here is potential to be applied in industry.

Acknowledgments This work was supported by the Tianjin Natural Science Foundation (No. 10JCYBJC09600, 10JCYBJC05000), National Natural Science Foundation of China (No. 21076162)

References

1. Elbein AD, Pan YT, Pastuszak I et al (2003) New insights on trehalose: a multifunctional molecule. Glycobiology 13:17–27
2. Kandror O, DeLeon A, Goldberg AL (2002) Trehalose synthesis is induced upon exposure of *Escherichia coli* to cold and is essential for viability at low temperatures. Proc Natl Acad Sci USA 99:9727–9732
3. Muller J, Wiemken A, Aeschbacher R (1999) Trehalose metabolism in sugar sensing and plant development. Plant Sci 147:37–47
4. Schiraldi C, Di Lernia I, De Rosa M (2002) Trehalose production: exploiting novel approaches. Trends Biotechnol 20:420–425
5. Satpathy GR, Trk Z, Bali R et al (2004) Loading red blood cells with trehalose: a step towards biostabilization. Cryobiology 49:123–136
6. Kouril T, Zaparty M, Marrero J et al (2008) A novel trehalose synthesizing pathway in the hyperthermophilic *Crenarchaeon Thermoproteus tenax*: the unidirectional TreT pathway. Arch Microbiol 190:355–369
7. Chen YS, Lee GC, Shaw JF (2006) Gene cloning, expression, and biochemical characterization of a recombinant trehalose synthase from *Picrophilus torridus* in *Escherichia coli*. J Agric Food Chem 54:7098–7104
8. Pan YT, Koroth EV, Jourdian WJ et al (2004) Trehalose synthase of *Mycobacterium smegmatis*. Eur J Biochem 271:4259–4269
9. Ma Y, Xue L, Sun DW (2006) Characteristics of trehalose synthase from permeablized *Pseudomonas putida* cells and its application in converting maltose into trehalose. J Food Eng 77:342–347
10. Zdzieblo A, Synowiecki J (2006) Production of trehalose by intramolecular transglucosylation of maltose catalysed by a new enzyme from *Thermus thermophilus* HB-8. Food Chem 96:8–13
11. Wang JH, Tsai MY, Lee GC et al (2007) Construction of a recombinant thermostable β-amylase-trehalose synthase bifunctional enzyme for facilitating the conversion of starch to trehalose. J Agric Food Chem 55:1256–1263
12. Wang JH, Tsai MY, Chen JJ et al (2007) Role of the C-terminal domain of *Thermus thermophilus* trehalose synthase in the thermophilicity, thermostability, and efficient production of trehalose. J Agric Food Chem 55:3435–3443
13. Tsusaki K, Nishimoto T, Nakada T et al (1997) Cloning and sequencing of trehalose synthase genen from *Thermus aquaticus* ATCC 33923. Biochim Biophys Acta 1334:28–32
14. Zhu Y, Zhang J, Wei D et al (2008) Isolation and identification of a thermophilic strain producing trehalose synthase from geothermal water in China. Biosci Biotechnol Biochem 72:2019–2024

15. Daly R, Hearn MTW (2005) Expression of heterologous proteins in *Pichia pastoris*: a useful experimental tool in protein engineering and production. J Mol Recognit 18:119–138
16. Zhu Y, Wei D, Zhang J et al (2010) Overexpression and characterization of a thermostable trehalose synthase from *Meiothermus ruber*. Extremophiles 14:1–8
17. Bradford MM (1976) A rapid and sensitive method for the quantitation of microgram quantities of protein utilizing the principle of protein-dye binding. Anal Biochem 72:248–254
18. Wang Q, Li Q, Xue J et al (2006) Characteristic and application of *Pichia pastoris* expresser. Biotechnol Lett 17:640–643
19. Cregg JM, Vedvick TS, Raschke WC (1993) Recent advances in the expression of foreign genes in *Pichia pastoris*. Nat Biotechnol 11:905–910

Chapter 24
Effect of Carbon Source on Fermentation Cultivation of *Streptococcosis suis* Vaccine Strain SD11

Yichun Wu, Lizhong Miao, Ming Li and Likun Cheng

Abstract The high cell-density cultivation technology of *Streptococcosis suis* vaccine strain SD11 in 10 L bioreactor was studied. The effect of different initial carbon sources on fermentation of *S. suis* vaccine strain SD11 were evaluated, and results indicated that the sucrose should be as initial carbon source. The opportune concentration of initial carbon sources was 4 g/L sucrose by analysing the effect of different sucrose concentrations on *S. suis* vaccine strain cultivation. The effect of different feeding substrate and residual glucose concentration on fermentation of *S. suis* vaccine strain SD11 were investigated, results showed that glucose solution was selected as feeding substrate and the residual glucose concentration should be controlled at low level. Applying the pH feedback feeding strategy, the concentration of residual glucose was maintained at a low level, the accumulation of lactic acid was 8.0 g/l, and both biomass and viable count improved obviously were 5.89 g/l, 7.02×10^9 cfu/ml, respectively.

Keywords *Streptococcosis suis* · Vaccine · Carbon sources · pH Feedback feeding

24.1 Introduction

Streptococosis was a kind of contagion, which was caused by the enteropathogenic strains of *Streptococcus* [1]. *Streptococcus suis* is a gram-positive bacterium that can cause meningitis, pneumonia, septicemia, sudden death, and other symptoms

Y. Wu (✉) · M. Li
Biological Engineering College of Binzhou Polytechnic, Binzhou 256603 Shandong, China
e-mail: wuyichun2002cn@yahoo.com.cn

L. Miao · L. Cheng
Animal Science and Veterinary Medicine Institute, Binzhou 256600 Shandong, China

T.-C. Zhang et al. (eds.), *Proceedings of the 2012 International Conference on Applied Biotechnology (ICAB 2012)*, Lecture Notes in Electrical Engineering 249,
DOI: 10.1007/978-3-642-37916-1_24, © Springer-Verlag Berlin Heidelberg 2014

in pigs, and it is also emerging as a zoonotic agent capable of causing severe invasion in humans via injured and inflamed skin or mucous membrane [2]. Based on capsular antigens, 35 serotypes (type 1/2 and 1–34) have been described. Serotype 2 of *S. suis* is generally thought to have the strongest pathogenicity, and also the most frequently reported serotype isolated from diseased animals worldwide [3]. Many strategies have been reported to prevent the *Streptococosis*, such as drug and immunization, and vaccine is an effective method for prevention and control of infectious diseases [1]. The preferred technology for production of *S. suis* vaccine strain was used by high cell-density cultivation.

Optimization of carbon source is a key factor for achieving high cell-density cultivation. Glucose is the preferred carbon source in bacterium cultivation as it is an inexpensive and readily utilizable carbon and energy source. Growth of *S. suis* vaccine strain on excess glucose causes the formation of acidic byproducts, the most common of which is lactic acid [4]. Lactic acid is a primary inhibitory metabolite in *S. suis* vaccine strain cultivation, and is detrimental to bacterial growth. The accumulation of lactic acid was decreased with the concentration of carbon source maintained an appropriate level, which could increase the viable count of *S. suis* vaccine strain. In production of L-threonine, the results of various carbon sources used in L-threonine fermentation showed that the maximum dry cell weight and yield of L-threonine obtained with sucrose as the initial carbon source [5]. In this study, *S. suis* vaccine strain SD11 fermentation with various initial carbon sources was compared. The effect of initial carbon source concentration, feeding substrates, and residual glucose concentration on *S. suis* vaccine strain SD11 fermentation was investigated. The concentration of initial carbon source was obtained, and a pH feedback feeding method was developed in *S. suis* vaccine strain SD11 fermentation.

24.2 Materials and Methods

24.2.1 Microorganism and Medium

The *S. suis* vaccine strain SD11 used in this study was isolated in our laboratory and stored in our laboratory.

The seed medium contained the components as follows: glucose 1 g/l, peptone 0.5 g/l, $MgSO_4 \cdot 7H_2O$ 0.05 g/l, KH_2PO_4 0.1 g/l, and blood serum 2 %. The medium for *S. suis* vaccine strain SD11 fermentation contained the following: source 4 g/l, peptone 0.5 g/l, $MgSO_4 \cdot 7H_2O$ 0.05 g/l, KH_2PO_4 0.1 g/l, and blood serum 2 %. The pH of both seed and fermentation media was adjusted based on specific experimental requirements.

24.2.2 Culture Methods

24.2.2.1 Fermentation in Automated Microbiology Growth Analysis Systems

A 500 ml baffled flask containing 150 ml of seed medium was inoculated with a single colony of *S. suis* vaccine strain SD11 and cultivated at 37 °C for 7 h. Thirty microlitre of this culture was inoculated into a 400 μl inoculum in Automated Microbiology Growth Analysis Systems (Bioscreen C) containing 350 μl fermentation medium and cultivated at 37 °C with shaking at normal amplitude for 7 h.

24.2.2.2 Fermentation in a Bioreactor

A 500 ml baffled flask containing 150 ml of seed medium was inoculated with a single colony of *S. suis* vaccine strain SD11 and cultivated at 37 °C for 7 h. Fed-batch fermentation was performed in 10 l jar fermenters. The seed culture was inoculated aseptically (10 % (v/v)) into 6 l of fermentation medium contained in a 10 l jar fermenters, and cultivated at 37 °C for 7 h. The pH was adjusted to 7.0 with 4 mol/l of NaOH during the whole cultivation period. The DO level was maintained at approximately 10 % saturation by adjusting the agitation and aeration rates. When the initial carbon source was depleted, 50 % (w/v) feeding substrate was fed into the fermenter to meet specific experimental requirements.

24.2.3 Analysis of Fermentation Process

The optical density (DO), pH, and temperature were measured automatically with electrodes attached to the fermenters. The OD was monitored by the Microbiology Growth Analysis Systems. Dry cell weight, viable count, and specific growth rate of this strain were determined as described previously [4]. The concentrations of glucose and lactic acid were monitored by an SBA-40E biosensor analyzer. The concentration of source was measured by the colorimetry of sulfuric acid-anthrone [6].

24.3 Results

24.3.1 Effect of Initial Carbon Source on S. suis *Vaccine Strain SD11 Fermentation*

Many kinds of sugar can be used as carbon source in *S. suis* vaccine strain fermentation. The effect of different carbon source on *S. suis* vaccine strain SD11 fermentation was investigated by adding 5 g/l glucose, 5 g/l sucrose, 5 g/l lactose,

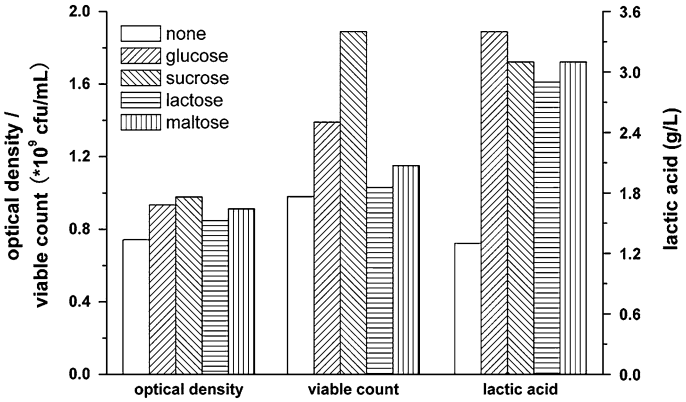

Fig. 24.1 Effect of initial carbon sources on fermentation of *S. suis* vaccine strain SD11

and 5 g/l maltose to the fermentation medium, respectively, which were carried out in Automated Microbiology Growth Analysis Systems.

Results of *S. suis* vaccine strain SD11 fermentation with various carbon sources are presented in Fig. 24.1. When no carbon source was added to the fermentation medium, the excretion of lactic acid was lowest, and the viable count was also lowest because of lack of carbon source. The accumulation of lactic acid was highest with glucose as initial carbon source. When the lactose used as initial carbon source, the accumulation of lactic acid was low, but both optical density and viable count were low, which showed that lactose was not an appropriate carbon source for this strain. The maximum optical density and viable count were obtained with sucrose as initial carbon source, indicating that sucrose is the optimal initial carbon source for *S. suis* vaccine strain SD11 fermentation.

24.3.2 Effect of Initial Carbon Source on S. suis *Vaccine Strain SD11 Fermentation*

Metabolic ways of bacterium were affected by the concentration of carbon source. The excretion of byproducts was decreased with an appropriate concentration of carbon source. The sucrose of 2 g/l, 4 g/l, 6 g/l, 8 g/l, and 10 g/l were selected as the initial carbon source in *S. suis* vaccine strain SD11 fermentation.

The effects of initial carbon source concentration on optical density and viable count are plotted in Fig. 24.2, along with the concentration of lactic acid. Concentration of lactic acid increased with increasing concentrations of sucrose. When the sucrose concentration was 2 g/l, optical density, viable count, and concentration were low. Both optical density and viable count decreased with sucrose concentration above 6 g/l. Too high or too low sucrose concentration were adverse

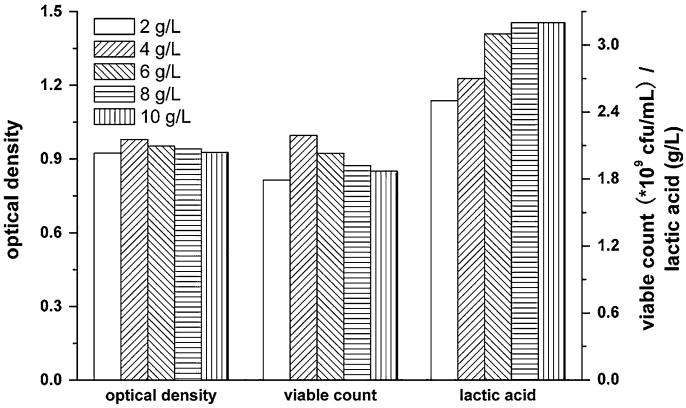

Fig. 24.2 Effect of sucrose concentrations on fermentation of *S. suis* vaccine strain SD11

to *S. suis* vaccine strain SD11 fermentation. Both optical density and viable count were highest with sucrose concentration at 4 g/l, and the initial sucrose concentration was selected at 4 g/l.

24.3.3 Effect of Feeding Substrate on S. suis *Vaccine Strain SD11 Fermentation*

Fed-batch culture fermentation was widely used in high cell-density cultivation. In fermentation process, nutriment was fed to satisfy the demand of strain growth. Glucose and sucrose were selected as the carbon source in feed stage of *S. suis* vaccine strain SD11 fermentation, and the concentration of carbon source was maintained at 5 g/l.

Results of *S. suis* vaccine strain SD11 fermentation with different feeding substrate are presented in Fig. 24.3. When sucrose was used as feeding substrate, the accumulation of lactic acid was low, both dry cell weight and specific growth rate were low. With sucrose or glucose as feeding substrate, the viable count was 4.57×10^9 cfu/ml and 5.34×10^9 cfu/ml, respectively. Thus, glucose should be selected as feeding substrate.

24.3.4 Effect of Residual Glucose Concentration on S. suis *Vaccine Strain SD11 Fermentation*

The "over-flow" metabolism occured with high glucose concentration. The concentrations of residual glucose were maintained at 1, 3, 5, and 7 g/l in *S. suis*

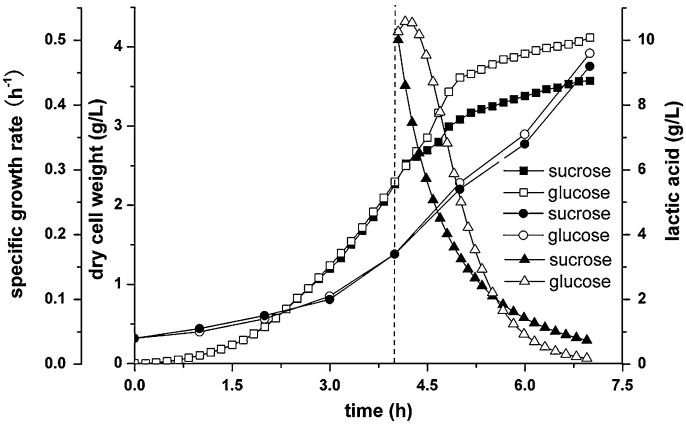

Fig. 24.3 Effect of feeding substrate on fermentation of *S. suis* vaccine strain SD11. Note: In Fig. 24.3, *square* represent dry weight cell, *circle* represent accumulation of lactic acid, *triangle* represent specific growth rate

vaccine strain SD11 fermentation. As shown in Fig. 24.4, the concentration of lactic acid increased with increasing the concentration of residual glucose, while both optical density and viable count decreased. High concentration of lactic acid was caused by high residual glucose concentration, leading to low optical density and viable count. The concentration of residual glucose should be controlled at a low level in *S. suis* vaccine strain SD11 fermentation.

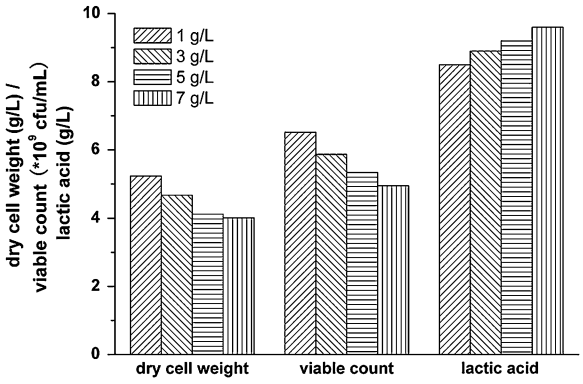

Fig. 24.4 Effect of concentrations of residual glucose on fermentation of *S. suis* vaccine strain SD11

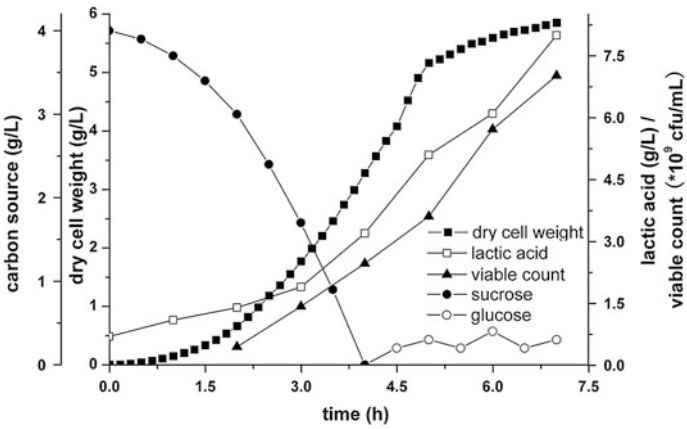

Fig. 24.5 Cultivation of *S. suis* vaccine strain SD11 with the pH feedback feeding method

24.3.5 Streptococcosis suis *Vaccine Strain SD11 Fermentation with a pH Feedback Feeding Method*

In fermentation process, many parameters can reflect the condition of carbon source, such as dissolved oxygen, pH, releasing rate of CO_2. When carbon source depleted, the pH increased due to increasing concentration of NH_4^+. The glucose solution was fed when the pH increased to 7.10.

Results of *S. suis* vaccine strain SD11 fermentation using the pH feedback feeding strategy are presented in Fig. 24.5. Applying this pH feedback feeding strategy, the concentration of residual glucose was maintained at the range of 0.2–0.4 g/l, the accumulation of lactic acid was low (8.0 g/l), dry cell weight increased to 5.89 g/l and the viable count reached 7.02×10^9 cfu/ml.

24.4 Discussion

Metabolic pathways of various carbon sources in *S. suis* vaccine strain SD11 were different. The metabolic pathway of sucrose was more complex than glucose [7]. Perturbation sugar rate of strain was low with sucrose as the initial carbon source, leading to low accumulation of lactic acid. In feed stage, sucrose could not satisfy the growth of strain because of vigorous growth of strain and low decomposition rate of sucrose, which was adverse to *S. suis* vaccine strain SD11 fermentation. In cultivation process, metabolic byproduct was accumulated because of "Crabtree" effect with high glucose concentration. In the cell of rCHO cultivation, a lot of lactic acid got excreted due to the too high glucose [8]. Byproduct was decreased by controlling the concentrations of initial carbon source and residual glucose at an

appropriate level [9]. Thus, 4 g/l of sucrose was used as initial carbon source and the residual glucose was maintained at a low level.

Many feeding strategies have been developed to achieve high cell-density cultivation. There are feedforward control feeding and feedback control feeding in fed-batch fermentation. The feedforward control feeding was up to the accuracy of kinetic model, and the feedback feeding control feeding depends on detection of fermentation parameters. Many feeding strategies based on pH have been developed. In butanol production by *Clostridium saccharoperbutylacetonicum*, a pH-controlled fed-batch culture resulted in not only acceleration of lactic acid consumption but also a further increase in butanol production [10]. A novel feeding method based on pH in which the carbon source and alkali were mixed together was proposed for lactic acid production, and the concentration of glucose and pH of the fermentation broth could be controlled synchronously at a pre-determined level during the entire process [11, 12]. With the development of computer, measurement, and feeding technology, the control strategy of *S. suis* vaccine strain SD11 fermentation will be optimized.

References

1. Du HM, Ding YC, Wang LL et al (2010) Pathogenic characteristics of four *Streptococcus suis* strains. Chin J Vet Sci 30(1):24–28
2. Xia XJ, Shen ZQ, Jiang SJ et al (2011) Prokaryotic expression of gene encoding glutamate dehydrogenase of *Streptococcus suis* serotype 2 and preparation of polyclonal antibodies against its expressed products. Animal Husbandry Feed Sci 3(5):15–19
3. Mai NT, Hoa NT, Nga TV et al (2008) *Streptococcus suis* meningitis in adults in vietnam. Clin Infect Dis 46(5):659–667
4. Cheng LK, Fu Q, Zhang SS et al (2012) Effect of the lactic acid by-prodcut on fermentation cultivation of swine *Streptococcosis* vaccine strain (ST171). Chin J Prev Vet Med 34(3):227–231
5. Chen N, Huang J, Feng ZB et al (2009) Optimization of fermentation conditions for the biosynthesis of L-Threonine by *Escherichia coli*. Appl Biochem Biotech 158(3):595–604
6. Huang J, Xu QY, Wen TY et al (2008) Metabolic flux analysis of L-Threonine biosynthesis strain under diverse dissolved oxgen conditions. Acta Microbiol Sinica 48(8):1056–1060
7. Shen DQ, Feng XY, Liu DQ et al (2009) Effect of different carbon sources on pyruvic acid production by using *lpd*A gene knockout *Escherichia coli*. Chin J Biotech 25(9):1345–1351
8. Gao L, You L, Zhu ML et al (2006) Growth and metabolism of rCHO cells in glucose-limited fed batch culture. J Chem Eng Chin Univ 20(1):74–78
9. Cheng LK, Huang J, Qin YF et al (2010) Effect of the byproduct-acetic acid on L-tryptophan fermentation. Microbiol Chin 37(2):166–173
10. Oshiro M, Hanada K, Tashiro Y et al (2010) Efficient conversion of lactic acid to butanol with pH-stat continuous lactic acid and glucose feeding method by *Clostridium saccharoperbutylacetonicum*. Appl Microbiol Biotech 87(3):1177–1185
11. Zhang C, Cong W, Shi SY (2010) Application of a pH feedback-controlled substrate feeding method in lactic acid production. Appl Biochem Biotech 162:2149–2156
12. Shen YL, Zhang Y, Sun AY et al (2004) High-level production of soluble tumor necrosis factor-related apoptosis-inducing ligand (Apo21/TRAIL) in high-density cultivation of recombinant *Escherichia coli* using a combined feeding strategy. Biotech Let 26:981–984

Chapter 25
Control Strategy of Specific Growth Rate in L-Tryptophan Production by *Escherichia coli*

Likun Cheng, Qingyang Xu, Jingbo Liang, Xixian Xie, Chenglin Zhang and Ning Chen

Abstract Specific growth rate is an important parameter in L-tryptophan production. In this study, variable specific growth rate fed-batch process was used and the maximum specific growth rate was controlled at 0.20, 0.25, and 0.30 h^{-1} respectively. The effects of different specific growth rate on dry cell weight, production of L-tryptophan, concentrations of by-products, NH_4^+ and K^+, and plasmid stability were investigated. With the maximum specific growth rate at 0.25 h^{-1}, dry cell weight increased to 45.37 g/L and L-tryptophan production reached 38.5 g/L. The plasmid stability was 96.2 % and concentration of acetic acid, lactic acid, and alanine was 1.12, 0.72, and 0.45 g/L. From the metabolic flux analysis of L-tryptophan biosynthesis with different specific growth rate, the metabolic flux of Glycolytic pathway, Tricarboxylic acid cycle, acetic acid, lactic acid, and alanine were decreased by 24.18, 17.48, 3.56, 3.34, and 4.0 % respectively and the metabolic flux of Pentose phosphate pathway and L-tryptophan were increased by 8.3 and 5.43 % with the maximum specific growth rate at 0.25 h^{-1} by comparing with that of the maximum specific growth rate at 0.30 h^{-1}, leading to a significant increase in L-tryptophan production. The maximum specific growth rate in L-tryptophan production should be controlled below 0.25 h^{-1}.

Keywords Specific growth rate · L-tryptophan · *Escherichia coli* · By-products · Metabolic flux analysis

L. Cheng · Q. Xu · J. Liang · X. Xie · C. Zhang · N. Chen (✉)
College of Biotechnology, Tianjin University of Science and Technology, Tianjin 300457, China
e-mail: ningch66@gmail.com

T.-C. Zhang et al. (eds.), *Proceedings of the 2012 International Conference on Applied Biotechnology (ICAB 2012)*, Lecture Notes in Electrical Engineering 249,
DOI: 10.1007/978-3-642-37916-1_25, © Springer-Verlag Berlin Heidelberg 2014

25.1 Introduction

L-tryptophan is an essential amino acid for humans and other animals, which is widely used in food, animal feed, and pharmaceutical industries [1, 2]. Process modification and genetic modification of L-tryptophan production by microbial fermentation in *E. coli* has been extensively studied [3, 4]. Zhao et al. constructed an L-tryptophan overproducing *E. coli* (Δ*Trp*R, Δ*Tna*A, Δ*Phe*A, Δ*Tyr*A, *Aro*F^{fbr} and *Trp*E^{fbr}D) from the wild-type *E. coli* W3110 by defined genetic modification methodology [2]. In L-tryptophan production, product formation increased, and the amount of by-products decreased by optimizing the glucose feed rate [1].

Specific growth rate is an important parameter in the fermentation process due to its impact on the plasmid stability and the formation of acetic acid [5]. Plasmid stability decreased with rise in specific growth rate and plasmid instability is a major reason for the decrease in the specific yield [6]. Acetic acid is a primary inhibitory metabolite in *E. coli* cultivation, and is detrimental to bacterial growth and formation of desired products [7]. The threshold growth rate for accumulation of acetic acid has been reported in defined media to be in the range of 0.14–0.17 h^{-1} for fed-batch process [6]. The acetic acid excretion is not observed when the specific growth rate of *E. coli* is lower than a certain threshold growth rate (μ_c), owing to the carbon limitation in continuous cultivations or the quality of carbon sources in batch cultures, and aerobic acetogenesis of *E. coli* has been proposed as a means of generating extra ATP to support faster growth [8]. From the study of *E. coli* K12 MG 1655 in accelerostat cultures, acetic acid accumulation began at $\mu = 0.34 \pm 0.01\ h^{-1}$ and two acetate synthesis pathways—phosphotransacetylase-acetate kinase (pta-ackA) and pyruvate oxidase (poxB)—contributed to the synthesis at the beginning of overflow metabolism, i.e., onset of acetic acid excretion [7].

In the variable specific growth rate fed-batch process, plasmid stability and specific yield of desired product were greater than that with constant specific growth rate fed-batch process [9]. The feeding rate of glucose was continuously adjusted in order to support the specific growth rate at a constant value [10]. A novel equation of feeding rate according to the experimental data could decrease the specific growth rate [9]. In this study, the variable specific growth rate fed-batch process in L-tryptophan production was achieved by adjusting feeding rate. The concentrations of by-products, NH_4^+, K^+, L-tryptophan and plasmid stability in L-tryptophan production with different specific growth rate were investigated, and distribution of metabolic flux in L-tryptophan production studied.

25.2 Materials and Methods

25.2.1 Microorganism and Medium

The L-tryptophan-producing strain *E. coli* TRTHΔpta used in this study was obtained from the early work in our laboratory [11] and stored at the Culture Collection of Tianjin University of Science and Technology, and maintained on Luria-Bertani (LB) agar containing 50 mg/L tetracycline.

The seed medium contained the components as follows: glucose 20 g/L, yeast extract 15 g/L, $(NH_4)_2SO_4$ 10 g/L, sodium citrate 0.5 g/L, $MgSO_4{\cdot}7H_2O$ 5 g/L, KH_2PO_4 1.5 g/L, $FeSO_4{\cdot}7H_2O$ 0.015 g/L, tetracycline 0.05 g/L, and vitamin B_1 0.1 g/L. The medium for L-tryptophan fermentation contained glucose 20 g/L, yeast extract 1 g/L, $(NH_4)_2SO_4$, 4 g/L, sodium citrate 2 g/L, $MgSO_4{\cdot}7H_2O$ 5 g/L, KH_2PO_4 5 g/L, and $FeSO_4{\cdot}7H_2O$ 0.1 g/L. The pH of both medium was adjusted to 7.0 with 4 mol/l NaOH.

25.2.2 Culture Methods

A 500-ml baffled flask containing 30 ml of seed medium was inoculated with a single colony of *E. coli* TRTHΔpta and cultivated at 36 °C, 200 rpm for 12 h. A 30-mL inoculum of this culture was added aseptically to a 5-l seed fermenter (Biotech-2002 Bioprocess controller, Baoxing, Shanghai, China) containing 3l of seed medium and cultivated at 36 °C for 16 h. The pH was adjusted to 7.0 with 25 % (w/w) ammonia during the whole cultivation period. The dissolved oxygen (DO) level was maintained at approximately 20 % saturation by adjusting the agitation and aeration rates.

Fed-batch fermentation was performed in 30 L jar fermenters (Biotech-2002 Bioprocess controller) containing 18 L of production medium in which seed culture was aseptically inoculated (10 % v/v). In the fermentation process of L-tryptophan, temperature was maintained at 36 °C and the pH was adjusted to 7.0 with 25 % (w/w) ammonia. The DO level was maintained at approximately 20 % saturation by adjusting the agitation and aeration rates. When the initial glucose was depleted, 80 % glucose solution (w/v) was fed into the fermenter to meet specific experimental requirements.

25.2.3 Analysis of Fermentation Products

DO, pH, and temperature were measured automatically with electrodes attached to the fermenters. Dry cell weight, plasmid stability, and concentration of alanine were assessed as described previously [12]. The concentrations of glucose and lactic acid were determined by an SBA-40E biosensor instrument (Biology Institute of Shandong Academy of Sciences, China). Concentrations of acetic acid,

NH_4^+, and K^+ were measured with a Bioprofile 300 A biochemical analyzer (Nova Biomedical, Waltham, MA, USA). L-tryptophan concentration in fermented broth was determined by high-pressure liquid chromatography using an Agilent 1200 instrument (Agilent Technologies, Santa Clara, CA, USA).

25.2.4 Metabolic Flux Analysis

The stoichiometric model of intracellular metabolism was constructed and the distribution of metabolic flux was calculated according to previous reports with slight modifications [11, 13]. The matrix function was solved using MATLAB 7.0 (Math Works).

25.3 Results and Discussion

25.3.1 Dry Cell Weight and L-Tryptophan Production with Different Specific Growth Rate

The specific growth rate was controlled by adjusting the feeding rate of glucose. Feeding profile was calculated from the equation as described previously [9, 10]. The maximum specific growth rate (μ_{max}) was controlled at 0.20, 0.25, and 0.30 h^{-1} respectively. The dry cell weight and L-tryptophan production with different specific growth rate are presented in Fig. 25.1. When the μ_{max} was controlled at 0.25 h^{-1}, the maximum dry cell weight (45.37 g/L) and L-tryptophan production (38.5 g/L) was obtained. Both dry cell weight and L-tryptophan production with μ_{max} at 0.20 h^{-1} were higher than those with μ_{max} at 0.30 h^{-1}.

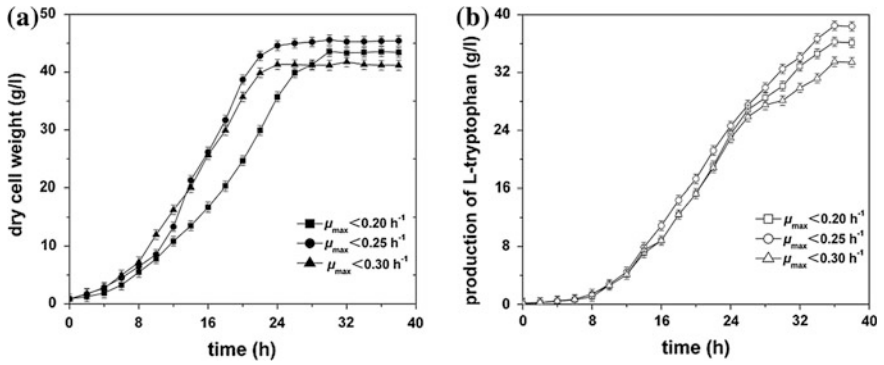

Fig. 25.1 Effect of different specific growth rate and dry cell weight and L-tryptophan production. (**a**) dry cell weight of TRTH Δ*pta* with different specific growth rate, (**b**) concentration of L-tryptophan with different specific growth rate

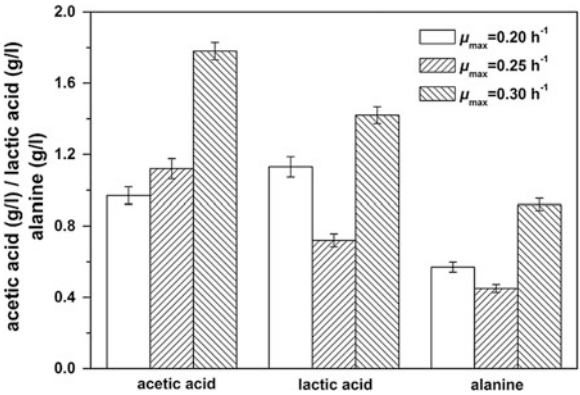

Fig. 25.2 Effect of different specific growth rate on accumulation of by-products

25.3.2 Concentrations of By-products with Different Specific Growth Rate

The by-products concentrations with different specific growth rate in L-tryptophan production are plotted in Fig. 25.2. The concentration of acetic acid increased with the increasing μ_{max} [14], and the accumulation of acetic acid with μ_{max} at 0.20, 0.25 and 0.30 h^{-1} were 0.97, 1.12, and 1.78 g/L, respectively. When the μ_{max} was 0.25 h^{-1}, concentration of lactic acid and alanine was 0.72 and 0.45 g/L. Excretion of lactic acid and alanine with μ_{max} at 0.20 h^{-1} or 0.30 h^{-1} were 1.13 and 0.57 g/L, 1.42 g/L, and 0.92 g/L, respectively. The excretion of by-products was highest with μ_{max} at 0.30 h^{-1}.

25.3.3 Concentrations of NH_4^+ and K^+ with Different Specific Growth Rate

In L-tryptophan production, $NH_3{\cdot}H_2O$ was the preferred neutralization reagent, and NH_4^+ concentration varied with additive amount of $NH_3{\cdot}H_2O$. NH_4^+ and K^+ are two important cations in L-tryptophan production. NH_4^+ can be used as nitrogen source, and K^+ is a cofactor for many important enzymes. The concentrations of the two cations with different specific growth rate are shown in Fig. 25.3. The concentration of NH_4^+ with μ_{max} at 0.30 h^{-1} was 129 mmol/L because of the increased excretion of by-products. 113 mmol/L and 96 mmol/L of NH_4^+ was accumulated with μ_{max} at 0.20 h^{-1} and 0.25 h^{-1}. High concentrations of NH_4^+ could decrease energy efficiency and inhibit growth of strain [15], and both biomass and L-tryptophan production increased significantly at concentration of NH_4^+ below 120 mmol/L [12]. The concentration of K^+ with different specific growth rate showed no difference, and K^+ was utilized in the fermentation process of L-tryptophan production.

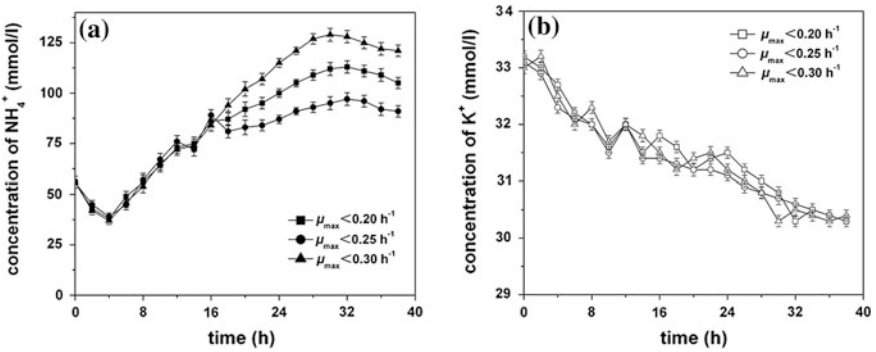

Fig. 25.3 Concentrations of NH_4^+ and K^+ with different specific growth

25.3.4 Plasmid Stability with Different Specific Growth Rate

The plasmid stability was determined every 4 h in the process of L-tryptophan fermentation. The plasmid stability decreased with the increasing specific growth rate. When μ_{max} was at 0.20 and 0.25 h^{-1}, the plasmid stability was 97.0 and 96.2 %, while the plasmid stability with μ_{max} at 0.30 h^{-1} was decreased to only 91.0 %. Short-chain acids could reduce the rate of RNA, DNA, protein, and lipid synthesis [16], and several proteins and genes were affected by acetic acid, particularly those involved in the *E. coli* transcription–translation machinery, the general stress response, and regulation [17]. High accumulation of lactic acid and acetic acid with μ_{max} at 0.30 h^{-1} could affect the transcription–translation machinery of plasmid, leading to lower plasmid stability. And high concentration of NH_4^+ was also adverse to the plasmid stability [12] (Fig. 25.4).

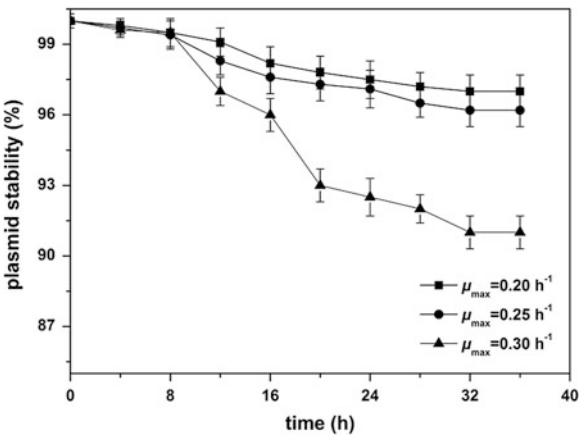

Fig. 25.4 Effect of different specific growth rate on plasmid stability in L-tryptophan fermentation

25.3.5 Metabolic Flux of L-Tryptophan Production with Different Specific Growth Rate

The strain ceased growth during the last period (28–38 h) of L-tryptophan fermentation, which was named the Pseudo-steady state. In the Pseudo-steady state, NADPH and $NADP^+$ are equivalent and the energy consumption is not equivalent to maintenance energy. The stoichiometric model in this study (Table 25.1) consists of 25 reactions and 20 compounds, and the degree of freedom is $25 - 20 = 5$, which means that the changing rate (mmol/h) of five other compounds should be measured to determine all of the reaction rates in the metabolic network. Glucose, L-tryptophan, acetic acid, lactic acid, and alanine were chosen for quantitation. All of the reaction rates (mmol/h) were normalized to the glucose uptake rate, which was defined as 100 %.

The distribution of metabolic flux in L-tryptophan production with different specific growth rate is shown in Fig. 25.5. The metabolic flux of Glycolytic pathway, Tricarboxylic acid cycle, lactic acid, and alanine with μ_{max} at 0.25 h^{-1} were 3.77, 103.56, 0.42, and 3.8 %, which were much lower than those decreased by 2.53 and 24.18 %, 4.14 and 17.48 %, 0.38 and 3.34 %, 2.6 and 4.0 % with μ_{max} at 0.20 h^{-1} or 0.30 h^{-1}, respectively. Compared with the μ_{max} at 0.30 h^{-1}, the metabolic flux of acetic acid decreased by 3.56 % and that of Pentose phosphate pathway and L-tryptophan production increased by 8.3 and 5.43 % with μ_{max} at 0.25 h^{-1}. An integrated optimization of the whole network lead to a significant increase in tryptophan production rate by decreasing the metabolic flux of Glycolytic with μ_{max} at 0.25 h^{-1} and Tricarboxylic acid cycle and increasing the metabolic flux of Pentose phosphate pathway [13].

Table 25.1 Reaction rate equation of metabolic nodes in L-tryptophan biosynthesis

Metabolic node	Reaction rate equation	Metabolic node	Reaction rate equation
Glc6P	$r1 - r2 - r11 = 0$	X5P	$r12 - r14 + r16 = 0$
F6P	$r2 - r3 + r15 - r16 = 0$	R5P	$r13 - r14 - r21 = 0$
GAP	$2r3 - r4 + r14 - r15 - r16 + r22 = 0$	S7P	$r14 - r15 = 0$
P3G	$r4 - r5 - r19 = 0$	E4P	$r15 + r16 - r17 = 0$
PEP	$r5 - r1 - r6 - r10 - 2r17 = 0$	Cho	$r17 - r22 = 0$
Pyr	$r1 + r6 - r7 + r22 - r23 - r25 = 0$	Glu	$r18 - r19 - r20 + r22 - r25 = 0$
AcCoA	$r7 - r8 - r24 = 0$	Gln	$r20 - r22 = 0$
α-KG	$r8 - r9 - r18 + r19 + r25 = 0$	PRPP	$r21 - r22 = 0$
OAA	$r9 - r8 + r10 = 0$	Ser	$r19 - r22 = 0$
Ru5P	$r11 - r12 - r13 = 0$	NADPH	$2r11 - r17 - r18 = 0$

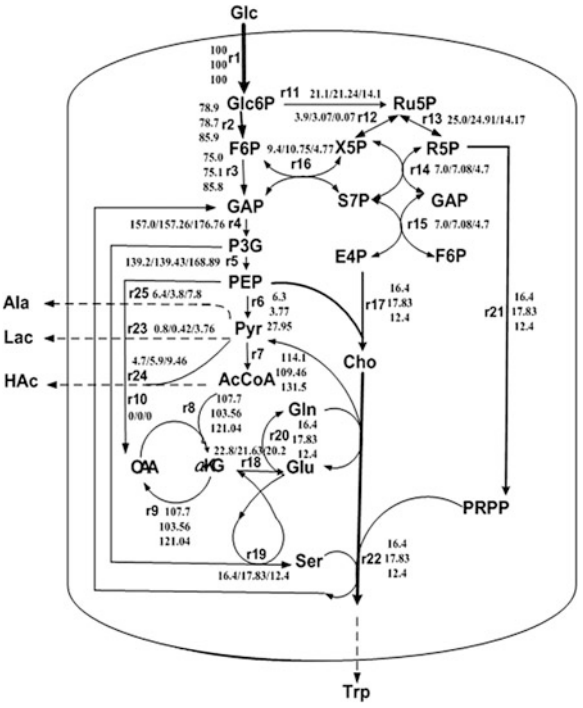

Fig. 25.5 Metabolic flux of L-tryptophan biosynthesis with different specific growth rate. The numbers of each reaction represent the metabolic flux with μ_{max} at 0.20, 0.25, and 0.30 h^{-1}, respectively

25.4 Conclusion

The μ_{max} of this L-tryptophan-producing *E. coli* strain TRTHΔpta in this study was controlled at 0.20, 0.25, and 0.30 h^{-1}, respectively. The maximum dry cell weight and L-tryptophan production obtained with μ_{max} at 0.25 h^{-1}. When the μ_{max} at 0.25 h^{-1}, concentration of acetic acid was low and plasmid stability was high, and lowest lactic acid as well as alanine were accumulated. The results of metabolic flux analysis of L-tryptophan biosynthesis with different specific growth rate showed that the metabolic flux of Glycolytic pathway, Tricarboxylic acid cycle and by-products decreased and the metabolic flux of Pentose phosphate pathway and L-tryptophan increased with the μ_{max} below 0.25 h^{-1}, which were of benefit for synthesis of L-tryptophan.

Acknowledgments This work was supported by the National Science and Technology Major Project of China for "Significant New Drugs Creation" (2008ZX09401-05), Key Projects in the National Science and Technology Support Program during the Eleventh Five-year Plan Period of China (2008BAI63B01) and the Program for Changjiang Scholars and Innovative Research Team in University (IRT 1166).

References

1. Dodge T, Gerstner J (2002) Optimization of the glucose feed rate profile for the production of tryptophan from recombinant *E. coli*. J Chem Technol Biotechnol 77:1238–1245
2. Zhao ZJ, Zou C, Zhu YX et al (2011) Development of L-tryptophan production strains by defined genetic modification in *Escherichia coli*. J Ind Microbiol Biotechnol 38:1921–1929
3. Ikeda M (2006) Towards bacterial strains overproducing L-tryptophan and other aromatics by metabolic engineering. Appl Microbiol Biotechnol 69:615–626
4. Liu Q, Cheng YS, Xie XX et al (2012) Modification of tryptophan transport system and its impact on production of L-tryptophan in *Escherichia coli*. Bioresour Technol 114:549–554
5. Yoon SK, Kang WK, Park TH (1994) Fed-batch operation of recombinant *Escherichia coli* containing *trp* promoter with controlled specific growth rate. Biotechnol Bioeng 43(10):995–999
6. Eiteman MA, Altman E (2006) Overcoming acetate in *Escherichia coli* recombinant protein fermentations. Trends Biotechnol 24(11):530–536
7. Nahku R, Valgepea K, Lahtvee PJ et al (2010) Specific growth rate dependent transcriptome profiling of *Escherichia coli* K12 MG1655 in accelerostat cultures. J Biotechnol 145(1):60–65
8. Shin S, Chang DE, Pan JG (2009) Acetate consumption activity directly determines to the level of acetate accumulation during *Escherichia coli* W3110 growth. J Microbiol Biotechnol 19(10):1127–1134
9. Khalilzadeh R, Shojaosadati SA, Bahrami A et al (2003) Over-expression of recombinant human interferon-gamma in high cell density fermentation of *Escherichia coli*. Biotechnol Lett 25:1989–1992
10. Suárez DC, Kilikian BV (2000) Acetic acid accumulation in aerobic growth of recombinant *Escherichia coli*. Process Biochem 5(9):1051–1055
11. Huang J, Shi JM, Liu Q et al (2011) Effects of gene *pta* disruption on L-tryptophan fermentation. Acta Microbiologica Sinica 51(4):480–487
12. Huang J, Shi JM, Huo WT et al (2011) The effects of NH_4^+ on L-tryptophan fermentation. Chin Biotechnol 31(3):55–60
13. Schmid JW, Mauch K, Reuss M et al (2004) Metabolic design based on a coupled gene expression-metabolic network model of tryptophan production in *Escherichia coli*. Meta Eng 6(4):364–377
14. Cheng LK, Wang J, Xu QY et al (2012) Effect of feeding strategy on L-tryptophan production by recombinant *Escherichia coli*. Ann Microbiol. doi:10.1007/s13213-012-0419-6
15. Yang ZN, Jiang M, Li J et al (2010) Effects of different neutralizing agents on succinate production by *Actinobacillus succinogenes* NJ113. Chin J Biotech 26(11):1500–1506
16. Cherrington CA, Hinton M, Chopra I (1990) Effect of short-chain organic acids on macromolecular synthesis in *Escherichia coli*. J Appl Bacteriol 68(1):69–74
17. Arnold CN, McElhanon J, Lee A et al (2001) Global analysis of *Escherichia coli* gene expression during the acetate-induced acid tolerance response. J Biotechnol 183:178–186

Chapter 26
Effect of Gene *FPS1* on Accumulation of Glycerol in *Zygosaccharomyces rouxii*

Yonghua Wei, Cong Wang, Xiaohong Cao and Lihua Hou

Abstract *Zygosaccharomyces rouxii* was applied in high-salt liquid state fermentation of soy sauce. The gene *FPS1* encoding Fps1p was analyzed in the *Z. rouxii* in order to investigate the effect of gene *FPS1* on glycerol accumulation. The sequence result showed that *FPS1* had an open reading frame of 2079 bp. It was found that the expression level of *FPS1* in the *Z. rouxii* decreased with the increase of osmotic stress. Furthermore, overexpression of *FPS1* could depress the salt-tolerance compared to the control.

Keywords *FPS1* · Glycerol · Salt-tolerance · *Zygosaccharomyces rouxii*

26.1 Introduction

Soy sauce is a traditional food condiment in Asian regions especially for Chinese and Japanese [1, 2]. And it is accepted by all over the world increasingly as its sharp flavor [3] and nutritional qualities [4]. There are high-salt liquid state fermentation soy sauce and low-salt solid state fermentation soy sauce in China. In comparison with the low-salt solid state fermentation soy sauce, high-salt liquid state fermentation soy sauce is more popular to most of consumers due to its unique taste and aroma. The addition of salt-tolerant *Zygosaccharomyces rouxii* into mash was applied to improve the flavor of soy sauce. However, the growth and metabolism of yeast cells are limited by the brine solution concentration

Y. Wei · C. Wang · X. Cao · L. Hou (✉)
Key Laboratory of Food Nutrition and Safety, Tianjin University of Science and Technology, Ministry of Education, Tianjin 300457, People's Republic of China
e-mail: lhhou@tju.edu.cn

Y. Wei
School of Biological Sciences and Engineering, Shaanxi University of Technology, Hanzhong 723001, People's Republic of China

T.-C. Zhang et al. (eds.), *Proceedings of the 2012 International Conference on Applied Biotechnology (ICAB 2012)*, Lecture Notes in Electrical Engineering 249,
DOI: 10.1007/978-3-642-37916-1_26, © Springer-Verlag Berlin Heidelberg 2014

exceeding 17 % [5, 6]. Accordingly, the osmoregulation is essential to subject to osmotic stress for *Z. rouxii*.

The production and accumulation of compatible solutes such as glycerol, which is partly controlled by the high osmolarity glycerol (HOG) signaling system, are key for osmoregulation of yeasts. Following a hyperosmotic shock, HOG signal transduction system is activated within several seconds. The glycerol is produced via a short branch of glycolysis consisting of two enzymatic steps [7, 8]. However, the glycerol accumulation is controlled by aquaglyceroporin Fps1p localized in the plasma membrane and encoded by *FPS1* genes. As a gated glycerol transport channel, it makes yeasts cells control rapidly and fine-tune the intracellular glycerol level [9]. However, the regulating mechanism of glycerol accumulation is still unclear. Thus, the transcription level of *FPS1* was studied in this work to clarify the effect of gene *FPS1* on glycerol accumulation. Besides, the engineered strains W303-YEp195-*FPS1* (WYF) and the control strain W303-YEp195 (WY) were constructed in order to analyze the effect of expression of *FPS1* on salt-tolerance of *S. cerevisiae*.

26.2 Materials and Methods

26.2.1 Strain, Medium and Cultivation Conditions

Z. rouxii and *S. cerevisiae* W303-1A (*MATa, leu2 ura3, trp1, his3, ade2, can1*) were cultivated in YPD medium (1 % w/v yeast extract, 2 % w/v peptone, and 2 % w/v glucose) and YPDN (a certain amount of NaCl dissolved in normal YPD substrate) or CM-URA medium (0.67 % w/v yeast nitrogen base without amino acids, 2 % glucose, and 0.192 % w/v CM-URA powder).

The high fidelity *E.coil* Top10 was cultivated in LB (0.5 % w/v yeast extract, 1 % w/v peptone, 1 % w/v NaCl, pH = 7.2) medium at 37 °C to propagate plasmid. The X-Gal LBA plate (50 ng/mL ampicillin, 0.5 mmol/L IPTG and 40 ug/mL X-Gal) was used to screen the colonies. The lithium acetate method was applied in transformation of plasmids into the strain W303-1A [10].

26.2.2 Plasmids and Strains Construction

PCR was performed using *easyPfu* DNA polymerase to clone the *FPS1* with the primers *FPS1*-up (GCCCCGGGGAATAAATCGGGGTCCGTAG) and *FPS1*-dn (GCGTCGACCATGGGAAACAAGAGATCAA). The sequencing vector and

PCR products were then digested with *Sma*I and *Sal*I, respectively. The PCR production digested was joined to pUC19 to obtain a plasmid pUC19-*FPS1* by ligation reaction. Then sequence of plasmid pUC19-*FPS1* was confirmed by DNA sequence analysis. Analogously, *FPS1* gene was cloned into the plasmid YEp195, forming the plasmids YEp195-*FPS1*. The YEp195-*FPS1* and YEp195 were transformed into W303-1A to construct the engineered strains W303-YEp195-*FPS1* (WYF) and W303-YEp195 (WY), respectively.

26.2.3 RNA Extraction and the Real-Time Quantitative PCR

Z. rouxii was cultivated in YPDN medium (0, 6, 12, and 18 %) at 30 °C. The cells (about 3×10^8) were centrifuged, washed, recollected, and frozen in liquid N_2. The total RNA was prepared using the trizol, following the operating instructions. The crude RNA was then treated with DNaseI to obtain high-purity RNA. The RT-PCR was performed to obtain cDNA with the RT kit. Aliquots (1.0 mg) of total RNA were used in the RT-PCR (42 °C 30 min, 85 °C 5 min).

Real-time quantitative PCR (QPCR) was used to investigation the expression level of *FPS1* in *Z. rouxii*. Then cDNA samples, the primers *FPS1*-R-up and *FPS1*-R-dn were used in the QPCR reaction. The nucleotide sequences of primers used were as follows: *FPS1*-R-up: TACGGGCGATACTTCTACGA; *FPS1*-R-dn: GCTGTTACTGCGGATATGAG; 18 s (128 bp) was used as internal reference with primers 18 s-up (CCAAGAACATGATGGCTGCT) and 18 s-dn (CTTGAAGAGCTCCTGGATGG) [11]. The annealing temperature of 58 and 55 °C were determined for QPCR of 18 s and *FPS1* short product, respectively.

26.2.4 The Salt-Tolerance Analysis

The biomass of engineered yeasts was evaluated by measuring the optical density of the culture at 600 nm. For analysis of the intracellular glycerol, the engineered yeasts were collected at the mid-log phase. The suspensions were centrifuged immediately at 5,000 rpm for 5 min and the supernatant was discarded. The harvested cells were washed with cold distilled water and recollected, and then samples were crashed as described by Li et al. [12]. The glycerol content was represented by dry cell weigh (DCW). The intracellular glycerol was quantified using an Aminex HPX-87H column and a refractive index detector (Shimadzu RID-10A). The 5 mM H_2SO_4 as eluent was used at a flow rate of 0.8 mL/min [12].

26.3 Results and Discussion

26.3.1 Sequence Analyses

The nucleotide sequence of analysis of recombinant plasmids pUC19-*FPS1* revealed the whole length of 2718 bp containing the sequences of promoter and terminator and an open reading frame (ORF) of 2079 bp, which encoded a 693 amino-acid protein, The nucleotide sequence of *FPS1* was identified. Its homology bases were completely different from that of *S. cerevisiae*. The results suggested *FPS1* was an important role in osmoregulation for *Z. rouxii*.

26.3.2 Structure Analyses

After sequencing, the secondary structures of Fps1p encoded by *FPS1* gene were analyzed further to investigate the physiological characterization of Fps1p using Anthepro software. As shown in Fig. 26.1, the results indicated structure composed of all alpha 4.46, all beta 3.17, alpha + beta 3.40, alpha/beta 3.56, and irregular 3.27. And a molecular weight of pI/Mw 6.135/75974.681 was predicted.

26.3.3 Expression of FPS1

The transcription levels of *FPS1* at different salt content were estimated using QPCR analysis. As shown in Fig. 26.2, the transcription levels of *FPS1* decreased with the increase of NaCl concentration, which indicated that expression levels of *FPS1* would be inhibited in hypertonic circumstances.

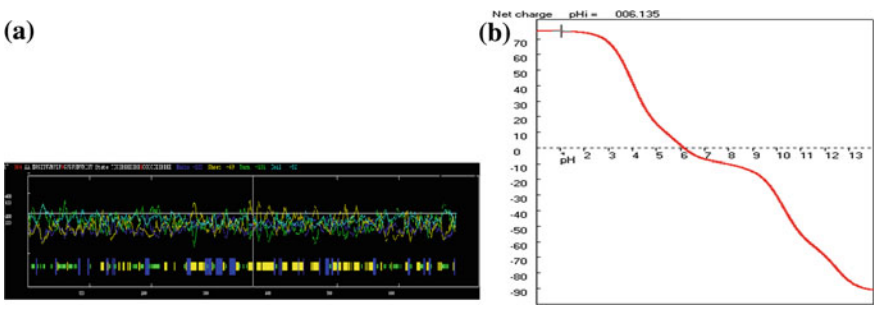

Fig. 26.1 The details of the second structure (**a**) and isoelectric point (**b**) of Fps1p

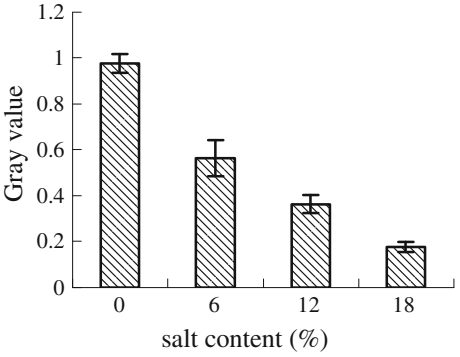

Fig. 26.2 Analysis of expression level of *FPS1* in Z. rouxii cultivated in the presence of 0–18 % NaCl by QPCR. Gray value = IOD of end products/IOD of internal reference

26.3.4 Salt-Tolerance Analyses

The engineered strains WYF and WY were obtained by transformation YEp195-*FPS1* and YEp195 into W303-1A, respectively. The resulting stains were then cultivated in YPDN with 12 % NaCl. Figure 26.3 indicated that the salt-tolerance of WYF was depressed compared to WY.

The intracellular glycerol content of WYF and WY under different salt stress was also measured quantitatively, respectively. As shown in Fig. 26.4, both of glycerol contents showed an incremental trend with the increase of NaCl concentration. At the same time, the glycerol contents of WY were significantly higher than WYF cultivated in same YPDN medium, which was according with the salt-tolerance of engineered strains.

The HOG signal transduction system is activated, and glycerol is produced within less than 1 min after a hyperosmotic shock. At the same time, the transcription levels of *FPS1* decrease and close glycerol export channel was closed to prevent glycerol leakage and accumulate glycerol [13, 14]. Accordingly, the

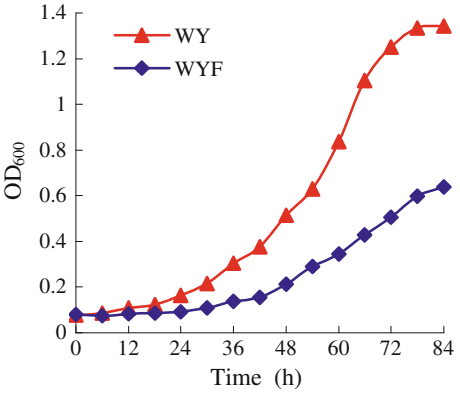

Fig. 26.3 Salt-tolerance analyses of engineered strains WY and WYF in the presence of 12 % NaCl

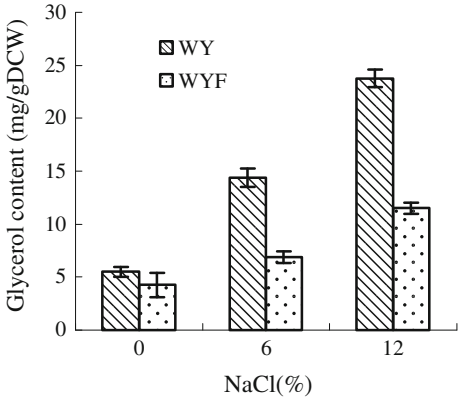

Fig. 26.4 Glycerol content of the engineered strains WYF and WY in the presence of 0, 6, and 12 % NaCl, respectively

salt-tolerance and glycerol content for WYF and WY with the increase of NaCl concentration, illustrating fine-tuning of Fps1p for osmoregulation of *Z. rouxii*.

However, the physiological role of Fps1p was to regulate export rather than uptake of glycerol under hyperosmotic conditions [13]. Oliveira et al. reported that multicopy *FPS1* could improve the diffusion rate of glycerol in *S. cerevisiae* [15]. Similarly, salt-tolerance and glycerol content of WYF were lower than those of WY under hyperosmotic conditions, which indicated that overexpression of *FPS1* would induce an opened Fps1p that was unable to accumulate glycerol.

26.4 Conclusion

This present study revealed that salt-tolerance of yeast had a positive correlation with the intracellular glycerol content. The reduction of expression level of *FPS1* in the *Z. rouxii* played an important role in accumulation of glycerol and enhancement of salt-tolerance. The overexpression of *FPS1* had an adverse effect on osmoregulation of yeast cells.

In addition, other genes, such as *GPD1, HOG1, PMA1*, and so on, should be also studied further in order to understand completely the mechanism why the *Z. rouxii* could resist to high osmotic circumstance during soy sauce fermentation.

Acknowledgments This work was supported by these projects in China (2013AA102106, 2012BAD33B04, 31371819, 2012GB2A100016, 2012AA022108, 31171731, 10ZCZDS0Y07000, 2012AA021303 and IRT1166).

References

1. Luo JQ, Ding LH, Chen XR et al (2009) Desalination of soy sauce by nanofiltration. Sep Pur Technol 66:429–437
2. Huang H (2004) Almanac of China's commerce. Almanac of China's Commerce Press, Beijing, pp 56–57
3. Van Der Sluis C, Tramper J, Wijffels RH (2001) Enhancing and accelerating flavor formation by salt-tolerant yeasts in Japanese soy-sauce processes. Trends Food Sci Tech 12:322–327
4. Li Y, Zhao HF, Zhao MM et al (2010) Relationships between antioxidant activity and quality indices of soy sauce: an application of multivariate analysis. Int J Food Sci Tech 45:133–139
5. Devantier R, Scheithauer B, Granato VS et al (2005) Metabolite profiling for analysis of yeast stress response during very high gravity ethanol fermentations. Biotechnol Bioeng 90:703–714
6. Jones RP (1989) Biological principles for the effects of ethanol. Enzyme Microb Tech 11:130–153
7. Ansell R, Granath K, Hohmann S et al (1997) The two isoenzymes for yeast NAD^+-dependent glycerol 3-phosphate dehydrogenase encoded by *GPD1* and *GPD2* have distinct roles in osmoadaptation and redox regulation. EMBO J 16:2179–2187
8. Norbeck J, Pahlman AK, Akhtar N et al (1996) Purification and characterization of two isoenzymes of DL-glycerol-3-phosphatase from Saccharomyces cerevisiae: identification of the corresponding GPP1 and GPP2 genes and evidence for osmotic regulation of Gpp 2p expression by the osmosensing mitogen-activated protein kinase signal transduction pathway. J Biol Chem 271:13875–13881
9. Hohmann S, Krantz M, Nordlander B (2007) Yeast Osmoregulation. Method Enzymol 428:29–45
10. Schiestl RH, Gietz RD (1989) High efficiency transformation of intact yeast cells using single stranded nucleic acids as carrier. Curr Genet 16:339–346
11. Watanabe Y, Akita H, Higuchi Y et al (2008) Heterologous expression of Na^+/H^+ antiporter gene (CvNHA1) from salt-tolerant yeast Candida versatilis in *Saccharomyces cerevisiae* Naþ-transporter deficient mutants. Biosci Biotech Bioch 72(4):1005–1014
12. Li LL, Ye YR, Pan L et al (2009) The induction of trehalose and glycerol in Saccharomyces cerevisiae in response to various stresses. Biochem Bioph Res Co 387:778–783
13. Tama's MJ, Luyten K, Sutherland FCW et al (1999) Fps1p controls the accumulation and release of the compatible solute glycerol in yeast osmoregulation. Mol Microbiol 31(4):1087–1104
14. Thorsen M, Di Y, Tangemo C et al (2006) The MAPK Fps1p modulates Fps1p-dependent arsenite uptake and tolerance in yeast. Mol Biol Cell 17:4400–4410
15. Oliveira R, Lages F, Silva-Grac M et al (2003) Fps1p channel is the mediator of the major part of glycerol passive diffusion in *Saccharomyces cerevisiae*:artefacts and re-definitions. Biochim Biophys Acta 1613(1–2):57–71

Chapter 27
Research on Enrichment Culture of *Bacillus subtilis* BI1

Depei Wang, Yingying Wang, Kele Li and Ying Yang

Abstract The fermentation medium and conditions of *Bacillus Subtilis* BI1 were accomplished using a variety of experimental design. Single factor experiments showed that the optimal concentration of fermentation medium were located to be 20 g/L sucrose, 10 g/L dusty yeast, 6.0 g/L K_2HPO_4, and 4.0 g/L KH_2PO_4. In the optimization of culture conditions, based on the results of Plackett–Burman design, liquid volume, inoculation amount, and culture time were identified to have significant effects on the absorbance of fermentation broth (10-fold diluted) and the maximum absorbance of 1.179 (OD_{600}) was resulted from the combination of liquid volume 39.49/250 ml, inoculation amount 4.05 %, and culture time 12.19 h. As a consequence, the viable count of *Bacillus Subtilis* BI1 obtained from fermentation broth could reach 3.0×10^9 cfu/ml.

Keywords *Bacillus Subtilis* BI1 · Medium optimization · Optimization of culture conditions · Response surface methodology

27.1 Introduction

As a nonpathogenic bacteria, *Bacillus Subtilis* can produce and secrete a variety of enzymes [1] and antibiotics [2]. So it is exploited for a wide range of applications, from the synthesis of metabolites [3] to the production of whole-cell biological

D. Wang (✉) · Y. Wang
Key Laboratory of Industrial Fermentation Microbiology, Ministry of Education, College of Biotechnology, Tianjin University of Science and Technology, Tianjin 300457, People's Republic of China
e-mail: wangdp@tust.edu.cn

K. Li · Y. Yang
College of Biotechnology, Tianjin University of Science and Technology, Tianjin 300457, People's Republic of China

T.-C. Zhang et al. (eds.), *Proceedings of the 2012 International Conference on Applied Biotechnology (ICAB 2012)*, Lecture Notes in Electrical Engineering 249,
DOI: 10.1007/978-3-642-37916-1_27, © Springer-Verlag Berlin Heidelberg 2014

agents used in human health [4], biological control [5], environmental protection [6], animal husbandry [7], and aquaculture [8]. *Bacillus Subtilis* has long been a subject of extensive studies on their biological activity products [9]. Some *Bacillus Subtilis* had been identified as producers of a wide range of antibacterial and antifungal agents, and we can use them as probiotics or competitive exclusion agents to control harmful bacterium [10].

The extensive applications of *Bacillus Subtilis* are often based on high-cell density bioreactor. It has been known that cultivation parameters are significant aspects to the high-density cell production, as well as key consideration in development of bioprocesses. The production of compounds or microbial cells is strongly influenced by the composition of the medium, which is in turn determined by the carbon sources, nitrogen sources, and inorganic salts. Therefore, optimization of these parameters is necessary for the overproduction of products our needs.

Optimization of media components by classical methods which involves the change of one variable at a time is extremely time consuming and expensive when a large number of variables are considered [11]. In order to overcome this difficulty and determine the interaction between the studied variables, an experimental factorial design and response surface method was employed for optimization [12].

A *Bacillus Subtilis* strain, denoted as BI1, was isolated from soil initially showed high antifungal activity [13]. Previous research has shown that *B. Subtilis* BI1 has a broad spectrum of activity against filamentous fungi. This study use single factor experiments and response surface methodology to select and optimize the factors which may have influences on the enrichment culture of *B. Subtilis* BI1. The purpose was to improve the viable count of *B. Subtilis* BI1 cell in fermentation broth rapidly, as well as to lay a solid foundation for the study of microbial agents.

27.2 Materials and Methods

27.2.1 Strains

Bacillus Subtilis BI1 strain was isolated from soil.

Candida albicans strain was kindly provided by the Life Science College of Nankai University.

27.2.2 Culture

Seed medium (g/L): peptone 10.0, beef extract 5.0, NaCl 5.0, pH 7.2–7.4.

Initial fermentation medium (g/L): glucose 5.0, NH_4NO_3 2.0, citrate sodium 1.0, $MgSO_4{\cdot}7H_2O$ 0.2, K_2HPO_4 4.0, KH_2PO_4 6.0, pH 7.0–7.2.

Initial fermentation conditions: pH 7.0, liquid volume 50 ml/250 ml, seed age 12 h, inoculation amount 2.0 %, culture temperature 37 °C, shaking speed 200 r/min and cultivating time 12 h.

27.2.3 Absorbance Measurement of B. Subtilis BI1 Fermentation Broth

The absorbance of 10-fold diluted fermentation broth was measured with a spectrophotometer at 600 nm.

27.2.4 The Growth Curve Determination of B. Subtilis BI1

Bacillus subtilis BI1 was cultured in a seed medium for 12 h at 37 °C. The growth of a bacterial population can be determined by inoculating 2 % seed broth into fermentation medium and the absorbance of the fermentation broth (5-fold diluted) can be measured to determine bacterial growth every hour for 24 h.

27.2.5 Dilution Plate Counting Method

To obtain a viable concentration, the fermentation broth was diluted in sterile saline in the proportion of one to ten. 100 μL diluted fermentation broth was dispersed in a Petri dish. The Petri dish was rotated carefully to make sure that the strain was equally distributed. Three repetitions were made with each dilution.

27.2.6 Single Factor Design

Based on the initial fermentation medium, single factor experimentation was designed. Made the composition of the medium or the addition of a component as a variable, other factors remained unchanged. The *B. Subtilis* BI1 was cultured according to the initial fermentation conditions.

Afterward, the absorbance (10-fold diluted) and viable count of the fermentation broth was measured.

27.2.7 Plackett-Burman Design

In order to select the significant factors, six independent variables were screened in twelve combinations organized according to the Plackett-Burman design [14]. All trials were performed in triplicate. The absorbance of the fermentation broth was measured as the responses.

The main effect of each variable was simply calculated as the difference between the average of measurements made at the high setting (+) and the average of measurements observed at the low setting (−) of that factor. Plackett-Burman experimental design is based on the first-order model:

$$Y = b_0 + \Sigma b_i x_i \tag{27.1}$$

where Y is the response (absorbance of the fermentation broth), b_0 is the model intercept and b_i is the linear coefficient, and x_i is the level of the independent variable. This model does not describe interaction among factors but it is used to screen and evaluate the important factors influenced the response.

27.2.8 Path of Steepest Accent (Descent)

The method of steepest ascent (descent) is a procedure for moving sequentially along the path of steepest ascent (descent), that is, in the direction of the maximum increase (decrease) is the response. Based on the results obtained from the Plackett-Burman design, the path of steepest ascent was designed.

27.2.9 Box-Behnken Design

In order to describe the nature of the response surface in the experimental region and elucidate the optimal concentrations of the most significant independent variables, a Box-Behnken design [15] was applied which is a response surface methodology (RSM). Factors of highest confidence levels namely; liquid volume (X_1), inoculation amount (X_2), and cultivating time (X_3) were prescribed into three levels (low, basal, high) coded, (−1, 0, +1). The central values (basal) chosen for experiment design were liquid volume 40 ml/250 ml, inoculation amount 4 %, cultivating time 12 h. In developing the regression equation the test factors were coded according to the equation [16].

$$x_i = (X_i - X_0)/\Delta X_i \tag{27.2}$$

where x_i is the coded variable of a factor, X_i is natural variable of the factor, X_0 is the value of the natural variable at the center point, and ΔX_i is the step change value.

According to the applied design, 17 combinations were executed and their observations were fitted to the following second order polynomial model:

$$Y = \beta_0 + \Sigma\beta_i x_i + \Sigma\Sigma\beta_{ij} x_i x_j + \Sigma\beta_{ii} x_i^2 \quad (27.3)$$

where Y is the measured response (absorbance of fermentation broth), b_0, intercept term, β_i, β_{ij}, and β_{ii} are, respectively, the measures of the effects of variables x_i, $x_i x_j$, and x_i^2. The variable $x_i x_j$ represents the first-order interactions between xi and x_j ($i < j$).

27.3 Results and Discussion

27.3.1 The Growth Curve of B. Subtilis BI1

Continuously determined the absorbance of the *B. Subtilis* BI1 fermentation broth (5-fold diluted). The growth curve of *B. Subtilis* BI1 was shown in Fig. 27.1.

0–2 h was the growth delay period with very few bacteria in the fermentation broth; 2–12 h was the logarithmic phase and the viable count increased sharply; in 12–18 h reached the stationary phase, there was a balance between cell growth and death; 18 h after the beginning of fermentation was the death phase, the viable count started to decline and the absorbance of fermentation broth began to decreased.

27.3.2 Optimization of Fermentation Medium

27.3.2.1 Carbon Source Screening Experiment

Took initial fermentation medium as the foundation, used glucose, sucrose, maltose, amylum, and lactose as carbon source separately, and the carbon source

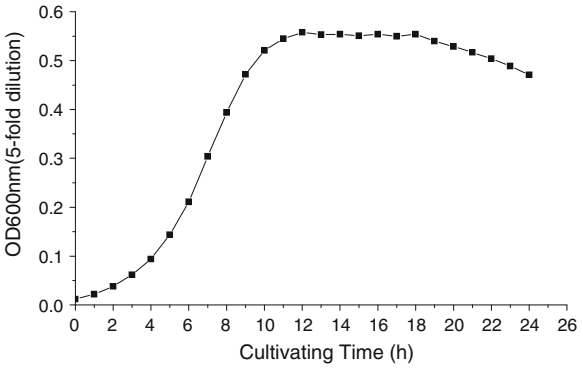

Fig. 27.1 The growth curve of *B. Subtilis* BI1

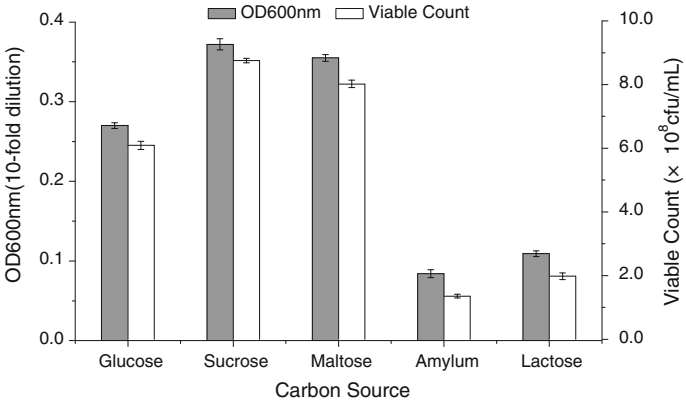

Fig. 27.2 Screening experiment of carbon source

additive amount was 5.0 g/L. The nitrogen source and inorganic salt remained unchanged. The *B. Subtilis* BI1 was cultured according to the initial fermentation conditions. Measured the absorbance (10-fold diluted) and viable count of the fermentation broth, and selected the best carbon source. The experiment result was shown in Fig. 27.2.

After the carbon source screening experiment, found that when sucrose was used as carbon source, the absorbance and viable count of the fermentation broth were highest, so chose sucrose as the best carbon source.

27.3.2.2 The Optimum Addition of Carbon Source

Took sucrose as carbon source of the fermentation medium and designed experiments to study the optimum addition of carbon source [17]. In a group of fermentation medium, added different amounts of carbon source. The *B. Subtilis* BI1 was cultured according to the initial fermentation conditions. Measured the absorbance (10-fold diluted) and viable count of the fermentation broth, and selected the optimum addition of carbon source. The experimental result was shown in Fig. 27.3.

After the research the optimum addition of carbon source was found. When added 20 g/L carbon source, the absorbance (10-fold diluted) and viable count of the fermentation broth were highest, so chose 20 g/L as the optimum addition of carbon source.

27.3.2.3 Inorganic Nitrogen Source Screening Experiment

Based on the initial fermentation medium, carbon source and inorganic salt remained unchanged. Then used KNO_3, NH_4Cl, NH_4NO_3, NH_4SO_4, CON_2H_4 as

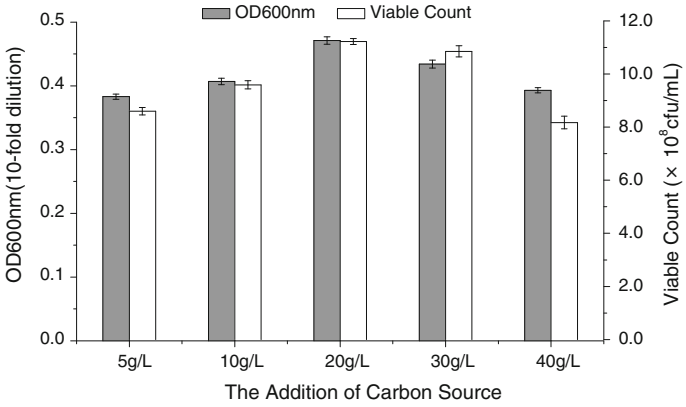

Fig. 27.3 The optimum addition of carbon source

nitrogen sources separately, and the inorganic nitrogen sources additive amount was 2.0 g/L. The *B. Subtilis* BI1 was cultured according to the initial fermentation conditions. Measured the absorbance (10-fold diluted) and viable count of the fermentation broth, and selected the best inorganic nitrogen sources. The experimental result was shown in Fig. 27.4.

After the inorganic nitrogen sources screening experiment,found that when NH_4NO_3 was used as nitrogen sources, the absorbance (10-fold diluted) and viable count of the fermentation broth were highest, so chose NH_4NO_3 as the best inorganic nitrogen sources.

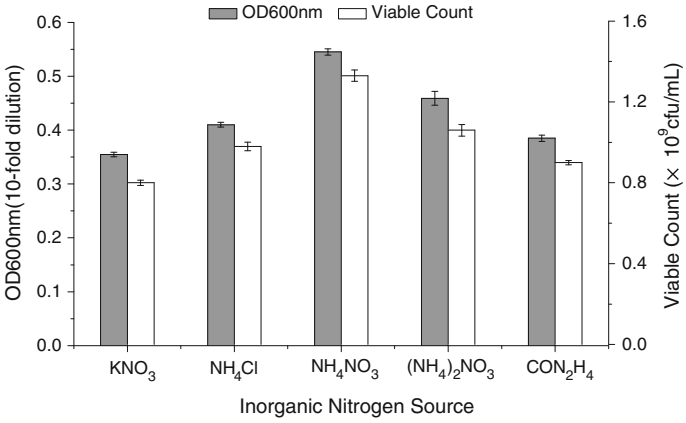

Fig. 27.4 Screening experiment of inorganic nitrogen

27.3.2.4 Organic Nitrogen Source Screening Experiment

Based on the initial fermentation medium, carbon source and inorganic salt remained unchanged. Then used corn steep powder, peptone, yeast extract, beef extract, and soy peptone as nitrogen sources separately, and the organic nitrogen sources additive amount was 2.0 g/L. The *B. Subtilis* BI1 was cultured according to the initial fermentation conditions. Measured the absorbance (10-fold diluted) and viable count of the fermentation broth, and selected the best organic nitrogen sources. The experimental result was shown in Fig. 27.5.

After the organic nitrogen sources screening experiment found that when yeast extract was used as nitrogen sources, the absorbance (10-fold diluted) and viable count of the fermentation broth were highest, so chose yeast extract as the best organic nitrogen sources.

The results of nitrogen source screening experiments showed that organic nitrogen was better than inorganic nitrogen sources, so chose the best organic nitrogen sources—yeast extract as the best nitrogen source.

27.3.2.5 The Optimum Addition of Nitrogen Source

Took yeast extract as the nitrogen source of fermentation medium and designed experiments to study the optimum addition of nitrogen source. In a group of fermentation medium, added different amounts of nitrogen source. The *B. Subtilis* BI1 was cultured according to the initial fermentation conditions. Measured the absorbance (10-fold diluted) and viable count of the fermentation broth, and selected the optimum addition of nitrogen source. The experimental result was shown in Fig. 27.6.

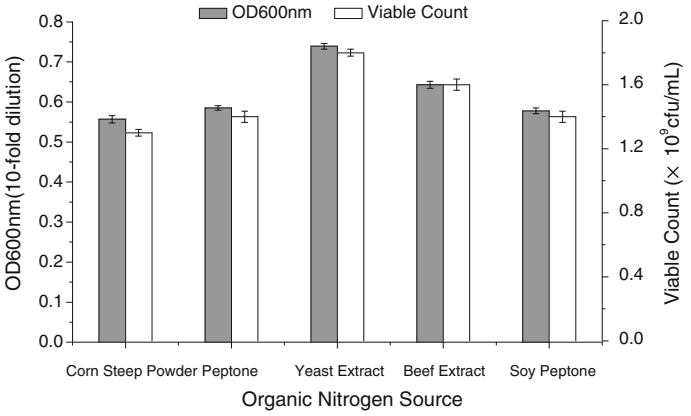

Fig. 27.5 Screening experiment of organic nitrogen

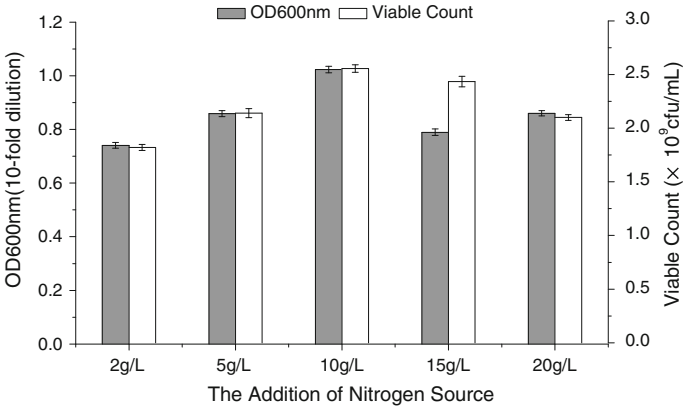

Fig. 27.6 The optimum addition of nitrogen source

After the research the optimum addition of nitrogen source was found. When added 10 g/L nitrogen source, the absorbance (10-fold diluted) and viable count of the fermentation broth were highest, so chose 10 g/L as the optimum addition of nitrogen source.

27.3.2.6 Optimization of Inorganic Salts

Experiment was designed to study the effects of inorganic salt on the enrichment culture of *B. Subtilis* BI1. The experimental result was shown in Fig. 27.7.

Finally, chose the B formula based on above experimental results.

According to all the experiments above, the optimal combination of the medium was as follows: sucrose 20 g/L, dusty yeast 10 g/L, Sodium Citrate 1.0 g/L, $MgSO_4 \cdot 7H_2O$ 0.2 g/L, K_2HPO_4 6.0 g/L, KH_2PO_4 4.0 g/L.

27.3.3 Optimization of Fermentation Conditions

27.3.3.1 Evaluation of the Most Significant Fermentation Condition

The initial fermentation conditions were pH 7.0, liquid volume 50 ml/250 ml, inoculation amount 2.0 %, culture temperature 37 °C, shaking speed 200 r/min, and cultivating time 12 h. The first problem was the most significant conditions should be found. The statistical software Design Expert 7.0 was used to design experiment and analyze data. Set up the experiment model with six actual factors (medium volume, pH, seed age, inoculum size, culture temperature, cultivating time) and five virtual factors. The design was applied under 12 different

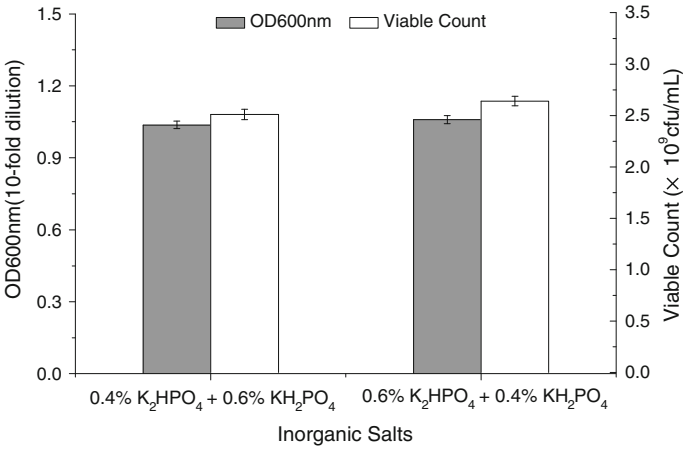

Fig. 27.7 Optimization of inorganic salts

fermentation conditions and each factor selected high and low level [18]. Experimental design and results (absorbance of 10-fold diluted fermentation broth) was shown in Table 27.1. Calculated the effect of various factors, and evaluated the importance. Levels of variables and analysis of main effect for Plackett-Burman was presented in Table 27.2.

By the software analysis, examined the effect of various factors. Took Factors X_1 for example, its effect level E $(x_1) = -0.2122$, showed that Factors X_1 had negative effect on the enrichment culture of *B. Subtilis* BI1 [19], so the absorbance of fermentation broth decreased with increasing medium volume. Consequently, X_1 should be reduced in the later experiments; the contribution of X_1 was significantly higher than other factors and the *p*-value of X_1 than 0.05, so X_1 was a significant factor for the response value. Identical to the above method, factors X_1 (medium volume), X_4 (inoculum size), X_6 (cultivating time) were significant factors for the enrichment culture of *B. Subtilis* BI1 ($p < 0.05$). On the other hand, factors X_2(pH), X_3 (seed age), X_5 (culture temperature) had no significant effect on response, so omitted them from steepest ascent experiment and Box-Behnken design in the following study. We obtained the following model in the coded variables. First-order Model Equation

$$Y_1 = 1.00 - 0.11 \times \boldsymbol{X}_1 + 0.042 \times \boldsymbol{X}_5 + 0.046 \times \boldsymbol{X}_6 \qquad (27.4)$$

27.3.3.2 The Path of Steepest Ascent Experiment

Based on the obtained first-order model equation, the path of steepest ascent was determined to find proper direction of changing variables. Increased or decreased the value of each factor according to the sign of the main effects to improve the

Table 27.1 Plackett-Burman experimental design and results

Trial	x_1	x_2	x_3	x_4	x_5	x_6	x_7	x_8	x_9	x_{10}	x_{11}	Y OD600 nm
1	1	1	−1	1	1	1	−1	−1	−1	1	−1	0.983
2	−1	1	1	−1	1	1	1	−1	−1	−1	1	1.065
3	1	−1	1	1	−1	1	1	1	−1	−1	−1	0.972
4	−1	1	−1	1	1	−1	1	1	1	−1	−1	1.123
5	−1	−1	1	−1	1	1	−1	1	1	1	−1	1.128
6	−1	−1	−1	1	−1	1	1	−1	1	1	1	1.170
7	1	−1	−1	−1	1	−1	1	1	−1	1	1	0.767
8	1	1	−1	−1	−1	1	−1	1	1	−1	1	0.935
9	1	1	1	−1	−1	−1	1	−1	1	1	−1	0.799
10	−1	1	1	1	−1	−1	−1	1	−1	1	1	1.098
11	1	−1	1	1	1	−1	−1	−1	1	−1	1	0.883
12	−1	−1	−1	−1	−1	−1	−1	−1	−1	−1	−1	1.028

Table 27.2 Levels of variables and analysis of main effect for Plackett-Burman

Factor	Code	Low levels (−1)	High levels (+1)	Effect	*p*-Value
Liquid volume (ml)	x_1	30	50	−0.2122	< 0.0001
pH	x_2	7	7.5	0.0092	0.6544
Seed age (h)	x_3	10	14	−0.0102	0.6204
Inoculation amount (%)	x_4	2	5	0.0845	0.0008
Culture temperature (C)	x_5	30	37	−0.0088	0.6660
Cultivating time (h)	x_6	9	13	0.0925	0.0005

Note $p \leq 0.05$ significant; $p \leq 0.01$ highly significant; $p \leq 0.001$ extremely significant; $p \geq 0.05$ Not significant

Table 27.3 The design and results of the steepest ascent experiment

Trial	X_1 Liquid Volume (ml)	X_2 Inoculation Amount (%)	X_3 Cultivating time (h)	OD600 nm (10-fold dilution)	Viable Count ($\times 10^9$cfu/ml)
1	30	3.0	10	1.025	2.5
2	35	3.5	11	1.052	2.6
3	40	4.0	12	1.136	2.8
4	45	4.5	13	1.095	2.7
5	50	5.0	14	0.978	2.4

absorbance of the fermentation broth. The path of steepest ascent started from the center of the factorial design and moved along the path in which the value of medium volume was decreased; in contrast, the values of inoculum size and cultivating time were increased. The design and results of the path of steepest ascent experiments was shown in Table 27.3. As was shown in Table 27.3, the absorbance reached a maximum when the value of liquid volume (X_1), inoculation amount (X_4), cultivating time (X_6) were 40 ml, 4.0 %, 12 h, respectively. It suggested that this point was close to the maximum response area.

27.3.3.3 Optimization of Fermentation Conditions by Box-Behnken Design

In order to approach the optimum response region, significant variables (liquid volume, inoculation amount, cultivating time) were further explored, each at three levels according to Box-Behnken design [20]. Experimental design and results (absorbance of 10-fold diluted fermentation broth) was shown in Table 27.4.

Statistic analysis by design expert 7.0 established a regression model for the enrichment culture of *B. Subtilis* BI1. The regression equation of the model was shown in equation 27.5:

Table 27.4 Box-Behnken experimental design and responses

Trial	X_1	X_2	X_3	Y (OD600 nm)
1	−1(35)	−1(3.5)	0(12)	1.076
2	1(45)	−1(3.5)	0(12)	1.071
3	−1(35)	1(4.5)	0(12)	1.100
4	1(45)	1(4.5)	0(12)	1.085
5	−1(35)	0(4.0)	−1(11)	1.097
6	1(45)	0(4.0)	−1(11)	1.067
7	−1(35)	0(4.0)	1(13)	1.119
8	1(45)	0(4.0)	1(13)	1.092
9	0(40)	−1(3.5)	−1(11)	1.080
10	0(40)	1(4.5)	−1(11)	1.095
11	0(40)	−1(3.5)	1(13)	1.107
12	0(40)	1(4.5)	1(13)	1.115
13	0(40)	0(4.0)	0(12)	1.164
14	0(40)	0(4.0)	0(12)	1.171
15	0(40)	0(4.0)	0(12)	1.170
16	0(40)	0(4.0)	0(12)	1.179
17	0(40)	0(4.0)	0(12)	1.175

$$Y = 1.17 - 9.625 \times 10^{-3} \times X_1 + 7.625 \times 10^{-3} \times X_2 + 0.012 \times X_3 - 2.5 \times 10^{-3} \times X_1 \times X_2 + 7.5 \times 10^{-4} \times X_1 \times X_3 - 1.75 \times 10^{-3} \times X_2 \times X_3 - 0.047 \times X_1^2 - 0.042 \times X_2^2 - 0.031 \times X_3^2 \quad (27.5)$$

Analysis of variance of regression model was shown in Table 27.5. The regression model p-value less than 0.01 implied the model was highly significant [18]. The p-value of lack of fit which is greater than 0.05 showed that it was not significant. P-values less than 0.05 indicate a model term is significant. In this case, A, D and F were significant model terms. Reliability analysis of the model was shown in Table 27.6. $R^2_{adj} = 97.10\%$, meant that the model can explained 97.10 % response value, only 2.90 % response value can not be explained [21]. CV (coefficient of variation) indicated the accuracy of the experiment. The higher the CV value, the lower the reliability of the experiment. In this experiment, CV = 0.6118 %, it showed that the experimental data was credibility and authentic [20]. "Adeq Precision" measures the signal to noise ratio. A ratio greater than 4 is desirable [22]. The ratio of 23.889 indicated an adequate signal. To sum up, the regression equation fitted to the proliferation culture of *B. Subtilis* BI1 well and it was a suitable model.

Figure 27.8 shows that there is a table point, which was also the maximum value point. Encoded value of three main factors ($x_1 = -0.103$, $x_2 = 0.091$, $x_3 = 0.187$) corresponding to the maximum responses value were obtained through ridge analysis. Actual values were predicted by substituting the respective

Table 27.5 Analysis of variance of regression model

Source	Sum of squares	DF	Mean square	F value	*p*-value
Model	2.5372×10^{-2}	9	2.8191×10^{-3}	60.5242	<0.0001
X_1	7.4113×10^{-4}	1	7.4113×10^{-4}	15.9113	0.0053
X_2	4.6513×10^{-4}	1	4.6513×10^{-4}	9.9858	0.0159
X_3	1.1045×10^{-3}	1	1.1045×10^{-3}	23.7126	0.0018
X_1 X_2	2.5000×10^{-5}	1	2.5000×10^{-5}	0.5367	0.4876
X_1 X_3	2.2500×10^{-6}	1	2.2500×10^{-6}	0.0483	0.8323
X_2 X_3	1.2250×10^{-5}	1	1.2250×10^{-5}	0.2630	0.6239
X_1^2	9.3605×10^{-3}	1	9.3605×10^{-3}	200.9618	<0.0001
X_2^2	7.3041×10^{-3}	1	7.3041×10^{-3}	156.8123	<0.0001
X_3^2	4.0203×10^{-3}	1	4.0203×10^{-3}	86.3112	<0.0001
Residual	3.2605×10^{-4}	7	4.6579×10^{-5}		
Lack of fit	1.9925×10^{-4}	3	6.6417×10^{-5}	2.0952	0.2436
Pure error	1.2680×10^{-4}	4	3.1700×10^{-5}		
Cor total	2.5698×10^{-2}	16			

Note $p \leq 0.05$ significant; $p \leq 0.01$ highly significant; $p \leq 0.001$ extremely significant; $p \geq 0.05$ Not significant

Table 27.6 Reliability Analysis of the model

Std.Dev	0.0068	R-Squared	0.9873
Mean	1.1155	Adj R-Squared	0.9710
C.V. (%)	0.6118	Adep Precision	19.7825

values in formula (27.2). This model predicted that the maximum of absorbance $OD_{600} = 1.174$ can be obtained when liquid volume (X_1) was 39.49 ml, inoculation amount (X_2) was 4.05 %, cultivating time (X_3) was 12.19 h.

The absorbance of fermentation broth (10-fold diluted) was 1.181 under optimized conditions, which was very close to the predictive value, suggesting that the optimization model was consistent with the actual situation.

27.3.4 Research on the Effects of Optimization

Bacillus. Subtilis BI1 was cultured according to the parameters before and after optimization of medium and culture conditions respectively. The absorbance of fermentation broth (10-fold diluted) and viable count were compared. After the optimization, absorbance of fermentation broth (10-fold diluted) reached 1.179 and viable count of *B. Subtilis* BI1 reached 3.0×10^9 cfu/ml, five times enhanced than before.

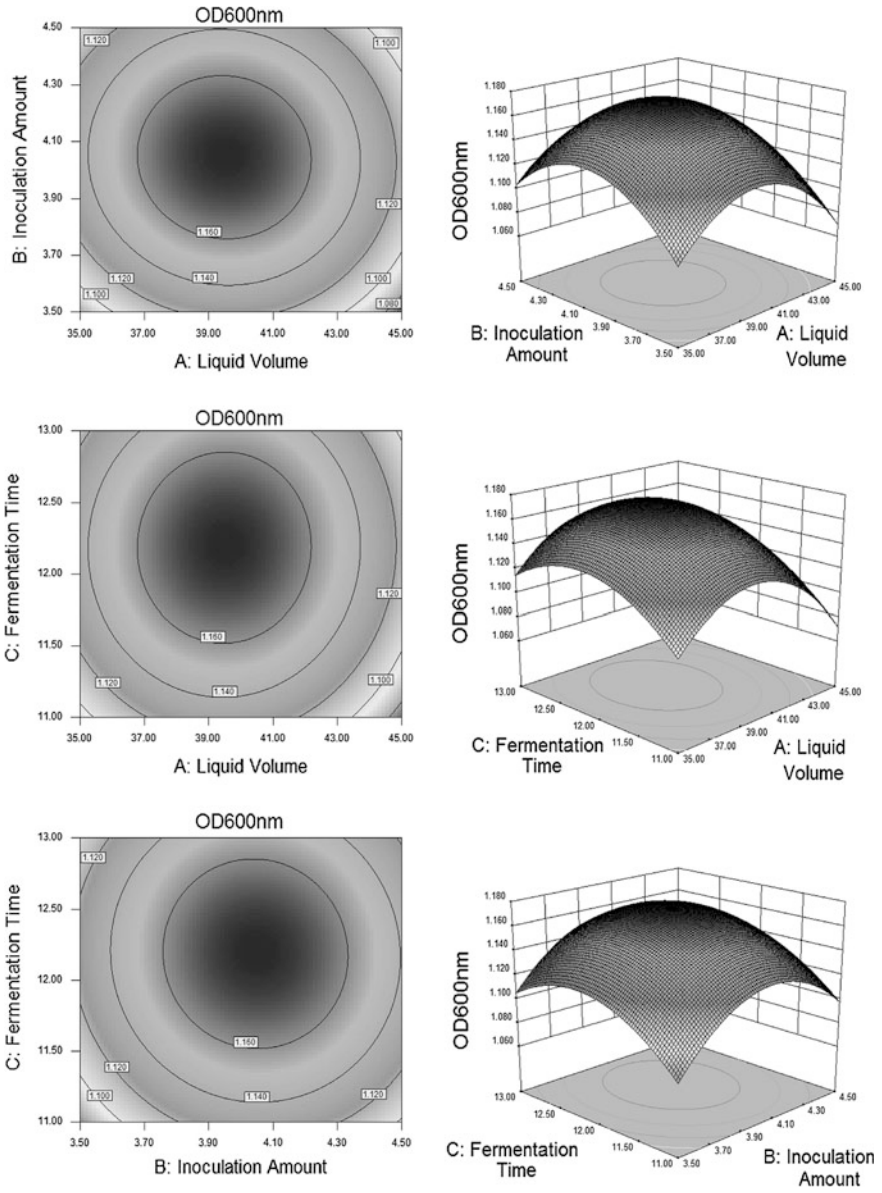

Fig. 27.8 Contour map and perspective view of the interactions

27.4 Conclusions

In this paper, fermentation medium and culture conditions for *B. Subtilis* BI1 were predicted to obtain maximum viable count. The optimized medium is as follows (g/L): glucose, 45; $NaNO_3$, 3.75; sucrose, 20; dusty yeast, 10; Sodium Citrate, 1.0; $MgSO_4 \cdot 7H_2O$, 0.2; K_2HPO_4, 6.0 and KH_2PO_4, 4.0. inoculation amount 4.05 %, culture temperature 37 °C, shaking speed 200 r/min and cultivating time 12.19 h are established for the maximum viable count 3.0×10^9 cfu/ml.

27.5 Discussions

Because of the potential use of *B. Subtilis*, submerged cultivation of bacteria is the best choice for their large-scale production. The optimal design of the culture media and conditions are very important aspects in the field of high-cell density cultivation. Optimization of media components and conditions by classical methods which involves the change of one variable at a time, is extremely time consuming and expensive when a large number of variables are considered. In order to overcome this difficulty and determine the interaction between the studied variables, an experimental factorial design and response surface method was employed for optimization [11]. Plackett-Burman design offers good and fast screening procedure and mathematically computes the significance of large number of factors in one experiment, which is time saving and maintains convincing information on each component [14]. Applying Box-Behnken designs in the optimization process for maximal production is an efficient method that tests the effect of factors interaction [8]. Besides, they convert bioprocess factors into mathematical models to predict where the optimum is likely to be located.

In the studies of Chen P.T [1], three critical medium components were selected by the Plackett–Burman design to optimize the medium formulation. As a consequence, the production of renilla luciferase reached 500 mg/L. The effect of cultivation conditions on *Bacillus Subtilis* growth and sporulation was investigated by Box–Behnken design in Sandra M. Monteiro's work [10]. Studies of the cultivation conditions led to an increase of the maximum concentration of vegetative cell from 2.6×10^9 cfu/ml to 2.2×10^{10} cfu/ml and the spore concentration from 4.2×10^8 spores mL^{-1} to 5.6×10^9 spores mL^{-1}.

In our studies,the fermentation medium and conditions of *Bacillus Subtilis* BI1 were optimized. First of all, the fermentation medium was optimized by single factor method. Then, the application of Plackett-Burman design filtered the more significant fermentation conditions. Next, the steepest ascent experiment to determine the area close to the maximum response value. Finally, established a regression model for the enrichment culture of *Bacillus Subtilis* BI1 by Box-Behnken design and predicted the response under the optimal conditions.

Compared with others research,more factors were investigated and more optimization strategy were used in our studies to obtain a better results. Comprehensive study led to a higher viable count. This is the difference and possible innovation in comparison with other research papers.

Experimental results show that the integration of optimization methods can construct target model effectively, and it outperforms single method obviously.

Acknowledgments This work was supported by Key Projects in the Tianjin Science & Technology Pillar Program (No. 12ZCZDNC01600).

References

1. Chen PT, Chang CJ, Chao YP (2010) Medium optimization and production of secreted Renilla luciferase in *Bacillus Subtilis* by fed-batch fermentation. Biochem Eng J 49:395–400
2. Mizumoto SJ, Shoda M (2007) Medium optimization of antifungal lipopeptide, iturin A, production by *Bacillus Subtilis* in solid-state fermentation by response surface methodology. Appl Microbiol Biotechnol 76:101–108
3. Abdel YR, El-Enshasy HA, Soliman NA (2009) Bioprocess development for production of alkaline protease by Bacillus pseudofirmus Mn6 through statistical experimental designs. Microbiol. Biotechnol 19:378–386
4. Sanders ME (2003) Probiotics: considerations for human health. Nutr Rev 61:91–99
5. Pusey PL, Wilson CL (1984) Postharvest biological control of stone fruit brown rot by *Bacillus Subtilis*. Plant Dis 68:753–756
6. Wu JY, Ye HF (2007) Characterization and flocculating properties of an extracellular biopolymer produced from a *Bacillus Subtilis* DYU1 isolate. Process Biochem 42:1114–1123
7. Bandyopadhyay P, Das Mohapatra PK (2009) Effect of a probiotic bacterium *Bacillus circulans* PB7 in the formulated diets: on growth, nutritional quality and immunity of Catla catla (Ham.). Fish Physiol Biochem 35:467–478
8. Balcázar JL, Tyrone RL (2007) Inhibitory activity of probiotic *Bacillus Subtilis* UTM 126 against *Vibrio* species confers protection against vibriosis in juvenile shrimp (*Litopenaeus vannamei*). Curr Microbiol 55:409–412
9. Schallmey M, Singh A, Ward OP (2004) Developments in the use of *Bacillus* species for industrial production. Can J Microbiol 50:1–17
10. Sandra MM, João JC, Adriano OH et al (2005) A procedure for high-yield spore production by *Bacillus Subtilis*. Biotechnol Progr 21:1026–1031
11. Rao YK, Tsay KJ, Wu WS (2007) Medium optimization of carbon and nitrogen sources for the production of spores from *Bacillus amyloliquefaciens* B128 using response surface methodology. Process Biochem 42:535–541
12. Tokcaer Z, Bayraktar E, Mehmetoğlu Ü (2006) Response surface optimization of antidipteran delta-endotoxin production by *Bacillus thuringiensis* subsp. *israelensis* HD 500. Process Biochem 41:350–355
13. Wang DP, Fang JH, Meng H et al (2010) Identification of BI1 and study on antagonistic capability. Chin j Antibiot 35:181–184
14. Taher A, Mohammad RG, Parviz N (2009) Multivariate optimization of molecularly imprinted polymer solid-phase extraction applied to parathion determination in different water samples. Anal Chim Acta 638:154–161
15. He GQ, Chen QH, JU XJ et al (2004) Improved elastase production by *Bacillus* sp. EL31410-further optimization and kinetics studies of culture medium for batch fermentation. J Zhejiang Univ-Sci B 5:149–156

16. Adinarayana K, Ellaiah P (2002) Response surface optimization of the critical medium components for the production of alkaline protease by a newly isolated *Bacillus* sp. J Pharm Pharmaceut Sci 5:272–278
17. Toru N, Michihiko K, Hideaki Y (1988) Optimum culture conditions for the production of benzonitrilase by *Rhodococcus rhodochrous* J1. Arch. Microbiology 150:89–94
18. Kalil SJ, Maugeri F, Rodrigues MI (2000) Response surface analysis and simulation as a tool for bioprocess design and optimization. Process Biochem 35:539–550
19. Venugopal P, Chandra TS (2000) Statistical optimization of medium components for enhanced riboflavin production by a UV-mutant of *Eremothecium ashbyii*. Process Biochem 36:31–37
20. Box GEP, Wilson KB (1951) On the experimental attainment of optimum conditions. J. R. Stat. Soc. B 13:1–45
21. Jin-CS Sze ML, Abdul RM (2011) Optimizing photocatalytic degradation of phenol by TiO2/GAC using response surface methodology. Korean J Chem Eng 28:84–92
22. Kaushik R, Saran S, Isar J et al (2006) Statistical optimization of medium components and growth conditions by response surface methodology to enhance lipase production by *Aspergillus carneus*. J Mol Catal B-Enzym 40:121–126

Chapter 28
Investigation on Electroporation: Mediated Transformation of *Chlorella ellipsoidea*

Zhihan Zuo, Feifei Qin, Yichen Zhang, Yichen Liu and Jinsheng Sun

Abstract *Chlorella ellipsoidea* is a kind of micro algae biological reactor. It is a suitable eukaryotic expression system for foreign proteins, and the bioactivity of the expressed protein is similar to the natural counterpart. However, introduction of foreign gene into *C. ellipsoidea* cells is the precondition for its efficient expression. In this paper the electroporation conditions to transform *C. ellipsoidea* including cultured medium, growth rate of *C. ellipsoidea*, voltage strength were systematically investigated. BG11 without Mg^{2+} was selected as the medium for cultivating *C. ellipsoidea*. The exponential phase cells were harvested and electroporated under different electric voltages. Voltage at the 630 V was identified to be optimal by determining the cells viability after electroporation. Under this condition, the plasmid pSC2 carrying *gfp* was successfully transformed into *C. ellipsoidea*. The *gfp* gene could continuously express for at least 7 days. (This work was financially supported by grants from the National Basic Research Development Program of China (973 programs, **2012CB114405**), National High-Tech Research and Development Program of China (863 programs, **2012AA092205** and **2012AA10A401**), National Key Technology Research and Development Program (**2011BAD13B07** and **2011BAD13B04**), Doctoral found of Tianjin normal university: **52X09010** and Open research found for city stage key laboratory of Tianjin normal university).

Keywords Cell viability · *Chlorella ellipsoidea* · Electroporation · Medium · Voltage strength

Z. Zuo · F. Qin · Y. Zhang · Y. Liu · J. Sun (✉)
College of Life Science, Tianjin Normal University, Tianjin Key Laboratory of Animal and Plant Resistance, Tianjin 300387, People's Republic of China
e-mail: jssun1965@yahoo.com.cn

T.-C. Zhang et al. (eds.), *Proceedings of the 2012 International Conference on Applied Biotechnology (ICAB 2012)*, Lecture Notes in Electrical Engineering 249,
DOI: 10.1007/978-3-642-37916-1_28, © Springer-Verlag Berlin Heidelberg 2014

28.1 Introduction

Unicellular green algea *Chlorella ellipsoidea* has long been regarded as a potential diet source due to its high protein content and various physiologically active substances [1]. This species is an essential phytoplankton used as live feed for fisheries with a high content of proteins and fatty acids. In addition, due to its fast growth and low cost, *C. ellipsoidea* is thus a promising candidate bioreactor for the large-scale production of value-added proteins. To make a *Chlorella* microalgal bioreactor, an appropriate genetic transformation system is needed to ensure the expression of the target gene in transgenic *Chlorella*. In the case of *Chlorella*, development of genetic transformation has been slow.

Many techniques are available for gene transformation of plant cells. Such as protoplasting, electroporation, particle bombardment, and *Agrobacterium*-mediated methods for higher plants [2]. For aglea, PEG-mediation method, electroporation, microinjection, particle bombardment, protoplasting, agitation with glass beads and silicon fibers are common methods [3]. However, genetic transformation of microalgae is usually quite transformed *Chlorella* were still relatively low.

The former two authors contributed equally to this study.

difficult due to the technical limitations of existing methods, and the expression levels of these foreign genes in

A plant ubiquitin gene promoter was used to drive the expression of a gene encoding mature rabbit neutrophil peptide-1 (NP-1) in *C. ellipsoidea* cells [4]. In another study, *C. ellipsoidea* was transformed with a vector containing the flounder growth hormone gene (fGH) under the control of the 35S promoter, and the phleomycin resistance *Sh ble* gene under the control of the Chlamydomonas *RBCS2* gene promoter. Over 400 μg fGH protein expression per one liter of culture containing 1×10^8 cells/mL was estimated by ELISA [5].

Therefore, effective transformation methods are urgently needed to be established for efficient expression of foreign genes in *Chlorella*. In this study, we optimized the conditions of the electroporation to transform *C. ellipsoidea* including cultured medium, growth rate of *C. ellipsoidea*, voltage strength.

28.2 Materials and Methods

28.2.1 Medium and Plasmid

C. ellipsoidea (Institute of Hydrobiology, Chinese Academy of Science) was used as the host cell for transformation. *Chlorella* was grown in BG11 medium [6] without Mg^{2+} in Erlenmeyer flasks, which was sterilized by autoclave sterilizer. Cultures in liquid medium or on the plate were grown at 25° ± 1 °C in an artificial climate incubator.

The plasmid pSC2 involves the *gfp* selection marker expression cassette was used for the selection of gene transfer in the host organism transformation.

28.2.2 Determination of Chlorella ellipsoidea Growth Rate

Chlorella ellipsoidea was inoculated in BG11 medium without Mg^{2+} to 10^6/mL initial concentration, and it was maintained at (25 ± 1) °C (with an illumination of 2500–3000 l×, under a light/dark cycle of 12:12). The growth rate of *C. ellipsoidea* was determined by counting cells in blood samples once per day.

Restrictionincision enzyme activity determination *of C. ellipsoidea* was obtained through cell freezing and thawing. Plasmid pSC2 was incubated with the lysed *C. ellipsoidea* cells in different buffer at 37 °C for 1 h to determine the degradation of the restriction enzyme for foreign DNA in *C. ellipsoidea*.

28.2.3 Preparation of Chlorella ellipsoidea Cells

Chlorella ellipsoidea was inoculated in 50 mL BG11 liquid medium in triangular flask in the biochemistry incubator at (25 ± 1) °C, with an illumination of 2500–3000 l×, under a light/dark cycle of 12:12, shake the flask three times per day.

Chlorella ellipsoidea cells in the exponential phase cultivated 11 days were collected by centrifuge at 5,000 rpm for 5 min in 1.5 mL eppendorf tube. The pellet was washed twice by BG11 medium without Mg^{2+} [7]. The resulting pellets were resuspended to a density of 1×10^8 cells/mL in electroporation buffer (10 mM KCl, 10 mM CaCl2, 40 mM Hepes, 400 mM mannitol, 400 mM sorbitol; pH−7.2). Then the cell suspension were kept on ice for 5–10 min [8, 9].

28.2.4 Electroporation and the Determination of Cell Viability

Suspension aliquots in volume 100 μL was transferred into a small electroporation cuvette and electroporated by using a Bio-Rad GenePulser Xcell apparatus (Bio-Rad, USA). The voltage was at different levels and the duration was 3 ms, after the electroporation, the cell suspension were kept on ice for 5–10 min. Then the cell suspension was dyed by FDA to determine the cell viability [10, 11].

The cell suspension was dyed to final concentration of 100 μg/mL of FDA of the cell suspension for 30 min in dark, and then 7 μL cell suspension was transferred to make microscopic slides. The slides were observed under the inverted fluorescence microscopy (OLYMPUS CKX41). Through calculating the dyed cells

and the whole cells at least 8 visual fields in one sample microscopy slide. The cell viability was calculated. The cell viability equals to the percentage that the dyed cells in the whole cells in one vision. And the viability of the voltage is the average value of the several visions. The suitable voltage of the electroporation is the voltage when the viability is about 50 % [12].

28.2.5 The Electroporation of Plasmid pSC2

Suspension aliquots of 100 μL in volume were mixed with plasmid pSC2 and milt DNA. The final concentration of plasmid pSC2 and the milt DNA were 10 μg/mL and 25 μg/mL, respectively. The final cell suspension was kept on ice for 5–10 min. Then transferred into an electroporation cuvette (Gene Pulser/MicroPulser Cuvette, 0.1 cm gap, Bio-Rad). The cell suspension was electroporated at 630 V and the duration was 3 ms. After electroporation, the cell suspension was kept on ice again. Finally, cells were transferred into 2 mL BG11 medium without Mg^{2+}, kept dark for 3 h, then observed under inverted fluorescence microscopy.

28.2.6 The **gfp** *Expression Duration*

The electroporation transformed *Chlorella* cells with plasmid pSC2 were normally incubated (12L: 12D). Cells with fluorescent were observed under inverted fluorescence microscopy at different time point. Through continuously observation of the cells, the *gfp* expression duration in *C. ellipsoidea* was determined.

28.3 Results and Discussions

28.3.1 The Optimization of the Medium

Plasmid pSC2 was used to determine the degradation affection of the restriction enzyme in *C. ellipsoidea* for foreign genes. When plasmid pSC2 was incubated with the lysed *C. ellipsoidea* cells, though the restriction enzyme in *C. ellipsoidea* cells is not purified, the plasmid has been cut into two pieces completely (Fig. 28.1). This result indicated the degradation of the restriction enzyme in *C. ellipsoidea* for foreign DNA is very strong. So it is difficult to transform foreign genes into *C. ellipsoidea* cells.

Due to the result, the medium of *C. ellipsoidea* must be optimized. Because Mg^{2+} is the activator of lots of enzymes in organism. The BG11 medium without

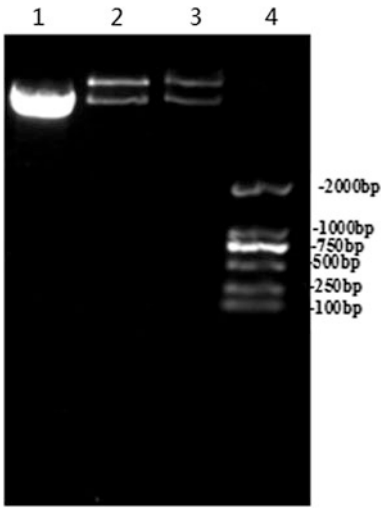

Fig. 28.1 The result of the *C. ellipsoidea* restriction enzyme reaction. *1* plasmid pSC2 restriction enzyme reaction, *2* plasmid pSC2 reacted with the restriction enzyme in H Buffer, *3* plasmid pSC2 reacted with the restriction enzyme in K Buffer, *4* DNA maker: DL 2000

Mg^{2+} would decrease the restriction enzyme activity of enzyme, which can improve the possibility of the foreign DNA transformation.

28.3.2 Determination of Chlorella ellipsoidea Growth Rate

Growth rate of *C. ellipsoidea* in BG11 without Mg^{2+} was determined by counting cells in blood samples once per day. Thus the growth curve of *C. ellipsoidea* was made (Fig. 28.2). From the result, conclusion can be made that under this condition *C. ellipsoidea* got into exponential phase from lag phase after 4 days. The period of 4 to 8 days was the early phase of exponential phase, 8 to 14 days was the middle phase of exponential phase, and 8 to 14 days was the late phase of exponential phase. After cultivating 16 days *C. ellipsoidea* entered the stationary phase. Owing to that the electroporation transformation efficiency of cells during

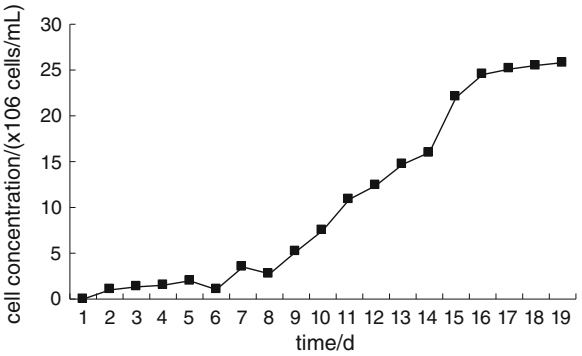

Fig. 28.2 Determination of *C. ellipsoidea* growth rate. Each time point represents an average value from three parallel flasks from each strain

the middle exponential phase was obviously higher than that during the early exponential phase or late exponential phase by under the same conditions [12], *C. ellipsoidea* cells cultivated in BG11 without Mg^{2+} for 11 days was selected as the material for electroporation transformation.

28.3.3 The Exploration of the Suitable Voltage

The transformation efficiency is superior when the viability is approximately 50 % after electroporation transformation [12]. Therefore, the optimal voltage value of the electroporation was selected through the calculating of electroporation viability. The survival rate was calculated by the percent of FDA dyed cells to the total cells in one vision, relative survival rate was the ratio of the survival rate after electroporation at different voltage to the survival rate without electroporating. The relationship between viability and voltage was shown in Tables 28.1, 28.2, 28.3.

Tables 28.1, 28.2 and 28.3 showed that along with the voltage strength rising, the viability decreasing. And the suitable voltage was between 610 and 624 V. For achieving 50 % of the relative survival rate, and for easily controlling the experiment, the 630 V was chosen as the suitable optimal voltage strength for electroporation.

28.3.4 The Electroporation of Plasmid pSC2

The green fluorescent protein (GFP) is a protein composed of 238 amino acid residues (26.9 kDa) that exhibits bright green fluorescence when exposed to light in the blue to ultraviolet range [13]. In cell and molecular biology, the *gfp* gene is

Table 28.1 The voltage and the related survival rate (1)

	No electroporated	500 V	700 V	900 V
Survival rate (%)	58.36	66.27	5.96	4.00
Relative survival rate (%)	100.00	113.55	10.21	6.85

Table 28.2 The voltage and the related survival rate (2)

Survival rate (%)	80.98	58.02	49.25	34.74	23.86
Relative survival rate (%)	100.00	71.64	60.81	42.89	29.46

Table 28.3 The voltage and the related survival rate (3)

	No electroporated	584 V	596 V	610 V	624 V
Survival rate (%)	59.94	41.65	46.08	36.10	32.22
Relative survival rate (%)	100.00	69.49	76.88	60.22	53.74

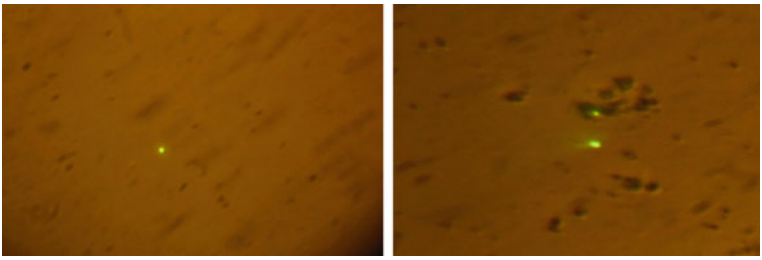

Fig. 28.3 Expression of pSC2 in *C. ellipsoidea* cells

Table 28.4 The *gfp* expressed cells with observed at different time point

Cultured time h	6	24	48	72	144	168
Average of transformed cells in each microscopic slides of sample	32	24	24	27	16	1

frequently used as a reporter of expression [14]. Aimed to make sure whether the foreign gene has been electroporated into the *C. ellipsoidea* cells. The plasmid pSC2 which carries the *gfp* gene was introduced into *C. ellipsoidea* and maintained in their genome through transformation. When plasmid pSC2 was electroporated into the cells, after at least 3 h, the fluorescent can be observed under the inverted fluorescence microscopy (Fig. 28.3) [15].

Figure 28.3 shows the *gfp* gene in pSC2 was expressed in *C. ellipsoidea* cells and the expressed green fluorescent protein could be observed distinctly under inverted fluorescence microscopy. This result indicates that the plasmid pSC2 with *gfp* gene has been electroporated into the *C. ellipsoidea* cells.

28.3.5 The gfp *Expression Duration*

The electroporated *Chlorella* cells with plasmid pSC2 were observed under inverted fluorescence microscopy at different time point. Table 28.4 showed the number of cells with fluorescent expressed by *gfp*. The result indicated that the *gfp* gene could continuously express for at least 7 days after transformation. When cells were incubated in BG11 without Mg^{2+} for 6 h after transformation, the transformation efficiency reached the highest value of 0.586 ‰. Transformation efficiency was calculated by the percent of the number of fluorescent expressed cells to the number of total cells observed.

28.4 Conclusions

In this paper, through optimizing the parameters of the electroporation of *C. ellipsoidea*, including *C. ellipsoidea* growth medium, growth rate of *C. ellipsoidea*, voltage strength. The conclusion could be made that *C. ellipsoidea* cultured in BG11 medium without Mg^{2+}, transformation efficiency of *C. ellipsoidea* would be increased. And 630 V is the suitable voltage for electroporation, under this voltage the plasmid pSC2 could be transferred into the algae cells and the fluorescent of *gfp* could be seen under the inverted fluorescence microscopy. During the period of observation of the transformed cells, the *gfp* gene could continuously express for at least 7 days.

References

1. Masato M, Irena H, Hiroyuki H et al (1994) Introduction of foreign DNA into *Chlorella saccharophila* by electroporation. Biotechnol Tech 8:821–826
2. EL-SHEEKH MM (1999) Stable transformation of the intact of *Chlorella kessleri* with high velocity microprojectiles. Biologia Plantrum 42:209–216
3. Wang CH, Wang YY, Qiao S et al (2007) Transient expression of the GUS Gene in a unicellular marine green alga, *Chlorella sp.* MACC/C95, via electroporation. Biotechnol Biotechnol Equip 12:180–183
4. Chen Y, Wang Y, Sun Y, Zhang L et al (2001) Highly efficient expression of rabbit neutrophil peptide-1 gene in *Chlorella ellipsoidea* cells. Curr Genet 39:365–370
5. Kim DH, Kim YT, Cho JJ et al (2002) Stable integration and functional expression of flounder growth hormone gene in transformed microalga, *Chlorella ellipsoidea*. Mar Biotechnol 4:63–73
6. Huo SH, Chen YB, Liu YP et al (2012) Experiment on microalgae cultivation in BG11 nutrient solution adding biogas slurry. Trans of the Chin Soc of Agric Eng 8:241–246
7. Lv PJ, Yan HX, Li J et al (2009) An optimal electroporation system for *Dunaliella salina*. Chin J Biotechnol 25:520–525
8. Li X (2004) Heterogeneous expression and protein purification of the rabbit defensin gene NP-1. BJFU
9. Wang YY (2005) Construction of a system of foreign genes in *Chlorella* sp. and expression of phytase. DLUT
10. Zhan LB, Liang WY, Qu JH et al (2005) The viability determination of cyanbacteria by double staining with fluoresce indiacetate and propidum iodide. Environ Chem 25:554–557
11. Lu SX (2010) Construction and transformation of expression vector into *Haematococcus pluvialis* by electroporation. SCUT
12. Lu SX, Chen G, Wei D (2010) Effect of electroporation conditions on cell viability of *Haematococcus pluvialis*. Mod food Sci. Technol 26:554–557
13. Prendergast F, Mann K (1978) Chemical and physical properties of aequorin and the green fluorescent protein isolated from *Aequorea forskålea*. Biochem 17:48–53
14. Phillips G (2001) Green fluorescent protein—a bright idea for the study of bacterial protein localization. FEMS Microbiol Lett 204:9–18
15. Zhang HS, Ye J, Tang XJ et al (2008) Expression of green fluorescent protein gene in A9 strain of *Spirulina platensis*. Acta Laser Biology Sinica 17:59–63

Chapter 29
Screening, Mutagenesis of *Brevibacterium flavum* for the Enhancement of L-Valine Production

Kun Cheng and Chaozheng Zhang

Abstract A L-valine production strain *Brevibacterium flavum* C1(Ile$^-$) was mutagenized using UV-irradiation and diethyl sulfate and was screened on the selective plates. The selective plates contained 4 g/L 2-thiazole-DL-alanine (2-TA) or 5 g/L α-aminobutyric acid (α-AB). After mutagenesis and selection, 1500 mutants were obtained, and 57 were found to be resistant to 2-thiazole-DL-alanine and α-aminobutyric acid. Following determination of the L-valine produced by these 57 mutants in fermentation medium in shaken cultures, a mutant CC5 (Ile$^-$, 2-TA^r, α-AB^r) showed highest L-valine production ability than the original strain.

Keywords *Brevibacterium flavum* · L-valine · Mutagenesis · Screening

29.1 Introduction

L-valine, an essential amino acid needed by human beings and animals, has great applications in food, flavoring, animal feeds, and so on. In addition, L-valine is also used as the precursor for the chemical synthesis of herbicides, drugs, and antibody. Currently, the annual consumption of L-valine amounts to several thousand tons globally. Due to the growing world market for L-valine, there is an increasing interest in the further development and optimization of its efficient production.

K. Cheng
Shandong NB Biotechnology Co., Ltd, Binzhou 256219, People's Republic of China

C. Zhang (✉)
Key Laboratory of Ministry of Education Industrial Fermentation Microbiology, Tianjin Key Laboratory of Industrial Microbiology, Tianjin University of Science and Technology, Tianjin 300457, People's Republic of China
e-mail: zhangchaozheng@tust.edu.cn

T.-C. Zhang et al. (eds.), *Proceedings of the 2012 International Conference on Applied Biotechnology (ICAB 2012)*, Lecture Notes in Electrical Engineering 249,
DOI: 10.1007/978-3-642-37916-1_29, © Springer-Verlag Berlin Heidelberg 2014

In general, the industrial production of L-valine is carried out mainly by fermentation using bacterial species such as *Corynebacterium pekineise* [1], *Corynebacterium glutacium* [2], *Escherichia coli* [3, 4], *Brevibacterium lactofermentum* [5, 6], *Serratia marcescens* [7], and *Brevibacterium flavum* [8, 9]. In order to achieve cost-effective production of L-valine, many researches have been carried out such as optimizing production process or developing improved production strains [10–12]. In this study, we attempt to develop a *B. flavum* strain giving improved yields through mutagenesis by UV-irradiation and diethyl sulfate and screening procedures.

29.2 Materials and methods

29.2.1 Strains

The L-valine producer *B. flavum* C1 (Ile^-) used in this study, which produced 12 g/L L-valine in shaken flasks, was obtained from Key Laboratory of Industrial Microbiology, Tianjin University of Science and Technology. This strain was an Ile auxotroph, and was not resistant to 1 g/L 2-thiazole-DL-alanine (2-TA) and 2 g/L α-aminobutyric acid (α-AB).

29.2.2 Media and Culture Conditions

The strain was maintained on complete medium (CM) agar slants and transferred on monthly basis. It was stored at 4 °C and utilized as stock inoculum. The complete medium was composed of the following (g/L): peptone 10, beef extract 10, yeast extract 5, NaCl 2.5, glucose 1, and pH was maintained at 7.2 [9]. Selective medium was utilized to isolate 2-TA-resistant mutants or α-AB-resistant mutants, and was prepared by the addition of 2-TA or α-AB to supplemental medium (SM). The supplemental medium was composed of the following (g/L): glucose 20, $(NH_4)_2SO_4$ 10, KH_2PO_4 1, $MgSO_4{\cdot}7H_2O$ 0.4, $FeSO_4{\cdot}7H_2O$ 0.01, $MnSO_4{\cdot}H_2O$ 0.01, V_H 300 μg, V_{B1} 100 μg, L-isoleucine 0.015, and pH was maintained at 7.0.

Cells grown on the slants were used to inoculate into 50 mL of seed medium. After 16 h of cultivation at 32 °C on a rotary shaker (200 rpm), this seed culture was transferred into 200 mL fermentative medium in 1000 mL baffled flasks under the same conditions. The fermentative medium used for L-valine production contained (g/L): glucose 80, corn liquid steep 20 mL, $(NH_4)_2SO_4$ 2, K_2HPO_4 1.2, $MgSO_4{\cdot}7H_2O$ 0.4, $MnSO_4{\cdot}H_2O$ 0.015, complex amino acid liquid 2 mL, and pH was adjusted at 7.2.

29.2.3 Mutagenesis

29.2.3.1 Ultraviolet (UV)-Mutagenesis

The single colony of *B. flavum* C1 was inoculated into 25 mL seed medium at 32 °C with shaking at 200 rpm for 16–18 h. The culture was diluted 50 fold into 50 mL seed medium and incubated under the same conditions to the exponential phase. Subsequently, cells were collected by centrifugation at 3500 rpm for 10 min. After three washes in sterile water, the cells were suspended in sterile water at a density of about 1.0×10^8 cells/mL.

About 10 mL of the cell suspension of *B. flavum* C1 was irradiated with a Phillips TUV-30-W-254 nm Lamp for 15 s at a distance of 30 cm. The mutagenesis was carried out in the dark to avoid photoreactivation repair. At this stage the drop in viability was about 75 %. The suspension was then diluted and spread onto the surface of SM agar containing 2 g/L or 4 g/L 2-thiazole-DL-alanine (2-TA). Plates were then incubated for 2 days at 32 °C, and the growing colonies were transferred on slants for further studies.

29.2.3.2 Diethyl Sulfate Mutagenesis

The procedure for diethyl sulfate (DES) mutagenesis was similar to that for UV-mutagenesis except that phosphate buffer (pH 7.0) was used to prepare the cell suspensions, and DES (Sigma, final concentration 0.5 % (v/v)) was used as the mutagenic agent. The cells were treated with DES for 30 min. After exposure, the cells were diluted with phosphate buffer and harvested by centrifugation. Then the diluted cell suspension was spread on the surface of SM agar containing 5 g/L α-aminobutyric acid (α-AB) and 4 g/L 2-TA. In addition, the mutagenesis procedure was not carried out in the dark. After DES treatment, a 70 % drop in viability was observed.

29.2.4 Determination of L-Valine

L-valine concentration in fermented broth was quantitatively determined using chemical colorimetry according to the report by Li et al. [13].

29.3 Results and Discussion

Several round mutagenesis were carried out, following subsequent selection of the mutants with increased L-valine production activity. A number of specific selection procedures have been adapted to improve the biosynthetic capacity of strains.

Table 29.1 2-TA or α-AB resistant mutants obtained after UV or DES mutagenesis

Mutagen	Number of resistant colonies	Number of resistant colonies with improved production characteristic
UV	521	7
UV	462	12
DES	517	57

Resistance to the L-valine analog had been demonstrated as an effective criterion to select mutants showing increased L-valine. Huang H H and Li F D isolated a mutant Corynebacterium 104 (2-TA^r, AHV^r, β-HL^r) after several round mutagenesis by UV and nitrosoguanidine (NTG), and the overproducer could accumulate L-valine more than 10 g/L [14]. Tsuchida et al. obtained a mutant *B. lactofermentum* 487 by the mutagenesis of NTG, which was resistant to 2-TA, could produce 31 g/L L-valine [15]. In our study, we also used 2-TA and α-AB as the L-valine analog. After exposure to UV or DES treatments, mutants resistant to 2-TA or α-AB were isolated (Table 29.1). At the first round mutagenization by UV, 521 mutants were isolated, characteristic of the best growth on the plates containing 2 g/L 2-TA. These cultures were initially evaluated for their L-valine production activity in flask on a rotary shaker, and 7 mutants showed an increase in the production of L-valine compared with the parental strain. The highest level of L-valine was produced by mutant A22 (21 g/L). Then A22 was subjected to UV-irradiation for the second time and the mutants were still screened on the plates containing 2-TA. Out of 462 selected colonies on the plates containing 4 g/L 2-TA, 12 mutants produced L-valine in amounts more than their original parental strain A22. Among these 12 mutants, B107 showed the greatest production ability (26.4 g/L).

To investigate the effect of chemical mutagens on the L-valine production, B107 was subjected to the DES treatment. At this round mutagenization, 57 mutants, among 517 colonies which were characterized by the best growth on the plates containing 5 g/L α-AB and 4 g/L 2-TA, exhibited the improved L-valine production ability than their parental strain B107 (data not shown). CC5 was the highest extracellular L-valine producer, with an ability (34.7 g/L) 1.31 and 2.89 times higher than that produced by B107 and its original strain C1, respectively. It was also noted that the improved L-valine production by overproducer CC5 was stable during subsequent subcultures.

29.4 Conclusion

It could be concluded that mutagenesis proved to be an effective technique to improve industrial microbial strains. Various mutagens had been used to obtain mutants with different characteristics. In our study, we selected UV and DES as the mutagens due to their convenient operation and application. An increment of about

189 % in L-valine production was achieved after mutagenesis of *B. flavum* C1. Similar results were also published after mutagenesis of L-valine producing strain by induction with various mutagens. In this respect, our results could be compared with data compiled by Wang X L et al., who improved L-valine production up to 50 % after mutagenesis of *C. pekineise* [16].

Acknowledgments The financial support of the Tianjin science and technology plan project (Science and technology innovation fund for small and medium-sized enterprises NO. 11ZXCXGX16300) is gratefully acknowledged.

References

1. Qu MB, Gong JH, Huang HR (1992) Research of oxygen-supplying and fed-batch control for L-valine fermentation. Chin J Biotechnol 8(2):184–191
2. Ratkov A, Georgiev T, Kristeva J et al (2000) Modelling of L-valine fed-batch fermentation process. The 22nd International Conference on Information Technology Interfaces, 397–402
3. Fusao T, Atsushi Y, Kenichi H et al (1999) Methods for producing L-valine and L-leucine. UP 5888783
4. Hiroshi M, Takayasu T, Shigeru N (1983) Method for producing L-valine by fermentation. UP 4391907
5. Katsurada N, Uchibori H, Tsuchida T (1993) L-valine producing microorganism and a process for producing L-valine by fermentation. EP 0287123
6. Iborra JL, Obon JM, Manjon A et al (1992) Analysis of a laminated enzyme membrane reactor for continuous resolution of amino acids-L-amino acid e.g. L-valine production by immobilized aminoacylase. Biotechnol Appl Biochem 15(1):22–30
7. hachatryan AG, Durgaryan SS, Martirosov SM (1986) Dependence of valine production by Serratia marcescens on the ion composition of the fermentation medium. Prikl Biokhim Mikrobiol 22(4):554–556
8. Mitsubishi-Petrochem et al (1989) Production of L-valine using glucose-containing aqueous solution with biotin auxotrophic Coryneform bacteria, e.g. Corynebacterium, Brevibacterium, etc.-*Brevibacterium flavum* fermentation in glucose culture medium. JP 094373
9. Ma L, Qin YF, Xu QY et al (2010) The effects of dissolved oxygen on L-valine in fermentation. Lett Biotechnol 21(4):509–514
10. Maija R, Longina P, Ilze D (2007) L-valine biosynthesis during batch and fed-batch cultivations of *Corynebacterium glutamicum*: relationship between changes in bacterial growth rate and intracellular metabolism. Process Biochem 42(4):634–640
11. Michel BT, Christian B, Christian W et al (2005) Application of model discriminating experimental design for modeling and development of a fermentative fed-batch L-valine production process. Biotechnol Bioeng 91(3):356–368
12. Bastian B, Mark ES, Tobias B et al (2008) *Corynebacterium glutamicum* tailored for high-yield L-valine production. Appl Microbiol Biotechnol 79(3):471–479
13. Li X. H, Chen N, Zhang KX (2003) Study on chemical colorimetry determination L-valine in fermented broth. Amino Acids Biotic Resour 25(4):55–57(in Chinese)
14. Huang HH, Li FD (1989) Studies on producing L-valine by fermentation. J Microbiol 9(2):1–8
15. Tsuchida T, Yoshinaga F, Kubota K (1975) Production of L-valine by 2-thiazolealanine resistant mutants derived from glutamic acid bacteria. Agric Biol Chem 39:1319–1322
16. Wang XL, Qu MB, Huang HR (1990) Fermentation of L-valine by a mutant. Microbiol China 5:276–279

Chapter 30
Reducing Impurities in Fermentation Broth for γ-Polyglutamic Acid Production by Medium Optimization Using *Bacillus licheniformis* CGMCC 3336

Changsheng Qiao, Lingfeng Lan, Shuai Zhang, Zheng Li and Huaxuan Hao

Abstract In this paper, the fermentation medium was optimized for the production of poly-(γ-glutamic acid) and reducing impurities in the fermentation broth using *Bacillus licheniformis* CGMCC3336. The results indicated that choline chloride, pyridoxine, arginine, glutamine, and methionine could effectively enhance γ-PGA production, individually. Especially, when 0.2 g/L methionine was added, the γ-PGA production was increased by onefold compared to the control. Flask fermentation was carried out using the optimized medium a 12.0 g/L γ-PGA was accumulated in the fermentation broth which was increased by three folds as compared to the control. Using the optimized medium a 30.3 g/L γ-PGA was accumulated in the fermentation broth in a 5 L bioreactor and impurities in the fermentation broth was reduced apparently. The results suggested that, choline chloride, pyridoxine, arginine, glutamine, and combined with methionine had the same effect on γ-PGA production as yeast extract.

Keywords Amino acid · *Bacillus licheniformis* · Impurities · Medium optimization · Poly-(γ-glutamic acid) · Vitamin

C. Qiao (✉) · L. Lan · S. Zhang
College of Biotechnology, Tianjin University of Science and Technology, Tianjin 300457, People's Republic of China
e-mail: qiaochangsheng@tust.edu.cn

Z. Li
School of Textiles, Tianjin Polytechnic University, Tianjin 300387, People's Republic of China

H. Hao
Tianjin Peiyang Biotrans Biotech Co., Ltd, Tianjin 300457, People's Republic of China

T.-C. Zhang et al. (eds.), *Proceedings of the 2012 International Conference on Applied Biotechnology (ICAB 2012)*, Lecture Notes in Electrical Engineering 249,
DOI: 10.1007/978-3-642-37916-1_30, © Springer-Verlag Berlin Heidelberg 2014

30.1 Introduction

γ-polyglutamic acid (γ-PGA) is a naturally occurring homopolyamide that is polymerized of L- and D-glutamic acid units via γ-amide linkages. γ-PGA is a versatile, water-soluble, edible, and biodegradable biopolymer [1], its molecular weight ranges between 100 and 1,000 KD [2]. Because of its unique physiochemical and biological properties, it may found applications in pharmaceutical industry, food processing, cosmetic industry, and agriculture [3].

Medium components have profound effect on the production of γ-PGA, much work has been done on the evaluation of the different kinds and amounts of carbon sources [4], nitrogen sources [5–7], and metal irons [6, 8] on the production of γ-PGA. Glucose, citric acid, and glycerol are found to be the best carbon sources for the accumulation of γ-PGA. Inorganic nitrogen sources such as NH_4Cl and $(NH_4)_2SO_4$, are mostly used in the production of γ-PGA. Metal irons are necessary for the success accumulation of γ-PGA, and also greatly affect the proportions of two isomers of glutamic acid in γ-PGA. The irons required for the production of γ-PGA by *Bacillus subtilis* are: Mn^{2+}, K^+, Fe^{3+}, Mg^{2+}, and Ca^{2+}. Mn^{2+} concentration has been found to regulate the proportion of L and D isomers of glutamic acid in γ-PGA.

For a broad application, the cost of bioproducts is one of the main factors determining the economics of a process. Reducing the costs of biopolymer production by optimizing the fermentation medium is the basic research objective of industrial application [9]. In previous studies of our lab, a semi-synthetic production medium was proposed for the production of γ-PGA using the strain as in this study. The fed-batch experiments carried out in a 200 L bioreactor indicated that for the successful accumulation of 40 g/L γ-PGA, the addition of 20 g/L yeast extract was essential. Although the production of γ-PGA was improved with the addition of yeast extract, however problems arise in the downstream. With the addition of yeast extract, the impurities were brought into the fermentation broth at the same time, and the color of the broth was not satisfied. Great effort in the downstream process was devoted to removing the impurities from the fermentation broth and decoloration [10]. The problems mentioned above were well solved in this study.

The objective of this study is to identify a basic salt medium with the addition of vitamins and amino acids for the effective production of γ-PGA at the same time to reduce impurities in the fermentation broth and lay the foundation for metabolic flux analysis and metabonomics analysis. The Plackett-Burman (PB) experimental design and Box-Behnken (BB) experimental design was applied in the production medium optimization.

30.2 Materials and Methods

30.2.1 Bacterial Strain and Medium

Bacillus licheniformis CGMCC3336 was used in the present study. The medium used for the maintenance contained (g/L): yeast powder 5.0, peptone 10, NaCl 5.0, and agar 20 (pH 7.2 ± 0.1). Bacterial cells in agar slants were incubated at 37 °C for 48 h and stored at 4 °C.

The seed medium contained (g/L): yeast extract 7.0, peptone 10, glucose 30, $K_2HPO_4 \cdot H_2O$ 0.5, $MgSO_4 \cdot 7H_2O$ 0.5, pH 7.2 ± 0.1.

For the production of PGA, a basal salt medium was used, which has the following composition (g/L): glucose 80, glutamic acid 80, NH_4NO_3 18, $MgSO_4 \cdot 7H_2O$ 0.5, $CaCl_2 \cdot 6H_2O$ 1.0, $FeSO_4 \cdot 7H_2O$ 0.01, NaCl 10. Initial pH of the medium was adjusted to 7.2 by using 5 N NaOH and/or 6 N HCl. The medium was sterilized in an autoclave for 20 min at 121 °C.

30.2.2 Inoculum and Fermentation

A loopful of cells from agar slant was transferred to 50 ml of the seed medium in a 500 ml conical flask and incubated at 37 °C and 220 rpm for 16 h. This was used as the inoculum. Fermentation was carried out in 500 ml baffled conical flask, each containing 50 ml of the sterile production medium. The medium was inoculated with 10 % (v/v) of the prepared inoculum. The flasks were incubated for 72 h on a rotary incubator at 37 ± 2.0 °C and 220 rpm. Fermentation was performed in a 5 L bioreactor (Jiangshu, China) with an initial broth volume of 3 L at 37 °C.

30.2.3 Effect of Different Vitamins on γ-Polyglutamic Acid Production

To study the effect of addition of different vitamins on γ-PGA production, nicotinic acid (VB_3), pantothenic acid (VB_5), pyridoxine (VB_6), riboflavin (VB_2), thiamine (VB_1), or choline chloride (VB_4) was added individually in the basal production medium.

30.2.4 Effect of Different Amino Acids on γ-Polyglutamic Acid Production

To study the effect of addition of amino acids on γ-PGA production, Arg, glycine (Gly), histidine (His), isoleucine (Ile), leucine (Leu), lysine (Lys), phenylalanine

(Phe), threonine (Thr), tyrosine (Tyr), valine (Val), Gln, cystine (Cys), Met, or tryptophan (Trp) was added individually in the basal production medium.

30.2.5 Screening of Nutrients Using Plackett-Burman Design

To identify factors that significantly influence γ-PGA production, fourteen variables at two levels were tested using a Plackett-Burman design (N = 20, with 4 controls). Design-Expert (version 8.0.6) was used for the experimental design and analysis of the data obtained.

30.2.6 Optimization of Nutrients Using Box-Behnken Design

To further optimize those critical factors identified via PB design, five independent variables, each at three levels with six replicates at the center points were tested using a BB design. The experimental result was used to fit a polynomial model:

$$\begin{aligned} Y = {} & \beta_0 + \beta_1 X_1 + \beta_2 X_2 + \beta_3 X_3 + \beta_4 X_4 + \beta_5 X_5 + \beta_{11} X_1^2 + \beta_{12} X_1 X_2 + \beta_{13} X_1 X_3 \\ & + \beta_{14} X_1 X_4 + \beta_{15} X_1 X_5 + \beta_{22} X_2^2 + \beta_{23} X_2 X_3 + \beta_{24} X_2 X_4 + \beta_{25} X_2 X_5 + \beta_{33} X_3^2 \\ & + \beta_{34} X_3 X_4 + \beta_{35} X_3 X_5 + \beta_{44} X_4^2 + \beta_{45} X_4 X_5 + \beta_{55} X_5^2 \end{aligned}$$

where Y was the yield of γ-PGA, β_0 was the intercept term, $\beta_{i\ (i=1,\ 2,\ 3,\ 4,\ 5)}$were linear coefficients, $\beta_{ij\ (i \neq j)}$ were interactive coefficients, $\beta_{ij\ (i=j)}$ were quadratic coefficients and $X_{i\ (i=1,\ 2,\ 3,\ 4,\ 5)}$ were coded independent variables. Design-Expert (version 8.0.6) was used for the experimental design and regression analysis of the data obtained.

30.2.7 Quantitative Analysis of γ-Polyglutamic Acid

When fermentation was terminated, an aliquot was withdrawn from the fermentation broth and centrifuged for 10 min at 15,000 rpm. 5 ml of the supernatant was poured into four volumes of ethanol to precipitate the γ-PGA. The precipitant containing crude γ-PGA was redissolved in deionized water at equal volume. Any insoluble contaminants were removed by filtration, the filtrate was reprecipitated and the precipitant was recovered. The final precipitant was redissolved in 25 ml deionized water, and then 5 ml of the solution was withdrawn, and was hydrolyzed using 6 N HCl of equal volume at 110 °C for 12 h. L-glutamic acid was determined enzymatically using a bioanalyzer (SBA-40E Shangdong Academy of Science). The γ-PGA yield was estimated by subtracting the amount of L-glutamic acid in the pre-hydrolysis solution from the amount of L-glutamic acid presented in the hydrolyzed solution.

30.3 Results and Discussion

30.3.1 Effect of Vitamins on γ-PGA Production

As shown in Fig. 30.1, γ-PGA production was enhanced with the addition of VB_4 and VB_6 at 0.1 and 0.001 g/L, respectively. Other vitamins have no or little effect on γ-PGA production. Among the vitamins that have been tested, only VB_4 and VB_6 have positive effect on γ-PGA production. VB_4 is required for synthesis of the phopholipids in cell membranes, methyl group metabolism [11]. In this study, the VB4 added into the medium serve as a methyl donor and facilitates protein synthesis, enhance strain's growth and γ-PGA production. VB_6 serves as the coenzyme of amino acid decarboxylases [12], vitamins was generally regards as growth factors. As a growth factor added into the medium, the γ-PGA production was enhanced.

30.3.2 Effect of Amino Acids on γ-Polyglutamic Acid Production

As shown in Fig. 30.2, γ-PGA yield was significantly increased with the addition of Met, Gln and Arg at 0.2, 0.5, and 0.44 g/L, respectively. Little effect on γ-PGA production has been found for Leu, Thr, His, Ile, Trp, and Gly. However, negative effect has been observed for Lys, Phe, Tyr, and Val on γ-PGA production. For those amino acids have been examined, enhancement of γ-PGA production was

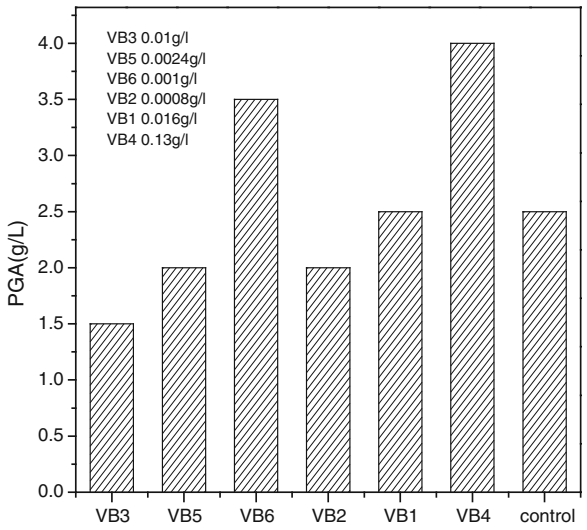

Fig. 30.1 Effect of vitamins on γ-PGA production (Data took from one of the three replications)

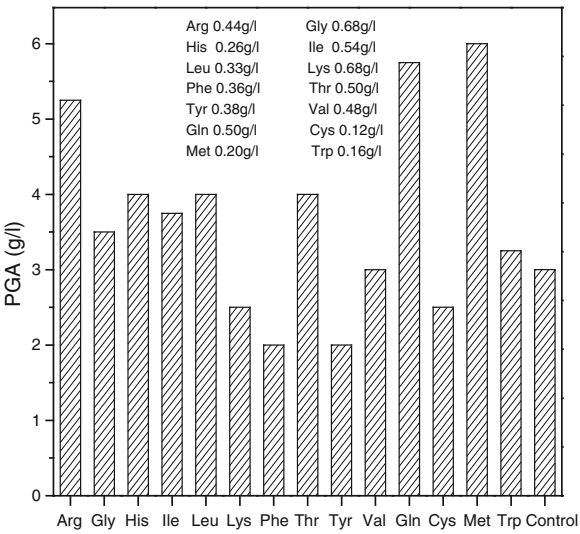

Fig. 30.2 Effect of different amino acids on γ-PGA production (Data took from one of the three replications)

found for Met, Gln, and Arg. Met as an important methyl donor functions the same as VB_4 [13], the growth of producer was accelerated in the presence of Met and VB_4. Previous studies of this strain has been shown that the γ-PGA synthesis was accompanied with cell growth, as cell growth was increased then the amount of γ-PGA accumulated in the broth was increased as well. The result that Gln increase the yield of γ-PGA was in accordance with the result of Kunioka's studies, it is suggested that Gln added to the medium activated enzymes in the pathway of γ-PGA synthesis [14]. This is the first report to enhance γ-PGA production by adding Arg, in the Bajaj's study the addition of Arg has a negative effect on γ-PGA production [15], which may due to the different strains used. As Arg and Gln are members of glutamate family, it is suggested that Arg activated enzymes involved in the pathway of γ-PGA synthesis.

30.3.3 Screening of Significant Nutrients Using Plackett-Burman Design

Fourteen variables at two levels (–1 for low level and +1 for high level) were analyzed for their effect on γ-PGA production using a PB design (Table 30.1). Twenty independent experiments were conducted according to the experimental design shown in Table 30.2, and each experiment was carried out in duplicates. The yield of γ-PGA for each experiment was also shown in Table 30.2. The software Design-Expert (version 8.0.6) was used for analysis of the variance of the experimental design, and calculate the coefficients, F values and significance levels for each variable, the results were shown in Table 30.3. As can be seen from the

Table 30.1 Nutrients for screening using PB design

Variable		Levels	
Code	Nutrient (g/l)	Low (–1)	High (+1)
X_1	Glucose	50	80
X_2	Glutamate	50	80
X_3	NH_4NO_3	18	27
X_4	NaCl	10	15
X_5	$MgSO_4{\cdot}7H_2O$	0.5	1.0
X_6	$CaCl_2{\cdot}6H_2O$	1.0	2.0
X_7	$FeSO_4{\cdot}7H_2O$	0.01	0.02
X_8	Arg	0.44	0.88
X_9	His	0.26	0.52
X_{10}	Leu	0.33	0.66
X_{11}	Thr	0.5	1.0
X_{12}	Met	0.2	0.4
X_{13}	V_{B4}	0.13	0.26
X_{14}	Gln	0.5	1.0
X_{15}	V_{B6}	0.001	0.002

Table 30.3, glutamate, $MgSO_4{\cdot}7H_2O$, Arg, Met, and Gln were the variables that have significant effect on γ-PGA production. For the other insignificant variables, if the calculated coefficient is positive then the higher level will be used in the following experiments, otherwise the lower level will be used. The optimum combinations of the five significant variables were further analyzed by a BB design.

30.3.4 Further Optimization of the Nutrients Using Box-Behnken Design

To arrive at an optimum combination, five nutrients above each at three levels with six replicates at the central point were carried out using a BB design (Table 30.4). Table 30.5 gave the design and results of experiments carried out by the BB design. The results obtained were analyzed by the software Design-Expert (version 8.0.6), the statistical analysis results were shown in Table 30.6, and the regression model was given as

$$\begin{aligned} Y = {} & 11.67 - 0.72X_2 + 0.22X_5 - 0.22X_8 + 0.53X_{12} + 0.12X_{14} - 2.21X_2^2 \\ & + 0.13X_2X_5 - 0.25X_2X_8 - 0.38X_2X_{12} - 0.38X_2X_{14} - 1.21X_5^2 + 0.13X_5X_8 - 0.25X_5X_{12} \\ & - 0.63X_5X_{14} - 1.54X_8^2 - 0.13X_8X_{12} + 0.13X_8X_{14} - 1.21X_{12}^2 + 0.38X_{12}X_{14} - 1.75X_{14}^2 \end{aligned}$$

where Y was the γ-PGA yield, X_i (i = 2,5,8,12,14) was the coded factors. As the F-test value of the model was 3.50 and the p value was 0.0018, so Eq. (2) was a significant model. Among model terms, X_2, X_2^2, X_5^2, X_8^2, X_{12}^2, and X_{14}^2 were

Table 30.2 Experimental design using the PB method for screening of nutrients (Data took from one of the three replications)

Run	X_1	X_2	X_3	X_4	X_5	X_6	X_7	X_8	X_9	X_{10}	X_{11}	X_{12}	X_{13}	X_{14}	X_{15}	PGA (g/L)
1	+1	+1	−1	−1	+1	+1	+1	+1	−1	+1	−1	+1	−1	−1	−1	9.5
2	−1	+1	+1	−1	−1	+1	+1	+1	+1	−1	+1	−1	+1	−1	−1	6.25
3	+1	−1	+1	+1	−1	−1	+1	+1	+1	+1	−1	+1	−1	+1	−1	3.75
4	+1	+1	−1	+1	+1	−1	−1	+1	+1	+1	+1	−1	+1	−1	+1	8.75
5	−1	+1	+1	−1	+1	+1	−1	−1	+1	+1	+1	+1	−1	+1	−1	7.5
6	−1	−1	+1	+1	−1	+1	+1	−1	−1	+1	+1	+1	+1	−1	+1	5.0
7	−1	−1	−1	+1	+1	−1	+1	+1	−1	−1	+1	+1	+1	+1	−1	5.0
8	−1	−1	−1	−1	+1	+1	−1	+1	+1	−1	−1	+1	+1	+1	+1	5.0
9	+1	−1	−1	−1	−1	+1	+1	−1	+1	+1	−1	−1	+1	+1	+1	3.75
10	−1	+1	−1	−1	−1	−1	+1	+1	−1	+1	+1	−1	−1	+1	+1	5.0
11	+1	−1	+1	−1	−1	−1	−1	+1	+1	−1	+1	+1	−1	−1	+1	3.5
12	−1	+1	−1	+1	−1	−1	−1	−1	+1	+1	−1	+1	+1	−1	−1	8.75
13	+1	−1	+1	−1	+1	−1	−1	−1	−1	+1	+1	−1	+1	+1	−1	3.5
14	+1	+1	−1	+1	−1	+1	−1	−1	−1	−1	+1	+1	−1	+1	+1	9.0
15	+1	+1	+1	−1	+1	−1	+1	−1	−1	−1	−1	+1	+1	−1	+1	10.25
16	+1	+1	+1	+1	−1	+1	−1	+1	−1	−1	−1	−1	+1	+1	−1	5.0
17	−1	+1	+1	+1	+1	−1	+1	−1	+1	−1	−1	−1	−1	+1	+1	8.75
18	−1	−1	+1	+1	+1	+1	−1	+1	−1	+1	−1	−1	−1	−1	+1	5.0
19	+1	−1	−1	+1	+1	+1	+1	−1	+1	−1	+1	−1	−1	−1	−1	6.25
20	−1	−1	−1	−1	−1	−1	−1	−1	−1	−1	−1	−1	−1	−1	−1	3.75

Table 30.3 Coefficients, *F* values and significance levels calculated from the PGA yield obtained in the screening experiments

Code	Coefficient	*F* value	Pr > |F|
X_1	0.16	1.37	0.3062
X_2	1.71	152.59	0.0002[a]
X_3	–0.31	5.08	0.0872
X_4	0.36	6.84	0.0591
X_5	0.79	32.27	0.0047[a]
X_6	0.063	0.20	0.6755
X_7	0.19	1.83	0.2476
X_8	–0.49	12.37	0.0245[a]
X_9	0.062	0.20	0.6755
X_{10}	–0.11	0.66	0.4626
X_{11}	–0.19	1.83	0.2476
X_{12}	0.56	16.46	0.0154[a]
X_{13}	–0.038	0.073	0.8002
X_{14}	–0.54	15.03	0.0179[a]
X_{15}	0.24	2.93	0.1618

[a] Statistically significant at 95 % of probability level

Table 30.4 Composition (g/L) of nutrients added to the substrate

Nutrient	–1	0	+1
X_2	87.5	91.25	95.0
X_5	1.125	1.1875	1.25
X_8	0.22	0.275	0.33
X_{12}	0.45	0.475	0.50
X_{14}	0.25	0.3125	0.375

significant with a probability of 95 % (Table 30.6). As shown in Table 30.6, interaction between the five nutrients had no significant influence on γ-PGA yield. The predicted maximum γ-PGA yield (11.818 g/L) derived from RSM regression was obtained when the initial concentration of glutamate, $MgSO_4 \cdot 7H_2O$, Arg, Met and Gln was 90.55, 1.1895, 0.272, 0.482, and 0.3172 g/L, respectively. The γ-PGA yield (12.0 g/L) in the optimum medium from three replications (i.e., 11.75, 12, and 12.25) was coincident with the predicted value, and the model was proven to be adequate. The final medium optimized with RSM was (g/L): glucose 80, glutamate 90.55, NH_4NO_3 18, NaCl 15, $MgSO_4 \cdot 7H_2O$ 1.1894, $CaCl_2 \cdot 6H_2O$ 2.0, $FeSO_4 \cdot 7H_2O$ 0.02, Arg 0.272, His 0.52, Leu 0.33, Thr 0.5, Met 0.481, VB_4 0.13, Gln 0.3173, and VB_6 0.002.

30.3.5 Production of γ-PGA in a 5 L Bioreactor

The production of γ-PGA was carried out in a 5 L bioreactor, containing 3 L of the initial optimized medium. As shown in Fig. 30.3, a 30.3 g/L γ-PGA was produced after 72 h of fermentation, and the γ-PGA production was corresponded to cell

Table 30.5 Experimental design using the BB design for optimization of nutrients (Data took from one of the three replications)

Run	Nutrients					PGA (g/l)
	X_2	X_5	X_8	X_{12}	X_{14}	
1	–1	–1	0	0	0	9.0
2	+1	–1	0	0	0	7.5
3	–1	+1	0	0	0	8.0
4	+1	+1	0	0	0	7.0
5	0	0	–1	–1	0	8.0
6	0	0	+1	–1	0	8.0
7	0	0	–1	+1	0	9.0
8	0	0	+1	+1	0	8.5
9	0	–1	0	0	–1	7.5
10	0	+1	0	0	–1	9.0
11	0	–1	0	0	+1	10.0
12	0	+1	0	0	+1	9.0
13	–1	0	–1	0	0	9.5
14	+1	0	–1	0	0	6.5
15	–1	0	+1	0	0	10.0
16	+1	0	+1	0	0	6.0
17	0	0	0	–1	–1	8.0
18	0	0	0	+1	–1	9.0
19	0	0	0	–1	+1	7.5
20	0	0	0	+1	+1	10.0
21	0	–1	–1	0	0	9.5
22	0	+1	–1	0	0	9.0
23	0	–1	+1	0	0	9.0
24	0	+1	+1	0	0	9.0
25	–1	0	0	–1	0	8.0
26	+1	0	0	–1	0	7.5
27	–1	0	0	+1	0	11.0
28	+1	0	0	+1	0	9.0
29	0	0	–1	0	–1	9.5
30	0	0	+1	0	–1	8.0
31	0	0	–1	0	+1	9.0
32	0	0	+1	0	+1	8.0
33	–1	0	0	0	–1	7.0
34	+1	0	0	0	–1	8.0
35	–1	0	0	0	+1	7.5
36	+1	0	0	0	+1	7.0
37	0	–1	0	–1	0	8.0
38	0	+1	0	–1	0	11.0
39	0	–1	0	+1	0	8.0
40	0	+1	0	+1	0	10.0
41	0	0	0	0	0	11.0
42	0	0	0	0	0	12.5
43	0	0	0	0	0	11.0
44	0	0	0	0	0	13.0
45	0	0	0	0	0	11.0
46	0	0	0	0	0	11.5

Table 30.6 Analysis of variance for the experiment results of the BB design

Factor	Coefficient	Sum of square	*F* value	Pr > |*F*|
X_2	–0.72	8.27	7.29	0.0123[a]
X_2^2	–2.21	42.56	37.53	0.0001[a]
X_5	0.22	0.77	0.68	0.4191
X_5^2	–1.21	12.74	11.24	0.0026[a]
X_8	–0.22	0.077	0.68	0.4191
X_8^2	–1.54	20.74	18.29	0.0002[a]
X_{12}	0.53	4.52	3.98	0.0570
X_{12}^2	–1.21	12.74	11.24	0.0026[a]
X_{14}	0.12	0.25	0.22	0.6428
X_{14}^2	–1.75	26.73	23.57	0.0001[a]
X_2X_5	0.13	0.063	0.055	0.8163
X_2X_8	–0.25	0.25	0.22	0.6428
X_2X_{12}	–0.38	0.56	0.50	0.4876
X_2X_{14}	–0.38	0.56	0.50	0.4876
X_5X_8	0.13	0.062	0.055	0.8163
X_5X_{12}	–0.25	0.25	0.22	0.6428
X_5X_{14}	–0.63	1.56	1.38	0.2516
X_8X_{12}	–0.13	0.063	0.055	0.8163
X_8X_{14}	0.13	0.063	0.055	0.8163
$X_{12}X_{14}$	0.38	0.56	0.50	0.4878
Model	11.67	79.30	3.50	0.0018[a]
Error		3.83		

[a] Statistically significant at 95 % of probability level

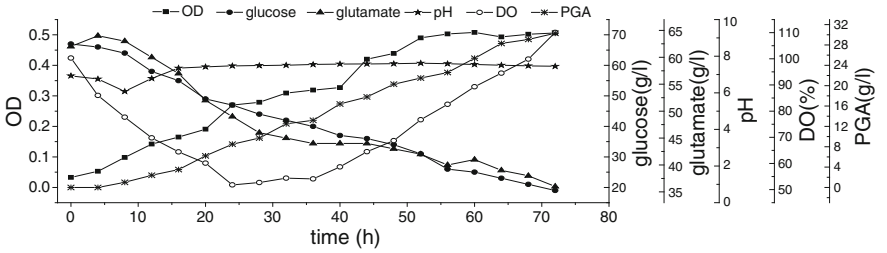

Fig. 30.3 The profiles of γ-PGA production in a 5 L bioreactor (Data took from one of the three replications)

growth. Glucose and glutamic acid was constantly consumed throughout the process. In the first 8 h, pH decreased from 7.0 to 6.08, and increased to 7.52 at 24 h, then slowly decreased to 7.28 at the end of the fermentation.

Our lab's previous studies shown that the addition of yeast extract was beneficial for cell growth and PGA production, however the impurities brought in the fermentation broth was less than satisfactory. In this study, the fermentation medium was optimized using response surface methodology, and the final medium

was consisted of chemically defined compounds. Using this medium the impurities in the fermentation broth was reduced apparently. It is suggested that VB_4, VB_6, Met, Gln together with Arg have the same effect on γ-PGA synthesis as yeast extract, in this way yeast extract can be replaced. Much effort in downstream can be reduced, the economics of the process becomes more promising.

30.4 Conclusions

In this study, in order to reduce impurities in fermentation broth and hence to facilitate the downstream process of γ-PGA production, a synthetic fermentation medium was identified by response surface methodology. The γ-PGA production was significantly increased with the addition of VB_4, VB_6, Met, Gln and Arg. A three folds increase of γ-PGA production as compared to the control was observed in the flask fermentation using the optimized medium, and impurities in the fermentation broth was reduced significantly. It is suggested that yeast extract could be totally replaced by VB_4, VB_6, Met, and Gln combined with Arg. The reason that those vitamins and amino acids could enhance γ-PGA production was not quite clear. Therefore, further studies should be carried out in the future.

References

1. Shih IL, Van YT (2001) The production of poly-(γ-glutamic acid) from microorganisms and its various applications. Bioresour Technol 79:207–225
2. Kubota H, Nambu Y (1996) Alkaline hydrolysis of poly(γ-glutamic acid) produced by microorganism. J Polymer Sci A Polym Chem 34:1347–1351
3. Margaritis A, Buescher MJ (2007) Microbial biosynthesis of polyglutamic acid biopolymer and applications in the biopharmaceutical, biomedical and food industries. Criti Rev Biotechnol 27:1–19
4. Ko YH, Gross RA (1998) Effects of glucose and glycerol on γ-poly(glutamic acid) formation by *Bacillus licheniformis* ATCC 9945a. Biotechnol Bioeng 57:430–437
5. Goto A, Kunioka M (1992) Biosynthesis and hydrolysis of poly(γ-glutamic acid) from *Bacillus subtilis* IFO3335. Biosci Biotechnol Biochem 56:1031–1035
6. Leonard CG, Housewright RD, Thorn CB (1958) Effects of some metallic ions on glutamyl polypeptide synthesis by *Bacillus subtilis*. J Bacterial 76:499–503
7. Troy FA (1973) Chemistry and biosynthesis of poly(γ-d-glutamyl) capsule in *Bacillus licheniformis*. I. properties of the membrane mediated biosynthetic reaction. J Biol Chem 248:305–315
8. Cromwick AM, Gross RA (1994) Effects of manganes (II) on *Bacillus licheniformis* ATCC9945A physiology and gama-poly(glutamic acid) formation. Int J Biol Macromol 17(5):259–267
9. Nadia A, Soliman Mahmoud M et al (2005) Polyglutamic acid (PGA) production by *Bacillus* sp. SAB-26: application of Plackett-Burman experimental design to evaluate culture requirements. Appl Micorbio Biotechnol 69:259–267

10. Ho GH, Ho TI, Hsieh KH et al (2006) γ-polyglutamic acid produced by bacillus subtilis (natto): structural characteristics, chemical properties and biological functionalities. J Chin Chem Soc 53(6):1363–1384
11. Zeisel SH, Blusztajn JK (1994) Choline and human nutrition. Annu Rev Nutr 14:269–296
12. Gunsalus IC, Bellamy WD, Umbreit WW (1945) The function of pyridoxine: conversion of members of the vitamin B_6 group into codecarboxylase. J Biol Chem 160:461–472
13. Park EI, Garrow TA (1999) Interaction between dietary methionine and methyl donor intake on rat liver betaine-homocysteine methyltransferase gene expression and organization of the human gene. J Biol Chem 274:7816–7824
14. Kunioka M (1995) Biosynthesis of poly (γ-glutamic acid) from L-glutamine, citric acid and ammonium sulfate in *Bacilus subtilis* IFO3335. Appl Microb Biotechnol 44:501–506
15. Bajaj IB, Singhal RS (2009) Enhanced production of poly (γ-glutamic acid) from *Bacillus licheniformis* NCIM 2324 by using metabolic precursors. Appl Biochem Biotechnol 159:133–141

Chapter 31
Scale-up of 5-keto-Gluconic Acid Production by *Gluconobacter oxydans* HGI-1

Yanyan Li, Shiru Jia, Cheng Zhong, Hongcui Wang, Ainan Guo and Xintong Zheng

Abstract *Gluconobacter oxydans* is known to oxidize glucose to gluconic acid (GA), and subsequently, to 2-keto-gluconic acid (2KGA) and 5-keto-gluconic acid (5KGA). 5KGA can be converted to L-(+)-tartaric acid which is important in industry. In order to increase the production of 5KGA, *G. oxydans* HGI-1 which converts GA only to 5KGA was chosen in this study. The fermentation process occurred in shake flask was studied in different inoculation, and 10 % inoculation amount was chosen. Furthermore, it was scaled-up to a 5-L stirred-tank fermenter, limitation of oxygen could not happen and pH could be adjusted by automated titration of 6 M KOH. 5KGA was accumulated up to 106.33 g/L in fermentation broth, while the strain was fed-batch cultured, the concentration of 5KGA was up to 179.4 g/L and the conversion rate of glucose was 89.0 %. *G. oxydans* HGI-1 was suitable for industrial production.

Keywords *Gluconobacter* · 5-ketogluconic acid · Scale-up · Fed-batch culture

31.1 Introduction

Gluconobacter oxydans, Gram-negative bacillus, belongs to the family of acetic acid bacteria. It is characterized by the ability of oxidizing a large number of organic compounds to corresponding acids and ketones [1] which can be found largely in the habitats. The natural habitats of this organism are flowers and fruits [2]. The organisms of *Gluconobacter* have been extensively used for industrial productions, such as the production of 6-amino-L-sorbose (precursor of the drug

Y. Li · S. Jia (✉) · C. Zhong · H. Wang · A. Guo · X. Zheng
Key Laboratory of Industrial Fermentation Microbiology, Ministry of Education, College of Biotechnology, Tianjin University of Science and Technology, Tianjin 300457, People's Republic of China
e-mail: jiashiru@tust.edu.cn

T.-C. Zhang et al. (eds.), *Proceedings of the 2012 International Conference on Applied Biotechnology (ICAB 2012)*, Lecture Notes in Electrical Engineering 249,
DOI: 10.1007/978-3-642-37916-1_31, © Springer-Verlag Berlin Heidelberg 2014

miglitol) and L-(−)-sorbose (synthesis of vitamin C) [3–6]. Other important products formed by *G. oxydans* are gluconic acid (GA), 2-keto-D-gluconic acid (2KGA), and 5-keto-D-gluconic acid (5KGA). 5KGA can be converted effectively to L-(+)-tartaric acid [7] which can be antioxidant and acidulant in the food industry, acidic reducing agent in the textile industry [8].

G. oxydans strains oxidize glucose in two separated enzyme systems [9]. Besides the membrane-bound enzymes, *G. oxydans* contains soluble glucose-oxidizing enzymes in the cytosol [10]. The former enzymes consist of a PQQ-dependent glucose dehydrogenase (GDH) oxidizing glucose to gluconic acid, a flavin-dependent gluconate-2-dehydrogenase (GA2DH) which catalyze gluconic acid to 2KGA [11], and a PQQ-dependent gluconate-5-dehydrogenase (GA5DH) catalyzing gluconic acid to 5KGA [12]. The later system is made up of the $NADP^+$-dependent enzymes glucose dehydrogenase and gluconate; NADP 5-oxidroreductase [13]. The later one played an important role in the production of 5KGA.

The optimum temperature and pH for *G. oxydans* were 25–30 °C and 5.5–6.0 [14], and amino acid is not necessary for the growth of the strain [15].

Recently, Herrmann et al. reported that the $NADP^+$-dependent GA-5-DH was overexpressed in a genetically engineered strain *G. oxydans* ATCC 621H, and the yield of 5KGA could be increased by resting cells of the strain [16] The yield was increased by 20 % in comparison with the yield obtained from the wild type. However, the formation of byproduct 2KGA prevented the higher yield of 5KGA. In this paper, some conditions of fermentation by *G. oxydans* HGI-1 which is a genetically modified strain and can oxidize glucose only to 5KGA finally without 2KGA were discussed.

31.2 Material and Method

31.2.1 Bacterial Strain and Media

G. oxydans HGI-1 was grown at 28 °C in seed culture consisting of 25 g mannitol, 5 g yeast extract, and 3 g peptone per liter [17] and it was maintained on the mannitol agar medium at 4 °C.

31.2.2 Shake Flask Culture

Conversion of glucose by *G. oxydans* was performed in shaking flasks with a shaking speed of 180 rpm at 30 °C. The production media contained 100 g glucose, 3.0 g corn starch, 1.67 of yeast extract, 1.5 g NH_4Cl, 0.1 g KH_2PO_4, 0.29 g $MgSO_4{\cdot}7H_2O$, 0.034 g $MnSO_4{\cdot}H_2O$, and 40 g $CaCO_3$ per liter. For the better growth of strain, the working volume was only 50 mL.

31.2.3 Fermenter Culture

Fermentations were carried out in a 5-L stirred-tank fermenter (Bailun, Bio-Technology Co., Ltd. Shanghai, China) with a working volume of 2.5 L. The media used contained 100 g glucose, 3.0 g corn starch, 1.67 g yeast extract, 1.5 g NH_4Cl, 0.1 g KH_2PO_4, 0.29 g $MgSO_4{\cdot}7H_2O$, 0.034 g $MnSO_4{\cdot}H_2O$, 0.34 g $CaCO_3$, and 0.3 ml antifoam per liter. The process performed at 30 °C with agitation speed of 750 rpm, and aeration rate of 1 vvm. During the process, 6 M KOH was used for pH regulation, and it was kept at 5.50 for the growth of cells [2]. In further experiment, fed-batch culture was performed. 300 mL of the feeding medium containing 200 g glucose was added to the vessel when the concentration of the glucose turned to 10 g/L. Glucose feeding was operated continuously in 2 h for one time.

31.2.4 Analytical Methods

The amount of biomass was measured by the optical density at 600 nm. $CaCO_3$ was used for neutralizing the acid produced by oxidation of glucose in flasks experiments, and its insolubility prevented the analysis of biotransformation. So, the addition of HCl is necessary in the measurement in order to dissolve the insoluble composition. Meanwhile, the measurement of substrate and product concentration was carried out in supernatant which was obtained after centrifugation at 8000 g for 10 min. Glucose was quantified by Biosensor (Biology Institute of Shandong, China) and 5KGA was determined by High Performance Liquid Chromatography (HPLC). A reversed-phase C18 HPLC-column (Thermo BDS HYPERSIL) was used for the separation of substances and 10 mM $HClO_4$ was used as the eluent (flow rate of 0.5 ml/min). The column temperature during chromatography was maintained at 25 °C and the product was detected by UV absorbance at 210 nm, and the peak of 5KGA appeared at 6.7 min.

31.3 Results and Discussion

31.3.1 Seed Culture

The morphology and physiological properties of microorganism cells are similar and steady in their exponential phase of growth, and they are suitable for the seed of fermentation [18]. *G. oxydans* HGI-1 on the mannitol agar medium was inoculated into the seed culture, and the flasks were placed at 28 °C with a shaking speed of 180 rpm. After culturing 20 h, the optical density at 600 nm reached 6.5 (Fig. 31.1). And then the seed culture for the fermentation was well prepared.

31.3.2 Inoculation Selection in Shaken Culture

In this experiment, 500-mL shake flasks were prepared with 50 mL culture in every flask. Different inoculation amounts (2, 5, and 10 % (v/v)) were inoculated into the fermentation.

The tendencies were similar to each other, however, the values were tremendous different. As it is shown in Fig. 31.2, glucose was used up after 24 h of incubation on condition that the inoculation was 10 %, while the concentration of glucose reduced to 0 when 2 % seed culture was inoculated. OD_{600nm} reached 3.30 and 1.06 when the inoculation was 10 and 2 %, respectively. In the fermentation process, pH dropped as glucose oxidating to acid, but $CaCO_3$ retarded the tendency.

The concentrations of 5KGA in the supernatant showed a marked difference (Fig. 31.3). When the inoculation was 10 %, 5KGA concentration reached 100 g/L which was the max value of three results. This conclusion was analogous to the data obtained by Marcel Merfort et al. [19]. When a small quantity of the cells were used for inoculation, high amounts of intermediate product gluconic acid were

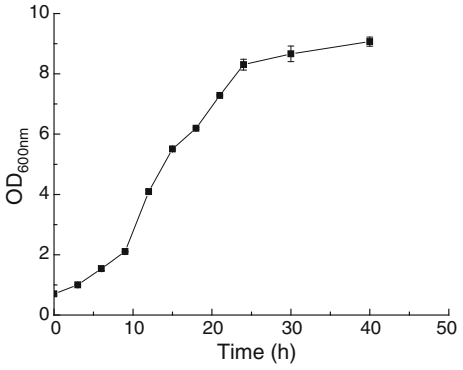

Fig. 31.1 The growth curve of *G. oxydans* HGI-1

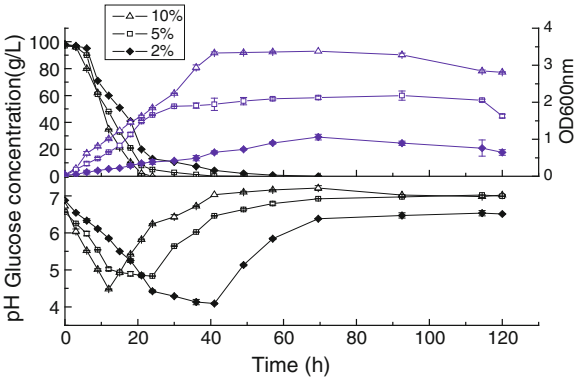

Fig. 31.2 Time-course of the biotransformation of glucose by *G. oxydans* HGI-1 in shake flasks at a shaking-speed of 180 rpm when the inoculation amounts were different. The inoculation amounts were 10 % (△), 5 % (□), 2 % (◆), and the *purple line* represented the optical density of cells at 600 nm

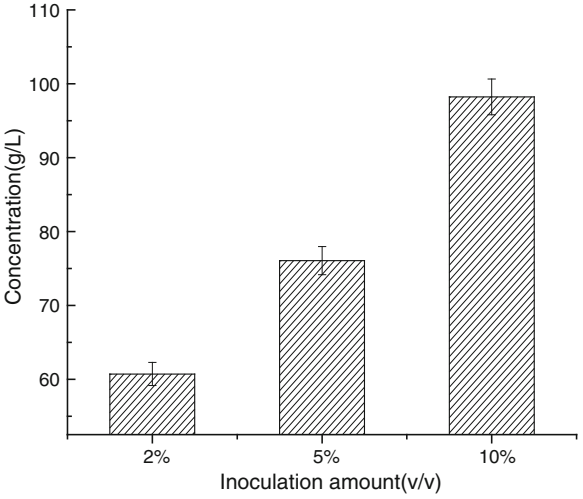

Fig. 31.3 Concentrations of 5KGA produced by *G. oxydans* HGI-1 at different inoculation amounts. The experiments were performed in the shake flasks at a speed of 180 rpm

accumulated, whereas larger inoculation amount allowed the fast conversion of gluconic acid to 5KGA, higher 5KGA concentration was present at the end of the cultivation.

31.3.3 Scale-up from Shake Flask into a Stirred-Tank Fermenter

Oxygen limitation appeared in the flasks culture, while sufficient oxygen was supplied in the fermenter by controlling the aeration rate. So the growth of cells and oxidation of glucose could be not limited by guaranteeing aeration rate of 1 vvm and stirred speed of 750 rpm. The results of the fermentation were shown in Fig. 31.4, and the conversion of glucose to acid made it necessary to add KOH tardily so that pH could be kept at 5.50 when glucose was not absent. And then it

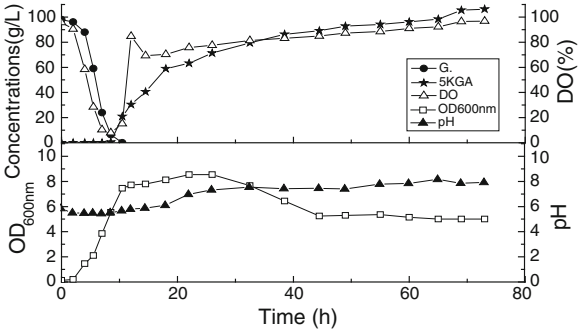

Fig. 31.4 Time-course of the biotransformation of glucose by *G. oxydans* HGI-1 in 5-L batch culture at an aeration rate of 1 vvm and a stirred speed of 750 rpm. pH was controlled by automated titration of 6 M KOH

rised as glucose which was completely used up by *G. oxydans* HGI-1 after 10.5 h of fermentation and alkaline potassium salt came into being. Kazunobu Matsushita et. al reported that 5KGA was catalyzed by a PQQ-dependent dehydrogenase and the enzyme was stable at alkaline pH around 8.0 [20].

The cells grew fast before glucose exhausted, and then the ascending trend came gentle. Optical density of cells at 600 nm reached up to 8.56 as the maximum and decreased later. Accumulation of 5KGA, the most important parameter, was 106.33 g/L after the fermentation, and the conversion rate of glucose was 85.08 %.

31.3.4 Fed-Batch Culture in a Stirred-Tank Fermenter

The fed-batch culture was also performed in a 5-L stirred-tank fermenter. 300 mL medium of 200 g glucose was added into the fermenter when the glucose turned to 10 g/L, and the results were shown in Fig. 31.5 Time-course of the biotransformation of glucose by *G. oxydans* HGI-1 in 5-L fed-batch culture at an aeration rate of 1 vvm and a stirred speed of 750 rpm. pH was controlled by automated titration of 6 M KOH.

The trends of pH and optical density at 600 nm were similar to that in Fig. 31.4. However, the specific values in two experiments were different, optical density at 600 nm was up to 15.2 which was twice that reached in former experiment. The increase of carbon source accounted for the improvement of optical density. After glucose exhausted, the pH was up to around 8.0 just as what mentioned above. Finally, the accumulation of 5KGA was up to 179.4 g/L and the glucose conversion rate was 89.0 %. Mustafa Elfari et al. reported that the concentration of 5KGA corresponds to 84 % of the glucose supplied [10]. So the conversion has reached a high point.

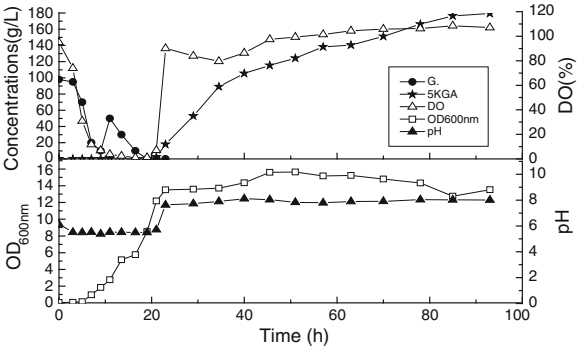

Fig. 31.5 Time-course of the biotransformation of glucose by *G. oxydans* HGI-1 in 5-L fed-batch culture at an aeration rate of 1 vvm and a stirred speed of 750 rpm. pH was controlled by automated titration of 6 M KOH

31.4 Conclusion

G. oxydans HGI-1 was suitable for producing 5KGA in an industrial process. When 10 % (v/v) seed culture was inoculated, the biotransformation was more effective than other cases. The yield of 5KGA was 106.33 g/L when *G. oxydans* HGI-1 was cultured in stirred-batch fermenter, and more yields (179.4 g/L) of 5KGA were obtained when it was fed-batch cultured. As a result, *G. oxydans* HGI-1 was suitable for the industrial production of 5KGA.

References

1. Asai T (1968) Acetic acid bacteria-classification and biochemical activities. University of Tokyo Press, Tokyo
2. Gupta A, Singh VK, Qazi GN et al (2001) *Gluconobacter oxydans*: its biotechnological applications. J Mol Microbiol Biotechnol 3:445–456
3. Deppenmeier U, Hoffmeister M, Prust C (2002) Biochemistry and biotechnological applications of *Gluconobacter* strains. Appl Microbiol Biotechnol 60:233–242
4. Macauley S, McNeil B, Harvey LM (2001) The genus *Gluconobacter* and its applications in biotechnology. Crit Rev Biotechnol 21:1–25
5. Herrmann U, Sahm H (2006) Application of *Gluconobacter oxydans* for biotechnologically relevant reactions. Appl Microbiol Biotechnol 73:443–451
6. Schedel M (2000) Regioselective oxidation of aminosorbitol with *Gluconobacter oxydans*, key reaction in the industrial 1-deoxynojirimycin synthesis. Biotechnol Biotransform 8:296–308
7. Matzerath I, Kläui W, Klasen R et al (1995) Vanadate catalysed oxidation of 5-keto-D-gluconic acid to tartaric acid: the unexpected effect of phosphate and carbonate on rate and selectivity. Inorg Chim Acta 237:203–205
8. Bestmann HJ, Philipp UC (1991) Enzymatische Synthese chiraler C4-Bausteine aus *meso*-Weinsäure. Angew Chem 103:78–79
9. Matsushita K, Toyama H, Adachi O (1994) Respiratory chains and bioenergetics of acetic acid bacteria. Adv Microb Physiol 36:247–301
10. Elfari M, Ha SW, Bremus C et al (2005) A *Gluconobacter oxydans* mutant converting glucose almost quantitatively to 5-keto-D-gluconic acid. Appl Microbiol Biotechnol 66:668–674
11. Shinagawa E, Matsushita K, Adachi O et al (1981) Isolation and purification of 2-ketogluconate dehydrogenase from *Gluconobacter melanogenum*. Agric Biol Chem 45:1079–1085
12. Sugisawa T, Hoshino T (2002) Purification and properties of membrane-bound D-sorbitol dehydrogenase from *Gluconobacter suboxydans* IFO 3255. Biosci Biotechnol Biochem 66:57–64
13. Klasen R, Bringer-Meyer S, Sahm H (1995) Biochemical characterization and sequence analysis of the gluconate:NADP 5-oxidoreductase gene from *Gluconobacter oxydans*. J Bacteriol 177:2637–2643
14. Macauley S, McNeil B, Harey LM (2001) The genus *Gluconobacter* and its applications in biotechnology. J. Mol. Microbiol 21:1–25
15. Gosselé F, Mooter MV, Verdonck L (1981) The nitrogen requirements of *Gluconobacter,* Acetobacter and Frateuria. Antonie Van Leeuwenhoek 47:289–296

16. Herrmann U, Merfort M, Jeude M (2004) Biotransformation of glucose to 5-keto-D-gluconic acid by recombinant *Gluconobacter oxydans* DSM 2343. Appl Microbiol Biotechnol 64:86–90
17. Silberbach M, Maier B, Zimmermann M (2007) Glucose oxidation by Gluconobacter oxydans: characterization in shaking-flasks, scale-up and optimization of the pH profile. Appl Microbiol Biotechnol 62:92–98
18. Lu FP (2007) Microbiology. China Light Industry Press: 162, Beijing
19. Merfort M, Herrmann U, Bringer-Meyer S et al (2006) High-yield 5-keto-D-gluconic acid formation is mediated by soluble and membrane-bound gluconate-5-dehydrogenases of *Gluconobacter oxydans*. Appl Microbiol Biotechnol 73:443–451
20. Matsushita K, Fujii Y, Ano Y (2003) 5-Keto-D-Gluconate production is catalyzed by a quinoprotein glycerol dehydrogenase, major polyol dehydrogenase, in *Gluconobacter* Species. Appl Environ Microbiol 69:1959–1966

Chapter 32
A New strategy for Quantitative Analysis of Ergothioneine in Fermentation Broth by RP-HPLC

Tao Zhou, Qi Liu, Wenxia Jiang and Ning Chen

Abstract An efficient and sensitive method was established for quantitative analysis of L-Ergothioneine during fermentation analyze by reversed-phase-high performance liquid chromatography (RP-HPLC). The method was carried out on two C18 columns (4.6 × 250 mm, 5 μm), and the isocratic mobile phase was 1 % methanol containing boric acid adjusted to a pH of 5.0 with a flow rate of 0.7 mL/min. An UV–VIS detector equipped with a wavelength of 257 nm was employed. The injection volume was 5 μL, with the columns temperature being 25 °C. The linearity, recovery, limit of detection (LOD) and quantification (LOQ), precision, repeatability, stability, and recovery were all tested and good results were obtained. The method was simple, rapid, accurate, and high sensitivity and could be utilized for the research and development of L-Ergothioneine in industry.

Keywords RP-HPLC · L-Ergothioneine · Fermentation broth

32.1 Introduction

L-Ergothioneine (2-Thiol-L-histidine-betaine, EGT) is a naturally occurring chiral amino acid biosynthesized in some bacteria and fungi but not in higher plants and animals [1]. A great number of rationales have been proposed to explain the universal presence of EGT and its accumulation and function in tissues, including

T. Zhou · N. Chen
College of Biotechnology, Tianjin University of Science and Technology, Tianjin 300222, China

T. Zhou · Q. Liu · W. Jiang (✉)
Tianjin Key Laboratory for Industrial Biological Systems and Bioprocessing Engineering, Key Laboratory of Systems Microbial Biotechnology, Tianjin Institute of Industrial Biotechnology, Chinese Academy of Sciences, Tianjin 300308, China
e-mail: jiang_wx@tib.cas.cn

T.-C. Zhang et al. (eds.), *Proceedings of the 2012 International Conference on Applied Biotechnology (ICAB 2012)*, Lecture Notes in Electrical Engineering 249,
DOI: 10.1007/978-3-642-37916-1_32, © Springer-Verlag Berlin Heidelberg 2014

a role for EGT as a factor in bioenergetics [2], immune regulator [3, 4], regulator of gene expression [5], divalent metal chelator [6–8], and ultraviolet ray filter [9], while its most important function is as an physiologic antioxidant and physiologic cytoprotectant [10–16].

EGT was first isolated from ergot fungus that devastated rye grain [17]. In aqueous solution, EGT exists as a thione-thiol tautomer, with the thione form predominating at physiological pH [18]. Therefore, EGT can instead other antioxidants (such as glutathione) and antiseptics due to its nontoxic and stability and would be applied to organ transplantation technology, cell preservation technology, pharmaceuticals industry, food software industry, functional food industry, animal feeding stuffs industry, cosmetic industry, biotechnology, and so on.

There were several methods for assaying EGT including chemical assay, spectrophotometry [19], and HPLC [20]. Currently, methods that utilize spectrophotometric analysis to detect ERG suffer from several serious drawbacks, for example, the sensitivity of the method was too low to be applied to microdetermination, certain compounds containing sulfhydryl group would interfere the detection. HPLC is a general method for assaying EGT at present. However, the process and products of the fermentation are extremely complex, it is hard to control and separate EGT and impurities using current HPLC assaying conditions.

This study reports a rapid, simple, sensitive, and accurate HPLC analysis of EGT during the process of fermentation, which is fit to qualitative, quantitative analysis and process control the production of EGT by fermentation, especially applied to in large-scale production.

32.2 Materials and Methods

32.2.1 Instruments and Reagents

Agilent 1260 series HPLC system equipped with a binary pump, online degasser, auto plate-sample, column oven, and ultraviolet detector (UV) was used in this experiment; MS was performed on an Agilent 6120 instrument (Agilent, MA); NMR experiments were performed on a Bruker AVIII600 MHz (Bruker BioSpin); magnetic stirring apparatus (WH240 plus, Wiggens); electronic analytical balance (AB204-S, METTLER TOLEDO).

L-(+)-Ergothioneine was purchased from Biomol International Inc. (purity $\geq$98 %); methanol and acetonitrile of HPLC grade was purchased from MERCK; all other chemicals were of analytical grade.

32.2.2 Pretreatment of the Samples

The mycelial fermentation broth was extracted at 90 °C and 500 rpm for 30 min on the magnetic stirring apparatus. Following filtration, the supernatant was collected and then centrifugal ultrafiltrated (12840 × g for 10 min at 4 °C) with 3 kDa of the retention molecular weight of the ultrafiltration membrane, the penetrant was the EGT sample.

32.2.3 Preparation of Standard Solution

10 mg of Authentic EGT was accurately weighted on the electronic analytical balance, transferred to volumetric flasks, and dissolved in purified water to assure the stock solution of 400 mg/L. Then the stock solution was diluted to five concentrations in the ranges of 40, 80, 120, 160, and 200 mg/L for calibration curve. All the solutions were filtrated by filter membrane of 0.22 μm as the final EGT standards.

32.2.4 Quantification of EGT by RP-HPLC

The analysis was carried out on two reversed-phase C18 columns (Eclipse XDB-C18) with each column being 4.6 × 250 mm, 5 μm particle size connected in tandem. Different HPLC parameters including mobile phase, column temperature, flow rate, and wavelength were examined and compared. Finally, the isocratic mobile phase was 1 % methanol containing boric acid adjusted to a pH of 5.0 with a flow rate of 0.7 mL/min. The injection volume was 5 μL, with the columns temperature being 25 °C. An UV–VIS detector equipped with a wavelength of 257 nm and comparing the peak area of the sample to peak areas obtained from different concentrations of the authentic standards as above.

32.2.5 Mass Spectroscopy Analysis

Regarding the conditions of MS, the nitrogen gas flow was 3 L/min, capillary temperature was regulated to 220 °C, spray voltage was set to 4.5 kV and capillary voltage was set at 10 v, analytical mode was electrogen ionization (ESI)—positive—scan, with the scan range of m/z being 50–450. For selected ion monitoring, m/z 230 was set for EGT.

32.2.6 Nuclear Magnetic Resonance Analysis

With regard to the conditions for NMR, the spectrometer frequency (SF) was set at 600.13, cumulative frequency (CF) was set to 64, with receiver gain (RG) being adjusted to 1440.

32.2.7 Validation of the Quantitative Analysis

Linearity, limits of detection and quantification, precision, repeatability, stability, and recovery were determined to validate the quantitative method.

32.3 Results and Discussion

32.3.1 Chromatographic Conditions

32.3.1.1 Selection of the Detection Wavelength

The DAD spectra were recorded between 190 and 380 nm. In the quantitative analysis, the wavelength was set at 257 nm to exhibit the vast majority of chromatography peaks and at 208 nm also exhibit a chromatography peak, but there were more impurity peaks at 208 nm, therefore, the wavelength was set at 257 nm.

32.3.1.2 Selection of the Mobile Phase

Different isocratic mobile phase compositions including methanol—water or acetonitrile—water containing different acids or salts such as sodium acetate buffer, acetic acid, boric acid, citric acid, formic acid, pyruvic acid, butyric acid, ethane diacid adjusted to a pH of 4.0–6.5. As a result, the separating effect was almost the same with the mobile phase system consisting of methanol or acetonitrile, considering acetonitrile is toxic and high cost, so the optimal mobile phase was 1 % methanol solution, and using boric acid adjusted to a pH of 5.0, it could be separated effectively between EGT and impurities and presented fairly shape of peak on this condition.

32.3.1.3 Influence of Flow Rate and Columns Temperature

Adjusted the flow rate from 0.3 to 1.3 mL/min, it affected separating effect scarcely, allowing for the pressure of the columns, the optimal flow rate was set on 0.7 mL/min.

When the columns temperature was set on 15–40 °C, the retention time of EGT was shorten with increasing temperature, but it did not affect the separating degree, consequently, the columns temperature was set on room temperature (25 °C).

32.3.2 Calibration Curves, the Limit of Detection and Quantification

A series of standard solutions of different concentrations (2.3) were used to determine the linear range of the analysis by the external standard method. Calibration curves were generated by plotting the peak areas versus the corresponding concentrations. The linearity of the calibration process was established, $y = 0.0405x + 5.0253$, x expressed area of peak and y expressed corresponding concentrations of EGT standard, correlation coefficient was 0.9999.

The diluted solution of EGT standard was further diluted to a series of concentrations with purified water for the purpose of obtaining the limit of detection LOD and the limit of quantification LOQ. They were determined at signal-to-noise (S/N) ratios of 3 and 10, respectively. As a result, the LOD for EGT was 10.4 μg/L and the LOQ was 34.7 μg/L.

32.3.3 Precision

The precision was conducted by five replicate injections of EGT standard solutions during a single day. An RSD value which was used to evaluate precision was 1.31 %, which indicated that the established method had a good and high precision.

32.3.4 Repeatability and Stability

Repeatability was investigated with five independently prepared sample solutions of EGT, one of which was injected into the apparatus at 0, 2, 4, 6, 8, 10, 14, and 24 h with repeated three times separately, to determine the stability of the solution. As shown in Fig. 32.1, the repeatability and stability RSD values of the EGT samples were 1.67 and 1.4 %.

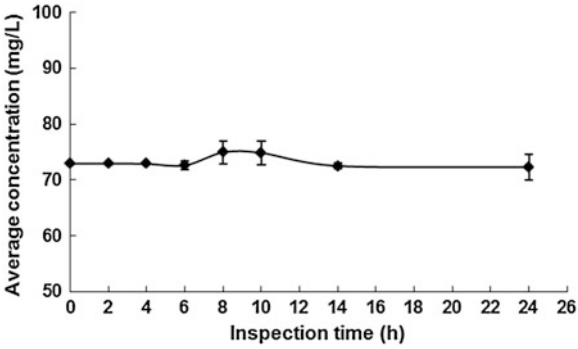

Fig. 32.1 Stability of EGT sample

32.3.5 Recovery

The recovery was determined by adding an accurately known amount of EGT standard at two different levels to the sample of EGT. As shown in Table 32.1, the average recoveries were 99.22 and 99.05 % with relative standard deviation (RSD) values of 0.43 and 0.55 %, which indicated that the absolute recovery of EGT meets the requirement of quantitative analysis.

32.3.6 Quantitative Analysis

Determined the EGT standard solutions and EGT samples respectively based on chromatographic conditions as Sect. 32.3.1, as shown in Figs. 32.2 and 32.3, the retention time of EGT was in between 7 and 8 min, under the optimized conditions, the EGT and impurities were separated well. The concentration of EGT in fermentation broth was 106 mg/L according to the standard curve.

Table 32.1 Recoveries of EGT

EGT	Background (μg/mL)	Added (μg/mL)	Found (μg/mL)	Recovery (*/ %)	Average Recovery (%)	RSD (%)
Sample 1	41.03	40.40	81.23	99.50	99.22	0.43
	41.03	40.40	81.03	99.01		
	41.03	40.40	80.88	98.64		
	41.03	40.40	81.33	99.75		
	41.03	40.40	81.1	99.18		
Sample 2	35.29	46.05	80.96	99.17	99.05	0.55
	35.29	46.05	81.28	99.87		
	35.29	46.05	80.64	98.48		
	35.29	46.05	80.94	99.13		
	35.29	46.05	80.7	98.61		

* Recovery = (Found − Background)/Added × 100 %

32.3.7 Qualitative Analysis by ESI–MS

Further ESI–MS analysis revealed prominent molecular ion [M + H] + peak at m/z 230 and [M + Na] + peak at m/z 252 of the component which was considered to be EGT in HPLC spectrum of a graph with 7.580 min of retention time in Fig. 32.3, which is in agreement with the molecular ion as well as the retention time of the authentic EGT, the compound was predicted for EGT, as shown in Fig. 32.4.

32.3.8 Qualitative Analysis by NMR

NMR analysis indicated ^{1}H-NMR of EGT standard and EGT in fermentation broth, as shown in Fig. 32.5, both the two spectrograms were basically the same.

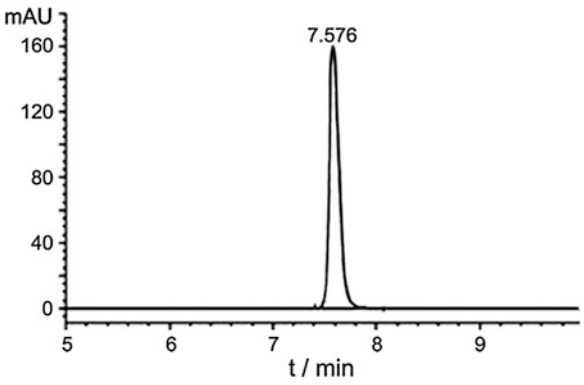

Fig. 32.2 HPLC chromatogram of EGT standard

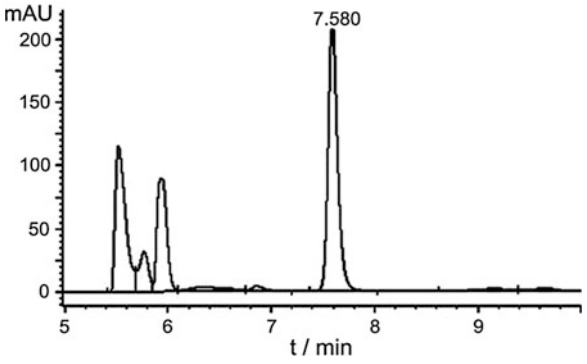

Fig. 32.3 HPLC chromatogram of EGT fermentation broth sample

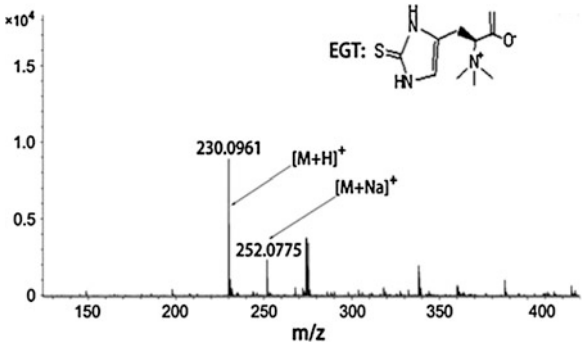

Fig. 32.4 MS spectrum of the component with 7.580 min of retention time in Fig. 32.3

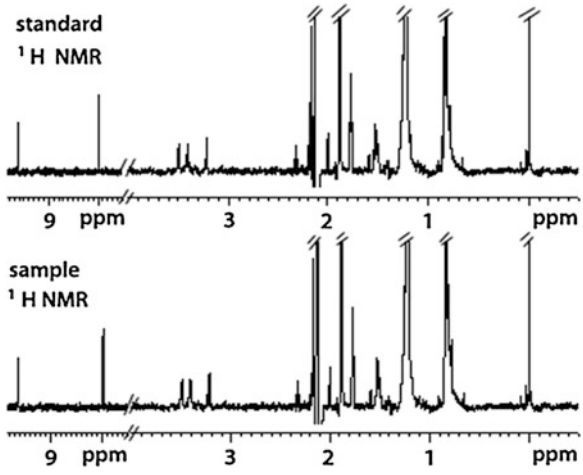

Fig. 32.5 ^{1}H-NMR spectrum of EGT standard and EGT in fermentation broth

32.4 Conclusion

A simple and efficient RP-HPLC method was developed to identify and evaluate the quality of EGT during fermentation, which offered good linearity, precision, repeatability, stability, and recovery. The method was applicable to quantification of massive fermentation and dynamic analysis of metabolites, which meet the technology and quality control requirements of EGT production by fermentation. Consequently, it laid foundation for industrial production, application development of EGT, and establishment of determining standard. Moreover, this method was easy to spread application and this study could provide reference for characterization of other similar natural bioactive metabolites.

Acknowledgments The authors acknowledge financial support from the Key Projects in the Tianjin Science and Technology Pillar Program, China (Grant No. 10ZCKFSY06300).

References

1. Weigand-Heller AJ, Kris-Etherton PM, Beelman RB (2012) The bioavailability of ergothioneine from mushrooms (*Agaricus bisporus*) and the acute effects on antioxidant capacity and biomarkers of inflammation. Prev Med 54:S75–S78
2. Kawano H, Higuchi F, Mayumi T, Hama T (1982) Studies on ergothioneine. VII. Some effects on ergothioneine on glycolytic metabolism in red blood cells from rats. Chem Pharm Bull 30:2611–2613
3. Laurenza I, Colognato R, Migliore L et al (2008) Modulation of palmitic acid-induced cell death by ergothioneine: evidence of an anti-inflammatory action. BioFactors 33:237–247
4. Rahman I, Gilmour PS, Jimenez LA et al (2003) Ergothioneine inhibits oxidative stress- and TNF-alpha-induced NF-kappa B activation and interleukin-8 release in alveolar epithelial cells. Biochem Biophys Res Commun 302:860–864
5. Gründemann Dirk (2012) The erghthioneine transporter controls and indicates ergothioneine activity-A review. Prev Med 54:S71–S74
6. Motohash N, Mori I, Sugiura Y, Tanaka H (1974) Metal-complexes of ergothioneine. Chem Pharm Bull 22:654–657
7. Motohashi N, Mori I, Sugiura Y (1976) Complexing of copper ion by ergothioneine. Chem Pharm Bull 24:2364–2368
8. Zhu BZ, Mao L, Fan RM et al (2011) Ergothioneine prevents copper-induced oxidative damage to DNA and protein by forming a redox-inactive ergothioneine–copper complex. Chem Res Toxicol 24:30–34
9. Pe Hartman, Hartman Z, Citardi Mj (1988) Ergothioneine, histidine, and two naturally occurring dipeptides as radioprotectors against gamma-irradiation inactivation of Bacteriophages T4 and P22. Radiation Res 114:319–330
10. Dong KK, Damaghi N, Kibitel J et al (2007) A comparison of the relative antioxidant potency of L-ergothioneine and idebenone. J. Cosmet. Dermatol. 6:183–188
11. Markova NG, Karaman-Jurukovska N, Dong KK et al (2009) Skin cells and tissue are capable of using L-ergothioneine as an integral component of their antioxidant defense system. Free Radic Biol Med 46:1168–1176
12. Damaghi N, Dong K, Smiles K et al (2008) The natural antioxidant L-ergothioneine and its receptor/transporter OCTN-1 participate in the skin's response to UVA-induced oxidative damage. J Am Acad Dermatol 58:AB111–AB111
13. Obayashi K, Kurihara K, Okano Y et al (2005) L-ergothioneine scavenges superoxide and singlet oxygen and suppresses TNF-alpha and MMP-1 expression in UV-irradiated human dermal fibroblasts. J Cosmet Sci 56:17–27
14. Song T-Y, Chen C-L, Liao J-W et al (2010) Ergothioneine protects against neuronal injury induced by cisplatin both in vitro and in vivo. Food Chem Toxicol 48:3492–3499
15. Deiana M, Rosa A, Casu V et al (2004) L-ergothioneine modulates oxidative damage in the kidney and liver of rats in vivo: studies upon the profile of polyunsaturated fatty acids. Clin Nutr 23:183–193
16. Paul BD, Snyder SH (2010) The unusual amino acid L-ergothioneine is a physiologic cytoprotectant. Cell Death Differ 17:1134–1140
17. Tanret C (1909) Sur une base nouvelle retiree du seigle ergote, l'ergothioneine Compt Rend 149:222–224
18. Hand CE et al (2005) Ab initio studies of the properties of intracellular thiols ergothioneine and ovothiol Bioorg. Med Chem Lett 15:1357–1360
19. Carlsson J, Kierstan MP, Brocklehurst K (1974) A convenient spectrophotometric assay for the determination of L-ergothioneine in blood. Biochem J 139(1):237–242
20. Dubost NJ, Beelman RB, Peterson D et al (2007) Identification and quantification of ergothioneine in cultivated mushrooms by liquid chromatography–mass spectroscopy. Int J Med Mushr 8:215–222

Chapter 33
Elimination of Carbon Catabolite Repression in *Bacillus subtilis* for the Improvement of 2,3-Butanediol Production

Weixi Liu, Jing Fu, Zhiwen Wang and Tao Chen

Abstract 2,3-butanediol is a vital platform compound, extensively used as liquid fuel and chemical raw material. In this study, *Bacillus subtilis* was engineered to utilize glucose and xylose for 2,3-butanediol production. Initially, the gene *araE* from *B. subtilis*, encoding the xylose transport protein AraE, was overexpressed under the control of the constitutive Pspac promoter. Subsequently, the xylose isomerase and xylulose kinase from *Escherichia coli*, encoded by the genes of *xylA* and *xylB* respectively, were introduced into *B. subtilis* genome. In mineral medium, the engineered strain BSUL02 is able to utilize D-glucose and D-xylose simultaneously to produce 2,3-butanediol. Under the fermentation conditions tested in this work, the recombinant strain BSUL02 could produce 3.1 g/L 2,3-butanediol from 10 g/L D-glucose and 5 g/L D-xylose, which sheds new light on a metabolic engineering strategy for commercial exploitation of lignocellulose to produce important building-block chemicals.

Keywords *Bacillus subtilis* · 2,3-Butanediol · Carbon catabolite repression · Xylose

33.1 Introduction

2,3-butanediol (BDO), also known as 2,3-butylene glycol, or dimethylethylene glycol [1], is an important platform chemical, which can be utilized to synthesize a series of vital products. For example, BDO can be used to produce 3-hydroxy-2-butanone, also named as acetoin, by dehydrogenation reaction catalyzed by alcohol dehydrogenase. Acetoin is a flavoring substance with pleasant smell,

W. Liu · J. Fu · Z. Wang · T. Chen (✉)
School of Chemical Engineering and Technology, Tianjin University, Tianjin 300072, People's Republic of China
e-mail: chentao@tju.edu.cn

T.-C. Zhang et al. (eds.), *Proceedings of the 2012 International Conference on Applied Biotechnology (ICAB 2012)*, Lecture Notes in Electrical Engineering 249,
DOI: 10.1007/978-3-642-37916-1_33, © Springer-Verlag Berlin Heidelberg 2014

which makes it a perfect candidate in food and beverage industry [2]. Methyl ethyl ketone is a product of the dehydration reaction, a major aviation fuel additive. Besides, BDO can also be converted to the strategic compound, 1,3-butadiene, which is a vital building block in synthetic rubber industry.

Conventionally, BDO can be synthesized from petroleum chemically. However, with the fluctuating price, depleting resources and environmental pollution problems, it necessitates the development of a sustainable, industrial, and environmentally benign chemical processes that would be able to shift our dependence on petroleum to the use of renewable resources. Biorefineries enable production of biofuels as well as building-block chemicals from biomass. BDO is a product of fermentative metabolism in many prokaryotic and eukaryotic microorganisms, such as *Bacillus* spp [3].

Bacillus subtilis, a rod-shaped and gram-positive bacterium, is a well-characterized organism and has served as a model for studies in biochemistry, genetics, and molecular biology [4]. Furthermore, with the improvement of genetic and molecular technology, *B. subtilis* could be transformed into platform strain for the modifiable chemicals production. It is naturally found in soil and vegetation [5] with a generally-recognized-as-safe (GRAS) status. Its nonpathogenic status, coupled with perfect secretion systems, makes *B. subtilis* one important commercial enzymes. Hitherto, many researchers have made *B. subtilis* as host organism to produce 1-butanediol [6], ethanol [5], lactate [7], and riboflavin, but few research groups have paid attention to take advantage of this bacterium to produce BDO.

Bacteria often sequentially utilize coexisting carbohydrates in environment, which is named as carbon catabolite repression (CCR). As glucose can make the fastest growth and is the priority selection of most microorganisms, CCR is also known as glucose effect. Without exception, this phenomenon exists in *B. subtilis* as well and the CCR mechanism limits its application for fermenting biomass sugar hydrolyzates. For example, the utilization of xylose-containing hydrolyzates from lignocellulose as a raw material for a fermentation process imposes many demands on *B. subtilis*, to which simultaneous utilization of glucose and xylose is desirable. However, preferential sugar utilization, as well as the transcriptional exclusion of less preferred sugars, turns out to be one of the major barriers in making the best use of sugar hydrolyzates to produce biochemicals. Elimination of CCR in microbial cell factories would mean an increase in the total sugar uptake by favoring pentose assimilation in addition to glucose [8]. Despite the reports about catabolite derepression in recombinant or mutant strains of *E. coli*, *Klebsiella oxytoca* [9], and *Clostridium acetobutylicum* [10], there are few tries in *B. subtilis* for catabolite derepression.

In this study, we constructed an engineered *B. subtilis* strain, in which CCR is eliminated by expression of heterologous xylose isomerase and xylulose kinase from *E. coli*, encoded by the genes of *xylA* and *xylB* respectively. Employing glucose and xylose as substrate, the engineered *B. subtilis* was able to utilize both of them simultaneously. Under the evaluated conditions in this work, the engineered strain BSUL02 could utilize glucose and xylose synchronously while the

main metabolites is BDO, which will shed new light on a metabolic engineering strategy to achieve efficient production of bio-based building blocks by sugar mixtures derived from the lignocellulosic biomass.

33.2 Materials and Methods

33.2.1 Bacterial Strains, Plasmids, and Genetic Manipulation

The strains and plasmids used in this study are listed in Table 33.1. *E. coli* Top10 was used for plasmids construction. All *Bacillus* strains used in this study were derived from *B. subtilis* 168Δupp, which was used as the wild type. DNA manipulations were carried out using standard techniques [11]. The transformation of *E. coli* and *B. subtilis* were performed by heat shock [11] and the competent cell method [12], respectively. Primers used for plasmid construction are listed in Table 33.2. Unless otherwise specified, for the adapted plasmid-bearing strain, antibiotics were added appropriately (kanamycin 5 μg/mL, ampicillin 100 μg/mL, and chloramphenicol 5 μg/mL).

Table 33.1 Strains and plasmids used in this study

Name	Relevant genotype	Source or reference
E. coli Top10	*F-, mcrAΔ(mrr-hsd RMS-mcrBC), φ80, lacZΔM15, △lacX74, recA1, araΔ139Δ(ara-leu)7697, galU, galK, rps, (Strr) endA1, nupG*	Laboratory stock
B. subtilis 168△upp	Wild type, △*upp*:: Kan	Laboratory stock
E. coli MG1655	F-, lambda-, *ilvG*-, *rfb*-50, *rph*-1	Laboratory stock
BSUL01	△*amyE*:: (Pspac-*araE*), △upp:: Kan, Cm^r, Kan^r	This study
BSUL02	△*amyE*:: (Pspac-*xylAB-araE*), △upp:: Kan, Cm^r, Kan^r	This study
pMUTIN4	Amp^r, Em^r	BGSC
pDG364	*B. subtilis* integration plasmid; Amp^r, Cm^r;	BGSC
pDG364-PA	Amp^r, Cm^r;	This study
pDG364-PXA	Amp^r, Cm^r;	This study
pHP13	Cm^r, Em^r;	BGSC
pHP13-PA	Cm^r, Em^r; Pspac-*araE*	This study
pHP13-PXA	Cm^r, Em^r; Pspac-*xylAB-araE*	This study

BGSC Bacillus Genetic Stock Center (http://www.bgsc.org/)

Table 33.2 Oligonucleotides used in this study

Primer name	Sequence[a] 5′ → 3′
araE-F	CCGGAATTCACATTCGGGAGGGCAGGGAA
L2-araE-B	CGCGGATCCTCATTTTATCCAAAGCTTTTC
Pspac-F	ATACCCTGCAGTTGTTGACTTTATCTACAAGGT
Pspac-B	GCGCCAATTGTCATTTTATCCAAAGCTTTTC
L1-xylAB-F	CCGGAATTCCCAAGGAGGGTATAGCTATG
L1-xylAB-B	CCGGAATTCTTACGCCATTAATGGCAGAAGT
L-PXA-F	CGCGGATCCTTGTTGACTTTATCTACAAGGT
amyE-F	CGATTCAAAACCTCTTTACTG
amyE-R	CCATTTAGCACGTAATCAAAG

[a] Underline stands for the restriction site

33.2.2 Bacterial Strains, Plasmids, and Genetic Manipulation

To engineer constitutive xylose metabolic pathway in *B. subtilis*, plasmids listed in Table 33.1 were constructed. First of all, the *araE* gene encoding xylose transportation protein was cloned from *B. subtilis* with primes *araE*-F and L2-*araE*-B. The PCR product of *araE* was cloned into pMUTIN4 to obtain pMUTIN4-*araE* via *Eco*RI/*Bam*HI restriction sites. Then, pHP13-PA was constructed by amplifying the Pspac promoter as well as the *araE* coding sequence from the plasmid pMUTIN4-araE with primers of Pspac-F and Pspac-B, digesting the PCR product with *Pst*I and *Mfe*I, and ligating into pHP13 cut with *Pst*I and *Eco*RI. Similarly, plasmid pHP13-PXA was constructed by amplifying *xylAB* of *E. coli* MG1655 from its genomic DNA with L1-xylAB-F and L1-xylAB-B, digesting the PCR product with *EcoR*I, and ligating into pHP13-PA in the right direction cut with the same enzymes.

The integration vector pDG364 was used to construct the following plasmids, pDG364-PA and pDG364-PXA. The Pspac promoter region and open reading frames of *araE* and *xylAB*, Pspac-*araE* and Pspac-*xylAB-araE*, were cloned from plasmids pHP13-PA and pHP13-PXA with the primers L-PXA-F and L2-*araE*-B, respectively. Further, the PCR products were digested with *Bam*HI and cloned into pDG364, generating the integrated plasmids pDG364-PA and pDG364-PXA. The pDG364 and its derivative integrated plasmids were selected by 50 μg/mL ampicillin without exception.

Through spizizen transformation, homologous recombination took place in a neutral site, *amyE*. The *B. subtilis* recombinants were further confirmed by observing amylase halo, PCR verification, and DNA sequencing with the primers of *amyE*-F and *amyE*-R.

33.2.3 Medium and Cultivation

Unless stated otherwise, all *E. coli* and *B. subtilis* strains were cultured in Luria–Bertani (LB) medium at 37 °C. The M9 minimal salt medium plus glucose, supplemented with tryptophan, was used for conical flask fermentation as *B. subtilis* 168 is tryptophan-deficient.

To prepare seed cultures, stains stored at −80 °C were streaked on LB agar plate containing kanamycin, and one colony was grown in 5 mL LB medium in test tubes at 220 rpm. After 12 h shaking at 220 rpm, 1 % (v/v) inocula was transferred to M9 medium. Subsequently, the precultures, which grown on M9 medium with 10 g/L glucose, of *B. subtilis* wild strain and engineered strain were used to inoculate to an initial OD_{600} of 0.05 in a 250 mL shaking flask with 100 mL M9 medium at 100 rpm.

33.2.4 Analytical Methods

Cell growth was determined by measuring turbidity at 600 nm (OD_{600}) with a UV–Vis spectrophotometer (TU-1901, Persee, Beijing, China). High-performance liquid chromatography (HPLC) analyses of fermentation products were performed as previously reported [3]. Glucose concentration was determined using a glucose analyzer (Model-SBA40, Shandong, China) and the other substrate, xylose, was analyzed by high pressure liquid chromatography.

33.3 Results and Discussion

33.3.1 Improvement for Xylose Metabolism by araE Gene Chromosomal Integration

Bio-refining industry is developing rapidly and gaining unprecedented momentum. Biorefinery integrates biomass conversion processes to produce fuels and chemicals. Lignocellulosic biomass from agricultural waste represents an abundant and cost-effective renewable energy source that is to date underutilized [13]. Therefore, catalytic conversion of this biorenewable feedstock to commodity chemicals has become a promising method for the future and may pacify the threats posed on fossil fuels. While extensive research efforts have been made to engineer efficient bio-technologies for lignocellulose utilization, the bioconversion of xylose, one of the main components of lignocellulose, remains a major obstacles. As to *B. subtilis*, the L-arabinose transporter araE is a non-specific xylose transporter [14]. The transcript of gene *araE* is induced by L-arabinose and restrained by the repressor araR. To confirm the effect of *ara*E gene on D-xylose utilization, plasmid pDG364-PA was

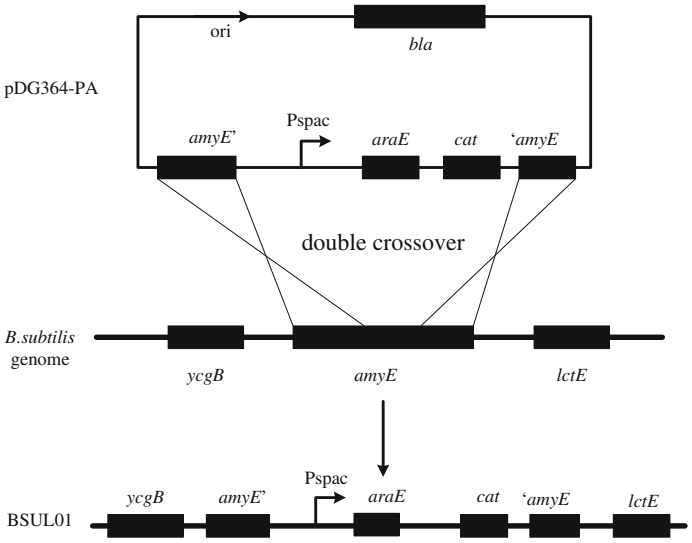

Fig. 33.1 Schematic diagram of the double crossover for construction of BSUL01

constructed as described above and transformed into *B. subtilis* 168Δupp at the site of *amy*E (Fig. 33.1). In the engineered strain BSUL01, one copy of *ara*E gene under the control of the constitutive Pspac promoter was introduced into the chromosomal DNA. To investigate the efficiency of xylose metabolism under aerobic conditions, the wild type strain B. subtilis 168Δupp and the engineered recombinant strain BSUL01 were cultivated in M9 medium at 220 rpm, while 10 g/L D-xylose was added to the medium as the sole carbon source. The optical density of strain growth and xylose concentration were monitored in the process of fermentation. The specific growth rate of strain BSUL01 on 10 g/L of D-xylose was noticeably different from that of wild type ($\mu = 0.107\ h^{-1}$ and $0.026\ h^{-1}$, respectively; Fig. 33.2). While *B. subtilis* 168Δupp could metabolize xylose, the OD was low even 3 days after inoculation. Strain BSUL01, however, could grow better on M9 medium than the wild strain, which was able to enter into stationary-phase within 30 h and xylose uptake was improved in the engineered strain. Therefore, the fermentative capacity of BSUL01 on xylose was improved by the overexpression of *araE*, which was consistent with the report of Park [14].

33.3.2 Simultaneous Utilization of Glucose and Xylose to Produce BDO by the Engineered B. subtilis

In *B. subtilis*, which prefers to catabolize glucose and begins to utilize xylose after the exhaustion of glucose, glucose repression is the consequence of a complex

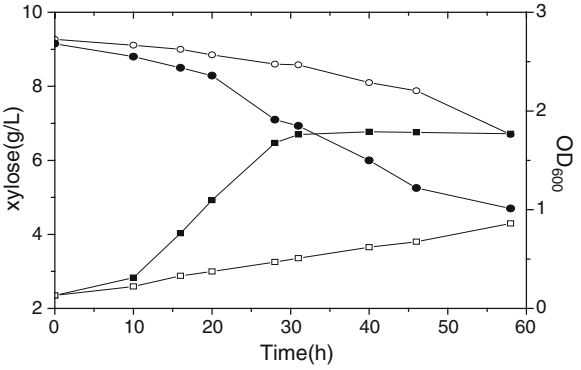

Fig. 33.2 Comparative microaerobic growth of *B. subtilis* 168Δupp (*unfilled symbols*) and BSUL01 (*filled symbols*) in mineral medium. The symbols were used: OD600 (*square*), xylose (*circle*)

cascade of events. This phenomenon is also referred as carbon catabolite repression, which exists in some other bacteria as well, such as *E. coli*. In *B. subtilis* not only the transportation pathway, but also a 14-bp cis-acting element located in the coding region of the gene *xylA* encoding xylose isomerase [15] and the repressor XylR, are involved in the carbon catabolite repression of xylose. Therefore, the presence of glucose in culture would prevent *B. subtilis* to assimilate xylose, resulting in the preferential utilization of glucose. Preferential utilization of glucose, as well as the exclusion of less preferred sugars in transcriptional level, turns out one of the major barriers in making the best use of sugar hydrolyzates to produce bio-based chemicals. Therefore, an artificial operon Pspac-*xylAB-araE* was constructed as described above and introduced to *B. subtilis* genome by double crossover afterwards, obtaining the engineered strain BSUL02.

In order to evaluate whether xylose is utilized efficiently in the presence of glucose, BSUL02 cells precultured in mineral medium containing 1 % (wt/vol) glucose was prepared and used to inoculate 100 mL of mineral medium containing 10 g/L glucose and 5 g/L xylose to give a final cell concentration of OD 0.05. According to Fig. 33.3, under the condition tested in this work, 10 g/L glucose was nearly exhausted during 30 h. As to the engineered strain BSUL02, it metabolized glucose and xylose synchronously to produce BDO. The parent strain *B. subtilis* 168Δupp, however, began to utilize xylose after the exhaustion of glucose. During this process, the parent strain only accumulated 2.7 g/L BDO, while the engineered strain could accumulate as much as 3.1 g/L BDO. Therefore, our work has demonstrated that the introduction of heterologous xylose isomerase and xylulose kinase could, to some extent, relieve CCR in *B. subtilis* and enhance the production of the vital platform building block.

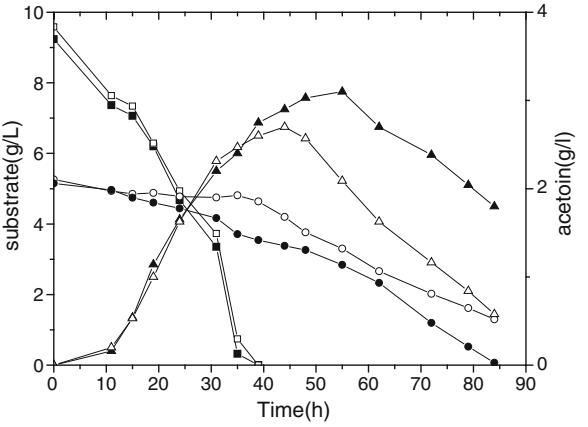

Fig. 33.3 BDO production and substrate uptake by *B. subtilis* 168△upp (*unfilled symbols*) and the recombinant BSUL02 (*filled symbols*) in mineral medium. The symbols were used: glucose (*square*), xylose (*circle*), and BDO (*upright triangle*)

33.4 Conclusion

In conclusion, the constitutive expression of gene *araE* under the control of Pspac promoter could make *B. subtilis* to utilize xylose. Further expression of heterologous xylose isomerase and xylulose kinase from *E. coli*, encoded by the genes *xylA* and *xylB*, allowed *B. subtilis* to derepress carbon catabolite repression and assimilate glucose and xylose simultaneously. In summary, we engineered *B. subtilis* to utilize glucose and xylose to produce acetoin in microaerobic condition.

Acknowledgments This work was supported by the National 973 Project (2012CB725203, 2011CBA00804), National Natural Science Foundation of China (NSFC-21176182), Natural Science Foundation of Tianjin (12JCYBJC12900) and the Research Fund for the Doctoral Program of Higher Education (20100032120014).

References

1. Syu MJ (2001) Biological production of 2,3-butanediol. Appl Microbiol Biotechnol 55(1):10–18
2. Huang M, Oppermann-Sanio FB, Steinbuchel A (1999) Biochemical and molecular characterization of the *Bacillus subtilis* acetoin catabolic pathway. J Bacteriol 181(12):3837–3841
3. Wang M, Fu J, Zhang X et al (2012) Metabolic engineering of *Bacillus subtilis* for enhanced production of acetoin. Biotechnol Lett 34:1877–1885
4. Kunst F, Ogasawara N, Moszer I et al (1997) The complete genome sequence of the gram-positive bacterium *Bacillus subtilis*. Nature 390(6657):249–256
5. Romero S, Merino E, Bolivar F et al (2007) Metabolic Engineering of *Bacillus subtilis* for ethanol production: lactate dehydrogenase plays a key role in fermentative metabolism. Appl Environ Microbiol 73(16):5190–5198

6. Li S, Wen J, Jia X (2011) Engineering *Bacillus subtilis* for isobutanol production by heterologous Ehrlich pathway construction and the biosynthetic 2-ketoisovalerate precursor pathway overexpression. Appl Microbiol Biotechnol 91(3):577–589
7. Zhang X-Z, Sathitsuksanoh N, Zhu Z et al (2011) One-step production of lactate from cellulose as the sole carbon source without any other organic nutrient by recombinant cellulolytic *Bacillus subtilis*. Metab Eng 13(4):364–372
8. Vinuselvi P, Kim MK, Lee SK et al (2012) Rewiring carbon catabolite repression for microbial cell factory. BMB Rep 45(2):59–70
9. Ji XJ, Nie ZK, Huang H et al (2011) Elimination of carbon catabolite repression in *Klebsiella oxytoca* for efficient 2,3-butanediol production from glucose-xylose mixtures. Appl Microbiol Biotechnol 89(4):1119–1125
10. Xiao H, Gu Y, Ning Y et al (2011) Confirmation and elimination of xylose metabolism bottlenecks in glucose phosphoenolpyruvate-dependent phosphotransferase system-deficient *Clostridium acetobutylicum* for simultaneous utilization of glucose, xylose, and arabinose. Appl Environ Microbiol 77(22):7886–7895
11. Sambrook J, Russell DW (2001) Molecular cloning: a laboratory manual, vol 2: CSHL press, Cold Spring Harbor
12. Anagnostopoulos C, Spizizen J (1961) Requirements for transformation in *Bacillus Subtilis*. J Bacteriol 81(5):741–746
13. Kawaguchi H, Vertes AA, Okino S et al (2006) Engineering of a xylose metabolic pathway in *Corynebacterium glutamicum*. Appl Environ Microbiol 72(5):3418–3428
14. Park YC, Jun SY, Seo JH (2012) Construction and characterization of recombinant *Bacillus subtilis* JY123 able to transport xylose efficiently. J Biotechnol 161:402–406
15. Kraus A, Hueck C, Gärtner D et al (1994) Catabolite repression of the *Bacillus subtilis* xyl operon involves a cis element functional in the context of an unrelated sequence, and glucose exerts additional xylR-dependent repression. J Bacteriol 176(6):1738–1745

Chapter 34
Metabolic Engineering of *Corynebacterium glutamicum* for Efficient Aerobic Succinate Production

Huihua Xia, Nianqing Zhu, Zhiwen Wang and Tao Chen

Abstract *Corynebacterium glutamicum* with deletions of succinate dehydrogenase complex and all known acetate-producing pathways still accumulates a certain amount of acetate as the by-product under aerobic conditions. In this study, a new approach to reduce acetate accumulation by engineering an acetate assimilation pathway in *C. glutamicum* was presented. Two enzymes of the acetyl-CoA synthase from *Escherichia coli* (*acs*) and *Bacillus subtilis* (*acsA*) were introduced into the strain SAX1 ($\Delta sdhABCD\Delta ldhA\Delta pta\Delta cat\Delta pqoP_{sod}$-$ppcP_{sod}$-*pyc*) background, resulting strain SAX2 and SAX3. Both modifications resulted in the elimination of acetate formation and overexpression of *acsA* had a higher succinate yield. Then, overexpressing the native citrate synthase encoded by *gltA* in the strain SAX3 resulted in a 65 % decrease in pyruvate yield and a 32 % increase in succinate yield (0.66 mol (mol·glucose)$^{-1}$) in 24 h. In shake-flask batch fermentations, the optimum strain produced 44.8 mM succinate with an average yield of 0.77 mol (mol·glucose)$^{-1}$ in 48 h.

Keywords Acetyl-CoA synthase · Aerobic condition · Citrate synthase · *Corynebacterium glutamicum* · Succinate production

34.1 Introduction

Succinate is considered as one of the important platform chemicals because of its extensive applications in many industrial fields. It can be converted to a wide range of products including specialty chemicals, food ingredients, green solvents, pharmaceuticals, and biopolymers [1–4]. Currently, for costly and ecological

H. Xia · N. Zhu · Z. Wang · T. Chen (✉)
School of Chemical Engineering and Technology, Tianjin University, Tianjin 300072, People's Republic of China
e-mail: chentao@tju.edu.cn

T.-C. Zhang et al. (eds.), *Proceedings of the 2012 International Conference on Applied Biotechnology (ICAB 2012)*, Lecture Notes in Electrical Engineering 249,
DOI: 10.1007/978-3-642-37916-1_34, © Springer-Verlag Berlin Heidelberg 2014

question, microbial production of succinate attracted great interest as more sustainable replacement for conventional petrochemical routes in recent years [1].

Succinate can be effectively produced by naturally isolated bacteria and recombinant organisms, such as *Actinobacillus succinogenes*, *Anaerobiospirillum succiniciproducens* [5], *Mannheimia succiniciproducens* [6], recombinant *Escherichia coli* [7–9], and engineered *Saccharomyces cerevisiae* [10]. Most of the succinate production processes of those engineered strains were all carried out under anaerobic conditions. However, it has been shown that anaerobic succinate production contained inherent disadvantages that were difficult to overcome, such as poor cell growth, slow carbon throughout, and limitation of NADH availability [11, 12]. Therefore, fully aerobic platforms have been designed and constructed [1, 11, 12].

Corynebacterium glutamicum is a rapidly growing gram-positive soil bacterium that can utilize a variety of sugars and organic acids as carbon sources and has been used for amino acids production for several decades [13]. Litsanov et al. reported that *C. glutamicum* lacking the succinate dehydrogenase complex showed greater potential for aerobic succinate production than other strains with equivalent genetic backgrounds [14]. The *sdhCAB*-deficient *C. glutamicum* strain accumulated succinate with a yield of 0.2 mol (mol·glucose)$^{-1}$ and formed acetate as the major by-product. Disrupting all known acetate formation pathways significantly reduced acetate production but not to the extent of complete abolishment [15].

In the present study, another approach, namely introducing exogenous acetate assimilation pathways, was presented aiming at further reducing acetate accumulation. Also, the native citrate synthase was overexpressed to redirect more carbon flux toward TCA cycle.

34.2 Materials and Methods

34.2.1 Strains, Plasmids and Media

All strains and plasmids used in this study, their sources and relevant characteristics are shown in Table 34.1. During plasmids construction, *E.coli* DH5α was used and cultured in lysogeny broth complex medium (LB). Plasmid DNA transferred into *C. glutamicum* was carried out by electroporation, and the recombinant strains were selected on brain heart infusion-sorbitol (BHIS) agar plates containing 25 μg mL^{-1} kanamycin.

34.2.2 Genetic Methods

For construction of plasmid pEC-XK99E-*acsA*, the *acsA* gene from *B. subtilis* was amplified from chromosomal DNA by PCR with primer pair acsA1/acsA2. The resulting fragment was digested with SacI and XbaI and ligated into SacI/XbaI-

Table 34.1 Bacterial strains and plasmids used in this study

Strain or plasmid	Relevant characteristics	Reference
Strains		
ATCC13032	*C. glutamicum* Wide type, biotin auxotrophic	ATCC[a]
SA	*C. glutamicum* △*ldh*△*pta*△*pqo*△*cat* P_{sod} *pyc* P_{sod} *ppc*,	Laboratory
SAX1	*C. glutamicum* △*ldh*△*pta*△*pqo*△*cat*△*sdh* P_{sod} *pyc* P_{sod} *ppc*, SA with an additional deletion of *sdhABCD*	This study
SAX2	*C. glutamicumΔldhΔptaΔpqoΔcatΔsdhPsod pyc Psod ppc(pEC-XK99E-acs)*	This study
SAX3	*C. glutamicumΔldhΔptaΔpqoΔcatΔsdh*P_{sod} *pyc* P_{sod} *ppc*(pEC-XK99E-*acs*)	This study
SAX4	*C. glutamicumΔldhΔptaΔpqoΔcatΔsdh*P_{sod} *pyc* P_{sod} *ppc*(pEC-XK99E-*acsA-gltA*),	This study
Plasmids		
pD*sacB*	derived from pK18*mobsacB,* for increasing expression of *sacB* under P_{trc}	Laboratory
pD*sacB*-△*sdhABCD*	pD*sacB* carrying up and downstream regions of *sdhABCD* operon	This study
pEC-xk99E	Kan^R; *C. glutamicum*/*E. coli* shuttle vector (P_{trc}, $lacI^q$; pGA1, $OriV_{C.g.}$, $OriV_{E.c.}$)	Laboratory
pEC-XK99E-*acs*	derived from pEC-XK99E, for overexpression of *acs* under the control of P_{trc}	This study
pEC-XK99E-*acsA*	derived from pEC-XK99E, for overexpression of *acsA* under the control of P_{trc}	This study
pEC-XK99E-*acsA-gltA*	derived from pEC-XK99E, for overexpression of *acsA* and *gltA* under the control of P_{trc}	This study

[a] ATCC, American Type Culture Collection

restricted vector pEC-XK99E. For construction of plasmid pEC-XK99E-*acs*, the *acs* gene from *E. coli* was amplified from chromosomal DNA by PCR with primer pair acs1/acs2. The resulting fragment was digested with SacI and XbaI and ligated into SacI/XbaI-restricted vector pEC-XK99E. For construction of plasmid pEC-XK99E-*acsA-gltA*, the *gltA* gene from *C. glutamicum* was amplified from chromosomal DNA by PCR with primer pair xbaIgltA1/sbfIgltA2. The resulting fragment was digested with XbaI and SbfI and ligated into XbaI/SbfI-restricted pEC-XK99E-*acsA*.

The in-frame deletion of *sdhABCD* operon in *C. glutamicum* was achieved via a two-step homologous recombination procedure using the suicide vector pD*sacB*. The flanking regions (approximately 800 bp each) of *sdhABCD* operon were amplified from chromosomal DNA using primer pairs sdh1/sdh2 and sdh3/sdh4. The flanking fragments were gel purified, mixed in equal amounts, and subjected to crossover PCR. The resulting fusion products containing the upstream and downstream regions were ligated into EcoRI/PstI-restricted pD*sacB* and then transformed into *C. glutamicum* by electroporation. The gene deletion was carried out as described previously [16]. The primers used in this study were shown in Table 34.2.

Table 34.2 Primes used in this study

Primes	Sequence (5′−3′)
acsA1	CTAGGAGCTCAAAGGAGGACAACCATGAACTTGAAAGCGTTACCAG
acsA2	CAGCTCTAGATTAATCCTCCATTGTTGACAG
acs1	CTAGGAGCTCAAAGGAGGACAACCATGAGCCAAATTCACAAACACACC
acs2	CAGCTCTAGATTACGATGGCATCGCGATAG
xbaIgltA1	AGGGTCTAGACCGTAATCCGGAAGAGTTT
xbaIgltA2	ATATCCTGCAGGGTTTCATGCAAAAACGGCCGA
sdh1	ATCGGAATTCTGATGCGCAATAACACCGGTA
sdh2	GCGAGTTCTGCGGTTCGCCTCCGTCGTAATTTTTCCGTGA
sdh3	GTAACTGCAGGGCCGGTTTCCTTGACGTAAC
sdh4	ATTACGACGGAGGCGAACCGCAGAACTCGCACTTGACCAC

34.2.3 Cultivation Conditions

For the precultivation of *C. glutamicum* strains, single clones were grown in 5 mL of modified CGIII medium containing 10 $g \cdot L^{-1}$ tryptone, 10 $g \cdot L^{-1}$ yeast extract, and 42 $g \cdot L^{-1}$ 3-morpholinopropanesulfonic acid (MOPS, as a buffering agent) (pH 7.4) at 30 °C and 220 rpm [17]. After incubation overnight, cells of the preculture were inoculated into modified CGIII medium supplemented with 55 mM glucose and 23 mM sodium bicarbonate and 42 $g \cdot L^{-1}$ of MOPS,which was carried out in shake-flask. Cultivations for succinate production were performed at 250 rpm and 30 °C. For induction, up to 1 mM of isopropyl β-D-1-thiogalactopyranoside (IPTG) was added to the culture medium.

34.2.4 Analytical Techniques

Extracellular organic acids were measured by HPLC (HP1100 LC, Agilent Technologies, USA) equipped with a cation-exchange column (HPX-87H, BioRad, USA), a UV absorbance detector (Agilent Technologies, G1315D), and an refractive index (RI) detector (Agilent Technologies, HP1047A) as previously described [9]. Succinate and acetate were measured by the RI detector while pyruvate and lactate were measured by the UV detector at 210 nm. Glucose concentration was monitored by using a SBA sensor machine (Institute of Microbiology, Shandong, China). Growth was determined by measuring the optical density at 600 nm (OD_{600}) and one unit of absorbance at 600 nm corresponded to 0.25 g cell dry weight (CDW) per liter.

34.3 Results and Discussion

34.3.1 Engineering an Aerobic Platform for Succinate Production in C. glutamicum

Starting with the wild-type ATCC13032, the genes of *pqo*, *pta*, and *cat* were disrupted and the native promoters of *ppc* and *pyc* were replaced by the strong promoter of the superoxide dismutase (*sod*), respectively. Also the *ldhA* gene encoding for lactate dehydrogenase was inactivated that avoided lactate accumulation in further strain improvement. Finally, the deletion of *sdhABCD* operon was introduced. All of those modifications resulting strain SAX1.

To test the strain SAX1 for its ability to produce succinate from glucose under aerobic conditions, shake-flask fermentations were carried out in accordance with the above described fermentation conditions (Fig. 34.1).

The strain SAX1 consumed glucose completely within 15 h. Also, it produced 31.5 mM succinate and 14.8 mM acetate at the end of the cultivation after 48 h. Furthermore, small amounts of pyruvate (6.3 mM) was formed simultaneously in the supernatant.

34.3.2 Introduction of Heterologous Acetate Assimilation Pathways

Previous attempts to allow succinate accumulation under aerobic conditions have been made by disrupting the succinate dehydrogenase complex as well as inactivating pathways leading to the synthesis of acetate [15].

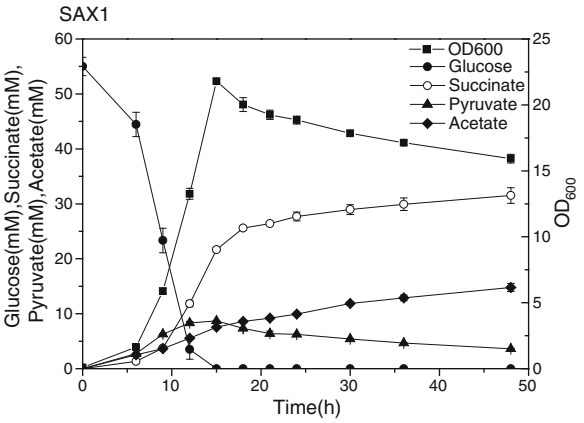

Fig. 34.1 The shake-flask batch fermentative results of the strain SAX1 in 48 h. Three independent fermentations were performed, showing comparable results

Despite that certain target genes involved in the acetate formation pathways were inactivated, 14.8 mM acetate with a yield of 0.26 mol (mol·glucose)$^{-1}$ was still accumulated in the supernatant by the strain SAX1. There might be other unclear pathways involved in the conversion of acetyl-CoA that is responsible for the remaining acetate formation. It has been previously reported that deletion of *aceE* gene encoding for E1 enzyme of pyruvate dehydrogenase complex could almost eliminate acetate accumulation under anaerobic conditions. Thus, other pathways involved in the conversion of acetyl-CoA might be responsible for the remaining acetate formation, whereas these pathways were yet unclear. Several target genes annotated as putative acetyltransferases, hydrolases, or dehydrogenases that have the potential contribution to acetyl-CoA conversion were described in previous studies [18, 19]. However, inactivation of one or more of these genes was time-consuming, and the influence on acetate production was uncertain. Introduction of an acetate assimilation pathway could address this conundrum. Exogenous ACS from *E. coli* and *B. subtilis* were expressed in the strain SAX1, respectively, resulting strain SAX2 and strain SAX3. The shake-flask fermentative results were shown in Fig. 34.2.

As we see, in batch cultivations, acetate was not detected by the high performance liquid chromatography in the strains SAX2 and SAX3. It showed there was no acetate accumulation. In the case of succinate production, strain SAX2 showed a 9.3 % increase in succinate yield as compared to strain SAX1, while strain SAX3 exhibited a 17.8 % enhancement. Also, both strains produced significant amounts of pyruvate in batch cultivations. Moreover, when compared with strain SAX2, strain SAX3 had 2.1 % higher succinate productivity and 23.1 % higher glucose consumption rate.

Taken together, these results indicated that the acetate assimilation pathway from *B. subtilis* was more effective. Therefore, strain SAX3 was chosen for further engineering.

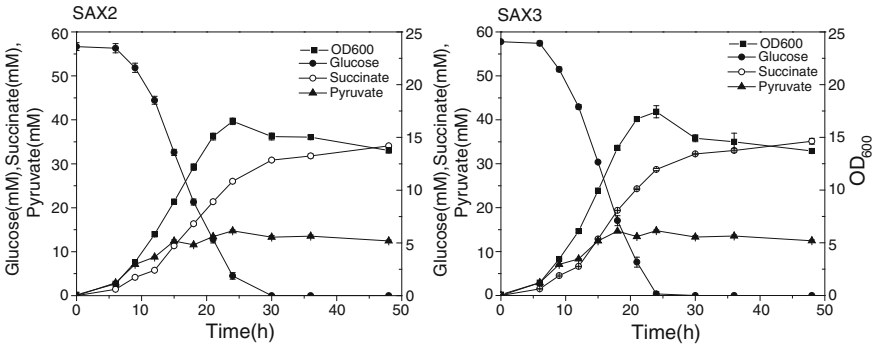

Fig. 34.2 The shake-flask batch fermentative results of the strains of SAX2 and SAX3 in 48 h. Three independent fermentations were performed, showing comparable results

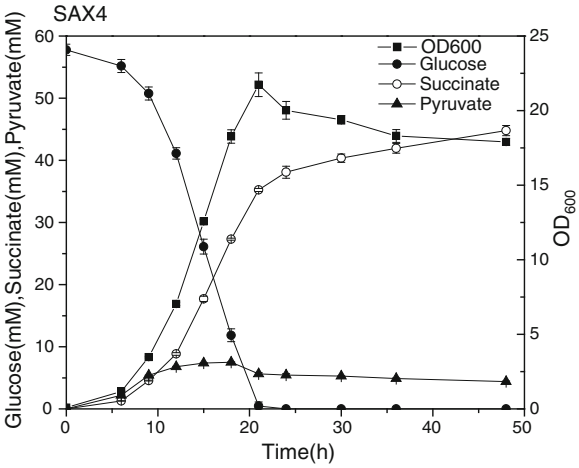

Fig. 34.3 The shake-flask batch fermentative results of the strain of SAX4 in 48 h. Three independent fermentations were performed, showing comparable results

34.3.3 Reduction of Pyruvate Formation by Overexpressing Citrate Synthase

As described above, strain SAX3 showed restricted growth as well as produced significant amounts of pyruvate (12.45 mM) as by-product. This was likely related to the introduction of a heterologous acetate assimilation pathway. The detrimental effect on growth was due to the accumulation of metabolic intermediates, such as acetyl coenzymeA [18]. If the formation rate of acetyl-CoA was higher than the condensation rate of acetyl-CoA and oxaloacetate, acetyl-CoA would accumulate. The elevated concentration of acetyl-CoA might affect several enzymes involved in the central metabolic pathways and results in accumulation of pyruvate as the major by-product in our strain. Citrate synthase can efficiently channel carbon flux toward the oxidative TCA cycle, as well as reduce the carbon accumulation at the pyruvate node [20]. Thus, the native citrate synthase *gltA* was overexpressed in the strain SAX3 aiming at driving more carbon flux toward the succinate synthesis pathway, resulting strain SAX4. The shake-flask fermentative results were shown in Fig. 34.3.

The strain SAX4 accumulated 4.38 mM pyruvate with the yield of 0.076 mol (mol·glucose)$^{-1}$, which was 62 % lower compared to strain SAX3. Moreover, the strain SAX4 produced 44.8 mM succinate and showed a 19.6 % increase in succinate yield compared to strain SAX3.

34.4 Conclusions

In conclusion, inactivation of the succinate dehydrogenase complex allowed the accumulation of succinate as an end-product of aerobic metabolism. The introduced acetate assimilation pathway from *B. subtilis* led to the elimination of

acetate production, it recovered wasted carbon and increased carbon flux toward succinate synthesis pathway. Overexpression of the native citrate synthase enhanced the condensation rate of acetyl-CoA and oxaloacetate, drove more carbon flux to the citrate which finally led to the secretion of succinate. Those efforts had made a significant contribution to the increase of succinate yield in the SAX1 background.

All in all, we reported the development of an efficient platform for aerobic production of succinate in *C. glutamicum.*

Acknowledgments This work was supported by the National 973 Project (2012CB725203, 2011CBA00804), National Natural Science Foundation of China (NSFC-21176182), Natural Science Foundation of Tianjin (12JCYBJC12900), and the Research Fund for the Doctoral Program of Higher Education (20100032120014).

References

1. Beauprez JJ, De Mey M et al (2010) Microbial succinic acid production: natural versus metabolic engineered producers. Process Biochem 45:1103–1114
2. Lee SY, Hong SH et al (2004) Fermentative production of chemicals that can be used for polymer synthesis. Macromol Biosci 4:157–164
3. Wendisch VF, Bott M et al (2006) Metabolic engineering of Escherichia coli and Corynebacterium glutamicum for biotechnological production of organic acids and amino acids. Curr Opin Microbiol 9:268–274
4. Zeikus JG, Jain MK et al (1999) Biotechnology of succinic acid production and markets for derived industrial products. Appl Microbiol Biotechnol 51:545–552
5. Beauprez JJ, Foulquie-Moreno MR et al (2011) Influence of C4-dicarboxylic acid transporters on succinate production. Green Chem 13:2179–2186
6. Lee SJ, Song H et al (2006) Genome-based metabolic engineering of Mannheimia succiniciproducens for succinic acid production. Appl Environ Microbiol 72:1939–1948
7. Blankschien MD, Clomburg JM et al (2010) Metabolic engineering of Escherichia coli for the production of succinate from glycerol. Metab Eng 12:409–419
8. Lee SJ, Lee DY et al (2005) Metabolic engineering of Escherichia coli for enhanced production of succinic acid, based on genome comparison and in silico gene knockout simulation. Appl Environ Microbiol 71:7880–7887
9. Sanchez AM, Bennett GN et al (2005) Novel pathway engineering design of the anaerobic central metabolic pathway in Escherichia coli to increase succinate yield and productivity. Metab Eng 7:229–239
10. Raab AM, Gebhardt G et al (2010) Metabolic engineering of Saccharomyces cerevisiae for the biotechnological production of succinic acid. Metab Eng 12:518–525
11. Lin H, Bennett GN et al (2005) Genetic reconstruction of the aerobic central metabolism in Escherichia coli for the absolute aerobic production of succinate. Biotechnol Bioeng 89:148–156
12. Lin H, Bennett GN et al (2005) Metabolic engineering of aerobic succinate production systems in Escherichia coli to improve process productivity and achieve the maximum theoretical succinate yield. Metab Eng 7:116–127
13. Becker J, Wittmann C (2011) Bio-based production of chemicals, materials and fuels - Corynebacterium glutamicum as versatile cell factory. Curr Opin Biotechnol 23:1–10
14. Litsanov B, Brocker M et al (2012) Glycerol as a substrate for aerobic succinate production in minimal medium with Corynebacterium glutamicum. Microb Biotechnol 6(2):189–195

15. Litsanov B, Kabus A et al (2011) Efficient aerobic succinate production from glucose in minimal medium with Corynebacterium glutamicum. Microb Biotechnol 5:116–128
16. Eggeling L, Bott M (2005) Handbook of Corynebacterium glutamicum. CRC Press, Boca Raton
17. Lee PC, Lee SY et al (2003) Biological conversion of wood hydrolysate to succinic acid by Anaerobiospirillum succiniciproducens. Biotechnol Lett 25:111–114
18. Underwood SA, Buszko ML et al (2002) Flux through citrate synthase limits the growth of ethanologenic Escherichia coli KO11 during xylose fermentation. Appl Environ Microbiol 68:1071–1081
19. Yasuda K, Jojima T et al (2007) Analyses of the acetate-producing pathways in Corynebacterium glutamicum under oxygen-deprived conditions. Appl Microbiol Biotechnol 77:853–860
20. Lin H, Bennett GN et al (2009) Chemostat culture characterization of Escherichia coli mutant strains metabolically engineered for aerobic succinate production: a study of the modified metabolic network based on metabolite profile, enzyme activity, and gene expression profile. Metab Eng 7:337–352

Chapter 35
Study on Submerged Fermentation Conditions for Intracellular Polysaccharide of *Cordyceps gunnii*

Kezhuang Sun, Zhenyuan Zhu, Lina Ding, Xiaocui Liu and Anjun Liu

Abstract Optimization of liquid culture conditions on the production of intracellular polysaccharide by *Cordyceps gunni* was carried out in submerged cultures. According to single test and the orthogonal design, the results showed that the fermentation condition was sucrose 4 %, peptone 1.0 %, KH_2PO_4 0.05 %, $MgSO_4$ 0.15 %, shaking rate 150 r/min, initial pH natural, inoculation rate 8 %. The maximum intracellular polysaccharide production of 217 mg/100 mL was achieved with the optimized culture conditions.

Keywords *Cordyceps gunnii* · Intracellular polysaccharide · Fermentation

35.1 Introduction

Cordyceps gunnii (berk.) Berk, a major entomogenous fungus, belongs to the Ascomycota, Pyrenomycetes, Sphaeriales, Clavicipitaceae, and parasites on the larvae of Hepialidae. It is also well known as the Chinese rare caterpillar fungus and has similar pharmacological activities to the famous Chinese traditional medicine *C. sinensis*. The anamorph of Paecilomyces gunii of *C. gunnii* has been isolated, verified, and identified [1]. Fermentation mycelia had efficacies of sedation, analgesia, enhancing memory, anti-tumor, protecting brain from oxygen deficiency, reducing the oxygen consumption of heart muscle in the case of oxygen deficiency, and improving the phagocytic effect of peritoneal macrophages in mice [2]. Many important secondary metabolic products were found in Paecilomyces gunii mycelia including cordycepin, cordycepic acid, polysaccharide and

K. Sun · Z. Zhu (✉) · L. Ding · X. Liu · A. Liu
Key Laboratory of Food Nutrition and Safety, Ministry of Education, College of Food Science and Biotechnology, Tianjin University of Science and Technology, Tianjin 300457, People's Republic of China
e-mail: zhyuanzhu@tust.edu.cn

T.-C. Zhang et al. (eds.), *Proceedings of the 2012 International Conference on Applied Biotechnology (ICAB 2012)*, Lecture Notes in Electrical Engineering 249,
DOI: 10.1007/978-3-642-37916-1_35, © Springer-Verlag Berlin Heidelberg 2014

anti-ultraviolet radiation constituents [3]. Consequently, it has received special attention for medicinal purpose due to its various physiological constituents [4–7].

Previous studies in our laboratory demonstrated that the intracellular polysaccharides (IPS) from the fermentation mycelia of *C. gunnii* possessed good antioxidation and anti-tumor effects [8, 9]. The aim of the present study was to optimize the cultivation conditions in a submerged culture that employed to simultaneously produce IPS via *C. gunnii* using the one-factor-at-a-time method and orthogonal experiment.

35.2 Materials and Methods

35.2.1 Material

C. gunnii berk (ZZY) used in this study was obtained from the Laboratory of Biological Resources and Functional Foods in Tianjin University of Science and Technology. The strain was maintained on potato dextrose agar (PDA) slants. The slant was incubated at 25 °C for 7 days, and then stored at 4 °C.

35.2.2 Inoculum Preparation

The activated mycelium was grown on PDA for 7 days. The seed culture was grown in a 250 ml Erlenmeyer flask at 25 °C on a rotary shaker incubator at 150 rpm for 4 days and the seed medium was composed of 2 % glucose, 1 % peptone, 0.3 % KH_2PO_4, 0.15 % $MgSO_4 \cdot 7H_2O$. The mycelium was then homogenized with a sterilized blender for 30 s and used as the inocula in the following experiments.

35.2.3 Fermentation and Mycelia Preparation

Fermentation medium was 4 % carbon, 1 % nitrogen, 0.3 % KH_2PO_4, 0.15 % $MgSO_4 \cdot 7H_2O$. And medium in the study was in accordance with the orthogonal design. The fermentation medium was inoculated with 8 % (v/v) the seed culture, and placed a 250 ml Erlenmeyer flask with 100 mL liquid at 25 °C on a rotary shaker incubator at 150 rpm for 5 days. The cultured mycelia of ZZY were separated from the medium and sufficiently rinsed with distilled water, then freeze-dried. We got dry powder of mycelia.

35.2.4 Orthogonal Layout

Media and cultural conditions were designed to meet the nutritional demands of the producer organism, the objectives of the process and the scale of the operation. The carbon source, nitrogen source, bioelements, growth factors, and initial pH (pH value of unsterilized culture broth) were regarded as correlated factors of the culture medium, in particular carbon and nitrogen source. Therefore, according to the varieties of media, we designed single factor experiments of carbon and nitrogen source in shake flask cultures. Based on the results of single factor test, the cultural conditions including carbon, nitrogen were further optimized by a L_9 (3^4) orthogonal test. The cultural factors and the levels of these factors are outlined in Table 35.1.

35.2.5 Analytical Methods

Intracellular polysaccharides (IPS) were extracted from dried mycelia (400 mg) by suspending the mycelia in 8 ml distilled water and 80 °C for 2 h, repeated three times. The extract gathered in one container, and was centrifuged at 4,500 g for 20 min, and the supernatant was collected that used for measuring the polysaccharide content. The polysaccharide content was measured by a phenol-sulfuric acid method.

35.3 Results and Discussion

35.3.1 Carbon Screening

The most commonly used carbon source is glucose, sucrose, soluble starch, which were used in this experiment for carbon screening. The results of the carbon source screening were observed (Table 35.2). The maximal IPS production was cultured in the sucrose medium.

Table 35.1 Experimental design

Factors	Sucrose (%)	Peptone (%)	K_2HPO_4 (%)	$MgSO_4 \cdot 7H_2O$ (%)
1	2	0.5	0.05	0.05
2	3	1	0.1	0.1
3	4	1.5	0.15	0.15

Table 35.2 Effect of various carbon on simultaneous production of mycelia and polysaccharide in submerged cultivation of *C. gunnii*

	Glucose 4 %	Sucrose 4 %	Soluble starch 4 %
Dry mycelia weight (g/100 mL)	1.246 ± 0.034	1.498 ± 0.043	1.114 ± 0.087
IPS (mg/100 mL)	91.3 ± 9.37	93 ± 6.84	73.24 ± 6.10

35.3.2 Effect of Sucrose Concentration on the Production of IPS

The effects of sucrose concentration on the mycelia growth and the production of IPS by ZZY in submerged cultivation are shown in Table 35.3. As sucrose concentration increased in range of 1–4 %, the mycelia weight was on an increase. It means that the suitable carbon can facilitate the cell growth. And the production of IPS was increasing identically. The maximal IPS production was 147.4 mg per 100 mL fermentation broth at 4 % sucrose medium.

35.3.3 Nitrogen Screening

The nitrogen sources are peptone, beef extract, yeast extract, which were used in this experiment for nitrogen screening. The results of the nitrogen source screening were observed in Table 35.4. The maximal IPS production was cultured in the peptone medium.

35.3.4 Effect of Peptone Concentration on the Production of IPS

The effects of peptone concentration on the mycelia growth and the production of IPS by ZZY in submerged cultivation are shown in Table 35.5. As peptone concentration increased in range of 0.5–2.5 %, the mycelia weight was not changed a lot. It means that the organic nitrogen sources can be suit for the cell growth. But the production of IPS was different. The maximal IPS production was 102.5 mg per 100 mL fermentation broth at 1 % peptone medium.

35.3.5 Optimization of IPS Production by Orthogonal

Table 35.6 summarizes the influence of the four factors (sucrose, peptone, KH_2PO_4, and $MgSO_4 \cdot 7H_2O$) on mycelial IPS production in *C. gunnii berk* ZZY.

Table 35.3 Effect of sucrose concentration on simultaneous production of mycelia and polysaccharide in submerged cultivation of *C. gunnii*

	1 % sucrose	2 % sucrose	3 % sucrose	4 % sucrose	5 % sucrose	6 % sucrose
Dry mycelia weight (g/100 mL)	1.022 ± 0.015	1.403 ± 0.016	1.432 ± 0.021	1.503 ± 0.079	1.265 ± 0.042	1.616 ± 0.041
IPS (mg/100 mL)	50.93 ± 6.96	101.72 ± 9.02	106.60 ± 2.25	147.39 ± 4.12	59.51 ± 8.56	149.40 ± 3.84

Table 35.4 Effect of various nitrogen sources concentration on simultaneous production of mycelia and polysaccharide in submerged cultivation of *C. gunnii*

	Peptone 1 %	Beef extract 1 %	Yeast extract 1 %
Dry mycelia weight (g/100 mL)	1.288 ± 0.024	1.268 ± 0.056	1.313 ± 0.029
IPS (mg/100 mL)	119.30 ± 6.83	76.18 ± 6.35	75.18 ± 7.09

Table 35.5 Effect of peptone concentration on simultaneous production of mycelia and polysaccharide in submerged cultivation of *C. gunnii*

	Peptone 0.5 %	Peptone 1.0 %	Peptone 1.5 %	Peptone 2.0 %	Peptone 2.5 %
Dry mycelia weight (g/100 mL)	1.683 ± 0.193	1.772 ± 0.049	1.683 ± 0.120	1.655 ± 0.017	1.599 ± 0.187
IPS (mg/100 mL)	93.48 ± 6.45	102.5 ± 2.69	90.05 ± 9.45	98.73 ± 3.05	94.61 ± 4.17

Table 35.6 Result of Orthogonal

Factors	1 Sucrose (%)	2 Peptone (%)	3 KH_2PO_4 (%)	4 $MgSO_4{\cdot}7H_2O$ (%)	IPS (mg/100 mL)
Test 1	2	0.5	0.05	0.05	97.357
Test 2	2	1	0.1	0.1	104.127
Test 3	2	1.5	0.15	0.15	79.263
Test 4	3	0.5	0.1	0.15	117.914
Test 5	3	1	0.15	0.05	107.876
Test 6	3	1.5	0.05	0.1	164.264
Test 7	4	0.5	0.15	0.1	216.844
Test 8	4	1	0.05	0.15	202.09
Test 9	4	1.5	0.1	0.05	123.826
I	93.582	144.038	154.57	109.686	
II	130.018	138.031	115.289	161.745	
III	180.92	122.451	134.661	133.089	
R	87.338	21.587	39.281	52.059	

The R value showed that sucrose was a more important factor than other culture conditions in the orthogonal layout L9(3^4). The R value of sucrose (87.338) was higher than that of peptone (21.587), KH_2PO_4 (39.281), and $MgSO_4{\cdot}7H_2O$ (52.059), hence sucrose indicated significantly influence.

In accordance with the results of the orthogonal layout, taking all the influencing factors and the results into consideration, the optimal cultural process of *C. gunnii berk* ZZY was considered as follows: media and cultural conditions including sucrose 4 %, peptone 0.5 %, KH_2PO_4 0.15 %, $MgSO_4{\cdot}7H_2O$ 0.1 %, natural pH, inoculum size 8 %, medium capacity 100 mL/250 mL flask, and culture time 5 days.

35.4 Conclusion

In this study, a process of submerged cultivation of *C. gunnii* for production of a bioactive compound, intracellular polysaccharide, was demonstrated.

The effects of major nutrients, i.e., carbon and nitrogen sources, on intracellular polysaccharide production were studied in order to obtain a suitable fermentation medium. Sucrose and peptone were optimal carbon and nitrogen sources for cell growth and intracellular polysaccharide production. According to the orthogonal layout design and analysis, an optimal carbon source (sucrose 4 %) and nitrogen source (peptone 0.5 %) were identified and a maximal intracellular production 217 ± 0.15 mg/mL was successfully obtained in same cultivation conditions. The fundamental information obtained in this work is beneficial for further development of *C. gunnii* cultivation process for production of intracellular polysaccharide on a large scale.

Acknowledgments This work was financially supported by National Agricultural Innovation Project (No. 2011GB2A100009) and the Foundation of Tianjin Educational Committee (No. 20090604).

References

1. Liang ZQ (1985) Isolation and identification of the conidial stage of *Cordyceps gunnii*. Acta Mycol Sinica 4:162–166
2. Liang ZQ, Liu AY, Dong XC et al (1991) In study and application of entomogenous fungi in China, division of entomogenous fungi, chinese society of mycology. China Agric Scientific Press 2:74–80
3. Huang JZ, Liang ZQ, Liu AY (1992) Protection on the anamorph of *Cordyceps pruinosa* Petch to anti-ultraviolet radiation in Bacillus thuringiensis. Southwest Chin J Agric Sci 5:63–67
4. Hou AI, Meng QF, An JS et al (2008) Isolation and purification of polysaccharides from *Cordyceps minlitaris* and its inhibition on the proliferation of rat glomerular mesangial cells. Chem Res Chinese U 24(5):584–587
5. Jiang YH, Jiang XL, Wang P et al (2008) The antitumor and antioxidative activities of polysaccharides isolated from Isaria farinose B05. Microbiol Res 163:424–430
6. Xiao JH, Chen DX, Fang N et al (2006) Growth arrest of human gastric adenocarcinoma cells by bioactive compounds of Cordyceps jiangxiensis (CaoMuWang) through induction of apoptosis. J Food Agric Environ 4:66–73
7. Sun YX, Wang SS, Li TB et al (2008) Purification structure and immunobiological activity of a new water-soluble polysaccharide from the mycelium of Polyporus albicans. Bioresource Technol 99:900–904
8. Liu AJ, Zhong YR, Zhu ZY et al (2008) Extraction, isolation and analysis of the polysaccharides from Cordyceps gunnii. Modern Food Sci Technol 24(1):28–31
9. Zhu ZY, Si CL, Zhong YR et al (2011) The purification and antioxidative activities in D-galactose-induced aging mice of a water-soluble polysaccharide from Cordyceps gunnii. J Food Biochem 35(1):303–322

Chapter 36
Deletion of Gene *recG* and its Susceptibility to Acetic Acid in *Escherichia coli*

Yu Zheng, Qi Han, Chunyue Jiang, Zhiqiang Nie and Min Wang

Abstract The gene *recG* encodes DNA helicase RecG which is involved in DNA replication, recombination, and repair. In this research, the λ Red homologous recombination system was used to delete *recG* gene of *Escherichia coli* resulting in the cut-off of part of the DNA repair pathway. The results showed that the *recG*-deficient mutant strain showed increasing significant growth disadvantages compared to the wild-type strain in the presence of acetic acid varied from 0.02–0.09 %. It was also observed that over 10-fold more *recG*-deficient mutant cells died than that of wild-type cells after shocking with 0.5 % acetic acid for 40 mins, specially, the mutant could not grow under 0.07 % acetic acid condition compared with the wild-type strain. The results showed that *recG*-deficient mutant strain is more susceptible to high concentration of acetic acid than the wild-type strain, indicating RecG may involve the repair of DNA damage caused by acetic acid.

Keywords Acetic acid · DNA helicase · *Escherichia coli* · Gene deletion · *recG*

36.1 Introduction

Acetic acid which can intensively inhibit cell growth and decrease the yields of target products during the fermentation processes is toxic for most bacteria. Three major aspects of cell functions may be affected by acidic conditions: the capacity for nutrient acquisition and energy generation, cytoplasmic pH homeostasis, and protection of proteins and DNA [1]. The available data suggest that cytoplasmic

Y. Zheng · Q. Han · C. Jiang · Z. Nie · M. Wang (✉)
Key Laboratory of Industrial Fermentation Microbiology, Ministry of Education, Tianjin Key Lab of Industrial Microbiology, College of Biotechnology, Tianjin University of Science and Technology, Tianjin 300457, People's Republic of China
e-mail: minw@tust.edu.cn

T.-C. Zhang et al. (eds.), *Proceedings of the 2012 International Conference on Applied Biotechnology (ICAB 2012)*, Lecture Notes in Electrical Engineering 249,
DOI: 10.1007/978-3-642-37916-1_36, © Springer-Verlag Berlin Heidelberg 2014

pH falls rapidly when cells are incubated at extremely acidic conditions [1]. For the organism which could survive when rapidly shifted to an acidic condition there must be some protective mechanisms that allow surface structures to remain functional and cytoplasmic proteins and DNA to be protected or repaired.

Acid-induced damage to the DNA may arise either through aberrant chemical reactions or via failure of repair. DNA repair has been implicated in the resistant bacteria to acidic pH [2–4]. And the previous data suggested enhanced DNA repair in acid-adapted cells [5]. One way of the DNA repair is recombinational repair including *recA* and *recG*. In *E. coli* and *Helicobacter pylori*, mutants defective in the *recA* were shown previously to be more acid sensitive than the wild-type strain, suggesting it's function in the repair of acid-induced DNA damage [5, 6]. In addition, overexpression of RecG whose function is DNA replication/repair from *Acetobacter aceti*, *Staphylococcus capitis*, and *E. coli*, increased the maximum biomass concentration attained by *E. coli* cultures grown in the presence of various weak organic acids and uncouples [7].

The RecG protein of *E. coli* are necessary for normal recombination and DNA repair, and they have been shown to help Holliday junction intermediates change into mature products by catalyzing branch migration [8, 9]. In this chapter, *E. coli* MG1655 mutant strain with targeted deletion of *recG* gene was constructed and the effect of inactive RecG on *E. coli* susceptibility to acetic acid has been investigated.

36.2 Materials and Methods

36.2.1 Bacterial Strains and Growth Conditions

The strain *E. coli* MG1655 and plasmids pKD46, pKD3, and pCP20 kindly provided by Professor B. Wanner (Purdue University) were used in this study. Luria–Bertani medium (with 2 % agar for solid medium) was used as the standard medium. *E. coli* was transformed by the $CaCl_2$ method or electroporation (25 μF, 400 Ω, 2.5 kV, with use of a 0.2 cm cuvette). All transformants were selected by antibiotic. Antibiotic concentrations used (μg/ml) were ampicillin (Ap) 100, chloramphenicol (Cm) 20. Both pKD46 and pCP20 show temperature-sensitive replication and can be simply cured by growth at 37 °C.

36.2.2 Construction of a recG*-Deficient Mutant of* E. coli

Gene knockout mutants were constructed by one-step inactivation method [10]. The chloramphenicol (Cm)-resistance gene was amplified by PCR with plasmid pDK3 as a template, using primers containing the *recG* gene recombination arm

(5′-ATGAAAGGTCGCCTGTTAGATGCTGTCCCACTCAGTTCCCTAACGG GGTATGGGAAT TAGCCATGGTCC-3′ and 5′-GCCCGCGCAGCTGGTG-TAACTGCGCCAGACCCAGACGCTCCGGGTTTTCGGT GAGGCTGGAGCT GCTTC-3′, and *recG* gene recombination arm up (nucleotide positions 1–50) and down (nucleotide positions 1701–1750) are underlined. For deleting *recG* gene, the PCR-generated fragment was introduced into *E.coli* MG1655 by electroporation, and Cm-resistant colonies were selected as candidate *recG*-deficient mutants. In the mutant strains, the target gene was replaced with a Cm-resistance gene flanked by FRT (FLP recognition target) sites. In order to amplify the intact *recG* gene, the Cm-replaced *recG* gene and the Cm-eliminated *recG* gene from *E. coli* MG1655 by PCR, a forward primer, 5′-GCCGACTGGTGGGCTACTAT-3′, and a reverse primer, 5′-CCGCAACAAAGACAAATGC-3′ were designed on the basis of the sequence data. After selection, the Cm-resistance gene was eliminated by using the helper plasmid pCP20.

36.2.3 Growth Assay

To test the growth of the mutants toward acetic acid, *E. coli* MG1655 cells and the mutant cells were grown overnight at 37 °C in LB medium. The overnight cultures were diluted to an OD_{600} of 0.02 in LB medium containing different concentration of acetic acid (0.03, 0.05, 0.07, and 0.09 %, v/v), and then grown at 37 °C. OD_{600} was monitored during growth.

36.2.4 Shock Experiments

To test the sensitivity of the mutants toward acetic acid, shock experiments were performed with much higher concentrations of acetic acid (0.5 %, v/v). Cells were grown overnight at 37 °C in LB medium, then diluted at a ratio of 1:100 into fresh LB medium, and grown at 37 °C to logarithmic phase with an OD_{600} of 2.0. The cultures were then diluted with fresh LB medium to an OD_{600} of 1.0, and acetic acid was added to final concentrations of 0.05 and 0.5 % (v/v). After incubation at 37 °C for different time, samples were removed and numbers of viable bacteria were determined by spreading serial dilutions onto LB agar. The cultures shocked for 30 min were serially diluted, and then plated onto LB/agar plates and incubated at 37 °C for 24 h.

36.3 Results and Discussion

36.3.1 PCR Analysis of the recG*-Deficient Mutant*

The RecG ORF is 2,079 bp long and encodes 693 amino acid residues. PCR was used to indicate the recombination and deletion of gene *recG* in *E. coli* MG1655, the result was shown in Fig. 36.1. In this case, a band of about 2.1 Kb was observed, as was the case for the intact *recG* fragment. Moreover, two bands of approximate 1.6 and 0.8 Kb were also detected, as were the cases for the Cm-replaced *recG* fragment and the Cm-eliminated *recG* deletion fragment, respectively. For further verification, the fragment from Cm-eliminated *recG* deletion mutants was sequenced, and the result revealed that a 1,375-nt deletion which could cause the inactive RecG protein was deleted.

36.3.2 Effect of recG *Deletion on the Growth of* E. coli *MG1655 Under Acidic Conditions*

To test whether *recG*-deficient mutant strain was more susceptible to the acetic acid, the growth of the strains was assayed by the OD_{600} value after 24 h cultivation in LB broth supplemented with different concentration of acetic acid. The growth of the strains was similar when the acetic acid concentration was below 0.05 %, however, the growth rates and cell masses of the parental strain during the exponential growth phase in LB medium were higher than those of the mutants. This result indicated that the inactivation of RecG partly affected DNA recombination and repair under common growth condition. While, in LB medium supplemented

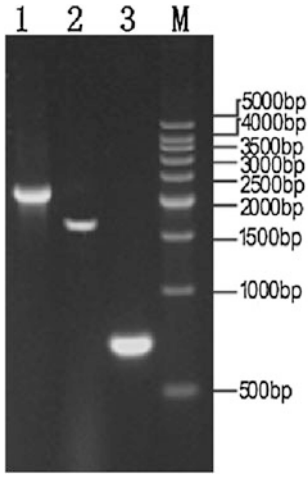

Fig. 36.1 PCR identification of *recG*-deficient mutants, *1* Wild-type strain; *2* Cm-replaced *recG*-deficient mutant; *3* Cm-eliminated *recG*-deficient mutant; *M* DNA Marker

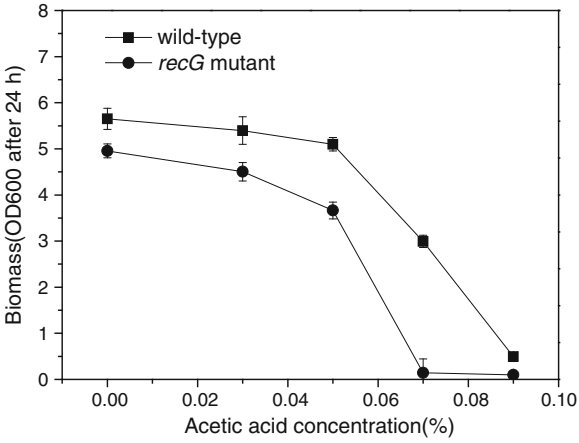

Fig. 36.2 Effect of RecG deletion on the growth of *E. coli* MG1655 under acidic conditions

with 0.05 % acetic acid, the *recG*-deficient mutant cells had a more obvious growth disadvantage (Fig. 36.2). The growth disadvantage of mutant was also significant compared with the control cells. After 24 h cultivation, the ratios of the OD of *recG*-deficient mutant to that of control strain were 87, 83, 67, and 5 % when the acetic acid concentration were 0, 0.03, 0.05, and 0.07 %, respectively. Specially, under 0.07 % acetic acid condition, the mutant could not grow, but the wild-type strain showed the significant growth advantage that OD_{600} values after 24 h was 3.1. Therefore, the *recG*-deficient mutant was more susceptible to high concentrations of acetic acid (above 0.05 %) compared with the wild-type cells.

36.3.3 Effect of recG *Deletion on the Growth of* E. coli *MG1655 Under Acid-Shock*

After short time of incubation in fresh LB medium supplemented with acetic acid, acidic survival curves for the *recG*-deficient strain and the wild-type strain were shown in Fig. 36.3a. With increasing shock time, the *recG*-deficient mutant showed a clearly increasing sensitivity to the acetic acid compared with the wild-type strain when exposed to both 0.05 and 0.5 % acetic acid. During the first 20 min of the 0.05 % acetic acid exposure, *recG*-deficient strain and the wild-type strain showed a similar pattern of sensitivity as compared with that of 0.5 % acetic acid exposure. A slightly higher susceptibility to 0.5 % acetic acid-shock for 40 min was observed in the mutant, and the mutant showed more than a 10-fold higher susceptible than the wild-type strain.

Furthermore, after shocking with 0.5 % acetic acid for 40 min, approximately 10-fold more wild-type cells survived compared with the *recG*-deficient mutant cells (Fig. 36.3b). However, the cell mass of *recG*-deficient mutant was almost the same as that of the parental strain under common condition.

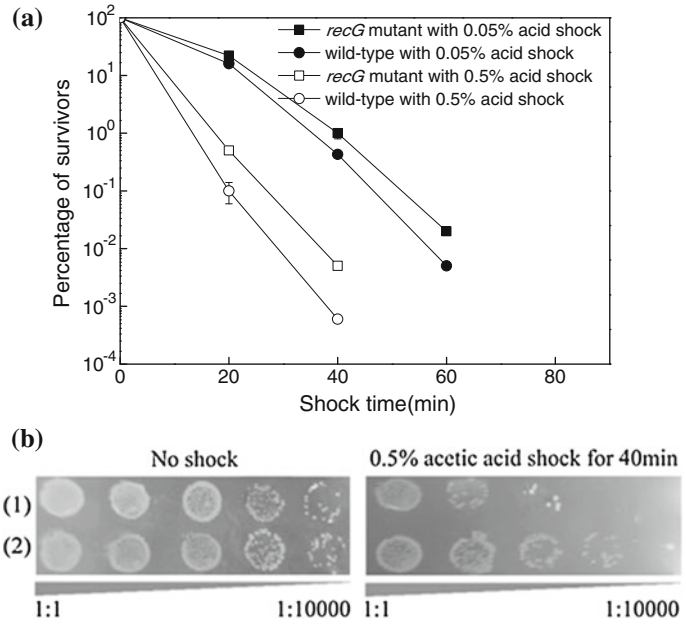

Fig. 36.3 Effect of RecG deletion on the survivors of *E. coli* MG1655 under acid-shock conditions. **a** Cells were cultured after the shock of 0.05 and 0.5 % acetic acid; **b** Cells were cultured after the shock of 0.5 % acetic acid for 40 min

These results indicated that the inactivation of *recG* was responsible for the susceptible to acid-shock. Since RecG is involved in diverse functions related to DNA metabolism, including DNA repair, the difference in the sensitivity to acid environments may be due to the relative difference in the ability to repair the lesions induced by acid.

36.4 Discussion

We have constructed a *recG*-deficient mutant of *E. coli* with the Red recombinant system which is a simple and highly efficient method to disrupt chromosomal gene. The *recG*-deficient mutant displayed an increasing growth disadvantages in the presence of acetic acid with a concentration from 0 to 0.09 %. The inactivation of *recG* was able to lessen cell viability under a shock of higher concentration acetic acid, indicating that *recG*-deficient mutant resulted in a slightly higher susceptibility to acid than the wild-type strain. These results implied that the RecG, DNA helicase displayed a critical role in resisting to acetic acid.

The experimental data suggested the increased sensitivity of the *recG*-deficient mutant compared with the wild-type *E. coli* strain to acid treatment may partly attribute to reduced capability of the repair-deficient strain to restore the damaged

DNA. Moreover, lesions induced by acidity were not efficiently repaired in the *recG*-deficient mutant strains and the unrepaired breaks might be a significant cause of cell death. It also has been previously demonstrated that inactivation of the *recG* genes in *E. coli* showed a clear increases in the susceptibilities to Cr(VI), mitomycin C, and UV radiation [8, 11, 12]. However, an adaptive response to one stress can often lead to cross-protection against other stresses [11]. Further evidence for this hypothesis comes from the firmly established low-pH-induced DNA damage in bacteria [13–16]. After being internalized, most damages caused single-strand breaks, DNA–DNA interstrand links, DNA-protein cross-links and nucleotide oxidation, among other modifications [17]. Some of these damages may be alleviated by the recombinational repair system, which has been widely studied in *E. coli* [18]. In this process, the RecG helicase and the RuvABC resolvase complex catalyzes branch migration of Holliday junction recombinational intermediates, leading to the restoration of undamaged DNA [18, 19]. Thus, the results presented here suggested that the RecG may be of physiological relevance in acidic environments, since acid-habituated *E. coli* exhibit a higher DNA repair activity [2].

Lastly, our results showed *recG*-deficient mutant strain is more susceptible to high concentration of acetic acid than the wild-type strain, and this is in agreement with the previously reported higher sensitivity of DNA repair mutants to weak organic acid and low-pH challenges [5, 16, 20]. In addition, the RecG promotes the rescue of replication forks that are stalled at damaged DNA [19, 21, 22], we presume that the mechanisms of helicase-mediated resistance to acid may be via DNA replication-repair.

Acknowledgments This work was supported by National High Technology Research and Development Program of China (2012AA022108), Program for Changjiang Scholars and Innovative Research Team in University (IRT1166), Doctoral Program Foundation of Institutions of Higher Education of China (20101208120003), National Natural Science Foundation of China (31201406), and Foundation of Tianjin University of Science and Technology (20110114).

References

1. Jordan SL, Glover J, Malcolm L et al (1999) Augmentation of killing of Escherichia coli O157 by combinations of lactate, ethanol, and low-pH conditions. Appl Environ Microbiol 65:1308–1311
2. Raja N, Goodson M, Chui WCM et al (1991) Habituation to acid in Escherichia coli: conditions for habituation and its effects on plasmid transfer. Appl Bacteriol 70:59–65
3. Raja N, Goodson M, Smith DG, Rowbury RJ (1991) Increased DNA damage by acid and increased repair of acid-damaged DNA in acid-habituated *Escherichia coli*. Appl Bacteriol 70:507–511
4. Bijlsma JJE, Lie-A-Ling M, Nootenboom CIC et al (2000) Identification of loci essential for the growth of Helicobacter pylori under acidic conditions. Infect Dis 182:1566–1569
5. Thompson SA, Blaser MJ (1995) Isolation of the *Helicobacter pylori recA* gene and involvement of the *recA* region in resistance to low pH. Infect Immun 63:2185–2193

6. Sinha RP (1986) Toxicity of organic acids for repair-deficient strains of *Escherichia coli*. Appl Environ Microbiol 51:1364–1366
7. Steiner P, Sauer U (2003) Overexpression of the ATP-dependent helicase RecG improves resistance to weak organic acids in *Escherichia coli*. Appl Microbiol Biotechnol 63:293–299
8. Lloyd RG, Buckman C (1991) Genetic analysis of the *recG* locus of *Escherichia coli* K-12 and of its role in recombination and DNA repair. Bacteriol 173:1004–1011
9. Whitby MC, Vincent SD, Lloyd RG (1994) Branch migration of Holliday junctions: identification of RecG protein as a junction specific DNA helicase. EMBO J 13:5220–5228
10. Datsenko KA, Wanner BL (2000) One-step inactivation of chromosomal genes in *Escherichia coli* K-12 using PCR products. Proc Natl Acad Sci USA 97(12):6640–6645
11. Hartke A, Bouche S, Gansel X et al (1995) UV-inducible proteins and UV-induced cross protection against acid, ethanol, H_2O_2 or heat treatments of *Lactobacillus lactis* subsp Lactis. Arch Microbiol 163:329–336
12. Miranda AT, Gonzalez MV, Gonzalez G et al (2005) Involvement of DNA helicases in chromate resistance by *Pseudomonas aeruginosa* PAO1. Mutat Res-Fund Mol M 578:202–209
13. Booth IR, Cash P, Byrne CO (2002) Sensing and adapting to acid stress. Anton Leeuw Int J G 81:33–42
14. Audia JP, Webb CC, Foster JW (2001) Breaking through the acid barrier: an orchestrated response to proton stress by enteric bacteria. Int J Med Microbiol 291:97–106
15. Foster JW (1995) Low pH adaptation and the acid tolerance response of *Salmonella typhimurium*. Crit Rev Microbiol 21:215–237
16. Hanna MN, Ferguson RJ, Li YH et al (2001) *uvrA* is an acid-inducible gene involved in the adaptive response to low pH in *Streptococcus mutans*. J Bacteriol 183:5964–5973
17. Friedberg EC, Walker GC, Siede W (1995) DNA Repair and muta-genesisM. ASM Press, Washington
18. West SC (1997) Processing of recombination intermediates by the RuvABC proteins. Annu Rev Genet 31:213–244
19. Sharples GJ, Ingleston SM, Lloyd RG (1999) Holliday junction processing in bacteria: insights from the evolutionary conservation of RuvABC, RecG and RusA. J Bacteriol 181:5543–5550
20. Cherrington CA, Hinton M, Mead GC et al (1991) Organic acids: chemistry, antibacterial activity and practical applications. Adv Microb Physiol 32:87–108
21. McGlynn P, Lloyd RG (2002) Genome stability and the processing of damaged replication forks by RecG. Trends Genet 18:413–419
22. Singleton MR, Scaife S, Wigley DB (2001) Structural analysis of DNA replication fork reversal by RecG. Cell 107:79–89

Chapter 37
Breeding of *Streptomyces diastatochromogenes* for Mass-Producing ε-Poly-L-Lysine by Composite Mutation

Shuai Song, Zhilei Tan, Fengzhu Guo, Xue Zhang, Qingchao Song and Shiru Jia

Abstract In order to improve the productivity of ε-Poly-L-Lysine (ε-PL) by *Streptomyces diastatochromogenes* Cbγ4, the selection and breeding of mass-producing strains were carried out through the single spore suspension treated with several groups of the composite mutation of NTG and UV and LiCl. The result showed that a high yield producing strain 6#−7 was obtained through 0.8 g/L NTG for 45 min, followed with UV irradiation for 45 s under magnetic stirring, and then through a series of screening, such as resistant plate, methylene blue plate, shake-flask screening. With the good genetic stability, the yield of ε-PL could reach 0.775 ± 0.046 g/L at 72 h, 42.2 % higher than the initial strain. Moreover, the mutant displayed a great potential for increasing productivity in later period of fermentation.

Keywords *Streptomyces diastatochromogenes* · ε-Poly-L-Lysine · Composite mutation · Screening

37.1 Introduction

Poly-ε-L-lysine (ε-PL) is a natural homopolyamide characterized by the peptide bond between α-carboxyl and ε-amino groups of L-lysine. The biopolymer with 25–30 residues was accidentally discovered as an extracellular material produced by filamentous actinomycetes group of *S. albulus* ssp. *Lysinopolymerus* strain 346 as a result of Shima and Sakai screening for Dragendorff's positive substances [1, 2]. The compound is biodegradable, water-soluble, good thermal stability,

S. Song · Z. Tan · F. Guo · X. Zhang · Q. Song · S. Jia (✉)
Key Laboratory of Industrial Microbiology, Ministry of Education, College of Biotechnology, Tianjin University of Science and Technology, Tianjin 300457, People's Republic of China
e-mail: jiashiru@tust.edu.cn

T.-C. Zhang et al. (eds.), *Proceedings of the 2012 International Conference on Applied Biotechnology (ICAB 2012)*, Lecture Notes in Electrical Engineering 249,
DOI: 10.1007/978-3-642-37916-1_37, © Springer-Verlag Berlin Heidelberg 2014

edible, and nontoxic toward human and the environment [3, 4]. Moreover, the biopolymer shows a wide range of antimicrobial activity [5] and antiphage action [6]. So as a novel biological preservative, ε-PL has been widely used as a food additive in Japan, Korea, and western countries [7, 8].

Due to its excellent biological properties, ε-PL and its derivatives attracted a great deal of attention and offered a wide range of unique applications such as lipase inhibitor, drug carriers, gene carriers, emulsifying agent, highly water absorbable hydrogels, interferon inducer, and biochip coatings [9–13].

To meet the great demand for ε-PL in such applications, the huge commercial production of ε-PL is considered indispensable. To improve the ε-PL productivity, by means of nitrosoguanidine treatment, Hiraki derived S-(2-aminoethyl)-L-cysteine (AEC) plus glycine-resistant mutants, 99 % found to be high producer, and No. 11011A showed maximum productivity of 2.11 mg/mL in a test-tube culture, which was 10 times higher than the wild strain *Lysinopolymerus* No. 346 [14]. In Japan ε-PL has been manufactured at the commercial scale by a fermentation process using the mutant of No. 346 [15], while domestic study still rest on the lab level. Up to date, the biosynthesis mechanism of ε-PL has not been clearly clarified, which makes the breeding a bottleneck problem. Many scholars are devoted to the breeding of desirable strains mass-producing ε-PL. In the present study, the initial strain *S. diastatochromogenes* Cbγ4 was treated with several groups of composite mutation of NTG and UV and LiCl, then followed with a couple of different resistance screenings to obtain the desirable strains.

37.2 Materials and Methods

37.2.1 Microorganism

The initial ε-PL producing strain Cbγ4, which was identified as *S. diastatochromogenes*, was isolated from soil samples of Hainan Island and preserved in our laboratory [16].

37.2.2 Culture Medium

The origin strain was maintained on modified Bennett's agar slant, which contained (per liter): glucose, 10 g; beef meat extract, 1 g; polypepton, 2 g; yeast extract, 1 g; and agar, 18 g, the pH adjusted to 7.7 with 2 M NaOH solution.

Medium M3G, which contained (per liter): glucose, 50 g; yeast extract (Oxoid Ltd., England), 5 g; $(NH_4)_2SO_4$, 10 g; $K_2HPO_4{\cdot}3H_2O$, 0.8 g; KH_2PO_4, 1.36 g; $MgSO_4{\cdot}7H_2O$, 0.5 g; $ZnSO_4{\cdot}7H_2O$, 0.04 g; $FeSO_4{\cdot}7H_2O$, 0.03 g, the pH adjusted

to 7.2 with NH_4OH solution (24–28 %, w/v), was used for both seed culture and production culture throughout the study.

The above media were autoclaved at 120 °C for 20 min, and in each case, glucose and yeast extract were autoclaved separately.

37.2.3 Culture Conditions

For seed culture, a loopful of the spore from the stock culture was inoculated into a 500-mL Erlenmeyer flask containing l00 mL M3G medium and cultured at 30 °C, 180 rpm on a rotary shaker for 30 h. For shake-flask production with two-stage fermentation, 100 mL M3G in 500-mL flask was inoculated with 6 % v/v of precultured seed culture and then cultured at 30 °C, 180 rpm for 72 h.

Batch culture was performed in a 5 L jar-fermenter with a 3 L working volume. 300 mL 30 h cultured seed broth was inoculated into 2.7 L sterilized M3G. With aeration 1–2 vvm and agitation 300–1,000 rpm, dissolved oxygen (DO) was controlled at about 30 % monitored with a DO electrode. The pH monitored with a pH electrode was kept 4.0 automatically with aqueous ammonia when pH dropped to below 4.0. The fermentation temperature remained at 30 °C with cooling water. When the remaining glucose (RG) of the broth in the tank was depleted, the batch fermentation was finished.

37.2.4 Mutagenesis Procedures

Based on the individual fatality rate of NTG and UV [17], the single spore suspension prepared in advance was treated with certain concentration of NTG for 45 min, followed with UV irradiation for several seconds under magnetic stirring, then kept in ice-water bath for 2 h.

37.2.5 Screening Procedures

37.2.5.1 Screening on Agar Plate

Firstly the design of resistant Bennett's agar plate and methylene blue M3G agar plates was carried out in Table 37.1.

The overnight cultured and diluted spore suspension samples were transferred onto the agar plates that contain couples of different resistance and incubated at 30 °C for several days. Based on colonial morphology and growth rate, the selected actinomycetes colonies were subcultured onto the methylene blue agar plates. Due to the electrostatic interaction, the strains having the largest ratios of

Table 37.1 The addition of resistance to the Bennet's agar plate

Label	The addition of resistance (mg/ml)						
	AEC	AHV[a]	Glycine	SG[b]	Threonine	Lysine	LiCl
a	10		5	5			5
b	15		5	5			5
c	10		5		4		5
d	15		5		4		5
e		2	5	5		2	5
f		4	5	5		4	5

[a] AHV (DL-β-Hydroxynorvaline); [b] SG (Sulfaguanidine)

the size of the transparent circle to the size of the colonies were transferred to further screen by shaking flask fermentation.

37.2.5.2 Screening by Flask Fermentation

Each selected colony was inoculated into a 500 ml flask containing 100 mL M3G medium and cultured at 30 °C on a rotary shaker (180 rpm). After incubation for 72 h, select the strains with the high ε-PL concentration in the culture broth to second flask screening with two-stage fermentation.

37.2.6 Analytical Methods

The Itzhaki method improved by our laboratory was adopted for determination of ε-PL concentration in the culture broth [18, 19]. The residual glucose was determined using a biosensor SBA-40C (Shandong academy of sciences). The pH was determined using an acidometer (FE20, Mettler Toledo). Biomass accumulation was determined using dry cell weight analysis.

37.3 Result and Discussion

37.3.1 Composite Mutation and Resistant Agar Plate Design

Figure 37.1 showed that the fatality rate reached 82.5 % when the concentration of NTG was 0.8 g/L, and based on that, we designed the composite mutation in Table 37.2.

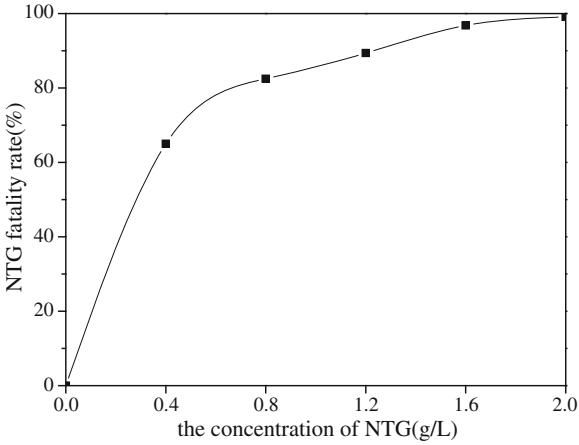

Fig. 37.1 The fatality rate of NTG on *Streptomyces diastatochromogenes*

Table 37.2 The scheme of composite mutation

Label	A	B	C	D
NTG (g/L)	0.6	0.8	0.8	1.0
UV (s)	60	30	45	30

37.3.2 Screening on Agar Plate and Shaking Flask

Based on colonial morphology and growth rate, 318 colonies from resistant agar plate were subcultured onto the methylene blue agar plates, from which 212 colonies were picked out for further screening with flask fermentation. Since the spore formation of some colonies on agar slant could not grow so well that only 170 strains were screened with flask fermentation. The results showed that 29 among them had remarkable performance for next screening with flask of two-stage fermentation. Finally, strain 6#−7 stood out with the highest ε-PL yield (0.775 ± 0.046 g/L), 42.2 % higher than the origin Cbγ4 (shown in Fig. 37.2). Moreover, the pH of the culture broth was 4.82 at 72 h, which was much higher than that of the other strains, so we prolonged the culture time for 6#−7. Figure 37.3 showed that in shaking flask with two-stage fermentation, as the culture time went on, the ε-PL productivity was increasing up to 1.318 g/L at 144 h, while the yield of Cbγ4 was slowly decreasing after 72 h. We could see that in the later period of fermentation the biomass and yield of the mutant were always higher than that of Cbγ4 till to the end.

Figure 37.4 demonstrated the fermentation performances of the mutant and origin strain in 5 L jar-fermenter with batch culture. At 48 h the ε-PL production of 6#−7 reached 3.24 g/L, 40.9 % higher than that of Cbγ4, 2.30 g/L, under the same culture conditions. Meanwhile, the mutant appeared to obtain larger biomass than the origin.

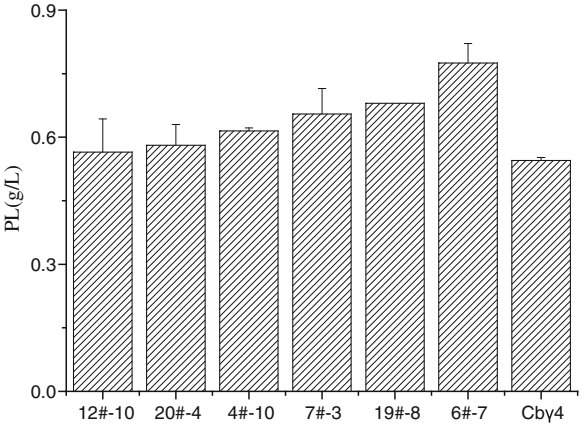

Fig. 37.2 The breeding results of screening with two-stage shaking flask fermentation

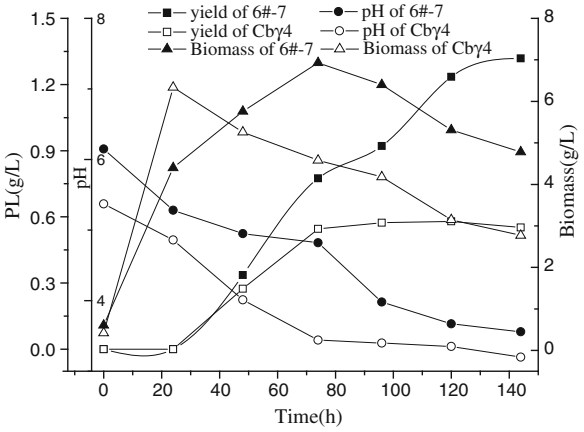

Fig. 37.3 Time profile of ε-PL production of 6#−7 and Cbγ4 in shaking flask with two-stage fermentation

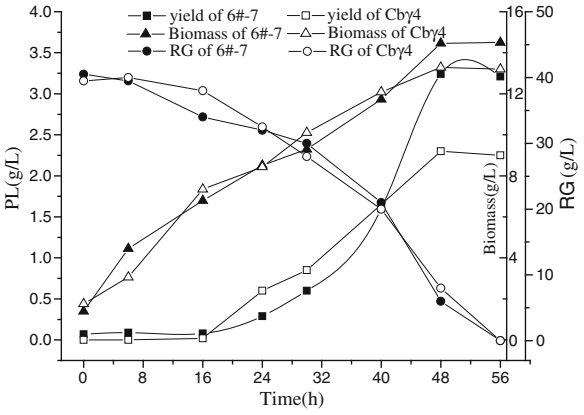

Fig. 37.4 Time profile of ε-PL production of 6#−7 and Cbγ4 in 5 L jar-fermenter in batch culture

Table 37.3 The genetic stability of mass-producing mutant strain 6#−7

Generation	1	2	3	4	5
The pH of culture broth	4.82	4.65	4.53	4.73	4.59
Biomass (g/L)	6.90	6.41	6.59	6.81	6.77
RG (g/L)	35	36.5	36	34	35.5
The yield of ε-PL (g/L)	0.775	0.738	0.749	0.746	0.753

Above all, it was not hard to see that the mutant displayed a great potential for increasing ε-PL productivity in later period of fermentation, so in the near future the fermentation conditions for 6#−7 would be intended to be optimized to tap its potentials for large-scale production industrially.

37.3.3 Genetic Stability Test

The strain 6#−7 was cultured in shaking flasks with two-stage fermentation for five generations, and the fermentation performance included the pH of the broth, biomass, RG, and the yield of ε-PL (shown in Table 37.3), indicated that its genetic characteristics were stable.

37.4 Conclusion

In this study, the original bacteria strain, *S. diastatochromogenes* Cbγ4 was treated with different composite mutant doses of NTG and UV, then the mutants were selected through a series of screening, such as resistant plate, methylene blue plate, shake-flask screening. Finally, a high yield producing strain 6#−7 was obtained through 0.8 g/L NTG for 45 min, followed with UV irradiation for 45 s under magnetic stirring, and then picked out from the resistant agar plate contained AEC 10 mg/mL, Glycine 5 mg/mL and Threonine 4 mg/mL. The experiments proved that 6#−7 had good genetic stability. With two-stage fermentation, the yield of ε-PL could reach 0.775 ± 0.046 g/L at 72 h, 42.2 % higher than the initial strain. Moreover, the mutant displayed a great potential for increasing productivity in later period of fermentation.

Acknowledgments This work was supported by the National Natural Science Foundation (21276197), the National High-tech R&D Program (863 Program, 2013AA102106) and the National Science and Technology Program of China (2011BAD23B05-3).

References

1. Shima S, Sakai H (1977) Polylysine produced by *Streptomyces*. Agric Biol Chem 41(9):1807–1809
2. Shima S, Sakai H (1981) Poly-L-lysine produced by *Streptomyces*. Part II. Taxonomy and fermentation studies. Agric Biol Chem 45:2497–2502
3. Hiraki J, Ichikawa T, Ninomiya S et al (2003) Use of ADME studies to confirm the safety of ε-polylysine as a preservative in food. Regul Toxicol Pharmacol 37(2):328–340
4. Shima S, Sakai H (1981) Poly-L-lysine produced by *Streptomyces*. Part III Chemical studies. Agric Biol Chem 45:2503–2508
5. Shima S, Matsuoka H, Iwamoto T et al (1984) Antimicrobial action of ε-poly-L-lysine. J Antibiot 37:1449–1455
6. Shima S, Fukuhara Y, Sakai H (1982) Inactivation of bacteriophages by ε-poly-L-lysine produced by *Streptomyces*. Agric Biol Chem 46:1917–1919
7. Hiraki J (2000) ε-Polylysine, its development and utilization. Fine Chem 29:18–25
8. Hiraki J (1995) Basic and applied studies on ε-polylysine. J Antibact Antifungal Agents 23:349–354
9. Ho YT, Ishizaki S, Tanaka M (2000) Improving emulsifying activity of ε-polylysine by conjugation with dextran through the Maillard reaction. Food Chem 68:449–455
10. Tsujita T, Takaichi H, Takaku T et al (2006) Antiobesity action of ε-polylysine, a potent inhibitor of pancreatic lipase. J Lipid Res 47(8):1852–1858
11. Kunioka M, Choi HJ (1995) Properties of biodegradable hydrogels prepared by γ-irradiation of microbial poly(ε-Lysine) aqueous solutions. J Appl Polym Sci 58:801–806
12. McKenzie DL (1999) Comparative gene transfer efficiency of low molecular weight polylysine DNA-condensing peptides. J Pept Res 54(4):311–318
13. Levine AS, Sivulich M, Wiernik PH, Levy HB (1979) Initial clinical trials in cancer patients of polyriboinosinic-polyribocytidylic acid stabilized with poly-lysine, in carboxymethylcellulose [poly(lCLC)], a highly effective interferon inducer. Cancer Res 39:1645–1650
14. Hiraki J, Hatakeyama M, Morita H et al (1998) Improved ε-poly-L-lysine production of an S-(2-aminoethyl)-L-cysteine resistant mutant of *Streptomyces albulus*. Seibutsu Kogaku Kaishi 76:487–493
15. Yoshida T, Nagasawa T (2003) ε-Poly-L-lysine: microbial production, biodegradation and application potential. Appl Microbiol Biotechnol 62(1):21–26
16. Jia S, Xu C, Tan Z, Cao W et al (2010) Isolation characterization of a new ε-poly-L-lysine-producing strain TUST-2. Acta Microbiologica Sinica 50(2):191–196 (in Chinese)
17. Shiru J, Huijun D, Junyun J et al (2004) The selection and breeding of ε-polylysine high-producing strain. Food Ferment Ind 30(11):14–17 (in Chinese)
18. Itzhaki RF (1972) Colorimetric method for estimating polylysine and polyarginine. Anal Biochem 50(2):569–574
19. Cao W, Tan Z, Yuan G et al (2007) Improvement of the assay method for ε-polylysine. J Tianjin Univ Sci Technol 22:9–11 (in Chinese)

Chapter 38
Study on Process Optimization for Bioemulsifier Production

Manman Wang, Xingbiao Wang, Chenggang Zheng, Yunkang Chang, Yongli Wang and Zhiyong Huang

Abstract A useful bioemulsifier was secreted by *Geobacillus* sp. XS2 isolated from an oil-contaminated soil sample from Yumen oil field in northern China. The extracellular bioemulsifier was able to form a stable oil/water emulsion. The effects of different bioemulsifier concentrations on cell growth and activity of fermentation broth with water-soluble and water-insoluble carbon sources were studied. Various carbon sources, nitrogen sources, and C/N ratios were screened, and the culture conditions such as pH and ventilation were optimized through the fermentation progress. After a series of steps of optimization, the maximum bioemulsifier production reached to 21.1 g/L ± 1.15 g/L and more than four times higher than that observed in the initial experiment. And the bacterial strain XS2 showed a good performance to adapt to the environment and strong potential for industrial applications.

Keywords Bioemulsifier · Emulsification activity · Fermentation optimization · *Geobacillus* sp.

M. Wang
College of Biotechnology, Tianjin University of Science and Technology, Tianjin 300457, People's Republic of China

X. Wang · Y. Chang · Z. Huang (✉)
Tianjin Key Laboratory for Industrial Biological Systems and Bioprocessing Engineering, Tianjin Institute of Industrial Biotechnology, Chinese Academy of Sciences, Tianjin 300308, People's Republic of China
e-mail: huang_zy@tib.cas.cn

C. Zheng
Petroleum Exploration and Production Research Institute, SINOPEC, Beijing 100083, People's Republic of China

Y. Wang (✉)
Lanzhou Institute of Geology, Chinese Academy of Sciences, Lanzhou 730000, People's Republic of China
e-mail: wyll6800@lzb.ac.cn

T.-C. Zhang et al. (eds.), *Proceedings of the 2012 International Conference on Applied Biotechnology (ICAB 2012)*, Lecture Notes in Electrical Engineering 249,
DOI: 10.1007/978-3-642-37916-1_38, © Springer-Verlag Berlin Heidelberg 2014

38.1 Introduction

A wide range of biosurfactants with surface activities were produced by various microorganisms [1]. The types of biosurfactants varied very much, including glycolipids, lipopeptides, lipoproteins, phospholipids, fatty acids, lipopolysaccharides, and polysaccharide-protein complexes [2]. Biosurfactants were divided into two classes according to their molecular weight. The high molecular weight biosurfactants, also called bioemulsifiers, were effectively in stabilizing emulsions, instead of efficiently lower surface and interfacial tensions as low molecular weight biosurfactants [3].

As an important member of the family of biosurfactants, many kinds of bioemulsifiers were studied and used in many industries for their significant advantages compared to their chemical counterparts [4, 5]. The characters of bioemulsifiers are as follows: (1) biodegradable, no secondary pollution; (2) nontoxic and harmfulless; (3) digestibly, can be used as food additives; (4) produce biosurfactant with industrial waste materials; (5) environmental compatibility. The most important is that bioemulsifiers can meet the needs of the green industry in this time of serious environmental pollution. In recent decades, researches on bioemulsifier were growing year by year. Emulsan, which produced by *Acinetobacter calcoaceticus* RAG-1, was one of the most well studied bioemulsifiers [6]. The biosynthesis of emulsan, as well as its chemical-physical properties and applications were studied by *Gutnick* [7–9]. An extracellular, water-soluble liposan which isolated from *Candida lipolytica*, strongly affected and stabilized oil-in-water emulsions and the strain could grow well and secrete liponsan with a variety of commercial vegetable oils [10]. A kind of bioemulsifier consisting of carbohydrates (50 %), protein (19.6 %), and lipids (10 %) was isolated from *Pseudomonas fluorescens* with gasoline as sole carbon source [11]. Alasan was a well-known bioemulsifier as well, it was a complex of an anionic, nondialyzable, alanine-containing heteropolysaccharide, and protein, isolated from *Acinetobacter radioresistens* [12]. Recently, a novel extracellular bioemuisifier which was produced by *Variovorax paradoxus* 7bCT5 was extracted and chemically characterized [13].

Biosurfactants, including bioemulsifiers, have been used widely in environmental restoration, cosmetics, oil exploitation, agriculture, and many other industries, especially in microbial enhanced oil recovery (MEOR) and bioremediation due to their diverse functional properties, such as surface activity, emulsifying, wetting, foaming, solubilizing, phase separation, and cleaning [14]. One of the important MEOR methods for bioemulsifier was to emulsify the crude oil, change the fluidity of the oil to improve the oil recovery efficiency [15, 16]. During the past years, great progress of MEOR technology was made in china, and field application tests were also carried out in Shengli and Daqing oil field. Biosurfactant-enhanced bioremediation of contaminated soil was a new technique [17], and typically, the recovery of hydrocarbons in contaminated sandy soil and sludge was improved greatly after disposed with biosurfactants [18]. At present, the main

limiting factors of extensive applications of biosurfactants were the lower productivity and lack of mass-production techniques. In this study, a bioemulsifier producing strain *Geobacillus* sp. XS2 was isolated and purified from crude oil-contaminated soil samples. This bacterium can be used in high temperature oilfield due to the thermophilic character. The bioemulsifier exhibited a promising potential for applications under extreme environmental conditions due to its thermostability, salt tolerance, acid, and alkali-resistance [19]. This study enhanced the bioemulsifier production through screening medium components, such as carbon sources, nitrogen sources, C/N ratios and optimizing culture conditions, and fermentation process, including fermentation time, pH, ventilation, and other parameters. The effects of different bioemulsifier concentrations on cell growth and activity of fermentation broth with water-soluble and water-insoluble carbon sources were also carried out. The most important significance of this study was provided some theoretical and experimental bases for further applications in different industries.

38.2 Materials and Methods

38.2.1 Bacterial Strain and Culture Conditions

The bioemulsifier producing bacterial strain, named XS2, was isolated from contaminated soil samples from Yumen oilfield, northern China. Minimal salt medium (MS) with crude oil of 1 % (w/v) was used to screen and isolate bacteria. The morphological, physiological, and phylogenetic properties suggested that the strain XS2 was a member of the genus *Geobacillus* [19]. MS medium (pH 7.0) as enrichment and production medium composed of (g/L H_2O): $NaNO_3$, 3; K_2HPO_4, 1.2; KH_2PO_4, 0.42; $FeSO_4$, 0.05; $MgSO_4$, 0.5; $CaCl_2$, 0.05; 1.0 ml of trace element solution which composed of (g/L H_2O): H_3BO_3, 0.25; $CuSO_4$, 0.5; $MnSO_4$, 0.5; $NaMoO_4$, 0.06; $ZnSO_4$, 0.7 [20]. Luria–Bertani (LB) medium, consisting of (g/L H_2O): peptone, 10; yeast extract, 5; NaCl, 10, was used as seed medium. All the medium used in this study were sterilized at 121 °C for 20 min. The bacterial cells were inoculated with 10 % (v/v) inoculum into 100 ml medium with 2 % carbon source and were cultivated in 250 ml flasks on a rotary shaker at 60 °C, 200 rpm for 24 h.

38.2.2 Optimization of Carbon and Nitrogen Sources

Different kinds of carbon sources and nitrogen sources (methionine, ammonium chloride, sodium nitrate, urea, tryptone) were screened in this study to determine the effects on cell growth and bioemulsifier production. The carbon sources used in

this study were listed as follows: 1-xylose, 2-fructose, 3-yeast extract, 4-galactose, 5-sucrose, 6-maltose, 7-mannose, 8-*n*-butanol, 9-acetic acid, 10-isooctane, 11-soybean oil, 12-gum sugar, 13-glucose, 14-lauric acid, 15-glycerol, 16-rhamnose, 17-liquid paraffin, 18-*n*-hexadecane, 19-lactose, 20-oleic acid, 21-malic acid, 22-citric acid, 23-fluorene, 24-anthracene, 25-soybean lecithin, 26-glutamic acid, 27-starch, 28-succinic acid, 29-alanine, 30-lactic acid, 31-methionine, 32-chitosan, 33-olive oil, 34-sodium carboxymethyl cellulose, 35-palmitic acid, and 36-stearic acid.

The best carbon source selected with different concentrations in range of 0 to 5 % (w/v) was added to MS medium to screen the best concentration. Different kinds of nitrogen sources were added to MS medium to screen the best nitrogen source for the cell growth and bioemulsifier production. Then different ratios of C/N by keeping a constant carbon source concentration were compared to screen the best ratio for the bioemulsifier production. After cultivation, the optical density (OD) and emulsification index (E24) of fermentation broth, bioemulsifier production was measured and used as screening indexes. Cell growth was detected by OD of fermentation broth at 600 nm with spectrophotometer (UV-1800, Shimadzu, Japan). The test methods of E24 and bioemulsifier production were introduced in the ensuing chapters.

38.2.3 Surface Activity

After incubated for 24 h, cells were removed by centrifugation at 10,000 rpm for 5 min, and the surface tension of the culture broth supernatant was measured by a tensiometer (JK99C, Zhongchen digital technology equipment CO. Ltd. Shanghai, China) at room temperature, according to the Ring method as previously described [21]. Measurements were carried out in triplicate and sterile MS medium were used as the negative control.

Emulsification index (E24) of bioemulsifier in the fermentation broth produced by XS2 strain was employed to quantify the emulsifying activity and the method was carried out as described previously with minimal modification [22]. A total of 2 ml cell-free supernatant was mixed with the same volume of liquid paraffin in a test tube, the mixture was vortexed for 5 min and then allowed to stand for 24 h at room temperature. The E24 (%) was calculated as the ratio of the emulsion layer height and the total liquid height, then multiplied by 100 %.

38.2.4 Preparation of Bioemulsifier

After incubated for 24 h, the culture broth was centrifuged at 10,000 rpm for 5 min to remove the cells and the supernatant was concentrated for 10 times by vacuum evaporation (R210, BüCH, Switzerland). The concentrated supernatant

was transferred to a flask with threefold volumes of methanol, then the flask was placed over night at 4 °C [23]. The mixture was centrifuged at 12,000 rpm, for 20 min at 4 °C. Then the precipitate was collected and washed twice with distilled water to obtain the crude bioemulsifier. The product was dried naturally to constant weight and then weighted.

The bioemulsifier with concentrations ranged from 0 to 2.5 % (w/v) was added to MS medium with glucose as sole carbon source to obtain higher productivity of the bioemulsifier. After incubation for 24 h, the OD of fermentation broth, E24, and bioemulsifier production were tested and the group without extra bioemulsifier was used as control. Cell surface lipophilicity (CSL) was measured by BATH test [24, 25] to prove the physiological significances on cell hydrophobic activity, when liquid paraffin was used as the sole carbon source.

38.2.5 Output Optimization in Fermentor

For the batch fermentation, glucose solution (40 %, w/v, 200 ml) which was sterilized separately was added to MS medium (4 L) in 7 L fermentor (BioFlo 110, NBS, USA). The initial culture conditions were set as: temperature 60 °C, pH naturally, stirring speed 500 rpm, ventilation 1.0 vvm to explore the situations of substrate-consumption, cell growth, and bioemulsifier production preliminarily. The stirring speed was set at different levels from 200 to 700 rpm to optimize the stirring speed and enhance the production of bioemulsifier. The pH was controlled at different values in different batches to guarantee optimum pH. During fermentation process, pH was maintained constantly by feeding acid (2 M HCl) and alkalis (2 M NaOH) automatically to offer a stable environment for cells.

Time course studies were carried out by measuring bioemulsifier productivity, OD, carbon, and nitrogen sources consumption. The temperature, pH, and dissolved oxygen (DO) were measured by electrode directly. Glucose concentration was measured by biosensor (SBA-40D, Huayan instrument and equipment CO. Ltd. Shanghai, China). The nitrate sodium concentration was measured by spectrophotometry at 220 nm [26].

Fed-batch fermentation was carried out under the optimized conditions to further increase the yield of bioemulsifier by relieving substrate inhibition. A 100 ml concentrated solution containing 400 g/L of glucose and 20 times concentrated MS medium were added to the fermentor at different points (8, 16, 24, 32 h) during fed-batch fermentation progress.

38.3 Results and Discussion

38.3.1 Optimization of Medium Components

38.3.1.1 Carbon Sources

The yield of bioemulsifier by strain *Geobacillus* sp. XS2 using 36 kinds of carbon sources (20 g/L) was measured. The results of preliminary screening showed that *Geobacillus* sp. XS2 can grow and produce bioemulsifier using most water-soluble and water-insoluble carbon sources. The order of the favorable carbon sources was as follows: saccharides > soybean oil > alkanes > organic acids > aromatic hydrocarbons > alcohols. After preliminary experiment, 14 carbon sources were selected with high OD and emulsifier activity for further screening, and the others with low OD (OD < 0.5) and low emulsifying activity (E24 < 50 %) were not pay attention in the next work. The OD of cell turbidity (OD), E24, and yield of bioemulsifier in each case were determined after cultivation for 24 h. The results were showed in Fig. 38.1. Among the 14 types of carbon sources detected, glucose was the best carbon source for bioemulsifier production combined with the data of OD and E24, and the biggest value of those three indexes were up to 4.6 g/L, 2.57, and 75 %, respectively. Furthermore, the E24 and bioemulsifier production were both higher than reported previously [13, 27].

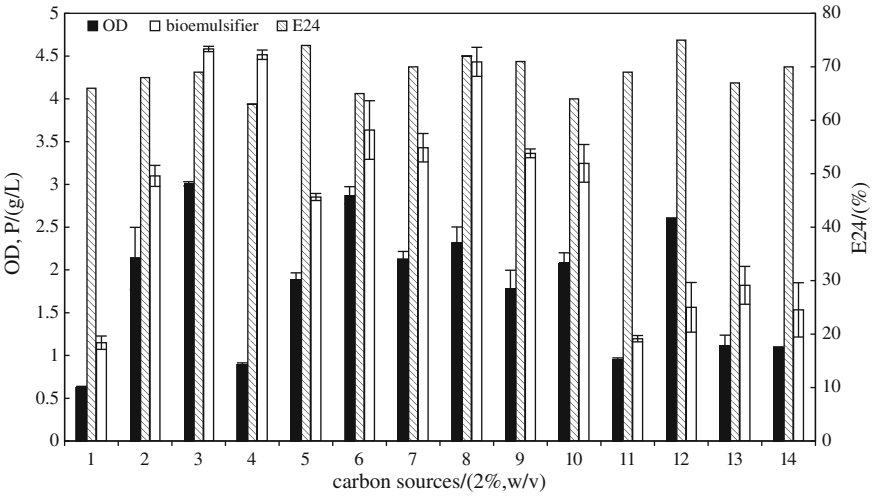

Fig. 38.1 Effects of different carbon sources on cell growth, E24 and bioemulsifier production by *Geobacillus* sp. XS2 grown on MS medium at 60 °C and 200 rpm. Carbon sources: 1-fructose, 2-galactose, 3-sucrose, 4-maltose, 5-isooctane, 6-soilbean oil, 7-arabia candy, 8-glucose, 9-rhamnose, 10-liquid paraffin, 11-lactose, 12-soybean lecithin, 13-starch, 14-chitosan

Considering the influence of carbon sources concentration on bioemulsifier production, different concentrations of glucose were added to MS medium to screen the best additive amount. The results indicated that the concentration of glucose had significant influence on the bioemulsifier production (Fig. 38.2). High concentration (≧3 %) of substrate potentially suppressed the cell growth and bioemulsifier production. The probable reason for this phenomenon was that high concentration of glucose may influence osmotic pressure of fermentation broth and further affect the substrate absorption by bacterial cells. From the results in Fig. 38.2, the concentration of glucose was set at 2 % for further study.

38.3.1.2 Nitrogen Sources and C/N Ratios

With glucose used as sole carbon source, the selection of nitrogen source affects the bioemulsifier production as represented in Fig. 38.3. Strain XS2 was able to product bioemulsifier with different kinds of nitrogen sources including methionine, ammonium chloride, sodium nitrate, urea, and tryptone. The results indicated that sodium nitrate was much more efficient in both cell growth and bioemulsifier yield than other nitrogen sources. It was reported that ammonium salts in the form of ammonium chloride can cause decrease of pH, restrain cell growth and bioemulsifier production [28]. The maximum emulsifying activity (71 %) and optimal bioemulsifier production (6.04 g/L) were obtained in medium with sodium nitrate. Nitrate was more favorable than ammonium salt and urea for biosurfactant production and the result was also demonstrated in other studies [29].

The C/N ratios were critical to improve the yield of bioemulsifier. Constant concentration of glucose (2 g/L) and different concentrations of sodium nitrate were chosen as carbon and nitrogen sources, respectively, to assay different C/N ratios. The maximum bioemulsifier production of 6.04 g/L was acquired at the C/N ratio of 20:3 (Fig. 38.4). The experiment was also performed in the nitrogen-limiting condition. OD of 0.88, E24 of 28 %, and bioemulsifier yield of 2.8 g/L were obtained without nitrogen source. The bioemulsifier production was

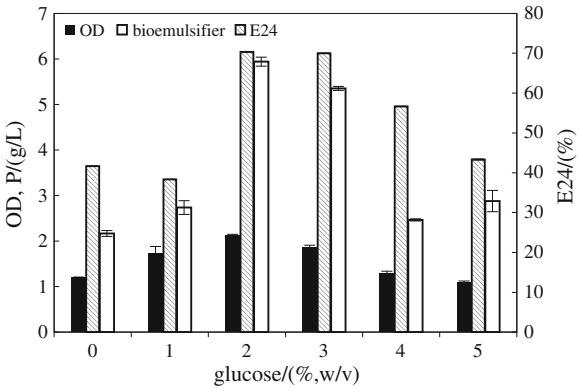

Fig. 38.2 Effects of different concentrations of glucose on cell growth, E24 and bioemulsifier production by *Geobacillus* sp. XS2 grown on MS medium at 60 °C and 200 rpm

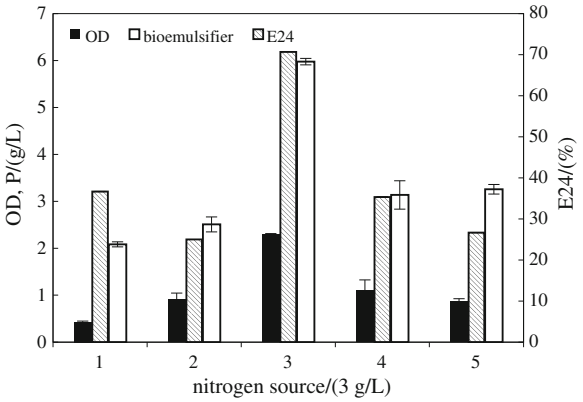

Fig. 38.3 Effects of different nitrogen sources on cell growth, E24 and bioemulsifier production by *Geobacillus* sp. XS2 grown on MS medium with 2 % glucose, Nitrogen sources: 1-methionine, 2-ammonium chloride, 3-sodium nitrate, 4-urea, 5-tryptone

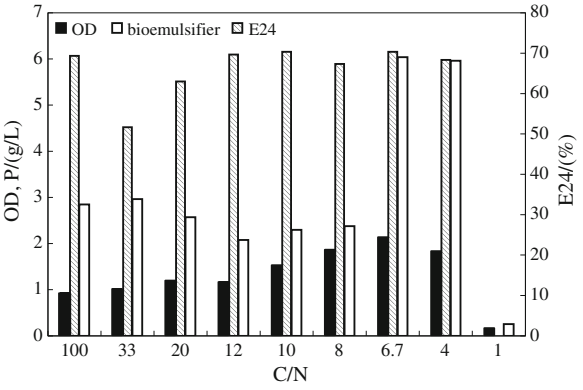

Fig. 38.4 Effects of different C/N (w/w) ratios on cell growth, E24 and bioemulsifier production by *Geobacillus* sp. XS2 using glucose and sodium nitrate as sole carbon source and nitrogen source, respectively

suppressed under nitrogen-limiting condition, and the results did not agree with the previous reports [30].

38.3.2 Characteristics of Crude Bioemulsifier

Crude bioemulsifiers with concentrations varied from 0 to 2.5 g/L were added to medium with glucose and liquid paraffin as sole carbon source, respectively. The results were described in Fig. 38.5. The results showed that the added bioemulsifier restrained cell growth when the cells grew on glucose (Fig. 38.5a), and both the final OD of the culture broth and bioemulsifier production were lower than controlled trial. This phenomenon may be caused by toxicity of extra bioemulsifier to fresh inoculum, leading to reduced cell growth rate, and emulsify activity. The increase of bioemulsifier yield and emulsifying activity (E24) along with the concentration of added bioemulsifier were probably attributed to external

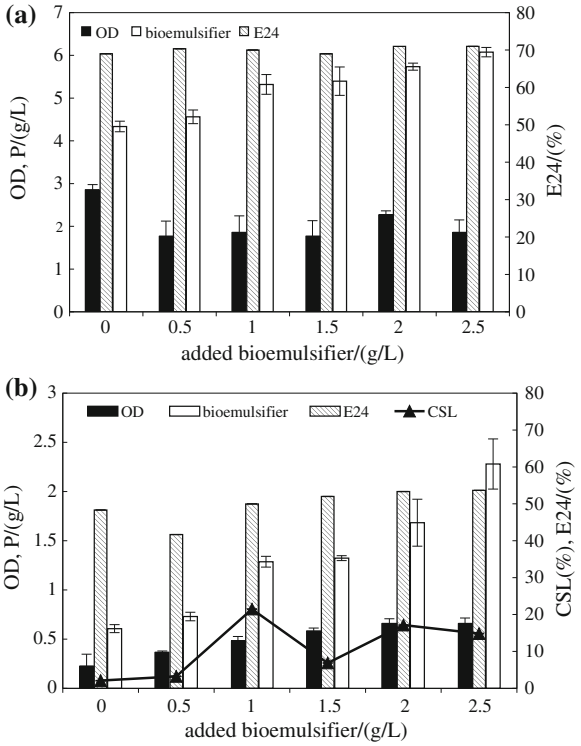

Fig. 38.5 Effects of added bioemulsifier on bacterial growth, E24 and bioemulsifier with *Geobacillus* sp. XS2 grown on MS medium with glucose (**a**) and liquid paraffin (**b**), respectively

bioemulsifier. But subtracting the added substrate, the actual bioemulsifier was constantly reduced along with the extra emulsifier addition. When cells grew with liquid paraffin as sole carbon source, the addition of bioemulsifier stimulated cell growth and enhanced the emulsifying activity (E24) of supernatant and CSL of the cells (Fig. 38.5b). This result was consistent with the reported cases previously [31]. The OD increased with concentrations of additives, and the biggest OD obtained in this study up to 0.7, however, the net production of bioemulsifier was not improved obviously. In addition, another point was that the bioemulsifier can increase cell surface hydrophobicity, and provide assistance for cells to uptake water-insoluble carbon sources. The decline of fermentation broth's surface tension was not prominent (52.66 mN/m), and this result confirmed these mainly existing emulsify mechanism of bioemulsifier [32]. In conclusion, the bioemulsifier studied in this study has excellent emulsifying activity, and potential applications in many industries, particularly in oil-contaminated soil remediation and MEOR-related technology.

38.3.3 Bioemulsifier Production Optimization in Fermentor

After the optimal culture conditions were obtained as described above, the scaling-up fermentation was carried out in 7 L fermentor and the fermentation parameters were also optimized with the initial conditions: load volume of the medium, 4 L; inoculation, 10 % (v/v); fermentation temperature, 60 °C; initial pH, 7.0; rotate speed, 300 rpm; ventilatory capacity, 1.0 vvm. The results showed that the OD, E24, and bioemulsifier production approach the maximum values with stirring speed of 550 rpm (Fig. 38.6a). During the fermentation process, pH decreased from 7.0 to 5.8 at the first 10 h and then increased to 8.8 in the rest of process. The stationary phase of strain XS2 became shorter because of pH fluctuated and lack of dissolved oxygen (maintained at 0 % from 4 to 10 h) during the batch fermentation progress, so the pH was maintained at different values in different batches and results were showed in Fig. 38.6b. To obtain high emulsify activity fermentation broth and high bioemulsifier output, 7.5 was selected as the best pH for

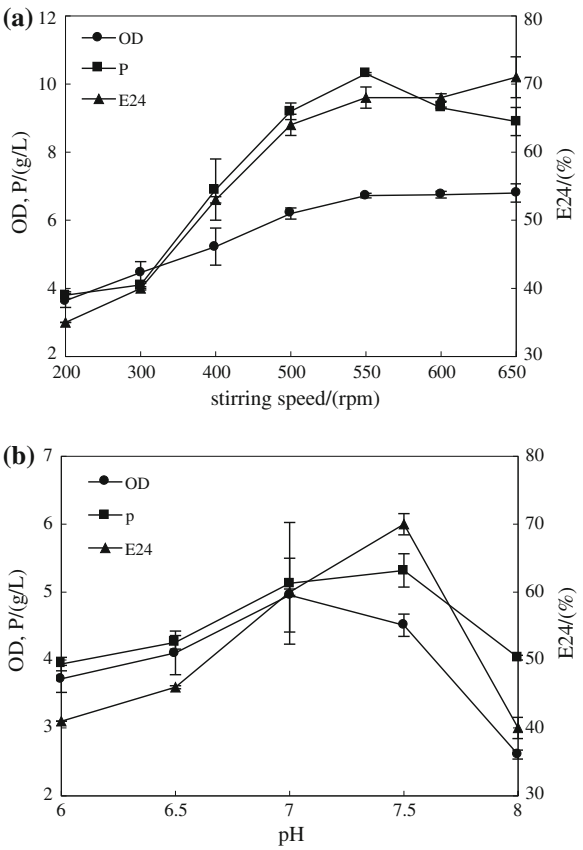

Fig. 38.6 OD, E24, and bioemulsifier production by *Geobacillus* sp. XS2 were obtained with different stirring speed (**a**) and different pH (**b**), respectively, in 7-L fermentor, fermentation conditions: temperature 60 °C, ventilatory capacity 1.0 vvm. Effects of stirring speed were investigated with initial pH of 7.0, and effects of pH were investigated with rotating speed of 300 rpm

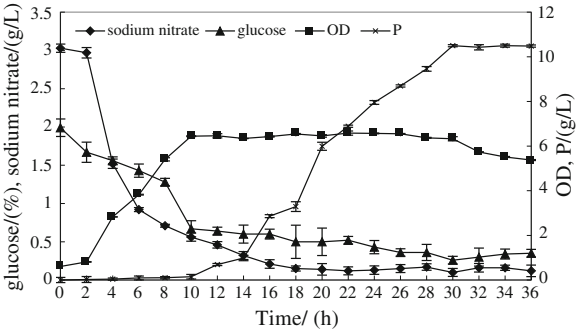

Fig. 38.7 Time course profiles of glucose concentration, nitrogen concentration, OD, and crude bioemulsifier yield in optimized medium and conditions in 7-L fermentor

further investigation. The ventilatory capacity was increased to 1.5 vvm in the later operation to meet oxygen requirement of XS2 cells.

The typical time course profile of the cell OD, bioemulsifier production, glucose, and sodium nitrate concentrations with optimized conditions were showed in Fig. 38.7. The notable reduction of substrate concentration and increase of cell density occurred simultaneously from 0 to 10 h, however, remarkable increase of bioemulsifier production proceeded during the fermentation time from 10 to 30 h. It can be predicted that the bioemulsifier may be a secondary metabolite and occurred at the stationary phase of the cell growth. The cell growth turned to decline phase after 30 h and the maximum OD of fermentation broth was 6.7 after 12 h of cultivation resulting in bioemulsifier production of up to 10.5 g/L.

A fed-batch fermentation of XS2 was carried out by feeding concentrated solutions at different time points (8, 16, 24, 32 h) to increase yield of bioemulsifier by relieving substrate inhibition. A 100 ml concentrated solution containing 400 g/L of glucose and 20 times concentrated MS medium was added to the fermentor every time. The experiment was terminated when the culture turned into death phase (36 h). The maximum cell density (OD) in fed-batch process reached 7.8 and final production of bioemulsifier reached 21.1 g/L $\pm$ 1.15 g/L. The yield of bioemulsifier produced by XS2 in this experiment indicated a potential capacity for industrial production and application.

38.4 Conclusion

In this study, the bioemulsifier was isolated from glucose fermentation broth of the bacterial strain *Geobacillus* sp. XS2. It was an efficient emulsifying agent and has potential applications in many industries. In present study, the yield of bioemulsifier was increased by a series of optimization techniques, including culture medium optimization (e.g., carbon sources and nitrogen sources screening), fermentation conditions optimization (e.g., pH, stirring speed, ventilation), and scaling-up fermentation system. After optimization, the maximum bioemulsifier

yield was more than four times (21.1 g/L ± 1.15 g/L) higher than initial yield (4.7 g/L ± 0.12 g/L). The results of this experiment indicated that the production of the bioemulsifier has possibility to further improve, and consequently to realized industrialization in the near future.

Acknowledgments This work was supported by Project of Chinese Academy of Sciences strategic science and technology special (XDA05120204), National Key Basic Research Program (2012CB214701-05), National Natural Science Foundation of China (Grant No. 51104106), West Light Foundation of The Chinese Academy of Sciences.

References

1. Ilori MO, Amobi CJ, Odocha AC (2005) Factors affecting biosurfactant production by oil degrading *Aeromona*s spp. isolated from a tropical environment. Chemosphere 61:985–992
2. Nitschke M, Pastore GM (2006) Production and properties of a surfactant obtained from *Bacillus subtilis* grown on cassava wastewater. Bioresour Technol 97:336–341
3. Rosenberg E, Ron EZ (1999) High- and low-molecular-mass microbial surfactants. Appl Microbiol Biotechnol 52:154–162
4. Makkar RS, Cameotra SS (1998) Production of biosurfactant at mesophilic and thermophilic conditions by a strain of *Bacillus subtillis*. J Ind Microbiol Biotechnol 20:48–52
5. Maier RM, Soberón-Chávez G (2000) *Pseudomonas aeruginosa* rhamnolipids: biosynthesis and potential applications. Appl Microbiol Biotechnol 54:625–633
6. Rosenberg E, Rubinovitz C, Gutnick DL et al (1979) Emulsifier of *Arthrobacter* RAG-1: isolation and emulsifying properties. Appl Environ Microbiol 37:402–408
7. Gutnick DL (1987) The emulsan polymer: perspectives on a microbial capsule as an industrial product. Biopolymers 26:S223–S240
8. Gutnick DL, Shabtai Y (1985) Exocellular esterase and emulsan release from the cell surface of *Acinetobacter calcoaceticus*. J Bacteriol 161:1176–1181
9. Belsky I, Gutnick DL, Rosenberg E (1979) Emulsifier of *Arthrobacter* RAG-1: determination of emulsifier-bound fatty acids. FEBS Lett 101:175–178
10. George MC, Michael CC (1985) Purification and characterization of liposan a bioemulsifier from *Candida lipolyticat*. Appl Environ Microbiol 50:846–850
11. Neu TR (1990) Emulsifying agent from bacteria isolated during screening for cell with hydrophobic surfaces. Appl Microbiol Biotechnol 32:521–525
12. Navon VS, Gottlieb A, Legmann R et al (1995) Alasan a new bioemulsifier from *Acinetobacter radioresistens*. Appl Environ Microbiol 61:3240–3244
13. Franzetti A, Gandolfi I, Raimondi C et al (2012) Environmental fate, toxicity, characteristics and potential applications of novel bioemulsifiers produced by *Variovorax paradoxus* 7bCT5. Bioresour Technol 108:245–251
14. Perfumo A, Rancich I, Banat IM (2010) Possibilities and challenges for biosurfactants use in petroleum industry. Adv Exp Med Biol 672:135–145
15. zobell CE (1946) Action of microorganisms on hydrocarbons. Bacteriol Rev 10:1–49
16. Zobell CE (1947) Bacterial release of oil from oil-bearing materials. World Oil 126:36–47
17. Foster J (1962) Hydrocarbons as substrates for microorganisms. Anton Leeuw Int J G 28:241–274
18. Thangamani S, Shreve GS (1994) Effect of anionic biosurfactant on hexadecane partitioning in multiphase systems. Environ Sci Technol 28:1993–2000
19. Zheng C, He J, Wang Y et al (2011) Hydrocarbon degradation and bioemulsifier production by thermophilic *Geobacillus pallidus* strains. Bioresour Technol 102:9155–9161

20. Yakimov MM, Timmis KN, Wray V et al (1995) Characterization of a new lipopeptide surfactant produced by thermotolerant and halotolerant subsurface *Bacillus licheniformis* BAS50. Appl Environ Microbiol 61:1706–1713
21. Lin SC, Minton MA, Sharma MM et al (1994) Structural and immunological characterization of a biosurfactant produced by *Bacillus licheniformis* JF-2. Appl Environ Microbiol 60:31–38
22. Cooper DG, Goldenberg BG (1987) Surface-active agents from two *Bacillus* species. Appl Environ Microbiol 53:224–229
23. Joshi S, Bharucha C, Desai AJ (2008) Production of biosurfactant and antifungal compound by fermented food isolate *Bacillus subtilis* 20B. Bioresour Technol 99:4603–4608
24. Rosenberg M (1984) Bacterial adherence to hydrocarbons: a useful technique for studying cell surface hydrophobicity. FEMS Microbiol Lett 22:289–295
25. Matz C, Jürgens K (2001) Effects of hydrophobic and electrostatic cell surface properties of bacteria on feeding rates of heterotrophic nanoflagellates. Appl Environ Microbiol 67:814–820
26. Zhu L, Yang X, Xue C et al (2012) Enhanced rhamnolipids production by *Pseudomonas aeruginosa* based on a pH stage-controlled fed-batch fermentation process. Bioresour Technol 117:208–213
27. Li X, Li A, Liu C et al (2012) Characterization of the extracellular biodemulsifier of *Bacillus mojavensis* XH1 and the enhancement of demulsifying efficiency by optimization of the production medium composition. Process Biochem 47:626–634
28. Abouseoud M, Maachi R, Amrane A et al (2008) Evaluation of different carbon and nitrogen sources in production of biosurfactant by *Pseudomonas fluorescens*. Desalination 223:143–151
29. Dutta JR, Dutta PK, Banerjee R (2004) Optimization of culture parameters for extracellular protease production from a newly isolated *Pseudomonas* sp. using response surface and artificial neural network models. Process Biochem 39:2193–2198
30. Benincasa M, Contiero J, Manresa MA et al (2002) Rhamnolipid production by *Pseudomonas aeruginosa* LBI growing on soapstock as the sole carbon source. J Food Hyg Soc Jpn 54:283–288
31. Hua X, Wu Z, Zhang H et al (2010) Degradation of hexadecane by *Enterobacter cloacae* strain TU that secretes an exopolysaccharide as a bioemulsifier. Chemosphere 80:951–956
32. Batista SB, Mounteer AH, Amorim FR et al (2006) Isolation and characterization of biosurfactant/bioemulsifier-producing bacteria from petroleum contaminated sites. Bioresour Technol 97:868–875

Chapter 39
Bacterial Cellulose/Hyaluronic Acid Composites: Preparation and Characterization

Yuanyuan Jia, Mingming Huo and Shiru Jia

Abstract The preparation and characterization of bacterial cellulose (BC)/hyaluronic acid (HA) nanocomposites are presented in this paper. BC/HA composites have been prepared by solution immersion method, biosynthesis method, and crosslink method. HA concentration (1, 10, and 12.5 g/L) was used as a variable factor. These materials were characterized by Field Emission Scanning Electron Microscopy (FESEM), Fourier Transform Infrared (FTIR) spectroscopy, and X-ray Diffraction (XRD). And tensile strength and young's modulus were tested for composites from solution immersion and biosynthesis. SEM graphs of the composites show that HA penetrated inside the cellulose network, filling the space of the network, and keeping a close interaction with the nanofibrils. FTIR spectra illustrate the integration of HA in the composites derived by solution immersion and crosslink method. The crystallinity index of all three composites was reduced slightly compared with pristine BC, known from XRD spectra. For composites from solution immersion and biosynthesis, the young's modulus and tensile strength of BC/HA have been improved compared with the pure BC. This is due to the enhanced hydrogen bonds offered by the interaction between HA and BC. In summary, all the three methods can provide composites of BC and HA. Further, biocompatibility tests will be carried out to evaluate these materials in terms of the potential applications on the biomedical field.

Keywords Bacterial cellulose · Composite · Crosslink · Hyaluronic acid

Y. Jia · M. Huo · S. Jia
Key Laboratory of Industrial Fermentation Microbiology, Ministry of Education, Tianjin 300457, People's Republic of China

Y. Jia (✉) · M. Huo
College of Material Science and Chemical Engineering, Tianjin University of Science and Technology, Tianjin 300457, People's Republic of China
e-mail: jiayuanyuan55@hotmail.com

T.-C. Zhang et al. (eds.), *Proceedings of the 2012 International Conference on Applied Biotechnology (ICAB 2012)*, Lecture Notes in Electrical Engineering 249,
DOI: 10.1007/978-3-642-37916-1_39, © Springer-Verlag Berlin Heidelberg 2014

39.1 Introduction

Cellulose is the most abundant biopolymer and has global economic importance, widely existing in plants. Cellulose is a water-insoluble polysaccharide used at an industrial scale for the manufacture of paper and films, or in the powder, natural, hydrolyzed, or derivative form [1]. In the early 1986s a new type of cellulose morphology was developed by Brown et al. [2]., known as bacterial cellulose or BC.

Bacterial cellulose (BC) is a nano-scale polyglucose generated from *Gluconacetobacter Xylinum*, possessing an interesting biocompatibility [3]. What is more, bacterial cellulose has a three-dimensional polymeric network, which is able to absorb and retain large volume of water, as well as possessing large surface area. So BC is widely used in medical fields, such as artificial skin for humans with extensive burns, artificial blood vessels for microsurgery, scaffolds for tissue engineering of cartilage, and wound dressing [4]. However, the pristine BC in specific applications has only single function, so the modification of the BC can improve is medical and mechanical properties. One of its drawback is the scarce of viscoelasticity; for example, when we press BC membrane, the water is easily squeezed out of the gel without recovery. Its structure is represented in Fig. 39.1.

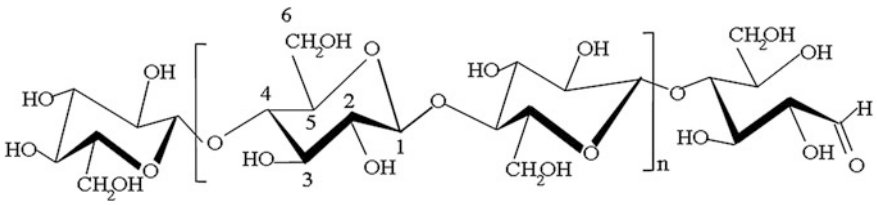

Fig. 39.1 The chemical formula of bacterial cellulose

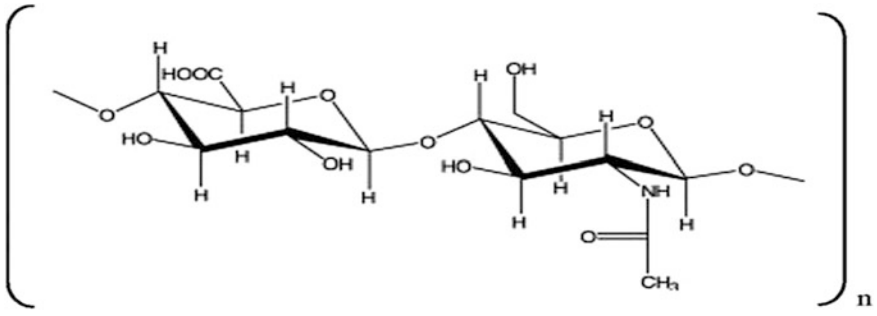

Fig. 39.2 The chemical formula of hyaluronic acid

Hyaluronic acid (HA), a naturally occurring polysaccharide, is widely distributed in animal tissues, and is a key precursor for most novel biomaterials. Its structure is represented in Fig. 39.2. Previous studies have reported its applications mainly in drug delivery vehicles, tissue engineering scaffolds, and tissue fillers [5–7].

HA is a double-molecular polysaccharide, which is different from other mucopolysaccharides, containing no sulfur. At present, it is accepted as the best moisturizing ingredient, known as the ideal natural moisturizing factor. Recently, some studies have found that water-soluble EDC (carbodiimide hydrochloride) [3] can be used as crosslinking agent to modify hyaluronic acid; the modified hyaluronic acid has a strong and controllable water absorption. During the reaction process of crosslinking, the product structure changes from unstable O-isoureide into stable N-ureide.

In this paper, we have considered three methods to cross BC and HA: solution immersion method, biosynthesis method, and crosslink method. The solution immersion method made the hyaluronic acid molecules enter the bacterial cellulose network to obtain composites. With biosynthesis method, the properties of BC were modified in situ during fermentation by forming BC/HA composite. Finally, we chose EDC to combine BC with HA. The Young's modulus and tensile strength of BC/HA crosslinked products were improved significantly. All the composites were characterized with FTIR and XRD, and other means.

39.2 Materials and Methods

39.2.1 Bacterial Strain

Glucose Acetobacter CGMCC No. 1.1812 was obtained from the industrial microbial key laboratory of Tianjin University of Science and Technology.

39.2.2 Production of Bacterial Cellulose

Bacterial cellulose was produced in culture dishes with the medium containing 25 (w/v) anhydrous dextrose, 7.5 (w/v) yeast extract, 10 (w/v) peptone, 10 (w/v) Na_2HPO_4, 10 (w/v) acetic acid, pH 6 buffered, and 121 °C sterilized. For inoculation, 200 μL bacterial suspension (*Acetobacter xylinum* mixed with glycerol) was added to each 250 ml culture medium, and the mixture was shaken vigorously. A 25 ml mixture was filled in one petri dish under sterile environment. Then they were allowed to cultivate in 30 °C, for about 3 or 4 days.

In order to remove the medium, the harvested BC membranes were boiled by 0.1 M NaOH. Then they were washed until pH 7.

39.2.3 Preparation of Bacterial Cellulose/Hyaluronic Acid Composites

39.2.3.1 Solution Immersion Method

Pharmaceutical grade native hyaluronic acid (above 1500 kDa) (purchased from Shangdong Freda Biopharm Co., Ltd) was dissolved at concentrations of 1, 10, and 12.5 g/L in distilled water. Soaked the BC membranes in HA solutions at 4 °C for 3 or 4 days till the concentration of remaining HA solutions did not change anymore.

39.2.3.2 Biosynthesis Method

The culture media of BC were supplemented with HA at concentrations of 1, 10, and 12.5 g/L. Then BC/HA composites were formed during biosynthesis [8].

39.2.3.3 Crosslink Method

The composite membranes prepared as 39.2.3.1 were immersed in 0.03 M EDC solution to obtain crosslinked BC/HA composites.

39.2.4 Characterization of BC/HA Composites

39.2.4.1 Field Emission Scanning Electron Microscope

Samples cut from the freeze-dried BC/HA and BC membranes were coated with a thin layer of evaporated gold, and the images were taken using a FESEM (1530 VP, LEO, Germany) with an acceleration voltage of 5.0 kV [9].

39.2.4.2 Fourier Transform Infrared Spectroscopy

Each membrane was air-dried in the form of a thin film. The spectra of the thin films were recorded using a FT-IR Spectroscopy (Brook Instrument Company), at wave numbers ranging from 4,000 to 400 cm^{-1}.

39.2.4.3 X-ray Diffraction

Measurements were performed using X-ray Diffraction (D/MAX-2500, SHIMADZU, Japan RIGAKU). The intensity of a Cu-Pd filter, 36 kV × 20 mA, was

measured in a 2θ range between 5° and 70°. The crystalline index was measured using the expression with the intensity of interference on the 020 crystalline plane and the amorphous contribution at $2\theta = 18°$, calculated by the expression, adapted from Revol et al. [10],

$$I_{CI} = \frac{I_{020} - I_{am}}{I_{020}} \times 100\,\%. \tag{39.1}$$

39.2.5 The Mechanical Measurements on BC/HA

The mechanical properties of BC/HA and BC were evaluated by computer-controlled electronic testing machine (CMT5000, Shenzhen), at 25 °C. In the stretching tests, a constant velocity 20 mm/min was adopted.

39.3 Results and Discussion

39.3.1 Morphology Observation of Spherical HA/BC Nanocomposites

Morphology of BC/HA composites is visualized in Fig. 39.3. As shown in Fig. 39.3a, bacterial cellulose presents a nanofibril network where each fibril is around 50–100 nm in width [11, 12]. Thanks to the numerous nano-pores in BC, HA can easily penetrate inside the cellulose network, keeping a close interaction with the nanofibrils. HA behaves like a glue, filling the spaces of the network. The well-dispersed HA can be seen in Fig. 39.3, which is consistent with FTIR. We can see from the Fig. 39.3c that the HA dispersed in BC through the biosynthesis method as well. It is believed that some particles are able to penetrate the BC nanofibrils and create a strong interaction with hydrogen bonding [13].

39.3.2 The FTIR Analysis

The FT-IR spectra of the BC composites at various blending ratios were measured from 400 to 4,000 cm^{-1} [14], as shown in Fig. 39.4. The BC spectra show a band at 1,646 cm^{-1}, which is attributed to the glucose carbonyl of cellulose. The interaction between BC and HA can be identified by the carbonyl and carboxyl group bands present in the range of 1,900–500 cm^{-1}. The HA spectra show that the absorption bands at about 1653.21, 1563.68, and 1320.18 cm^{-1} are characteristic of the amide I, II, and III band, respectively [15]. From Fig. 39.4b, there is little difference between the spectra of composites BC/HA and that of BC, and

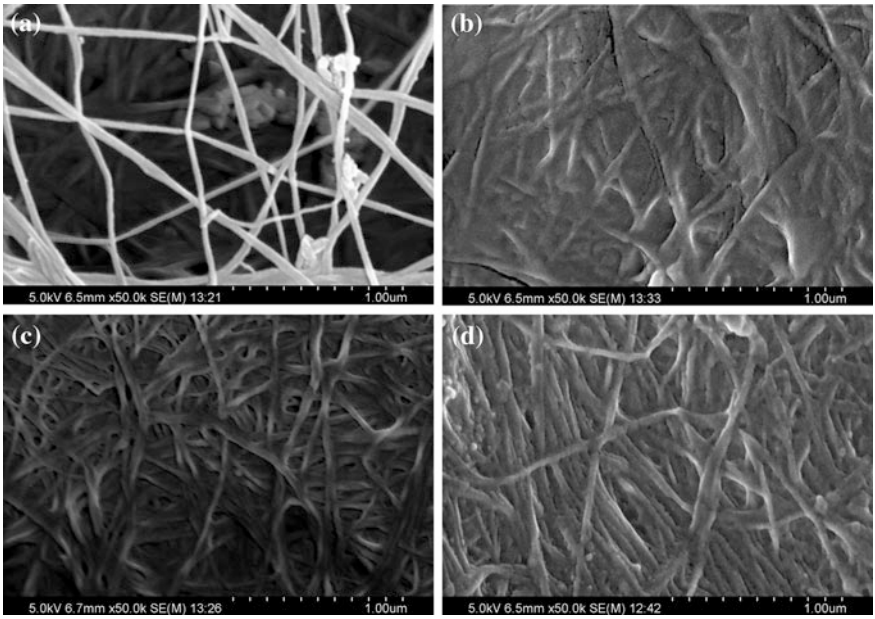

Fig. 39.3 The morphology of BC and BC/HA composite. **a** Pristine BC, **b** HA/BC composite from solution immersion method, **c** HA/BC composiste from biosynthesis method, **d** HA/BC composite from crosslink

there are no peaks of amide I, II, and III bands, implying that the composites from biosynthesis method have less content of HA. However, we can see from part label a and c, the composites have the absorption bands at about 1653.21 and 1563.68 cm^{-1}, which are attributed to amide I and II bands. This has proved the presence of HA in the materials.

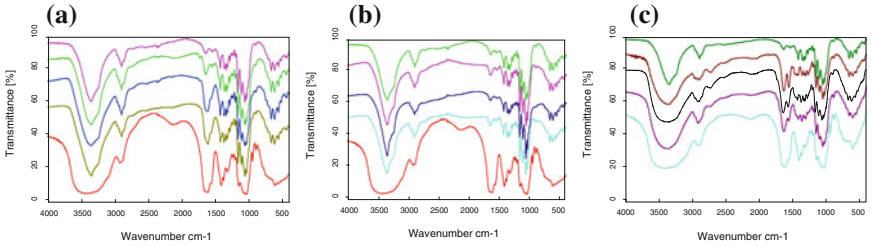

Fig. 39.4 FT-IR spectra of composites from **a** solution immersion from *top to down*: BC, 1.0, 10, and 12.5 g/L HA, **b** biosynthesis: BC from *top to down*: BC, 1.0, 10, and 12.5 g/L HA and **c** crosslink method in different concentration of HA from *top to down*: BC, 1.0, 10, and 12.5 g/L HA

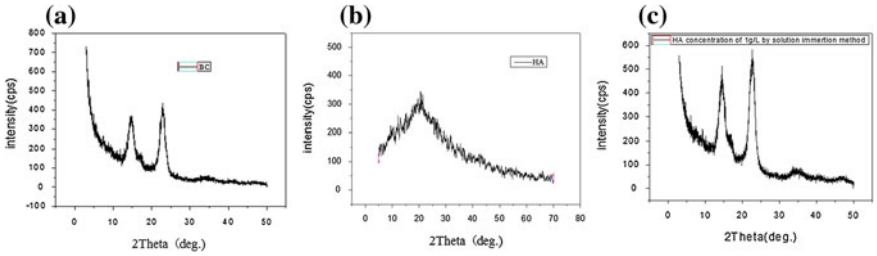

Fig. 39.5 XRD patterns of **a** BC, **b** HA, **c** HA/BC composite

39.3.3 The X-Ray Diffraction Analysis

The XRD patterns of the HA/BC film prepared form concentration of 1 g/L HA is shown in Fig. 39.5c. In the case of pristine BC, three characteristic peaks centered at 14.8°, 16.7°, and 22.7° are observed, corresponding to the typical profile of cellulose I allomorph [16, 17]. According to equation 39.1, the relative crystallinity index CI of BC is 83.9 %, and that of the composites are 81.8, 81.2, and 80.1 % (biosynthesis method, HA 1, 10, and 12.5 g/L), 81.8, 81.0, and 79.6 % (solution immersion method, HA 1, 10, and 12.5 g/L). The characteristic 2θ peaks of BC appear in the spectra of HA/BC. After the incorporation of HA, the CIs decrease with the increase of HA concentration, which means that the HA in the composites disturbs the aggregation and crystallization of the BC matrix [18–20].

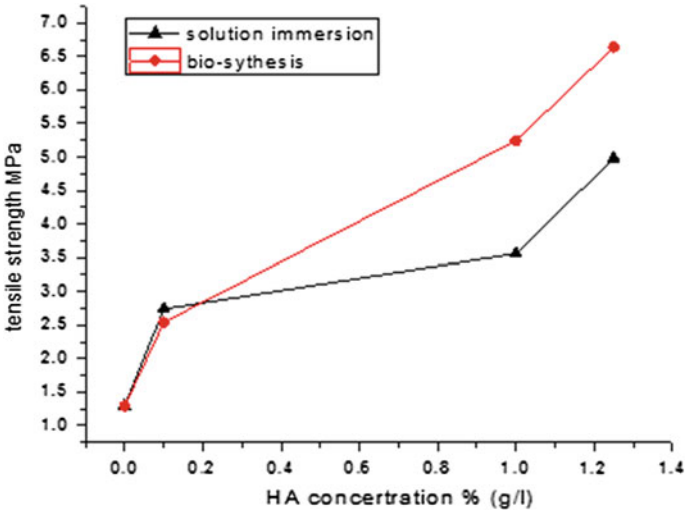

Fig. 39.6 Tensile strength of HA/BC composites

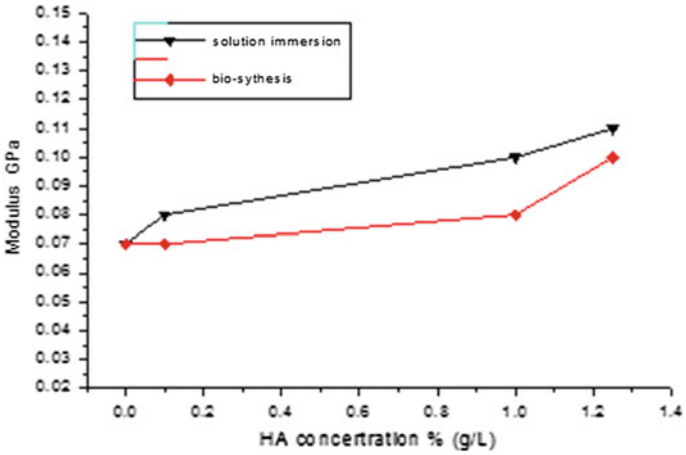

Fig. 39.7 Young's modulus of HA/BC composites

39.3.4 The Mechanical Measurements

We can see from Figs. 39.6 and 39.7 that for composites from solution immersion and biosynthesis, the tensile strength and modulus are increased with HA contents in the materials, which mean that the mechanical strength is improved significantly by incorporating HA in BC. The improvement in tensile strength of composites from biosynthesis is more significant than that of the materials from immersion; while the trend of Young's modulus is opposite. Since the mechanical properties of the materials have been modified significantly compared with that of pristine BC, we can infer that the two methods realize integration of BC and HA.

39.4 Conclusions

Integration of BC/HA has been achieved by three methods, proved by morphology observation, FTIR, and XRD. The content of HA in the composites from biosynthesis is relatively low, known from FTIR spectra. However, tensile strength and young's modulus of these composites are enhanced. SEM graphs show that HA penetrates inside the cellulose network, filling the space of the network and keeping a close interaction with the nanofibrils. The crystallinity indexes of three composites are decreased slightly compared with pristine BC. Since the two compositions, BC and HA, have excellent biocompatibility, the obtained composites have the potentiality to find application on the field of biomedical material, such as tissue engineering scaffolds, artificial skin, and so on. Further tests will be performed to evaluate their performance on this issue.

Acknowledgment The authors wish to acknowledge the Science and Technology Agency of Jilin Province for the financial support of Project No. 200905136. The work is also supported by Tianjin Municipal Education Commission for the Project No. 20100602.

References

1. Marco Lima GD, Sierakowski MR, Faria Tischer PCS et al (2011) Characterisation of bacterial cellulose partly acetylated by dimethylacetamide/lithium chloride. Mater Sci Eng C 31:190–197
2. Brown AI (1886) On an acetic ferment which forms cellulose. Chem Soc 49:432
3. Chang ST, Chen LC, Lin SB et al (2012) Nano-biomaterials application: Morphology and physical properties of bacterial cellulose/gelatin composites via crosslinking. Food Hydrocolloid 27:137–144
4. Jung HH, Nasrullah SH, Mazhar UI et al (2011) Bacterial cellulose production from a single sugar-linked glucuronic acid-based oligosaccharide. Process Biochem 46:1717–1723
5. Sannino A, Pappada S, Madaghiele M et al (2005) Crosslinking of cellulose derivatives and hyaluronic acid with water-soluble carbodiimide. Polymer 46:11206–11212
6. Weiss C (1998) In: Laurent T (ed) The chemistry, biology and medical applications of HA and its derivatives. Portland Press, London, pp 255–266
7. Larsen NE (1998) In: Laurent T (ed) The chemistry, biology and medical applications of HA and its derivatives. Portland Press, London: 267–281
8. Zhu AM, Feng YH, Lin Q et al (2010) Biosynthesis and characterization of bacterial cellulose/hyalurionic acid composites. J Cellulose Sci Technol 18:1–6
9. Yang G, Xie JJ, Hong F et al (2012) Antimicrobial activity of silver nanoparticle impregnated bacterial cellulose membrane: Effect of fermentation carbon sources of bacterial cellulose. Carbohydr Polym 87:839–845
10. Revola JF, Dieteicha ND, Goring DAI (1987) Effect of mercerization on the crystallite size and crystallinity index in cellulose from different sources. Can J Chem 65:1724–1725
11. Zhang W, Chen SY, Hu WL et al (2011) Facile fabrication of flexible magnetic nanohybrid membrane with amphiphobic surface based on bacterial cellulose. Carbohydr Polym 1760–1767
12. Hu WL, Chen SY, Xu QS et al (2011) Solvent-free acetylation of bacterial cellulose under moderate conditions. Carbohydr Polym 83:1575–1581
13. Zhu HX, Jia SR, Wan T et al (2011) Biosynthesis of spherical Fe_3O_4/bacterial cellulose nanocomposites as adsorbents for heavy metal ions. Carbohydr Polym 86:1558–1564
14. Pedro C, Joana AS, Mendes et al (2011) Utilization of residues from agro-forest industries in the production of high value bacterial cellulose. Bioresource Technol 102:7354–7360
15. Wu Y (2012) Preparation of low-molecular-weight hyaluronic acid by ozone treatment. Carbohydr Polym 89:709–712
16. Feng YY, Zhang XQ, Shen YT et al (2012) A mechanically strong, flexible and conductive film based on bacterial cellulose/graphene nanocomposite. Carbohydr Polym 87:644–649
17. Katepetch C, Rujiravanita R (2011) Synthesis of magnetic nanoparticle into bacterial cellulose matrix by ammonia gas-enhancing in situ co-precipitation method. Carbohydr Polym 86:162–170
18. Yang JZ, Yua JW, Fan J et al (2011) Biotemplated preparation of CdS nanoparticles/bacterial cellulose hybrid nanofibers for photocatalysis application. J Hazard Mater 189:377–383
19. Marta MS, Amparo LR, Lagaron JM (2011) Optimization of the nanofabrication by acid hydrolysis of bacterial cellulose nanowhiskers. Carbohydr Polym 85:228–236
20. Lee BH, Kim HJ, Yang HS (2012) Polymerization of aniline on bacterial cellulose and characterization of bacterial cellulose/polyaniline nanocomposite films. Curr Appl Phys 12:75–80

Part II
Food Biotechnology

Chapter 40
A Review of Research on Polysaccharide from *Coriolus versicolor*

Feifei Wang, Limin Hao, Shiru Jia , Qizhi Wang, Xiaojuan Zhang and Shuang Niu

Abstract In recent years, edible and medicinal fungi attract more and more interest for their various biological functions and they have become a research focus. Polysaccharide of *Coriolus versicolor* is isolated from *Coriolus versicolor* or its broth, and gained much attention from the industries of medicine, food, cosmetics and even chemistry, and so on because of its superior biological activity and functions. This paper reviews the recent studies on polysaccharide from *Coriolus versicolor*, about its structure, properties, fermentation, purification, application, market, and prospects. It is also a comprehensive survey of polysaccharide for further research and development.

Keywords Fungal polysaccharide · *Coriolus versicolor* · Polysaccharide · Review

40.1 Introduction

As well as the polysaccharide from plants, the fungal polysaccharide is the polymer condensated of aldose and ketose with glycosidic bond. Among these polysaccharide molecules composed of monosaccharide, the polysaccharides combined with proteins or peptides are called glycoproteins. They are present in

F. Wang · L. Hao · S. Jia (✉) · S. Niu
Key Laboratory Industrial Fermentation Microbiology, University of Science and Technology, Tianjin 300457, People's Republic of China
e-mail: jiashiru@tust.edu.cn

L. Hao
e-mail: hlm2005@tust.edu.cn

F. Wang · L. Hao · Q. Wang · X. Zhang · S. Niu
The Quartermaster Equipment Institute of GLD of PLA, Beijing 100010, People's Republic of China

T.-C. Zhang et al. (eds.), *Proceedings of the 2012 International Conference on Applied Biotechnology (ICAB 2012)*, Lecture Notes in Electrical Engineering 249,
DOI: 10.1007/978-3-642-37916-1_40, © Springer-Verlag Berlin Heidelberg 2014

the fruiting body, mycelium, and the fermented broth of fungi [1]. As a kind of natural biological macromolecule, fungal polysaccharide has gained wide attention because of its wide range of edible and nontoxic characteristics. Currently, there are 651 species and 7 subspecies of fungi which come from 182 genus of basidiomycetes containing anti-tumor and immunomodulatory polysaccharides [2].

Coriolus versicolor (CV), known as *Yunzhi* in China, is a mushroom belonging to species of the Basidiomycetes class of fungi, which has been widely used as a magic drug to treat cancer and immune deficiency related illnesses [3]. *Coriolus versicolor* was recorded in the Compendium of Materia Medica by Li Shizhen during the Ming Dynasty in China, as being beneficial to health and able to bring longevity if consumed regularly [4].

Coriolus versciclor polysaccharide contains extracellular polysaccharide (EPS) from submerged fermented broth, crude polysaccharide (CVPS) extracted from its fruiting body and protein-polysaccharide (glycopeptide) isolated from the deep layer-cultivated mycelia which include Yunzhi polysaccharopeptide (PSP) and polysaccharide Kureha (PSK, Krestin) from the Cov-1 and CM-101 strains of *Coriolus versicolor*, respectively [5].

40.2 Structure and Properties

There are some differences both in molecular weight and structure of extracted *Yunzhi* polysaccharide due to varied strains, culture conditions, and other factors. The medium component also affects the molecular weight of the polysaccharide [6]. Both products (PSK and PSP) have a molar mass of approximately 100 kDa [7]. The EPS contains predominantly glucose and small amounts of galactose, mannose, arabinose, and xylose. The main EPS is composed of β-1, 3/β-1, 6-linked D-glucose molecules [8], while PSP and PSK contain α-1, 4 and β-1, 3 glucosidic linkages in their polysaccharide moieties (Fig. 40.1) [4, 9]. D-glucose is the major monosaccharide present while arabinose and rhamnose are the other principal monosaccharides in PSP. However PSK contains fucose, galactose, mannose, and xylose [10, 11].

PSP and PSK are light or dark brown powders that are still stable in hot water. The compounds are odorless and tasteless polysaccharopeptides and do not have a definite melting point. The PSP/PSK polymers are soluble in water but insoluble in methanol, pyridine, chloroform, benzene, and hexane. The aqueous solution of PSP (1 g/100 ml water) is neutral, with a pH value of between 6.6 and 7.2. The α_D^{25} (specific rotation) value of the PSP solution is in the range of 0–30° [12].

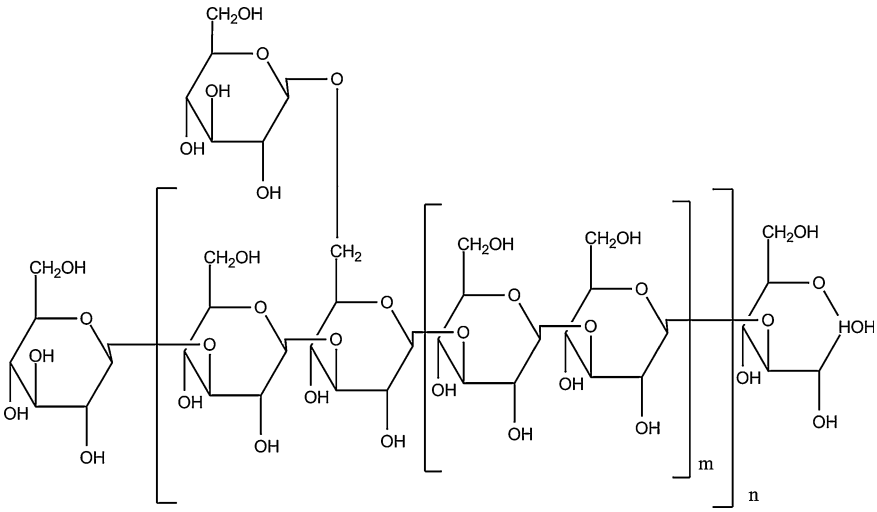

Fig. 40.1 Typical partial structures of polysaccharide portions of the polysaccharide peptide (PSP) of COV-1 strain of *Coriolus versicolor* [9]

40.3 Extraction and Purification

Typically, the polysaccharide is extracted repeatedly with hot water and the combined extract is concentrated by evaporation under vacuum or ultrafiltration. The concentrate is subjected to fractional precipitation using ammonium sulfate or alcohol. Precipitates are redissolved, dialyzed, and may be further purified by chromatographic methods. The solution of the purified product is concentrated and spray dried [5].

40.4 Fermentation

There are some advantages in submerged fermentation, such as little influence on the external environment, high pace of fermentation, ease of amplification, etc., it has become a major production method all over the world.

The culture medium plays an important role in the submerged fermentation, including the necessary carbon and nitrogen sources and other growth factors. The methodology of experimental factorial design and response surface analysis permitted determination of the optimal initial glucose concentration (13.8 g/L) and pH (5.5) to obtain EPS production (642.9 mg/L) by *Coriolus versicolor*, meanwhile the highest production of EPS (0.7 g/L) was obtained with the optimum medium (YM) after cultivating for 9 days at 28 °C using an orbital shaker at 180 r/min [13]. In addition, vitamin, mineral elements, and other growth factors are also

important factors for regulating the fungal growth and polysaccharide production of *Coriolus versicolor*. For example, polysaccharide production can be altered by adding different types of fatty acids or alcohols during the fermentation process. The mechanism of their inhibition or promotion to the formation of polysaccharide may be that they affect the structure and composition of the cell membrane, increase osmotic pressure, or directly affect the level of the enzyme involved in polysaccharide synthesis [14].

There are shake-flask cultivation and bioreactor cultivation for submerged fermentation. The former is applied to small-scale experiment in lab and the latter is generally carried out in large-scale for industrial production. Final biomass of 3.75 g/L and EPS of 4.1 g/L were attained after 12 days when synthetic minimal medium (20 g/L glucose, 20 mL/L salt stock solution, and 1 mg/L thiamine) and 30 L low-shear bioreactor cultivation technique were used [8], which increased by 5.9 times than those of previous report [13]. Using complex media compounds (potato dextrose broth and peptone) in an agitated submerged fermentation (50 L), Yoshikumi [15] obtained 4 g/L representing a total of extracellular and intracellular polysaccharopeptide from *Coriolus versicolor* by hot water extraction of 18 g/L mycelia after 7 days. Except for synthetic media, Cui [16] obtained 8.9–10.6 g/L biomass and 1132–1150 mg/L EPS using milk permeate as substrate after 7 days of fermentation. Moreover, Tavares established a new method to assess production of EPS by tracking the rheology of medium [13].

The reports about solid-state cultivation of CVPS are very few. Yadav and Tripathi used wheat bran and wheat straw to cultivate *Coriolus versciclor* when supplying with water, 1.0 % (g/100 mL) superphosphate and 1.5 % urea as extra nutrition and established the optimum fermentation conditions: 55 % water, pH 5.5, 30 °C , 21 days. Because there are a lot of problems for solid-substrate fermentation such as poorly control, labor-intensive, and environment vulnerably, submerged fermentation becomes the first choice [17].

40.5 Application

Coriolus versicolor polysaccharide has been widely studied as a medicinal fungus because of its antitumor, antioxidant, and immunity improving activities. For example, *Coriolus versicolor* methanol extract exerted pronounced anti-melanoma activity, both directly through antiproliferative and cytotoxic effects on tumor cells and indirectly through promotion of macrophage anti-tumor activity [18]. PSP and PSK indirectly inhibited the growth of various tumors by regulating immune function and improving the host immune response [19, 20]. DPPH radical scavenged for E-PPS and I-PPS, produced by liter of medium, was equivalent to 2.115 ± 0.227 and 1.374 ± 0.364 g of ascorbic acid, respectively. Moreover, these complexes showed a protective effect in the oxidation of erythrocyte membranes and the ability to inhibit the hemolysis and methemoglobin synthesis in stressed erythrocytes [6]. Thus, the results suggest that both extracellular and

intracellular polysaccharides produced by *Coriolus versicolor* are important bioactive compounds with medicinal potential. The latest research showed that the water extract from *Coriolus versicolor* did not cause remarkable adverse effect in SD rats [21].

40.6 Market and Prospects

As limited resources of wild *Coriolus versicolor*, the method of submerged culture mycelium except for the use of wild and cultivated ones is adopted to make food additives and healthcare products, which has been reported all over the word. But the filtrate of submerged fermentation is always overlooked or even abandoned. The studies on extracellular extract of *Coriolus versicolor* are relatively fewer than PSP and PSK.

Since polysaccharides have prominent biological activities and a wide range of medical applications in the functional food and medicine, the development and utilization of polysaccharides resources have become a critical concern of food science, natural medicine, biochemistry, and life science. In recent decades, both the domestic and foreign relevant science and technology personnel have carried out extensive research work in separation, purification, identification of chemical composition, and structure–activity relationship of biological activity of CVPS, and they have also achieved gratifying results. But efforts should be made in the following aspects: (1) In theory, we should thoroughly study and understand the structure–activity relationship of biological activity of CVPS, the mechanism of action with target cells and a series of follow-up biological effects. (2) In terms of product research and development, the techniques of extraction, purification, and identification need to be improved to obtain uniform composition and enhance the technological content of products. (3) It is necessary to further discuss on the metabolic pathway and the action mechanism of physiological and pharmacological activity after polysaccharides enter into bodies. (4) It is an important research part to study configuration differences and physiological activity of CVPS from different strains and the biological activity of polysaccharide derivatives. While it is also significant to extend the research on new functions of CVPS.

Fungal polysaccharide has been widely used as new resource in health food, medicine, cosmetics, and other areas. Therefore, the intensive study of function, structure–activity, activity, metabolic pathway of CVPS which is one of the members of this family will produce a certain market effect on system development of fungal polysaccharide. It also has the guiding significance for the research of other edible polysaccharide. In the near future, the CVPS products will create more potential applications in medicine, health care, functional food, and other fields along with widespread popularization and application of biological engineering technology.

Acknowledgments This work was financially supported by the National Natural Science Foundation of China (Grant No.31171662,No.21006072) and Innovative Research Team in University(IRT1166).

References

1. Xu JT (1997) Chinese medicinal mycology [M]. Beijing Medical University & Beijing Union Medical College Unionsverlag
2. Wasser SP (2002) Medicinal mushrooms as a source of antitumor and immunomodulating polysaccharides. Appl Microbiol Biotechnol 60:258–274
3. Yang QY (1999) History, present status and perspectives of the study of Yun Zhi polysaccharopeptide. In: Yang QY (ed) Advance research in PSP. The Hong Kong Association for Health Care Limited, Hong Kong, pp 5–15
4. Ng TB (1998) A review of research on the protein-bound polysaccharide (polysaccharopeptide, PSP)from the mushroom *Coriolus versicolor* (Basidiomycetes: Polyporaceae). Gen Pharmacol 30:1–4
5. Cui J, Chisti Y (2003) Polysaccharopeptides of *Coriolus versicolor*: physiological activity, uses, and production. Biotechnol Adv 21:109–122
6. Arteiro JMS, Martins MR, Salvador C, et al (2011) Protein–polysaccharides of *Trametes versicolor*: production and biological activities. Med Chem Res 21:937–943
7. Ng TB (1998) A review of research on the protein-bound polysaccharide polysaccharopeptide, (PSP) from the Mushroom *Coriolus versicolor* (Basidiomycetes: Polyporaceae). Gen Pharmacol 30:1–4
8. Rau Udo, Kuenz Anja, Wray Victor et al (2009) Production and structural analysis of the polysaccharide secreted by *Trametes Coriolus versicolor* ATCC 200801. Appl Microbiol Biotechnol 81:827–837
9. Zhou YL, Yang QY (1999) Active principles from *Coriolus* sp. In: Yang QY (ed.), Advanced Research in PSP[M]. Hong Kong: The Hong Kong Association for Health Care Limited 111–124
10. Wang HX, Ng TB, Liu WK et al (1996) Polysaccharide–peptide complexes from the cultured mycelia of the mushroom *Coriolus versicolor* and their culture medium activate mouse lymphocytes and macro-phages. Int J Biochem Cell Biol 28:601–607
11. Cheng G-Y, Wu G-R, Zhou Y-Z, et al (1998) Extraction and characterization of proteoglycan from the mycelium of *Polystictus versicolor* (L.) Fr. by submerged culture. Zhiwu Ziyuan Yu Huanjing 7:19–23
12. Hotta T, Enomoto A, Yoshikumi C, et al (1981) Protein-bound polysaccharides. US Patent 4, 271, 151
13. Tavares APM, Agapito MSM, Coelho MAZ (2005) etal. Selection and optimization of culture medium for exopolysaccharide production by *Coriolus (Trametes) versicolor*. World J Microbiol Biotechnol 21:1499–1507
14. Yang FC, Ke YF, Kuo SS (2000) Effect of fatty acids on the mycelial growth and polysaccharide formation by Ganoderma lucidum in shake flask cultures. Enzyme Technol 27:295–301
15. Yoshikumi C, Wada T, Fujii M, et al (1978b) Recovery of a polysaccharide with therapeutic action. German Patent DE 2, 731, 570
16. Cui J, Goh KKT, Archer R et al (2007) Characterisation and bioactivity of protein-bound polysaccharides from submerged-culture fermentation of *Coriolus versicolor* Wr-74 and ATCC-20545 strains. J Ind Microbiol Biotechnol 34:393–402
17. Yadav JS, Tripathi JP (1991) Optimization of cultivation and nutrition conditions and substrate pretreatment for solid-substrate fermentation of wheat straw by *Coriolus versicolor*. Folia Microbiol 36:249–301

18. Harhaji LJ, Mijatovic S, Maksimovic-Ivanic D, et al (2008) Anti-tumor effect of *Coriolus versicolor* methanol extract against mouse B16 melanoma cells: in vitro and in vivo study. Food Chem Toxicol 46:1825–1833
19. Lee CL, Yang XT, Wan JMF (2006) The culture duration affects the im-munomodulatory and anticancer effect of polysaccharopeptide derivedfrom *Coriolus versicolor*. Enzyme Microbial Technol 38:14–21
20. Jiménez-Medina E, Berruguilla E, Romero I et al (2008) The immunomodu-lator PSK induces in vitro cytotoxic activity in tumour cell lines viaarrest of cell cycle and induction of apoptosis. BMC Cancer 8:78
21. Hor SY, Ahmad M (2011) Acute and subchronic oral toxicity of *Coriolus versicolor* standardized water extract in Sprague-Dawley rats. J Ethnopharmacol 137:1067–1076

Chapter 41
Antimicrobial Effects of Aqueous Extracts Obtained from Fallen Leaves of *Ginkgo biloba*

Wuyuan Deng

Abstract The filter paper method was used to study the antimicrobial effects of aqueous extracts obtained from fallen leaves of *Ginkgo biloba* on the common environment contaminative microorganisms. The influences of temperature, ultraviolet light, and pH value on the antibacterial activity were also evaluated. The results showed the aqueous extracts could inhibit all the tested strains at the different extents. The extracts had the strongest antibacterial function against *Pseudomonas aeruginosa* and the effect was greater in higher extracts concentration. The aqueous extracts had excellent thermal stability but poor ultraviolet stability and could maintain good antimicrobial effect in a broad range of pH values.

Keywords Antimicrobial effect · Aqueous extracts · Fallen leaves of *Ginkgo biloba* · Filter paper method

41.1 Introduction

Ginkgo biloba is a precious species and belongs to *Ginkgo* genus of the *Ginkgoaceae*. The *Ginkgo* leaf has important medicinal values because of its several kinds of active components such as flavonoids, lactones, phenols, etc. At present, for fully exploiting and utilizing the ginkgo leaves, extracting flavone and lactone from it is the main pathway, because these two components have obvious therapeutic effects on cardiovascular and cerebral diseases. However, their content in ginkgo leaves varied with seasons. The data showed that the content of ginkgolide in green ginkgo leaves is higher than in yellow leaves. Furthermore, it is

W. Deng (✉)
Experiment and Teaching Resources Management Center,
Yibin University, Yibin 644007, People's Republic of China
e-mail: dengwuyuan78@163.com

T.-C. Zhang et al. (eds.), *Proceedings of the 2012 International Conference on Applied Biotechnology (ICAB 2012)*, Lecture Notes in Electrical Engineering 249,
DOI: 10.1007/978-3-642-37916-1_41, © Springer-Verlag Berlin Heidelberg 2014

reported that both the contents of flavone and ginkgolide in yellow leaves are fewer [1, 2]. So now, supplies of the green ginkgo leaves often fall short of our demand, but there are relatively few developments and utilizations of yellow ginkgo leaves. China is the largest country producing and exporting ginkgo in the world. Now its ginkgo output shares 90 % of the world [3]. Most of the ginkgo leaves are abandoned when they become fallen leaves, which generates enormous waste of resources and does not fully exploit the ginkgo resource. Therefore, how to efficiently utilize this natural resource needs to be urgently settled.

Many studies have demonstrated that gingko leaf extract has antimicrobial activity [4–7], but most of the experimental materials used in these researches were fresh ginkgo leaves; antimicrobial effect of fallen leaves of ginkgo is barely reported. Therefore, this paper focuses on fallen ginkgo leaves and discusses their antimicrobial effects on the common environment contaminative microorganisms, which may be the direction for further development of gingko resource in China.

41.2 Materials and Methods

41.2.1 Plant Materials and Tested Strains

Fallen ginkgo leaves were collected from Yibin University. *Bacillus subtilis, E*scherichia *coli*, *Staphylococcus aureus, Pseudomonas aeruginosa*, and *Proteus vulgaris* were supplied by the microbiology laboratory of Yibin University, China.

41.2.2 Preparation of Extracts

The fallen ginkgo leaves were washed and dried in the shade, cut into pieces, and crushed to powder [8]. One hundred grams of the powdered material was soaked in 250 ml of distilled water and agitated mechanically at room temperature for 6 h, and then centrifuged and the supernatant was sterilized by filtration with 0.2 μm of filter membrane. The extracts (its concentration was regarded as 100 %, hereinafter referred to as "original aqueous extracts") obtained was stored at 4 °C when not in use.

41.2.3 Preparation of Inoculum

All the inoculum of bacteria mentioned above were prepared by cultivating cells in beef cream-peptone culture medium for 24 h at 37 °C. These cell suspensions were diluted with sterile saline to provide initial cell counts of about 10^7–10^8 CFU/ml.

41.2.4 Antibacterial Activity Test of Original Aqueous Extracts

The antibacterial activity of the original aqueous extracts obtained from fallen leaves of *Ginkgo biloba* was carried out by filter paper method [9–13]. 0.1 mL of inoculum was evenly spread on agar using a glass rod spreader. Sterile filter paper (diameter 6 mm) was impregnated with the extracts and placed on the culture medium. For control, disks were impregnated with sterile distilled water. After 30 min, plates were turned upside down and incubated at 37 °C for 48 h. The diameter of the clear zone around the disk was measured and expressed in millimeters as its antimicrobial activity.

41.2.5 Antibacterial Activity Test of Different Concentration of the Aqueous Extracts

The antibacterial activities of the extracts with different concentrations were determined. The concentrations tested were 100.0, 50.0, 25.0, and 12.5 %. Appropriate volume of original aqueous extracts was added to sterile distilled water (v/v) to obtain the desired concentrations cited above. The tested strain was *Pseudomonas aeruginosa* (the following tested strains were the same). Sterile distilled water was used as controls.

41.2.6 Heat Stability Test

The antibacterial activities of the original aqueous extracts heated in 60, 80, 100, and 121 °C for 30 min were determined, sterile distilled water and extracts at room temperature (about 28 °C) were used as controls.

41.2.7 UV Stability Test

To evaluate the influences of UV irradiation on the antimicrobial effects of the extracts obtained from fallen ginkgo leaves, the original aqueous extracts were exposed to ultraviolet irradiation for 0, 5, 10, 15, 20, and 25 min, respectively before their antibacterial activity tests.

41.2.8 pH Stability Test

To determine the stability of the extracts under different pH, the pH values in original aqueous extracts were adjusted to 2, 4, 6, 8, 10, 12 with HCL solution or NaOH solution before their antibacterial activity tests; unadjusted extracting solution and sterile distilled water were used as controls.

41.3 Results and Discussion

41.3.1 Antibacterial Activity of Original Aqueous Extracts

The aqueous extracts of fallen ginkgo leaves could inhibit all the tested strains at the different extents. The extracts have the strongest antibacterial function against *Pseudomonas aeruginosa* as shown in Fig. 41.1. But variance analysis showed that there are no significant difference among these groups of various tested strains ($F < F_{0.05}$). It indicated that there was no marked difference in the antimicrobial effects of aqueous extracts on the different tested strains. Ginkgo leaves contain ginkgolic acid, ginkgol, and some other antifungal substances. It is reported that ginkgolic acid, predominant antibiotic composition, is hardly soluble in water, but soluble in organic solvents [14]. If the extracting agent in this experiment was replaced with ethanol, we can expect that the content of antifungal substances in the extracts obtained from the fallen leaves of *Ginkgo biloba* could be increased, and the antimicrobial effects could be stronger.

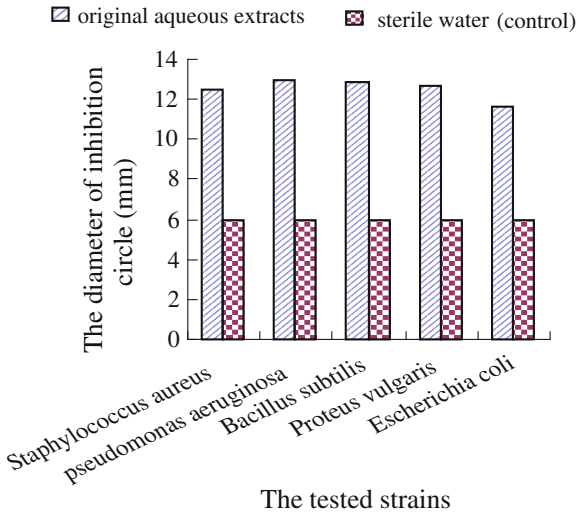

Fig. 41.1 The antimicrobial effect of the original aqueous extracts obtained from fallen ginkgo leaves

41.3.2 Antibacterial Activity of Different Concentration of the Extracts

Like the results of many other antibacterial experiments [15–20], the antimicrobial effect of the aqueous extracts obtained from fallen leaves of *Ginkgo biloba* was associated with extracts concentration, as shown in Fig. 41.2, the effect was stronger in higher extracts concentration. Variance analysis showed that there were significant differences among these different concentration groups ($F > F_{0.01}$).

41.3.3 Stability Test of the Aqueous Extracts

The results of heat stability test showed that the aqueous extracts had excellent thermal stability as shown in Fig. 41.3. Although the antibiotic activities decreased as the heat treatment temperature increased, the scale of reduction of effects was small. There was no significant difference among the groups by analysis of variance ($F < F_{0.05}$). It indicated that the antibiotic effect of the aqueous extracts of fallen ginkgo leaves was not changed obviously after different heat treatment. But the extracts had poor ultraviolet stability, its antibiotic activities began to fall rapidly after UV irradiation for 5 min (Fig. 41.4), and there were significant differences among these groups after exposed to UV irradiation for different times ($F > F_{0.01}$). The experimental results indicated that different UV irradiation time had different impact on the antibiotic activities of the extracts. So UV irradiation

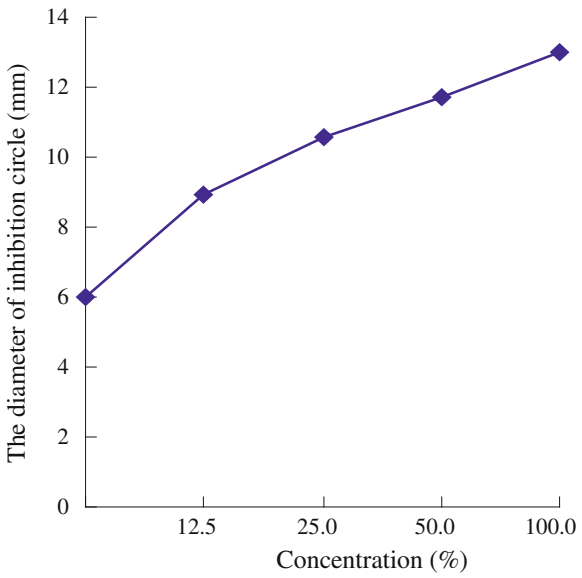

Fig. 41.2 The antimicrobial effect of different concentration of the aqueous extracts obtained from fallen ginkgo leaves

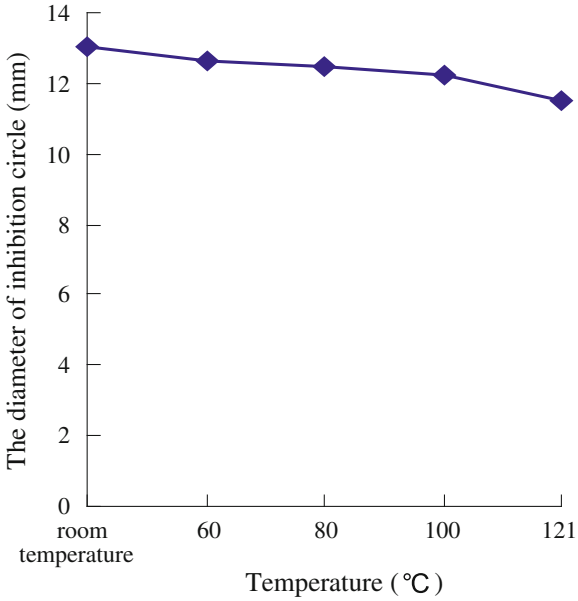

Fig. 41.3 The influence of heat treatment on the antimicrobial effect of the aqueous extracts obtained from fallen ginkgo leaves

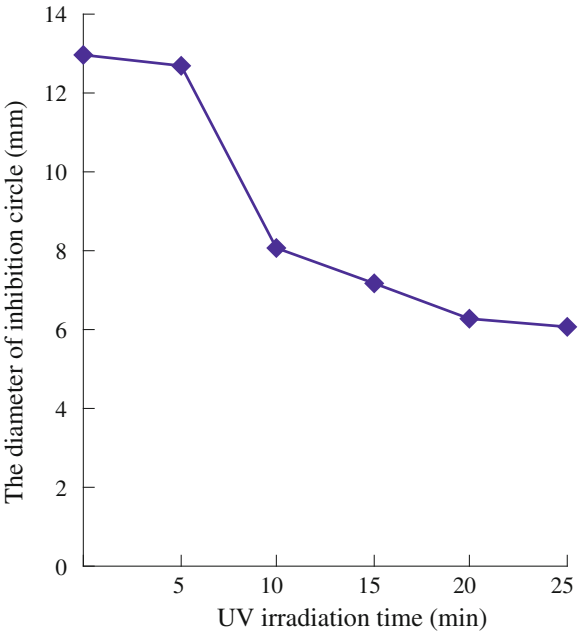

Fig. 41.4 The influence of UV irradiation on the antimicrobial effect of the aqueous extracts obtained from fallen ginkgo leaves

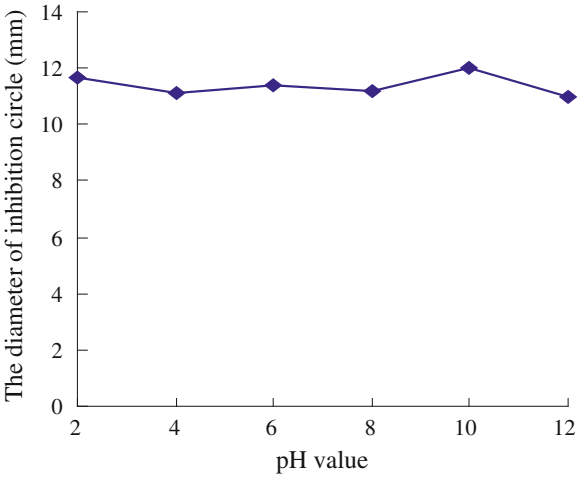

Fig. 41.5 The influence of pH value on the antimicrobial effect of the aqueous extracts obtained from fallen ginkgo leaves

should be avoided in practical production of related products. Treated by various pH values, the extracts of fallen ginkgo leaves could maintain good antimicrobial effects in a broad range of pH values (Fig. 41.5), but the effects under different pH values were different ($F > F_{0.01}$). Within the range of pH values in this experiment, when pH was 10, the extracts exhibited the strongest antibacterial function.

41.4 Conclusions

The extracts of ginkgo leaves have been developed into all kinds of drugs, health foods, and cosmetics sold in China and abroad [21]. Besides, its anti-bactericidal characters will promote the development and utilization of *Ginkgo biloba* leaves toward a wider prospect. Our results showed that the aqueous extracts obtained from fallen leaves of *Ginkgo biloba* had excellent thermal stability and could maintain good antimicrobial effect in a broad range of pH values. Therefore, it may be further processed and developed into some new products. If the considerable resources of abandoned fallen ginkgo leaves are developed into natural antiseptic, it will result in notable economic, environmental, and social benefits.

Acknowledgments This research is supported by the Science and Technology Plan Project of Sichuan Provincial Education Department (12ZB344) and the key project of Sichuan Science and Technology Department (2010JY0145). The author expresses her great thanks to the microbiology lab of Yibin University for providing the tested strains.

References

1. Zhang L, Tang XF, Sun GT (2011) Picking and storage of Ginkgo leaves. Mod Agric Sci Tech 24:239–239, 241 (Chinese)
2. Zhang XD, Ma, LZ, Shao BX (2006) Progress of preparation of total flavanoid in leaves of ginko biloba L. Chin J Card Med 11(5):385–387 (Chinese)
3. Geng JZ (2011) Research progress of health factors in *Ginkgo biboba* Linn. Am Ac Bi Resour 33(1):63–66, 83 (Chinese)
4. Qu XH, Xin YF, Zhang KY (2010) Comparative study of different extracting methods on antibacterial effect of *Ginkgo biloba* active substances. Shandong Agric Sci 4:62–64 (Chinese)
5. Xu Y, Wang SY (2006) Effect of restraining bacterium on Ginkgo leaves. Food Res Dev 27(10):64–66 (Chinese)
6. Li Y, Yang XY, Lin YX et al (2006) Comparison of in vitro antibacterial effect of Ginkgo leaves extract. Hubei Agric Sci 45(4):503–505 (Chinese)
7. Sheng JG., Huang DY (2005) The researches on extraction technology and antimicrobial characteristics of the *Gingko biloba* extract. Sci Technol Cereals Oil Food 13(5):16–18 (Chinese)
8. Huo GH, Ga YY, Chen MH (2005) Study on the antifungal components in the leaf of *Sapium sebiferum*. Food Ferm Ind 31(3):52–56 (Chinese)
9. Shan WR, Li JX, Liu HF (2010) Study on the inhibitory effects of different active materials screened by the filter paper on cotton verticillium wilt. Chin Agric Sci Bull 19:285–289 (Chinese)
10. Zhang J, Wang Y, Zhang F (2009) Mensurating the antiseptic activity of extracts from *Artemisia annua* L. to mold with the filter paper method. Hubei Agric Sci 48(5):1153–1154 (Chinese)
11. Gong JW, Hu BF, Yan LL (2011) Comparative study on bacteriostasis of extracts from Zanthoxylum bungeanum. Guangdong Agric Sci 38(24):57–58 (Chinese)
12. Xiao FY, Gao YF, Yin JJ (2011) Study on antimicrobial activity on *Lonicera chrysantha* extracts. Northern Hortic 13:177–179 (Chinese)
13. Liu XL, Hou SJ (2009) Study on anti-microbial activities of potato skin. J Xichang Coll (Nat Sci) 23(4):35–37 (Chinese)
14. Li WH, Wang J, Li DW (2004) Technical process of extraction from the testa of *Ginkgo biloba* L. and the application for preparation of biotic pesticide. Chem Eng (China) 32(2):69–72 (Chinese)
15. Kang ML (2012) Study on bacteriostasis of onion. J Anhui Agric Sci 40(5):2604–2607 (Chinese)
16. Ma HM, Zhang YH, Chen XL (2012) Bacteriostasis of different extracts from impatiens balsamina L. Stem on bacteria. J Henan Agric Sci 41(1):126–128 (Chinese)
17. Li WC, Shi WJ, Gu YF (2011) Antibacterial effect of different extract of Pulsatilla chinensis (Bunge) regel in vitro. J Trad Chin Vet Med 13(2):38–40 (Chinese)
18. Yu LH, Li XL, Lan H (2010) Effect of bacteriostaticon penicillium italicumin stored citruses by using the extracts of Ginkgo bilobaleaves. Food Mach 6:60–62 (Chinese)
19. Wang YN, Zheng L, Li L (2010) Study on bacteriostasis of onion juice. Guizhou Agric Sci 12:56–58 (Chinese)
20. Xu GF, Wang HS, Liu MJ (2010) Primary study on the inhibition effect of acetone extracts from rhus typhina leaves. Chin Agric Sci Bull 26(12):242–246 (Chinese)
21. Li ZQ (2007) Researching and producing of healthy food from Ginkgo leaf. Stor Process 7(1):53–54 (Chinese)

Chapter 42
Effects of *IAH1* Gene Deletion on the Profiles of Chinese Yellow Rice Wine

Longhai Dai, Cuiying Zhang, Jianwei Zhang, Yanan Qi and Dongguang Xiao

Abstract Acetate esters are the representative flavor-active esters responsible for the fruity odors of Chinese yellow rice wine. The *IAH1* gene, encoding an ester-hydrolyzing esterase, was deleted in the industrial *Saccharomyces cerevisiae* RY-1, and the engineered strain IY-1 was obtained. Then, Chinese yellow rice wine brewing was simulated using the parental strain RY-1 and the engineered strain IY-1, respectively. The results showed that after 6 days of fermentation, fermentation profiles as well as components of the resulting yellow rice wine were so similar except for the ethyl acetate production. The content of ethyl acetate in the yellow rice wine fermented with IY-1 was 47.4 $mg \cdot L^{-1}$ which increased by 46.3 % than that of the parental strain RY-1, while isoamyl acetate and isobutyl acetate were not detected in both RY-1 and IY-1. The results demonstrate that deletion of *IAH1* gene in industrial yeast strain could increase ethyl acetate production in Chinese yellow rice wine.

Keywords *Saccharomyces cerevisiae* · *IAH1* · Ethyl acetate · Chinese yellow rice wine

42.1 Introduction

Chinese yellow rice wine is one of the most three ancient wines in the world, which has its distinct flavor, high nutrition, and health functions. In Chinese yellow rice wine brewing, rice starch is saccharified by the mixed strains of koji and then the liberated glucose is fermented to ethanol by *Saccharomyces*

L. Dai · C. Zhang (✉) · J. Zhang · Y. Qi · D. Xiao
Key Laboratory of Industrial Fermentation Microbiology, Ministry of Education, Tianjin Industrial Microbiology Key Laboratory, College of Biotechnology, Tianjin University of Science and Technology, Tianjin 300457, People's Republic of China
e-mail: cyzhangcy@tust.edu.cn

T.-C. Zhang et al. (eds.), *Proceedings of the 2012 International Conference on Applied Biotechnology (ICAB 2012)*, Lecture Notes in Electrical Engineering 249,
DOI: 10.1007/978-3-642-37916-1_42, © Springer-Verlag Berlin Heidelberg 2014

cerevisiae. The two steps proceed simultaneously, which is a characteristic compared with the fermentation system of other alcohol production in the world. During fermentation processes, yeast cells produce a broad range of aroma-active substances which greatly affect the complex flavor of Chinese yellow rice wine [1–7]. Though formed only in trace amount, acetate esters are the most important contributor of all the flavor-active to the odor, they are responsible for the highly desired fruity character of Chinese yellow rice wine [8–11].

Acetate esters in Chinese yellow rice wine are mainly ethyl acetate (solvent-like aroma) and trace amount of isoamyl acetate (banana flavor) and isobutyl acetate (fruity-like aroma), which are produced in the primary fermentation [12–15]. These esters are synthesized from correlated alcohol and acetyl coenzyme A (CoA) by alcohol acetyltransferase (AATFase) in yeast, and hydrolyzed by the *IAH1*-encoded esterase at the same time [16–18].

The yeast strain used for fermentation plays a vital role in the production of esters [19]. However, Chinese yellow rice wine yeast displays very poorly in the ethyl esters production. With the purpose of increase acetate esters, in this study, we constructed *IAH1*-deficient diploid Chinese yellow rice wine yeast by recombinant DNA technology, and detected the fermentation profiles of the resulting mutants so as to offer prospects for the development of excellent yeast starter strains for high-quantity Chinese yellow rice wine production.

42.2 Materials and Methods

42.2.1 Strains, Media, and Culturing Conditions

Commercial yellow rice wine yeast strain RY-1 was screening from Angel Yeast (Hubei, China) and used as parent to spore to get haploids RY-a1 and RY-α3. Recombinant diploid IY-1 was fusing by engineered haploids IY-a1 and IY-α3, all of which the *IAH1* gene were deleted. *Escherichia coli* DH5α was used as a host for plasmid amplification and grown at 37 °C in a Luria–Bertani medium (1 % Bacto tryptone, 1 % NaCl, and 0.5 % yeast extract), Ampicillin was added into the media at a final concentration of 100 $\mu g \cdot mL^{-1}$. YPD medium (2 % glucose, 2 % peptone, 1 % yeast extract) was used to culture the yeast strains at 30 °C, G418 was added into the media at a final concentration of 600 $\mu g \cdot mL^{-1}$ to select the yeast transformants. Agar (2 %) was used to solidify media. The seed was cultivated by wort (prepared by treating freshly smashed malt with water at 65 °C for 2 h and adjusting the sugar content of wort to 12° Brix) at 28 °C.

42.2.2 Recombinant DNA Methods and Plasmid Construction

Standard procedures for the isolation and manipulation of DNA [20] were used in this study. Restriction enzymes, T4 DNA-ligase, and Expand highfidelity DNA polymerase (TaKaRa Biotechnol, Dalian, China) were used in the enzymatic manipulation of DNA, according to the recommends of the supplier. The primers used for plasmids construction and verification of recombinant yeast in this study are listed in Table 42.1. The 253 bp of IA (amplified by primers IA-F and IA-R) fragment upstream of *IAH1*, and 229 bp of IB (amplified by primers IB-F and IB-R) fragment downstream of *IAH1* were amplified via PCR with the genomic DNA of RY-1 as template, and Kan antibiotic gene for G418 resistance was amplified (amplified by primers Kan-F and Kan-R) via PCR from plasmid pUG6 (presented by Professor Hegemann JH, Heinrich-Heine-University Düsseldorf). The IA, IB, Kan fragments were inserted into the pUC19 multiple cloning site sequentially and with the same direction to form the deletion plasmid pUC-IABK.

42.2.3 Construction of Recombinant S. cerevisiae Haploid

The gene disruption cassette IA-Kan-IB was amplified by PCR with the primer pair IA-F/IB-R from plasmid pUC-IABK and transformed to yeast haploids RY-a1 and RY-α3 using the previously described lithium acetate procedure [21]. After transformation, the yeast cells were plated on YPD medium containing 600 $\mu g \cdot mL^{-1}$ of G418.

Table 42.1 Primers used in this work[a]

Primers	Sequence (5′ → 3′)
Primers for plasmids construction	
IA-F	CCAAGCTT CCCTTGGAAAACGTTCA
IA-R	GCGGATCCATTTGGTCACAGTTTAAG
IB-F	GCGGATCC ATGCAGTAATCCTTTGTA
IB-R	CGGAATTC AATTTCTATGTATCTCTC
Kan-F	GCGGATCCCAGCTGAAGC TTCGTAC
Kan-R	GCGGATCCGCATAGGCCA CTAGTGG
Primers for recombinant yeast verification	
I–S	TTCGCGTACCGTAGGTCAGCAAT
K–S	CGGATAAAATGCTTGATGGTCGGA
K-X	CGGTTGCATTCGATTCCTGTTTGT
I-X	TGATCTACACGAATAACACGGTCC

[a] The restriction site introduced in each primer is indicated by an underline

42.2.4 Fermentation Experiments

Yeast cells were precultured in 5 mL wort medium at 28 °C for 12 h, then 1 mL of the preculture was used to inoculate 100 mL of wort medium in 250-mL Erlenmeryer flasks at 28 °C for 24 h. A total of 100 g rice was dipped in water for 72 h at 25 ~ 30 °C. The dipped rice was washed, and then cooked for 40 ~ 50 min; the cooked rice was cooled at room temperature, and then transferred into 500 mL flasks. Finally, 10 g mature wheat koji, 105 mL water (consisting of 60 mL clean water and 45 mL serofluid), and 30 mL second-preculture of yellow rice wine yeast were added into the flasks. The mixture was fermented at 28 °C for 6 days [22]. The weight loss of CO_2, ethanol production, residual reducing sugar, and contents of certain aroma components were determined after fermentation. All fermentations were performed in triplicate.

42.2.5 Gas Chromatography Analysis

The yellow rice wine broth was filtered and distilled after fermentation and used for GC analysis. The analysis of volatile compounds was carried out on an Agilent 7890C GC coupled to an Agilent G4512A autosampler and injector. Amyl acetate was used as the internal standard. The column used was a HP-INNOWax polyethylene glycol (higher limit temperature 260 °C; LabAlliance), which is an organic coated fused silica capillary column with 30 m × 320 μm i.d. and a 0.5 μm coating thickness. Nitrogen was used as the carrier gas and the temperature of the flame ionization detector (FID) was adjusted to 250 °C. The injector temperature was 230 °C, the split ratio was 25:1, and the injection volume was 1.0 μL. The oven temperature program was as follows: 50 °C for 0 min, followed by an increase to 62 °C at 2 °C min^{-1}, and then an increase to 200 °C (0 min) at 15 °C min^{-1} for 0 min.

42.3 Results and Discussions

42.3.1 Verification of Recombinant S. cerevisiae Haploid

G418-resistant colonies were confirmed by PCR with primer pairs I–S/K–S and K–X/I–X. The results showed that both the 1,559 bp band with I–S/K–S and the 1,167 bp band with I–X/K–X could be amplified from engineered haploids IY-a1 and IY-α3, but could not from the parental haploids RY-a1 and RY-α3 (Fig. 42.1). Then the amplified 1,559 bp and 1,167 bp PCR products were further sequenced, revealing a complete match to the sequence as the expected result from double

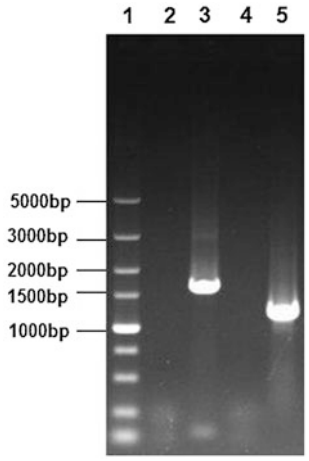

Fig. 42.1 PCR verification of *IAH1* gene deletion mutants. Lane *1* was DL 5000 ladder marker, lane *2* PCR fragment (negative control) from parental haploid RY-a1 genomic DNA with pair I–S/K–S, lane *3* PCR fragment from the engineered IY-a1 genomic DNA with pair I–S/K–S, lane *4* PCR fragment (negative control) from parental haploid RY-a1 genomic DNA with pair K-X/I-X, lane *5* PCR fragment from engineered IY-a1 genomic DNA with pair K–X/I–X

homologous recombinant between the recombinant cassette and the *IAH1* gene in haploid yeast.

42.3.2 Construction of the Recombinant Diploid Yeast Strain

Two recombinant haploids I-a1 and I-α3 with perfect fermentation performances and ethyl acetate production were chosen for mating and then verified by PCR using the method just as the haploid (data not shown).

42.3.3 Effects of IAH1 *Gene Deletion on Fermentation Performances of the Yellow Rice Wine Yeast*

Simulation of Chinese yellow rice fermentation was carried out using the engineering strains IY-1, IY-a1, IY-α3 and parental strains RY1, RY1-a1, and RY1-a1 at 28 °C, respectively. Total loss of CO_2, ethanol production and residual reducing sugar were measured after 6 days of fermentation (Table 42.2). As shown in Table 42.2, after 6 days of fermentation, the weight loss of CO_2 and the content of alcohol were so similar between the engineered yeasts and its parental strains. And the residual reducing sugars of all the strains were lower than 1 g/100 mL, which

Table 42.2 Fermentation performances of the yellow rice wine yeast[a]

Strain	Weight loss (g)	Ethanol (%)	Glucose (g/100 mL)
RY-1	30.5 ± 0.2	13.8 ± 0.1	0.70 ± 0.08
RY-a1	31.0 ± 0.2	13.8 ± 0.1	0.62 ± 0.13
RY-α3	30.9 ± 0.2	14.1 ± 0.1	0.48 ± 0.12
IY-1	30.7 ± 0.3	14.1 ± 0.1	0.66 ± 0.22
IY-a1	30.8 ± 0.1	14.0 ± 0.1	0.60 ± 0.10
IY-α3	30.5 ± 0.2	13.8 ± 0.1	0.41 ± 0.17

[a] Results are averages from three parallel independent experiments. Values are mean ± S.D. of three different tests

indicated that the fermentation was relatively thorough and the deletion of *IAH1* gene had no influence on the fermentation performances of engineered strains.

42.3.4 *Effects of* IAH1 *Gene Deletion on the Production of Volatile Flavor Compounds*

After fermentation at 28 °C for 6 days, the yellow rice wines were filtered and distilled. The concentrations of the ethyl esters and higher alcohols in the samples were then determined through GC analysis (Table 42.3). Analysis of the general components of the yellow rice wine showed that there was no difference between that produced with the parental strains and those produced with the engineered strains, except for the concentration of ethyl acetate. As shown in the Table 42.3, the ethyl acetate concentration in the yellow rice wines fermented by RY-1, RY-a1, and RY-α3 were 32.4, 35.2, and 36.3 $mg{\cdot}L^{-1}$, while the content of ethyl acetate produced by engineered strains IY-1, IY-a1, and IY-α3 were 47.4, 49.3, and 50.2 $mg{\cdot}L^{-1}$, which increased by 46, 39, and 39 %, respectively. Isoamyl acetate and isobutyl acetate were not detected in all the strains all through the study.

Ethyl esters were synthesized by AATFase and hydrolyzed by esterase at the same time. Also it had been proved that the accumulation of ethyl esters was

Table 42.3 Volatile flavor compounds productions of the yellow rice wine yeast

Strain	Ethyl acetate ($mg{\cdot}L^{-1}$)	Isoamyl acetate ($mg{\cdot}L^{-1}$)	Isobuty acetate ($mg{\cdot}L^{-1}$)	Isoamyl alcohol ($mg{\cdot}L^{-1}$)	Isobuty alcohol ($mg{\cdot}L^{-1}$)
RY-1	32.4 ± 1.3	ND	ND	353.2 ± 3.5	168.1 ± 8.5
RY-a1	35.2 ± 0.5	ND	ND	347.5 ± 5.1	159.4 ± 4.2
RY-α3	36.3 ± 0.5	ND	ND	343.2 ± 2.6	149.4 ± 5.7
IY-1	47.4 ± 0.4	ND	ND	358.6 ± 4.3	161.2 ± 6.3
IY-a1	49.3 ± 1.5	ND	ND	349.6 ± 7.1	155.2 ± 3.5
IY-α3	50.2 ± 0.3	ND	ND	353.4 ± 5.2	153.0 ± 3.6

controlled by a balance of activity of AATFase and Iah1p-esterase. In this study, isoamyl acetate and isobutyl acetate were not detected in all the strains all through the study. We speculate that the major rate-limiting factor for accumulation of isoamyl acetate and isobutyl acetate is the activity of AATFase in the fermentation mash, so the deletion of *IAH1* gene has little influence on isoamyl acetate and isobutyl acetate accumulation. To increase isoamyl acetate and isobutyl acetate content in Chinese yellow rice wine, yeast strain with higher AATFase activity should further be screened.

42.4 Conclusion

In this study, an engineered industrial strain IY-1 produced 46 % higher ethyl acetate than that of parental strain RY-1 was obtained through the deletion of *IHA1* gene. Negligible influence was observed on the fermentation profile between the parental strains and engineered strains. The study is encouraging, which makes us better understand the metabolism of ethyl esters and provides an approach for the screening of excellent yeast strain so as to improve the quality of Chinese yellow rice wine.

Acknowledgments This work was supported by the program for Changjiang Scholars and Innovative Research Team in University (IRT1166), the 863 (Hi-tech research and development program of China) program under contract NO.SS2012AA023408, and the Youth Foundation of Application Base and Frontier Technology Project of Tianjin, China (12JCQNJC06500).

References

1. Fujii T (1994) Molecular cloning, sequence analysis and expression of the yeast alcohol acetyltransferase gene. Appl Environ Microbial 60:2786–2792
2. Fujii T, Yoshimoto H, Tamai Y (1996) Acetate ester production by *Saccharomyces cerevisiae* lacking the *ATF1* gene encoding the alcohol acetyltransferase. J Ferment Bioeng 81:538–542
3. Minetoki T (1992) Alcohol acetyl transferase of sake yeast. J Brew Soc Jpn 87:334–340
4. Plata C (2003) Formation of ethyl acetate and isoamyl acetate by various species of wine yeasts. Food Microbiol 20:217–224
5. Peddie H (1990) Ester formation in brewery fermentations. J Inst Brew 96:327–331
6. Mason AB, Dufour JP (2000) Alcohol acetyltransferase and the significance of ester synthesis in yeast. Yeast 16:1287–1298
7. Kobayashi M, Shimizu H, Shioya S (2008) Beer volatile compounds and their application to low-malt beer fermentation. J Biosci Bioeng 106:317–323
8. Meilgaard MC (1975) Flavor chemistry of beer flavor and threshold of 239 aroma volatiles. MBAA Tech Q 12:151–168
9. Malcorps P, Dufour JP (1992) Short-chain and medium-chain aliphatic ester synthesis in *Saccharomyces cerevisiae*. Eur J Biochem 210:1015–1022

10. Nordström K (1963) Formation of ethyl acetate in fermentation with brewer's yeast IV: metabolism of acetyl coenzyme A. J Inst Brew 69:142–153
11. Minetoki T (1992) Alcohol acetyl transferase of sake yeast. J Brew Soc Jpn 87:334–340
12. Yoshimoto H, Fujiwara D, Momma T (1998) Characterization of the *ATF1* and *Lg-ATF1* genes encoding alcohol acetyltransferases in the bottom fermenting yeast *Saccharomyces pastorianus*. Ferment Bioeng 86:15–20
13. Meilgaard MC (2001) Effects on flavour of innovations in brewery equipment and processing: a review. J Inst Brew 107:271–286
14. Verstrepen KJ (2003) Expression levels of the yeast alcohol acetyltransferase genes *ATF1*, *Lg-ATF1*, and *ATF2* control the formation of a broad range of volatile esters. Appl Environ Microbiol 69:5228–5237
15. Meilgaard MC (1975) Flavor chemistry of beer. I. Flavor interaction between principal volatiles. MBAA Tech Q 12:107–117
16. Fukuda F, Yamamoto N (2008) Brewing properties of sake yeast whose *EST2* gene encoding isoamyl acetate-hydrolysing esterase was disrupted. J Ferment Bioeng 85:101–106
17. Fukuda F, Yamamoto N (2008) Balance of activities of alcohol acetyltransferase and esterase in *Saccharomyces cerevisiae* is important for production of isoamyl acetate. Appl Environ Microbiol 64:4076–4078
18. Lilly M, Lambrechts MG (2006) The effect of increase yeast alcohol acetyltransferase and esterase activity on the flavour profiles of wine and distillates. Yeast 23:641–659
19. Lambrechts MG, Pretorius IS (2000) Yeast and its importance to wine aroma. S Afr J Enol Vitic 21:97–129
20. Sambrook J, Russell DW (2001) Molecular cloning: a laboratory manual, 3rd edn. CSHL press, New York
21. Gietz RD, Woods RA (2002) Transformation of yeast by lithium acetate/single-stranded carrier DNA/polyethylene glycol method. Methods Enzymol 350:87–96
22. Zhang JW, Zhang CY, Dai LH et al (2012) Effects of overexpression of the alcohol acetyltransferase-encoding gene *ATF1* and deletion of the esterase-encoding gene *IAH1* on the flavour profiles of Chinese yellow rice wine. Int J Food Sci Tech 47:2590–2596

Chapter 43
Investigation of Bacterial Diversity in Traditional Meigui Rice Vinegar by PCR-DGGE Method

Jieyan Shi, Ye Liu, Wei Feng, Xiong Chen, Yanglin Zhu and Xinle Liang

Abstract Denaturing gradient gel electrophoresis (DGGE) was applied to investigate the bacterial community in traditional Meigui rice vinegar produced in Zhejiang province, China. The V3 regions of 16S rDNA were amplified with universal primers (GC-338F and 518R). Nine dominant DGGE bands were isolated, cloned, and sequenced. They were most similar to *Acetobacter pasteurianus*, *A. aceti, Lactobacillus delbrueckii subsp bulgaricus*, *Gluconobacter oxydans*, *Leuconostoc mesenteroides subsp mesenteroides*, *Lb. reuteri*, *Lb. casei*, and *Lb. acidophilus.* Of which, *A. pasteurianus* and *Lb. delbrueckii subsp bulgaricus* are two dominant species, and occur along the whole acetic acid fermentation process. *Lb. bulgaricus*, *G. oxydans*, and *A. pasteurianus* dominated in the last phase of the fermentation. *G. oxydans* is first identified in the Meigui rice vinegar broth, and occurs in the last phase. The DGGE profile also indicated that bacterial community transition took place at the initial stage at which acetic acid fermentation stage started.

Keywords Meigui rice vinegar · DGGE · 16S rDNA · Microbial diversity

J. Shi · Y. Zhu · X. Liang (✉)
College of Food and Biotechnology, Zhejiang Gongshang University, Hangzhou 310035, People's Republic of China
e-mail: dbiot@mail.zjgsu.edu.cn

Y. Liu · W. Feng
Xi Hu Brewing Coporation, Hangzhou 310027, People's Republic of China

X. Chen
Open Funding of Key Fermentatin Engineering Lab of Hubei Industrial Univerisity, Wuhan, People's Republic of China

T.-C. Zhang et al. (eds.), *Proceedings of the 2012 International Conference on Applied Biotechnology (ICAB 2012)*, Lecture Notes in Electrical Engineering 249,
DOI: 10.1007/978-3-642-37916-1_43, © Springer-Verlag Berlin Heidelberg 2014

43.1 Introduction

Wine vinegar is primarily produced with an enological tradition in European countries (e.g., balsmic vinegar in Italy, and sherry vinegar in Spain) [1]. In Northeastern regions of Asia, such as Japan and China, vinegar has been traditionally produced from cereals, primarily rice [2]. Vinegar fermentation from cereals requires a saccharification step in addition to the alcohol fermentation and oxidation of ethanol to acetic acid. In China, the saccharification of rice is conducted by moulds such as *Aspergillus oryzae*. Alcohol fermentation with yeast is performed either after saccharification process or at the meanwhile as saccharification. The alcoholic medium is used for acetic acid fermentation. For acetate production there are two well-defined methods, traditional static surface fermentation and modern submerged fermentation [3].

"Meigui rice vinegar", one famous traditional rice vinegar in China, has been manufactured since the 1900s at Zhejiang Province. This type of rice vinegar is produced in a ceramic jar (1,000 L volume) with rosy color, sort sweet, soft and sterling aroma, and particular flavor, referred as "Meigui rice vinegar". The brewing process is completely unique, the whole process (i.e., saccharification, alcohol fermentation, and acetic acid fermentation) proceeds within the same jar, and without any controls such as the temperature, aeration, and pure culture inoculation. The materials are used: steamed rice, water, and natural microbial community from the environment; no additional microorganisms are inoculated during the fermentation process. Jar fermentation begins often at the spring only, continues to winter or next spring. The diversity and succession of microorganisms involved in jar vinegar fermentation are of considerable interest, since there are three microbiological precesses simultaneously or sequentially in a single jar; furthermore, no pure microorganisms are used for inoculation. Microbiological studies of vinegar fermentation have been reported by convertional cultivation approaches. Recently, culture-independent techniques such as 16S rRNA genes, have suggested the existence of a vast undiscovered microbial diversity, and been applied to analyze food ecosystems. In the case of vinegar bacteria, it has been reported that conventional plate counts were considerably lower than the fluorescence optical counts of microbial cells from industrial acetatoers.

DGGE is a well documented culture-independent method for analysis of microbial communities in environmental and food samples [4]. Compared to traditional culturing, these methods, generally based on nucleic acids such as the 16S rRNA gene, aim at obtaining both a qualitative and a semi-quantitative picture of a microbial community without the need to isolate and culture its single components [5]. However, it has previously been demonstrated that while these techniques are valuable, there is a need to use a combined system to overcome the bias of the "culture-(in)-dependent-only" approach [6, 7]. Therefore, culture-independent and cultivation methods should be applied in parallel for population dynamics and biodiversity studies. Recently, such an approach was applied to study the bacterial community traditional fermentation food [8–13].

In this paper, we applied the denaturing gradient gel electrophoresis (DGGE) method technique to analyze the dynamic of bacterial communities in Zhejiang Meigui rice vinegar during the fermentation process.

43.2 Materials and Methods

43.2.1 Vinegar Samples

Twenty samples from Hangzhou Niangzhao Shipin Factory were collected. The vinegar samples were centrifuged at 4 °C, 9,000 r/min for 5 min, and then the bacterial cells in the suspension was harvested by centrifugation at 4 °C, 12,000 r/min for 5 min the precipitate was stored at −70 °C.

43.2.2 Bacterial DNA Extraction

The genomic DNA of each strain was extracted using a modification of the cetyltrimethylammonium bromide method [14]. In brief, the cells were washed with sterile distilled water. Then the pellets were suspended in saline EDTA buffer (0.15 M NaCl and 1 M EDTA, pH 8.0). The cell lysis was induced by addition of 10 mg ml^{-1} lysozyme solution. After addition of 10 mg ml^{-1}RNAse, the tube was incubated at 37 °C for 30 min. Proteinase K (20 mg ml^{-1}) was added and the incubation was done at 37 °C for 60 min. Afterwards, 40 µl of 25 % sodiumdodecyl sulfate (SDS) solution was added and incubated at 65 °C for 10 min, then 180 µl of a 5 M sodium acetate solution was assed and the cell polysaccharides were eliminated by the addition of 100 µl of 2 % cetyltrimethylammonium bromide (CTAB) solution and centrifuged at 10,000 × g for 10 min. Chromosomal DNA was further twice purified by extraction with chloroform/isoamylic alcohol (25:1, v/v), precipitated by transferring the upper aqueous phases to new tubes and adding twice cold absolute ethanol. The chromosomal DNA was resuspended in 100 µl of highly purified H_2O. The size of the DNA was checked by 1 % agarose gel electrophoresis in 1X TAE buffer (40 mM tris base, 20 mM acetic aced glacial, 1 mM EDTA 0.5 M, pH 8.0) with a 23 Kb DNA ladder (TaKaRa, China) as size marker. The gel was visualized by ethidium bromide staining under UV light.

43.2.3 PCR Amplification of the V3 Region of 16S rDNA

The V3 region of 16S rRNA gene was amplified for bacterial community analysis. The primers used to amplify the V3 region were as follows: 338f (5′-ACTCCTA CGGGAGGCAGCAG-3′) and 518r (5′-ATTACCGCGGCTGCTGG-3′) [15] GC-clamp (5′-CGCCGCCGCGCGC GGCGGGCGGGGCGGGGGCACGGGGGG-3′)

were attached to the 5′ end of primer 338f [16]. Amplification was performed in a final volume of 50 ml containing 1 × PCR buffer, 1.5 mM $MgCl_2$, 0.2 mM dNTPs, 2.5 UI Taq- polymerase (TaKaRa, China), 0.2 mM each primer, and the template DNA. In order to increase the specificity of amplification, a touchdown PCR was performed using an annealing temperature of 10 °C above the expected annealing temperature of 55 °C [17]. The temperature from 65 °C was decreased by 1 °C each second cycle until the touchdown temperature of 55 °C was reached. Ten additional cycles were carried out at 55 °C. A denaturizing step of 95 °C for 1 min was used and extension was performed at 72 °C for 3 min with a final extension of 10 min at 72 °C which finished the amplification cycle. The PCR products (5 ml) were analyzed by electrophoresis in agarose gel [18].

43.2.4 DGGE Analysis

DGGE analysis was carried out on the DcodeTM Universal Mutation Detection System (Bio-Rad, USA). Electrophoresis was performed with 1 mm-thick 6 % polyacrylamide gels (acrylamide-bisacrylamide, 37.5:1) submerged in 1 × TAE buffer (40 mM Tris, 40 mM acetic acid, 1 mM EDTA; pH 8.0) at 60 °C. Approximately, 600–800 ng of PCR product from environmental samples and 100 ng of PCR product from cultures were applied to individual lanes in the gel [17]. The following electrophoresis conditions were selected based on the results of perpendicular DGGE and time travel experiments. The perpendicular electrophoresis was performed at 80 V for 1 h in a linear 0–100 % denaturant agent gradient (100 % denaturant agent was defined as 7 M urea and 40 % deionized formamide). After electrophoresis, the gels were stained in 1 × TAE solution containing ethidium bromide (50 μg/ml) for 10 min and photographed under UV transillumination and analyzed by Quantity One software (Bio-Rad).

43.2.5 Sequencing of 16S rDNA Regions

Selected DGGE bands were excised from the denaturing gels, eluted in 30 μl of sterile water, and incubated over night. And 5 μl of diffused DNA supernatant was used as template for reamplification with primers F338-GC and R518. The e-amplified PCR products were examined by DGGE to confirm that single bands were present at the same positions. Sequencing was carried out by TaKaRa using ABI PRISM^{TM} 377XL DNA Sequencer. To determine the closest known relatives of the partial 16S rDNA sequences obtained, searches were performed in public data libraries with the BLAST.

43.3 Results and Discussion

43.3.1 Mega DNA Extraction and PCR Process of V3 of 16S rDNA

In the same genomic DNA samples for template, primers like F338-GC/R518 with not GC splint primer and GC splint were used. All use touchdown PCR reaction procedure. The length of PCR products is about 230 bp. Parallel DGGE profiles of PCR products of 16S rDNA with different primers (Fig. 43.1). The DGGE profiles of different PCR products were performed and supported a good seperation when F338-GC/R518 used as the primers (Fig. 43.1b).

43.3.2 DGGE Optimization

The denaturing range and time of electrophoresis were optimized in our study (Fig. 43.2). Between a gradient of denaturant concentrations of 35–55 %, the DNA fragments displayed reduced mobility(Fig. 43.2a). Moreover, the fragments of different sequences were separated absolutely. After that time travel experiments with the mixture of PCR products were conducted to determine the optimal electrophoresis time. PCR products were loaded into a gel every 0.5 h and electrophoresis at 150 V (Fig. 43.2b). Bands were defined most clearly and showed reduced mobility for 4.0 h. Thus, the electrophoresis conditions were obtained at 150 V, 60 °C for 4 h.

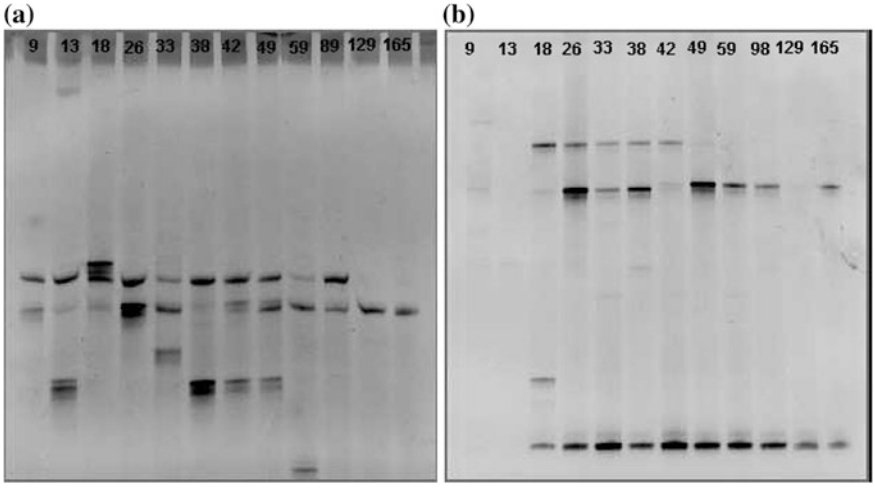

Fig. 43.1 Parallel DGGE profiles of PCR products of 16S rDNA with different primers. Primers, **a** F338/R518; **b** F338-GC/R518

43.3.3 DGGE Profile of the Bacterial Community of Meigui Vinegar Fermentation Process

The transition of the bacterial community throughout the fermentation process is shown in Fig. 43.3. In the DGGE profiles, the brighter bands represent the dominant bacteria [19]. DNA sequences of eight representative bands were determined and blasted in Genbank (Table 43.1), whereas the other bands were not determined due to the failure, to reproducibly amplify the excised bands. Comparison of V3 regions of 16S ribosomal DNA sequences similarity revealed that the dominating microbial species were *Acetobacter pasteurian*, *Lactobacillus delbrueckii subsp bulgaricus*, *Gluconobacter oxydans*, *Leuconostoc mesenteroides subsp mesenteroides*, *Lactobacillus reuteri*, *Lactobacillus casei*, *Lactobacillus acidophilus NCFM*.

The DGGE profile indicated that there are dramatic difference about bacterial community between "Fahua" phase and fermentation phase. The "Fahua" phase was characterized by bands related to *Leu. mesenteroides*, *Lb. reuteri*, *Lb. casei*, *Lb. casei,* and *A. pasteurianus*. *Lb. reuteri* (band 2) was detectable from day 13 to day 49. *A. pasteurianus* and *Lb. bulgaricus* occurred along the whole fermentation

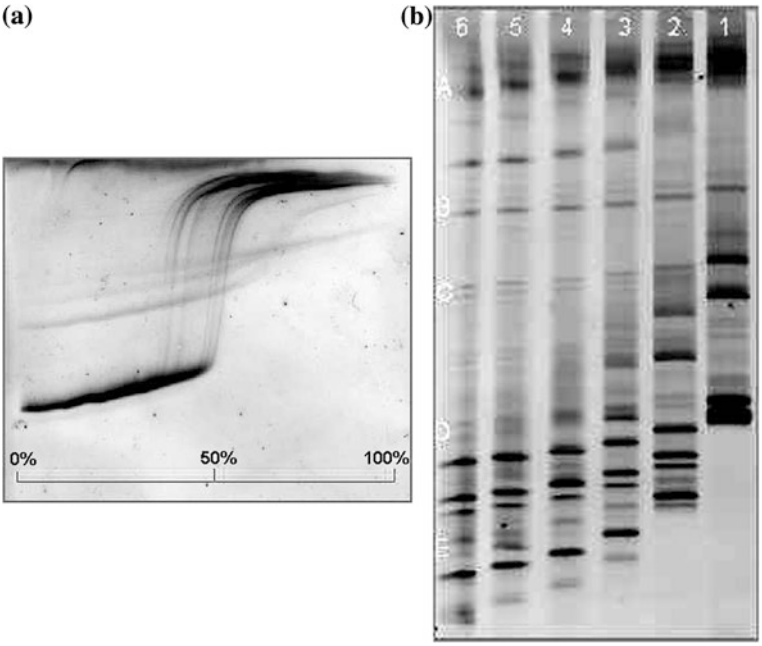

Fig. 43.2 Optimizatin of DGGE process. **a** perpendicular DGGE profiles of PCR products. **b** DGGE profile under diferent start-up time of time travel. Star-up time: lane *1*, 1.5 h; lane *2*, 2.0 h; lane *3*, 2.5 h; lane *4*, 3.0 h; lane *5*, 3.5 h; lane *6*, 4.0 h

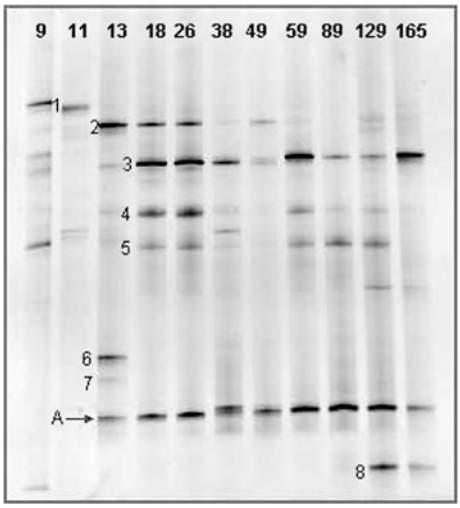

Fig. 43.3 DGGE profiles of bacteria in the whole fermentation process (from 9 to 165 days)

Table 43.1 Phylogenetic affiliation of DGGE bands in Fig. 43.3

Band#	Phylogenetic affiliation	Similarity (%)
1	*Leuconostoc mesenteroides subsp. mesenteroides*	87
2	*Lactobacillus reuteri*	92
3	*Lactobacillus delbrueckii subsp. bulgaricus*	95
4	*Lactobacillus acidophilus NCFM*	99
5	*Acetobacter aetic*	98
6	*Lactobacillus casei*	99
7	ND	–
8	*Gluconobacter oxydans*	97
A	*Acetobacter pasteurianus*	99

ND, not determined

process, while *G. oxydans* was first identified in the rose vinegar, just occurred in the last phase. Only *Lb. bulgaricus*, *G. oxydans*, and *A. pasteurianus* dominated in the last phase of the fermentation.

43.4 Conclusion

In this study, PCR-DGGE analysis demonstrated the clear succession of microbial communities during the fermentation process of Zhejiang Meigui rosy rice vinegar. The DGGE profile indicated dynamic changes in the bacterial population at the transition from saccharification phase to alcohol fermentation, and acetic acid

fermentation phase. Moreover, the bacterial population during the fermentation process were distinct from that observed in the starting materials. The similar change of microbial community also happened in the Japanese rice vinegar [2]. However, the bacteria which was determined by DGGE was different in these two case, there are five bacteria determined in the Japanese rice vinegar, i.e., *Lb. fermentum*, *Lactococcus lactis*, *Pediococcus acidilactici*, *Lb. acetotolerans,* and *A. pasteurianus*. In the Meigui rice vinegar DGGE process showed that the following species would be dominants, *A. pasteurianus*, *A. aetic, Lb. delbrueckii subsp. bulgaricus*, *G. oxydans*, *Leu. mesenteroides subsp mesenteroides*, *Lb. reuteri*, *Lb. casei*, and *Lb. acidophilus.* Of which, *A. pasteurianus* and *Lb. delbrueckii subsp bulgaricus* are two dominant species, and occurred along the whole acetic acid fermentation process. *Lb.bulgaricus*, *G.oxydans*, and *A.pasteurianus* dominated in the last phase of the fermentation. *G. oxydans* is first identified in the Meigui rice vinegar broth, and occurred in the last phase too. The DGGE profile also indicated that bacterial community transition took place at the the initial stage when acetic acid fermentation stage started.

Acknowledgments The work was financially supported by National Nature and Science foundation of China (3117175), Nature and Science foundation of Zhejiang Province (Y3100609), and Open Funding of Key Fermentation Engineering Lab of Hubei Industry University (2010Y053).

References

1. Gullo M, Giudici P (2008) Acetic acid bacteria in traditional balsamic vinegar: phenotypic traits relevant for starter cultures selection. Int J Food Microbiol 125:46–53
2. Haruta S, Ueno S, Egawa I et al (2006) Succession of bacterial and fungal communities during a traditional pot fermentation of rice vinegar assessed by PCR-mediated denaturing gradient gel electrophoresis. Int J Food Microbiol 109:79–87
3. Tesfaye W, Morales ML, Garcia-Parrilla MC et al (2002) Wine vinegar: technology, authenticity and quality evaluation. Trends Food Sci Technol 13:12–21
4. Kusar D, Avgustin G (2012) Optimization of the DGGE band identification method. Folia Microbiol 57:301–306
5. Nakatsu CH, Torvik V, Ovreas L (2000) Soil community analysis using DGGE of 16S rDNA polymerase chain reaction products. Soil Sci Soc Am J 64:1382–1388
6. Ritz K, Wheatley RE, Griffiths BS (2007) Effects of animal manure application and crop plants upon size and activity of soil microbial biomass under organically grown spring barley. Biol Fert Soils 24:372–377
7. Oger JC, El-Baradei G, Delacroix-Buchit A (2008) Bacterial biodiversity of traditional Zabady fermented milk. Int J Food Microbiol 121:295–301
8. Wu JJ, Ma YK, Zhang FF et al (2012) Biodiversity of yeasts, lactic acid bacteria and acetic acid bacteria in the fermentation of "Shanxi aged vinegar", a traditional Chinese vinegar. Food Microbiol 30:289–297
9. Lv XC, Weng X, Zhang W et al (2012) Microbial diversity of traditional fermentation starters for Hong Qu glutinous rice wine as determined by PCR-mediated DGGE. Food Control 28:426–434

10. Tanaka Y, Watanabe J, Mogi Y (2012) Monitoring of the microbial communities involved in the soy sauce manufacturing process by PCR-denaturing gradient gel electrophoresis. Food Microbiol 31:100–106
11. Liang ZB, Drijber RA (2008) A DGGE-cloning method to characterize arbuscular mycorrhizal community structure in soil. Soil Bio Biochem 40:956–966
12. Bouity MD, Frigon JC (2008) Comparison of treatment efficacy and stability of microbial populations between raw and anaerobically treated liquid pig manure, using PCR-DGGE and 16S sequencing. Can J Microbiol 54:83–90
13. He F, Huang D, Liu L (2008) A novel PCR-DGGE-based method for identifying plankton 16S rDNA for the diagnosis of drowning. Forensic Sci Int 176:152–156
14. Knapp JE, Chandlee JM (1996) RNA/DNA mini-prep from a single sample of orchid tissue. Biotechniques 21:54–56
15. Tae WK, Jun HL, Sung EK et al (2009) Analysis of microbial communities in doenjang, a Korean fermented soybean paste, using nested PCR-denaturing gradient gel electrophoresis. Int J Food Microbiol 131:265–271
16. Fushuku S, Fukuda K (2008) Inhomogeneity of fecal flora in separately reared laboratory mice, as detected by denaturing gradient gel electrophoresis (DGGE). Exp Anim 57:95–99
17. Cherif H, Ouzari H, Marzorati M et al (2008) Bacterial community diversity assessment in municipal solid waste compost amended soil using DGGE and ARISA fingerprinting methods. World J Microb Biotechnol 24:1159–1167
18. Yoshida A, Seo Y, Suzuki S et al (2008) Actinomycetal community structures in seawater and freshwater examined by DGGE analysis of 16S rRNA gene fragments. Mar Biotechnol 10:554–563
19. Zidkova K, Kebrdlova V (2007) Detection of variability in apo(a) gene transcription regulatory sequences using the DGGE method. Clin Chim Acta 376:77–81

Chapter 44
The Effect of Co-Culture on Production of Blue Pigment by *Streptomyces coelicolor* M145 with *Bacillus subtilis* as Auxiliary

Fengyun Sun, Shuxin Zhao, Shichao Wang and Peng Chen

Abstract The aim of this study was to determine the effect of co-culture on production of blue pigment by *Streptomyces coelicolor* M145 with *Bacillus subtilis* as auxiliary. Preliminarily *B. subtilis* was found to have positive effect to increase the blue pigment. Then two *B. subtilis* (AS1.398 and WB600) were used to evaluate the amount and time of inoculation. The results demonstrated when 1 % of the *B. subtilis* AS1.398 or WB600 that the concentration was about 1×10^{10} cells/mL was added after 48 h' fermentation of the *S. coelicolor*, the yield of blue pigment can increase about 30–40 % than single culture. Further, research was going on to try to find the substances that stimulate blue pigment. It could be approximately proved that these substances should be in cells of *B. subtilis*, and might be heat stable due to a similar result between live and heat-killed cells.

Keywords *Bacillus subtilis* · Blue pigment · Co-culture · *Streptomyces coelicolor*

44.1 Introduction

As one of the three essential colors, the blue pigments play an indispensable role in our daily life. Generally, blue pigments are divided into two certain kinds, natural and synthetic pigments. Although the synthetic pigments are mainly used as colorants in food or cosmetic industry, it is found that the synthetic colors are hardly nutrients, and some of them are toxic [1–3] to some extent. So the natural pigments, safer than synthetic ones, are being increasingly emphasized. Natural blue

F. Sun · S. Zhao (✉) · S. Wang · P. Chen
College of Biotechnology, Tianjin University of Science and Technology, Tianjin 300457, People's Republic of China
e-mail: zsx999@tust.edu.cn

T.-C. Zhang et al. (eds.), *Proceedings of the 2012 International Conference on Applied Biotechnology (ICAB 2012)*, Lecture Notes in Electrical Engineering 249,
DOI: 10.1007/978-3-642-37916-1_44, © Springer-Verlag Berlin Heidelberg 2014

pigments are mainly derived from plants, which often have restricted habitats. And many researchers have devoted themselves to the new ways to produce natural blue pigments such as microbial fermentation [4, 5].

Streptomyces coelicolor, a Gram-positive bacterium, basically lives in the soil. In laboratory research, the common practice is to use single culture [6, 7]. However, in nature microorganisms are consisted of complex mixtures of different species [8–10]. And these species may interact with each other which result in the production of some important bioactive compounds [11, 12]. In this study, *S. coelicolor* M145 was cultivated with *B. subtilis* AS1.398 or WB600 to evaluate the increase in blue pigment production. The related property of substances that stimulated blue pigment was also studied preliminarily [13].

44.2 Materials and Methods

44.2.1 Microorganisms and Media Composition

Streptomyces coelicolor M145 was grown in the liquid medium with the following composition (g/L): soluble starch 20, yeast extract powder 5, and NaCl 5. LB agar was used for the maintenance of *B. subtilis* AS1.398 and *B. subtilis* WB600.

44.2.2 Preparation of Inoculum

Inocula of *S. coelicolor* and *B. subtilis* were prepared as follows [14, 15]: two inoculating loops of *S. coelicolor* from agar slant was cultured into flasks containing 50 mL liquid medium and incubated at 30 °C and 200 r/min for 24 h. Another few loops of *B. subtilis* AS1.398 or WB600 from an overnight culture on LB agar was cultured into test tubes with 5 mL liquid medium and incubated at 37 °C for 12 h.

44.2.3 Cultivation in Shake Flasks

The single cultures of *S. coelicolor* were prepared at 30 °C and 200 r/min for 10 d. And in the co-cultures, the overnight grown culture of *B. subtilis* at 1 % (v/v) level was added to the broth that has already fermented for 48 h. In research about amount and time of inoculation of *B. subtilis* AS1.398 or WB600, the amount was at 1, 3 and 5 %, respectively, and the adding time was at 24, 48 and 72 h, respectively.

Further, study was going on that both live and heat-killed supernatant and cells suspension of *B. subtilis* AS1.398 and WB600 at 1×10^{10} cells/mL and 1 % (v/v) level were inoculated into *S. coelicolor* fermented broth. The preliminary treatment of *B. subtilis* fermented broth was as follows: it was centrifuged at 10,000 r/min for 10 min. The supernatant was treated with membrane filtration, and the deposition were washed for 3 times and then resuspended in equal volume of sterile saline. The number of *B. subtilis* cells was adjusted to be approximately at the level of 1×10^{10} cells/mL by adding sterile saline. The supernatant and *B. subtilis* cells suspension was placed in boiling water for 30 min if necessary [16].

44.2.4 Analyses

The fermented broth was centrifuged at 8,000 r/min for 15 min. The supernatant, containing extracellular blue pigment, was diluted with moderate distilled water and detected at 580 nm by a spectrophotometer [17–19]. Then a certain amount of deposition was immersed in 70 % of alcohol solution that is 10 times as heavy as the deposition at 60 °C for 1 h to extract the intracellular blue pigment, and the testing method was same with that of extracellular pigment. Another certain amount of deposition was dried in a drying oven to count the moisture content of microbial cells. The calculation formulas of extracellular and intracellular blue pigment were as follows:

$$\text{Extracellular pigment value} = \text{OD}_{580} \times 10\,(\text{U/mL}) \tag{44.1}$$

$$\text{Intracellular pigment value} = \frac{10 \times \text{OD}_{580}}{m \times (1 - a)}\,(\text{U/g}) \tag{44.2}$$

Among the formula (2), m means the wet weight of sample, which was obtained by weighing the sample directly. And a means the moisture content of microbial cells. It was a ratio of the dry weight and wet weight of the sample.

44.3 Results and Discussion

44.3.1 Preliminary Analysis About S. coelicolor *M145 Interaction with* B. subtilis *AS1.398 in Liquid Medium*

Table 44.1 gives the values of intracellular and extracellular blue pigment in the co-culture which increased markedly compared with the control that the extracellular and intracellular blue pigment production was only 12.20 U/mL and

Table 44.1 Effect of *B. subtilis* AS1.398 on the yield of blue pigment

	Co-culture
Extracellular blue pigment production (U/mL)	47.20
Intracellular blue pigment production (U/g)	198.37

138.64 U/g, respectively. It approximately proved that *B. subtilis* AS1.398 gave *S. coelicolor* M145 an advantage to synthesize blue pigment.

44.3.2 Optimizing the Amount and Time of B. subtilis *AS1.398 and WB600 Inoculation*

In some other co-culture experiments, the amount and time of inoculation was found to be important [20]. As can be seen in Fig. 44.1, the production of extracellular and intracellular blue pigments at 1 % level was 86.7 U/mL and 318.59 U/g, while the control was only 54.3 U/mL and 221.41 U/g, respectively. The positive effect of *B. subtilis* at 3 % level or 5 % level was lower than that of 1 % level.

In Fig. 44.2, the best time of *B. subtilis* AS1.398 inoculation was at 48 h. In this case, the production of intracellular blue pigment was 238.65 U/g, while in the control it reached only 176.74 U/g. The yield decreased when *B. subtilis* was added at 0 h or 24 h, and the positive effect was not obvious if the inoculating time was delayed.

Similar to the effect of *B. subtilis* AS1.398, the suitable amount and time of *B. subtilis* WB600 inoculation was also 1 % and 48 h (Figs. 44.3 and 44.4), respectively. Although *B. subtilis* AS1.398 produced neutral protease and *B. subtilis* WB600 did not, their effect on blue pigment production were similar. So it

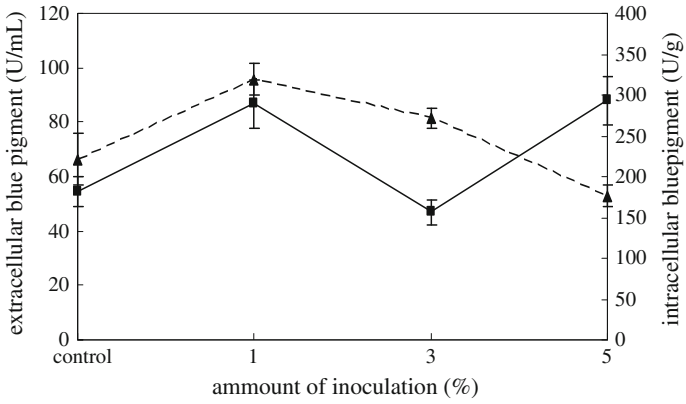

Fig. 44.1 Production of extracellular and intracellular blue pigment (*continuous line* with *filled square* and *dotted line* with *filled triangle*, respectively) by *S.coelicolor* M145 in single culture and in the cultures elicited with *B.subtilis* AS1.398 at amounts of 0, 1, 3, and 5 %

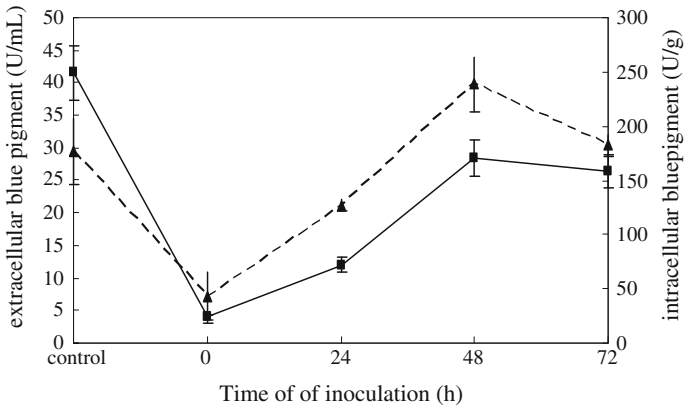

Fig. 44.2 Production of extracellular and intracellular blue pigment (*continuous line* with *filled square* and *dotted line* with *filled triangle*, respectively) by *S.coelicolor* M145 in single culture and in the cultures elicited with *B.subtilis* AS1.398 at timing of 0, 24, 48, and 72 h

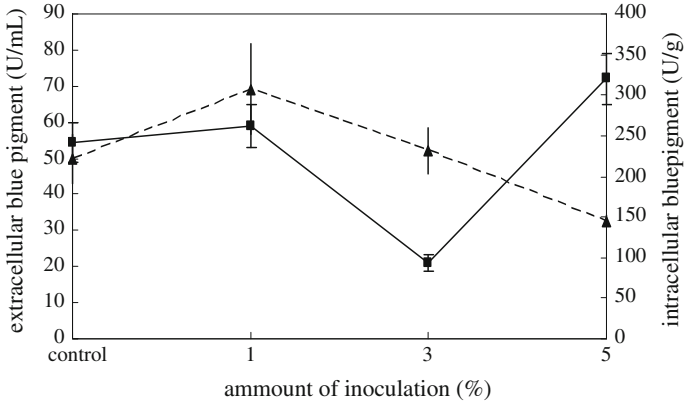

Fig. 44.3 Production of extracellular and intracellular blue pigment (*continuous line* with *filled square* and *dotted line* with *filled triangle*, respectively) by *S.coelicolor* M145 in single culture and in the cultures elicited with *B.subtilis* WB600 at amounts of 0, 1, 3, and 5 %

was approximately proved that the neutral protease may not be the active constituent.

44.3.3 Analysis About Effective Constituents in B. subtilis *that Increase the Blue Pigment*

Further experiments about substances that stimulated blue pigment were going on. Live or heat-killed supernatant of *B. subtilis* AS1.398 at 1 % (v/v) level was added

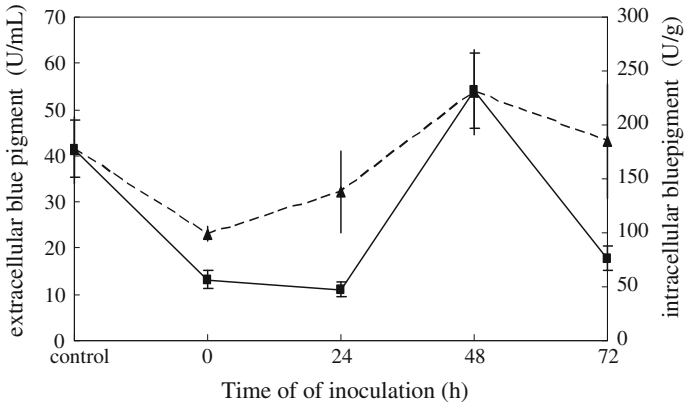

Fig. 44.4 Production of extracellular and intracellular blue pigment (*continuous line* with *filled square* and *dotted line* with *filled triangle*, respectively) by *S.coelicolor* M145 in single culture and in the cultures elicited with *B.subtilis* WB600 at timing of 0, 24, 48, and 72 h

to the *S. coelicolor* culture. And the production of blue pigment was similar to the control. The yield of pigment markedly increased when the live or heat-killed cells suspension of *B. subtilis* AS1.398 was added (Fig. 44.5). It was deduced preliminarily that the effective constituents were in *B. subtilis* AS1.398 cells.

Moreover, both live and heat-killed cells were favorable to the blue pigment, which were approximately similar. It suggested that these effective substances might be heat resistant materials.

Similar to the effect of *B. subtilis* AS1.398, the blue pigment was also enhanced after adding *B. subtilis* WB600 cells (Fig. 44.6). And the effect of supernatant was not obvious.

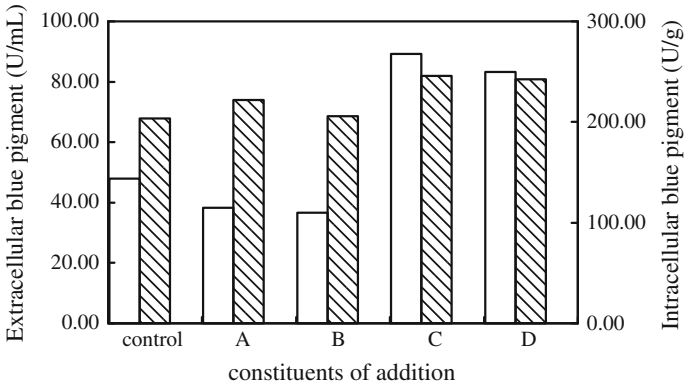

Fig. 44.5 Production of extracellular and intracellular blue pigment (the *blank strip* and *diagonal strip*, respectively) in single culture and in the cultures elicited with different constituents (*A*, *B*, *C*, and *D* stand for supernatant, heat-killed supernatant, live cells and heat-killed cells, respectively)

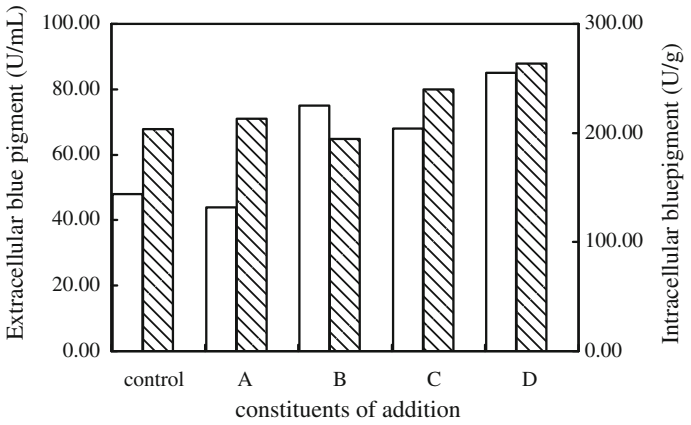

Fig. 44.6 Production of extracellular and intracellular blue pigment (the *blank strip* and *diagonal strip*, respectively) in single culture and in the cultures elicited with different constituents (A, B, C, and D stand for supernatant, heat-killed supernatant, live cells and heat-killed cells, respectively)

44.4 Conclusion

Based on these results, when *B. subtilis* AS1.398 and WB600 that the concentration was about 1×10^{10} cells/mL were added to *S. coelicolor* M145 cultures, the blue pigment production was increased about as much as 30–40 % compared with that in single culture. And their suitable amount and time of inoculation were 1 % and 48 h, respectively. The positive constituents might be intracellular and heat resistant. Our study supports the use of interspecies interactions to enhance the production of blue pigment. The fact that live and heat-killed cells of *B. subtilis* are positive for the enhancement may be useful for the industrial fermentation. And further research is needed to study more properties of these effective constituents.

Acknowledgments We would like to acknowledge Professor Zhao, Shichao Wang, and Peng Chen for many useful discussions.

References

1. Lu L, Cui H-L, Chen Y-N et al (2002) Isolation and identification of Streptomyces sp. and assay of its exocellular water-soluble blue pigments. Folia Microbiol 47:493–498
2. Hechun Z, Jixun Z, Keman S et al (2006) A kind of potential food additive produced by Streptomyces coelicolor: Characteristics of blue pigment and identification of a novel compound, k-actinorhodin. Food Chem 95:186–192
3. Vining LC (1990) Functions of secondary metabolites. Annu Rev Microbiol 44:395–427

4. Leonid V, Bystrykh, Miguel A et al (1996) Production of actinorhodin-related ‘‘blue pigments’’ by Streptomyces coelicolor A3(2). J Bacteriol 2238–2244
5. Hobbs G, Frazer CM, Gardner DCJ et al (1989) Dispersal growth of Streptomyces coelicolor in liquid culture. Appl Microbiol Biotechnol 31:272–277
6. Kang SG, Jin W, Bibb M et al (1998) Actinorhodin and undecylprodigiosin production in wild-type and relA mutant strains of Streptomyces coelicolor A3(2) grown in continuous culture. FEMS Microbiol Lett 168:221–226
7. Wright LF, Hopwood DA (1996) Actinorhodin is a chromosomally determined antibiotic in Streptomyces coelicolor A3(2).Gen Microbiol 289–297
8. Khalid J, Kadhum L, Ferda M (2011) Elicitation of Streptomyces coelicolor with E. coli in a bioreactor enhances undecylprodigiosin production. Biochem Eng J 53:281–285
9. Haileia W, Zhifang R, Ping L et al (2011) Improvement of the production of a red pigment in Penicillium sp. HSD07B synthesized during co-culture with Candida tropicalis. Bioresource Technol 102:6082–6087
10. Oh DC, Jensen PR, Kauffman CA et al (2005) Libertellenones, Induction of cytotoxic diterpenoid biosynthesis by marine microbial competition. Bioorgan. Med Chem 13:5267–5273
11. Pettit RK (2009) Mixed fermentation for natural product drug discovery. Appl Microbiol Biot 83:19–25
12. James GA, Beaudette L, Costerton JW (1995) Interspecies bacterial interactions in biofilms. J Ind Microbiol 15:257–262
13. Bibb M (1996) The regulation of antibiotic production in Streptomyces coelicolor A3 (2). Microbiology 142:1335–1344
14. Sevcikova B, Kormanec J (2004) Differential production of two antibiotics of Streptomyces coelicolor A3 (2), actinorhodin and undecylprodigiosin, upon salt stress conditions. Arch Microbiol 181:384–389
15. Elibol M, Ulgen K, Kamaruddin K et al (1995) Effect of inoculum type on actinorhodin production by Streptomyces coelicolor A3 (2). Biotechnol Lett 17:579–582
16. Khalid J, Kadhum L, Ferda M (2011) Streptomyces coelicolor increases the production of undecylprodigiosin when interacted with Bacillus subtilis. Biotechnol Lett 33:113–118
17. Rasool KA, Wimpenny JWT (1982) Mixed continuous culture experiments with an antibiotioc-producing Streptomycete and Escherichia coli. Microbial Ecol 8:267–277
18. Doull JL, Vining LC (1990) Nutritional control of actinorhodin prouction by Streptomyces coelicolor A3 (2): suppressive effects of nitrogen and phosphate. Appl Microbiol Biot 32:449–454
19. Ozergin-Ulgen K, Mavituna F (1993) Actinorhodin production by Streptomyces coelicolorA3 (2): kinetic parameters related to growth, substrate uptake and production. Appl Microbiol Biotechnol 40:457–462
20. Thaler JS, Fidantsef AL, Bostock RM (2002) Antagonism between jasmonate and salicylate-mediated induced plant resistances: effects of concentration and timing of elicitation on defense-related proteins, herbivore, and pathogen performance in tomato. J Chem Ecol 28:1131–1159

Chapter 45
The Application of Salting-Out in the Analysis of Methoxy-Phenolic Compounds in Pu-erh Tea

Chao Wang, Liping Du, Yan Lu, Tao Li, Jianxun Li, Wei Li, Dongguang Xiao, Changwen Li and Yongquan Xu

Abstract This paper presents the application of salting-out in the analysis of methoxy-phenolic compounds in pu-erh tea by using headspace solid microextraction (HS-SPME) combined with gas chromatography mass spectrometry (GC/MS). At first, the influences of extraction and the best extraction condition were investigated, include SPME fibers, extraction time and extraction temperature. Under the optimum condition, the salting-out performances of NH_4Cl, KCl, NaCl, $MgCl_2$, Na_2SO_4, $(NH_4)_2SO_4$ and $C_6H_5O_7Na_3$ were studied. Sodium citrate exhibits the highest extraction efficiency. Compared with unsalted, the total peak area of methoxy-phenolic compounds increased by 2.8 times with sodium citrate added. With $C_6H_5O_7Na_3$, the proposed method affords wide of linearity, good linear regression coefficients (0.992–0.999), detection limits varied from 1.54 to 14.53 ng/g and the relative standard deviations for repeatability were below 10 %. Recovery was ranged from 82.05 to 112.04 % and the relative standard deviations were below 10 %.

Keywords Pu-erh tea · Methoxy-phenolic compounds · Headspace solid microextraction · Salting-out effect

C. Wang · L. Du (✉) · Y. Lu · T. Li · J. Li · W. Li · DongguangXiao
Key Laboratory of Industrial Fermentation Microbiology, Tianjin Industrial Microbiology Key Laboratory, Ministry of Education, College of Biotechnology, Tianjin University of Science & Technology, Tianjin 300457, People's Republic of China
e-mail: dlp123@tust.edu.cn

C. Li · Y. Xu
Yunnan Tasly Biology Tea Technology Limited Incorporation, Yunnan 665000, People's Republic of China

T.-C. Zhang et al. (eds.), *Proceedings of the 2012 International Conference on Applied Biotechnology (ICAB 2012)*, Lecture Notes in Electrical Engineering 249,
DOI: 10.1007/978-3-642-37916-1_45, © Springer-Verlag Berlin Heidelberg 2014

45.1 Introduction

Pu-erh tea, a famous Chinese special post-fermented tea mainly produced in Yunnan Province of China, which is traditionally made with leaves from old, wild tea trees of a variety known as "broad leaf tea", Camellia sinensis (L.) O. Kuntze var. assamica Kitamura [1, 2]. Pu-erh tea is prepared by first parching the green tea leaves and then fermenting them with microorganisms, such as Aspergillus sp [3]. It has attracted more attention especially in China and some other Asian countries because of its beneficial health effects and special flavor and taste [4].

Volatile methoxy-phenolic compounds were the key compounds in pu-erh tea, most of them produced in large amounts during the post-fermentation process that is a unique process in the manufacturing of pu-erh tea due to the microbial metabolic activities and auto-oxidation. These compounds contribute to the special stale and woody flavor of pu-erh tea [5, 6]. Moreover, it is also one of the most important indicators for its market price. However, little investigation has been carried out on the of the pu-erh tea, and the exactly concentration of methoxy-phenolic compounds remain unknown yet.

Salt addition can improve the extraction efficiency since it modifies the solubility of the molecules into the sample matrix. This process is called "salting-out" [7]. Analytes solubility usually decreases as salt concentration increases. The decrease in analytes solubility can improve sensitivity by promoting analytes partitioning into the stationary phase.

In recent years, solid phase microextraction (SPME) has been become a widespread technique in the analysis of volatile and medium volatile compounds from gases, liquids, and solids with a diverse matrix composition, which eliminates most drawbacks to extracting volatile and semi-volatile compounds, including high cost and excessive preparation time. SPME technique provides as a convenient and reproducible method for tea analysis, appears more suitable for the analysis of aromatic characteristic components [8, 9].

The aim of this work is to investigated the influences of different salts on the extraction efficiency of volatile methoxy-phenolic compounds, and select the best salt and its concentration.

45.2 Materials and Methods

45.2.1 Sample and Reagents

Pu-erh tea sample was supplied by Yunnan Tasly Biology Tea Technology Limited Incorporation (Simao, Yunnan, China).

Ethyl decanoate (internal standard, ≥99 %), 1,2,3-trimethoxybenzene (98 %), 3,4-dimethoxytoluene (≥97 %), 1,2,3-trimethoxy-5-methylbenzene (97 %), 1-methoxy-4-(1-propenyl)-benzene (≥99 %) 1,2,4-trimethoxybenzene (97 %), 1,2-dimethoxybenzene (99 %), and Ethanol (≥99.5 %) were purchased from

Sigma (St. Louis, MO, USA). All the salts (analytical quality) were purchased from Aladdin (Shanghai, China). Pure water was obtained from a Milli-Q purification system (Millipore, Bedford, USA).

45.2.2 Instruments

The samples were analysed on an Agilent-7890A Gas chromatograph directly interfaced with Agilent 5975C MSD (Agilent USA). A capillary column HP-5MS (30 m × 0.25 mm i.d., 0.25 μm film thickness) was employed. 100 μm PDMS, 85 μm PA, 75 μm CAR-PDMS, 70 μm CW-DVB, 65 μm PDMS-DVB, and 50/30 μm DVB-CAR-PDMS were purchased from Supelco (Bellefonte, PA, USA). Before use, they were conditioned in accordance with the manufacturer's specifications. The operating conditions were the following: Injector temperature 250 °C; injection mode splitless; EI 70 eV; interface temperature 280 °C; ion source temperature 230 °C; quadrupole temperature 150 °C; mass scan range 30–500 AMU. Oven temperature was programmed from 50 °C (held for 3 min) to 125 °C at 2 °Cmin and kept for 5 min, heated to 180 °C at 6 °Cmin and kept for 3 min, and finally raised to 250 °C at 15 °C min. Helium (percentage purity >99.999 %), at a flow of 1 ml/min, was used as carrier gas. The identification of the peaks was obtained through mass spectrometry by comparing the MS fragmentation pattern with those of the standards and mass spectrum of the unknown peaks with those stored in the NIST 08 GC–MS library, retention time of the standards obtained under the same conditions.

45.2.3 Optimization of Extraction Conditions

HS-SPME is an equilibrium technique that requires a previous optimization of the extraction parameters that can affect extraction efficiency [10]. Thus, in the first stage, the main factors that affect the SPME process were studied to determine the most suitable conditions for the analysis of volatile methoxy-phenolic compounds in pu-erh tea, included types of fiber coating, extraction time, and extraction temperature.

Five conditions were kept constant during optimization process, including a 100 ml headspace vial with a screw cap and a PTFA septum (Agilent), 1:3 of brewing proportion of tea and water, 15 min equilibrium, agitation of the sample was performed at 400 rpm, desorption time of 5 min. All analysis, were carried out four times.

45.2.3.1 Fiber Coating

The fiber coating used influences the chemical nature of the extracted analyte that is established by their characteristic polarity and volatility [10–13]. In this study,

six commercial SPME fibers: 100 μm PDMS, 85 μm PA, 75 μm CAR-PDMS, 70 μm CW-DVB, 65 μm PDMS-DVB, and 50/30 μm DVB-CAR-PDMS were evaluated and compared. Fiber performance was evaluated using 6 g pu-erh tea. The sample vial was equilibrated for 15 min at 60 °C water bath followed by fiber exposure to the headspace over the sample for 60 min. Finally, fiber was exposed in the GC injector for 5 min.

45.2.3.2 Extraction Time

Time of extraction is an important factor that controls analytes recoveries by the fiber [12]. To study the effect of time in the extraction procedure, five extraction times (40 min, 50 min, 60 min, 70 min, 80 min) were investigated using the selected fiber. The pu-erh tea (6 g) was placed in a 100 mL vial and conditioned for 15 min at 60 °C. The fiber was exposed to the headspace over the sample for selected times. Finally, fiber was exposed in the GC injector for 5 min.

45.2.3.3 Extraction Temperature

Extraction temperature is also an important factor that influence compounds extraction, such that has an effect on the equilibrium during extraction. Samples heated at appropriate temperature prove to be extracted more successfully [14]. To study the effect of temperature in the extraction procedure, five extraction temperatures (40 °C, 50 °C, 60 °C, 70 °C, 80 °C) were evaluated using the selected fiber. The pu-erh tea (6 g) was placed in a 100 mL vial and conditioned for 15 min at selected temperatures. The fiber was exposed to the headspace over the sample for 60 min. Finally, fiber was exposed in the GC injector for 5 min.

45.2.4 The Effect of Salting-Out

Matrix effects as its ionic strength can also influence the mechanism of the mass transfer [15]. In SPME procedure salt addition can improve the extraction efficiency, because it modifies the solubility of the volatiles into the sample matrix [7, 16, 17]. In order to corroborate this statement, under the above studied optimum conditions, the salt effect on SPME adsorption for pu-erh tea volatile methoxyphenolic compounds was investigated through adding different types of salts and different amount of salt.

45.2.4.1 Types of Salt

To study the effect of types of salt in the extraction procedure, eight salts (NH_4Cl, KCl, NaCl, $MgCl_2$, Na_2SO_4, $(NH_4)_2SO_4$, $C_6H_5O_7Na_3$) were investigated at two

levels (0 %, 30 %). The pu-erh tea (6 g) was placed in a 100 mL vial, added a certain amount of salt and conditioned for 15 min at selected temperatures. The fiber was exposed to the headspace over the sample for 60 min. Finally, fiber was exposed in the GC injector for 5 min.

45.2.4.2 Amount of Salting

In order to investigate the effect of amount of salt on the extraction efficiency, varied amounts (5 %, 15 %, 25 %, 30 %, 35 %, 40 %) of selected salt were added to the pu-erh tea sample. The pu-erh tea (6 g) was placed in a 100 mL vial, added a certain amount of selected salt and conditioned for 15 min at 6 °C The fiber was exposed to the headspace over the sample for selected times. Finally, fiber was exposed in the GC injector for 5 min.

45.3 Result and Discussion

45.3.1 Optimization of HS-SPME Conditions

45.3.1.1 Selection of Optimal Type of Fiber Coating

The selection of a suitable fiber is an important step in SPME optimization [18]. The extraction efficiency of SPME depends greatly on the value of the distribution constant of analytes partitioned between the sample and the fiber coating material [19]. In this study, six different fiber coatings (PDMS, PA, CAR-PDMS, CW-DVB, PDMS-DVB, DVB-CAR-PDMS) were evaluated to determine the effectiveness of fiber coating type on the headspace extraction efficiency of volatile compounds from pu-erh tea. Figure 45.1 shows the capacity of six different fiber coatings for extraction of volatile methoxy-phenolic compounds of pu-erh tea at the same condition. 75 μm CAR-PDMS exhibited the highest responses for analytes. So the 75 μm CAR-PDMS was selected for the future experiments.

45.3.1.2 Extraction Time

Absorption-time profiles for 75 μm CAR-PDMS were presented in Fig. 45.2. For analytes, the best extraction efficiency was achieved at 60 min. As the extraction time was increased further, the peak area of total volatiles decreased. This decrease may be attributed to reverse diffusion of analytes form fiber to sample in an attempt to maintain the partition equilibrium. So 60 min were selected for the future experiments.

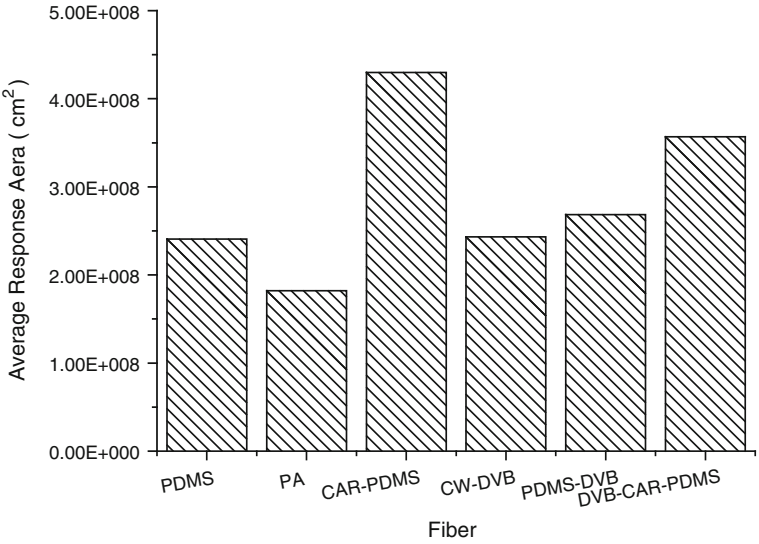

Fig. 45.1 Effect of six types of fiber on the efficiency of extraction of volatile methoxy-phenolic compounds

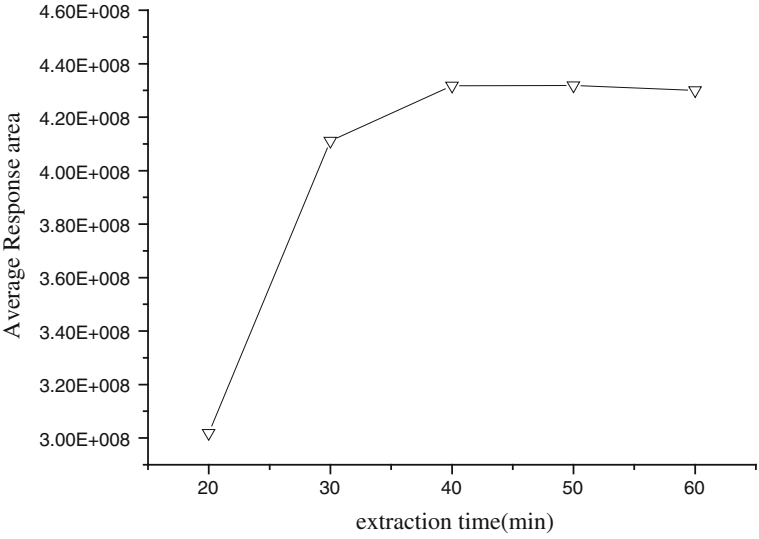

Fig. 45.2 Effect of extraction time on the efficiency of extraction of volatile methoxy-phenolic compounds

45.3.1.3 Extraction Temperature

Extraction temperature plays an important role in the extraction process by controlling the diffusion rate of analytes into the coating [20]. For this extraction, the influence of temperature in the extraction yield was investigated varying the temperature between 40 and 80 °C.

The extraction-temperature profile obtained for the analytes using 75 μm CAR-PDMS fiber, was shown in Fig. 45.3. With the temperature increasing, the peak area of volatile compounds of pu-erh was found to vary significantly, which reached to maximum at 70 °C because increasing the temperature improved the mobility of the volatiles through liquid and gas phase, increasing the extraction efficiency. Temperatures higher than 70 °C provided a decrease of sensitivity for the volatile compounds of pu-erh tea probably due to a decrease in the partition coefficients between the fiber coating material and the sample headspace. A temperature of 70 °C was finally selected for the future study.

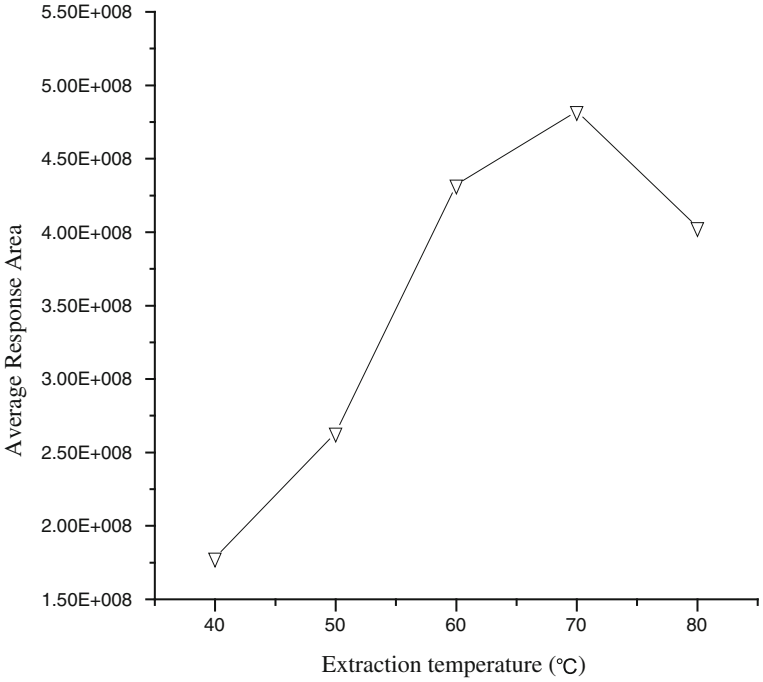

Fig. 45.3 Effect of extraction temperature on the efficiency of extraction of volatile methoxyphenolic compounds

45.3.2 The Effect of Salting-Out

45.3.2.1 Effect of Different Types of Salts

The impact of different types of salt on the extraction of volatile methoxy-phenolic compounds was investigated. Figure 45.4 illustrates the extraction efficiency of volatile methoxy-phenolic compounds in the use of different kinds of salts, such as NH_4Cl, KCl, NaCl, $MgCl_2$, Na_2SO_4, $(NH_4)_2SO_4$, and $C_6H_5O_7Na_3$. Obviously, KCl, $MgCl_2$ and $C_6H_5O_7Na_3$ exhibit higher extraction efficiency, $C_6H_5O_7Na_3$ exhibit the highest extraction efficiency. Compared with unsalted, it clearly exhibited an increasing trend with the concentration of 30 % of eight salts. So $C_6H_5O_7Na_3$ was selected for the future study.

45.3.2.2 Effect of Different Concentrations of Salt

In order to evaluate the effect of the ionic strength on the extraction of volatile methoxy-phenolic compounds four concentrations (5–40 %, w/v) of $C_6H_5O_7Na_3$ were selected. The results on the influence of $C_6H_5O_7Na_3$ concentration added to the sample are shown in Fig. 45.5. It is indicated that the total peak area of analytes extracted exhibited an increasing trend with increase of concentrations of

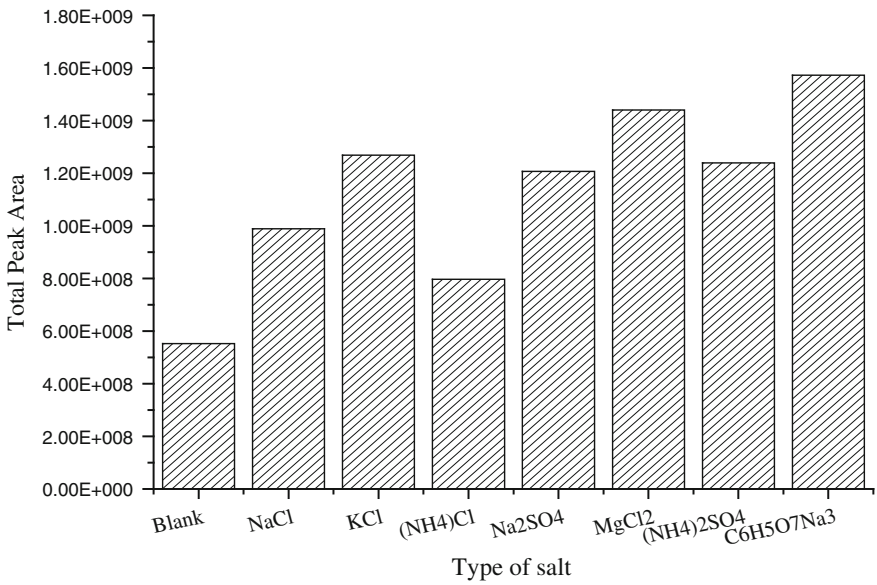

Fig. 45.4 Effect of type of salt on the efficiency of extraction of volatile methoxy-phenolic compounds

$C_6H_5O_7Na_3$. Above 30 %, with the increase of concentration of salt, the increasing trend was not significantly changed. Therefore, 30 % (w/v) of $C_6H_5O_7Na_3$ was selected for the rest of experiments.

45.3.3 Method Validation

The linearity of the proposed method was evaluated under the optimization conditions. Six volatile methoxy-phenolic compounds at five levels were performed. The concentration range of each analyte and the correlation coefficients (R^2) shown in Table 45.1. The correlation indicated a good linearity for the analytes. In addition, the repeatability and the method detection limits are also presented. The repeatability of the method was determined by the relative standard deviation (RSD). The values of the RSD were below 10 % for all analytes, which is considered satisfactory for this type of analysis. The LODs of six methoxy-phenolic compounds were estimated on the basis of the lowest detectable peak that had signal three times of the background noise (signal/noise = 3). Owing to the high selectivity and sensitivity of CAR/PDMS coating, low detection limits were

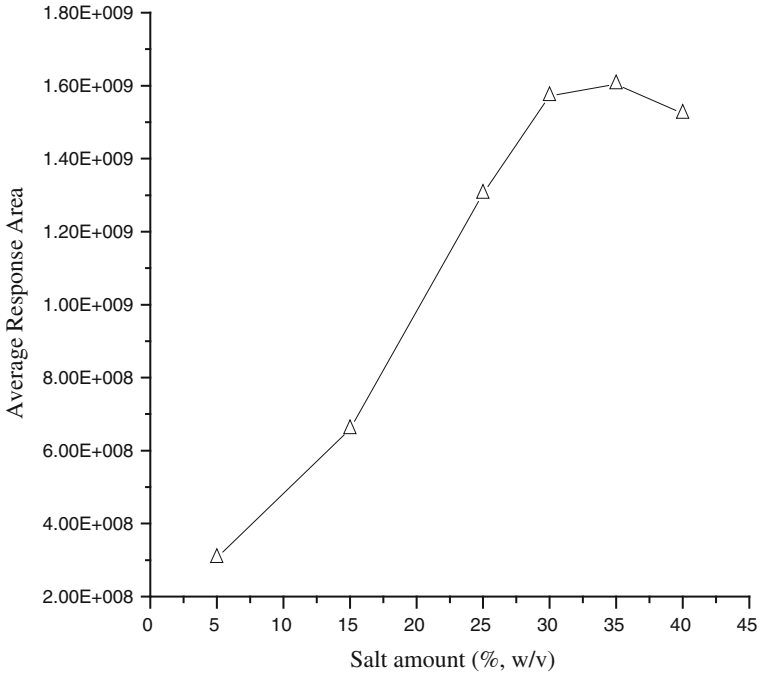

Fig. 45.5 Effect of salt concentration on the efficiency of extraction of volatile methoxy-phenolic compounds

Table 45.1 Ranges of Concentration (n = 5), Regression Coefficients (R^2), Limits of Detection (LOD), Relative Standard Deviations (% RSD) of Repeatability, and Recovery

Compound	Linear range (μg/g)	R^2	LOD (ng/g)	RSD (%)	Add content (μg/g)	Recovery (%)	RSD (%)
1,2-dimethoxybenzene	0.15–30.03	0.992	14.53	9.02	0.30	92.21	8.84
3,4-dimethoxytoluene	0.071–7.07	0.997	2.31	7.25	0.71	98.06	5.90
1-methoxy-4-(1-propenyl)-benzene	0.033–3.30	0.990	1.54	8.31	0.33	112.04	9.58
1,2,3-trimethoxybenzene	0.167–33.33	0.998	3.01	6.54	1.67	96.34	5.73
1,2,4-trimethoxybenzene	0.145–28.91	0.992	3.39	8.34	1.45	82.05	9.08
1,2,3-trimethoxy-5-methylbenzene	0.05–10.0	0.999	2.58	4.62	0.50	86.56	7.64

achieved for the six volatile methoxy-phenolic compounds. The LODs of six methoxy-phenolic compounds were ranged from 1.54 ng/g to 14.53 ng/g.

To evaluate the accuracy of the optimized method, a recovery study for each analyte was performed in real pu-erh tea sample. For this purpose, known quantities of the six analytes (Table 45.1) were added to pu-erh tea sample. The recoveries and the repeatability of the method are listed in Table 45.1. The recoveries obtained from the high level range from 82.05 to 112.04 %. The precision of the determination of the pu-erh tea sample is also satisfactory for the analytes. The RSD values are below 10 %.

45.4 Conclusion

In the present study, we have developed an efficiency method (salting-out) for determining volatile methoxy-phenolic compounds in pu-erh tea, based on the use of SPME. Under the optimization condition, sodium citrate showed the highest extraction efficiency. Compared with unsalted, the total peak area of methoxy-phenolic compounds increased by 2.8 times with sodium citrate added. Meanwhile, the proposed method affords wide of linearity, good linear regression coefficients (0.992–0.999), detection limits varied from 1.54 to 14.53 ng/g and the relative standard deviations for repeatability were below 10 %. Recovery was ranged from 82.05 to 112.04 % and the relative standard deviations were below 10 %. Owing to the low detection limits and good repeatability the developed methodology can be used to determine the content of volatile methoxy-phenolic compounds in various pu-erh tea samples.

Acknowledgments This work was financially supported by the program of National High Technology Research and Development Program of China (863 Program) (Grant No. SS2012AA023408), the Cheung Kong Scholars, and Innovative Research Team Program in University of Ministry of Education, China (Grant No. IRT1166).

References

1. Ku KM, Kim J, Park HJ et al (2010) Application of metabolomics in the analysis of manufacturing type of pu-erh tea and composition changes with different postfermentation year. J Agr Food Chem 58:345–352
2. Lu CH, Hwang LS (2008) Polyphenol contents of Pu-Erh teas and their abilities to inhibit cholesterol biosynthesis in Hep G2 cell line. Food Chem 111:67–71
3. Kubot K, Sumi S, Tojo H et al (2011) Improvements of mean body mass index and body weight in preobese and overweight Japanese adults with black Chinese tea (Pu-Erh) water extract. Nutr Res 31:421–428
4. Qian ZM, Guan J, Yang FQ et al (2008) Identification and quantification of free radical scavengers in pu-erh tea by HPLC-DAD-MS coupled online with 2,2′-Azinobis(3-ethylbenzthiazolinesulfonic acid) diammonium salt assay. J Agr Food Chem 56:11187–11191
5. Lv HP, Zhong QS, Lin Z et al (2012) Aroma characterisation of pu-erh tea using headspace-solid phase microextraction combined with GC/MS and GC-olfactometry. Food Chem 130:1074–1081
6. Xu X, Yan M, Zhu Y (2000) Influence of fungal fermentation on the development of volatile compounds in the puer tea manufacturing process. Eng Life Sci 4:382–386
7. Pizarro C, Perez-del-Notario N, Gonzalez-Saiz JM (2007) Optimisation of a headspace solid-phase microextraction with on-fiber derivatisation method for the direct determination of haloanisoles and halophenols in wine. J Chromatogr A 1143:26–35
8. Llompart M, Lourido M, Landin P et al (2002) Optimization of a derivatization-solid-phase microextraction method for the analysis of thirty phenolic pollutants in water samples. J Chromatogr A 963:137–148
9. Canosa P, Rodriguez I, Rubi E et al (2005) Optimization of solid-phase microextraction conditions for the determination of triclosan and possible related compounds in water samples. J Chromatogr A 1072:107–115
10. Charry-Parra G, DeJesus-Echevarria M, Perez FJ (2011) Beer volatile analysis: optimization of HS/SPME coupled to GC/MS/FID. J Food Sci 76:C205–C211
11. Lambropoulou DA, Albanis TA (2001) Optimization of headspace solid-phase microextraction conditions for the determination of organophosphorus insecticides in natural waters. J Chromatogr A 922:243–255
12. Ducki S, Miralles-Garcia J, Zumbe A et al (2008) Evaluation of solid-phase micro-extraction coupled to gas chromatography-mass spectrometry for the headspace analysis of volatile compounds in cocoa products. Talanta 74:1166–1174
13. Pontes M, Marques JC, Câmara JS (2007) Screening of volatile composition from Portuguese multifloral honeys using headspace solid-phase microextraction-gas chromatography–quadrupole mass spectrometry. Talanta 74:91–103
14. Beceiro-Gonzalez E, Guimaraes A, Alpendurada MF (2009) Optimisation of a headspace-solid-phase micro-extraction method for simultaneous determination of organometallic compounds of mercury, lead and tin in water by gas chromatography-tandem mass spectrometry. J Chromatogr A 1216:5563–5569
15. Brás I, Santos L, Alves A (2000) Monitoring organochlorine pesticides from landfill leachates by gas chromatography–electron-capture detection after solid-phase microextraction. J Chromatogr A 891:305–311
16. Saison D, De Schutter DP, Delvaux F et al (2008) Optimisation of a complete method for the analysis of volatiles involved in the flavour stability of beer by solid-phase microextraction in combination with gas chromatography and mass spectrometry. J Chromatogr A 1190:342–349
17. Pizarro C, Perez-del-Notario N, Gonzalez-Saiz JM (2010) Optimisation of a simple and reliable method based on headspace solid-phase microextraction for the determination of volatile phenols in beer. J Chromatogr A 1217:6013–6021

18. Canosa P, Rodriguez I, Rubi E et al (2006) Optimisation of a solid-phase microextraction method for the determination of parabens in water samples at the low ng per litre level. J Chromatogr A 1124:3–10
19. Perestrelo R, Barros AS, Rocha SM et al (2011) Optimisation of solid-phase microextraction combined with gas chromatography-mass spectrometry based methodology to establish the global volatile signature in pulp and skin of Vitis vinifera L. grape varieties. Talanta 85:1483–1493
20. Geerdink RB, Breidenbach R, Epema OJ (2007) Optimization of headspace solid-phase microextraction gas chromatography-atomic emission detection analysis of monomethylmercury. J Chromatogr A 1174:7–12

Chapter 46
Effects of *NTH1* Gene Deletion and Overexpressing *TPS1* Gene on Freeze Tolerance in Baker's Yeast

Mingyue Wu, Cuiying Zhang, Xi Sun, Guanglu Wang, Yanwen Liu and Dongguang Xiao

Abstract The content of trehalose is widely believed to be a major determinant of stress resistance in *Saccharomyces cerevisiae*. A neutral trehalase gene, *NTH1*, is involved in trehalose degradation and *TPS1* encoding trehalose biosynthesis enzyme is improtant to trehalose accumulation in *S. cerevisiae*. In this research, the responses of two engineering strains, the deletion of *NTH1* (Δ*nth1*) and overexpression *TPS1* (Δ*nth1* + *TPS1*), were investigated to freezing stresses. High trehalose accumulation and growth activity were observed in Δ*nth1* + *TPS1* strain after freezing stress induction. Our results indicated that high trehalose accumulation can make yeast cells resistant freezing stress.

Keywords *Saccharomyces cerevisiae* · Freeze tolerance · *NTH1* · *TPS1* · Trehalose

46.1 Introduction

Freeze-tolerant yeasts are necessary as the process for manufacturing bread from frozen dough widely used in the baking industry [1, 2]. Trehalose, a nonreducing disaccharide (a-D-glucopyranosyl-[1,1]-a-D-glucopyranoside), has been reported to play a dual role of a stress protectant of the integrity of cytoplasmic membrane and reserved carbohydrate providing the energy necessary for correct renaturation of proteins during stress recovery [3, 4].

It described that three trehalases are involved in trehalose hydrolysis in *Saccharomyces cerevisiae* [5, 6]: (1) a neutral trehalase encoded by the *NTH1*

M. Wu · C. Zhang (✉) · X. Sun · G. Wang · Y. Liu · D. Xiao
Key Laboratory of Industrial Fermentation Microbiology, Tianjin Industrial Microbiology Key Laboratory, Ministry of Education, College of Biotechnology, Tianjin University of Science and Technology, Tianjin 300457, People's Republic of China
e-mail: cyzhangcy@tust.edu.cn

T.-C. Zhang et al. (eds.), *Proceedings of the 2012 International Conference on Applied Biotechnology (ICAB 2012)*, Lecture Notes in Electrical Engineering 249,
DOI: 10.1007/978-3-642-37916-1_46, © Springer-Verlag Berlin Heidelberg 2014

gene; (2) a putative trehalase Nth2p encoded by the *NTH2* gene, which is a homolog of the *NTH1* gene; (3) the acid trehalase encoded by the *ATH1* gene. It suggested that *NTH1* and *ATH1* disruptant, respectively, strains exhibited higher freeze tolerance and intracellular trehalose levels than the parental strains [7].

In *S. cerevisiae,* trehalose is synthesized from glucose and glucose-1-phosphate by two consecutive enzymatic reactions catalyzed by trehalose-6-phosphate synthase,defined as Tre6P, and trehalose-6-phosphate phosphatase. The two proteins are encoded by the genes *TPS1* and *TPS2*, respectively [8–10].

Previous studies reported that thermotolerance, growth rate, and ethanol fermentation ability of the yeast strain were improved by overexpressing *TPS1* [11, 12]. The responses to various environmental stresses of the *TPS1*- and TPS2-overexpressing triple deletion (Δ*nth1* Δ*ath1* Δ*nth2*) strains were higher than that in the original laboratory strain as Siraje Arif Mahmud reported [4].

As a result of these findings, we became interested in studying the influence of the deletion of the *NTH1* gene and the overexpression of the *TPS1* gene on freezing stressor, with a view to obtain a freeze-tolerant industrial baker's yeast strain.

46.2 Materials and Methods

46.2.1 Media and Cultivation Conditions

Escherichia coli strain DH5α was incubated in Luria–Bertani medium added ampicillin resistance for plasmid maintenance.

Yeast strains were routinely cultured in YEPD medium at 30 °C. The yeast mutants were screened on YEPD plates added G418 additionally to 800 μg/mL. Molasses medium (10 ∼ 12° Brix molasses, contains 5 g/L yeast extract, 0.5 g/L $(NH_4)_2SO_4$, pH 5.5) and low sugar model liquid dough (LSMLD, 2.5 g/L $(NH4)_2SO_4$, 5 g/L urea, 16 g/L KH_2PO_4, 5 g/L Na_2HPO_4, 0.6 g/L $MgSO_4$, 2.25×10^{-2} g/L nicotinic acid, 5×10^{-3} g/L Ca-pantothenate, 2.5×10^{-3} g/L thiamine, 1.25×10^{-3} g/L pyridoxine, 1×10^{-3} g/L riboflavin, 5×10^{-4} g/L folic acid) medium are used for fermentation assay. Besides, the mixed sugar LSMLD medium contained 40 g/L glucose [13].

46.2.2 Measurement of Cell Mass Yield and Leavening Ability

A certain volume molasses culture was centrifugated at 5,000 rpm for 5 min, washed with sterile water twice, and dried overnight at 105 °C. The weight of the dry yeast cell was defined as the cell mass yield (g dry yeast/L).

The leavening ability in the lean dough of all the yeasts was determined by the SJA fermentograph (Type JM451, Sweden) according to the CNS (Chinese National Standards of the Yeast using in Food Processing). Lean dough was composed of 280 g flour, 150 mL water, 4 g salt, and 6 g fresh yeast (the moisture content was 68 %). The dough was stirred evenly and speedily for 5 min at 30 °C ± 0.2 °C, put the dough into the box of the fermentation chamber. Keep the records of the CO_2 production for 60 min at 30 °C [14].

46.2.3 Survival Rate Analysis

For evaluating the growth behavior of *S. cerevisiae* after freezing stress, 36-h stationary cultures in YEPD was transferred into 100 mL of molasses medium in a Sakaguchi flask to cell growth reached stationary phase and the cells harvested by centrifugation were washed twice with distilled water. Then the harvested cells were inoculated to 100 mL LSMLD and the culture was maintained at −20 °C for 21 days.

The cell samples were thawed at 35 °C to the temperature that reached 30 °C. Thawed samples at appropriate dilutions were spreaded on YEPD agar plates for determining cell viability.

46.2.4 Measurement of Intracellular Trehalose Content

The cells harvested by centrifugation were washed twice with sterile water to obtain fresh yeast cells. 0.1 g of fresh yeast cells was treated violently with 4 mL of 0.5 mol/L trichloroethanoic acid and incubated in ice bath on oscillator every 10 min for 1 h. The shocked samples were centrifugated and washed twice using washing solution, then all the supernatants were obtained and used for measuring the trehalose content [15]. The trehalose concentration in the supernatant was determinated by sulfuric anthrone reaction and the absorbance was measured at 630 nm [16]. The cell dry weight, described as 2.1, was used for calculating the trehalose content (mg/g dry cell).

46.2.5 Plasmids and Strains Construction

Plasmids, strains, and primers used in the current work are listed in Tables 46.1 and 46.2, respectively. Yeast strains (BY14α) and *E. coli* strain DH5α used in this study were obtained from the Yeast Collection Center of Tianjin Industrial Microbiology Key Laboratory of Tianjin University of Science and Technology,

Table 46.1 Strains and plasmids used in the current study

Strains and plasmids	Relevant features	Reference or source
Strains		
BY14α	*MAT*α (haploid derived from BY14 strain)	This study
Δ*nth1*	*MAT*α *nth1*:: AKB	This study
Δ*nth1* + *TPS1*	*MAT*α *nth1*::AKPTB	This study
DH5α	*E. coli* strain	Our lab
Plasmids		
pUC-NBAK	A-*KanMX*-B	Our lab
pPGK1	*bla* LEU2 $PGK1_P$-$PGK1_T$	Lilly [17]
pUC19	*Cloning vector*	Our lab
pUC-PGK	pUC19 + PGK_P + PGK_T	This study
pUC-TNBAK	A-*KanMX*-PGK_p-*TPS1*-PGK_T-B	This study

Table 46.2 Primers used in the present study[a]

Primers	Sequence (5′–3′)
TPS1-F	CCGCTCGAGATGACTACGGATAACGCT
TPS1-R	CCGCTCGAGGGGTTCATCAGTTTTTGG
PGK-F	CGCGGATCCTCTAACTGATCTATCCAAAACTGA
PGK-R	CGCGGATCCTAACGAACGCAGAATTTTC
NA-U	CCGGAATTCCGTCTTCTTCCATTGTCTT
NB-D	ACATGCATGCCTAGGTTATCTATGCTGTCT
Y1-U	ATCATCATCTGTAATCGCTTCACC
Y1-D	CCTTTTATATTTCTCTACAGGGGCG
Y2-U	TACAGCGGTAAAGTTTCTATGAGCA
Y2-D	TAGGTTGTATTGATGTTGGACGAGT
Y3-U	TTTTCTCTTTCCCCATCCTTTACGC
Y3-D	TCAGAATGTATGTCCATGATTCGCC

[a] The restriction site introduced in each primer is indicated by an *underline*

P. R. China. The recombinant strains (Δ*nth1* and Δ*nth1* + *TPS1*) were constructed by homologous recombination and overexpression method.

The recombinant plasmid pUC-NBAK used for *NTH1* deletion was presented by our previous experiment [18]. The fragment containing *PGK* promoter and terminator was cloned into vector pUC19 from pPGK1 to obtain the plasmid pUC-PGK. Plasmid pUC-TNBAK, a recombinant plasmid for overexpressing *TPS1* was constructed by the following procedure (Fig. 46.1). The fragment of *TPS1* was amplified from BY14α genomic DNA using primer pair *TPS1*-F and *TPS1*-R both containing the *Xho I* restriction sites. The PCR product was inserted into vector pUC-PGK to create the plasmid pUC-PGKT. The sequence encoding *PGKT* was amplified using primer pair *PGK*-F and *PGK*-R both containing the *BamH I* restriction sites. The PCR product *PGKT* was inserted into plasmid pUC-NBAK to create the recombinant plasmid pUC-TNBAK. The recombinant cassette fragments A-*KanMX*-B and A-*KanMX*-PGK_P-*TPS1*-PGK_T-B were transferred into yeast cells using a lithium acetate procedure, described previously [19]. The two

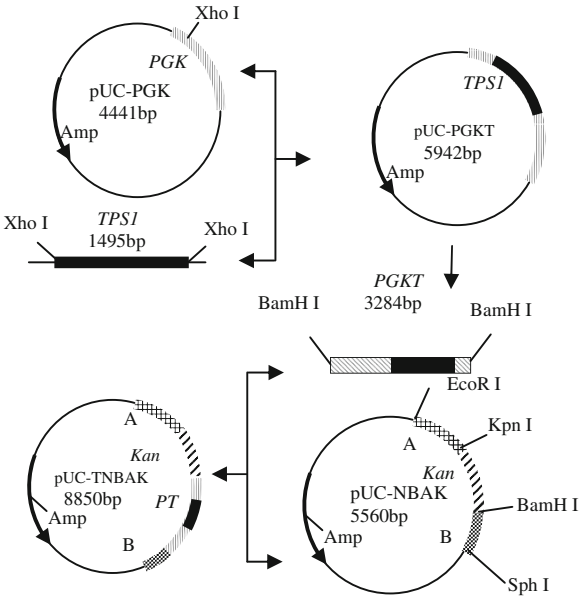

Fig. 46.1 Construction of plasmid pUC-TNBAK

recombinant strains were verified by primer pairs Y1-U, Y1-D/Y2-U, Y2-D and *PGK*-F, *PGK*-R/Y1-U, Y1-D/Y3-U, Y3-D, respectively.

46.3 Results and Discussion

46.3.1 Construction of NTH1 *Deletion and* TPS1 *Overexpression Mutants*

The primer pairs Y1-U,Y1-D/Y2-U, Y2-D/Y3-U, Y3-D, and *PGK*-F,*PGK*-R were designed to verify the recombinant mutants. The result in Fig. 46.2 showed that the target bands could be obtained from genome of the mutants using the validation primers, but could not from the parental strain. The PCR products sequencing results (data not shown) were the further proof to verify that the recombinant cassette fragments and were successfully integrated into the yeast genome.

46.3.2 Fermentation Characteristics

The cell mass yield in stationary phase of the mutants and the parental strain in the same medium and culture conditions illustrated that deletion of *NTH1* and overexpression of *TPS1* have no influence on the growth of the baker's yeast strains.

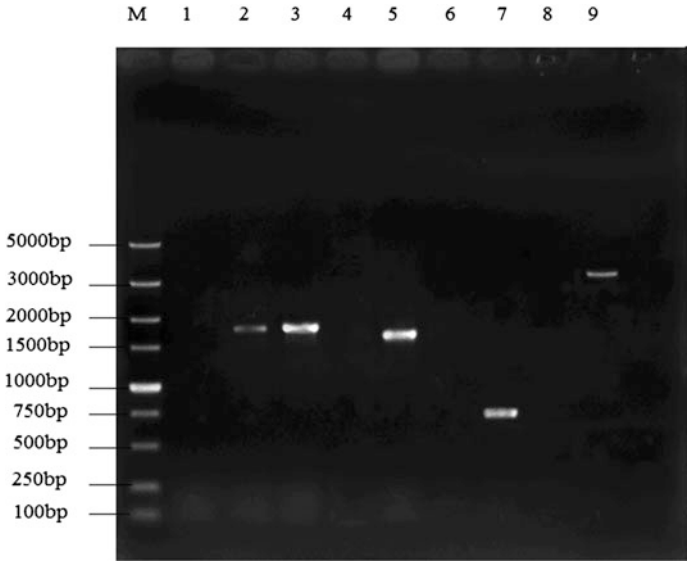

Fig. 46.2 PCR validation of the mutants. *M*, maker DL5000; *1*, *2*, *3*, segments amplified with Y1-U and Y1-D primers from BY14α, Δ*nth1*, Δ*nth1* + *TPS1*, respectively; *4*, *5*, Results amplified with Y2-U and Y2-D primers from BY14α and Δ*nth1*, respectively; *6*, *7*, PCR products from BY14α and Δ*nth1* + *TPS1* with primers Y3-U and Y3-D; *8*, *9*, $PGK1_P$ + TPS1 + $PGK1_T$ segments amplified with *PGK*-F and *PGK*-R primers from BY14α and Δ*nth1*α + *TPS1*

The glucose and maltose metabolisms were understood by detecting the direct leavening ability in lean dough. From the results above, it can be concluded that the leavening ability in lean dough was almost the same either before or after *NTH1* gene deletion and *TPS1* gene overexpression, while certain elevations of the growth ability and intracellular trehalose content of mutants Δ*nth1* and Δ*nth1* + *TPS1* after freezing in −20 °C were detected. The deletion of *NTH1* could reduce decomposition rate of trehalose, thus improving the freezing tolerance of yeast, but the effection was not obvious in this work, while the recombinant strain Δ*nth1* + *TPS1* exhibited the highest survival rate (almost 100 %) and the most intracellular trehalose content (156.1 mg/g dry cell) compared with the parental strain.The detailed information of data are listed in Table 46.3.

Table 46.3 Fermentation characteristics of parental strain and mutants[a]

Strains	BY14α	Δ*nth1*	Δ*nth1* + *TPS1*
Cell mass yield (g dry yeast/L)	8.67	8.70	8.60
Leavening ability in lean dough (mL)	895.4	882.9	887.3
Cell viability after freezing (%)	46.67	63	99.23
Trehalose contents (mg/g dry cell)	107.4	119.3	156.1

[a] Data are averages from three independent experiments

46.4 Conclusion

The objective of this research was to gain better insight into the relationship between trehalose metabolism under stressed condition and *NTH1* and *TPS1* genes in baker's yeast BY14α. Previous studies reported that neutral trehalase is the main factor in trehalose decomposition. In our study, the results showed that *NTH1* deletion could increase intracellular trehalose content and cell survival rate after freezing but not obviously, while the combined effect of *TPS1* overexpression and *NTH1* deletion played a more important role on trehalose accumulation. It was suggested that integrative overexpression of *TPS1* gene and deletion of *NTH1* gene could protect cells against stress condition. Excellent baker's yeast strain was obtained, which is effective to improve the development of bread making.

Acknowledgments The current study was financially supported by the National Natural Science Foundation of China (31171730), program for Changjiang Scholars and Innovative Research Team in University (IRT1166), and Major Project of Research Program on Applied Fundamentals and Advanced Technologies of Tianjin (10JCZDJC16700).

References

1. Takagi H, Iwamoto F, Nakamori S (1997) Isolation of freeze-tolerant laboratory strains of *Saccharomyces cerevisiae* from proline-analogue-resistant mutants. Appl Microbiol Biotechnol 47:405–411
2. Jiang Z, Qi J, Den H et al (2002) Screening the freeze-tolerant yeast strains. J China Agric Univ 7:87–91
3. Hirasawa R, Yokoigawa K, Isobe Y et al (2001) Improving the freeze tolerance of bakers' yeast by loading with trehalose. Biosci Biotechnol Biochem 65:522–526
4. Mahmud SA, Hirasawa T, Shimizu H (2010) Differential importance of trehalose accumulation in *Saccharomyces cerevisiae* in response to various environmental stresses. J Biosci Bioeng 109:262–266
5. Zahringer H, Burgert M, Holzer H et al (1997) Neutral trehalase Nthlp of *Saccharomyces cerevisiae* encoded by the *NTH1* gene is a multiple stress responsive protein. FEBS Lett 412:615–620
6. Ren Y, Liu J, Dai X et al (2003) Genes involved in biosynthesis and metabolism of trehalose and their use in biotechnology. Acta Microbiologica Sinica 43:821–825
7. Shima J, Hino A, Yamadalyo C et al (1999) Stress tolerance in doughs of *Saccharomyces cerevisiae* trehalase mutants derived from commercial Baker's yeast. Appl Environ Microbiol 9:2841–2846
8. Bonini BM, Dijck PV, Thevelein JM (2003) Uncoupling of the glucose growth defect and the deregulation of glycolysis in *Saccharomyces cerevisiae tps1* mutants expressing trehalose-6-phosphate-insensitive hexokinase from *Schizosaccharomyces pombe*. Biochim Biophys Acta 1606:83–93
9. Lee J, Hai T, Pape H et al (2008) Three trehalose synthetic pathways in the acarbose-producing *Actinoplanes* sp. SN223/29 and evidence for the TreY role in biosynthesis of component. Appl Microbiol Biotechnol 80:767–778
10. Gancedo C, Flores C (2004) The importance of a functional trehalose biosynthetic pathway for the life of yeasts and fungi. FEMS Yeast Res 4:351–359

11. An M, Tang Y, Mitsumasu Liu Z et al (2011) Enhanced thermotolerance for ethanol fermentation of *Saccharomyces cerevisiae* strain by overexpression of the gene coding for trehalose-6-phosphate synthase. Biotechnol Lett 33:1367–1374
12. Guo Z, Zhang L, Ding Z et al (2011) Minimization of glycerol synthesis in industrial ethanol yeast without influencing its fermentation performance. Metab Eng 13:49–59
13. Jiang TX, Xiao DG, Gao Q (2008) Charactrisation of maltose metabolism in lean dough by lagging and non-lagging baker's yeast strains. Annal Microbiol 58:655–660
14. Zhang Y, Xiao DG, Zhang CY et al (2012) Effect of *MIG1* gene deletion on glucose repression in Baker's yeast. Adv Mater Res 396–398:1531–1535
15. Sharma SC (1997) A possible role of trehalose in osmotolerance and ethanol tolerance in *Saccharomyces cerevisiae*. FEMS Microbiol Lett 152:11–15
16. Ferreir JC, VMFP, Panek AD (1996) Comparison of three different methods for trehalose determination in yeast extracts. Food Chem 60:251–254
17. Lilly M, Lambrechts MG, Pretorius IS (2000) Effect of increased yeast alcohol acetyl transferase activity on flavor profiles of wine and distillates. Appl Environ Microbiol 66:744–753
18. Hao X (2010) Study on higher alcohols metabolize and tolerance of *Saccharomyces cerevisia*. Tianjin University of Science and Technology, Tianjin
19. Zhang JW, Zhang CY, Dai LH et al (2012) Effects of overexpression of the alcohol acetyltransferase-encoding gene *ATF1* and deletion of the esterase-encoding gene *IAH1* on the flavour profiles of Chinese yellow rice wine. Int J Food Sci Tech 47:2590–2596

Chapter 47
Synergistic Effects of Sakacin C2 in Combination with Food Preservatives

Dapeng Li, Xiaoyan Liu and Yurong Gao

Abstract Synergistic effects of sakacin C2 in combination with nisin and several chemical preservatives against *Staphylococcus aureus* ATCC 63589 and *Escherichia coli* ATCC 25922 were investigated. Methyl paraben, propyl paraben, nisin, and sodium nitrite notably increased inhibitory effect of sakacin C2 against these two indicators. Inhibitory effects of sakacin C2 (10 AU/ml) against *S. aureus* ATCC 63589 were increased to 71.6 %, 61.3 %, 58.9 %, and 56.2 % from 41.3 % in the presence of methyl paraben (0.16 g/L), propyl paraben (0.16 g/L), nisin (5 mg/L), and sodium nitrite (0.1 g/L), respectively. Inhibitory effects of sakacin C2 against *E. coli* ATCC 25922 were respectively increased to 45.8 %, 44.1 %, 41.2 %, and 47.6 % from 29.3 % in the presence of methyl paraben (0.16 g/L), propyl paraben (0.16 g/L), nisin (5 mg/L), and sodium nitrite (0.1 g/L), even though nisin could not inhibit Gram-negative bacteria. These synergistic actions may be beneficial to broaden the application range, improve the efficiency, and decrease the dosage of bacteriocins from LAB and chemical preservatives in the food industry.

Keywords Sakacin C2 · Nisin · Parabens · Sodium nitrite · Synergistic effects

47.1 Introduction

Bacteriocins produced by lactic acid bacteria (LAB) are antimicrobial peptides or proteins with activity mainly against Gram-positive bacteria and are generally regarded as safe [1]. The use of bacteriocins from LAB is a promising ongoing development in the food industry. Bacteriocins from *Lactobacillus sakei* species have gained great attention, because they have been extensively used as starter in

D. Li (✉) · X. Liu · Y. Gao
Food College, Heilongjiang Bayi Agricultural University, Daqing 163319, People's Republic of China
e-mail: dpengl@163.com

T.-C. Zhang et al. (eds.), *Proceedings of the 2012 International Conference on Applied Biotechnology (ICAB 2012)*, Lecture Notes in Electrical Engineering 249,
DOI: 10.1007/978-3-642-37916-1_47, © Springer-Verlag Berlin Heidelberg 2014

fermented meat products [2]. Sakacin C2 is a novel bacteriocin produced by *L. sakei* C2 isolated from traditional Chinese fermented cabbage [3]. Sakacin C2 has broad antimicrobial activity against not only some Gram-positive bacteria but also some Gram-negative bacteria, and that is different from other bacteriocins from *L. sakei* because their inhibition spectra are limited to some Gram-positive bacteria. The broad inhibitory spectrum and strong stability of sakacin C2 suggested its good prospect for application in food preservation.

Hurdle technology has been developed for the realization of nutritious, stable, safe, and economical foods in the recent years [4]. It employs the combination of different antimicrobial agents or techniques to achieve mild but effective preservation [5]. Although bacteriocins from LAB have good safety, their efficacy tends to be limited if applied alone [6]. The synergistic effects of bacteriocins with other factors including other antimicrobial agents were extensively researched for food preservation. The synergistic effects of food chemical preservatives methyl paraben, propyl paraben, and ethylenediaminetetraacetic acid (EDTA) in combination with acidocin CH5 and bacteriocin D10 were reported [7]. The synergistic effects of lactocin 705, enterocin CRL35, and nisin in both broth and meat system also indicated that the combined use of LAB bacteriocins may be more effective in preventing the emergence of bacteriocin-resistant *Listeria* population [8]. Beyond these, synergistic effects have been reported between mesenterocins 52A and 52B [9], and between nisin and curvaticin 13 [10]. Nevertheless, all these synergistic effects were observed against Gram-positive bacteria susceptible to all antimicrobial agents tested. The synergistic effects of bacteriocins from LAB in combination with other antimicrobial agents against Gram-negative bacteria are seldom researched even though many of Gram-negative bacteria such as *E. coli* and *Salmonella typhimurium* are food-borne pathogens. The majority of bacteriocins from LAB didnot show inhibitory activity against Gram-negative bacteria because cell membrane of Gram-negative bacteria is a complex barrier system for many antimicrobial agents. Therefore, bacteriocins and antimicrobial agents or processes used as hurdle technology against Gram-negative are gradually getting people's attention.

The objective of this work is to evaluate the synergistic effects of sakacin C2 in combination with nisin, methyl paraben, propyl paraben, or sodium nitrite against *S. aureus* ATCC 63589 and *E. coli* ATCC 25922 in broth.

47.2 Materials and Methods

47.2.1 Bacterial Strains and Culture Conditions

L. sakei C2 (The GenBank access number: EU586177) producing sakacin C2 was isolated from Chinese traditional fermented cabbage and stored in MRS broth with 20 % (v/v) glycerol at −20 °C.. Before use, they were grown twice in MRS broth

and statically incubated at 30 °C for 18 h. *S. aureus* ATCC 63589 and *E. coli* ATCC 25922 were obtained from China General Microbiological Culture Collection Center (CGMCC, Beijing, China). They were stored in nutrient broth plus 10 % glycerol at −20 °C. Before use, they were grown twice in nutrient broth at 37 °C with constant shaking at 100 rpm for 12 h.

47.2.2 Preparation of Sakacin C2

Sakacin C2 was purified from the cell-free supernatant of *L. sakei* C2 using cold ethanol, Sephadex G50 column chromatography, and high-performance liquid chromatography (HPLC). Briefly, cell-free supernatant (pH 6.0) of *L. sakei* C2 was concentrated to one-tenth of the original volume and then precipitated by 4-fold volume cold ethanol (4 °C). By rotary vacuum evaporation, the supernatant was concentrated to one-fifth of the volume. Then the sample was eluted by a Sephadex G50 column chromatography system (1.0 cm × 160 cm) at a flow rate of 0.5 ml/min for 8 h. The fractions with inhibitory activity were pooled, concentrated by vacuum lyophilization, and diluted to 0.2 g/ml with distilled water. 2 ml of this sample was finally injected onto reverse-phase C18 HPLC column (5.0 mm × 100 mm, Daqing Sanxing Mechanical Manufacture Company, China), eluted with 50 % (v/v) methanol aqueous solution at a flow rate of 1.0 ml/min and checked with UV detection at 210 nm (25 °C). The fractions with inhibitory activity were collected and stored at −20 °C.

47.2.3 Determination of Bacteriocin Activity of Sakacin C2 Preparation

Bacteriocin activity (AU/ml) was determined using *S. aureus* ATCC 63589 as indictor. Briefly, 50 microliter of 2-fold serial dilutions of sakacin C2 preparation were transferred into wells on nutrient soft agar plates seeded with *S. aureus* ATCC 63589 and incubated for 18 h at 30 °C. Bacteriocin activity (AU/ml) was defined as the reciprocal of the highest dilution by 2-fold serial dilution showing a clear inhibition zone [11].

47.2.4 Inhibitory Effects of Sakacin C2 Against S. aureus *ATCC 63589 and* E. coli *ATCC 25922*

Sterile nutrient broth supplemented with sakacin C2 preparation (0–30 AU/ml) was used to detect inhibitory effects of sakacin C2 against *S. aureus* ATCC 63589 or *E. coli* ATCC 25922. Sterile nutrient broth without sakacin C2 preparation was used as control. Sterile nutrient broth were inoculated with 1 % overnight culture

of *S. aureus* ATCC 63589 or *E. coli* ATCC 25922 and incubated at 37 °C with constant shaking at 100 rpm. After 12 h of incubation, values of the optical density (OD) of cell cultures were measured at 600 nm.

47.2.5 Determination of the Inhibitory Effect

The following equation was used to determine inhibitory effect (I): $I = 100 - 100 \times \mathrm{OD}/\mathrm{OD}_0$ [%], where OD_0 was the optical density of the control, and OD was the optical density of cell culture containing sakacin C2 preparation.

47.2.6 Effect of Food Preservatives on the Inhibitory Effect of Sakacin C2

Sterile nutrient broth containing sakacin C2 (10 AU/ml) and supplemented with propyl paraben (0.02–0.16 g/L), methyl paraben (0.02–0.16 g/L), nisin (1–5 mg/L), or sodium nitrite (0.02–0.10 g/L) was used to determine the effect of food preservatives on the inhibitory effect of sakacin C2. Food chemical preservatives (propyl paraben, methyl parabens, and sodium nitrite) and nisin were respectively purchased from Wuxi Lu's Food Additive Co LTD (China) and Zhejiang Silver Elephant Bioengineering Co., Ltd (1×10^6 IU/g, China). Sterile nutrient broth supplemented with propyl paraben, methyl parabens, nisin, or sodium nitrite but without sakacin C2 was used as control. Samples were incubated at 37 °C with constant shaking with 100 r/min for 12 h and the inhibitory effect was calculated.

47.2.7 Statistical Analysis

Each experiment was repeated three times. Data analysis was carried out using Microsoft Excel (version 2003).

47.3 Results

47.3.1 Inhibitory Effects of Sakacin C2 Against S. aureus *ATCC 63589 and* E. coli *ATCC 25922*

In order to find the suitable bacterion activity of sakacin C2 used to research the effect of food preservatives on its inhibitory effects against *S. aureus* ATCC 63589 and *E. coli* ATCC 25922, inhibitory effects of different activity of sakacin C2 (0–30 AU/ml) were detected.

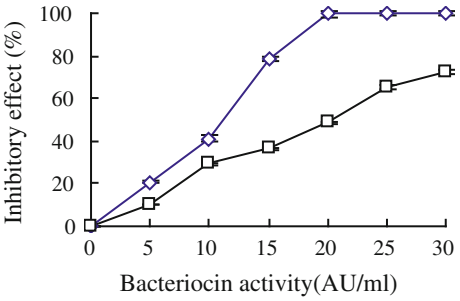

Fig. 47.1 Inhibitory effects of sakacin C2 against *S. aureus* ATCC 63589 and *E. coli* ATCC 25922. (◇): Inhibitory effects of sakacin C2 against *S. aureus* ATCC 63589; (□): Inhibitory effects of sakacin C2 against *E. coli* ATCC 25922

Inhibitory effects of sakacin C2 against *S. aureus* ATCC 63589 and *E. coli* ATCC 25922 respectively attained 100 % and 48.7 % when 20 AU/mL sakacin C2 was added (Fig. 47.1). These results showed that *S. aureus* ATCC 63589 was more sensitive than *E. coli* ATCC 25922 to sakacin C2. Added 10 AU/ml sakacin C2, inhibitory effects against *S. aureus* ATCC 63589 and *E. coli* ATCC 25922 were respectively 41.3 % and 29.3 %. Therefore, 10 AU/ml sakacin C2 were used for further experiments.

47.3.2 Effect of Methyl Paraben on the Inhibitory Effects of Sakacin C2

Inhibitory effects of methyl paraben against *S. aureus* ATCC 63589 and *E. coli* ATCC 25922 were not detected when its concentration was not higher than 0.16 g/L. However, inhibitory effects of sakacin C2 (10 AU/ml) against these two indicators were increased in presence of 0.02-0.16 g/L methyl paraben (Fig. 47.2). Inhibitory effects of sakacin C2 (10 AU/ml) against *S. aureus* ATCC 63589 and *E. coli* ATCC 25922 were respectively increased from 41.3 to 71.6 % and from 29.3 to 45.8 % in the presence of 0.16 g/L methyl paraben (Fig. 47.2).

47.3.3 Effect of Propyl Paraben on the Inhibitory Effects of Sakacin C2

Even at the highest concentration of propyl paraben (0.16 g/L), its inhibitory effects against both *S. aureus* ATCC 63589 and *E. coli* ATCC 25922 were not observed (Fig. 47.3). Similarly to methyl paraben, propyl paraben also increased the inhibitory effects of sakacin C2 (10 AU/ml) against these two indicators. Inhibitory effects of sakacin C2 (10 AU/ml) against *S. aureus* ATCC 63589 and *E. coli* ATCC 25922 were respectively increased from 41.3 to 61.3 % and from 29.3 to 44.1 % in the presence of 0.16 g/L methyl paraben (Fig. 47.3).

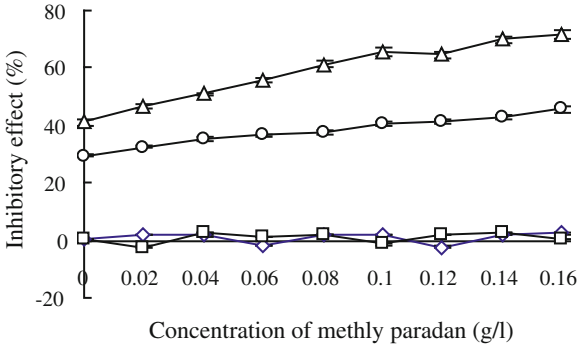

Fig. 47.2 Effect of methyl paraben on the inhibitory effects of sakacin C2. (△): Inhibitory effects of sakacin C2 (10 AU/ml) against S. aureus ATCC 63589 in presence of 0–0.16 g/L methyl paraben; (○): Inhibitory effects of sakacin C2 (10 AU/ml) against E. coli ATCC 25922 in presence of 0–0.16 g/L methyl paraben; (◇): Inhibitory effects of methyl paraben against S. aureus ATCC 63589 without sakacin C2; (□): Inhibitory effects of methyl paraben against E. coli ATCC 25922 without sakacin C2

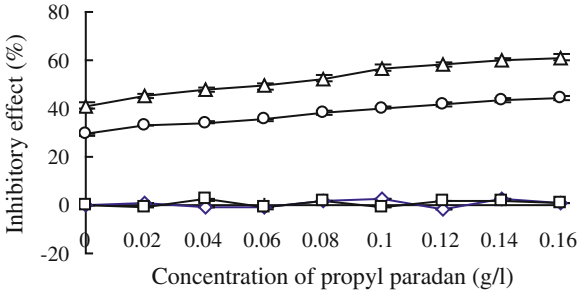

Fig. 47.3 Effect of propyl paraben on inhibitory effects of sakacin C2. (△): Inhibitory effects of sakacin C2 (10 AU/ml) against *S. aureus* ATCC 63589 in presence of 0–0.16 g/L propyl paraben; (○): Inhibitory effects of sakacin C2 (10 AU/ml) against *E. coli* ATCC 25922 in presence of 0–0.16 g/L propyl paraben; (◇): Inhibitory effects of propyl paraben against *S. aureus* ATCC 63589 without sakacin C2; (□): Inhibitory effects of propyl paraben against *E. coli* ATCC 25922 without sakacin C2

47.3.4 Effect of Nisin on the Inhibitory Effects of Sakacin C2

No inhibition of these two indicators was observed when nisin (1–5 mg/L) was used individually (Fig. 47.4). However, inhibitory effects of sakacin C2 (10 AU/ml) against *S. aureus* ATCC 63589 and *E. coli* ATCC 25922 were respectively increased from 41.3 to 58.9 % and from 29.3 to 41.2 % in the presence of 5 mg/L nisin (Fig. 47.4). It is noteworthy that nisin also increased the inhibitory effects of sakacin C2 against *E. coli* ATCC 25922 although nisin used individually couldnot inhibit *E. coli* ATCC 25922.

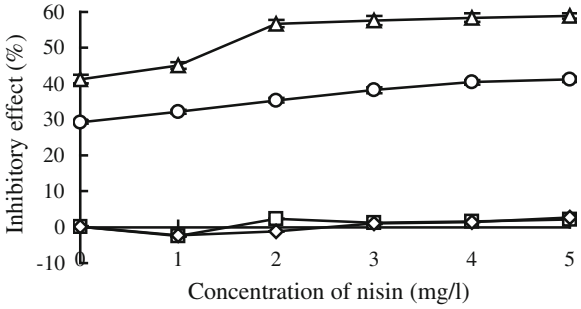

Fig. 47.4 Effect of nisin on inhibitory effects of sakacin C2. (△): Inhibitory effects of sakacin C2 (10 AU/ml) against *S. aureus* ATCC 63589 in presence of 0–5 mg/L nisin; (○): Inhibitory effects of sakacin C2 (10 AU/ml) against *E. coli* ATCC 25922 in presence of 0-5 mg/L nisin; (□): Inhibitory effects of nisin against *S. aureus* ATCC 63589 without sakacin C2; (◇): Inhibitory effects of nisin against *E. coli* ATCC 25922 without sakacin C2

47.3.5 Effect of Sodium Nitrite on the Inhibitory Effects of Sakacin C2

As shown in Fig. 47.5, inhibitory effects of sakacin C2 (10 AU/ml) against *S. aureus* ATCC 63589 and *E. coli* ATCC 25922 were respectively increased from 41.3 to 56.2 % and from 29.3 to 47.6 % in the presence of 0.1 g/L sodium nitrite, while no inhibition of two indicator strains was detected when sodium nitrite (0.02–0.1 g/L) was used individually. From these results, the synergistic inhibitory action of sakacin C2 and sodium nitrite against *S. aureus* ATCC 63589 and *E. coli* ATCC 25922 was detected.

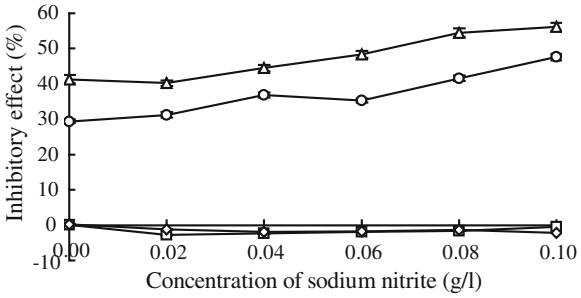

Fig. 47.5 Effect of sodium nitrite on the inhibitory effects of sakacin C2. (△): Inhibitory effects of sakacin C2 (10 AU/ml) against *S. aureus* ATCC 63589 in presence of 0–0.10 g/L sodium nitrite; (○): Inhibitory effects of sakacin C2 (10 AU/ml) against *E. coli* ATCC 25922 in presence of 0–0.10 g/L sodium nitrite; (□): Inhibitory effects of sodium nitrite against *S. aureus* ATCC 63589 without sakacin C2; (◇): Inhibitory effects of sodium nitrite against *E. coli* ATCC 25922 without sakacin C2

47.4 Discussion

Parabens have been widely used as antimicrobial agents against Gram-positive bacteria, yeasts, and molds in foods and drugs for over 50 years. In vegetables, fruit juices, baked goods, sauces, frozen dairy products, and fats and oils, the used concentration of propyl paraben is between 0.045 and 0.2 %. The concentration of methyl paraben used in food is between 0.03 and 0.4 % [12]. Methyl paraben and propyl paraben both increased inhibitory effects of sakacin C2 against *S. aureus* ATCC 63589 and *E. coli* ATCC 25922 (Fig. 47.2 and Fig. 47.3). Although the combined effects of propyl parabens and methyl paraben in combination with bacteriocins such as acidocin CH5 and bacteriocin D10 against Gram-positive bacteria have been studied [7], the inhibitory effects of these two substances in combination with bacteriocins from LAB against Gram-negative have not been reported so far.

Nisin is a polycyclic antibacterial peptide against Gram-positive spoilage and pathogenic bacteria used in processed cheese, meats, beverages, etc. However, nisin cannot inhibit Gram-negative bacteria except when it combined with chelators and rapid chilling [13, 14]. Nisin is commonly used in the food at a range between 1 and 25 mg/kg. Nisin contains unusual amino acids having binding specificity for lipid II (the component of bacterial cell) [15]. In this paper, study showed that inhibitory effects of sakacin C2 against *S. aureus* ATCC 63589 and *E. coli* ATCC 25922 were increased in the presence of 5 mg/L nisin (Fig. 47.4). Synergistic effects of nisin in combination with pediocin AcH and curvaticin 13 against Gram-positive bacteria have been reported [10, 16]. However, synergistic action of nisin and other bacteriocins from LAB against Gram-negative bacteria have not been reported. These results may imply that the combined use of two antimicrobial agents may be advantageous to produce a synergistic effect what make the individual antimicrobial agent effective at low concentration even when indictor strain is sensitive to one antimicrobial agent but not sensitive to another.

As a chemical preservative used in the food industry, sodium nitrite serves a dual purpose since it is used not only to cure meats like ham, bacon, and hot dogs but also prevent the growth of some pathogenic bacteria such as *Clostridium botulinum* and *Listeria monocytogenes*. However, sodium nitrite was found to form carcinogenic nitrosamines in meats containing sodium nitrite when exposed to high temperatures [17]. Therefore, usage of sodium nitrite has been carefully regulated in cured products in the United States and residual levels of nitrite have decreased to 200 mg/kg in the past 20 years. Reducing the usage concentration of sodium nitrite by synergistic action of sodium nitrite and biopreservative generally regarded as safety, may be a feasible and effective method. However, research about this has not been reported so far. In this paper, study showed that sodium nitrite in combination with sakacin C2 had notably synergistic action against *S. aureus* ATCC 63589 and *E. coli* ATCC 25922.

At present, all these synergistic effects were observed on strains susceptible to antimicrobial agents mainly Gram-positive bacteria. There have not reports about

synergistic effects of bacteriocin from LAB and other antimicrobial agents on Gram-negative so far. This paper reports that sakacin C2 can be combined with nisin, methyl paraben, propyl paraben, or sodium nitrite to produce more effective activity against *S. aureus* ATCC 63589 (a typical Gram-positive bacteria) and *E. coli* ATCC 25922 (a typical Gram-negative bacteria) in broth even though nisin could not inhibit Gram-negative bacteria. This might be beneficial to broaden the application range, improve the efficiency, and decrease the dosage of bacteriocins from LAB and chemical preservatives in the food industry.

Acknowledgment This research was funded by Young Science Mainstay Subject of the Education Department of Heilongjiang Province (1155G38).

References

1. Cleveland J, Montville TJ, Nes IF et al (2001) Bacteriocins: safe, natural antimicrobials for food preservation. Int J Food Microbiol 71:1–20
2. Ross RP, Morgan S, Hill C (2002) Preservation and fermentation: past, present and future. Int J Food Microbiol 79:3–16
3. Gao YR, Jia SR, Gao Q et al (2010) A novel bacteriocin with a broad inhibitory spectrum produced by Lactobacillus sakei C2, isolated from traditional Chinese fermented cabbage. Food Control 21:76–81
4. Lee SY (2004) Microbial safety of pickled fruits and vegetables and hurdle technology. Int J Food Safety 4:21–32
5. Leistner L (2000) Basic aspects of food preservation by hurdle technology. Int J Food Microbio 55:181–186
6. Gálbez A, Abriouel H, López RL et al (2007) Bacteriocin-based strategies for food biopreservation. Int J Food Microbiol 120:51–70
7. GiesováM Chumchalová J, Plocková M (2004) Effect of food preservatives on the inhibitory activity of acidocin CH5 and bacteriocin D10. Eur Food Res Technol 218:194–197
8. Vignolo G, Palacios J, Farías ME et al (2000) Combined effect of bacteriocins on the survival of various Listeria species in broth and meat system. Curr Microbiol 41:410–416
9. Limonet M, Revol-Junelles AM, Cailliez-Grimal C et al (2004) Synergistic mode of action of mesenterocins 52A and 52B produced by Leuconostoc mesenteroides subsp. Mesenteroides FR52. Curr Microbiol 48:204–207
10. Bouttefroy A, Millière JB (2000) Nisin-curvaticin 13 combinations for avoiding the regrowth of bacteriocin resistant cells of Listeria monocytogenes ATCC 15313. Int J Food Microbiol 62:65–75
11. Xiraphi N, Georgalaki M, Van Driessche G et al (2006) Purification and characterization of curvaticin L442, a bacteriocin produced by Lactobacillus curvatus L442. Antonie Van Leeuwenhoek 89:19–26
12. Golden R, Gandy J, Vollmer G (2005) A review of the endocrine activity of parabens and implications for potential risks to human health. Cri Rev in Toxicol 35:435–458
13. Belfiore C, Castellano P, Vignolo G (2007) Reduction of Escherichia coli population following treatment with bacteriocins from lactic acid bacteria and chelators. Food Microbiol 24:223–229
14. Cao-Hoang L, Marechal PA, Le-Thanh M et al (2008) Synergistic action of rapid chilling and nisin on the inactivation of Escherichia coli. Appl Microbiol Biotechnol 79:105–109

15. Hasper HE, Kramer NE, Smith JL et al (2006) An alternative bactericidal mechanism of action for lantibiotic peptides that target lipid II. Sci 313:1636–1637
16. Hanlin MB, Kalchayand N, Ray P et al (1993) Bacteriocins of lactic acid bacteria in combination have greater antibacterial activity. J Food Pro 56:252–255
17. Bills DD, Hildrum KI, Scanlan RA et al (1973) Potential precursors of N-nitrosopyrrolidine in bacon and other fried foods. J Agric Food Chem 21:876–877

Chapter 48
Purification and Characterization of Antifungal Lipopeptide from *Bacillus amyloliquefaciens* BI_2

Depei Wang, Kele Li, Yingying Wang, Ying Yang and Jian Zhang

Abstract *Bacillus amyloliquefaciens* BI_2 isolated from straw feed was shown to be antagonistic against *Aspergillus flavus*. Crude extract of antagonistic substance was obtained by ultrafiltration, nanofiltration, acid precipitation, and solvent extraction and it was stable to high temperature, different pH value, and several proteinases. Then the pure substance was isolated and purified by Sephadex G-15 column chromatography and prepared thin-layer chromatography. Oil-film collapsing, emulsification of toluene and on-plate hydrolysis experiments showed the compound was cyclic peptide, and its molecular structure was determined by UV absorption spectrum and infrared absorption spectrum following the amino acid analysis, ESI–MS and MS–MS. It showed that isolated compound consists of three homologues with molecular mass 1,008, 1,022 and 1,036 Da, and bearing a cyclic structure. Meanwhile, it also showed that antifungal substance had absorption peak at 206 nm. All of those indicated that the isolated substance belongs to the homologues of surfactin.

Keywords *Bacillus amyloliquefaciens* BI_2 · Antifungal substance · Purification · Lipopeptide

48.1 Introduction

Aspergillus flavus is one of the major of spoilage organisms of several moist grains and nut products such as peanuts, corn, and certain nuts. Aflatoxins which are highly toxic, mutagenic, and carcinogenic to human being and animals are its secondary metabolites. Meanwhile, *A. flavus* is also a human pathogen, which can

D. Wang (✉) · K. Li · Y. Wang · Y. Yang · J. Zhang
College of Biotechnology, Tianjin University of Science and Technology, Tianjin 300457, People's Republic of China
e-mail: wangdp@tust.edu.cn

T.-C. Zhang et al. (eds.), *Proceedings of the 2012 International Conference on Applied Biotechnology (ICAB 2012)*, Lecture Notes in Electrical Engineering 249,
DOI: 10.1007/978-3-642-37916-1_48, © Springer-Verlag Berlin Heidelberg 2014

cause aspergillosis and onychomycosis [1, 2]. Therefore, there is interest in developing biological control methods which can inhibit the growth of pathogen and decrease toxin content. *Bacillus species* are the ideal candidates to use as biocontrol agents because they are safe and easily cultivated in a low-cost culture medium. In addition to, their spore can tolerate adverse conditions and many physicochemical factors such as high temperature and ultraviolet radiation. Previous studies showed that isolations of *Bacillus sp.* have been used successfully in the field of biological control of *A. flavus*.

Bacillus sp., can synthesize a variety of metabolites with antibacterial and/or antifungal activity. Bacteria of the genus *Bacillus* produce a variety of antibiotics which are classified as ribosomal or nonribosomal and which mostly have a molecular weight of less than 2,000 Da. Nonribosomally synthesized circular oligopeptides contain the lipopeptides fengycin, iturin, surfactin, plipastatin and the phosphono-oligopeptide, rhizocticin. The ribosomal antibiotics include TasA, subtilosin, sublancin, and so on [3, 4]. Generally speaking, lipopeptides have a variety of biological activities including antibacterial, antifungal, antiparasitic, antitumoural, and antiviral activities. Meanwhile, Comparing with chemical agents, lipopeptides are safe and friendly to environment because they are derived from *Bacillus sp.*, which will be widely used in agriculture and food industry.

In our previous study, we have isolated a antagonistic bacteria of the genus *Bacillus* which was identified as *Bacillus amyloliquefaciens* and strongly inhibited plant pathogens such as *A. flavus*, *Rhizoctonia cerealis*, *Fusarium Oxysporum*, *Alternaris solani*, *Bipolaris maydis*, *Rhizoctonia solani*. We have also found that *B. amyloliquefaciens* BI_2 secretes at least two kinds of antifungal substances. The purpose of this study was to isolate, purify, and characterize the lipopeptide-like compound which can partially inhibit the mycelial growth and has no effect on spore germination.

48.2 Materials and Methods

48.2.1 Microorganisms

Bacterial antagonist, strain BI_2, was isolated from straw feed and identified as *B. amyloliquefaciens*. *A. flavus* was kindly provided by the College of Food Engineering and Biotechnology of Tianjin University of Science and Technology.

48.2.2 Media and Culture Conditions

BI_2 was cultured in a seed medium (pH = 7.2) containing 0.5 % beef extract, 1 % peptone, 0.5 % NaCl, and 1 % glucose for 12 h at 37 °C with shaking, and then

2 % the resulting culture was inoculated into 65 mL aliquots of the fermentation medium (pH 7.5) dispensed in a 250 mL flask. The components of fermentation medium include 0.5 % beef extract, 0.5 % soluble starch, 0.5 % NaCl, 1.2 % $NaNO_3$, 1.2 % corn steep liquor, 0.06 % tween 80, and 2 % sodium glutamate. The fermentation was carried out at 30 °C under shaking conditions at 200 r/min for 36 h.

48.2.3 Agar Well Diffusion Assay

Mycelial plugs from the edges of fungal cultures were placed in the centre of the Petri plate, containing PDA medium for *A. flavus*. After incubation at 30 °C to allow vegetative growth, samples were added to the well which was formed by puncher and which had a distance of 2 cm away from the edge of the mycelia colony. After the plates were incubated for 60 h at 30 °C, the inhibition of mycelial growth was assessed by measuring the semidiameter of the inhibition zone [5].

48.2.4 Preparation of Crude Extract

The cell-free supernatant was obtained by centrifugation at 10,000×g for 20 min and the precipitate was discarded. The fermentation broth was collected by means of ultrafiltration (MWCO, 5 kDa) and nanofiltration (MWCO, 600 Da). The pH of the fermentation broth was adjusted to 2 with 6 N concentrated HCl. The precipitate was collected by centrifugation at 10,000 rpm for 20 min at 4 °C and was extracted twice with two times volume of methanol. The combined extracts were concentrated in a rotary evaporator and crude extract was obtained [6]. Then crude preparation was stored at 4 °C for further analysis.

48.2.5 Effects of Heat, pH and Enzymes on Antifungal Activity

To analyze thermal stability, the crude extract was exposed to temperatures ranging 50 °C to 100 °C for 30 min, and 121 °C for 20 min. The pH stability of crude extract was determined by adjusting the pH range from 2 to 12. To evaluate the stability of protease, samples were treated at 37 °C for 1 h with 1 mg/mL final concentration of the following enzymes: trypsin, papain, and pepsin. Then samples were boiled for 5 min to inactivate the enzyme [7]. After the treatment, the samples (1 mg/mL) were tested for antifungal activity against the mycelium growth of *A. flavus*.

48.2.6 Purification of Crude Extract

The crude extract was applied to a Sephadex G-15 (1.5 × 32 cm) column which was connected to a FPLC system (Bio-Rad, USA) and had been equilibrated with distilled water, then the samples were eluted with distilled water at a flow rate of 1 mL/min. The absorbance was monitored at 210 nm, and the fractions showing antimicrobial activity were pooled and freeze-dried. Then antifungal compound was dissolved in methanol and spotted on the preparative silica gel plate G. The compound was further separated by TLC in solvent system: Butanol–pyridine–water–acetic acid (10:6:3:1). One of the plates was dipped into ninhydrin solution (0.2 g ninhydrin in 100 mL ethanol), heated at 110 °C for 20 min. The cooled TLC plate was placed in a sealed bottle contained 1 mL concentrated HCl and heated at 110 °C for 2 h. Ninhydrin solution was used again and the plate was heated to display color. Target substance was detected as white spots by spraying water and gentle warming. The spots were scrapped off the preparative TLC plate and extracted by methanol, and the compounds were purified to homogeneity by the preparative thin-layer chromatography [8].

48.2.7 Assay of Oil-Film Collapsing and Emulsification Activity

The purified compound was dissolved in PBS buffer and evaluated for biosurfactant activity through a oil-film collapsing assay. A 100 μL of liquid paraffin was placed on the surface of distilled water in Petri dishes, and a oil film was immediately formed. Then, 10 μL of solution was gently placed in the center of the oil film. The emulsification activity was assessed by the method of emulsification of toluene. The solution was diluted with distilled water to a final volume of 3 mL and added to 0.5 mL of toluene. Then the mixture was vigorously shaken for 2 min. Control is the PBS buffer [9].

48.2.8 Mass Spectrometry and Amino Acid Analysis

The purified compound was dissolved in methanol and analyzed by ESI–MS and MS–MS (Finnigan CO., LCQ Advantayc MAX, USA). The electrospray source was operated at a spray voltage of 4.5 kV, a capillary voltage of 10 V, and capillary temperature of 220 °C. The equipment was run in a positive and negative ion mode, and the collision energy was set at 50 % for the CID experiment [10]. Sample was hydrolyzed in 6 M HCl at 110 °C for 24 h in sealed tubes. Amino acid analysis with 2,4-dinitrofluorobenzene method was carried out on a Vertex XB C18 column (250 × 4.6 mm). Peaks were detected at 360 nm with a UV

monitor (Agilent Technologies, 1100 series, UV detector, USA) and the system was operated at a flow rate of 1 mL/min. The column temperature was held at 35 °C and the mobile phase consisted of acetonitrile, water, and 10 mm Sodium acetate buffer (pH 6.4). Amino acids were estimated by comparison with amino acid standard products.

48.2.9 Ultraviolet and Infrared Absorption Spectrum

Ultraviolet absorption was analyzed by ultraviolet spectrometer. Infrared spectroscopy was carried out on a Fourier transform infrared spectrometer (BRUKER, VECTOR22, Germany). Infrared spectra was collected between 400 and 4,000 wave numbers (per centimeter).

48.2.10 Antifungal Activity of the Purified Substance

Antifungal activity of the purified antibiotic was tested against the mycelium growth of *A. flavus* with the agar well diffusion method. 100 μL of antibiotic (250 μg/mL) was added to the hole and the inhibition of mycelium growth was assessed after incubation. Control is the PBS buffer (50 mm, pH 7.5).

48.3 Results and Discussion

48.3.1 Antifungal Activity and Stability of Crude Extract

The crude extract inhibited the mycelium growth of *A. flavus*, but not for the residue dissolved in PBS buffer. The antimicrobial substance was stable in the pH range from 2 to 12. The inhibitory activity remained unchanged by temperature at 121 °C for 20 min, and by treatment with all the proteolytic enzymes tested. It showed that crude extract was stable to high temperature, different pH value, and several proteinases.

48.3.2 Purification of the Active Compound

The crude extract with antifungal activity was then purified on a Sephadex G-15 column (Fig. 48.1). Two peaks were obtained and the second peak showed the antifungal activity. The further separation was carried out by preparative TLC and

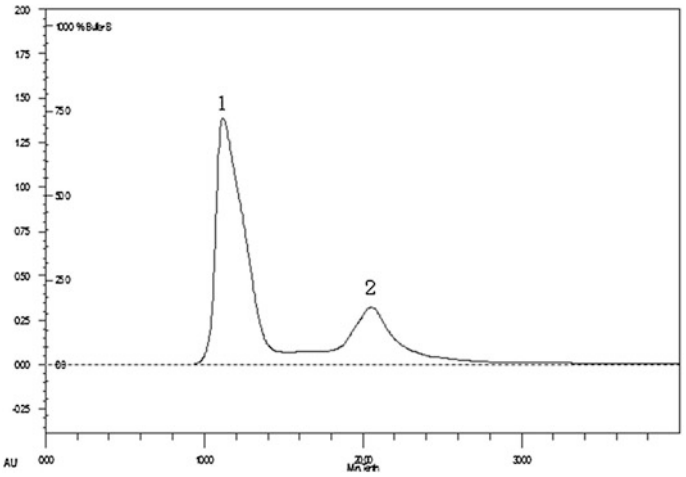

Fig. 48.1 Gel chromotagraphy on a Sephadex G-15 Column (1.5 × 32 cm)

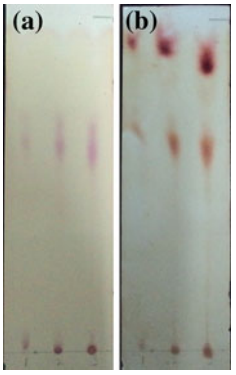

Fig. 48.2 TLC of antifungal substance collected from Sephadex G-15.
a Unacidized, **b** acidized

two spots with $Rf_1 = 0.87$ and $Rf_2 = 0.60$ were obtained (Fig. 48.2). The compound with $Rf_1 = 0.87$ can inhibit the mycelium growth of *A. flavus*.

48.3.3 Property of the Purified Compound

When the sample was gently placed in the center of the oil film, a clear halo became visible under light. The emulsified phenomenon was observed after the mixture of sample and toluene was vigorously shaken. After TLC analysis, the results (Fig. 48.2) showed that there was no color with Rf = 0.87 before hydrolysis, but colored spots appeared at the same place after hydrolysis. This phenomenon indicated that cyclic peptides were broken down to free amino acids in

the existence of concentrated HCl at high temperature and then colored by ninhydrin. These properties can preliminarily deduce that antifungal compound is a lipopeptide.

48.3.4 Mass Spectrometry and Amino Acid Analysis

The molecular weight of the purified compound was determined by ESI–MS analysis. The mass spectra (Fig. 48.3) showed a series of ion peaks at [M + H] m/z = 1,009.89; 1,023.32; 1,037.05 and [M + Na] m/z = 1,046.97; 1,059.15. A series of mass peaks with an intervals of 14 Da are observed for lipopeptide with different numbers of methylene groups in fatty acid chains. Ion peak with m/z = 1,059.00 was selected as parent ion for further MS–MS analysis. Partial data of fragment ion was shown in Fig. 48.4. Product ions of m/z 945.75; 832.70; 716.86 and 618.96 can be explained as the gradual losses of Leu–Leu–Asp–Val from the N-terminal amino acid of the entire molecule. Similarly, fragment ions of m/z 707.71; 549.69; 481.55 and 382.57 can be interpreted as the gradual losses of Leu–Leu-Val from the C-terminal amino acid [11]. HPLC method was carried out to further determine amino acid composition. The results (Fig. 48.5) showed that lipopeptide is consisted of Asp, Leu, Val, Glu with a mole ratio of 1:4:1:1. Therefore, the amino acid sequence of lipopeptide represents Glu–Leu–Leu–Val-Asp–Leu–Leu. These results indicated that the lipopeptide was similar to surfactin.

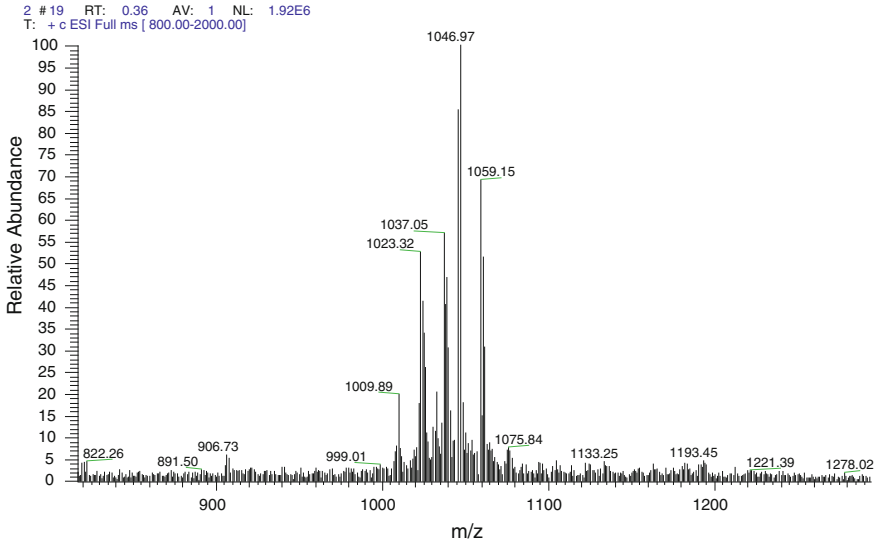

Fig. 48.3 ESI–MS of purified lipopeptide produced by BI_2

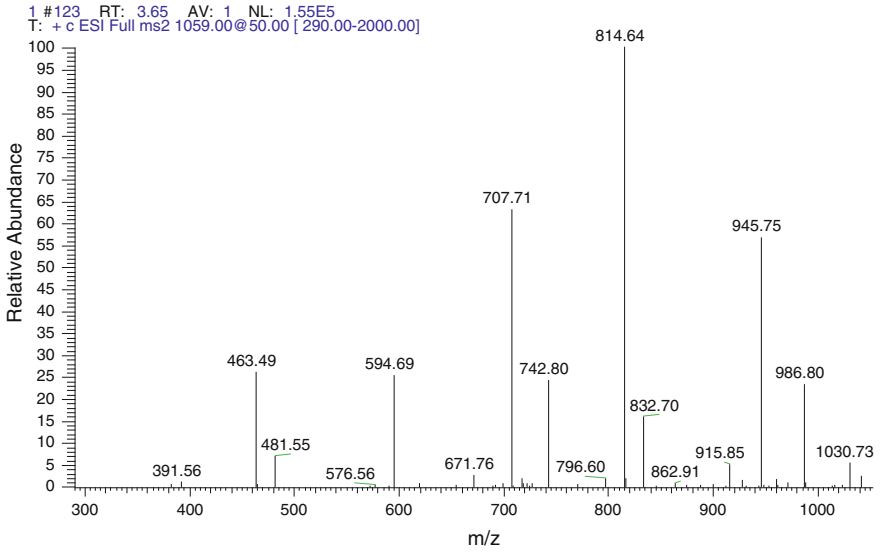

Fig. 48.4 MS–MS spectrum of precursor ion of *m/z* 1,059.00

48.3.5 Ultraviolet and Infrared Spectrometry

The UV absorption spectrum of the lipopeptide was examined between 200 and 400 nm. Figure 48.6 showed absorbance at 206 and 230 nm, which was corresponding to characteristic absorption of peptide bonds. There was minor absorbance peak at 280 nm and no appreciable absorbance above 300 nm. The ultraviolet spectrum was compatible with a polypeptide. The infrared spectrum was shown in Fig. 48.7. Characteristic absorption bands at 1,650, 1,541, 1,272 cm^{-1} indicated that the purified substance contains peptide bonds. Particularly, strong bands indicated the presence of a peptide component at 1,650 resulting from the stretching mode of the C=O bond, at 1,541 resulting from the deformation mode of the N–H bond and at 1,272 resulting from the stretching mode of the C–N bond [12]. Bands that result from C–H stretching (2,958, 2,871, 2,929 cm^{-1}) and C–H bending (1,468, 1,388 cm^{-1}) indicated the presence of aliphatic chain. A lactone ring was suggested by the absorption at 1,732 cm^{-1}. These results were similar to surfactin which can inhibit the mycelium growth of *A. flavus* (Fig. 48.8).

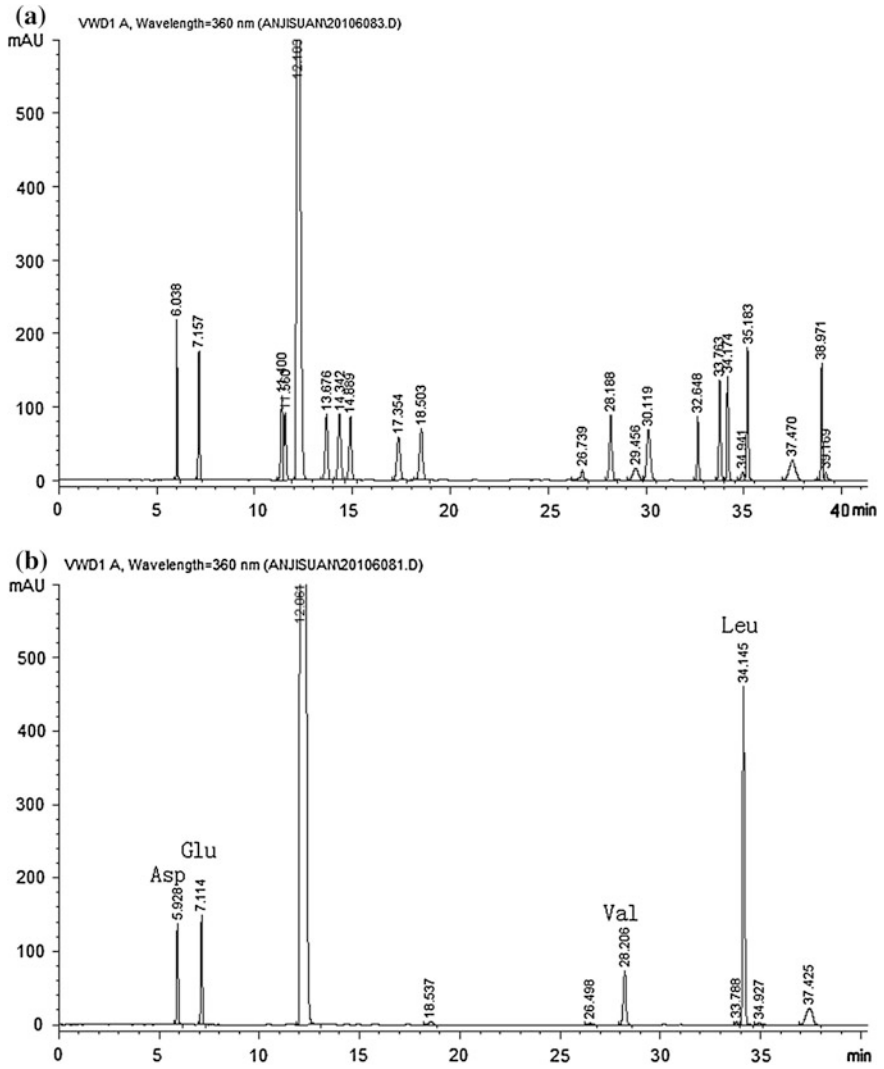

Fig. 48.5 The chromatograph of amino acids determined by HPLC. **a** Standard amino acid, **b** hydrolysate of surfactin

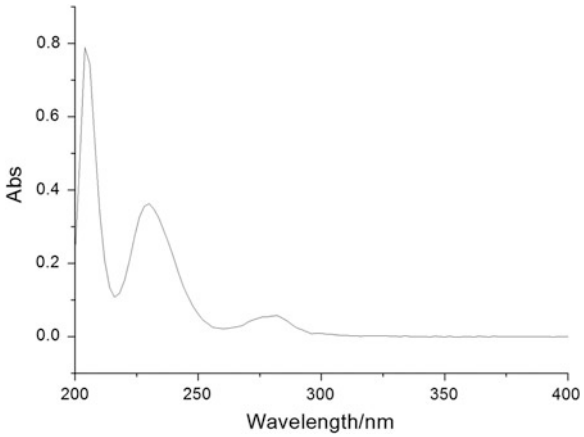

Fig. 48.6 Ultraviolet spectra of purified substance produced by BI_2

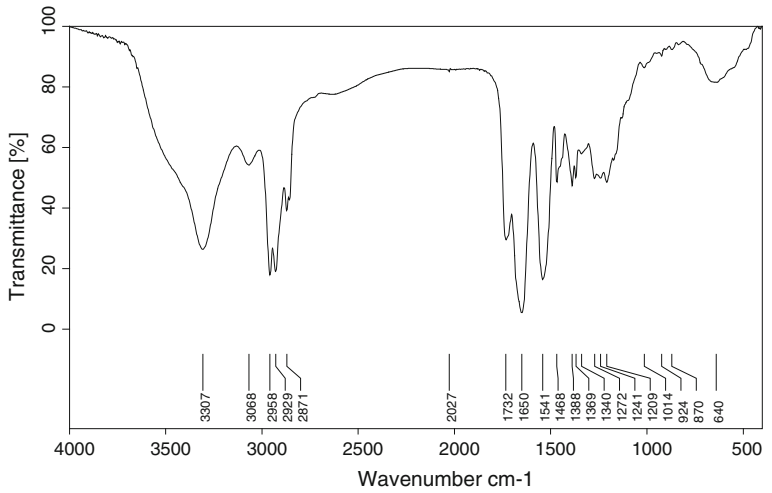

Fig. 48.7 FTIR spectra of purified substance produced by BI_2

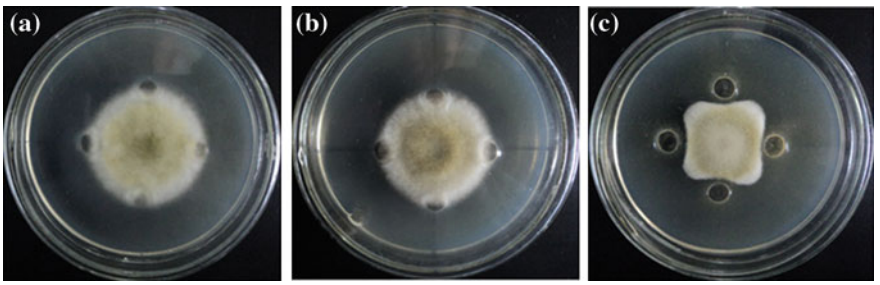

Fig. 48.8 Antifungal activity of fractions from preparative TLC plate. **a** Control, **b** fraction 1 ($Rf_2 = 0.6$), **c** fraction 2 ($Rf_1 = 0.87$)

48.4 Conclusion

In this study, ultrafiltration and nanofiltration were used as the effective means of separation. Lipopeptide compound was purified by Sephadex G-15 column chromatography and prepared thin-layer chromatography according to its property and antifungal activity. Finally, lipopeptide compound was identified as surfactin. *A. flavus* can widely invade crops such as peanuts, maize, and produce aflatoxins. Because of its antifungal activity against *A. flavus*, the surfactin-like compound may be useful as potential biocontrol agents.

Acknowledgments This research received financial support from the National Natural Science Foundation of China (No. 31101275) and National Science and Technology Support Program (No. 2012BAK17B11).

References

1. Bluma RV, Etcheverry MG (2006) Influence of *Bacillus spp*. isolated from maize agroecosystem on growth and aflatoxin B1 production by *Aspergillus section Flavi*. Pest Manag Sci 62:242–251
2. Cho KM, Math RK, Hong SY et al (2009) Iturin produced by *Bacillus pumilus* HY1 from Korean soybean sauce (kanjang) inhibits growth of aflatoxin producing fungi. Food Control 20:402–406
3. Moyne AL, Shelby R, Cleveland TE et al (2001) Bacillomycin D: an iturin with antifungal activity against *Aspergillus flavus*. J Appl Microbiol 90:622–629
4. Tamehiro N, Okamoto-Hosoya Y, Okamoto S et al (2002) Bacilysocin, a Novel Phospholipid Antibiotic Produced by *Bacillus subtilis* 168. Antimicrob Agents Ch 46:315–320
5. Li J, Yang Q, Zhao L-h et al (2009) Purification and characterization of a novel antifungal protein from *Bacillus subtilis* strain B29. J Zhejiang Univ Sci B 10:264–272
6. Sivapathasekaran C, Mukherjee S, Samanta R et al (2009) High-performance liquid chromatography purification of biosurfactant isoforms produced by a marine bacterium. Anal Bioanal Chem 395:845–854
7. Benitez LB, Velho RV, Lisboa MP et al (2011) Isolation and characterization of antifungal peptides produced by *Bacillus amyloliquefaciens* LBM5006. J Microbiol 48:791–797
8. Grangemard I, Bonmatin JM, Bernillon J et al (1999) Lichenysins G, a novel family of lipopeptide biosurfactants from *Bacillus licheniformis* IM 1307: production, isolation and structural evaluation by NMR and mass spectrometry. J Antibiot (Tokyo) 52:363–373
9. Sang-Cheol L, Kim S-H, Park I-H et al (2010) Isolation, purification, and characterization of novel fengycin S from *Bacillus amyloliquefaciens* LSC04 degrading-crude oil. Biotechnol Bioproc E 15:246–253
10. Sun L, Lu Z, Bie X et al (2006) Isolation and characterization of a co-producer of fengycins and surfactins, endophytic *Bacillus amyloliquefaciens* ES-2, from *Scutellaria baicalensis* Georgi. World J Microb Biot 22:1259–1266
11. Kim KM, Lee JY, Kim CK et al (2009) Isolation and characterization of surfactin produced by *Bacillus polyfermenticus* KJS-2. Arch Pharm Res 32:711–715
12. Yakimov MM, Timmis KN, Wray V et al (1995) Characterization of a new lipopeptide surfactant produced by thermotolerant and halotolerant subsurface *Bacillus licheniformis* BAS50. Appl Environ Microbiol 61:1706–1713

Chapter 49
The Effect of the Enzyme on the Liquid-State Fermentation of Pu'er Tea

Tao Li, Liping Du, Chao Wang, Peng Han, Dongguang Xiao, Changwen Li and Yongquan Xu

Abstract In order to investigate the effect of the enzyme on the liquid-fermentation of sun dried green tea of Yunnan large leaf, three enzymes were used, including cellulase, pectinase, and flavourzyme. On the base of single factor experiments, the optimal design with the content of the theabrownines was carried out using response surface methodology (RSM). It is feasible to optimize the enzyme in the process of the liquid-state fermentation of Pu'er tea by RSM. Pretreated the raw material under the optimal concentration combination of enzyme, the content of theabrownines of fermentation broth is 27.14 %, which is 18.00 % higher than CK.

Keywords Pu'er tea · Liquid-state fermentation · Enzyme · Theabrownines

49.1 Introduction

Pu'er tea is a Chinese special post-fermentation tea which is produced by the use of tea leaves from Yunnan tea variety [*Camellia sinensfs* (Linn.) var. *assamica* (Masters) Kitamura] [1]. Pu'er tea with its distinctive, earthy taste, and deep reddish color is known in China for its properties related to health. Numerous medicinal functions of the tea have been confirmed by modern scientific

T. Li · L. Du (✉) · C. Wang · P. Han · D. Xiao
Key Laboratory of Industrial Fermentation Microbiology, Ministry of Education, Tianjin University of Science and Technology, Tianjin 300457, People's Republic of China
e-mail: dlp123@tust.edu.cn

T. Li · L. Du · C. Wang · P. Han · D. Xiao
Tianjin Industrial Microbiology Key Lab, College of Biotechnology, Tianjin University of Science and Technology, Tianjin 300457, People's Republic of China

C. Li · Y. Xu
Yunnan Tasly Deepure Biological Tea Group Co., Ltd, Pu'er 665000, People's Republic of China

T.-C. Zhang et al. (eds.), *Proceedings of the 2012 International Conference on Applied Biotechnology (ICAB 2012)*, Lecture Notes in Electrical Engineering 249,
DOI: 10.1007/978-3-642-37916-1_49, © Springer-Verlag Berlin Heidelberg 2014

researches. Aided in digestion and fat metabolism, Pu'er is efficacious to hypoglycemic, hypolipidemic, anti-mutagenic, and anti-cancer [2–8]. Polyphenols and tea pigment are the main active substance in the tea. The changes of polyphenols played a decisive role on its color, taste, and other sensory quality in the process of the quality formation. Studies have shown that polyphenols in the dried green tea decreased (60 %), while the theabrownins significantly increased along the fermentation, which not only impacts the dense and bright of tea liquor majorly, but also affects the brown of the bottom. Therefore, it is essential to further improve quality and the yield of the tea by the use of new technology.

In the present studies, changes of substances during the pile-fermentation process of Yunnan Pu'er tea have shown that theabrownins and other complex compounds which are favorable for the quality of Pu'er tea are generated along with the oxidation and condensation of polyphenols, decomposition of protein, and amino acids, the digestion of carbohydrates as well as the polymerization and condensation between different products. With the continuous researches on the liquid-state fermentation of Pu'er tea and the development of the studies on enzymatic application, the content of the particular enzymes is targeted to improve the flavor substance in the tea according to their specificity, efficiency, and mild reaction condition. So it has been a major research focusing on the tea processing to enhance the quality and output of Pu'er tea.

In this study, cellulase, pectinase, and flavourzyme were added to investigate the effect of the enzyme on the liquid-state fermentation of Pu'er tea. On the base of single factor experiments, the optimal experiments carried out with the content of the theabrownines using the Box–Behnken experimental design.

49.2 Materials and Methods

49.2.1 Materials

Sun dried green tea of Yunnan large leaves was supplied by Yunnan Tasly Biology Tea Technology Limited Incorporation (Simao, Yunnan, China); cellulase, pectinase, flavourzyme were supplied by Tianjin Honour Development Technology Co., Ltd (Tianjin, China). All chemicals (analytical grade) were purchased from Guangfu chemical industry (Tianjin, China). Pure water was obtained from a Milli-Q purification system (Millipore, Bedford, USA).

49.2.2 Methods

49.2.2.1 Pretreatment of the Sun Dried Green Tea of Yunnan Large Leaf and Flask Fermentation

Xu et al. [9] have established the process for the liquid-state fermentation of Pu'er tea as follow: Solid–liquid ratio is 3:80 (g/mL). Firstly, 3 g grinded tea was soaked in 20 mL distilled water for water bath at 35 °C which lasts 20 min, and then filtered to get the filtrate and precipitate. The precipitate was subsequently subjected to mix with 60 mL boiled water for water bath at 100 °C which lasts 15 min and then for the second filtration to obtain the compounds in the leaves. Finally, mix the filtrate in the two steps hereinbefore.

All experiments were carried out in 250-mL flasks containing 50-mL mixture which has been pretreated. These flasks were incubated at 30 °C for 96 h on a rotary of 120 rpm, and then the temperature was changed into 50 °C and kept for 48 h.

In order to select the best adding style of the enzyme with the index of the content of theabrownins, three adding styles were investigated. The first one is to add 1.875 g grinded tea to 50 mL enzyme solution (according to the solid–liquid ration 3:80) for the fermentation. The second one uses 20 mL enzyme solution to replace the 20 mL distilled water in the process hereinbefore. And the last one is to get 45 mL the mixture and then add enzyme solution (10×) for the fermentation.

49.2.2.2 Optimization and Validation Procedures

In this study, the optimal concentration of three kinds of enzyme (cellulose, pectinase, flavourzyme) was firstly evaluated via single factor experiments. The concentrations of enzyme at five levels ranging from 10 to 50 U/mL were studied. Based on the single factor experiments, response surface methodology (RSM) was utilized to optimize the best conditions.

Design-Expert 6 software (Stat-Ease Inc., Minneapolis, USA) was employed for a three-level-three-factor Box–Behnken design, which requires 15 experiments as shown in Table 49.1 in this study. X_1, X_2, and X_3 are the coded values of cellulose, pectinase, and flavourzyme, respectively. The three levels for variables were cellulose (30, 40, 50 U/mL), pectinase (20, 30, 40 U/mL), flavourzyme (10, 20, 30 U/mL). The experimental data were compared with the fitted values predicted by the response regression equations in order to verify the accuracy of final reduced models.

Table 49.1 Scheme and results of response surface design for optimizing the concentration of the enzymes

Run	Coded level		
	X_1	X_2	X_3
1	−1	0	−1
2	1	0	1
3	0	0	0
4	1	−1	0
5	1	1	0
6	0	−1	−1
7	0	1	1
8	0	0	0
9	0	1	−1
10	0	−1	1
11	−1	1	0
12	−1	−1	0
13	−1	0	1
14	0	0	0
15	1	0	−1

49.3 Results and Discussion

49.3.1 Selection of the Adding Style

Three adding styles of the enzyme into the system of the liquid-state fermentation were carried out. The effect of adding style on the content of theabrownins of the Pu'er Tea of Liquid-state Fermentation was showed in Fig. 49.1.

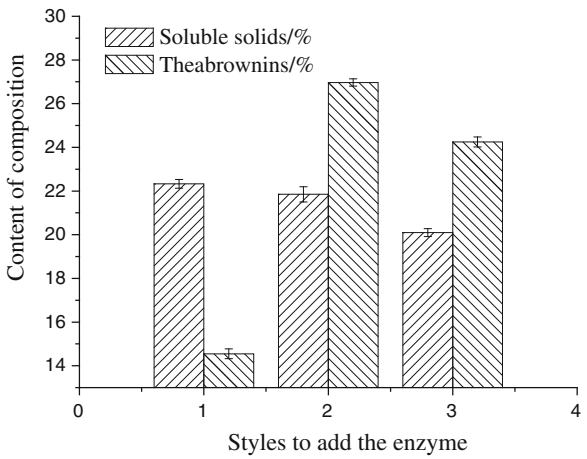

Fig. 49.1 Effect of adding style of the enzyme on the content of soluble solid and theabrownins

Cellulase was able to make the material of tea cell wall to be partially hydrolyzed, increasing the permeability of the cell wall, in order that the dissolution of amino acids, polyphenols was promoted, and part of the insoluble polysaccharides was converted to soluble ones, thereby enhancing the content of the water extracts which promoted the growth of microorganism. At the same time, the destruction of the cell wall can indirectly promote metabolic and enzymatic oxidation. As shown in Fig. 49.1, yield of theabrownins and soluble solids by the second adding style are highest which may caused by the increased precursor of theabrownins as well as the growth and reproduction of microorganism most among the three, one resulting the highest evaluation of theabrownins and soluble solid. So the second adding style was selected for the further study.

49.3.2 Single Factor Investigations

Soluble solids, theabrownins, polyphenols, polysaccharide, and amino acids were the major chemical compounds, among which theabrownins is considered to play a decisive role on the quality of Pu'er tea. Hence, content of theabrownins along with soluble was accounted as response variables in further optimization study solids. In order to determine the optimal concentration of three kinds of enzyme, the effect of concentration (ranging from 10 to 50 U/mL) of the enzymes was studied.

Cellulase, a multicomponent enzyme consisting of three different enzymes (endocellulases, cellobiohydrolase, and β-glucosidases) is responsible for the bioconversion of cellulose into soluble sugar [10]. As mentioned above, increase in soluble sugar results in the increase of soluble solid and the growth enhancement of some microorganism whose growth is based on soluble sugar. As shown in Fig. 49.2 both soluble solid and theabrownins increased and then decreased with

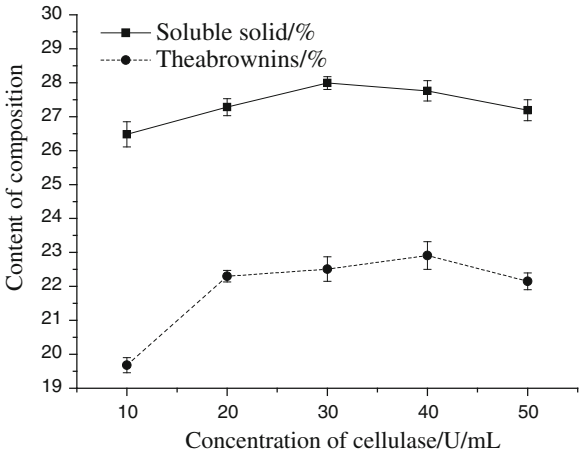

Fig. 49.2 Impact of the cellulase concentration on the content of soluble solid and theabrownins

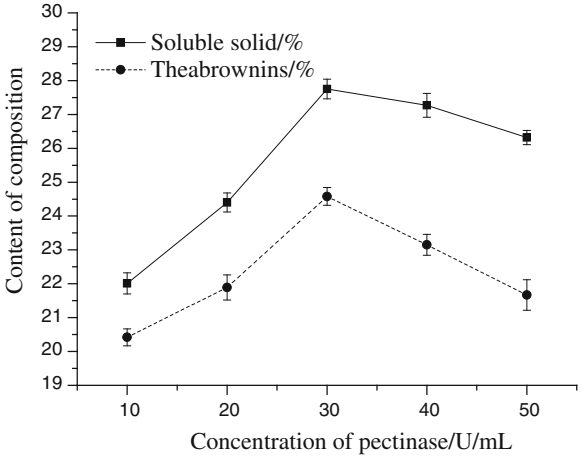

Fig. 49.3 Impact of the pectinase concentration on the content of soluble solid and theabrownins

the increase in concentration of cellulase ranging from 10 to 50 U/mL. Soluble solid and theabrownins reached the maximum when the concentration of cellulase was 30 and 20 U/mL, respectively.

Pectine is the major component of the middle lamella of the plant cell wall and acts as a sort of "glue" to hold plant cells into a structure [11]. Pectinase degrades the pectin substances between cells to separate the plant cells from the organization, and along with cellulase to promote the release of intracellular starch, lipids, proteins, etc. As shown in Fig. 49.3, both soluble solid and theabrownins reached the maximum when the concentration of pectinase was 30 U/mL.

Flavourzyme is able to degrade the insoluble polyphenol polymers in the tea as well as the protein in tea polysaccharides resulting the increase of polyphenols, soluble polysaccharides, and the water content of the material which led to the ultimately promotion of the theabrownins generation. As shown in Fig. 49.4, both

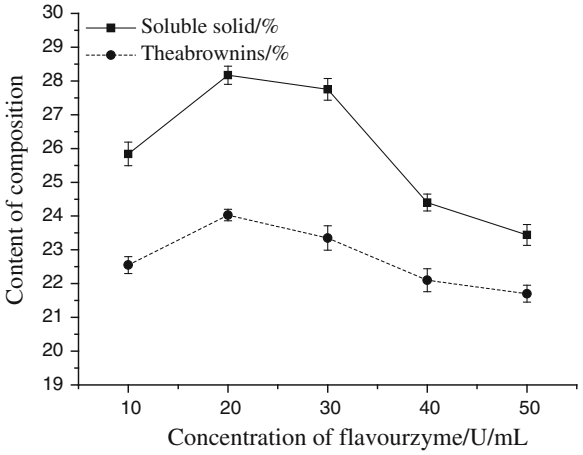

Fig. 49.4 Impact of the flavourzyme concentration on the content of soluble solid and theabrownins

soluble solid and theabrownins reached the maximum when the concentration of flavourzyme was 20 U/mL.

49.3.3 The Box–Behnken Design

Following single factor investigations, appropriate level of enzyme concentration was obtained according to the Box-Behnken design. The model coefficients were calculated by backward multiple regression and were validated by ANOVA. Applying multiple regression analysis to the experimental data, the following second-order polynomial equation was found to explain the theabrownins content (%):

$$Y = 26.83 - 0.48X_1 + 1.07X_2 + 1.07X_3 - 1.88X_1^2 - 2.24X_2^2 - 2.41X_3^2 - 0.61X_1X_2 + 1.44X_1X_3 + 0.83X_2X_3$$

where Y is the predicted theabrownins content (%); X_1, X_2, and X_3 are the coded values of cellulose, pectinase, and flavourzyme, respectively.

On the basis of the experimental values, statistical testing was carried out for ANOVA (Table 49.2). The analysis of variance (ANOVA) for the regression model which demonstrates that the model is highly significant indicates that the effect of linear coefficients in the equation is the most significant, followed by the interaction coefficients, indicating that the response to changes in the value of the relative complexity. The goodness of fit of the model can be checked by the determination coefficient (R^2). The value of adjusted R^2 (0.8649) indicated that only 13.51 % of the total variations was not explained by this model. Meanwhile, the value of determination coefficient ($R^2 = 0.9518$) indicates good relation between the experimental and predicted values of the response.

The three-dimensional response surfaces are shown in Fig. 49.5. It is evident that the response surface convex in nature suggesting that there are well-defined optimum conditions. The less prominent interaction of cellulase, pectinase, and flavourzyme are also shown by the almost circular nature of the contour plot,

Table 49.2 Analysis of variance for the regression equation

Source	Degree of freedom	Seq SS	Adj SS	Adj MS	*F*-value	*P*
Regression	9	8.7551	78.7551	8.7506	10.96	0.008
Linear	3	20.1072	20.1072	6.7024	8.40	0.021
Square	3	6.1138	46.1138	15.3713	19.25	0.004
Interaction	3	12.5341	12.5341	4.1780	5.23	0.053
Residual	5	3.9917	3.9917	0.7983		
Lack-of-fit	3	3.9904	3.9904	1.3301	2100.22	0.000
Pure error	2	0.0013	0.0013	0.0006		
Sum	14	2.7468				
$R^2 = 95.18$ %; R^2 (Adj) = 86.49 %						

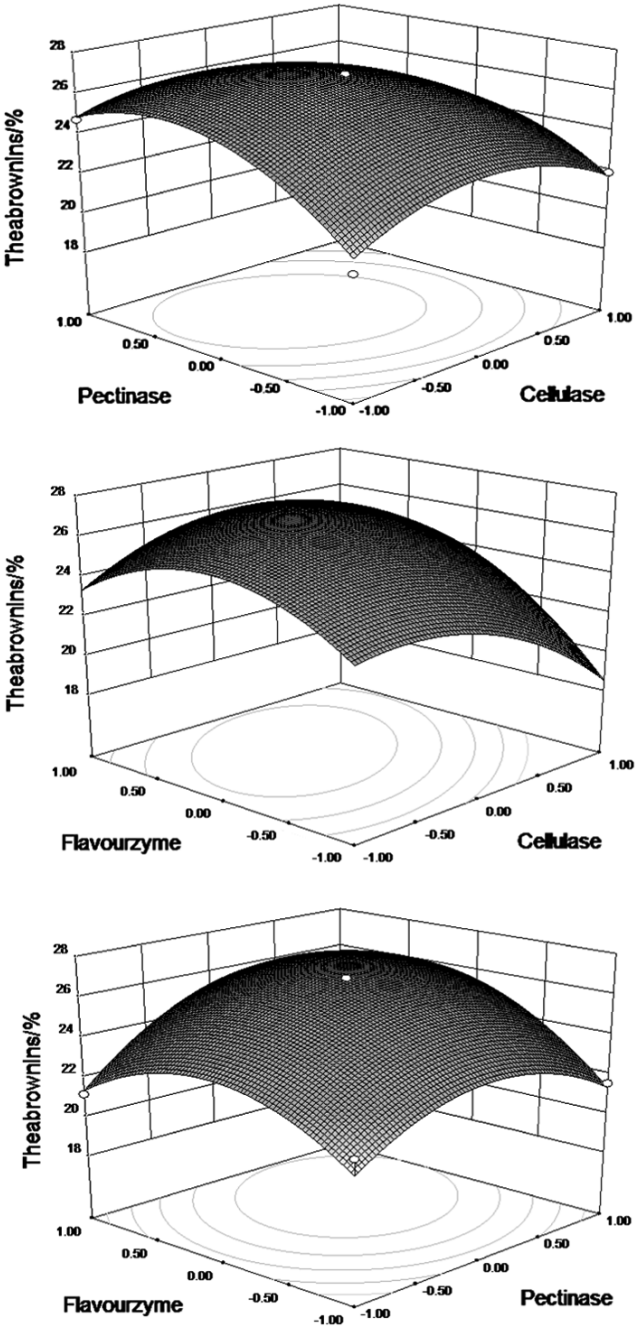

Fig. 49.5 Response surface and contour maps for each of the two factors interact

which coincides with the significance test of the regression coefficient. It is obvious from the plot that theabrownins content (%) has a maximum point in the studied region.

To sum up, the model predicted a maximum content of theabrownins 27.14 %, which is improved 18.00 % compared with the blank. The optimum concentration of cellulase, pectinase, flavourzyme is 39.40, 33.00, and 22.90 U/mL, respectively.

49.4 Conclusion

Liquid-state fermentation which is a novel approach for the fermentation of Pu'er tea using the using tea leaves from Yunnan tea variety [*Camellia sinensfs* (Linn.) var. *assamica* (Masters) Kitamura] as raw material contribute to shorten the fermentation cycle, reduce labor intensity, and improve labor productivity. This is a stable technique which can improve the quality of fermented tea, simultaneously. Adding of enzyme was study using Box–Behnken experimental design combined with RSM to improve the content of theabrownins which is regard as the most important composition for the quality of Pu'er tea. In this study, the optimum concentration of cellulase, pectinase, flavourzyme was determined at 39.40, 33.00, and 22.90 U/mL, respectively. Under the optimum condition, the content of theabrownins was 27.14 %. Furthermore, the relative standard deviation of the replicate was <5.0 %. The developed procedure was applied to the liquid-state fermentation for the sun dried green tea of Yunnan large leaves.

Acknowledgments This work was financially supported by the Cheung Kong Scholars and Innovative Research Team Program in University of Ministry of Education, China (Grant No. IRT1166) and Training Programs of Innovation and Entrepreneurship for Undergraduates (program number 201210057047).

References

1. Fang X, Li B, Chen D et al (2008) Review on functional components and mechanism of quality formation of Puer tea. Food Sci Technol 29(6):313–316
2. Delerive P, Martin-Nizard F, Chineni G et al (1999) Peroxisome proliferators-activated receptor activators inhibit thrombin induced endothel-in-1 production in human vascular endothelial cells by inhibiting the activator protein-1 signaling pathway. Circ Res 85(3):394–402
3. Kuo K, Weng M, Chiang C et al (2005) Comparative studies on the hypolipidemic and growth suppressive effects of oolong, black, Pu-erh, and green tea leaves in rats. J Agric Food Chem 53(2):480–489
4. Lu C, Hwang L (2008) Polyphenol contents of Pu-erh teas and their abilities to inhibit cholesterol biosynthesis in hep G2 cell line. Food Chem 111(1):67–71
5. Lin J, LinShiau S (2006) Mechanisms of hypolipidemic and anti-obesity effects of tea and tea polyphenols. Mol Nutr Food Res 50(2):211–217

6. Chiang C, Mengshih W, Shoeiyn L et al (2005) Pu-erh tea supple-mentation suppresses fatty acid synthase expression in the rat liverthrough downregulating Akt and JNK signalings as demonstrated in human hepatoma HepG2 cells. Oncol Res 16(3):119–128
7. Pin D, Gow C, Wen J et al (2004) Effects of Pu-erh tea on oxidative damage and nitric oxide scavenging. J Agric Food Chem 52(26):169–176
8. Wang B, Yu H, Lee W et al (2008) Protective effects of pu-erh tea on LDL oxidation and nitric oxide generation in macrophage cells. LWT-Food Sci Technol 41(6):1122–1132
9. Xu R, Du L, Hao R et al (2012) Study on technology of liquid natural fermentation of Pu'er tea. Sci Technol Food Ind 33(11):243–246 (in Chinese)
10. Li C, Yoshimoto M, Fukunaga K et al (2007) Characterization and immobilization of liposome-bound cellulase for hydrolysis of insoluble cellulose. Bioresour Technol 98:1366–1372
11. Vatanparast M, Hosseininaveh V, Ghadamyari M et al (2012) Pectinase and cellulase activity in the digestive system of the elm leaf beetle, *Xanthogaleruca luteola* Muller (Coleoptera: Chrysomelidae). J Asia-Pac Entomol 4(15):555–561

Chapter 50
Enhancing the Concentration of 4-vinylguaiacol in Top-Fermented Wheat Beers by SPSS Software

Yunqian Cui, Mingguang Zhu, Chunling Wang, Xiaohong Cao and Nuo Xu

Abstract Despite being considered undesirable in bottom-fermented beers, 4-vinylguaiacol is a well-known aroma compound found in top-fermented beers. In this paper, effects of wheat malt proportion, mash-in temperature, boiling time, and fermentation temperature on the production of 4-vinylguaiacol in top-fermented wheat beers were investigated. By means of the SPSS software, the optimal technology of enhancing the 4-vinylguaiacol concentration was obtained, i.e., the cloned yeast strain W303+padc was selected, wheat malt proportion was 40 %, mash-in temperature was 37 °C, boiling time was 90 min, and fermentation temperature was 20 °C. Under the optimal conditions, the 4-vinylguaiacol concentration was approximately 2.238 mg/L. Meantime, an approximately equation between the 4-vinylguaiacol concentration and wheat malt proportion, mash-in temperature, boiling time, fermentation temperature was determined, i.e., the concentration of 4-vinylguaiacol = 1.10156 + 0.05005 × wheat malt proportion − 0.02443 × mash-in temperature + 0.00024 × boiling time + 0.09688 × fermentation temperature.

Keywords 4-vinylguaiacol · Top-fermented wheat beers · SPSS software

Yunqian Cui and Mingguang Zhu contributed equally to this work.

Y. Cui · N. Xu
Shandong Provincial Key Laboratory of Microbial Engineering, Shandong Polytechnic University, Jinan 250353, People's Republic of China

M. Zhu · C. Wang · X. Cao (✉)
College of Bioengineering, Tianjin University of Science and Technology, Tianjin 250353, People's Republic of China
e-mail: cuiyunqian@yahoo.com.cncaoxh@tust.edu.cn

M. Zhu
Novozymes (China) Investment Co. Ltd, Shanghai Office, Beijing 200336, People's Republic of China

T.-C. Zhang et al. (eds.), *Proceedings of the 2012 International Conference on Applied Biotechnology (ICAB 2012)*, Lecture Notes in Electrical Engineering 249,
DOI: 10.1007/978-3-642-37916-1_50, © Springer-Verlag Berlin Heidelberg 2014

50.1 Introduction

Despite being considered undesirable in bottom-fermented beers, 4-vinylguaiacol is a well-known aroma compound found in top-fermented beers [1]. The selection of a suitable yeast strain is vitally important for enhancing the concentration of 4-vinylguaiacol in top-fermented wheat beers, which is the primary method to control the final concentration. According to previous researches [1–3], the POF phenotypes of 4 top-fermenting yeast strains stocked in our laboratory were assessed. On this basis, the typical POF+ top-fermenting yeast strain W303-1A is transformed by molecular cloning, and through some laboratory-scale fermentation experiments, the cloned yeast strain W303+padc of high yield 4-vinylguaiacol concentration was obtained [4].

It is known to all that ferulic acid is the precursor of 4-vinylguaiacol [5], and the effect of barley malt and wheat malt varieties, degree of grinding, stirring regime, mashing pH, and time on release of ferulic acid has been studied, the highest ferulic acid content is found by using Scarlett barley malt, Beaufort wheat malt, mashing pH 5.8, and stirring regime 200 r/min [6]. Thus, above brewing materials, methods and the cloned yeast strain W303+padc were used to carry out laboratory-scale mashing and fermentation experiments, and the interrelation between the formation of 4-vinylguaiacol and wheat malt proportion, mashing-in temperature, boiling time, and fermentation temperature was investigated in detail by SPSS software to further enhance the concentration of 4-vinylguaiacol in top-fermented beers.

50.2 Materials and Methods

50.2.1 Materials and Reagents

Scarlett barley malt was provided by Zhongliang Malt Division (Dalian, China). Wheat malt was obtained from Weyermann (Bamberg, Germany). Hops were supplied from Barth-Haas Group (Beijing, China), which contained 4.9 % α-acids (Analytica-EBC). HPLC grade 4-vinylguaiacol (2-methoxy-4-vinylphenol) and ferulic acid were purchased from Sigma-Aldrich (Shanghai, China). Other reagents were all of analytical grade.

50.2.2 Propagation of Top-Fermenting Yeast Strain W303+padc

Top-fermenting yeast strain W303+padc was obtained by cloning in former study [4]. Yeast cells were cultured in yeast peptone dextrose (YPD) medium (10 g/L

yeast extract, 20 g/L peptone, and 20 g/L glucose), Solid media contained 20 g/L agar, and yeast strains were cultured at 30 °C.

The cloning yeast strain W303+padc was inoculated into three tubes of 10 mL liquid YPD, respectively, with a transfer needle. They were incubated in a shaking table at 25 °C, 230 r/min. When they grew up, the yeast strains were propagated to 300 mL at 1:10 ratio step by step, which can be used in laboratory-scale mashing and fermentation experiments.

50.2.3 Laboratory-Scale Mashing and Fermentation Experiments

Milling: Malt milling is finished by EBC standard mill (Bühler Company, Germany), and milling type is dry milling. When milling barley malts, the millstone gap was adjusted to "5.5", i.e., the grinding space was 0.55 mm, then the husk was ground as whole as possible, and the kernel was ground as pieces as possible. When wheat malts were ground, the millstone gap was adjusted to "2", i.e., the grinding spacing was 0.2 mm, then the wheat malt was ground as pieces as possible.

Mashing-in: Mashing was accomplished by LB 8 automatic mashing instrument (Lochner Company, Germany). The ratio of malts and water was 1:4. According to Chinese National Beer Standard GB4927-2008 [7], the proportion of wheat malt was set to 40, 70, and 100 %, respectively. The malts weight of each mashing cup was 75 g, so the total amount of eight mashing cups in one batch was 600 g.

Mashing technology: Infusion mashing method was adopted. According to the LB 8 automatic mashing experiment illustration, the temperature of mashing-in was determined as 37, 40, and 45 °C, respectively. The following processes were used respectively:

Test 1: 37 °C (20 min) → 45 °C (30 min) → 52 °C (40 min) → 65 °C (70 min) → 72 °C (15 min) → 78 °C (10 min);
Test 2: 40 °C (20 min) → 45 °C(30 min) → 52 °C(40 min) → 65 °C(70 min) → 72 °C (15 min) → 78 °C (10 min);
Test 3: 45 °C(30 min) → 52 °C(40 min) → 65 °C(70 min) → 72 °(15 min) → C78 °C(10 min)

Lautering: Lautering was finished with eight layers of gauze and a glass funnel. Turbid wort was recirculated until the wort was clear, and then lautering was started. The limpid wort was filled into clean 5000 mL triangular flask. The concentration of the first wort was measured by sugar meter attached temperature (10–20°P). Sparging water was added several times. The temperature of sparging water is 78 °C, and the amount is 2500 mL or so. The concentration of mixed wort was measured by sugar meter attached temperature at any time, to prevent the wort

concentration too high or too low. If the final concentration was 11°P, the concentration of mixed wort was approximately controlled at 9.7°P.

Wort boiling: the mixed wort in 5,000 mL triangular flask was boiled by electric cooker. Boil time was 70, 90, and 110 min, respectively. According to the experimental design, the time and dosage of hop addition were adopted as follows:

When boiling time is 70 min: starting boiling → 10 min (1 g of hops) → 30 min (1.5 g of hops) → 60 min (0.5 g of hops) → 70 min (stop boiling).
When boiling time is 90 min: starting boiling → 10 min (1 g of hops) → 40 min (1.5 g of hops) → 80 min (0.5 g of hops) → 90 min (stop boiling).
When boiling time is 110 min: starting boiling → 10 min (1 g of hops) → 50 min (1.5 g of hops) → 100 min (0.5 g of hops) → 110 min (stop boiling).

The concentration of final wort was measured to control at 11°P.

Fermentation: Boiled wort was cooled to about 20 °C, and then was poured into 2 L PET bottle. The propagated yeast strain W303+padc was pitched into the bottle. Then the cap was tightened and the bottle was turned up and down, so that the wort and yeast strains were mixed thoroughly. The bottles were placed in incubators of 16, 18, and 20 °C for fermentation, respectively, at this time the bottle cap was semi-closed state. When the apparent extract was 3.8-4.2°P, the open lid of the PET bottle was closed until the diacetyl content of the green beer was reduced below 0.1 mg/L. The temperature was then decreased to 0 °C in refrigerator and the secondary fermentation continued for more than 5 days.

50.2.4 Analysis of Ferulic Acid and 4-vinylguaiacol Concentration

The ferulic acid and 4-vinylguaiacol levels were determined by Shimadzu HPLC using a method described by Shinohara et al. [3]. The HPLC system consisted of a LC-10Avp pump, a 7725i Sample injector, a Shimadzu UV-Vis detector, and a N2000 data analyzer (Zhejiang University, Hangzhou, China). The samples were analyzed using a 15 cm × 4.6 mm i.d. packed column (no. 6042278, C18, Hitachi, Tokyo) eluted with water/acetonitrile/phosphoric acid (599/400/1,V/V) at a flow rate of 1 mL/min. The UV detector was operated at 230 nm.

50.2.5 Data Analysis

All mashing and fermentation experiments were repeated three times. The data results were represented in the form of mean ± standard deviation. By the analysis of SPSS software, the optimizing technology of enhancing the concentration of 4-vinylguaiacol in top-fermented beers was determined, and the approximate equation of calculating the content of 4-vinylguaiacol was also obtained.

50.3 Results and Discussion

50.3.1 The Effect of Wheat Malt Proportion, Mash-in Temperature, Boiling Time and Fermentation Temperature on 4-vinylguaiacol

4-vinylguaiacol is abundant in top-fermented wheat beers, which is produced by thermal decarboxylation of ferulic acid, and more is formed by the decarboxylation of cinnamic acid decarboxylase of yeast. In order to study the effect of wheat malt proportion, mash-in temperature, boiling time, and fermentation temperature on 4-vinylguaiacol, laboratory-scale mashing, and fermentation experiments were carried out. The content of 4-vinylguaiacol in finished beer was determined by high performance liquid chromatography. There were four factors and three levels, so requiring total experiments are $3^4 = 81$, and each experiment was repeated three times. The concentration of 4-vinylguaiacol was counted in excel, then the mean values and standard deviations were calculated. Results were recorded in Table 50.1.

50.3.2 Data Analysis

Data in Table 50.1 was analyzed by SPSS software, and results were shown in Fig. 50.1. According to Fig. 50.1, the optimizing technology of enhancing the concentration of 4-vinylguaiacol in top-fermented beers was determined: cloning yeast strain W303+padc was selected, wheat malt proportion was 40 %, mash-in temperature was 37 °C, boiling time was 90 min, and fermentation temperature was 20 °C.

The optimizing technology of enhancing the concentration of 4-vinylguaiacol in top-fermented beers has been determined from Fig. 50.1, and the theoretical analysis of it as follows:

It is well-known to all that ferulic acid is the precursor of 4-vinylguaiacol. When wheat malt was added, the content of ferulic acid in the wort was decreased significantly (Fig. 50.2). From Fig. 50.2, the content of ferulic acid decreased 12 % when 50 % Beaufort wheat malt was added. As ferulic acid in the wort decreased, the concentration of 4-vinylguaiacol would be lower. Therefore, in the experiments of 3 different wheat malt proportions (40, 70 and 100 %), the concentration of 4-vinylguaiacol in the final beer brewed with 40 % wheat malt was the highest. In fact, if the wort was made of 100 % barley malt, the concentration of 4-vinylguaiacol in the finished beer would be higher (shown in Fig. 50.3). Of course, this is not in compliance with Chinese National Beer Standard GB4927-2008 (dosage of wheat malt is at least 40 %).

Table 50.1 The 4-vinylguaiacol levels of various wheat proportion, mash-in temperature, boiling time and fermentation temperature during brewing

No.	Wheat malt proportion	Mash-in temperature (°C)	Boiling time (min)	Fermentation temperature (°C)	Content of 4-vinylguaiacol (mg/L)
1	60:40	37	70	16	1.8427 ± 0.0012
2	60:40	40	70	16	1.7758 ± 0.0113
3	60:40	45	70	16	1.6320 ± 0.0089
4	60:40	37	90	16	1.7583 ± 0.1003
5	60:40	40	90	16	1.7636 ± 0.0074
6	60:40	45	90	16	1.6558 ± 0.0152
7	60:40	37	110	16	1.8158 ± 0.1320
8	60:40	40	110	16	1.7890 ± 0.1034
9	60:40	45	110	16	1.6646 ± 0.0099
10	60:40	37	70	18	2.0421 ± 0.0158
11	60:40	40	70	18	1.9674 ± 0.0362
12	60:40	45	70	18	1.8425 ± 0.1003
13	60:40	37	90	18	2.0483 ± 0.0118
14	60:40	40	90	18	1.9735 ± 0.0122
15	60:40	45	90	18	1.8489 ± 0.1013
16	60:40	37	110	18	2.0540 ± 0.2002
17	60:40	40	110	18	1.9542 ± 0.1033
18	60:40	45	110	18	1.8545 ± 0.0041
19	60:40	37	110	20	2.1947 ± 0.0111
20	60:40	40	110	20	2.1996 ± 0.1078
21	60:40	45	110	20	2.0452 ± 0.0533
22	60:40	37	70	20	2.2327 ± 0.0001
23	60:40	40	70	20	2.1573 ± 0.0034
24	60:40	45	70	20	2.0329 ± 0.0470
25	60:40	37	90	20	2.2383 ± 0.0032
26	60:40	40	90	20	2.1638 ± 0.0901
27	60:40	45	90	20	2.0384 ± 0.1076
28	30:70	37	70	16	1.7923 ± 0.2237
29	30:70	40	70	16	1.7172 ± 0.3356
30	30:70	45	70	16	1.5923 ± 0.7003
31	30:70	37	90	16	1.8058 ± 0.4339
32	30:70	40	90	16	1.7230 ± 0.1790
33	30:70	45	90	16	1.5981 ± 0.1077
34	30:70	37	110	16	1.8046 ± 0.0113
35	30:70	40	110	16	1.7183 ± 0.0578
36	30:70	45	110	16	1.6041 ± 0.0993
37	30:70	37	70	18	1.9825 ± 0.0570
38	30:70	40	70	18	1.9079 ± 0.0783
39	30:70	45	70	18	1.7823 ± 0.0115
40	30:70	37	90	18	1.9883 ± 0.0003
41	30:70	40	90	18	1.9134 ± 0.0074
42	30:70	45	90	18	1.7889 ± 0.0188

(continued)

Table 50.1 (continued)

No.	Wheat malt proportion	Mash-in temperature (°C)	Boiling time (min)	Fermentation temperature (°C)	Content of 4-vinylguaiacol (mg/L)
43	30:70	37	110	18	1.9941 ± 0.0007
44	30:70	40	110	18	1.9197 ± 0.0089
45	30:70	45	110	18	1.7945 ± 0.0459
46	30:70	37	110	20	2.1840 ± 0.0987
47	30:70	40	110	20	2.1095 ± 0.0560
48	30:70	45	110	20	1.9843 ± 0.0118
49	30:70	37	70	20	2.1723 ± 0.0447
50	30:70	40	70	20	2.0977 ± 0.1013
51	30:70	45	70	20	1.9720 ± 0.0007
52	30:70	37	90	20	2.1784 ± 0.0023
53	30:70	40	90	20	2.1034 ± 0.0047
54	30:70	45	90	20	1.9786 ± 0.0115
55	0:100	37	70	16	1.7687 ± 0.0582
56	0:100	40	70	16	1.6936 ± 0.10001
57	0:100	45	70	16	1.5680 ± 0.2030
58	0:100	37	90	16	1.7742 ± 0.1780
59	0:100	40	90	16	1.6993 ± 0.1016
69	0:100	45	90	16	1.5747 ± 0.0078
61	0:100	37	110	16	1.7806 ± 0.0101
62	0:100	40	110	16	1.7032 ± 0.0099
63	0:100	45	110	16	1.5803 ± 0.0402
64	0:100	37	70	18	1.9588 ± 0.0108
65	0:100	40	70	18	1.8832 ± 0.0705
66	0:100	45	70	18	1.7582 ± 0.0589
67	0:100	37	90	18	1.9644 ± 0.0334
68	0:100	40	90	18	1.8890 ± 0.0114
69	0:100	45	90	18	1.7644 ± 0.0207
70	0:100	37	110	18	1.9703 ± 0.0363
71	0:100	40	110	18	1.8959 ± 0.0262
72	0:100	45	110	18	1.7703 ± 0.0008
73	0:100	37	110	20	2.1606 ± 0.0049
74	0:100	40	110	20	2.0803 ± 0.0023
75	0:100	45	110	20	1.9607 ± 0.0189
76	0:100	37	70	20	2.1480 ± 0.0302
77	0:100	40	70	20	2.0730 ± 0.0003
78	0:100	45	70	20	1.9485 ± 0.0110
79	0:100	37	90	20	2.1540 ± 0.0126
80	0:100	40	90	20	2.0790 ± 0.0072
81	0:100	45	90	20	1.9548 ± 0.0109

According to former researches [6, 8], the most relevant enzyme about release of ferulic acid was cinnamoyl esterase. Of course, the other arabinoxylan degrading enzymes which are esterified with ferulic acid (e.g., β-endo-xylanase, β-

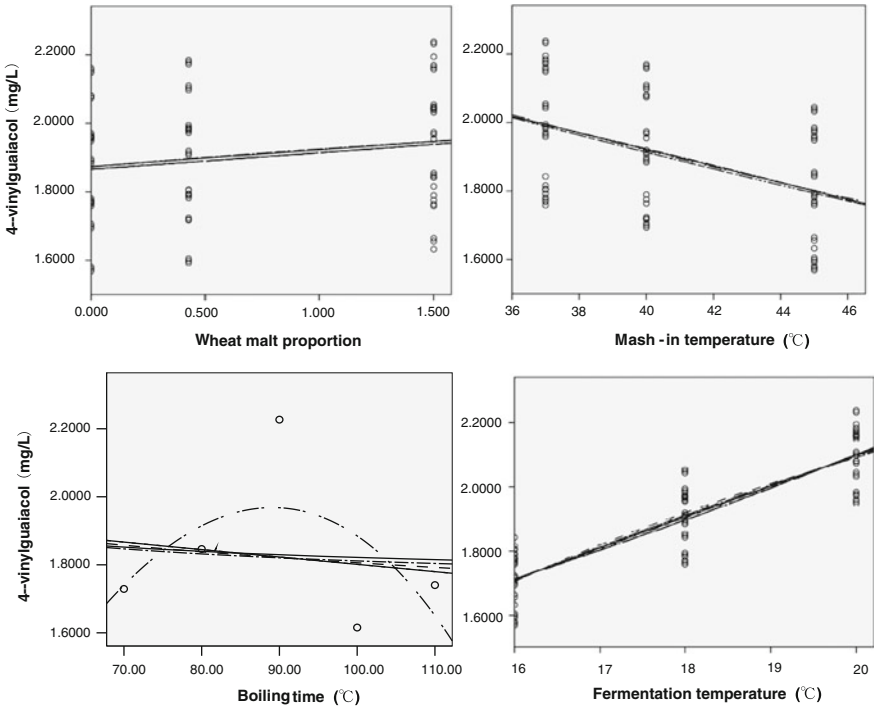

Fig. 50.1 Effects of various brewing conditions on the 4-vinylguaiacol concentrations by SPSS software

D-xylan glycosidase, α-L-furan Arabia glycosidases) are also of importance. The optimal temperature of Cinnamoyl esterase, *β*-endo-xylanase, and *β*-L-xylan glucosidase was 30, 45, and 50 °C, respectively. However, α-L-furan Arabia

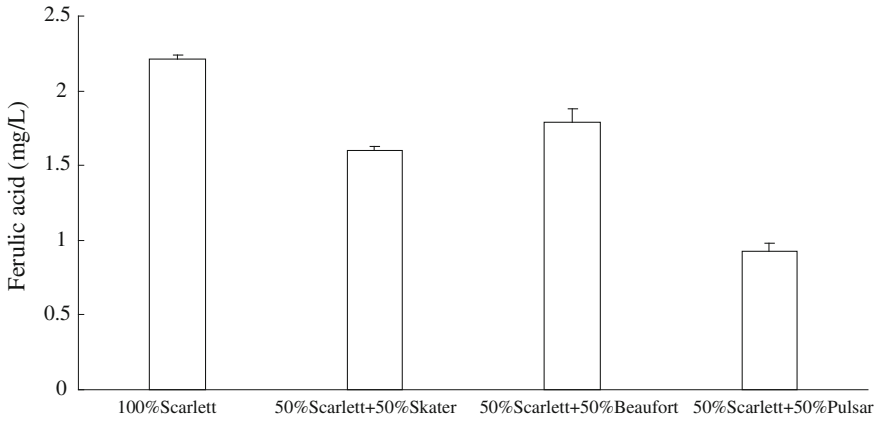

Fig. 50.2 Effect of the addition of wheat malt on ferulic acid

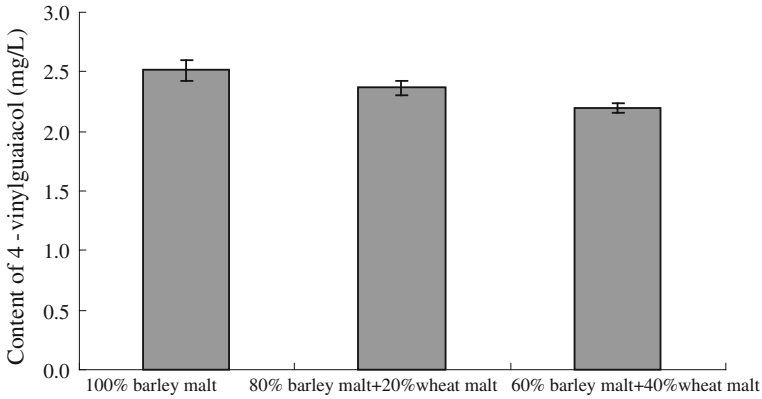

Fig. 50.3 Effects of wheat malt proportion on the 4-vinylguaiacol levels

glycosidase is not sensitive to warming-up, and it will gradually be inactive until 70 °C. When the mashing-in temperature was 37 °C, many varieties of enzymes will be easy to released. Once the enzymes reached their optimum temperature, they would immediately play their roles, and the 4 kinds of enzymes will synergistically work (closer to the optimum temperature of cinnamoyl esterase), which is conducive to the release of ferulic acid, so the content of 4-vinylguaiacol in finished beer was higher.

In the optimizing conditions of enhancing 4-vinylguaiacol levels from Fig. 50.1, the content of 4-vinylguaiacol was higher when the boiling time was 90 min. A small amount of 4-vinylguaiacol was produced by thermal decarboxylation of ferulic acid in the wort during boiling. At the same time, 4-vinylguaiacol will partly volatilize because of evaporation. Possibly, when the boiling time was less than 90 min, the formation of 4-vinylguaiacol would be greater than the volatilization of 4-vinylguaiacol. The differential of 4-vinylguaiacol between the formation and volatilization was gradually decreased, and at this time the content of 4-vinylguaiacol in the final wort would be higher if the boiling time was

Table 50.2 Effect of various technology conditions on the 4-vinylguaiacol levels by SPSS software

Model	Unstandardized coefficients		Standardized coefficients	*t*	Sig.
	B	Std. error	Beta		
Constant	1.10156	0.02355		46.77972	0.00000
Wheat malt proportion	0.05005	0.00213	0.17469	23.45003	0.00000
Mash-in temperature	−0.02443	0.00041	−0.44595	−59.86421	0.00000
Boiling time	0.00024	0.00008	0.02207	2.96319	0.00406
Fermentation temperature	0.09688	0.00082	0.87516	117.48123	0.00000

increased. When boiling time is more than 90 min, the formation of 4-vinylguaiacol would be less than the volatilization of 4-vinylguaiacol, and the differential of 4-vinylguaiacol was gradually increased between the formation and volatilization, the content of 4-vinylguaiacol in the final wort would be lower if the boiling time was increased, thereby the concentration of 4-vinylguaiacol would be also fewer in finished beer.

According to German Purity Beer Law, the fermentation temperature of wheat beer should be between 15 and 25 °C to highlight its unique different flavor and aroma from the bottom-fermented beer. In the optimizing process conditions of formation of 4-vinylguaiacol obtained from Fig. 50.1, the content of 4-vinylguaiacol was higher when fermentation temperature was 20 °C, which was consistent with previous researches [9]. Thus, if the same yeast strains and the same mashing process are adopted, the larger content of 4-vinylguaiacol was obtained when the fermentation temperature was higher.

By the analysis of SPSS software, the optimizing conditions of the formation of 4-vinylguaiacol were obtained. Meantime, the approximate equation for calculating 4-vinylguaiacol levels can be also obtained through the multiple linear regression of SPSS software (Table 50.2). That is: the concentration of 4-vinylguaiacol = 1.10156 + 0.05005 × wheat malt proportion-0.02443 × mashing-in temperature + 0.00024 × boiling time + 0.09688 × fermentation temperature. According to the above calculation equation, if the same raw materials are used as above (water, barley malt, wheat malt, hops, top-fermenting yeast), once wheat malt proportion, mashing-in temperature, boiling time, and fermentation temperature are determined, the concentration of 4-vinylguaiacol in final beer will be approximately calculated out.

Acknowledgments We are grateful for technical assistance of Professor Tongcun Zhang, Xuegang Luo, Nan Wang, Xinghua Liao, and Zhipeng Liu from Tianjin University of Science and Technology in China in genetic cloning of W303+padc yeast strains.

References

1. Vanbeneden N, Gils F, Delvaux F et al (2008) Formation of 4-vinyl and 4-ethyl derivatives from hydroxycinnamic acids: occurrence of volatile phenolic flavour compounds in beer and distribution of Pad1 activity among brewing yeasts. Food Chem 107(1):221–230
2. Thurston PA, Tubb RS (1981) Screening yeast strains for their ability to produce phenolic off-flavours: a simple method for determining phenols in wort and beer. J I Brew 87(3):177–179
3. Shinohara T, Kubodera S, Yanagida F (2000) Distribution of phenolic yeasts and production of phenolic off-flavours in wine fermentation. J Biosci Bioeng 90(1):90–97
4. Cui YQ, Cao XH, Li SS, Thamm L, Zhou GT (2010) Enhancing the concentration of 4-vinylguaia-col in top-fermented beers-a review. J Am Soc Brew Chem 68(2):77–82
5. Coghe S, Benoot K, Delvaux F et al (2004) Ferulic acid release and 4-vinylguaiacol formation during brewing and fermentation: indications for feruloyl esterase activity in *Saccharomyces cerevisiae*. J Agr Food Chem 52(3):602–608

6. Vanbeneden N, Roey TV, Willems Filip, Delvaux F, Delvaux FR (2008) Release of phenolic flavour precursors during wort production: influence of process parameters and grist composition on ferulic acid release during brewing. Food Chem 111(1):83–91
7. GB4927-2008. Chinese National Standard: Beer (2008) Chinese Standard Press, Beijing
8. Bamforth CW, Kanauchi M (2001) A simple model for the cell wall of the starchy endosperm in barley. J I Brew 107:235–240
9. Schmidt G (1978) Rund um das Hefeweizenbier. Brauwelt 580–592:638–652

Chapter 51
Research on Characteristic Aromatic Compounds in Jujube Brandy

Ying Shu, Zhisheng Zhang, Zhenqiang Wang, Hui Ren and Huan Wang

Abstract Aromatic compounds in jujube brandy were extracted by liquid–liquid extraction (LLE) and identified and quantified by gas chromatography–mass spectrometry (GC–MS). A 60 compounds were identified in the samples, including propanoic acid, 2-hydroxy-,ethyl ester, furfural, hexanoic acid, ethyl ester, heptanoic acid, ethyl ester, octanoic acid, ethyl ester, nonanoic acid, ethyl ester, decanoic acid, ethyl ester, dodecanoic acid, ethyl ester, ethyl tridecanoate, 9- tetradecenoic acid, tetradecanoic acid, ethyl ester, pentadecanoic acid, ethyl ester, methyl palmitate, E-11-hexadecenoic acid, ethyl ester, (E)-9-octadecenoic acid ethyl ester, hexadecanoic acid, ethyl ester, and ethyl oleate (total relative content was 81.70 %) and they are characteristic flavor of jujube brandy.

Keywords Aromatic compounds · Brandy · Gas chromatography–mass spectrometry · Jujube

51.1 Introduction

Chinese jujube is a native fruit of china and has a long history of over 2,500 years. It has been commonly used as a drug in traditional Chinese medicine and has also been commonly used as food, food additive, and flavorant for thousands of years. The Chinese share of world jujube production is about 90 % and its production has in increased in the last 10 years due to the demands for food and pharmaceutical applications [1–4].

Aroma profile is important in brandy, as it contributes to the quality of the final product. It is due to the combined effects of several volatile compounds mainly

Y. Shu · Z. Zhang (✉) · Z. Wang · H. Ren · H. Wang
College of Food Science and Technology, Agricultural University of Hebei, Baoding 071001 Hebei Province, People's Republic of China
e-mail: zzs324@126.com

T.-C. Zhang et al. (eds.), *Proceedings of the 2012 International Conference on Applied Biotechnology (ICAB 2012)*, Lecture Notes in Electrical Engineering 249,
DOI: 10.1007/978-3-642-37916-1_51, © Springer-Verlag Berlin Heidelberg 2014

alcohols, esters, acids, alkane, and other minor components already present in the fruit and being formed during the fermentation and maturation process [5]. In the present investigation, characterization of volatile aroma nature of the jujube brandy was studied using gas chromatography coupled with mass spectrometry (GC–MS). This study will contribute a great deal toward a program aimed at the enhancement of the quality of the product derived from one of the china's traditional fruits, jujube.

51.2 Materials and Methods

51.2.1 Materials

Jujube brandies were supplied by a local jujube brandy factory of Hebei province and stored at room temperature.

51.2.2 Reagents and Standards

Dichloromethane (HPLC grade) and anhydrous sodium sulfate (Analytical grade) were purchased from Kemiou (Tianjin, China).

51.2.3 Extraction of Volatile Compounds

A 100 ml of sample was extracted with 100, 50 ml Dichloromethane in separate funnel, respectively, the organic phase was collected and filtered through glass wool and dried over anhydrous sodium sulfate into a round-bottom flask. The extract was concentrated to 1 ml using rotary evaporator in a 35 °C water bath, the extract was then filtered through 0.22 μm filter, hermetically capped, then stored in a freezer (−20 °C) until GC–MS analysis.

51.2.4 Gas Chromatography–Mass Spectrometry Analysis

An Agilent 7890A GC system with a split/splitless injector and interfaced with an Agilent 5975C mass spectrometer was used for sample analysis. The injector was set at 250 °C. Agilent MSD ChemStation Software (E.02.00 493 version) was used to control the system. For separation, a HP-5MS (30 m × 250 μm i.d. × 0.25 μm film thickness) was used. Helium was the carrier gas. Analyses were performed at

programmed temperature starting from 50 °C for 4.5 min, then increased at 10 °C/min to 70 °C, followed by an increase of 7 °C/min to 280 °C at which the temperature was kept constant for 5 min. The total run time was 41.5 min.

For the MS system, the temperature of the transfer line, quadrupole, and ionization source were 250, 150, 230 °C, respectively. Electron impact mass spectra were recorded at 70 eV ionization voltages. The acquisitions were performed in Scan mode (from 40 to 500 amu). Peak identification was carried out by analogy of mass spectra with those of the mass library (NIST05).

51.2.5 Statistical Analysis

Each experiment was repeated three times and results are expresses as mean. The data were analyzed using Microsoft excel to determine the compounds percentages in jujube brandy.

51.3 Results and Discussion

The extract of jujube brandy was analyzed by GC–MS to know the volatile components and different types of eaters and alcohols, from the analysis nearly sixty compounds were identified. Figure 51.1 shows chromatogram of volatile compounds obtained LLE approach. The number of peak is much higher, so are the areas. Table 51.1 shows the volatile compounds of jujube brandy, expressed as means (%) for the three times. Esters, the compounds showing the highest values in the analyses of volatiles, were identified in jujube brandy. Among the ester

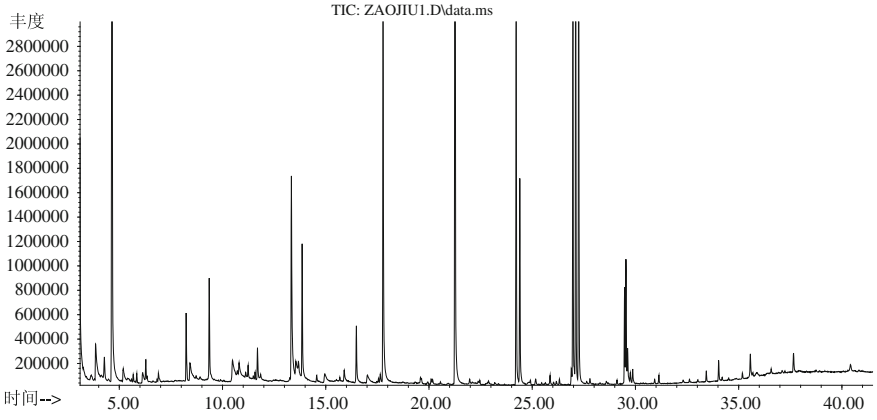

Fig. 51.1 GC-MS chromatogram of the volatile compounds in jujube brandy

Table 51.1 Aroma compounds results of jujube brandy by GC/MS

S.No.	Retention time (RT)	Name of the compounds	Molecular formula	Molecular weight	Percentage (%)	Odour descriptor [6–19]
Acids						
1	24.226	9-Tetradecenoic acid	$C_{14}H_{26}O_2$	226.19	5.74	Fresh, floural
Alcohols						
2	3.097	1-Butanol, 2-methyl-	$C_5H_{12}O$	88.09	1.98	Rancid almonds, pungent
3	3.642	1-Pentanol	$C_5H_{12}O$	88.09	0.18	Alcohol
4	3.857	2,3-Butanediol	$C_4H_{10}O_2$	90.07	1.5	Butter, creamy
5	6.134	1-Hexanol	$C_6H_{14}O$	102.1	0.39	Green, grass
6	11.495	Linalool oxide trans	$C_{10}H_{18}O_2$	170.13	0.19	Sweet, fruity
7	27.8	Hexadeca-2,6,10,14-tetraen-3-ol, 3,7,11,15-tetramethyl-	$C_{20}H_{34}O$	290.26	0.11	Flowery, fruity,
8	35.882	Stigmasterol, 22,23-dihydro-	$C_{29}H_{50}O$	414.39	0.37	–
	Total				4.72	
Alkanes						
9	5.849	Propane, 1,1-diethoxy-2-methyl-	$C_8H_{18}O_2$	146.13	0.15	–
10	8.243	Butane, 1,1-diethoxy-3-methyl-	$C_9H_{20}O_2$	160.15	1.24	–
11	11.579	Hexane, 1,1-diethoxy-	$C_{10}H_{22}O_2$	174.16	0.25	–
12	14.565	Cyclohexene, 2-ethenyl-1,3,3-trimethyl-	$C_{11}H_{18}$	150.14	0.17	Floural
13	15.519	Octane, 1,1-diethoxy-	$C_{12}H_{26}O_2$	202.19	0.18	–
14	20.559	.alpha.-Calacorene	$C_{15}H_{20}$	200.16	0.06	–
15	27.643	1,15-Hexadecadiene	$C_{16}H_{30}$	222.24	0.08	–
16	31.14	Dodecane	$C_{12}H_{26}$	170.2	0.34	–
	Total				2.47	
Esters						
17	4.279	Butanoic acid, ethyl ester	$C_6H_{12}O_2$	116.08	0.62	Sour fruit, strawberry, fruity
18	4.653	Propanoic acid, 2-hydroxy-, ethyl ester	$C_5H_{10}O_3$	118.06	13.4	Lactic, raspberry
19	5.679	Butanoic acid, 3-methyl-, ethyl ester	$C_7H_{14}O_2$	130.1	0.16	Banana, sweet fruity

(continued)

Table 51.1 (continued)

S.No.	Retention time (RT)	Name of the compounds	Molecular formula	Molecular weight	Percentage (%)	Odour descriptor [6–19]
20	6.287	1-Butanol, 3-methyl-, acetate	$C_7H_{14}O_2$	130.1	0.42	Fresh, banana
21	6.348	1-Butanol, 2-methyl-, acetate	$C_7H_{14}O_2$	130.1	0.16	Fresh, banana
22	6.90	Pentanoic acid, ethyl ester	$C_7H_{14}O_2$	130.1	0.32	Apple, fruity
23	9.36	Hexanoic acid, ethyl ester	$C_8H_{16}O_2$	144.12	2.19	Floral, fruity, apple peel, pear, ester
24	10.719	2-Furancarboxylic acid, ethyl ester	$C_7H_8O_3$	140.05	0.39	Fruity, mushroom, smoked
25	10.804	Pentanoic acid, 2-hydroxy-4-methyl-, ethyl ester	$C_8H_{16}O_3$	160.11	1.37	Fruity, ester, mint, orange
26	11.696	Heptanoic acid, ethyl ester	$C_9H_{18}O_2$	158.13	0.82	Fruity
27	13.339	Benzoic acid, ethyl ester	$C_9H_{10}O_2$	150.07	4.76	Ripen fruit
28	13.556	Butanedioic acid, diethyl ester	$C_8H_{14}O_4$	174.09	0.93	Cheese, earthy, spicy
29	13.861	Octanoic acid, ethyl ester	$C_{10}H_{20}O_2$	172.15	2.84	Ripe fruits, pear, sweety, floral, fruity, exotic and passion fruit
30	14.958	Benzeneacetic acid, ethyl ester	$C_{10}H_{12}O_2$	164.08	0.63	Fruity, floral, rose, honey
31	15.898	Nonanoic acid, ethyl ester	$C_{11}H_{22}O_2$	186.16	0.56	Floral, fruity
32	17.021	Benzenepropanoic acid, ethyl ester	$C_{11}H_{14}O_2$	178.1	0.43	Sweet, fruity, honey
33	17.645	Ethyl 9-decenoate	$C_{12}H_{22}O_2$	198.16	0.16	Light fruity, fatty
34	17.78	Decanoic acid, ethyl ester	$C_{12}H_{24}O_2$	200.18	6.6	Sweet, fruity, dry fruits, grape
35	19.596	Undecanoic acid, ethyl ester	$C_{13}H_{26}O_2$	214.19	0.13	Fresh, floural
36	21.265	Dodecanoic acid, ethyl ester	$C_{14}H_{28}O_2$	228.21	14.89	Sweet, floral, fruity, cream
37	22.886	Ethyl tridecanoate	$C_{15}H_{30}O_2$	242.22	0.17	Fresh, floural
38	24.403	Tetradecanoic acid, ethyl ester	$C_{16}H_{32}O_2$	256.24	3.37	Sweet fruity, butter, fatty odor
39	25.868	Pentadecanoic acid, ethyl ester	$C_{17}H_{34}O_2$	270.26	0.2	Fresh, floural
40	26.323	Methyl palmitate	$C_{17}H_{34}O_2$	270.25	0.09	Fatty, rancid, fruity, sweet
41	26.901	Dibutyl phthalate	$C_{16}H_{22}O_4$	278.15	0.28	Sweet
42	26.976	E-11-Hexadecenoic acid, ethyl ester	$C_{18}H_{34}O_2$	282.26	5.68	Floral, fruity
43	27.111	(E)-9-Octadecenoic acid ethyl ester	$C_{20}H_{38}O_2$	310.29	6.8	Fresh, floural
44	27.255	Hexadecanoic acid, ethyl ester	$C_{18}H_{36}O_2$	284.27	8.05	Fatty, rancid, fruity, sweet

(continued)

Table 51.1 (continued)

S.No.	Retention time (RT)	Name of the compounds	Molecular formula	Molecular weight	Percentage (%)	Odour descriptor [6–19]
45	28.595	Heptadecanoic acid, ethyl ester	$C_{19}H_{38}O_2$	298.29	0.09	–
46	29.479	Linoleic acid ethyl ester	$C_{20}H_{36}O_2$	308.27	1.43	Fruity, butter
47	29.545	Ethyl Oleate	$C_{20}H_{38}O_2$	310.29	2.05	Fruity, butter
48	29.626	9-Octadecenoic acid, ethyl ester	$C_{20}H_{38}O_2$	310.29	0.76	Fresh, floural
49	29.756	8-Octadecenoic acid, methyl ester, (E)-	$C_{18}H_{34}O_2$	296.27	0.25	Fresh, floural
50	29.87	Octadecanoic acid, ethyl ester	$C_{19}H_{36}O_2$	312.3	0.33	Wax
51	34.037	1,2-Benzenedicarboxylic acid, mono(2-ethylhexyl) ester	$C_{16}H_{22}O_4$	278.15	0.37	–
Total					81.7	
Ketone						
52	8.43	Benzaldehyde	C_7H_6O	106.04	1.18	Almond
53	10.488	Benzeneacetaldehyde	C_8H_8O	120.06	1.39	Hawthorne, honey, sweet
54	11.242	2-Furaldehyde diethyl acetal	$C_9H_{14}O_3$	170.09	0.76	–
55	25.173	2-Pentadecanone, 6,10,14-trimethyl-	$C_{18}H_{36}O$	268.28	0.16	–
	Total				3.49	
Phenol						
56	16.486	Benzene, (2,2-diethoxyethyl)-	$C_{12}H_{18}O_2$	194.13	1.11	–
57	19.954	Phenol, 2,4-bis(1,1-dimethylethyl)-	$C_{14}H_{22}O$	206.17	0.06	–
58	20.182	Naphthalene, 1,2,3,5,6,8a-hexahydro-4,7-dimethyl-1-(1-methylethyl)-, (1S-cis)-	$C_{15}H_{24}$	204.19	0.1	–
	Total				1.27	
Other						
59	5.195	Furfural	$C_5H_4O_2$	96.02	0.54	Smoked, floral, fruity
60	20.935	4(1H)-Pteridinone, 5,6,7,8-tetrahydro-6-methyl-	$C_7H_{10}N_4O$	166.09	0.07	–
	Total				0.61	

– Mean unknown

compounds, most of the esters were ethyl ester and only two acetates (1-Butanol, 3-methyl-, acetate and 1-Butanol, 2-methyl-, acetate) were detected, this fact maybe attributed to the control of Fermentation process. In this study, the ester compounds were in C3–C8 straight chain fatty acid ethyl ester which contribute to fruity and floral sensory properties to the jujube brandy. Linalool oxide trans, one of the most important monoterpene, was the only terpene compound. 9-Tetradecenoic acid is only acid compound which are responsible for fresh, floral, this may be due to the esterification of these acids with alcohols that result into esters. The alcohols compounds that contribute sweet, creamy, and 1-Hexanol, which responsible for resin flavor and green grass odor, are the third major part of the jujube brandy volatile.

51.4 Conclusion

In conclusion, 60 aromatic compounds were identified and quantified by (GC–MS) in jujube brandy, including propanoic acid, 2-hydroxy-, ethyl ester, furfural, hexanoic acid, ethyl ester, heptanoic acid, ethyl ester, octanoic acid, ethyl ester, nonanoic acid, ethyl ester, decanoic acid, ethyl ester, dodecanoic acid, ethyl ester, ethyl tridecanoate, 9-tetradecenoic acid, tetradecanoic acid, ethyl ester, pentadecanoic acid, ethyl ester, methyl palmitate, E-11-hexadecenoic acid, ethyl ester, (E)-9-octadecenoic acid ethyl ester, hexadecanoic acid, ethyl ester, and ethyl oleate(total relative content was 81.70 %), and they are characteristic flavor of jujube brandy.

References

1. Mu QY, Chen JP, Zhang BS (1999) Identification of volatile fragrant compounds of Chinese dates by gas chromatography-mass spectrometry (GC-MS) analysis. Trans CSAE 15(3):251–255
2. Pu YF, Zhang N, Li SG (2011) Analysis of the nutritional components and volatile components of Zizyphus jujube cv.Dongzao in the south of xin jiang. J Anhui Agri Sci 39(13):7715–7717, 7720
3. Zhu FM, Li J, Gao HS et al (2010) Study on aromatic ingredients of the golden silk jujube and the Shanxi zizyphus jujube. China Food Addit 3:119–124
4. Li JW, Liu PF, Shao DD et al (2007) Nutritional composition of five cultivars of Chinese jujube. Food Chem 103(2):454–460
5. Verzera A, Ziino M, Scacco A et al (2008) Volatile compound and sensory analysis for the characterization of an Italian white wine from "Inzolia" grape. Food Anal Methods 1(2):144–151
6. Wang YF, Yang HF, Sun CY et al (2010) Analysis of flavoring compositions of cabernet sauvignon ice grape wine. Liquor-Making Sci Technol 1:107–109, 113
7. Li H, Li J, Wang H et al (2007) Study on aroma components in cabernet sauvignon wines from Changli original producing area. J Northwest A & F University (Nat Sci Ed) 35(6):94–98

8. Hui RH, Hou DY, Li TC (2004) Extraction and analysis on volatile constituents of the fruit in Zizyphus jujuba Mill. Chin J Analyt Chem 32(3):325–328
9. Li H, Tao YS, Kang WH et al (2006) Wine aroma analytical investigation progress on GC. J Food Sci Biotechnol 25(1):99–104
10. Peinado RA, Moreno J, Medina M et al (2004) Changes in volatile compounds and aromatic series in sherry wine with high gluconic acid levels subjected to aging by submerged flor yeast cultures. Biotechnol Lett 26:757–762
11. Lopez R, Ezpeleta E, Sanchez I et al (2004) Analysis of the aroma intensities of volatile compounds released from mild acid hydrolysates of odourless precursors extracted from Tempranillo and Grenache grapes using gas chromatography-olfactometry. Food Chem 88:95–103
12. Cullere L, Escuderro A, Cacho JF (2004) GC-O and chemical quantitative study of the six premium quality Spanish aged red wines. J Agric Food Chem 52:1653–1660
13. Gomez MJ, Cacho JF, Ferreira V et al (2007) Volatile components of Zalema white wines. Food Chem 100:1464–1473
14. José MO, Isabel MA, Óscar MP et al (2004) Characterization and differentiation of five "Vinhos Verdes" grape varieties on the basis of monoterpenic compounds. Anal Chim Acta 513:269–275
15. Styger G, Prior B, Bauer FF (2011) Wine flavor and aroma. I Ind Microbiol Biotechnol 38:1145–1159
16. Li JM, Song CB, He PC (1998) Advances in aroma components of grape and wine. Acta Univ Agric Boreali-occidentalis 26(5):105–109
17. Li H (2001) Aromatic components in grape. Sino-Overseas Grapevine Wine 6:43–44
18. Zhang MX, Wu YW, Duan CQ (2008) Progress in study of aromatic compounds in grape and wine. Scientia Agricultura Sinica 41(7):2098–2104
19. Wang H, Li H, Liu LP et al (2005) Analysis of aroma components of pineapple wine by gas chromatography-mass spectrometry. J North West Sci-Tech Univ Agri For (Nat Sci Ed) 33(4):143–146

Chapter 52
Characterization of Bacterial Community of "Hetao" Strong-Flavor Chinese Liquor Daqus by PCR–SSCP

Na Hai and Lin Yuan

Abstract "Daqu" is a fermentation starter that is used to initiate fermentations for the production of Chinese liquor. The total DNA extracted from Daqu samples were used as a template for PCR with universal primers of 16S rRNA. The amplicons were analyzed using single-strand conformational polymorphism (SSCP). It was observed that the bacterial SSCP profile indicated high diversity. The results showed that *Leuconostoc citreum*, *Weissella cibaria*, *Acetobacter pasteurianus*, and *Lactobacillus mindensis* were the most dominant species. Based on the SSCP analysis, a few differences in community structure were found between Daqu samples.

Keywords Strong-flavor liquor · Daqu · Bacterial community · PCR-SSCP

52.1 Introduction

The Chinese liquor is one of the six distilled liquor in the world, because of its unique fermentation process and product style. Strong-flavor liquor is the typical style in the Chinese liquor [1]. Daqu is natural fermentation of mold, bacteria, and yeast. Daqu is a starter to affect liquor quality during the further fermentation. Several researches have been studying on liquor microorganisms in Daqu [2, 3], pit mud, and fermented grains [4, 5] through traditional culture-dependent methods. Culture-dependent methods have many shortages, such as time consuming and lack of uncultured species [6, 7]. Amann and the other people found that the cultivated kinds of the microorganisms are less than 10 % of the total microorganisms [8]. In the past decade, a large amount of the new molecular biology

N. Hai · L. Yuan (✉)
College of Life Science, Inner Mongolia University, Huhhot 010021,
People's Republic of China
e-mail: yuan0079@163.com

T.-C. Zhang et al. (eds.), *Proceedings of the 2012 International Conference on Applied Biotechnology (ICAB 2012)*, Lecture Notes in Electrical Engineering 249,
DOI: 10.1007/978-3-642-37916-1_52, © Springer-Verlag Berlin Heidelberg 2014

approaches have been proven to be the powerful tools to study the microbial diversity in environmental samples [9–12].

Single-strand conformational polymorphism (SSCP) is able to separate the single-stranded DNA which has the differences in the length and the secondary structure. SSCP has been used to study the succession of bacterial communities [13], rhizosphere communities [14, 15], bacterial population changes in an anaerobic bioreactor [16], and AMF species in roots [17, 18]. This article analyzed the structure and the succession of the bacterial community of Strong-flavor liquor Daqu by PCR–SSCP.

52.2 Materials and methods

52.2.1 Daqu Sample

All of the Daqu samples were collected from Hetao Liquor Industry Group in the west of China. The Daqu samples were collected and stored in the sealed plastic bags at 4 °C. The DNA extraction was performed within 5 d.

52.2.2 DNA Extraction

The total DNA was extracted using the method described by Zhang Rui with slight modifications [19]. One mL of the extraction buffer (100 mM Tris–HCl, 100 mM EDTA, 100 mM Na_3PO_4, 1.5 M NaCl, and 1 % CTAB, pH8.0) was added to 0.5 g Daqu sample. The mixture was incubated at 37 °C for 90 min. Next, 200 μL of 20 % SDS and 10 μL lysozyme were added. The mixture was incubated at 65 °C for 90 min and then centrifuged at 5,500 rpm for 10 min. The supernatant was transferred into a new tube. 750 μL of the extraction buffer and 75 μL of 20 % SDS were added. The mixture was incubated at 65 °C for 20 min and then centrifuged at 5,500 rpm for 5 min. The supernatant was transferred into a new tube. 600 μL of a mixture of chloroform and isoamyl alcohol (vol/vol, 24:1) was added and then centrifuged at 12,000 rpm for 10 min at 4 °C. The supernatant was transferred into a new tube. This step was repeated. Then, 480 μL of cold isopropanol was added to precipitate the DNA at −20 °C for 1 h. The solution was centrifuged at 12,000 rpm for 10 min. The DNA pellet was washed using 200 μL of cold 70 % ethanol. After drying, the pellet was suspended in 30 μL of 0.1 × TE (10 mM Tris, 1 mM EDTA, pH 8.0). The DNA was quantified by electrophoresis using 1 % agarose gel and subsequently diluted to 10 ng/μL.

52.2.3 PCR Amplification

Amplification of the partial sequence of 16S rDNA was performed with the universal primers Com1 (5′-CAG CAG CCG CGG TAA TAC-3′) and Com2 (5′-CCG TCA ATT CCT TTG AGT TT-3′). The PCR reaction was performed in a 25 μL volume, containing 10 ng genomic DNA, 0.2 mM dNTPs, 2.0 mM $MgCl_2$, 0.2 μM of each primer, and 0.5 U Taq polymerase (Sangon, China). All amplifications were performed with an initial denaturing at 95 °C for 5 min, followed by 30 cycles of 95 °C for 60 s, 55 °C for 60 s, and 72 °C for 90 s, and a final elongation at 72 °C for 4 min. The PCR products were quantified by electrophoresis using 1 % agarose gel. Amplified PCR products were cleaned using a DNA fragment purification kit (Takara, Dalian, China).

52.2.4 SSCP Analysis

About 5 μL of purified PCR product was denatured by adding 10μL of deionized formamide loading buffer (98 % (vol/vol) deionized formamide, 10 mM EDTA, 1 mg/ml xylene cyanol FF, 1 mg/ml bromophenol blue) at 95 °C for 10 min and then resolved by 10 % polyacrylamide (29:1) gel electrophoresis in 1 × TBE buffer at 300 V for 10 h. Gels were silver stained according to standard procedures [20].

52.2.5 Sequencing of SSCP Bands

The bands of interest were excised from the gel using a sterile blade and incubated 10 min at 100 °C in distilled water to allow DNA diffusion out of the polyacrylamide matrix. The solution was used directly for further amplifications. Excised bands were reamplified using the universal primers Com1 and Com2 as described previously. For further sequencing analysis, every PCR product was ligated into pMD19-T easy vector (Takara, Japan), and plasmid DNA was extracted from randomly selected clones and screened for inserts of the expected size and correct SSCP migration properties. For each band, three clones that yielded a single band co-migrating with the original band were sequenced with an automatic sequencer (Sangon, China). To determine the closest known relatives of the partial rRNA sequences obtained, searches were performed in GenBank.

52.3 Results and Discussion

52.3.1 SSCP Analysis

SSCP profiles of Daqu samples collected at different time are shown in Fig. 52.1. The microorganism diversity of samples increased at first and then decreased during the whole fermentation process. There was high diversity in Daqu at the middle stage of fermentation. After about 10 days of fermentation, six special bright band appeared and the corresponding species became the predominant microbe ultimately, such as band 7 and band 8. Some bands disappeared slowly during the fermentation, such as band 9. At the same time, the microorganism quantity of the samples changed during the whole fermentation process. Some bands brighten gradually, such as band 8. Some bands getting dark gradually, such as band 2.

The main bands of the sample collected from different time exhibited little differences during the fermentation. This means that the bacterial community during the whole fermentation has the similar structure. At the same time, the banding profile difference shows that the bacterial community has polymorphism.

52.3.2 Sequencing of the Main Bands in SSCP Profiles

Four dominant bands (1–4) in the SSCP profile were sequenced and identified. Their closest relatives found in the GenBank database are listed in Table 52.1. The most dominant bands (bands 1–4) in samples at different time were related most closely to lactic acid bacteria. This result indicated that the majority of microorganisms died because of the decrease of oxygen content and increase of acidity

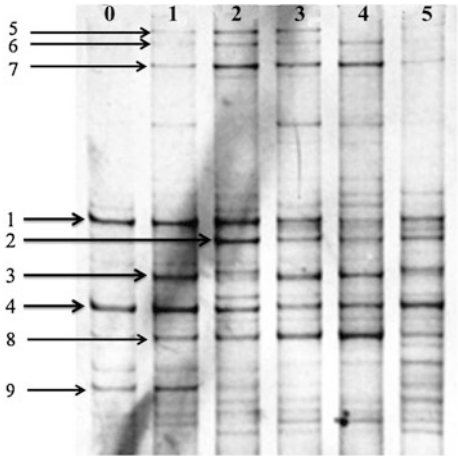

Fig. 52.1 SSCP profiles of 16S rRNA V4–V5 regions of the Daqu samples collected at different time. lane *0*: fermentation 0d, lane *1*: fermentation 10d, lane *2*: fermentation 20d, lane *3*: fermentation 30d, lane *4*: fermentation 40d, lane *5*: fermentation 50d

Table 52.1 Sequencing results of selected bands from the SSCP profiles

Band no.	Closest relative microorganism
1	*Leuconostoc citreum*
2	*Weissella cibaria*
3	*Acetobacter pasteurianus*
4	*Lactobacillus mindensis*

and alcohol concentration during the fermentation, and only lactic acid bacteria could endure the extreme environment and became the most predominant species. This result agrees with that of the research of Zhang [21].

52.4 Conclusion

The Chinese liquor quality is correlated to many factors, such as production techniques, grains, the local geographic environment around the liquor production factories [3], and Daqu. Daqu is a mixture of grains, micro-organisms, enzymes, and aroma precursors [22]. Although the same style liquor contains uniform key flavor components, production techniques, and geographic environment will result in the different evolvement of microorganism community in Daqu. After solid-form distillation, the different types and concentration of microorganism in the distillate influence liquor quality. In the Chinese liquor fermentation process, Daqu is equivalently the seed. So the composition and the function of the microorganisms in the Daqu are important to investigate. The structure and diversification course of microorganism community in Daqu during the fermentation process produced in Inner Mongolia were analyzed through PCR–SSCP analysis. At the interim of fermentation, there was high diversity of microorganisms in Daqu. With the fermentation time, many microorganisms could not endure the changes of microenvironment and were led to death. At the end of fermentation, lactic acid bacterium became the major predominant species.

References

1. Hu YS (2000) Thinking of the wine industry ecology and development. Liquor 1:222–231
2. Shi AH, Guan JK, Zhang WP et al (2001) Analysis of microbial species in Xufang Daqu and determination of the dominant microbes. Liquor Mak Sci Technol 108:26–28
3. Wang HY, Zhang XJ, Zhao LP et al (2008) Analysis and comparison of the bacterial community in fermented grains during the fermentation for two different styles of Chinese liquor. J Ind Microbiol Biotechnol 35:603–609
4. Xiong CX (1994) Research on changes of microbes and materials in Zaopei during fermentation of strong aroma style liquor. Liquor Mak Sci Technol. 62:25

5. Wu ZY, Zhang WX, Zhang QS (2009) Developing new sacchariferous starters for liquor production based on functional strains isolated from the pits of several famous Luzhou-flavor liquor brewers. J Inst Brew 115:111–115
6. Tsai YL, Olson BH (1991) Rapid method for direct extraction of DNA from soil and sediments. Appl Environ Microbiol 57:1070–1074
7. Miller DN, Bryant JE, Madsen EL et al (1999) Evaluation and optimization of DNA extraction and purification procedures for soil and sediment samples. Appl Environ Microbiol 65:4715–4724
8. Amann RI, Ludwig W, Schleifer KH (1994) Identification of uncultured bacteria: a challenging task for molecular taxonomists. ASM News 60:360–365
9. Gich F, Garcia-Gil J, Overmann J (2001) Previously unknown and phylogenetically diverse members of the green nonsulfur bacteria are indigenous to freshwater lakes. Arch Microbiol 177:1–10
10. Schneegurt MA, Kulpa CF (1998) The application of molecular techniques in environmental biotechnology for monitoring microbial systems. Biotechnol Appl Biochem 27:73–79
11. Atlas RM, Sayler G, Burlage RS et al (1992) Molecular approaches for environmental monitoring of microorganisms. Biotechniques 12:706–717
12. Madsen EL (1998) Epistemology of environmental microbiology. Environ Sci Technol 32:429–439
13. Peters S, Koschinsky S, Schwieger F et al (2000) Succession of microbial communities during hot composting as detected by PCR-single-strand- conformation-polymorphism based genetic profiles of small-subunit rRNA genes. Appl Environ Microbiol 66:930–936
14. Schwieger F, Tebbe C (1998) A new approach to utilize PCR single-strand-conformation-polymorphism for 16S rRNA gene based microbial community analysis. Appl Environ Microbiol 64:4870–4876
15. Schmalenberger A, Schwieger F, Tebbe CC (2001) Effect of primers hybridizing to different evolutionarily conserved, regions of the small-subunit rRNA gene in PCR-based microbial community analyses and genetic profiling. Appl Environ Microbiol 67:3557–3563
16. Zumstein E, Moletta R, Godon JJ (2000) Examination of two years of community dynamics in an anaerobic bioreactor using fluorescence polymerase chain reaction single-strand conformation polymorphism analysis. Environ Microbiol 2:69–78
17. Simon L, Levesque RC, Lalonde M (1993) Identification of endomycorrhizal fungi colonizing roots by fluorescent singlestrand conformation polymorphism-polymerase chain reaction. Appl Environ Microbiol 59:4211–4215
18. Kjoller R, Rosendahl S (2000) Detection of arbuscular mycorrhizal fungi in roots by nested PCR and SSCP. Plant Soil 226:189–196
19. Zhang R, Cao H, Cui ZL (2003) Extraction and purification of total DNA in soil microbial. J Micro 43:276–282
20. Cho JC (2000) Computer-assisted PCR single strand conformation polymorphism analysis for assessing shift in soil bacterial community structure during bioremediational treatments. World J Microbiol Biotechnol 12:3
21. Zhang WX, Qiao ZW, Shigematsu T et al (2005) Analysis of the bacterial community in Zaopei during production of Chinese Luzhou-Xavor liquor. J Inst Brew 111(2):215–222
22. Wang HY, Gao YB, Fan QW et al (2011) Characterization and comparison of microbial community of different typical Chinese liquor Daqus by PCR–DGGE. Lett Appl Microbiol 53:134–140

Chapter 53
Analysis of Functional Components in Submerged-Fermentation Mycelium and Fruit Body of *Grifola frondosa*

Jia Li, Zhenyu Wang, Ping He and Tong-Cun Zhang

Abstract The contents of three main functional components including amino acids, microelements, and polysaccharides were determined in submerged- fermentation mycelium and compared with data of fruit body in *Grifola frondosa*. The results showed that the contents of three main functional components in mycelium were higher than or as same as the fruit body. This indicated that submerged-fermentation mycelium was not only better in output and period than traditional culture method, but also better in nutrient components than fruit body. So the process of submerged-fermentation has very bright future in mycelium production of *G. frondosa*.

Keywords *Grifola frondosa* · Submerged-fermentation · Mycelium · Functional component

53.1 Introduction

Grifola frondosa, known as maitake, hen-of-the-woods, and *Polyporus frondosus*, is one of the macrofungi, belonging to *Polyporus* (*Basidiomycotina*, *Aphyllophorales*, *Polyporaceae*) [1].

G. frondosa has highly nutritional and medical value and is one kind of extremely precious high-grade mushroom fungus, both in food and drug fields. At least eight kinds of amino acids, that human body needs essentially, are rich in *G. frondosa*. Moreover there are proteins, carbohydrates, vitamins, and

J. Li
College of Biological and Pharmaceutical Engineering, Wuhan Polytechnic University, Wuhan 430023, People's Republic of China

Z. Wang · P. He · T.-C. Zhang (✉)
Institute of Life Science, Wuhan University of Science and Technology, Wuhan 430065, People's Republic of China
e-mail: zhangtongcun@wust.edu.cn

T.-C. Zhang et al. (eds.), *Proceedings of the 2012 International Conference on Applied Biotechnology (ICAB 2012)*, Lecture Notes in Electrical Engineering 249,
DOI: 10.1007/978-3-642-37916-1_53, © Springer-Verlag Berlin Heidelberg 2014

microelements in *G. frondosa*. *G. frondosa* can be used to treat urination, edema, beriberi, liver cirrhosis, ascites, diabetes, hypertension, obesity, and other diseases [2–7]. In recent years, some researchers reported that the glucan of *G. frondosa* had the obvious effects for enhancing immunity and inhibiting tumor, and was non-toxic [8–10]. As a high-grade health care food, *G. frondosa* is very popular in Japan, Singapore, and other countries' markets and is regarded as a treasure in the area of edible fungus, so that the price of *G. frondosa* is increasingly high.

In nature, there are very few wild *G. frondosa*. At present, the production of *G. frondosa* is mainly artificial cultivation, however, this situation has caused many shortcomings, including covering bigger area, lasting longer period for producing, having unstable output, being sensitive to climates and environmental factors, and so on. For the past few years, with the rapid development of fermentation engineering, the method of liquid submerged-fermentation technology for the production of *G. frondosa* has arose. Liquid submerged-fermentation method which can make the production of *G. frondosa* to be industrialized has many advantages, such as shorter producing cycle, higher yield, more stable quality, and so on. But the research about whether the content of functional components in liquid submerged-fermentation of *G. frondosa* is lower or higher than in fruit body is still not reported. Therefore, we determined the contents of three mainly functional components, including amino acids, microelements, and polysaccharides in submerged-fermentation mycelium of some strains and compared the data with the fruit body of *G. frondosa*. The results could be considered to be applied in this technological development of *G. frondosa*.

53.2 Materials and Methods

53.2.1 Experimental Materials

53.2.1.1 Strains

Gr1, Gr2, Gr3, Gr4, Gr5 which were tested are the lab-saving strains of *G. frondosa*.

53.2.1.2 Submerged-Fermentation Medium

PDA liquid medium

53.2.1.3 Submerged-Fermentation

The strains were inoculated into submerged-fermentation medium and cultured at 26 °C and shaken at 150 r·min^{-1}. After 7 days, the thalli were collected.

53.2.2 Experimental Methods

53.2.2.1 Content Determination of Amino Acid

(1) Proteolysis [11]

The sample (80 mg) was put into hard—glass hydrolysis tube and was mixed with hydrochloric acid (6 N) until the sample was dissolved. And then the tube was sealed and maintained at 110 °C in an oven for 24 h to make the sample completely hydrolyzed. When the hydrolysate was cooling, opening the pipe, the hydrolyzed sample was put into crucible, dried in boiling water bath, washed several times, and dried again. After the last step of drying, suitable amount of sodium hydroxide was added and the sample was put at room temperature for 4 h. The final sample solution, added appropriate amount of 0.02 N hydrochloric acid, was centrifuged in 10000 $r \cdot min^{-1}$ for 20 min. After the solution was diluted, it was analyzed by analyzer machine (Japanese Hitachi—835-50 type automatic amino acid analyzer) and the machine working conditions was column temperature 53 °C, buffer pump pressure 90 $kg \cdot cm^{-2}$, quantity of flow 0.225 $ml \cdot min^{-1}$, sample quantity 50 μl.

(2) Free amino acid determination

The sample was added 4 % sulfosalicylic acid to precipitate proteins and centrifuged at 15000 $r \cdot min^{-1}$ for 20 min. The supernatant fluid was taken to be analyzed by the machine (Japanese Hitachi—835-50 type automatic amino acid analyzer).

53.2.2.2 Determination of Microelements

(1) Determination of Ca, P, Fe, K, Zn, Cu, Na, Cr

The sample (0.8 g) was put into 50 ml beaker and dropped 4 ml concentrated HNO_3. If, after added the HNO_3, the reaction was not fierce, the beaker can be put on a hot plate for heating, until no brown NO_2 released so far. The above operations were repeated until the solution turned into colorless or light yellow. The beaker was added 1 ml concentrated hydrochloric acid and heated to generate white smoke. If the solution was still black, then, add 2–3 ml concentrated HNO_3 and heat the solution to generate white smoke. The solution was taken out for a while until it turned to be cold, added 2–3 ml water and heated to generate white smoke. Repeat this operation (adding acid–water) one more time, the solution should be colorless or very light yellow. At last, the solution was added with water for 10 ml constant volume for the next processing. During the preparation of the sample, a control group would be tested for each of the same species of samples. The content determinations of inorganic elements were tested by the ICAP9000

plasma spectrometer produced by American Jarrell—Ash company. The standard curves of the tested elements were prepared in advance. The samples were adjusted according to the standard curves, and then multi- elements were tested according to time integral equation at the same time. The results of the content of measured elements were printed directly.

(2) Determination of Se

The standard application fluid (0.0, 0.1, 0.2, 0.3, 0.4, 0.5 ml) was put into 15 ml centrifuge tubes, added deionized water to constant volume of 10 ml, then added 2 ml concentrated hydrochloric acid respectively, blended with 1 ml potassium ferricyanide solution, and made standard working curves.

The sample (0.5 g) was added with 10 ml mixed acid (nitric acid and perchloric acid to 4:1 mixed) in a 150 ml tall canister beaker, covered by surface plate, and digested coldly for one night. The next day, the beaker was put in a hot plate for heating, and timely added the mixed acid. When the solution turned into clear, colorless, and with white smoke, the heating should continue until the residual volume turned to 7 ml or so. The reaction system was cooled down, added 5 ml 6 $mol \cdot L^{-1}$ hydrochloric acid, heated continually until the solution turned into clear, colorless, and with white smoke. At the time, hexavalent Se has completely reduced into quadrivalence Se. The reaction was cooled down, transferred, and added deionized water to constant volume of 50 ml in a volumetric flask. A blank control was made at the same time. 10 ml sample of digested solution was absorbed in 15 ml centrifuge tube, added 2 ml concentrated hydrochloric acid and 1 ml potassium ferricyanide solution. The reaction system was blended and analyzed by the machine (AFS-230 type of atomic fluorescence spectrometer).

53.2.2.3 Determination of Polysaccharide

(1) Drawing standard curve

Glucose (2–3 g) was dried for 3–4 h to remove moisture at 105 °C. Glucose (0.02 g dry weight) was added in deionized water to constant volume of 200 ml. The solution was taken respectively 0, 0.2, 0.3, 0.4, 0.5, 0.6, 0.7, 0.8 ml, added water to 2 ml, add 1 ml 5 % phenol, slowly added 5 ml concentrated sulfuric acid, heated in 100 °C water bath for 20 min, cooled down, and measured absorbance at 489 nm. The regression equation of standard curve was calculated.

(2) Determination of sample's polysaccharide

Dried bacteria powder sample was weighed for 0.2 g into a 50 ml centrifuge tube, added 30 ml 85 % ethanol, heated in 60 °C water bath for 1 h, and shook one time for every 10–15 min until blended. The system was centrifuged at 12000 $r \cdot min^{-1}$ for 20 min. The supernatant was discarded and the tube with precipitation was boiled in 150–200 ml distilled water for 1 h, filtered by cotton,

added distilled water to constant volume of 200 ml. 0.5 ml of the solution (if the measured value was beyond the standard curve range, the sample volume for taking should be reduced or increased accordingly) was measured accurately, added distilled water to 2 ml, added 1 ml 5 % phenol, 5 ml concentrated sulfuric acid, heated in 100 °C water bath for 20 min. The absorbance was determined, substituted regression equation, and calculated the content of polysaccharide.

53.3 Results and Discussion

53.3.1 Content Determination Results of Amino Acid in Submerged-Fermentation Mycelium of G. frondosa

The results of amino acid content in mycelium and fruit body of *G. frondosa* are shown in Table 53.1.

The protein of submerged-fermentation mycelium was hydrolyzed. The result shows that it contains 18 kinds of amino acids generally higher than the fruit body, of which the content of 8 kind of human essential amino acid, including Ile, Leu, Lys, Met, Phe, Thr, Trp, Val is higher. Some researches showed that, in most of the food, the content of Trp was lower [2], however, the content of Trp in *G. frondosa* was relatively higher. So when *G. frondosa* and other foods were eaten at the same time, it can have a complementary action for proteins' intake, so that the amino acid ratio can be made closer to the model of human needs. And the amino acid content of the mycelium from submerged-fermentation is not reduced, which explains that the adoption of submerged-fermentation industrial production of *G. frondosa* does not affect the contents of amino acid in the products.

Lacking some data during the pretreatment of samples is due to, because of the use of acid hydrolysis method, Try was destroyed, Asn and Gln turned into Asp and Glu, cysteine was oxidized to cystine.

53.3.2 Content Determination Results of Microelements in Submerged-Fermentation Mycelium of G. frondosa

The results of microelements content in mycelium and fruit body [2] of *G. frondosa* are shown in Table 53.2.

Among them, the content of Ca, P, and Na in mycelium are far higher than the fruit body, the content of K and Zn in mycelium and fruit body are almost the same, and the content of Fe, Se, Cu, and Cr of mycelium is relatively lower than the fruit body. According to the relevant research, microelements, especially Ca,

Table 53.1 Comparison of amino acids contents between submerged-fermentation mycelium and fruit body of *G. frondosa*

Type of amino acid	Contents of amino acid (g·100 g^{-1} dry sample)				
	Fruit body[a]	Protein hydrolysis of submerged-fermentation mycelium[b]		Free amino acid of submerged-fermentation mycelium[b]	
		Gr1	Gr2	Gr1	Gr2
Ile	0.986	2.0066	1.4260	0.1659	0.1361
Leu	2.538	2.6065	1.7415	0.0684	0.0863
Lys	1.739	1.9793	1.4045	0.1283	0.0896
Met	0.433	0.4491	0.3348	0.4000	0.2612
Cys	0.117	0.4638	0.4580	0.1162	0.0795
Phe	0.861	1.6692	1.1295	0.7214	0.5005
Tyr	0.601	0.9665	0.7369	0.1214	0.0587
Thr	1.267	1.8026	1.2792	0.2706	0.1913
Trp				0.0360	0.0289
Val	1.233	2.7730	1.9799	0.2266	0.1848
Arg	1.690	2.3152	1.6645	0.2421	0.1861
His	0.590	1.0724	0.7866	0.0617	0.0467
Ala	1.448	2.5954	1.8109	0.3567	0.2905
Asp	2.444	3.7114	2.7159	0.3470	0.2928
Glu	3.753	5.1341	3.9407	0.3406	0.2838
Gly	1.262	2.1285	1.5051	0.1183	0.0855
Pro	1.153	2.5228	1.9413	0.6133	0.4211
Ser	1.412	1.6463	1.0999	0.1564	0.1385
Tau				0.4157	0.3061
NH_3		0.9074	0.6676	0.0379	0.0289
Total amino acids	23.53	36.7502	26.6230	4.9446	3.6959

[a] Results from the Ministry of Agriculture Quality Inspection Center, the Institute of Nutrition and Food Hygiene in Chinese Academy of Preventive Medicine [2]

[b] Results determined in Guangdong Institute of Entomology. The data are the average value based on three experiments

Fe, Zn, Cu, Cr is necessary to ensure the various metabolic response in human body to be normal, so microelements is also an important indicator for evaluating the healthcare function of *G. frondosa*. From Table 53.2, the content of microelements in mycelium is generally close to fruit body of *G. frondosa*. Another important thing is the microelement content of submerged-fermentation mycelium of *G. frondosa* is far below the maximum of safety limit [12] provided by the state for food and drugs, so these microelements contained in the mycelium of submerged-fermentation of *G. frondosa* are safe to the human body. Therefore, the mycelium of submerged-fermentation of *G. frondosa* can replace the fruit body of *G. frondosa* in the aspect of the healthcare function.

Table 53.2 Comparison of microelements' contents between submerged-fermentation mycelium and fruit body of *G. frondosa*

Type of element	Content of microelements ($\mu g \cdot g^{-1}$ dry weight)		
	Fruit body[a]	Mycelium of Gr1[b]	Mycelium of Gr2[b]
Ca	176	5420	6810
P	7210	12300	12400
Fe	526	79.28	77.24
K	16380	14400	12700
Zn	175	108.4	98.31
Se	0.4	0.117	0.110
Cu	39.7	6.72	8.01
Na	386	3410	2690
Cr	11.6	2.80	2.24

[a] Results from the Ministry of Agriculture Quality Inspection Center, the Institute of Nutrition and Food Hygiene in Chinese Academy of Preventive Medicine [2]
[b] Results determined in Testing Center of Sun yat-sen university. The data are the average value based on three experiments

53.3.3 *Content Determination Results of Polysaccharide in Submerged-Fermentation Mycelium of* G. frondosa

The comparison results of polysaccharide content between mycelium and fruit body of *G. frondosa* are shown in Fig. 53.1.

Modern medical research showed that the polysaccharide of *G. frondosa* is a kind of immune activation adjuvant and the main functional component in *G. frondosa* [13]. From the results of polysaccharides determination, the average values of polysaccharides content in submerged-fermentation mycelium of *G. frondosa* are between 9 and 12 % based on three times of the test. Among them, the value of Gr1 is the highest, about 11.60 %, then Gr5, Gr4, and Gr3, is 10.74, 10.66, and 10.17 %, respectively, Gr2 is the lowest, at 9.04 %. And the content of

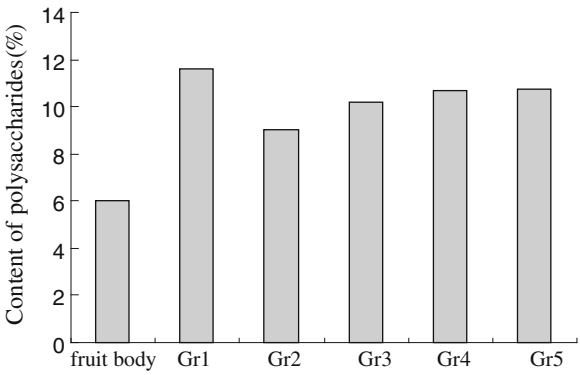

Fig. 53.1 Comparison of polysaccharides' contents between submerged-fermentation mycelium and fruit body of *G. frondosa*

polysaccharides in fruit body of *G. frondosa* is about 5–7 %, which is obviously lower than that of the mycelium. Moreover, there is a certain amount of *G. frondosa* polysaccharides in the fermented liquids, therefore fermentation medium also has a certain application value.

From the above results, we think using the method of submerged-fermentation to produce the mycelium of *G. frondosa* can make not only the output and production potential far higher than the fruit body of *G. frondosa* produced by cultivation methods, but also the two indexes, including amino acid and polysaccharide, obviously more than the fruit body of *G. frondosa* produced by artificial cultivation, and the microelements content of mycelium close to the fruit body. Thus, submerged-fermentation method for the industrial production of *G. frondosa* has great developmental potential.

In addition, almost all the indexes of Gr1 are relatively higher than other strains. Therefore, we preliminarily think that Gr1 is more suitable for submerged-fermentation industrial production of *G. frondosa* than others.

Acknowledgments This study was supported by the part of National High Technology Research and Development Program (China "863" Program) (2008AA10Z336), Wuhan Science and Technology R&D program and the scientific research funds of Wuhan University of Science and Technology (2006XY36). We thank Guangdong Institute of Entomology and Testing Center of Sun Yat-sen University for the assistant of testing the content of amino acid and microelements.

References

1. Xu JT (1997) Chinese medicinal mycology. Union Press of Beijing Medical University and Peking Union Medical College, Beijing, pp 707–717
2. Qiu JP, Sun PL, Zhong WH (1998) High-production cultivation and trophic analysis of *Grifola frondosa*. Edible Fungi China 17(3):31–33
3. Shen Q, Royse DJ (2001) Effects of nutrient supplements on biological efficiency, quality and crop cycle time of maitake (*Grifola frondosa*). Appl Microbiol Biotechnol 57:74–78
4. Shen Q, Royse DJ (2002) Effects of genotypes of maitake (*Grifola frondosa*) on biological efficiency, quality and crop cycle time. Appl Microbiol Biotechnol 58:178–182
5. Shih IL, Chou BW, Chen CC et al (2008) Study of mycelial growth and bioactive polysaccharide production in batch and fed-batch culture of *Grifola frondosa*. Bioresour Technol 99:785–793
6. Montoya S, Orrego CE, Levin L (2012) Growth, fruiting and lignocellulolytic enzyme production by the edible mushroom *Grifola frondosa* (maitake). J Microbiol Biotechnol 28:1533–1541
7. Nishiwaki T, Asano S, Ohyama T (2009) Properties and substrate specificities of proteolytic enzymes from the edible basidiomycete *Grifola frondosa*. J Biosci Bioeng 107(6):605–609
8. Suzuki K, Hashimoto S, Oikawa S et al (1989) Antitumor and immunomodulating activities of a beta-glucan from liquid-cultured *Grifola frondosa*. Chem Pharm Bull (Tokyo) 37(2):410–413
9. Cui FJ, Tao WY, Xu ZH et al (2007) Structural analysis of anti-tumor heteropolysaccharide GFPS1b from the cultured mycelia of *Grifola frondosa* GF9801. Bioresour Technol 98:395–401

10. Gu CQ, Li JW, Chao FH et al (2007) Isolation, identification and function of a novel anti-HSV-1 protein from *Grifola frondosa*. Antiviral Res 75:250–257
11. Han R, Lin QF, Zhang SS et al (1993) Free amino acid compositions and concentrations of *Xenorhabdus* spp. cultures. Nat Enemies Insects 15(3), 129–134
12. Zhou JL, Chen XS (2004) Tolerable upper intake level on vitamins and minerals. J Hygiene Res 33(6):771–773
13. Xing ZT, Zhou CY, Pan YJ et al (1999) Rencent chemical and pharmacological studies on polysaccharide constituent of *Grifola frondosa*. Acta Edulis Fungi 6(3):54–58

Chapter 54
Quantitative Identification and Antioxidant Activity In Vitro of Phenolic Compounds from the Old Leaves of *Toona sinensis*

Changjin Liu, Hongying Wan, Jie Zhang and Zetian Hua

Abstract In the present study, HPLC methodology was developed for the simultaneously determining the major phenolic compounds such as rutin, gallic acid, quercetin, and kaempferol in the old leaves of *Toona sinensis*. The results showed that the percentage contents of rutin, gallic acid, quercetin, and kaempferol were (1.55 ± 0.01) %, (0.87 ± 0.02) %, (2.27 ± 0.05) %, and (1.31 ± 0.01) % from purified phenolics of *Toona sinensis* old leaves respectively. Antioxidation activity of *Toona sinensis* phenolics before purified and after purified were studied, the results indicated that the purified phenolics in *Toona sinensis* old leaves had a significant capacity for scavenging DPPH free radical and superoxide anion radical but less effective on scavenging hydroxyl radical. The phenolics existed in *Toona sinensis* leaves showed obvious antioxidant effect on soybean oil, which could be as an alternative natural antioxidant.

Keywords *Toona sinensis* · Phenolic compounds · HPLC · Antioxidation

54.1 Introduction

Toona sinensis (*TS*) Roemor, a perennial deciduous tree also called "Xiangchun," is a kind of native plant in China. It has been cultivated for more than 2300 years [1]. The tender leaves and stem have been used for the treatment of enteritis, carminative, itch, and dysentery in the oriental medicine [2]. Its young leaves can

C. Liu · H. Wan (✉) · J. Zhang · Z. Hua
Key Laboratory of Food Nutrition and Safety, Ministry of Education, Tianjin University of Science and Technology, Tianjin 300457, People's Republic of China
e-mail: anjing_jaychou@126.com

C. Liu · Z. Hua
China National Japonica Rice Research and Development Center, Tianjin 300457, People's Republic of China

T.-C. Zhang et al. (eds.), *Proceedings of the 2012 International Conference on Applied Biotechnology (ICAB 2012)*, Lecture Notes in Electrical Engineering 249,
DOI: 10.1007/978-3-642-37916-1_54, © Springer-Verlag Berlin Heidelberg 2014

be used as a kind of vegetable called "Xiangchun Ya" in China and thus is known as a "tree Vegetable" [3]. The edible leaves have been used as an oriental medicine for treating dysentery, rheumatoid arthritis, enteritis, gastric ulcers, itchiness, and cancer [4]. Various biological activities of *TS* leaf extracts have been reported, including antioxidant effects [5], anti-cancer [6], and anti-diabetes [7] as well as the suppressing brain degeneration in senescence-accelerated mice [8] and inhibiting Leydig cell steroidogenesis [9]. Meanwhile, several methods have been employed for the analysis of ingredients in *TS*. Gradient reversed-phase high performance liquid chromatography (HPLC), ^{1}HPLC-mass, CE-ED [10], and thin-layer chromatography (TLC) are the most powerful analytical methods [11]. Antioxidant compounds extract from the plant extract antioxidant compounds potentiate body's antioxidant defense or act as antioxidant and they are antioxidants of choice because of their safety over the synthetic ones [12]. So in recent years, considerable attention has been directed toward identification of natural antioxidants derived from plant, which may be possibly used for human consumption [13]. The purposes of this study are to quantify four kind of phenolic compounds from leaves of *TS* by HPLC and measure the antioxidant activity as well in vitro.

54.2 Materials and Methods

54.2.1 Chemicals

Rutin, gallic acid, quercetin, and kaempferol were purchased from the National Institute for the Control of Pharmaceutical and Biological Products. Methanol was of HPLC grade from Tianjin concord technology Co. Ltd. AB-8 macroporous resin was purchased from resin processing plant of Southern pharmaceutical group. All other chemicals used in this study were of analytical grade and supplied by Tianjin Jiangtian Chemical Co. Ltd.

54.2.2 Plant Materials

The old leaves used for this investigation were collected from Teda campus of Tianjin University of Science and Technology on the autumn of 2010. After oven-dried at 55 °C, the leaves were screened after swashed to obtain a powder in the granular size of 60 meshes and stored in the dry dark place for preservation.

54.2.3 Preparation of Plant Extracts

One kilogram of *TS* powder was extracted by 15 L 60 % ethanol (in water, V/V) at 60 °C for 2 h with the aid of ultrasonic waves. Then the mixture was filtered and the residue was extracted again under the same conditions. The two ethanol solutions were combined and evaporated to dryness under reduced pressure to obtain crude phenolic (CP) extracts of *TS*. Part of CP powder was added to 1 L distilled water and shaken vigorously to form a suspension followed by extraction using ethyl acetate for three times. The ethyl acetate fraction was chromatographed on an AB-8 resin column flushed subsequently by adequate distilled water and triple column volume of 70 % ethanol (in water, V/V). Then the 70 % ethanol fraction was evaporated to dryness under reduced pressure to obtain purified phenolic (PP) extracts of *TS*. 20.0 mg of CP, PP, vitamin C (VC), and citric acid were dissolved with absolute ethanol and adjusted to 10 ml in volumetric flasks respectively to obtain sample solutions (2.0 mg/ml) for determining antioxidant activity in vitro.

54.2.4 Preparation of Standards

Rutin, gallic acid, quercetin, and kaempferol standard compounds were completely dissolved with methanol completely. The solutions were adjusted in a 10 ml volumetric flask to obtain a stock solution with the concentration of 40.00, 28.00, 70.00, 21.00 μg/ml, respectively. 1.25, 2.50, 5.00, and 7.50 ml of the stock solution were diluted with methanol and adjusted to four 10 ml in volumetric flasks for making calibration curves accordingly.

54.2.5 Sample Preparation

A 10.0 mg of PP powder was dissolved with methanol in a 10 ml volumetric flask to obtain a solution without acid hydrolysis. A 8 ml of 80 % methanol (in water, V/V) and hydrochloric acid (4.0 mol/L) was added to a test tube with a plug, containing 10.0 mg of PP powder. After refluxing for 2 hours in a water bath at 78 °C, the solution was filtered into a 10 ml volumetric flask and made up to the volume with 80 % methanol (in water, V/V) to obtain a solution after acid hydrolysis. All prepared sample solutions including standard solutions were filtered through 0.45 μm membrane filter prior to the injection into the HPLC system.

54.2.6 Analysis of Phenolic by HPLC

A new method for quantitative analyses of phenolic in *TS* was developed using high performance liquid chromatography (HPLC). The conditions were obtained as follows: The separation was performed on an Agilent C_{18} column (250 × 4.6 mm, 5.0 μm). Methanol (phase A) and 0.1 % phosphoric acid solution (phase B) were used as mobile phase for gradient elution at a flow rate of 1.0 ml/min. The linear gradient of A was at 30 % (0 min), 38 % (4 min), 60 % (7 min), 70 % (9 min), 75 % (15 min), and 30 % (20 min). Column temperature was 40 °C. The wavelength at 255 nm was utilized for the quantitative analysis. The injection volume was 10 μl.

54.2.7 Hydroxyl Radical Scavenging Activity

Hydroxyl radical scavenging activity was determined by the Fenton reaction [14] with slightly modified. A 1.0 ml sample solution of CP, PP, vitamin C (VC), and citric acid was mixed with 2.0 ml of $FeSO_4$ (1.8 mmol/L) and 1.5 ml of salicylic (1.8 mmol/L) ethanol solution in each test tube respectively. The reaction is initiated by adding 0.1 ml of 0.03 % H_2O_2 (in water, V/V) into the mixture. All the reaction solutions were diluted with ethanol and adjusted to 10 ml and in a water bath at 37 °C for 30 min. The absorbance at 510 nm was measured using a spectrophotometer. A blank solution was prepared same as above except that the sample was replaced with distilled water. The equation for calculation of hydroxyl free radical scavenging activity rate (*H*) was as following:

$$H\ (\%) = \frac{A_0 - A_x}{A_0} \times 100\ \% \tag{54.1}$$

where A_0 is the absorbance of control, A_s is the absorbance of sample.

54.2.8 Superoxide Radical Scavenging Activity

Superoxide radical scavenging activity was determined following a method described by Md. Nur Alam [15] with slight modification. 0.4 ml of CP, PP, VC, citric acid solution (2 mg/ml), and 0.4 ml of pyrogallol (30 mmol/L) were mixed with 1.6 ml of Tris–HCl buffer (pH 8.9) and 0.7 ml of brilliant green (20 mmol/L) in every test tube with a plug respectively. The reaction solution was made up to 10 ml with distilled water. A blank solution was prepared as mentioned above except that the sample was replaced with distilled water. The mixture was shaken vigorously and allowed to stand at room temperature for 15 min. The decrease in absorbance of the resulting solution was then measured by spectrophotometer at

625 nm against distilled water. The superoxide radical scavenging activity rate (S) was calculated using the equation:

$$S\,(\%) = \frac{A_2 - A_1}{A_0 - A_1} \times 100\,\% \tag{54.2}$$

where A_0 is the absorbance of control, A_1 is the absorbance of pyrogallol, A_2 is the absorbance of sample solution.

54.2.9 DPPH Radical Scavenging Activity

DPPH radical scavenging activity was determined toward a method quoted from Yongjing Liu with slightly modified [16]. Stock solution of DPPH with the concentration of 2.0×10^{-4} mol/L was dissolved with absolute ethanol. A 0.4 ml of all sample solutions mentioned above was mixed with 4.0 ml stock solutions of DPPH in the reaction tubes respectively. All the reaction solutions were made up to 8 ml with absolute ethanol at last. The mixture was shaken vigorously and kept in the dark for 30 min. The absorbance was measured by the spectrophotometric method at 517 nm against absolute ethanol. The DPPH radical scavenging activity rate (D) was calculated using the following equation:

$$D\,(\%) = \left(1 - \frac{A_i - A_j}{A_c}\right) \times 100\,\% \tag{54.3}$$

where A_c is the absorbance of a mixed solution of 4.0 ml DPPH and 4.0 ml absolute ethanol; A_i is the absorbance of a mixture of 4.0 ml DPPH, 0.4 ml sample and 3.6 ml absolute ethanol; A_j is the absorbance of 0.4 ml sample and 7.6 ml absolute ethanol.

54.2.10 Sample Preparation and Measurement of Peroxide Value

A 100.0 mg of CP, PP, VC, and tea polyphenols (TP) powder were adjusted to 10 ml in volumetric flasks dissolved with absolute ethanol severally to obtain antioxidant solutions (10.0 mg/ml). A 1 ml of all the solutions was added to the samples of soybean oil respectively. All the samples (50 g each) were placed in reagent bottles with narrow necks, without stoppers and stored in an oven at 65 °C. Control sample was placed under the same storage condition. Analyses were carried out after regular intervals of every 2 days. Three parallel samples of each category were analyzed to fulfill the requirements for statistical analysis. Measurement was made at regular intervals following official method (GB/T5538-1995) [17]. Peroxide value (POV) was calculated by the following formula:

$$POV(meq/kg) = \frac{c(V_1 - V_2) \times 1000}{m} \tag{54.4}$$

where c is the concentration of standard sodium thiosulfate solution (mol/L), V_1 is the volume of standard sodium thiosulfate solution consumed by sample (ml), V_2 is the volume of standard sodium thiosulfate solution consumed by blank control (ml), and m is the sample quality (g).

54.3 Results and Discussion

54.3.1 Chromatograph and Calibration Curves

A representative HPLC chromatogram of the standards, the HPLC chromatograms of *TS* solution before and after acid hydrolysis was shown in Figs. 54.1, 54.2, and 54.3 respectively. In the range of 6.000–48.000 μg/ml for rutin, 3.500–28.000 μg/ml for gallic acid, 8.750–70.000 μg/ml for quercetin, 2.625–21.000 μg/ml for kaempferol, good correlation of linearity has been achieved. The regression equations and correlation coefficients determined for the references were

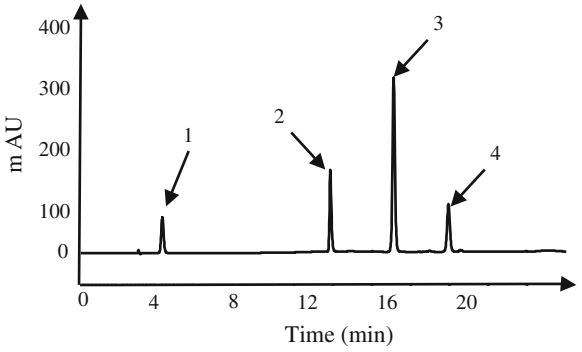

Fig. 54.1 HPLC of standard rutin (*1*), gallic acid (*2*), quercetin (*3*), and kaempferol (*4*)

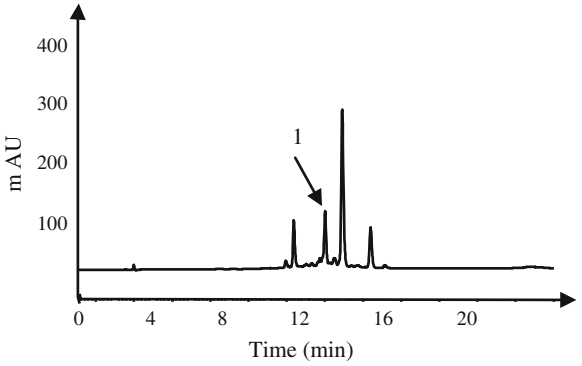

Fig. 54.2 HPLC of rutin (*1*) from extract of *TS* before acid hydrolysis

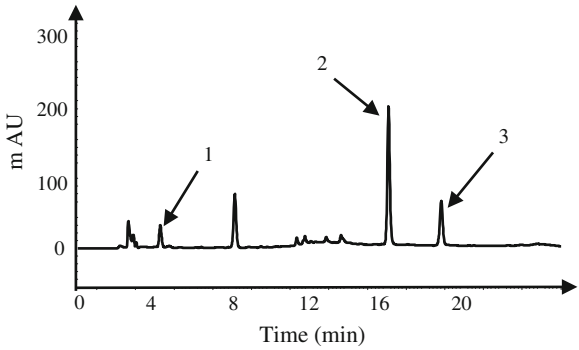

Fig. 54.3 HPLC of gallic acid (*1*), quercetin (*2*), and kaempferol (*3*) from extract of *TS* after acid hydrolysis

$y = 21175.7520x - 15359.9512$, $R^2 = 0.9997$, $y = 20332.2178x - 9613.2012$, $R^2 = 0.9998$, $y = 43707.5752x - 135139.4683$, $R^2 = 0.9995$, $y = 37216.9640x - 11854.6280$, $R^2 = 0.9999$.

54.3.2 Quantitative Determination of Phenolic Compounds

All prepared sample solutions were analyzed using the HPLC system. The content of each compound was determined by the corresponding regression equation and was summarized in Table 54.1.

54.3.3 Hydroxyl Radical Scavenging Activity

CP and PP of the *TS* extract both scavenged hydroxyl radicals significantly (Fig. 54.4). The hydroxyl radicals were generated by Fenton's type reaction with VC and citric acid to form the comparisons. At a concentration of 0.20 mg/ml, citric acid showed the highest scavenging activity among VC with (82.93 ± 0.05) % of hydroxyl radicals followed by PP (30.85 ± 0.80) % and CP (15.16 ± 0.06) %. CP showed a relatively lower hydroxyl radical scavenging activity compared with others, which was much lower than that of citric acid, only one-sixth of it. The results of CP and PP showed that *TS* extract was not quite effective on hydroxyl radical scavenging activity.

Table 54.1 Quantitative results of phenolic compounds from PP (mean ± standard deviation; $n = 5$)

Phenolic	Rutin	Gallic acid	Quercetin	Kaempferol
Percentage content (%)	1.55 ± 0.01	0.87 ± 0.02	2.27 ± 0.05	1.31 ± 0.01

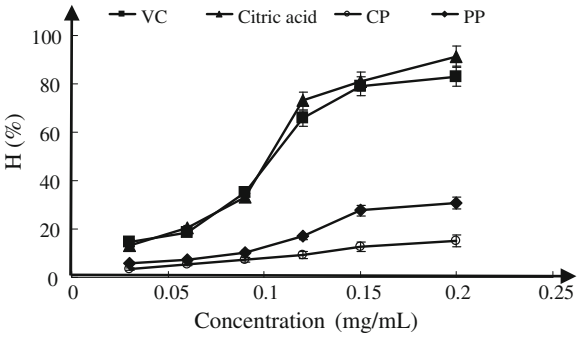

Fig. 54.4 Elimination capacity of sample solutions on Hydroxyl radical

54.3.4 Superoxide Radical Scavenging Activity

Superoxide radical, contributing to tissue damage and various diseases, is harmful to cellular components as a precursor of more reactive oxygen species [18]. The scavenging activities of the reaction solutions on superoxide radicals were shown in Fig. 54.5. It was found that the superoxide scavenging activities of the extract increased with the augment of their concentration. When the concentration went up to 0.20 mg/ml, the superoxide scavenging activities were (90.17 ± 1.42) % for VC, (85.37 ± 1.31) % for citric acid, (15.57 ± 1.13) % for CP, and (74.67 ± 0.75) % for PP. CP showed an obviously lower superoxide radical scavenging activity compared with the others. The superoxide radical scavenging activity of *TS* was improved after purification.

54.3.5 DPPH Radical Scavenging Activity

The DPPH scavenging activity of four sample solutions was shown in Fig. 54.6. VC displayed the highest DPPH radical scavenging activity of (89.99 ± 1.31) % at the concentration of 0.20 mg/ml, whereas CP and PP were showed

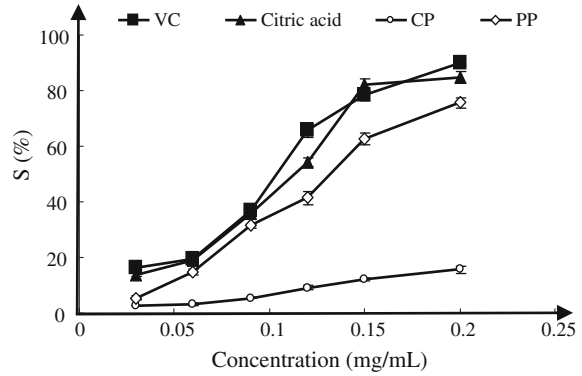

Fig. 54.5 Elimination capacity of sample solutions on superoxide radical scavenging activity

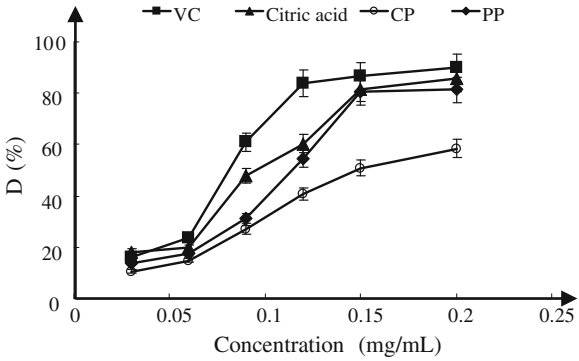

Fig. 54.6 Elimination capacity of sample solutions on DPPH

(58.41 ± 1.49) % and (81.32 ± 1.24) % inhibition at the same concentration, respectively. The scavenging effect of PP at a concentration of 0.20 mg/ml was nearly equal to that of 0.09 mg/ml citric acid (54.37 ± 0.61) %. The clearance increased by adding the concentration of PP, but the clearance became steady after the concentration of PP reached to 0.15 mg/ml concentration.

54.3.6 Development of Peroxide Value During Storage of Soybean Oil

The POV is a common method to determine the early stages of fat oxidation. According to Economou [19], the oil will become obviously rancid when the POV reaches 20–40 meq/kg. Oxidation of oil can be monitored by the development of POV. A continuous increase in POV with the increase in storage period was observed for all the samples (Fig. 54.7). The storage temperature was set at 65 °C to accelerate the reaction [20]. Initially, POV increased slowly, but it started increasing near fourth day of storage and went on increasing further with storage

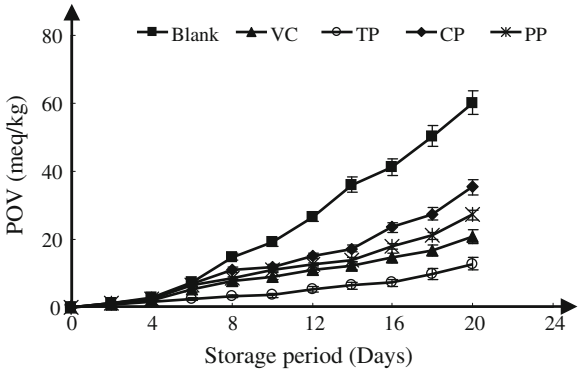

Fig. 54.7 Peroxide value (POV) of soybean oil samples under accelerated storage

period. Among the samples, TP as a useful natural antioxidant exhibited the lowest POV at all the stages, while CP showed the highest. The result in Fig. 54.7 was shown that addition of CP and PP resulted in effective protection in soybean oil system. 0.02 % by the addition of CP and PP, POV of control was decreased from (60.17 ± 0.11) meq/kg to (35.36 ± 0.54) meq/kg and (27.25 ± 0.46) meq/kg respectively after 20 days' storage at 65 °C. Thus, it could be concluded that *TS* extract had a stable antioxidant effect on edible oil.

54.4 Conclusion

In the present study, a simple, accurate, and rapid HPLC method was developed and this is the first publication of a HPLC determination of four kinds of phenolic compounds from extract of *TS* at the same time. The assay is reproducible, sensitive and has been fully validated. To seek a method for acid hydrolysis optimization, the influence on the acid hydrolysis procedure, the concentration of hydrochloric acid, the time of acid hydrolysis, and the temperature of acid hydrolysis were investigated. The optimum conditions were screened, which were performed under 4 mol/LHCl, 80 % methanol (in water, *V/V*) at water bath of 78 °C for 2 hours. The results of antioxidant activity of *TS* were indicated that PP had a strong capacity for scavenging DPPH free radical and superoxide anion radical but feeble effect on scavenging hydroxyl radical. The effect of scavenging was intensified as the addition of CP and PP increased. Meanwhile, PP played a notable role on the ability of antioxidant on soybean oil.

References

1. Wang PH (2008) *Toona sinensis* leaf extract alleviates hype-glycemia via altering adipose glucose transporter 4. Food Chem Toxicol 46:2554–2560
2. Liao JW, Chung YC, Yeh JY, Lin YC (2007) Safety evaluation of water extracts of *Toona sinensis* Roemor leaf. Food Chem Toxicol 45:1393–1399
3. Hsu HK, Yang YC, Hwang JH, Hong SJ (2003) Effects of *Toona sinensis* leaf extract on lipolysis in differentiated 3T3-L1 adipocytes. Kaohsiung J Med Sci 19:3855–3890
4. Hseu YC, Lin WH, Chang CS (2011) *Toona sinensis* (leaf extracts) inhibit vascular endothelial growth factor (VEGF)-induced angiogenesis in vascular endothelial cells. J Ethnopharmacol 134:111–121
5. Hsu YC, Chen SC, Yech YJ, Wang L (2008) Antioxidant activity of *Antrodia camphorata* on free radical-induced endothelial cell damage [J]. J Ethnopharmacol 118:237–245
6. Chang HC, Hung WC, Huang MS, Hsu HK (2002) Extract from the leaves of *Toona sinensis* Roemor exerts potent antiproliferative effect on human lung cancer cells. Am J Chinese Med 30:307–314
7. Hsieha TJ, Liub TZ, Chia YC et al (2004) Protective effect of methyl gallate from *Toona sinensis* (Meliaceae) against hydrogen peroxide-induced oxidative stress and DNA damage in MDCK cells. Food Chem Toxicol 42:843–850

8. Liao JW, Hsu CK, Wang MF, Hsu WM, Chan YC (2006) Beneficial effect of *Toona sinensis* on improving cognitive performance and brain degeneration in senescence-accelerated mice. Br J Nutr 96:400–407
9. Poon SL, Leu SF, Hsu HK, Liu MY, Huang BM (2005) Regulatory mechanism of *Toona sinensis* on mouse leydig cell steroidogenesis. Life Sci 76:1473–1487
10. Wang WY, Geng CH, Zhang YL, Ye JN (2007) CE-ED separation and determination of seasonal content variations of some active ingredients in *Toona sinensis* leaves. Chromatographia 66:697–701
11. Hsieh MM, Chen CY, Hsieh SL, Hsieh SF (2006) Separation of phenols from the leaves of *Toona sinensis* (Meliaceae) by capillary electrophoresis. J Chin Chem Soc 53:1203–1208
12. Krishnaiah D, Sarbatly R, Nithyanandam R (2010) A review of the antioxidant potential of medicinal plant species. Food Bioprod Process 14:240–246
13. Zhang LH, Li L, Li YX, Zhang YH (2008) In vitro antioxidant activities of fruits and leaves of pomegranate. Acta Horticulturae 765:31–34
14. Wen XB, Miao F, Zhou L, Zhang M, He Q (2012) In vitro antioxidant activity of *Parnassia wightiana* extracts. Chin J Nat Med 10(3):190–195
15. Alam MN, Bristi NJ, Rafiquzzaman M (2012) Review on in vivo and in vitro methods evaluation of antioxidant activity. Saudi Pharm J 4(2):77–86
16. Liu YJ, Chen D, Qiu HX (2012) In vitro antioxidant effect of the total flavones of *citrus aurantium* L. var *Daidai* Tanaka fruit. Chin J Mod Appl Pharm 29(2):99–103
17. Ahn JH, Kim YP, Seo EM, Choi YK, Kim HS (2008) Antioxidant effect of natural plant extracts on the microencapsulated high oleic sunflower oil. J Food Eng 84:327–334
18. Halliwell B, Gutteridge JC (1999) Free radicals in biology and medicine. Oxford University Processing 10(6):449–450
19. Economou KD, Oreopoulou V, Thomopoulos CD (1991) Antioxidant activity of some plant extracts of family Labiatae. J Am Oil Chem Soc 68(2):109–113
20. Wanasundra UN, Shahidi F (1994) Stabilization of canola oil with flavonoids. Food Chem 50:33–36

Chapter 55
Optimization of Submerged Culture for Exopolysaccharides Production by *Morcella esculenta* and its Antioxidant Activities In Vitro

Lihong Fu, Jinju Wang, Sheng Xu, Liming Hao and Yanping Wang

Abstract *Morcella esculenta* is an excellently edible and delicious morel mushroom found growing in China, Japan, and other Asian countries. Polysaccharides extracted from fungi have shown a variety of medical activities; however, the industrial large-scale production of *Morcella esculenta* can not be achieved now due to the natural conditions. So this paper is concerned with optimization of submerged culture conditions for mycelial growth and exopolysaccharides (EPS) production of *Morcella esculenta.* by airlift fermentation. And the antioxidant activities of EPS were revealed by various free radical scavenging assays in vitro. The optimal medium constituents were determined as follows: (g/L): glucose 20 g/L, peptone 4.5 g/L, KH_2PO_4 0.8 g/L, and $MgSO_4{\cdot}7H_2O$ 1.0 g/L. The optimum parameters of liquid culture were temperature 25 °C, cultivation time 5 d, rotary speed 140 rpm, and initial pH 6.0. This optimization strategy in shake flask culture leads to a mycelia yield of 4.93 ± 0.28 g/L, and EPS production of 1.65 ± 0.28 g/L, respectively. Under optimal culture conditions, the maximum mycelia and EPS concentration in a 7 L airlift tower loop reactor were 6.13 g/L and 2.12 g/L for the first report, which were considerably higher than those obtained in preliminary studies that indicated the EPS production was closely correlated to the mycelia growth by *Morcella esculenta*. Futuremore, the EPS demonstrated positively antioxidant potential on 1,1-diphenyl-2-picrylhydrazyl radical scavenging, reducing power, and hydroxyl radical scavenging. These findings may provide the basis for the popular use of EPS in functional food or medicine.

Keywords *Morcella esculenta* · Airlift fermentation · Exopolysaccharides · Antioxidant activity

L. Fu · J. Wang · S. Xu · Y. Wang (✉)
Key Laboratory of Food Nutrition and Safety, Ministry of Education, Tianjin University of Science and Technology, Tianjin 300457, People's Republic of China
e-mail: ypwang@tust.edu.cn

L. Hao
The Quartermaster Institute of the General Logistics Department of P.L.A, Beijing 100010, People's Republic of China

T.-C. Zhang et al. (eds.), *Proceedings of the 2012 International Conference on Applied Biotechnology (ICAB 2012)*, Lecture Notes in Electrical Engineering 249,
DOI: 10.1007/978-3-642-37916-1_55, © Springer-Verlag Berlin Heidelberg 2014

55.1 Introduction

Morcella esculenta is a species of fungus in the Morchellaceae family of the Ascomycota. It is one of the most readily recognized of all the edible mushrooms and medical fungi [1]. Modern medical research shows that *Morcell*a of fruiting body and mycelia has variety of medicinal activities, such as antioxidant, antivirus, anti-fatigue, immunomodulating, and anti-tumor [2–4]. However, commercial extract from the fruiting body of morel mushrooms has not been largely obtained till now. Submerged culture is viewed as a promising alterative for producing valuable substances. In recent years, stirring type fermenting reactor is usually used to study submerged culture of fungus such as *Ganoderma lucidum*, and *Paecilomyces tenuipes*, Such as *Ganoderma lucidum*, and *Paecilomyces tenuipes* [5, 6]. However, the shear stress usually causes adverse effects on mycelial morphology, product formation, and yields in stirred-tank reactors.

The airlift reactors do not require mechanical agitation and do not have mechanical parts, the shear stress is considerably less than that in stirred-tank reactors [7], so it is suitable for cultivation of fungus. However, it has not yet been reported on the fermentation of *Morcella esculenta* by airlift reactors.

Reactive oxygen species (ROS) include free radicals such as superoxide, hydroxyl, and peroxyl, which lead to oxidative stress related diseases like aging, cancer, and arteriosclerosis [8]. Therefore, it is increasingly becoming attractive in employing antioxidants from natural sources for natural products to replace synthetic antioxidants, due to their adverse effects and toxic properties. However, there have been few reports about the antioxidant activities of EPS from mushroom, such as *P. nebrodensis* and *Agaricus blazei* [9, 10]. This study will research antioxidant activities of EPS from *Morcella esculenta* by airlift fermentation.

The purpose of this study is to optimize the submerged culture conditions to produce the mycelia and EPS by *Morcella esculenta*. In order to maintain mycelial morphology, preserve exopolysaccharides formation, and enhance yields, the first research on the airlift tower loop reactor was used for large-scale submerged fermentation of *Morcella esculenta*. The information obtained is considered fundamental and useful to the development of the fungus cultivation on a large scale. At the same time, the study also determined the antioxidant activities of EPS in vitro. The antioxidant activity of EPS was investigated to provide some evidence for the development and application of functional food or polysaccharide drug.

55.2 Materials and Methods

55.2.1 Microorganism and Inoculums Preparation

The strain *Morcella esculenta* was maintained on potato dextrose agar (PDA) slants. The slants were incubated at 25 °C for 13 d. All strains were initially

incubated on PDA medium in a Petri dish for 13 d at 25 °C. A 10 units of active mycelia agar squares (0.5 cm × 0.5 cm) were obtained by a sterilized self-designed cutter and inoculated into a 500 mL Erlenmeyer flask containing 100 ml of the PDA seed culture medium at 140 rpm for 4 d.

55.2.2 Cultivation in Shake Flask

The flask culture experiment was performed in 500 mL containing 100 mL of media after inoculation 5 % (v/v) of the seed culture. The media compositions were determined according to the experiment design. The initial fermentation medium consisted of the following: 20 g/L glucose, 3 g/L peptone, 1.0 g/L $MgSO_4 \cdot 7H_2O$, 1.0 g/L KH_2PO_4 with natural pH. The culture was incubated at 25 °C on an Erlenmeyer flask 140 rpm for 5 d. All analyses were carried out in triplicate to minimize errors.

55.2.3 Fermentation in a Bioreactor

The fermentation medium was carried out in a fully instrumented and computer controlled 7 L airlift fermentator (Biotech, 10QS-2002, Shanghai). The fermentation medium was inoculated with 5 % (v/v) of the seed culture. The fermentation medium was the same with shake flask culture. Unless otherwise specified, fermentations were performed under the following conditions: temperature, 25 °C; ventilation, 0.5 Nm^3/h; initial pH 6.0; working volume, 5 L.

55.2.4 Analytical Methods

Mycelial biomass was determined gravimetrically after vacuum filtration and drying for 24 h at 50 °C to a constant weight. The resulting culture filtrate was vigorously mixed with 4 vol chilled ethanol and kept overnight at 4 °C. The precipitated exopolysaccharides was centrifuged at 5,438 g for 10 min discarding the supernatant. The precipitate of pure EPS was dried at 50 °C. Residual fructose in the fermentation liquid was assayed by the DNS method. The pH was measured with a digital pH meter.

55.2.5 Preparation of EPS

Under the optimal conditions of producing EPS, the culture filtrates of *Morcella esculenta* were collected by vacuum filtration and condensed to one-fourth of their

total volume using a rotary evaporator under reduced pressure at 55 °C. The crude polysaccharide fraction was obtained from the culture filtrates through precipitation with 4 vol chilled ethanol and left for overnight at 4 °C. The precipitated EPS was separated by centrifugation (5,348 × g for 10 min) and the EPS pallet was dissolved in distilled water at 60 °C, then repeated ethanol precipitation steps and dialyzed for 2d at 4 °C. The sample was lyophilized, which was applied to detect the antioxidant activities in vitro.

55.2.6 In Vitro Assay of Antioxidant Property of EPS

The antioxidant activities of EPS were measured by means of reducing power, free-radical, and hydroxyl radicals scavenging activity. The reducing power of EPS was determined by the method of Oyaizu [11]. The 1,1-diphenyl-2-picrylhydrazyl (DPPH) radical scavenging activity was measured according to the method of Bektas [12]. The assay of hydroxyl radical scavenging activity was assayed as described by Chung and Osawa [13].

55.3 Results and Discussion

55.3.1 Effects of Carbon and Nitrogen Sources

Culture medium is important to the yield of fermentation products, and carbon and nitrogen sources generally play a significant role because these nutrients are directly linked with cell proliferation and metabolite biosynthesis [14, 15]. Usually, carbohydrates are important carbon and energy sources for cultured cells. To choose the optimal carbon sources, various carbon sources were used to check their influence on growth conditions of the fungus. As shown in Fig. 55.1a, the glucose could promote mycelium formation and the highest amount of mycelia (3.90 ± 0.20 g/L) was obtained, which happened to be suitable carbon sources for the mycelial growth of several mushrooms in submerged cultures [16].

The effect of five different nitrogen sources on the yield of mycelium is summarized in Fig. 55.1b. The maximum mycelium production (about 4.61 ± 0.15 g/L) was detected when peptone was served as the nitrogen source for submerged cultivation of *Morcella esculenta*, which had significant advantage over the other four carbon sources. In agreement with other mushrooms, organic nitrogen sources were more favorable than inorganic nitrogen sources for the mycelial growth [17].

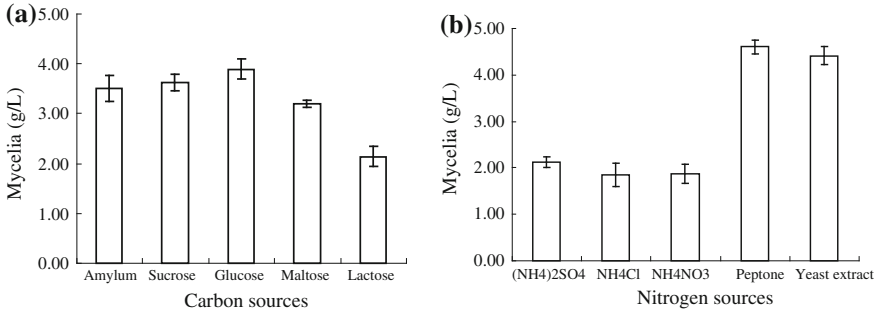

Fig. 55.1 Effects of carbon sources (**a**) and nitrogen sources (**b**) on the mycelial growth of *Morcella esculenta*. *Morcella esculenta* was cultured for 5 d at 25 °C in medium containing 2 % of carbon sources, 0.3 % nitrogen sources, 0.1 % KH_2PO_4, 0.1 % $MgSO_4{\cdot}7H_2O$, natural conditions of pH

55.3.2 *Effect of Initial Maltose and Yeast Extract Concentrations*

Based on the above results, glucose and peptone were selected as carbon and nitrogen sources in subsequent studies. The effect of initial glucose and peptone concentrations on mycelial growth was shown in Fig. 55.2a and b. The highest mycelial production was obtained at 20 g/L initial glucose. As to initial peptone concentration, 4 g/L was suitable for mycelial growth by submerged culture of *Morcella esculenta*.

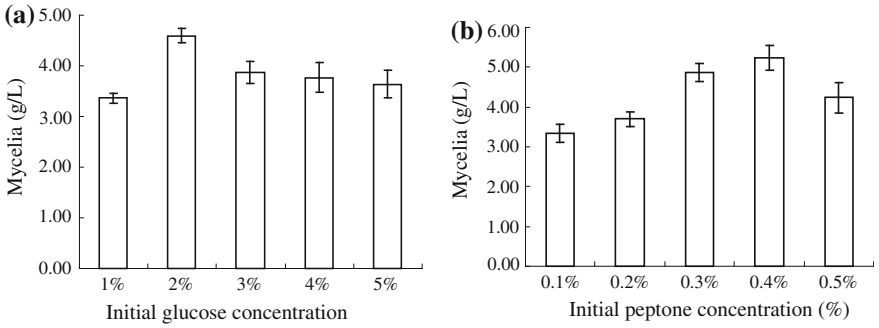

Fig. 55.2 Effects of initial glucose (**a**) and peptone concentrations (**b**) on mycelia production of *Morcella esculenta*. *Morcella esculenta* was cultured for 5 d at 25 °C in medium containing different concentration of peptone and glucose, 0.1 % KH_2PO_4, 0.1 % $MgSO_4{\cdot}7H_2O$, natural conditions of pH

55.3.3 Optimization of Initial pH and Temperature

In order to investigate the effect of initial pH on mycelial growth, *Morcella esculenta* was cultivated with different initial pH (4.0–9.0) in shake flask cultures. Maximum mycelium yield was obtained with an initial pH of 6.0 (Fig. 55.3a). It has been reported that the initial pH for mycelial growth was also low value for a wide variety of mushrooms [18, 19]. So we used an initial pH 6.0 for following studies.

The organism was cultivated at temperatures ranging from 20 to 30 °C. The result was shown in Fig. 55.3b, it was found that maximum yield was obtained at 25 °C for mycelium. We decided to use 25 °C as the fermentation temperature for the subsequent study because mycelium was the primary concern.

55.3.4 Orthogonal Matrix Method

To investigate the relationships between variables of medium components and their concentrations for mycelial growth and EPS production, the orthogonal matrix L9 (3^4) method could be used. According to preliminary experiments, we selected and varied three levels as shown in Table 55.1.

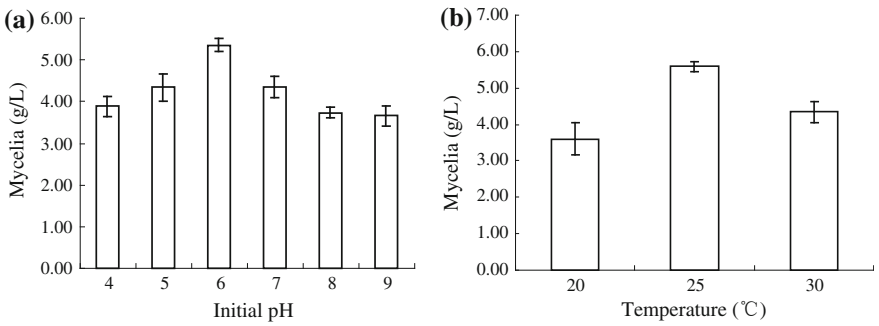

Fig. 55.3 Effect of initial pH (**a**) and temperature (**b**) on mycelia production of *Morcella esculenta*. *Morcella esculenta* was cultured for 5 d at 25 °C, the medium contain 2 % of glucose, 0.4 % of peptone, 0.1 % KH_2PO_4, 0.1 % $MgSO_4 \cdot 7H_2O$

Table 55.1 Experimental factors and their levels for orthogonal projects

Level	Glucose A(g/L)	Peptone B(g/L)	KH_2PO_4 C(g/L)	$MgSO_4 \cdot 7H_2O$ D(g/L)
1	15	3.5	0.8	0.8
2	20	4.0	1.0	1.0
3	25	4.5	1.2	1.2

Table 55.1 illustrates the factor allocations of the orthogonal matrix, in which the letters A, B, C, and D represent the glucose, peptone, KH_2PO_4, and $MgSO_4{\cdot}7H_2O$ concentration, respectively. In the course of optimization experiments, the fermentation temperature, initial pH, agitation rate, and culture period were fixed at 25 °C, 6.0, 140 rpm, and 5 d, respectively.

To obtain the optimal levels or composition of each factor, the intuitive analysis based on statistical calculation using the data in Table 55.2. The results were as follows: to obtain a high mycelial growth and EPS, the optimum composition were 20 g/L glucose, 4.5 g/L peptone, 0.8 g/L KH_2PO_4, 1.0 g/L $MgSO_4{\cdot}7H_2O$. To confirm these data, experiments were carried out using these nutrient concentrations and 4.93 ± 0.28 g/L of mycelial biomass and 1.65 ± 0.28 g/L of EPS were obtained that showed EPS production was closely correlative to the mycelia growth by *Morcella esculenta*. This implied that the selected conditions were the most suitable in practice.

According to the magnitude order of R (Max Dif), the order of effect of all factors on mycelial growth and EPS production could be determined. The order of effects of factors on mycelial growth was glucose > peptone > KH_2PO_4 > $MgSO_4{\cdot}7H_2O$. The order of effects of factors on EPS was glucose > peptone > $MgSO_4{\cdot}7H_2O$>KH_2PO_4. This result pointed out that the effect of glucose was more important than that of other nutrients.

55.3.5 Fermentation Results in Fermentator

Figure 55.4 shows the typical time courses of mycelial growth and EPS production in a 7 L airlift fermentator under optimal culture conditions. The exponential

Table 55.2 Application of L9 (3^4) orthogonal projects to the mycelia and EPS production by *Morcella esculenta*

Run	A	B	C	D	Mycelia (g/L)	EPS (g/L)
1	1	1	1	1	4.84 ± 0.26	1.33 ± 0.11
2	1	2	2	2	4.37 ± 0.35	1.05 ± 0.09
3	1	3	3	3	4.70 ± 0.21	1.48 ± 0.17
4	2	1	2	3	4.51 ± 0.16	1.25 ± 0.29
5	2	2	3	1	4.38 ± 0.40	1.42 ± 0.21
6	2	3	1	2	4.93 ± 0.28	1.65 ± 0.28
7	3	1	3	2	3.76 ± 0.56	0.87 ± 0.18
8	3	2	1	3	3.81 ± 0.39	0.94 ± 0.25
9	3	3	2	1	4.04 ± 0.38	1.27 ± 0.17
k_1'	1.29 ± 0.12	1.15 ± 0.19	1.31 ± 0.21	1.34 ± 0.16		
k_2'	1.44 ± 0.26	1.14 ± 0.18	1.19 ± 0.18	1.19 ± 0.18		
k_3'	1.03 ± 0.20	1.47 ± 0.21	1.26 ± 0.19	1.22 ± 0.24		
R′	0.41 ± 0.46	0.33 ± 0.39	0.05 ± 0.03	0.15 ± 0.07		

The results are represented as Mean ± SD of three replicates

growth phase of *Morcella esculenta* occurred from 0 to 6 d. The growth of cell biomass increased steadily for the first 5 d, with corresponding depletion of sugar concentration. The maximum mycelial biomass indicated 6.13 g/L after 5 d of fermentation. At the same time, highest EPS yield reached 2.12 g/L that indicated the EPS production was closely correlative to the mycelial growth by *Morcella esculenta*. And they showed slightly higher level than those in shake flask cultures. The initial pH of the fermentation broth of *Morcella esculenta* sharply ascended to 6.12 for the first 1d, then dropped for the rest of fermentation period.

55.3.6 Antioxidant Activity of EPS

Antioxidant activities have been performed to various reactions and mechanism. In this experiment, the antioxidative activities of EPS from *Morcella esculenta* in vitro were evaluated using different biochemical methods of reducing power activity, DPPH radical, and hydroxyl radical scavenging assay which was compared with control ascorbic acid.

Figure 55.5a shows that the hydroxyl radical scavenging activity of EPS was concentration-dependent and higher than ascorbic acid at the dosage range of 0–1.3 mg/mL, the scavenging capacity of EPS rapidly increased with the continually increasing its concentrations. The EC50 value of EPS for hydroxyl radical

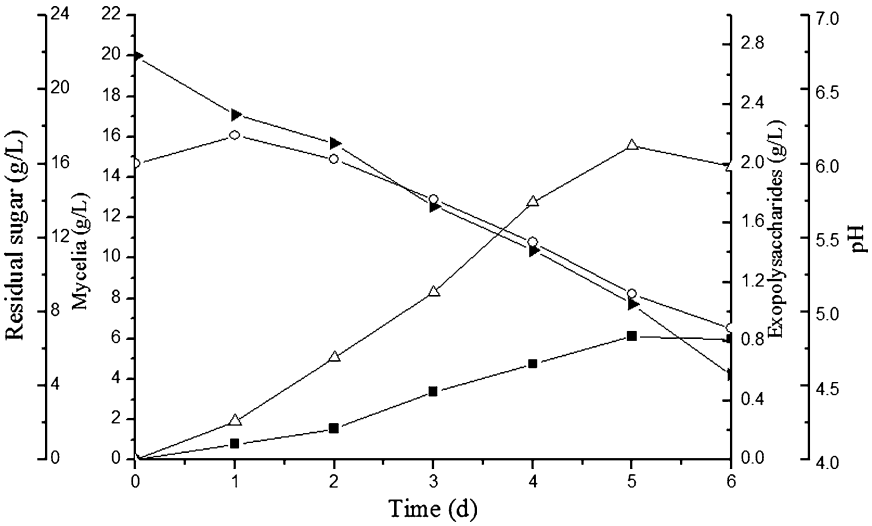

Fig. 55.4 Time courses of submerged culture of *Morcella esculenta* in 7 L fermentator ■ Mycelia; △ Exopolysaccharides; ▲ Residual sugar; ○ pH; *Morcella esculenta* was cultured for 6 d at 25 °C in medium containing 2 % of glucose, 0.45 % of peptone, 0.08 % KH_2PO_4, 0.12 % $MgSO_4 \cdot 7H_2O$, pH 6.0

scavenging activity was 0.86 ± 0.02 mg/mL, which was significantly lower than ascorbic acid (2.94 ± 0.04 mg/mL). Paulrag [20] reported that the scavenging ability of EPS from *Streptococcus phocae PI80* on hydroxyl radicals was 50 ± 1 % at 0.9 mg/mL, which was almost close with this study. It was reported that the hydroxyl radical is another important free radical, which can react with all biomacromolecules in living cells and induce severe damage to the adjacent macromolecule [21].

As shown in Fig. 55.5b, EPS and ascorbic acid to DPPH radical scavenging activity were directly proportional to their concentrations. The EC50 values of DPPH radical scavenging activity were 1.09 ± 0.03 mg/mL for EPS and 0.002 ± 0.001 mg/mL for ascorbic acid. Although the inhibition percentage of EPS was slightly lower than that of ascorbic acid, it reached 66.6 ± 1.49 % at 1.3 mg/mL, indicating that the EPS affects the scavenging of the free-radical.

It can be seen from Fig.55.5c that the reducing capacity of EPS was remarkably lower than that of ascorbic acid. The reducing power (absorbance at 700 nm) of EPS was 0.16 ± 0.02 at a dose of 0.163 mg/mL, slightly higher than that (0.13 ± 0.05) at 0.2 mg/mL in *P. nebrodensis* [22], showing that the EPS from *Morcella esculenta* has potential antioxidant activities. During the assay of

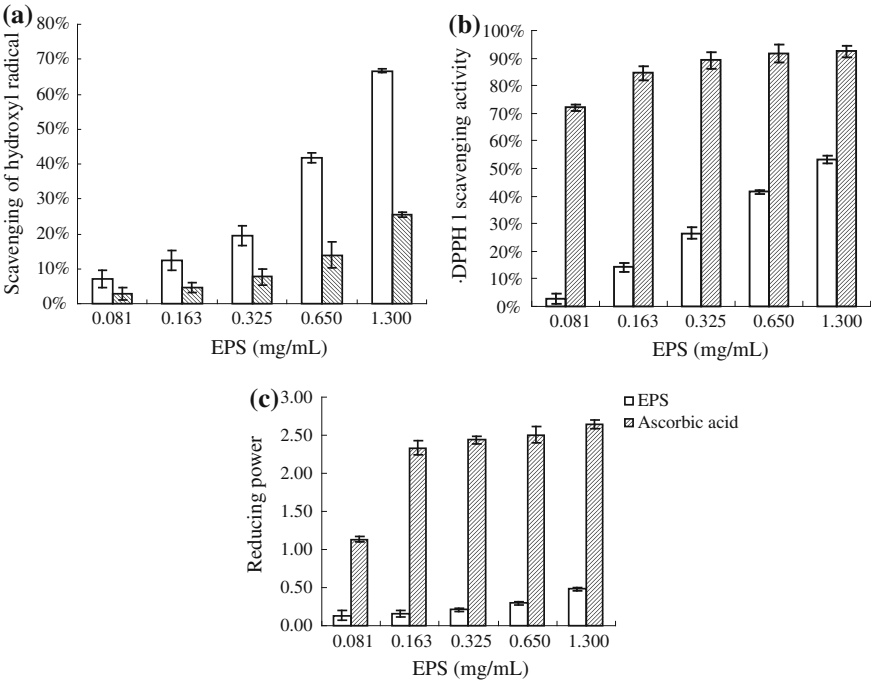

Fig. 55.5 Scavenging effect of EPS from *Morcella esculenta* and ascorbic acid on hydroxyl radical (**a**), DPPH radical (**b**) and reducing power (**c**), the results are represented as Mean ± SD of the three independent data

reducing power, the capability of antioxidant compounds to reduce Fe^{3+}/ferricyanide complex to its ferric form, which was monitored by absorbance of Perl's Prussian blue formation at 700 nm [23].

55.4 Conclusion

The process parameters for submerged cultivation of *Morcella esculenta*, including carbon source, nitrogen source, initial pH and temperature, were optimized to obtain mycelium and EPS. The fermentation process was then scaled up to the 7 L airlift fermentator. To date, there was no report on airlift cultivation of mycelia and EPS by *Morcella esculenta* and antioxidant activities of EPS in vitro. The result showed *Morcella esculenta* could be effectively cultivated in airlift fermentation for mycelial growth and exopolysaccharide production. Mycelium and EPS were much higher than that in shake flask culture. The fundamental information obtained in this work was beneficial for further development of *Morcella esculenta* cultivation. In vitro antioxidant assays showed strong antioxidant capability of EPS, especially scavenging of hydroxyl and DPPH radicals. The results suggest that EPS from *Morcella esculenta* may be a better alternative natural source with antioxidant activity as healthy food grade adjunct. However, the biological activities and antioxidant mechanism of EPS need to be investigated in future.

Acknowledgments The authors gratefully acknowledge the nancial support by the National Natural Science Foundation of China (No. 31171662).

References

1. Negi CS (2006) Morels (*Morchella* spp.) in Kumaun Himalaya. Nat Prod Radian 5:306–310
2. Nitha B, Janardhanan KK (2008) Aqueous-ethanolic extract of morel mushroom mycelium *Morchella esculenta*, protects cisplatin and gentamicin induced nephrotoxicity in mice. Food Chem Toxicol 46(9):3193–3199
3. Dong Y, Gao X, Li TT et al (2008) Study on in vitro antioxidation of *Marasmius androsaceus* extracellular polysaccharides. Food Res Dev 29:45–48
4. Wasser SP (2002) Medicinal mushrooms as a source of antitumor and immunomodulating polysaccharides. Appl Microbiol Biotechnol 60(3):258–274
5. Berovic M, Habijanic J, Zore I et al (2003) Submerged cultivation of *Ganoderma lucidum* biomass and immunostimulatory effects of fungal polysaccharides. J Biotechnol 103(1):77–86
6. Xu CP, Kim SW, Hwang HJ et al (2003) Optimization of submerged culture conditions for mycelial growth and exo-biopolymer production by *Paecilomyces tenuipes C240*. Process Biochem 38:1025–1030
7. Prihardi K, Kengo K, Toshiharu I et al (2002) Production of ε-polylysine in an airlift bioreactor (ABR). J Biosci Bioeng 93:274–280
8. Darley UV, Halliwell B (1996) Blood radicals: relative nitrogen species relative oxygen species transition metal ions and the vascular system. Pharm Res 13(5):649–662

9. Liu X, Zhou B, Lin R et al (2010) Extraction and antioxidant activities of intracellular polysaccharide from *Pleurotus* sp. mycelium. Int J Biol Macromol 47(2):116–119
10. Atsuko N, Takashi TJ, Hideaki H (2011) Ipomoea batatas and *Agarics blazei* ameliorate diabetic disorders with therapeutic antioxidant potential in streptozotocin-induced diabetic rats. J Clin Biochem Nutr 48(3):194–202
11. Oyaizu M (1986) Studies on products of browning reactions: antioxidative activities of products of browning reaction prepared from glucosamine. Jpn J Nutr 44:307–315
12. Bektas T, Munevver S, Akpulat HA et al (2006) Screening of the antioxidant potentials of six Salvia species from Turkey. Food Chem 95:200–204
13. Chung SK, Osawa T (1998) Hydroxy radical scavengers from white mustard (*Sinapis alba*). Food Sci Biotechnol 7:209–213
14. Kim SW, Xu CP, Hwang HJ et al (2003) Production and characterization of exopolysaccharides from an enthomopathogenic fungus *Cordyceps militaris NG3*. Biotechnol Prog 19(2):428–435
15. Zou X (2005) Optimization of nutritional factors for exopolysaccharide production by submerged cultivation of the medicinal mushroom *Oudemansiella radicata*. World J Microb Biot 21:1267–1271
16. Jonathan SG, Fasidi IO (2001) Effect of carbon, nitrogen and mineral sources on growth of *Psathyerella atroumbonata* (Pegler), a nigerian edible mushroom. Food Chem 72:479–483
17. Jung IC, Kim SH, Kwon YI et al (1997) Cultural condition for the mycelial growth of *Phellinus igniarius* on chemically different medium and grains. Korean J Med Mycol 25:133–142
18. Fang QH, Zhong JJ (2002) Effect of initial pH on production of ganoderic acid and polysaccharide by submerged fermentation of *Ganoderma lucidum*. Process Biochem 37:769–774
19. Winder RS (2006) Cultural studies of *Morchella elata*. Mycol Res 110(Pt 5):612–623
20. Kanmani P, Kumar RS, Yuvaraj N et al (2011) Production and purification of a novel exopolysaccharide from lacticacid bacterium *Streptococcus phocae PI80* and its functional characteristics activity in vitro. Bioresource Technol 102:4827–4833
21. Gülçin I (2006) Antioxidant and antiradical activities of L-carnitine. Life Sci 78(8):803–811
22. Sheng W, Wu P, Guo H et al (2008) Studies on anti-oxidation activity of polysaccharide and exopolysaccharide extracted from *Pleurotus nebrodensis*. Forest prod Special Chi 94:8–10
23. Chung YC, Chang CT, Chao WW et al (2002) Antioxidative activity and safety of the 50 ethanolic extract from red bean fermented by *Bacillus subtilis IMR-NK1*. J Agric Food Chem 50(8):2454–2458

Chapter 56
Effect of Trehlose on Anti-Aging of Steamed Bread

Yunfeng Hu, Xiujuan Li and Qingli Zhou

Abstract By the method of adding trehalose, mixtures (trehalose with the enzyme preparation) to delay the aging of steamed bread, and using Texture Analyzer with texture analysis to evaluate the quality of steamed bread. The results showed that trehalose can improve steamed bread specific volume, hardness, and springiness and it can also improve the initial quality of steamed bread and slow down the aging of steamed bread at the concentration of 3 %; Compared with using the trehalose or Novamyl® Steam alone, further adding 50 ppm of enzymes after added 3 % trehalose can have a better improvement on the specific volume, hardness, and resilience of steamed bread and can better delay the aging of steamed bread.

Keywords Steamed bread · Trehalose · Aging · Texture

56.1 Introduction

Steamed bread is one of Chinese traditional features, and it is the representative of Chinese food in baking. Flour is the main raw material for making steamed bread, and fermented with yeast in a certain temperature and humidity, and then the flour is formed and steamed, the steamed bread could be got with the shape of the hemispherical or strip. The steamed bread with good quality has a bright white surface, soft texture, flexible, and chewing the sweet. However, after 24 h storage, steamed bread will soon be aging, which could lead to structural hardening, loss of soft texture, and after aging the starch is harden and difficult to re-water, digest,

Y. Hu (✉) · X. Li
Tianjin University of Science and Technology, Tianjin 300457, China
e-mail: hu-yf@163.com

Q. Zhou
Tianjin Center of Food Processing Engineering, Tianjin 300457, China

T.-C. Zhang et al. (eds.), *Proceedings of the 2012 International Conference on Applied Biotechnology (ICAB 2012)*, Lecture Notes in Electrical Engineering 249,
DOI: 10.1007/978-3-642-37916-1_56, © Springer-Verlag Berlin Heidelberg 2014

and absorb. Therefore, if manufacturers want to make steamed bread to be industrial products with large-scale production and sales, the main issues is to prevent the steamed bread hardens in the logistics process. Studies have shown that the crystallization of amylopectin and the interaction between protein and starch molecules are the main factor for the steamed bread's hardening, and add enzymes, improvers, fat soy flour, saccharides, hydrocolloids, etc., can be appropriately delay the aging of steamed bread [1–7].

Trehalose, also known as yeast sugar, is a kind of non-reducing disaccharide composed of two glucose molecules through the semi-acetal hydroxyl, and widely present in bacteria, algae, yeast, lower plants, insects, and other invertebrates. Trehalose has a wide range of applications in the food, pharmaceutical industrial, cosmetic, and agricultural fields since it is chemical stability, non-toxic, moderate sweetness, and can protect the organism's organization and function of macr-molecules and the activity in high temperature, freezing, drying dehydration, high osmotic pressure, and other adverse circumstances [8, 9]. It has been reported that trehalose may very well prevent the variability of proteins in frozen, refrigerated or dry condition. Adding trehalose in the protein-containing foods can be very effective in protecting the natural structure of protein molecules; moreover, the flavor and texture of the food remain unchanged [10–16].

This paper aims to measure the changes in physical properties of steamed bread during storage at room temperature by Texture Analyzer, by which to characterize the effects of trehalose on steamed bread's aging, expect to provide a new solution for the preservation and anti-aging of the steamed bread.

56.2 Experimental Materials and Methods

56.2.1 Materials

Flour: Jinniu household flour; Yeast: Anqi active dry yeast; Sugar: commercially available white sugar; Trehalose: Sinozyme Biological Engineering Co., Ltd; Novamyl® Steam: Novozymes Biotechnology Co., Ltd. All of the above materials are food-grade.

56.2.2 Main Instruments and Equipment

Texture Analyzer (TA.XT.Plus Texture Analyzer, British Stable Micro System Company); Incubator (MJ-180 mold incubator, Shanghai Hede Experimental Equipment Co., Ltd); Electronic balance (JJ precision electronic balance, Changshu Shuangjie Test Instrument Factory).

56.2.3 Methods

56.2.3.1 Basic Formula of Steamed Bread

The basic recipe of steamed bread is as Table 56.1.

56.2.3.2 Process of Making Steamed Bread

Activate the yeast with sugar (5 min, 38 °C) → weigh flour and knead into dough → fermentation at 38 °C for 2 h → knead again → forming → fermentation at 38 °C for 30 min → steaming 20 min → finished product

56.2.3.3 Determination of Indicators

Determination of specific volume: Weighing a whole steamed bread which have been cooled for 1 h after steaming, get the quality. Using the method of replacement of the measurement with millet to measure the volume of steamed bread and accurate to 0.5 ml. Take 3 of representative sample to be measured, take the average of measured data of three times as a result.

Specific volume of steamed bread (ml/g) = volume of steamed bread (ml)/quality of steamed bread (g).

Determination of physical properties: Using TA-XT-plus type Texture Analyzer, select the cylindrical probe P/36R, TPA model for testing conditions, pre-test speed 1 mm/s, test speed 5 mm/s, after test speed 5 mm/s, settling time 3 s, test mode: pushing, downward pressure on the distance of 10 mm, Compression rate of 40 %. Take 3 of each sample to be measured, take the average of measured data of three times as a result. Select the hardness, springiness, resilience in the resulting data as valid data [17].

56.2.3.4 Experimental Methods

(1) According to the amount of flour to add 1, 2, 3 % of the trehalose into flour. After fermentation, knead again, forming, fermentation again, steaming to get different products of steamed bread. After cooling, take them into plastic trays,

Table 56.1 The basic recipe of steamed bread

Ingredients	Quality of ingredients (m/g)
Flour	500
Yeast	5
Water	265

and sealed with plastic wrap, then storage at room temperature (about 20 °C). Take the steamed bread which was not added trehalose as the control group, then take the samples to measure at certain time in the 96 h of storage and repeat 3 times for measuring. The evaluation of measuring includes hardness, resilience, springiness, and specific volume.

(2) According to the amount of flour to add 3 % of trehalose and 50 ppm of Novamyl® Steam into flour. After fermentation, knead again, forming, fermentation again, steaming to get different products of steamed bread. After cooling, take them into plastic trays, and sealed with plastic wrap, then storage at room temperature (about 20 °C). Take the steamed bread which were not added trehalose as the control group, then take the samples to measure at certain time in the 48 h of storage and repeat 3 times for measuring. The evaluation of measuring includes hardness, resilience, springiness and specific volume.

56.3 Results and Discussion

56.3.1 The Effect of Trehalose on Specific Volume of Steamed Bread

The effect of trehalose on specific volume of steamed bread is shown in Table 56.2. Generally, trehalose can increase the specific volume of steamed bread. Specifically, the specific volume of steamed bread has a positive correlation with the amount of trehalose. The specific volume is 2.76, which is more than 2.75, when the 2 % of trehalose is added. Particular, after 3 % of trehalose is add, the specific volume of Steamed bread reaches to 2.78, which is increased more than 5 % compared with the control group. The addition of trehalose could happen to increase the specific volume of steamed bread significantly.

56.3.2 The Effect of Trehalose on Hardness of Steamed Bread

Hardness is the measure of how resistant solid matter is to various kinds of permanent shape change when a force is applied. Hardness value is the first time to wear red when the pressure of the sample peak and it is a number from a hardness

Table 56.2 The effect of trehalose on specific volume of steamed bread

Samples	Specific volume
Blank	2.65
1 % of Trehalose	2.70
2 % of Trehalose	2.76
3 % of Trehalose	2.78

testing scale that indicates the ability of a material to resist scratching and penetration. In food science the property of matter commonly described as the resistance of external force, such as squeeze pressure and chewing force. In general, hardness is negatively correlated with quality of the steamed bread. The bigger the hardness value, the greater resistance it has to deformation, and the greater difficult to be chewed.

The relationship between hardness value and time is shown in Fig. 56.1. On the whole, the hardness of steamed bread has a time-dependent increase and a negative correlation with the concentration of trehalose. However, during the first 48 h, the hardness increases greatly. After 48 h, a slight increase in the hardness of steamed bread is observed in Fig. 56.1. During the first 6 h, there is slight difference between the hardness of the control group and that of the steamed bread added 3 % trehalose, however, the difference significantly increases after 48 h. Therefore, the trehalose could improve the percentage changes in the hardness of steamed bread.

56.3.3 *The Influence of Trehalose on Resilience of Steamed Bread*

Resilience of the steamed bread is closely related with its quality. The relationship can be describe as the greater the resilience value of the steamed bread is, the more soft, bouncy, sty, and refreshing the steamed bread tastes.

These curves are shown in Fig. 56.2 are extraordinarily similar. The first stage, which can be characterized by a major change in resilience of the steamed bread, mainly take place in the first 24 h, and the four groups changes similarly. After 48 h, a slight change happens to the four groups. In the storage process of steamed bread, the resilience of the group, in which the 3 % trehalose is added, is slightly

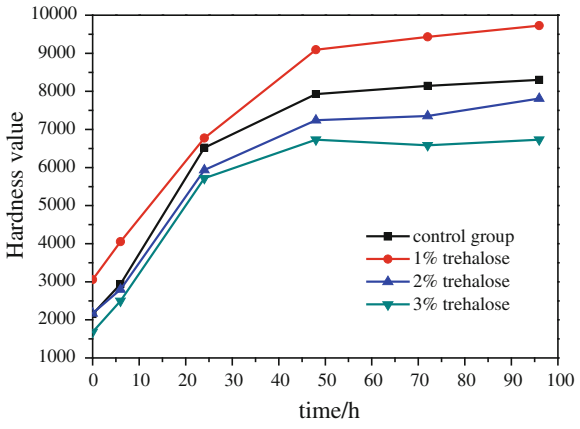

Fig. 56.1 The relationship between hardness value and time

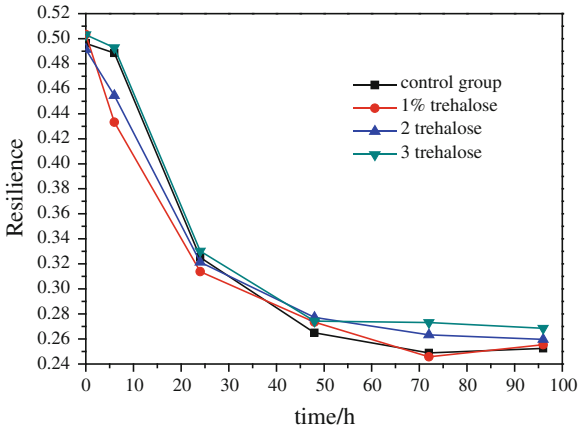

Fig. 56.2 The relationship between resilience and time

higher than that of the control group. On the whole, it is not efficient way of improvement the quality of the steamed bread by increasing the resilience value of the steamed bread with adding trehalose.

56.3.4 The Influence of Trehalose on Springiness of Steamed Bread

The springiness of steamed bread is also important to the quality and taste of it, and the principle is just like the relationship between resilience of steamed bread and its quality described above.

The relationship between springiness of steamed bread and time is shown in Fig. 56.3. The trehalose has a great influence on the springiness of steamed bread, and the springiness value increases as the increase in the amount of added trehalose, and it decreases with time extending. Compared with the experimental groups, the control group varies slightly after 24 h, however, the experimental groups vary greatly and differently. As is shown in Fig. 56.3, the curves of groups, which is added 2 and 3 % trehalose respectively, is always above the curve of the control group. This indicates that there is some extent incensement in springiness of steamed bread in these two groups, compared with the control group. However, the group added 1 % trehalose, in which the springiness is bigger than that of control group before 65 h and it is less than that of control group after 65 h, is much different from other experimental groups. Therefore, the added trehalose can improve the springiness of the steamed bread, and the optimum amount of trehalose is 3 %.

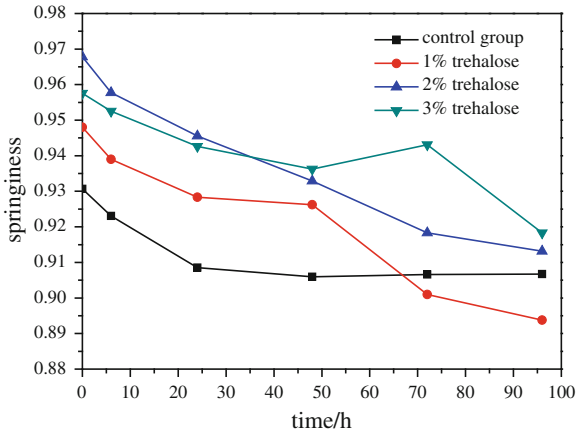

Fig. 56.3 The relationship between springiness of steamed bread and time

56.3.5 The Influence of Mixtures of Trehalose and Novamyl® Steam on Quality of Steamed Bread

Novamyl® Steam is a kind of special anti-aging enzyme for steamed bread and produced by Novozymes (China) Investment Co., Ltd, its main ingredient is malt amylase then supplemented by other enzymes or additives which could improve the quality of steamed bread and slow down the aging of steamed bread. In previous experiments by our group, we have studied the effect of improving the quality of steamed bread from Novamyl® Steam, the results show that during the three concentrations of 25, 50, 75 ppm, the concentrations of 50 ppm have the best improvement on the quality of steamed bread. In this paper, adding 3 % trehalose and 50 ppm of Novamyl® Steam together, to study the affect on the quality of steamed bread and anti-aging effect by using Novamyl® Steam in conjunction with trehalose.

Experimental results show that mixtures can improve the quality of steamed bread and delay steamed bread's aging better than trehalose. Mixtures can make the specific volume of steamed bread 15.2 % higher than the control group's leading to the initial hardness of steamed bread got a good improvement. The hardness value of steamed bread which added mixtures is significantly lower than that of control group during the storage period, and 19.3 % lower than that of control group after 48 h. Mixtures can also significantly improve the initial resilience of steamed bread and have the resilience of steamed bread always higher than that of control group in the storage process; mixtures can also significantly improve the initial springiness of steamed bread and make the steamed bread which has been stored for 24 h has the same springiness value as control group's which only have been stored for 6 h.

56.4 Results and Discussion

(1) Trehalose plays a good role on improving the specific volume, hardness and springiness, it can improve the initial quality of steamed bread and slow down the aging of steamed bread, and 3 % is the best dosage of the three concentrations of trehalose of 1, 2, 3 %. Trehalose could play a role on the aging of steamed bread and may has a relationship with the ability that trehalose can protect organisms and biological macromolecules non-specifically.
(2) Adding 50 ppm of Novamyl® Steam and 3 % of trehalose together can make marked improvement in the specific volume, hardness, resilience, and springiness of steamed bread than use trehalose or Novamyl® Steam alone, especially in the improvements in specific volume, hardness, and resilience of steamed bread, so it can delay the aging of steamed bread better.

References

1. Kerch G, Zicans J, Meri RM (2010) The effect of chitosan oligosaccharides on bread staling. J Cereal Sci 52:491–495
2. Sim SY, Aziah AAN, Cheng LH (2010) Characteristics of wheat dough and Chinese steamed bread added with sodium alginates or konjac glucomannan. Food Hydrocolloids 25:951–957
3. Gomes-Ruffi CR, da Cunha CR, Almeida EL et al (2012) Effect of the emulsifier sodium stearoyl lactylate and of the enzyme maltogenic amylase on the quality of pan bread during storage. LWT Food Sci Technol 49:96–101
4. Guarda A, Rosell CM, Benedito C et al (2004) Different hydrocolloids as bread improvers and antistaling agents. Food Hydrocolloids 18:241–247
5. Moayedallaie S, Mirzaei M, Paterson J (2009) Bread improvers: comparison of a range of lipases with a traditional emulsifier. Food Chem 122:495–499
6. Mouliney M, Lavery B, Sharma R et al (2011) Waxy durum and fat differ in their actions as improvers of bread quality. J Cereal Sci 54:317–323
7. Timasheff SN (1993) The control of protein stability and association by weak interactions with water: how do solvents affect these processes? Annu Rev Biophys Biomol Struct. doi:10.1146/annurev.bb.22.060193.000435
8. Sasano Y, Haitani Y, Hashida K et al (2011) Simultaneous accumulation of proline and trehalose in industrial baker's yeast enhances fermentation ability in frozen dough. J Biosci Bioeng 113:592–595
9. Sola-Penna M, Meyer-Fernandes JR (1998) Stabilization against thermal inactivation promoted by sugars on enzyme structure and function: why is trehalose more effective than other sugars?. Arch Biochem Biophys doi:10.1006/abbi.1998.0906
10. Parrou JL, Jules M, Beltran G et al (2005) Acid trehalase in yeasts and filamentous fungi: localization, regulation and physiological function. FEMS Yeast Res 5:503–511
11. Kim YS, Huang WN, Du GC et al (2008) Effects of trehalose, transglutaminase, and gum on rheological, fermentation, and baking properties of frozen dough. Food Res Int 41:903–908
12. Gadd GM, Chalmers K, Reed RH (1987) The role of trehalose in dehydration resistance of Saccharomyces cerevisiae. FEMS Microbiol Lett. doi:10.1111/j.1574-6968.1987.tb02551.x
13. Gujral HS, Rosell CM (2003) Functionality of rice flour modified with a microbial transglutaminase. J Cereal Sci 39:225–230
14. Hino A, Mihara K, Nakashima K (1990) Trehalose levels and survival ratio of freeze-tolerant versus freeze-sensitive yeasts. Appl Environ Microbiol 56:1386–1391

15. Hsu K, Hoseney RC, Seib PA (1979) Frozen dough.2. Effects of freezing and storing conditions on the stability of yeasted doughs. Cereal Chem 56:424–426
16. Huang WN, Kim YS, Li XY et al (2008) Rheofermentometer parameters and bread specific volume of frozen sweet dough influenced by ingredients and dough mixing temperature. J Cereal Sci 48:639–646
17. Huang S, Quail K, Moss R et al (1995) Objective methods for the quality assessment of northern-style chinese steamed bread. J Cereal Sci 21:49–55

Chapter 57
Development of HPLC Method for Determination of the Content of Tyramine in Rice Wine

Xuewu Guo, Lina Li, Yefu Chen and Dongguang Xiao

Abstract The method of detecting the contents of tyramine in rice wine by HPLC was developed. The chromatographic separation was performed in an analytical column, C18 (4.6 × 150 mm ID, 5 μm) and a UV detector was used with wavelengths at 278 nm. The mobile phase was 0.02 mol/L disodium hydrogen-acetonitrile (v: v 85:15), 10 % phosphoric acid adjusted pH = 8.4, with a flow rate was 0.8 ml/min, the column temperature was 35 °C. The results showed that the correlation coefficients were greater than 99.9 %, the limit of detection was 0.7 mg/L, the repeatability (RSD = 1.1 %), reproducibility (RSD = 2.91 %), and accuracy were of satisfying quality. The recovery was more than 97 %. This method has been successfully applied for the content of tyramine in rice wine.

Keywords Tyramine · HPLC · Rice wine

57.1 Introduction

Biogenic amines are low molecular weight and formed by the descarboxylation reaction from corresponding free amino acids by microbial activity in many foods and especially in fermented food products (Fig. 57.1) [1, 2].

Tyramine, 4-(2-aminoethyl)phenol, is one of the hazards and highest content in biogenic amines [3]. Trace amounts of Tyramine do not usually represent any health hazard to individuals. For many drugs synthesis, Tyramine is the necessary initial substance [4], and is also one of the important components of active cells and has obvious dilation and shrinkage effect to muscle and vascular. Large

X. Guo · L. Li · Y. Chen · D. Xiao (✉)
Key Laboratory of Industrial Fermentation Microbiology, Ministry of Education Tianjin Industrial Microbiology Key Lab, College of Biotechnology, Tianjin University of Science and Technology, Tianjin 300457, People's Republic of China
e-mail: xiao99@tust.edu.cn

T.-C. Zhang et al. (eds.), *Proceedings of the 2012 International Conference on Applied Biotechnology (ICAB 2012)*, Lecture Notes in Electrical Engineering 249,
DOI: 10.1007/978-3-642-37916-1_57, © Springer-Verlag Berlin Heidelberg 2014

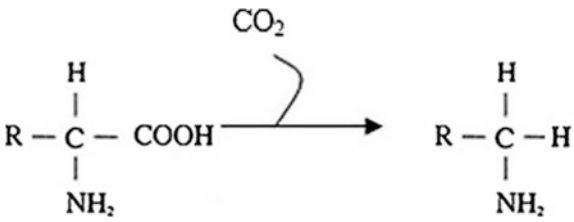

Fig. 57.1 The main production way of biogenic amines in fermented food. The catalyst of this reaction is tyrosine decarboxylation enzymes

amounts of tyramine can make the person elevated blood pressure and even poisoning [5–8].

Many methods have been developed for the determination of biogenic amines in fermented foods, for example, gas chromatography, capillary electrophoretic method (CE), thin-layer chromatography (TLC), and high performance liquid chromatography (HPLC) [9]. At present, HPLC method is the most widely used and convenient method. But, most of the biogenic amines need be derived by HPLC for lacking fluorescence or ultraviolet absorption [10–13]. Angela used dansyl chloride as derived reagent before chromatographic detection by HPLC to determine the content of eight biogenic amines in Chilean young varietal wines [14]. Mardiana developed a method to determine of the biogenic amines (tryptamine, putrescine, cadaverine, histamine, tyramine, spermidine) in food samples using dansyl chloride as derived reagent by HPLC [15]. These methods have high cost and time-consuming, and the repeatability and reproducibility are not satisfying.

In this paper, a rapid and accurate method of determination without derivative action of tyramine content in rice wine was developed. The method was based on the benzene structure with the ultraviolet absorption characteristics in tyramine, and it was necessary to ensure the quality of rice wine.

57.2 Materials and Methods

57.2.1 Materials

Tyramine, HPLC grade, purity is greater than 99.9 %, was purchased from Sigma (St. Louis, MO, USA). Acetonitrile, HPLC grade, was obtained from KaiTong (Tianjin, China). Phosphoric acid, 85 %, analytically pure (Tianjin, China), Sodium phosphate dibasic dodecahydrte, analytically pure, (Tianjin, China); Distilled water.

57.2.2 Solution Preparation

Tyramine standard fluid (mother solution): take 10 mg tyramine (HPLC grade, purity is greater than 99.9 %) with the capacity of mobile phase to 10 mL

as 1 mg/mL tyramine standard fluid; The mobile phase: 0.02 mol/L disodium hydrogen-acetonitrile (v: v 85:15), 10 % phosphoric acid adjusted pH = 8.4; 10 % Phosphoric acid: take 85 % Phosphoric acid 10 mL to the capacity of 85 mL with distilled water; 0.02 mol/L disodium hydrogen: take sodium phosphate dibasic dodecahydrte 0.7160 g and add water to dissolve to 100 mL; rice wine fermented liquid, centrifugal, 0.2 μm filter.

57.2.3 Instruments and Equipment

High performance liquid chromatography, Agilent, Germany; Ultraviolet detector, Agilent, Germany; One over ten thousand balance, Mettler Toledo (Shanghai, China); Numerical control ultrasonic cleaning device, Hengao, Tianjin, China; Diaphragm vacuum pump, Tianjin, China; Centrifugal machine, Eppendorf, Germany; pH meter, Mettler Toledo, Shanghai, China.

57.2.4 Chromatographic Condition

Chromatographic column: C18 (4.6 × 150 mm ID, 5 μm); column temperature: 35 °C; flow rate: 0.8 ml/min; UV detector: 278 nm.

57.2.5 The Preparation of the Standard Solution

Take different volumes of the mother liquor tyramine (1000 μl, 900 μl, 800 μl, 600 μl, 500 μl, 300 μl, 200 μl, 100 μl), add mobile phase to the capacity of 1 mL to get tyramine standard fluids with different density.

57.3 Results and Discussion

57.3.1 HPLC Chromatogram of Tyramine Standard Fluid

Under the condition of column temperature: 35 °C; flow rate: 0.8 ml/min; UV detector: 278 nm, the retention time of tyramine was 4.445 min. This result proves tyramine can be directly tested without derivative reaction (Fig. 57.2).

57.3.2 The Establish of Standard Curve

The standard curve was constructed using tyramine standard solutions. The corresponding regression equation and other characteristic parameters are shown in

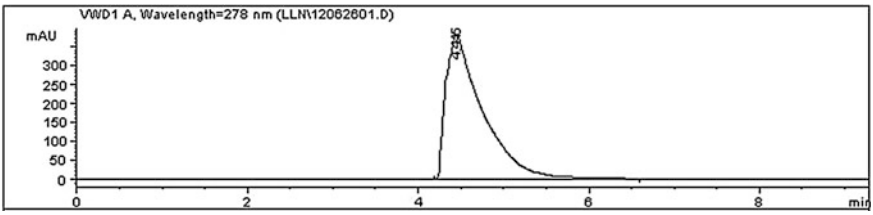

Fig. 57.2 HPLC chromatograms of Tyramine standard fluid

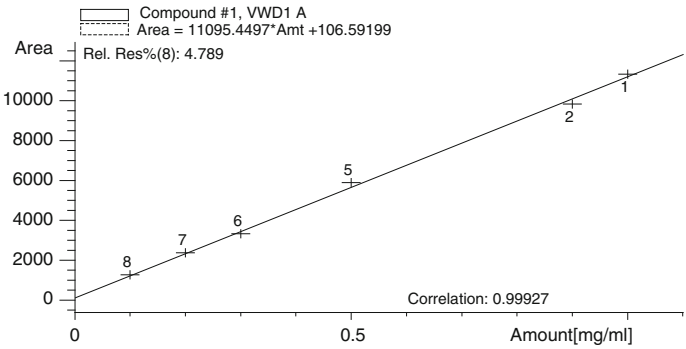

Fig. 57.3 The standard curve of Tyramine standard solutions

Fig. 57.3. LOD [16], defined as three times the basis of signal-to-noise ratio, for tyramine was 0.7 mg/L with coefficients of determination greater than 0.999. The results showed that the analytical curves exhibited excellent linear behavior over the examined concentration range.

57.3.3 The Repeatability and Reproducibility

The repeatability and reproducibility of the method were evaluated. The Tyramine standard fluid was performed seven times by duplicate under optimum conditions during a working day to determine repeatability and three replicate analyses of the same sample were made on three different days to determine reproducibility. Tables 57.1 and 57.2 showed the results of the test for repeatability and reproducibility. The relative standard deviations (RSD) were less than 3 % for both reproducibility and repeatability. Considering these RSD values, the repeatability and reproducibility are satisfactory. These results indicate that this method can be applied as quantitative analyses of tyramine.

Table 57.1 Precision of the method for determination the repeatability

Compound	Repeatability ($n = 6$ mg/L)						
	1	2	3	4	5	6	RSD (%)
Tyramine Standard fluid	28.8	28.8	27.7	28.5	28.9	28.4	1.56

Table 57.2 Precision of the method for determination the reproducibility

Compound	Reproducibility ($n = 3$) Date			
Tyramine standard fluid	2012.6.6	2012.6.7	2012.6.8	RSD (%)
	28.8	29.2	27.6	2.91

57.3.4 The Determination of Tyramine in Rice Wine

The chromatogram of the rice wine sample without tyramine addition was showed in Fig. 57.4, the results prove the presence of tyramine in rice wine, and the retention time was 4.399 min.

Figure 57.5 represents the chromatogram of the rice wine sample with tyramine standard fluid addition (v: v 1:1) and the amount of tyramine addition was 0.5 mg. The retention time of tyramine was 4.292 min, and the amount of detected tyramine was higher than the amount in Fig. 57.4 obviously. The results demonstrate that the recovery of tyramine can be obtained according to the different amounts between Figs. 57.4 and 57.5.

57.3.4.1 The Recovery of Tyramine

The accuracy was estimated by means of recovery assays. Different amount of tyramine addition in rice wine samples to determine the recovery of tyramine was performed (Table 57.3), the concentrations of tyramine were 500 mg/L, 400 mg/L, 300 mg/L, respectively. The accuracy was satisfying for the recovery higher than 98 %.

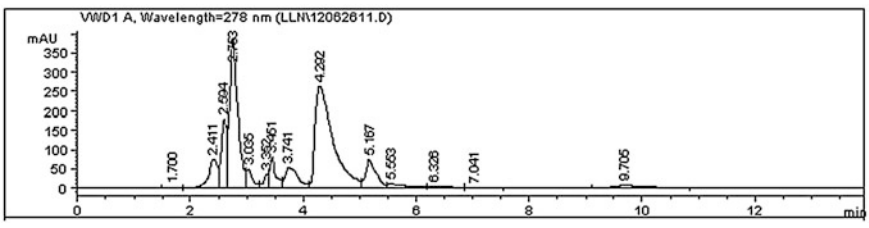

Fig. 57.4 HPLC chromatograms of sample rice wine

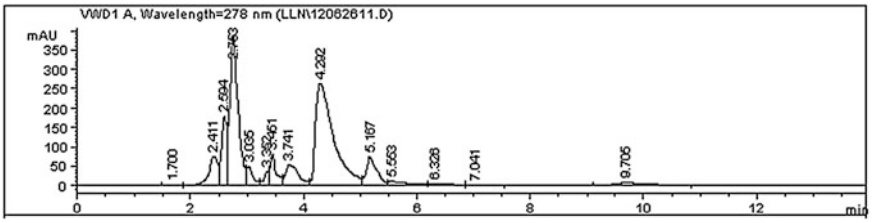

Fig. 57.5 HPLC chromatograms of sample rice wine with tyramine standard fluid addition

Table 57.3 The recovery of tyramine in rice wine with tyramine standard fluid addition by HPLC

Rice wine	No addition (mg/L)	Amount addition (500 mg/L)	Amount addition (400 mg/L)	Amount addition (300 mg/L)	Average recovery	RSD (%)
Amount found	28.8	525.6	420.1	325.7	98.7 %	0.8

Percent recovery = (amount found-amount no addition)/(amount addition) × 100 [13]

57.4 Conclusions

The amount of tyramine detected by our method was similar to the reported in previous works in rice wine by derivative action. This HPLC method makes possible the identification of tyramine in rice wine without derivative and also promotes a sensitive, precise, and accurate procedure for their quantification. The method would be very useful for the analysis of other foods and by-products fermented like measure of theirs sanitary and nutritional quality.

Acknowledgments This work was financially supported by the program of National High Technology Research and Development Program of China (863 Program) (Grant No. SS2012AA023408), the Cheung Kong Scholars and Innovative Research Team Program in University of Ministry of Education, China (Grant No. IRT1166), and the National Science and Technology Support Program under contract NO. 2012BAK17B11-05.

References

1. Halasz A, Barath A, Holzapfel WH (1999) The biogenic amine content of beer; the effect of barley, malting and brewing on amine concentration. Chem and Mate Sci 208:418–423
2. Anderson MC, Hasan F, McCrodden JM et al (1993) Monoamine oxidase inhibitors and the cheese effect. Neurochem Res 18:1145–1149
3. Stratton J, Hutkins R, Taylor S (1991) Biogenic amines in cheese and other fermented foods: a review. J Food Protect 54:460

4. McCabe-Sellers BJ, Staggs CG, Bogle ML (2006) Tyramine in foods and monoamine oxidase inhibitor drugs: a crossroad where medicine, nutrition, pharmacy, and food industry converge. J Food Compos Anal 19:S58–S65
5. Leuschner RG, Heidel M, Hammes WP (1998) Histamine and tyramine degradation by food fermenting microorganisms. Int J Food Microbiol 39:1–10
6. Arena M, Manca de Nadra M (2001) Biogenic amine production by Lactobacillus.J Appl MicrobioI 90:158-162
7. Caruso M, Fiore C, Contursi M et al (2002) Ormation of biogenic amines as criteria for the selection of wine yeasts. World J Microb Biot 18:159–163
8. Stratton J, Hutkins R, Taylor S (1991) Biogenic amines in cheese and other fermented foods: a review. J Food Protect 54:460–470
9. Armagan (2007) A review: Current analytical methods for the determination of biogenic amines in foods. J Agr Food Chem 103:1475–1486
10. Innocente N, Biasutti M, Padovese M et al (2007) Determination of biogenic amines in cheese using HPLC technique and direct derivatization of acid extract. J Agr Food Chem 101:1285–1289
11. Hwang DF, Chang SH, Shiua CY et al (1997) High-performance liquid chromatographic determination of biogenic amines in fish implicated in food poisoning. J Chromatogr B 693:23–30
12. Shalaby AR (1996) Significance of biogenic amines to food safety and human health. Food Res Int 29:675–690
13. Bueno-Solano C, Lopez-Cervantes J (2012) HPCL determination of histamine, tyramine and amino acids in shrimp by-products. J Brazil Chem Soc 23:096–102
14. Pinedaa A, Carrascoa J, Pena-Farfalb C et al (2012) Preliminary evaluation of biogenic amines content in Chilean young varietal wines by HPLC. Food Control 23:251–257
15. Saaid M, Saad B, Ali ASM et al (2009) In situ derivatization hollow fibre liquid-phase microextraction for the determination of biogenic amines in food samples. J Chromatogr A 1216:5165–5170
16. Dias FS, Lovillo MP, Barroso CG et al (2010) Optimization and validation of a method for the direct determination of catechin and epicatechin in red wines by HPLC/fluorescence. Microchem J 96:17–20

Chapter 58
Effect of Milk Basic Protein from Cheese Whey on Rat Bone Metabolism

Hong-ni Wang, Hui-ping Liu, Dong Ting and Ping-wei Liu

Abstract The work investigated the effect of milk basic protein (MBP) from cheese whey on bone metabolism of rats. Totle 80 SD female rats were used in the work. The rats were randomly separated into 10 groups by gavaging different doses of MBP. The normal low-dose, normal media-dose, and normal high-dose were applied 5.0, 10.0, and 15.0 mg/kg body weight (BW) MBP in the rat diet, respectively. The ovx low-dose, ovx media-dose, and ovx high-dose were gavaged the same dose MBP with normal groups. The normal control, ovx control, and sham-operated were fed distilled water, and positive control was fed by casein phosphopeptides (CPP). After 12 weeks, bone mineral density (BMD), the osteocalcin, and serum calcium were increased with concomitant decrease in alkaline phosphatase (ALP) activity at low-dose groups. However, it had little effect on BMD, ALP, the osteocalcin, and serum calcium at media-dose and high-dose of MBP.

Keywords Milk basic protein · BMD · ALP activity · Bone metabolism

58.1 Introduction

Milk basic protein (MBP) has important implications in strengthening the bone by stimulating into bone cell proliferation and inhibiting the activity of osteoclasts. It is one of the best "medicines" to prevent osteoporosis. With the deepening of the aging of society, osteoporosis increased in the elderly, especially postmenopausal woman [1]. At present, more than 75 million people suffered from osteoporosis in American, England, and Japan. The latest research shows that the osteoporosis is existed in childhood which has been considered age-related diseases in China.

H. Wang · H. Liu (✉) · D. Ting · P. Liu
Key Laboratory of Food Nutrition and Safety, Tianjin University of Science & Technology, Tianjin 300457, People's Republic of China
e-mail: liuhuiping111@163.com

T.-C. Zhang et al. (eds.), *Proceedings of the 2012 International Conference on Applied Biotechnology (ICAB 2012)*, Lecture Notes in Electrical Engineering 249,
DOI: 10.1007/978-3-642-37916-1_58, © Springer-Verlag Berlin Heidelberg 2014

Milk has a significant preventive effect on osteoporosis [2]. There are several micronutrients in the milk, such as calcium, lactose, and CPP which can affect bone metabolism. Specifically, there is a trace element in the cheese whey called milk basic protein (MBP) with alkaline isoelectric point, the heat and digestive enzymes cannot destroy its function [3–5]. The Snow Brand Milk Products Co. Ltd found the MBP in the milk through 10 years of research from 1989 to 2000. In addition, there was little report on metabolism of purified MBP and most studies of MBP were remaining in the crude extract stage.

In order to providing further experimental evidence of MBP to prevent the osteoporosis, the objective of this research is to study the effect of milk basic protein (MBP) from cheese whey on bone metabolism of rats, the bone mineral density (BMD), alkaline phosphatase (ALP), osteocalcin, and serum calcium. The changes observed in bone metabolism by examining the femur weight, ash weight, and bone calcium result in larger errors. So the BMD and ALP were examined to increase the accuracy of the experiment. It is well known that menopause mainly causes trabecular bone loss. By calculating the selected indicators of the right femur of the vox rats, the effect of MBP on bone loss will be tested.

58.2 Materials and Methods

58.2.1 Chemicals and Reagents

Chemicals required for the assays Pelltobarbitalum Natricum was purchased from Sigma.

Chemical Co. (St. Louis, MO, USA). Cation exchange resin (D072) and Sephadex G-100 was purchased from Pharmacia (Uppsala, Sweden). CPP was of food grade (ShangHai Natural Bio-engineering, Co., Ltd.). Other chemicals and reagents used were of analytical grade.

58.2.2 Preparation of MBP

MBP was obtained from cheese whey. Cheese whey was defatted by centrifugation and loaded onto a column that had been packed with cation exchange resin (D072). The column was sufficiently washed with demonized water and the bound protein was eluted with 0.05 mol/L phosphate-buffered saline (PBS, pH7.2) solution. The crude milk basic protein was purified by Sephadex chromatography (Sephade G-100). The MBP was obtained by freeze-drying, after dialysis of the eluted fraction in a cellulose membrane (MD34, Solarbio Science & Technology, Co., Ltd.) tube. the purity of the MBP extracted was determined by the method of optical density scanning [6] the purity is 83.55 %.

58.2.3 Animals and Treatment

A total of 80 female Sprague–Dawley rats weighing 230 ± 15 g (12 weeks of age) were used in this study. All animals were obtained from the Center of Animal Laboratory of Medical Department of Peking University, and adapted to the vivarium for one week before treatment began. Mice were group-housed (four mice per cage) with free access to standard rodent chow and tap water, and kept in a constant temperature (23 ± 1 °C) and humidity (60 ± 10 %) environment under a 12 h light/dark cycle (light on 07:30–19:30 h). All animals were handled in accordance with the guidelines of the Principle of Laboratory Animal Care (NIH Publication No. 85–23, revised 1985).

Animals were randomly assigned to ten groups (n = 8), 32 rats were ovariectomized, and 8 rats received a sham operation. After the recovery period, the ovx rats were separated into four groups, i.e., vehicle control group, ovx low-does, ovx media-dose, ovx high-dose, MBP at 5.0,10.0 and 15.0 mg/kg BW were applied in rat diet, and ovx control, sham was fed distilled water; The other rats were used for normal low-dose, normal media-dose, normal high-dose, normal control, and positive control. Normal groups were fed like the ovx groups and the positive control was gavaged CPP (3.0 %). The above groups were labeled as follows: A: positive control; B: normal control; C: normal low-dose; D: normal media-dose; E: normal high-dose; F: sham; G: ovx control; H: ovx low-does; I: ovx media-dose; J: ovx high-dose. Animal body weights were obtained weekly to determine the effects of MBP on body weight and to adjust the injection volumes. After 12 weeks, the rats were deprived of food overnight and weighed, then were anesthetized by CO_2 inhalation and sacrificed by aortic exsanguinations. At the same time, the femur and tibiae were excised immediately, carefully removed the soft tissue and muscle, and stored at 4 °C until further use.

58.2.4 Femur Weight and Ash Weight

The right femur of every groups were drying to constant weight in the oven (105 °C), weighed the ash weight after ashing them in the muffle (500 ∼ 600 °C) [7].

58.2.5 Measurement of BMD

The bone mineral density was measured according to the method of Peterson et al. [8]. The rats right femurs mineral density was measured by QDR-4500w DEXA (Prodigy, GE lunar, Hologic, USA).

58.2.6 Measurement of ALP

The ALP procedure was performed according to the standard protocol of the ALP kit [9]. The blood was separated by centrifugation at 1000 g for 20 min at 4 °C, and particulates were removed from the supernatants by centrifugation, and the samples were stored at −70 °C until used. The sample diluent (50 μL) was added to each well and then 50 μL/well of ALP standard or HRP marked by affinity element supernatant sample was applied. The plate was then covered with an adhesive strip and incubated for 1 h at 37 °C. Each well was aspirated and washed, and the process was repeated four times. The 0.1 mg/mL of affinity streptomycin-HRP (80 μL/well) was added, covered with a new adhesive strip, and incubated for 30 min at 37 °C. The washing process was repeated four times. The substrate solution (50 μL/well) was added and incubated for 30 min at 37 °C. Finally, the stop solution (50 μL/well) was added and the optical density of each well determined within 30 min, using an ELISA reader (Bio-Rad, Hercules, CA) at a test wavelength of 450 nm and a reference wavelength of 540 nm.

58.2.7 Measurement of Calcium

The calcium contents of blood serum and right femur were determined according to the methods of Russell et al. [10] by AA-6800 atomic absorption spectrometry (Shmidzu, Japan). Briefly, the samples were digested to colorless and transparent,then they were completely transferred to 100 mL volumetric flasks separately and add distilled water to 100 mL. Atomic absorption spectrometry of sample solutions and calcium standard solution were performed using a calcium hollow cathode lamp. The electric current of the lamp is 4 mA, slit width is 0.1 mm, air and acetylene flow rate are 0.12 L/min and 1.4 L/min, burner height is 8 mm, and at the test wavelength of 422.7 nm.

58.3 Statistical Analysis

The data reported in the tables were the mean values with SD, and the figures are expressed as means with 95 % confidence intervals. Analysis of variance was used to compare the results of sham and control groups with the results of the other groups. Analysis of covariance and Student's *t* test was used to compare the results of sham and control group with the results of the other groups. The treatment differences were given with 95 % confidence intervals. The SPSS 11.5 software (SPSS Inc., Chicago, IL, USA) was used to analyze data. The results were expressed as mean ± standard error of the mean. A value of $P < 0.05$ was considered statistically significant.

58.4 Results and Discussion

58.4.1 Results

58.4.1.1 Effect on Body Weight

The body weight was measured by scale (Table 58.1). Increase in body weight of every group was observed during the interventions. During the first 3 weeks the body weight did not significantly differ between the groups ($P > 0.05$). At the end of the study the body weight varied significantly between the groups. The weight gain was lower in the normal group, sham group, and positive group than in the vox group, and no significant difference between the every normal group, so do the vox group. Therefore, the ovx groups gained more weight as expected, because of the estrogen which will lose in postmenopausal.

58.4.1.2 Effect on Femur Weight and Ash Weight

The change in femur weight (Fig. 58.1a) and ash weight (Fig. 58.1b) of each group is the same basically. At the end of experiment, the vox groups are significantly lower than the normal groups and the sham. The ovx low-does is significantly higher than the ovx control, the ovx media-dose, and the ovx high-dose is higher than the ovx control too, but dose not have a significant. The normal control is distinctive with the normal low-dose, the normal media-dose, the normal high-dose, and the positive control.

Table 58.1 Effect on body weight by MBP ($\overline{X} \pm S$, $n = 8$)

Groups	N	0 week	3 week	6 week	12 week
A	8	230.51 ± 5.99a	283.55 ± 7.52a	294.11 ± 9.04a	323.57 ± 14.58a
B	8	231.25 ± 6.27a	280.51 ± 6.31a	290.55 ± 6.57a	316.66 ± 10.08a
C	8	232.04 ± 4.79a	276.88 ± 11.55a	288.57 ± 8.21a	321.45 ± 11.74a
D	8	229.59 ± 8.57a	277.54 ± 9.06a	293.65 ± 7.44a	325.51 ± 9.78a
E	8	230.73 ± 7.45a	282.21 ± 5.39a	291.76 ± 10.45a	311.65 ± 15.98a
F	8	231.57 ± 5.67a	271.88 ± 6.88a	295.63 ± 6.51a	310.62 ± 10.04a
G	8	233.01 ± 4.42a	289.38 ± 7.16a	341.25 ± 8.90b	353.75 ± 10.93b
H	8	231.83 ± 3.69a	291.57 ± 7.41a	337.84 ± 10.57b	351.21 ± 12.47b
I	8	231.53 ± 4.89a	285.33 ± 9.21a	341.66 ± 9.87b	346.84 ± 18.40b
J	8	231.89 ± 5.99a	293.66 ± 10.58a	343.57 ± 8.56b	351.11 ± 13.64b

* A: positive control; B: normal control; C: normal low-does; D: nomal media-does; E: nomal high-does; F: sham; G: ovx control; H: ovx low-does; I: ovx media-does; J: ovx high-does

58.4.1.3 Effect on Bone Mineral Density

The right femur bone mineral density of the SD rats was tested in this experiment in order to demonstrate the effects of MBP on bone (Fig. 58.2). The bone mineral density decreased significantly when the rats were ovariectomized, but the process will slow down if given the MBP to the rats. The all gavage groups of ovariectomized are significantly higher than ovx control except ovx high-dose, at the same time, they all are lower than the normal groups. In the normal groups, the normal control is significantly lower than the positive control and the normal low-dose, but it is just like the sham. There is no significant difference between the positive control and the normal low-dose; it shows that effects of MBP on bone are same to effects of CPP on bone.

58.4.1.4 Effect on ALP Activity

ALP is an indicator reflecting the bone formation, Involving in osteoblast formation, differentiation process. The research of Duda shows that the ALP activity will increase when the women were postmenopausal and osteoporosis. This maybe related to the estrogen which will decline when the women were postmenopausal, and this also maybe related to the faster bone transformation and more active osteoblast.

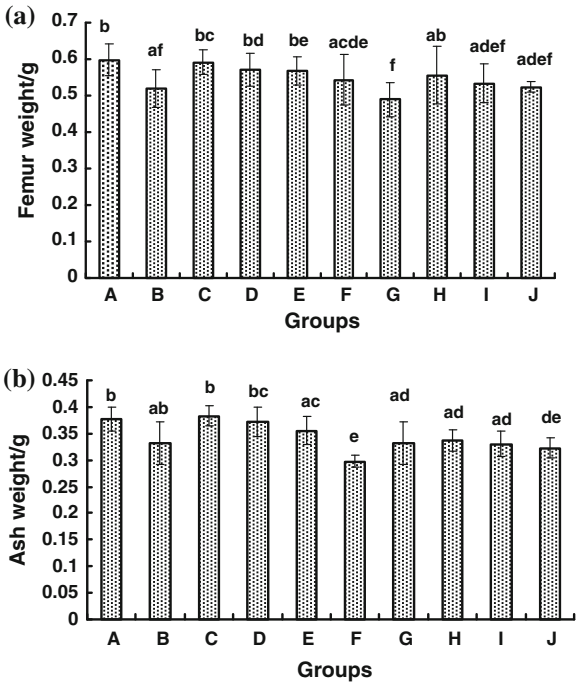

Fig. 58.1 Effect on femur weight/g. **a** and ash weight **b** by MBP ($\overline{X} \pm S$, n = 8) (aP < 0.05 vs. A; bP < 0.05 vs. B; cP < 0.05 vs. F; dP < 0.05 vs. G) *A* positive control; *B* normal control; *C* normal low-does; *D* nomal media-does; *E* nomal high-does; *F* sham; *G* ovx control; *H* ovx low-does; *I* ovx media-does; *J* ovx high-does

In the Fig. 58.3, all the vox groups are significantly higher than all the normal groups and sham. The ovx low-does and the ovx media-dose are significantly lower than the ovx control, there is no statistically significant between ovx high-dose and ovx control. The MBP also has the function to reducing the ALP activity in normal rats; the normal low-dose is significantly lower than normal control and no statistically significant to the positive control (CPP group).

58.4.1.5 Effects on Bone Calcium and Serum Calcium

The change in calcium content is one of the indicators which reflect the bone health directly. This study found that all the vox groups have calcium loss in different levels.

For bone calcium, the ovx low-does are significantly higher than ovx control but lower than normal control (Fig. 58.4a). In the normal groups, low-dose and positive control is significantly higher than normal control, but there is no diversity between the two. The normal media-dose and normal high-dose have no statistical significance to the normal control.

The change in serum calcium is the same to bone calcium on the whole (Fig. 58.4b). The sham has no diversity to the normal control. However, because

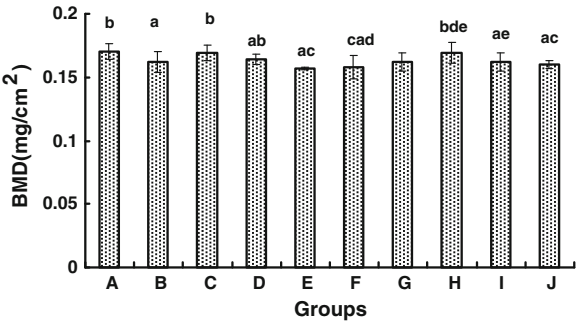

Fig. 58.2 Effect on Bone Mineral Density by MBP ($\overline{X} \pm S$, n = 8) (aP < 0.05 vs. A; bP < 0.05 vs. B; cP < 0.05 vs. F; dP < 0.05 vs. G) *A* positive control; *B* normal control; *C* normal low-does; *D* nomal media-does; *E* nomal high-does; *F* sham; *G* ovx control; *H* ovx low-does; *I* ovx media-does; *J* ovx high-does

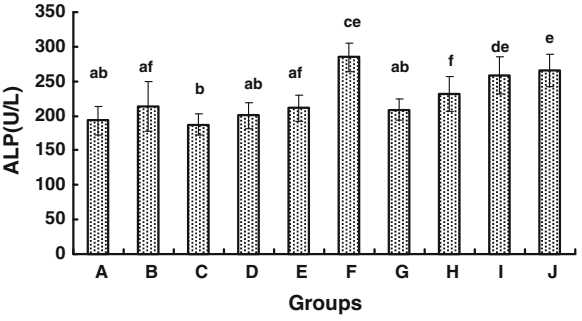

Fig. 58.3 Effect on ALP activity by MBP ($\overline{X} \pm S$, n = 8) (aP < 0.05 vs. A; bP < 0.05 vs. B; cP < 0.05 vs. F; dP < 0.05 vs. G) *A* positive control; *B* normal control; *C* normal low-does; *D* nomal media-does; *E* nomal high-does; *F* sham; *G* ovx control; *H* ovx low-does; *I* ovx media-does; *J* ovx high-does

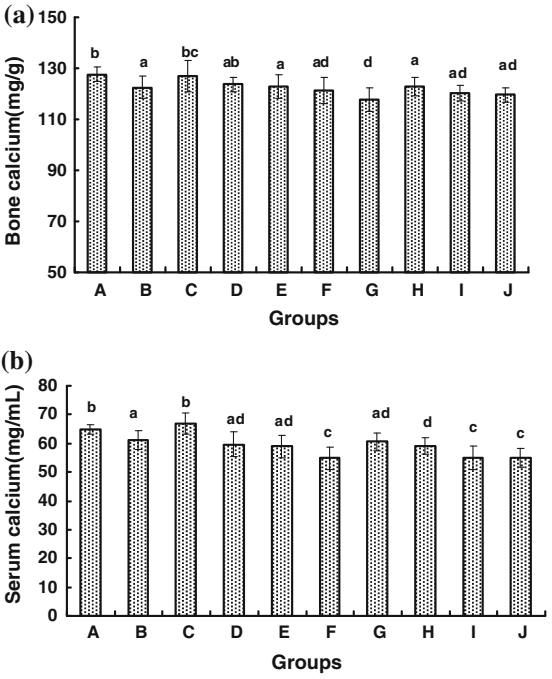

Fig. 58.4 Effect on bone calcium. **a** and surum calcium **b** by MBP ($\overline{X} \pm S$, n = 8) (aP < 0.05 vs. A; bP < 0.05 vs. B; cP < 0.05 vs. F; dP < 0.05 vs. G) *A* positive control; *B* normal control; *C* normal low-does; *D* nomal media-does; *E* nomal high-does; *F* sham; *G* ovx control; *H* ovx low-does; *I* ovx media-does; *J* ovx high-does

of the ovariectomized make the calcium lose faster; all the vox groups are significantly lower than normal control. As garaging MBP, the serum calcium lose becomes slower and the ovx low-does is significantly higher than ovx control.

58.4.2 Discussion

Ovariectomized SD rats are used as a model of osteoporosis to examine the effect of MBP on bone loss. Ovariectomy causes bone loss, because of the estrogen deficiency. However, the MBP can prevent the bone loss in the ovx rats was proved in this research.

The normal rats and the vox rats were gavaged by different doses of MBP solution. After 12 weeks, there are different changes in the selected indicators of every group. The weight of all the vox groups is significantly higher than the sham and normal groups; This maybe connected to the abnormal lipid metabolism caused by the declining estrogen, but within the normal and vox groups there is no significant change. It means that the MBP has no effect on body weight. In the vox group, all the selected indicators of the ovx low-dose are significantly higher than the ovx control (the ALP is lower); the indicators of the ovx media-dose are higher too, but not statistically significant; the effect of ovx high-dose is not obvious.

The MBP has effect not only on the vox groups but also on the normal groups. Compared with the normal control, all the selected indicators of the normal low-dose are significantly improved. But compare with the positive control, there was no significant difference, its shows that the MBP has the same effects on bone to the CPP which already has proved. The normal media-dose and normal high-dose have no significant impact on the bone. These results suggest that the MBP has obvious effect on osteoporosis at 5 mg/kg BW, while there is aslo effect at 10 mg/kg BW, but not significant.

In conclusion, the bone of SD rats will lose when it ovariectomized, in the wake of this, all the selected indicators will go down (ALP go up). The MBP could help to improve those indicators and could reduce the incidence of osteoporosis. Whether this can be used as measures of the nutritional prevention and treatment of primary osteoporosis, and is subject to human clinical validation. At the same time, these results thus indicate that MBP cannot heal the osteoporosis, because it is difficult to reverse when bone loss occurs. The best way to against the osteoporosis is prevention [11].

58.5 Conclusion

By measuring the BMD,ALP,Osteocalcin, and serum calcium of different doses of MBP in normal rats and ovarian rat model of vitality, and comparing with the gavage CCP group rats, the results show that the MBP has the same effects on bone to the CPP; the MBP has obvious effect on osteoporosis at 5 mg/kg BW. In addition, the study indicates that MBP cannot heal the osteoporosis.

Acknowledgments The authors acknowledge the financial support of the Tianjin scientific and technological project (Project number 08ZHNZNC02500), Scientific research foundation for Talents from Tianjin University of Science and Technology (project number 20080420).

References

1. Rodriguez MA, Garcia EC (2002) Role of Ca2+ and vitamin D in the prevention and treatment of osteoporosis. Pharmacol Ther 93:37–49
2. Yasuhiro M, Atsushi S (2002) Cystatin C in milk basic protein (MBP) and its inhibitory effect on bone resorption in vitro. Biosci Biotech Bioch 66(12):2531–2536
3. Hiroshi K (2005) Biological significance of milk basic protein (MBP) for bone health. Food Sci Technol Res 11(1):1–8
4. Yasuhiro T, Yukihiro T (2001) Milk basic protein promotes bone formation and suppresses bone resorption in healthy adult men. Biosci Biotech Bioch 65(12):1353–1357
5. Seiichiro A, Takao K (2005) A controlled trial of the effect of milk basic protein (MBP) supplementation on bone metabolism in healthy menopausal women. Osteoporos Int 16:2123–2128

6. Anuradha SN, Prakash V (2009) Altering functional attributes of proteins through cross linking by transglutaminase —A case study with whey and seed proteins. Food Res Int 42:1259–1265
7. Tsuchita H, Goto T, Shimizu T et al (1996) Dietary casein phosphopepetides prevent bone loss in aged ovariectomised rats. J Nutr 126:86-93
8. Peterson C, Eurell J, Erdman J (1995) Alterations in calcium intake on peak bone mass in the female rat. J Bone Miner Res 10:81–95
9. Duda R Jr, O'Brien JF, Katzmann JA et al (1988) Concurrent assays of circulating bone Glap rotein and bone alkaline phosphatase: effects of sex, age, and metabolic bone disease. J Clin Endocr Metab 66(5):9512957
10. Russell TT, Avudaiappan M, Sutada L et al (2001) Animal models for osteoporosis. Rev Endocr Metab Dis 2:117
11. Kanis JA (1996) Estrogens, the menopause, and osteoporosis. Bone, 19 (s):1852190

Chapter 59
Isolation, Identification of Strains Producing Membranes from the Contaminated Apple Vinegar and Analysis of the Membranes

Yuenan Wang, Zhiqiang Nie, Yu Zheng, Min Wang and Jingyao Wang

Abstract Fruit vinegar, such as apple vinegar, is very popular throughout the world because of its health functions and special flavors. However, lots of flocculent membrane were frequently found during fruit vinegar production and storage process, which seriously affected the product by decreasing the concentration of acetic acid and bringing vinegar turbidness. In this research, a total of 106 bacterial strains were isolated from the contaminated apple vinegar samples and five (named B1, B2, B3, B4, B16) of them, which could produce leathery membranes, were isolated and subsequently identified as *Gluconacetobacter europaeus* by methods of morphology, physiology, biochemical characteristic, and 16S rDNA sequence analysis. Scanning electron microscopy and X-ray diffraction were used to observe and compare the structure of the membranes, and the component of the membranes which was determined as bacterial cellulose was analyzed by Fourier transform infrared spectroscopy.

Keywords Fruit vinegar · Bacterial cellulose · Gluconacetobacter · Membrane

59.1 Introduction

Vinegar is one of the necessities in daily dietary. It is usually used as seasonings and preservatives in food preparation and watered down as drink [1]. Vinegar is widely produced from rice, malt, or various other raw materials. Moreover, fruit

Y. Wang · Z. Nie · Y. Zheng · M. Wang (✉)
Key Laboratory of Industrial Fermentation Microbiology, Key Laboratory of Industrial Microbiology, Ministry of Education, College of Biotechnology, Tianjin University of Science and Technology, Tianjin 300457, People's Republic of China
e-mail: minw@tust.edu.cn

J. Wang
Tianjin Nankai High School, Tianjin, People's Republic of China

T.-C. Zhang et al. (eds.), *Proceedings of the 2012 International Conference on Applied Biotechnology (ICAB 2012)*, Lecture Notes in Electrical Engineering 249,
DOI: 10.1007/978-3-642-37916-1_59, © Springer-Verlag Berlin Heidelberg 2014

vinegars which are made from fruits or fruit wines, such as apple vinegar, lemon vinegar, are perceived as a healthy beverage and are becoming popular throughout the world [2]. Fruit vinegars are rich in organic acids, amino acids, vitamins, mineral substances, and so on [3]. Meanwhile, they have the advantages of deliciousness, fashion, and health. Many reports indicated that fruit vinegars have functions of antioxidant and anti-microbial [4–6]. They can prevent inflammation and hypertension [7], decrease serum cholesterol and triacylglycerol [8], decrease the glycemic index of carbohydrate food for people with or without diabetes [9, 10], and also reduce food intake for diet control [11].

Submerged pure-culture fermentation techniques have been widely used for fruit vinegars production with lots of advantages such as high mechanization, sanitary operation, high utilization ratio of raw material, and high yield. However, leathery membranes were frequently discovered in fermentor and pipeline during the fruit vinegar production and storage process. Those membranes not only affect the air and liquid flow but also inhibit the growth of the acetic acid bacteria by blocking the pipeline. Also, they may decrease the yield of acetic acid and affect the quality of the product of fruit vinegar. It has been reported that some kind of bacteria could produce the membranes. However, they were difficult to be eliminated. In this research, strains which produced the membrane were isolated from the contaminated apple vinegar and the structure and property of the membrane were investigated.

59.2 Materials and Methods

59.2.1 Sample and Medium

The contaminated apple vinegar with membranes was from an apple vinegar factory in Hebei Province, China. The strains which produced membranes were grown in GYPMS medium which consisted of (per liter): glucose 50 g, yeast extract 6 g, peptone 10 g,$MgSO_4 \cdot 7H_2O$ 2 g, sodium citrate 1 g, ethanol 35 mL, pH 6.8 [12]. The strains were stored in GYC slant medium which consisted of (per liter): glucose 50 g, yeast extract 10 g, $CaCO_3$ 30 g and agar 20 g, ethanol 35 mL, pH 6.8 at 4 °C. Before inoculation ethanol was added to the sterilized culture medium.

59.2.2 Strains Isolation and Identification

The contaminated apple vinegar samples (4 mL) were added to GYPMS medium (40 mL) for enrichment incubation at 30 °C for 2 days with shaking at 160 rpm. Then, 0.1 mL fermentation broth was spread on GYC plates and incubated at 30 °C

for 3–5 days [13]. Colonies formed on the plates were then incubated in GYPMS medium at 30 °C to determine the ability of producing membranes.

The strains isolated were identified to species level by following physiological and biochemical tests: (i) Morphology observation under the light microscope, (ii) Gram stain of the strains, (iii) catalase production, (iv) growth on 3 % ethanol in the presence of 5 % acetic acid, (v) growth in presence of 30 % (w/v) D-glucose, and (vi) acid production from different carbon sources [14, 15].

The 16S rDNA was amplified by PCR with primers 27f (5′-AGAGTTTGATCCTGGCTCAGG-3′) and 1492r (5′-ACGGCAACCTTGTTACGAGTT-3′). PCR products were ligated into pMD-18T Vector after purification according to the manufacturer's instructions (TaKaRa, Dalian, China). The 16S rDNA sequences were blasted with nucleotide sequences in the GreenGenes database. Phylogenetic and molecular evolutionary analyses of these sequences were conducted with neighbor-joining method.

59.2.3 Collection of the Membranes

The strains were inoculated to the sterile GYPMS medium and incubated at 30 °C for 24 h with shaking at 160 rpm. Then, it was transferred into fresh GYPMS medium with 10 % inoculum (v/v). This cultivation was performed at 30 °C without shake for 7 days to produce the membrane. Then, the membranes were treated with 0.1 mol/L NaOH solution at 100 °C for 30 min, and then washed 5 times with sterilized deionized water to remove the cell and medium [16]. Purified membranes were dried in vacuum oven at −50 °C for 24 h [17].

59.2.4 Scanning Electron Microscopy Observation

The structure of the membranes was monitored using JEOL JSM 6380 Scanning Electron Microscope. The samples were sputter coated with gold (30 μm thick). The accelerating potential was 15 kV [18]. Photographs of representative areas of the samples were taken at 20000 magnifications.

59.2.5 X-ray Diffraction Analysis

The structure of the membranes could also be tested using a X-ray diffractometer (Copper target 40 kv, 200 mA, Kα 0.154 nm, Shimazu, Japan). The diffraction diagram was compared with the known data [19].

59.2.6 Fourier Transform Infrared Spectroscopy (FTIR) Analysis

The components of the membrane samples were determined using a Fourier transform infrared spectrometer (Vector 22, Bruke). Each membrane sample of 10 mg was prepared for test [20]. The FTIR spectra were compared with the known spectra in the documents [21].

59.3 Results and Discussion

59.3.1 Isolation and Identification of Strains Producing Membranes

A total of 106 bacterial strains with different morphology were isolated from the contaminated apple vinegar. Colonies formed after 3 days on GYC plates at 30 °C. After incubating the colonies in GYPMS medium, five strains of them (named B1, B2, B3, B4, B16) which produced membranes were isolated. The colors of the colonies, the morphological characteristics of the membranes and the biochemical characteristics of the five strains were listed in Tables 59.1 and 59.2. In liquid medium, the membranes produced by strains B1 and B4 were thicker and harder than those of others. Moreover, the production of membranes by strain B1 was faster than others.

The five strains were difficult to be picked out from the plate medium. Transparent circle observed from the GYC plates suggested that they could produce some acids. Observed under light microscope, they were unspore forming, bending or straight rods, single or double, and gram negative. SEM microscope observation showed that the shapes of five strains were atrichia, bending, or straight and cell surfaces were smooth and size was (0.45 – 2.20) × (0.4 – 1.50) μm.

Table 59.1 The color of colonies and morphological of membranes

Tests	B1	B2	B3	B4	B16
Color of the colony (GYC medium)	Pale brown	Light brown	Light gray	Light yellow	
Color of the membrane (GYPMS medium)	Dark brown	Light brown	Dark brown	Light brown	Light brown
Hardness of the membrane (GYPMS medium)	+++	++	+	+++	+
Thickness of the membrane (GYPMS medium)	+++	++	+	++++	+

Note + Degree of hardness or thickness

Table 59.2 The biochemical identification of five strains

Tests	Five strains
Growth on 3 % (v/v) ethanol in the presence of 5 % acetic acid	+
Growth only in presence of acetic acid, ethanol and glucose	−
Growth in presence of 30 % D-glucose	−
Growth on 8 % (v/v)ethanol	+
Growth on ammonium salts as the only nitrogen source	−
Catalase	+
Production of brown pigment	−
Growth in pH 4.5	+
Growth on methanol as carbon source	−
Growth on D-glucose as carbon source	+

Note − Negative, + Positive

The 16S rDNA of five strains showed a high similarity (99 %) to *Gluconacetobacter* sp. and the sequences were submitted to GreenGenes database. According to Bergey's Manual of Determinative Bacteriology, 9th ed., morphological and biochemical characteristics of the five strains such as growth on 3 % (v/v) ethanol in the presence of 5 % acetic acid and growth on 8 % (v/v) ethanol showed that the five strains all belonged to *Gluconacetobacter europaeus*, but they were not a same strain. A phylogenetic tree based on the genotypic similarities was established using the method of neighbor-joining, as shown in Fig. 59.1. Generally, *G. europaeus* was founded in vinegar or fruits juice which contained sugars. Some strains of *G. europaeus* were also used in submerged cultures and trickling generators for industrial production of vinegar [14]. But some of them may produce cellulose which could contaminate the vinegar.

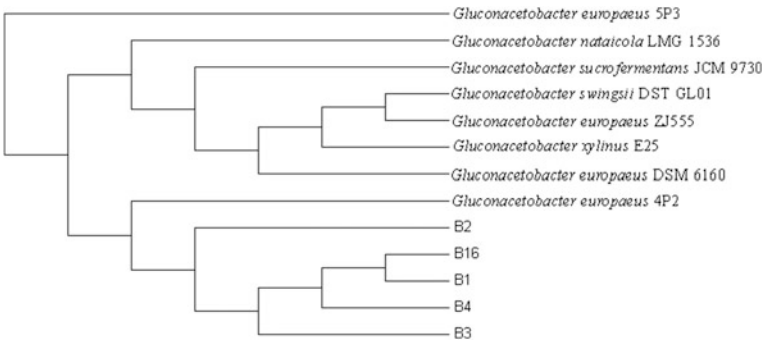

Fig. 59.1 The phylogenetic tree based on 16S rDNA sequence

59.3.2 Scanning Electron Microscopy Observation of the Membranes

The residual medium, protein and cells cannot be completely removed from the surface of the membranes only by washing with water [21]. However, they could be removed by treating with 0.1 mol/L NaOH solution at 100 °C for 30 min. The dried membranes produced in GYPMS medium exhibited certain toughness and were difficult to be ruptured. SEM was used to observe the structure of the membranes, as shown in Fig. 59.2. It was clearly described that the surface morphologies and structures of five membranes were similar but different in size. They showed a typical microfibrillar structure, mesh-like, and porous appearance, and also contained some fiber cluster, which were similar with the known bacterial cellulose [18]. The fiber cluster which interweaved into a complex network was parallel with each other and had much pore space in arrangement. This may be the reason why the membrane had a certain toughness and stress strength.

59.3.3 X-ray Diffraction Analysis

The data of 2θ and d-value could be used to identify the components of the membranes. The X-ray diffraction diagrams of the membranes were similar with the known data [20] of bacterial cellulose (as shown in Table 59.3). Thus, the components of the membranes were likely to be bacterial cellulose. Generally, the bacterial cellulose contained crystalline region and amorphous region. The ratio of the crystalline region related to the tensile strength, Young's modulus, and hardness of the bacterial cellulose. If the crystalline region occupied a large proportion in the whole, the crystallinity and the stability of the tensile strength, Young's modulus, and hardness of the bacterial cellulose will be high. Through improving the fermentation conditions of the strains, the crystallinity could be increased to meet the need of productions.

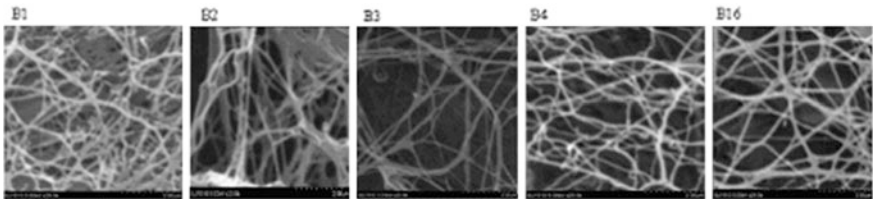

Fig. 59.2 The SEM image of membranes (×20000)

Table 59.3 The X-ray diffraction analysis of membranes produced by strains

Sample	2θ			d-value	
Membrane by B1	14.44°	16.02°	22.74°	6.1285	3.9072
Membrane by B2	14.44°	16.80°	22.62°	6.1292	3.9274
Membrane by B3	14.42°	16.78°	22.82°	6.2577	3.8936
Membrane by B4	14.42°	16.88°	22.72°	6.1369	3.9243
Membrane by B16	14.44°	16.58°	22.62°	6.0956	3.9173
Bacterial cellulose	14.69°	16.69°	22.83°	6.1037	3.9038

59.3.4 FTIR Analysis

The FTIR spectra of the five membranes produced by strain B1, B2, B3, B4, B16 were compared to the known spectra [21] of bacterial cellulose. The infrared spectrums of the five membranes were showed in Fig. 59.3. The major stretching peak associated with –OH groups on the glucose rings and water molecules took place between 3300 and 3400 cm^{-1}. The C–H stretching vibration bands of $-CH_2$ and $-CH$ groups were observed as a broad band centered at about 2897 cm^{-1}, whereas bending bands of these groups were observed at 1428–1205 cm^{-1}. The structure of conjugate diene and aromatic was observed at 1630 cm^{-1}. The absorption peak at 1205–1036 cm^{-1} was the characteristic peak of glycosidic linkages. The FTIR spectra of the five membranes were similar with the known spectra [18] indicating that the components of the membranes were bacterial cellulose. The bacterial cellulose was known as a kind of biopolymer which comprised of β-D-glucopyranose units linked together through β-1,4 glycosidic linkages. Because of the unique structure and special properties, bacterial cellulose has a broad perspective for application in

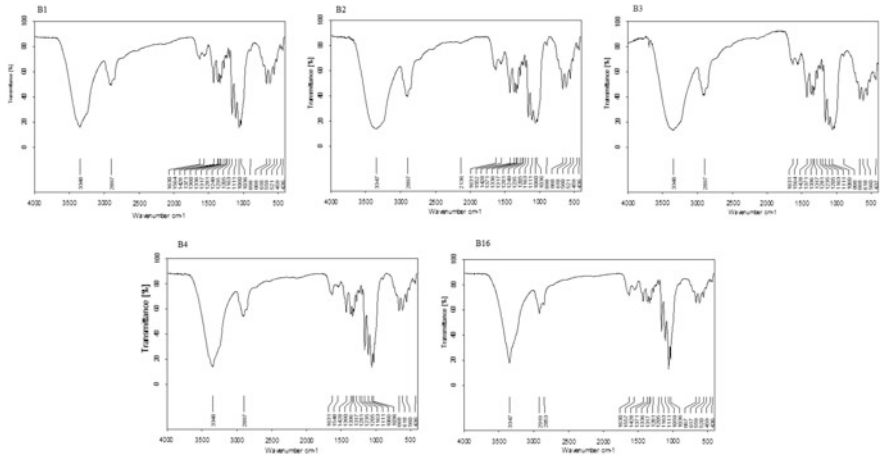

Fig. 59.3 The infrared spectrum of membranes

different fields, including medicine, paper, foods, textiles, binding agents. Beside, it could also be used as biomedical materials in practical application such as artificial skins, blood vessels, and so on.

59.4 Conclusion

Leathery membranes were frequently found in fruit vinegar contaminated by microorganisms during production and storage process, which seriously affected the quality of the fruit vinegar. The membranes continuously accumulated and blocked the pipeline. Moreover, the membranes were difficult to be eliminated in the production process because of its high toughness and special structure. In this research, five strains which could produce membranes were isolated from the contaminated apple vinegar and were identified as *G. europaeus* but they were not a same strain by methods of morphological, physiological, biochemical characteristic, and 16S rDNA sequence analysis. Additionally, the components of the membranes were determined as bacterial cellulose by methods of scanning electron microscopy, X-ray diffraction, and Fourier transform infrared spectroscopy.

This study revealed the causing of the membrane production in fruit vinegar, also, this study was beneficial to prevent the contamination in industrial applications.

Acknowledgments This work was supported by National High Technology Research and Development Program of China (2013AA102106), Program for Changjiang Scholars and Innovative Research Team in University (IRT1166), National Natural Science Foundation of China (31201406).

References

1. Lin JT, Liu SC, Shen CY et al (2011) Comparison of various preparation methods for determination of organic acids in fruit vinegars with a simple ion-exclusion liquid chromatography. Food Anal Method 4:531–539
2. Liu F, He Y, Wang L et al (2011) Detection of organic acids and pH of fruit vinegars using near-infrared spectroscopy and multivariate calibration. Food Bioprocess Tech 4:1331–1340
3. Chang RC, Lee HC, Ou ASM (2005) Investigation of the physicochemical properties of concentrated fruit vinegar. J Food Drug Anal 13:348–356
4. Dávalos A, Bartolomé B, Gómez-Cordovés C (2005) Antioxi-dant properties of commercial grape juices and vinegars. Food Chem 93:325–330
5. Karapinar M, Gönül SA (1992) Effects of sodium bicarbonate, vinegar, acetic and citric acids on growth and survival of *Yeriniae ntrocolitica*. Int J Food Microbiol 16:343–347
6. Medina E, Romero C, Brenes M et al (2007) Antimicr-obial activity of olive oil, vinegar, and various beverages against foodbrone pathogens. J Food Protect 70:1194–1199
7. Murooka Y, Yamshita M (2008) Traditional healthful fermented products of Japan. J Ind Microbiol Biot 35:791–798

8. Fushimi T, Suruga K, Oshima Y et al (2006) Dietary acetic acid reduces serum cholesterol and triacylglycerols in rats fed a cholesterol-rich diet. Brit J Nutr 95:916–924
9. Sugiyama M, Tang AC, Wakaki Y et al (2003) Glyce-mic index of single and mixed meal foods among common Japanese foods with white rice as a reference food. Eur J Clin Nutr 57:743–752
10. Johnston CS, Kim CM, Bullar AJ (2004) Vinegar improves insulin sensitivity to a high-carbohydrate meal in subjects with insulin resistance or type 2 diabetes. Diabetes Care 27:281–282
11. Östman E, Granfeldt Y, Persson L et al (2005) Vinegar supplementation lowers glucose and insulin responses and increases satiety after a bread meal in healthy subjects. Eur J Clinical Nutr 59:983–988
12. Hestrin S, Schramm M (1954) Factors affecting production of cellulose at the air/liquid interface of a culture of *Acetobacter xylinum*. Biochem J 58:345
13. Yamada Y, Okada Y, Kondo K (1976) Isolation and characterization of polarly flagellated intermediate strains in acetic acid bacteria. J Gen Appl Microbiol 22:237–245
14. Holt JG (2004) Bergey′s manual of determinative bacteriology, 9th edn. Williams and Wilkins, Baltimore
15. Garrity GM, Holt JG (2005) Bergey′s manual of systematic bacteriology, 2nd edn. Springer-Verlag, New York
16. Czaja W, Romanovic ZD, Brown RM (2004) Structural investigations of microbial cellulose produced in stationary and agitated culture. Cellulose 11(3/4):403–411
17. Krystynowicz A, Czaja W, Wiktorowskaj A (2002) Factors affecting the yield and properties of bacterial cellulose. J Ind Microbiol Biot 29(4):189–195
18. Karahan AG, Akoglu A, Cakir I et al (2011) Some properties of bacterial cellulose produced by new native strain *Gluconacetobacter* sp. A06O2 obtained from Turkish vinegar. J Appl Polym Sci 121:1823–1831
19. Han XJ (2008) Modern instrumental analysis experiment. Harbin Industry University Press, Harbin, pp 188–191 (In Chinese)
20. Zhang YF, Lu HM, Zhang FJ et al (2008) Study on the producing membrane strain separation in the progress of wash vinegar production and the membrane component. J Cellulose Sci Tech 16:62–65
21. Klemm D, Schumann D, Udhardt U et al (2001) Bacterial synthesized cellulose-artificial blood vessels for microsurgery. Prog Polym Sci 26(9):1561–1570

Chapter 60
Antibacterial Activity and Mechanism of Action of 10-HDA Against *Escherichia coli*

Xiaohui Yang, Tengfei Wang and Ruiming Wang

Abstract 10-HDA (10-hydroxy-2-decenoic acid), an unsaturated fatty acid, is the main active component of royal jelly. It has been demonstrated that 10-HDA possesses remarkable antibacterial activities. However, it is unclear in terms of the underlying antibacterial mechanism of 10-HDA. In our study, we showed that 10-HDA has obvious effects against Gram-negative bacteria and its antibacterial activity was not affected by pH and temperature. 10-HDA was shown to change membrane ionic conductivity and resulted in the leakage of K^+, Ca^{2+}, and Mg^{2+} from bacterial cells, suggesting that 10-HDA was able to compromise the integrity of the bacterial membranes. By detecting the 260 nm absorbing materials, it was showed that the membrane integrity was damaged and resulted in the leakage of large molecules. The results suggested that 10-HDA could damage the permeability and integrity of bacterial cell membrane, leading to the outflow of important large molecules from the cell and its eventual death.

Keywords 10-HDA · Antibacterial mechanism · Escherichia coli · Membrane permeability

Xiaohui Yang and Tengfei Wang contributed equally to this article.

X. Yang · T. Wang · R. Wang (✉)
Key Laboratory of Shandong Microbial Engineering, Qilu University of Technology, Jinan 250353, China
e-mail: ruiming3k@163.com

T. Wang
Key Laboratory of Industrial Microbiology, Ministry of Education, Qilu University of Technology, Tianjin 300457, China

T.-C. Zhang et al. (eds.), *Proceedings of the 2012 International Conference on Applied Biotechnology (ICAB 2012)*, Lecture Notes in Electrical Engineering 249,
DOI: 10.1007/978-3-642-37916-1_60, © Springer-Verlag Berlin Heidelberg 2014

60.1 Introduction

10-HDA (10-hydroxy-2-decenoic acid), an unsaturated fatty acid, is the main active component of royal jelly, which has been mainly found in the royal jelly by now. It has been demonstrated that 10-HDA possesses remarkable biologic activities in antibacterial [1, 2], immunoregulation [3], antioxidative [4, 5], collagen production promoting [6, 7], and antitumour activities [8–10].

The presence of antimicrobial activity in RJ secreted from the pharyngeal glands of the honeybee has been documented for more than 60 years [11–13]. The inhibitory activity of RJ against both Gram-positive and Gram-negative bacteria has been demonstrated. Antibacterial activity of ether-soluble fraction of RJ was rather stronger than that of raw RJ (containing 10-HDA). It was point out that the main component of ether-soluble fraction was 10-HDA occupying 38 % of total acids [12, 14]. The antibacterial activity of 10-HDA against *Bacillus subtilis*, *Staphylococcus aureus*, *Escherichia coli* was stronger than that of the other C_{10} fatty acids [15]. Extracts of royal jelly as well as its isolated compounds were studied for their antimicrobial activity against two Gram-positive bacteria, *S.aureus* (ATCC 25923) and *S. epidermidis* (ATCC 12228); four Gram-negative bacteria, *E. coli* (ATCC 25922), *Enterobacter cloacae* (ATCC 13047), *Klebsiella pneumoniae* (ATCC 13883), and *Pseudomonas aeruginosa* (ATCC 227853); the oral pathogens Gram-positive bacteria, *Streptococcus mutans* and *Streptococcus Viridans*, and three human pathogen fungi, *Candida albicans* (ATCC 10231), *C. tropicalis* (ATCC 13801), and *C. glabrata* (ATCC 28838). The results of these tests showed the antimicrobial activity of 10-HDA against above strains [2].

The studies of 10-HDA against microorganisms have been reported, however, until recently it is unclear about the underlying antibacterial mechanism of 10-HDA. In this paper, to understand the antibacterial activity and acting mechanism of 10-HDA deeply, we investigated the mechanism of inhibition to *E. coli* by analyzing the bacteria growth, membrane permeability, and release of 260 nm absorbing materials from bacterial cells following treatment with 10-HDA. For the first time, we offer evidences to indicate that 10-HDA could damage the permeability and integrity of bacterial cell membrane, lead to the important intracellular materials flow out from cell and finally caused bacteria to die.

60.2 Material and Method

60.2.1 Reagents

10-HDA was purchased from Shanghai Gongshuo Biotechnology Company limited (Shanghai, China). The purity of 10-HDA is higher than 99 %. The 10-HDA was dissolved in ethanol, and kept frozen at −20 °C. The stock solutions of 10-HDA were diluted to the desired concentration.

60.2.2 Organism, Medium, and Cultivation

The strains of *E. coli* CICC23657, *S. aureus* CICC10384, *B.subtilis* CICC20037, *Saccharomyces cerevisiae* CICC31466, *S. cerevisiae* CICC32298 were purchased from China Center of Industrial Culture Collection (CICC) and conserved in our laboratory. Luria–Bertani (LB) medium (final pH 7.0 ± 0.2) contained the following: 5.0 g yeast extract, 10 g tryptone, and 10 g sodium chloride. LB medium was used for aerobic cultivation of *E. coli* (Gram-negative bacteria) and *S. autes*, *B. subtilis* (Gram-positive bacteria) at 37 °C. YEPD medium (final pH 6.0 ± 0.2) contained the following: 20 g peptone, 10 g yeast extract, and 20 g glucose. YEPD medium was used for aerobic cultivation of *S. cerevisiae* at 30 °C. The solid medium was supplemented with 2 % agar in LB medium and YEPD medium.

60.2.3 Antimicrobial Activity of 10-HDA

Antimicrobial activity of 10-HDA was determined by Oxford cup diffusion method. The sterile four Oxford cups were symmetrically placed in the culture medium plate. The ethanol solution of 200 μl of different concentrations of 10-HDA was added to the Oxford cup. The ethanol solution without 10-HDA was used as blank control. The radii of the zones of inhibition obtained were measured with a caliper. The experiments were repeated in triplicate on one occasion. The average radii of the inhibition zones were calculated.

60.2.4 The Antibacterial Effect of 10-HDA Solution in Different pH to **E.coli**

10-HDA solution were adjusted to different pH value at pH 3.5–9.5 by phosphate buffer solution to detect the stability of antibacterial effect of 10-HDA. The experiments were repeated in triplicate, and the average radii of the inhibition zones were calculated by the disk diffusion method.

60.2.5 The Antibacterial Effect of 10-HDA Solution in Different Temperature to **E.coli**

10-HDA solution were processed respectively for 30 min under different temperatures at −18, 0, 10, 30, 50, 70, and 90 °C. The experiments were repeated in triplicate, and the average radii of the inhibition zones were calculated by the disk diffusion method.

60.2.6 *Effect of 10-HDA on the Growth of* E. coli

Growth curves of *E. coli* exposed to 10-HDA were determined based on the absorbing value of OD600. *E. coli* were grown in LB medium and incubated overnight at 37 °C. Then, 200 μl *E. coli* bacterial suspension in a logarithmic growth phase (18 h) was prepared for an antibacterial test. 10-HDA solution was added to the cultures with the final concentration of 1.0 mg/ml 10-HDA. The cultures were incubated at 37 °C for 24 h. The ethanol solution without 10-HDA was used as control. The final concentration of ethanol added to the liquid medium was less than 3 % (v/v). The antibacterial activity was estimated periodically by measuring the turbidity of the culture medium at 600 nm with UV–vis spectrophotometer (Rayleigh, UV-9200, Beijing, China). Each batch experiment was carried out in triplicate, and the results were reported as an average of three replicates.

60.2.7 *Effect of 10-HDA on the Leakage of Ions from* E. coli *Cell*

Escherichia coli bacterial suspension in a logarithmic growth phase (18 h) was prepared, then the suspension was washed by stroke-physiological saline solution twice and kept suspended again. 10-HDA solution was added to the cultures with the final concentration of 10-HDA of 1.0 mg/ml. The cultures were incubated at 37 °C, 150 rpm for 24 h. The ethanol solution without 10-HDA was used as control. The final concentration of ethanol added to the liquid medium was less than 3 % (v/v). 5 mL suspension was taken every 15 min, then was centrifugated 5 min at 6000 rpm. K^+, Ca^{2+} and Mg^{2+} concentration of supernate were detected with atomic emission method.

60.2.8 *Effect of 10-HDA on the Release of 260 nm Absorbing Materials*

The *E.coli* was cultivated to later logarithmic phase as previously described. 10-HDA ethanol solution of 1.0 mg/ml was added into suspension. Meanwhile, the blank control group and the negative control group were set up. The *E. coli* suspension was incubated at 37 ± 2 °C with shaking at 150 rpm, and 5 ml of these suspensions were pipetted into centrifuge tubes at 3, 5, 7 h, and centrifuged for 5 min at 8000 rpm. Every supernatant was carefully removed and diluted into absolute ethanol, the absorbance was measured on 260 nm to indicate changes of nucleic acid leakage.

60.3 Results

60.3.1 Antimicrobial Activity of 10-HDA

Results showed that 10-HDA had significant inhibitory effects against *E. coli* CICC23657, *B. subtilis* CICC20037, and *S. aureus* CICC10384, but had none against fungi, such as *S. cerevisiae* CICC31466 and *S. cerevisiae* CICC32298 (Table 60.1). And the antibacterial activity of 10-HDA against Gram-negative bacteria (*E. coli*) was more susceptible to Gram-positive bacteria (*B. subtilis* and *S. aureus*).

60.3.2 The Antibacterial Effect of 10-HDA Solution in Different pH to E. coli

The experimental results were shown in Fig. 60.1. The result showed that there was no obvious changes of inhibitory zone radii by 10-HDA at different pH. When 10-HDA was adjusted to pH 6.5–9.5, the size of the inhibition zones did not decrease too much. Therefore, the change in the antibacterial activity was not caused by different pH of 10-HDA solution. Our study suggests that the antibacterial activity of 10-HDA were not affected by different pH.

60.3.3 The Antibacterial Effect of 10-HDA Solution in Different Temperature to E. coli

The 10-HDA solution was stored respectively for 30 min in −18, 0, 10, 30, 50, 70, 90 °C, and the inhibition zone radius were determined by disk diffusion method. The results were shown in Fig. 60.2. 10-HDA had an excellent antibacterial effect

Table 60.1 The inhibitory effect of 10-HDA by oxford cup method

10-HDA concentration ($mg \cdot mL^{-1}$)	Inhibitory zone radii (mm)				
	E. coli CICC23657	*B. subtilis* CICC20037	*S. aureus* CICC10384	*S. cerevisiae* CICC31466	*S. cerevisiae* CICC32298
0	0	0	0	0	0
0.625	6.9	6.4	5.7	0	0
1.25	6.1	7.7	6.6	0	0
2.5	10.7	9.2	8.3	0	0
5.0	12.4	11.3	9.7	0	0
10.0	13.6	12.2	11.3	0	0

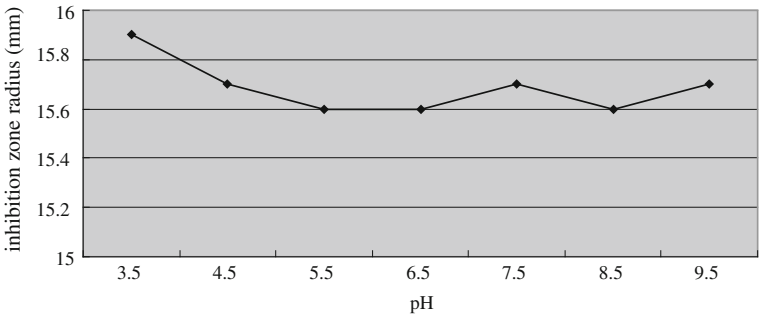

Fig. 60.1 The antibacterial effect of 10-HDA solution in different pH to *E. coli*

in different temperature conditions, and the inhibition zone radii from 15.9 to 16.3 mm. The result suggested that 10-HDA has good stability with the change of temperature.

60.3.4 Growth Curve of E. coli *Exposed to 10-HDA*

The growth curve of *E. coli* treated with 10-HDA was shown in Fig. 60.3 by measuring optical density at 600 nm. Under absence of 10-HDA, *E. coli* reached exponential phase rapidly. But exposed to 1.0 mg/ml of 10-HDA, *E. coli* cells growth were lagged to 15 h, which prolonged the lag phase of *E. coli*, and the concentration of *E. coli* was lower than blank control in the stabilization phase. This result indicated that 10-HDA could effectively inhibit the proliferation and growth of *E. coli*.

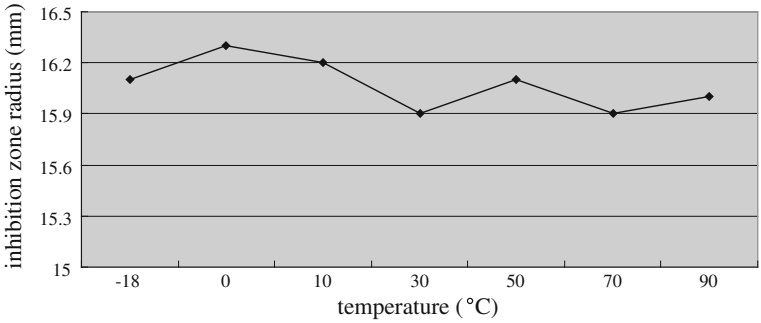

Fig. 60.2 The antibacterial effect of 10-HDA solution in different temperature to *E. coli*

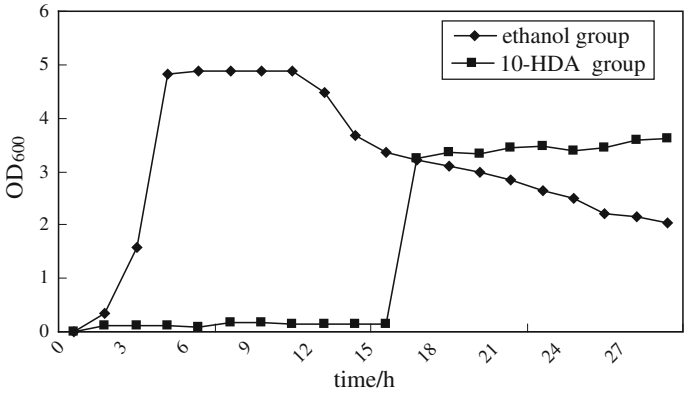

Fig. 60.3 Growth curves of *E. coli* cells exposed to1 mg/ml 10-HDA and unexposed to 10-HDA

60.3.5 Effect of 10-HDA on the Leakage of Ions from E.coli *Cell*

The concentration of K^+, Ca^{2+}, and Mg^{2+} were detected by atomic emission spectrometer after reaction of 10-HDA. As shown in Fig. 60.4a, b, c, when *E. coli* cultivation time prolonged, K^+, Ca^{2+}, and Mg^{2+} concentration in supernate in blank group changed gentlly, the same results were shown in ethanol control. While all three ions' concentration in 10-HDA group increased as time prolonged. The concentration was higher than blank group and ethanol group at 15 min and reached highest at 45 min. After incubation of 10-HDA for 45 min, the ions concentration were stable, which indicated that 10-HDA can destroy the permeability and integrity of the bacterial membranes, resulted in the leakage of K^+, Ca^{2+}, and Mg^{2+}.

60.3.6 Effect of 10-HDA on Leakage of 260 nm Absorbing Material from E. coli

From Fig. 60.5, we could see that there was no obvious change of 260 nm absorbing material from cell in blank group. The same outcome was shown in ethanol group. While the release of 260 nm in group added in 10-HDA was increased as time incubation prolonged, which indicated that 10-HDA can break the integrity of *E. coli* cell membrane resulted in release of macromolecule substance, such as DNA and RNA.

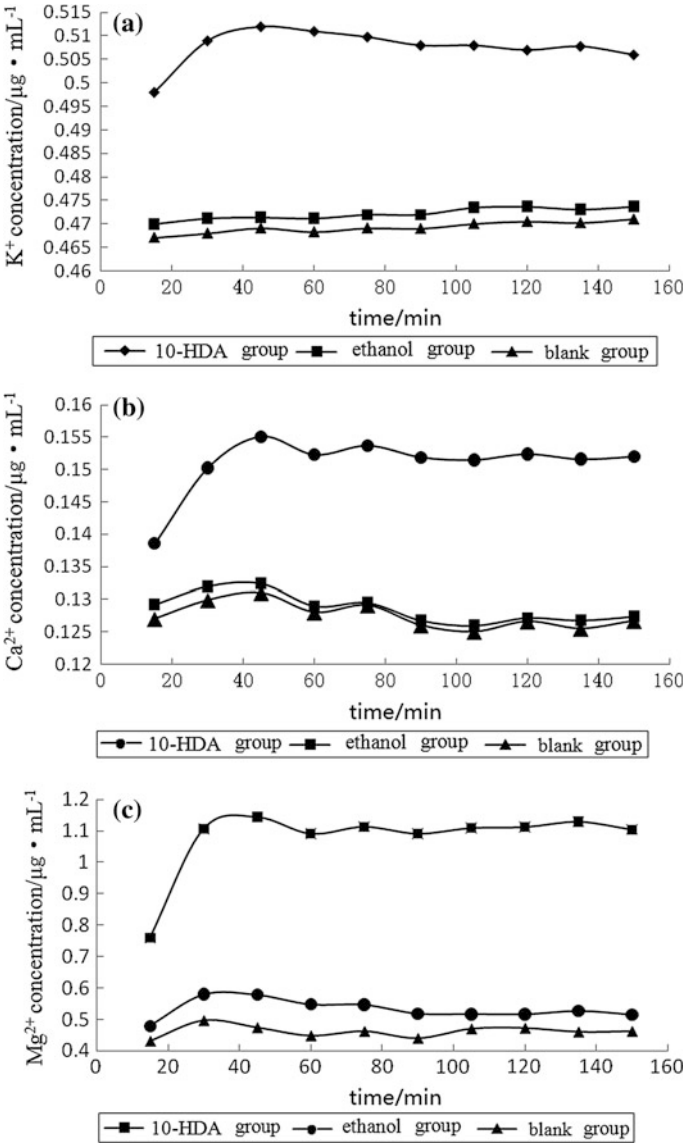

Fig. 60.4 **a** K^+ concentration in *E. coli*. Supernate added in 10-HDA detected by atomic emission spectrometer, **b** Ca^{2+} concentration in *E. coli*. Supernate added in 10-HDA detected by atomic emission spectrometer, **c** Mg^{2+} concentration in *E. coli*. Supernate added in 10-HDA detected by atomic emission spectrometer

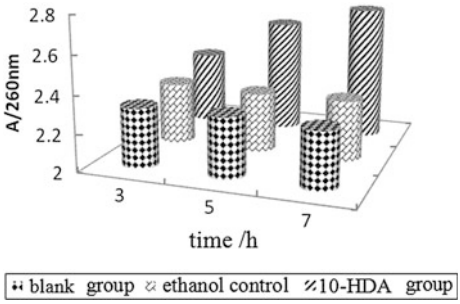

Fig. 60.5 Effect of 10-HDA on leakage of 260 nm absorbing material from *E.coli*

60.4 Discussion and Conclusion

In our study, we first detected the antibacterial activity of 10-HDA against *E. coli*, *B.subtilis*, *S. aureus*, and *Saccharomyces cerevisiae by* oxford cup method. And the results showed that 10-HDA has obvious effect against Gram-negative bacteria and its antibacterial activity was not affected by different pH and temperature, which indicated that the stability of 10-HDA against bacteria.

To understand the antibacterial mechanism of 10-HDA to Gram-negative bacteria, we selected *E. coli* as model to study the effect of 10-HDA. As is shown in Fig. 60.3, the growth curve of *E. coli* included three phases: lag phase, exponential phase, and stabilization phase. However, decline phases in each growth curve could not be revealed because we only assayed the total numbers of bacteria, including live and dead ones, based on the value of OD600. The result indicated that 10-HDA could effectively inhibit the proliferation and growth of *E. coli*.

Furthermore, the acting mechanism of 10-HDA on *E. coli* was investigated by analyzing the leakage of ions and release of 260 nm absorbing materials from bacterial cells following treatment with 10-HDA. The experimental results indicated that 10-HDA changed ionic conductivity, resulted in the leakage of K^+, Ca^{2+}, and Mg^{2+} from bacterial cell, suggesting that 10-HDA was able to destroy the permeability and integrity of the bacterial membranes. It has been estimated that approximately 3.5 million molecules of LPS cover three quarters of the surface of *E. coli*, with the remaining quarter composed of membrane proteins. Evidence from genetic and chemical experiments have proved that the LPS layer of the outer membrane plays an essential role in providing a selective permeability barrier for *E. coli* and other Gram-negative bacteria. And mutant altered LPS structures could increase permeability compared with that of native cells [16]. K^+, Ca^{2+}, and Mg^{2+} adsorped by LPS not only to increase the tenacity of cell wall but also to keep enzyme activity as important elements. While 10-HDA with terminal carboxyl group can be dissociated to $[HOCH_2(CH_2)_8COO^-]$ and $[H^+]\circ[HOCH_2(CH_2)_{8-}COO^-]$ can competitive adsorption of inorganic ions attached to LPS, which resulted in leakage of LPS, and cut down the tenacity of cell wall, then lead to cell death. Also we can infer enzyme activity which was inhibited because of decrease of the ion concentration, thus disturb bacterial normal growth.

By detecting the 260 nm absorbing materials using a UV–Vis spectrophotometer, it was showed that the membrane integrity was damaged and resulted in the leakage of large molecules such as DNA, RNA materials. Youqing Xu [17] find that polyunsaturated fatty acid interfere and affect DNA synthesis in bacterial nucleus such as *E. coli.* The experiments in Beijing Medical University drawed similar conclusion [18]. In conclusion, the combined results suggested that 10-HDA could damage the permeability and integrity of bacterial cell membrane, lead to the important intracellular materials flow out from cell and finally caused bacteria to die.

Acknowledgments This work was supported by grants from the National Natural Science Foundation of China (No: 31171727 and 31201281).

References

1. Blum MS, Novak AF, Taber S (1959) 10-Hydroxy-delta 2-decenoic acid, an antibiotic found in royal jelly. Science 130:452–453
2. Melliou E, Chinou I (2005) Chemistry and bioactivity of royal jelly from Greece. J Agric Food Chem 53:8987–8992
3. Vucevica D, Mellioub E, Vasilijica S et al (2007) Fatty acids isolated from royal jelly modulate dendritic cell-mediated immune response in vitro. Int Immunopharmacol 7:1211–1220
4. Nagai T, Inoue R, Suzuki N, Nagashima T (2006) Antioxidant properties of enzymatic hydrolysates from royal jelly. J Med Food 9:363–367
5. Nagai T, Sakai M, Inoue R et al (2001) Antioxidative activities of some commercially honeys, royal jelly and propolis. Food Chem 75:237–240
6. Satomi KM, Iwao O, Shimpei U et al (2004) Identification of a collagen production-promoting factor from an extract of royal jelly and its possible mechanism. Bioscience, Biotechnol Biochem 68:767–773
7. Park HM, Wang EH, Lee KG et al (2011) Royal jelly protects against ultraviolet β–induced photoaging in human skin fibroblasts via enhancing collagen production. J Med Food 14:899–906
8. Townsend GF, Morgan JF, Hazlett B (1959) Activity of 10-hydroxydecenoic acid from Royal Jelly against experimental leukaemia and ascitic tumours. Nature 183:1270–1271
9. Townsend GF, Morgan JF, Toinai S et al (1960) Studies on the in vitro antitumor activity of fatty acids 10-Hydroxy-2-decenoic acid from royal jelly. Cancer Res 20:503–510
10. Nakaya M, Onda H, Sasaki K (2007) Effect of royal jelly on bisphenol A-induced proliferation of human breast cancer cells. Biosciences, Biotechnol Biochem 71:253–255
11. Boukraa L, Meslem A, Benhanifia M et al (2009) Synergistic effect of starch and royal jelly against *Staphylococcus aureus* and *Escherichia coli*. J Altern Complem Med 15:755–757
12. Eshraghi S, Seifollahi F (2003) Antibacterial effects of royal jelly on different strains of bacteria. Iran J Public Health 32:25–30
13. Mccleskey CS, Melampy RM (1939) Bactericidal properties of royal jelly of the honeybee. J Econ Entomol 32:581–587
14. Kitahara T, Sato N, Ohya Y et al (1995) The inhibitory effect of ω-hydroxy acids in royal jelly extract on sebaceous gland lipogenesis. J Dermatol Sci 10:75–75
15. Yatsunami K, Echigo T (1985) Antibacterial action of royal jelly. Bull Fac Agric Tamagawa Univ 25:13–22

16. Amro NA, Kotra LP, Wadu-Mesthrige K et al (2000) High-resolution atomic force microscopy studies of the *Escherichia coli* outer membrane: structural basis for permeability. Langmuir 16:2789–2796
17. Youqing Xu, Shaonan Pang, Zhaokun Ding et al (2011) Effect of gene expression and mechanism on polyunsaturated fatty acid. Feed Industry 32(2):56–60
18. Jingyao Xu, Baoqin Ren (2000) Study and utilization of royaljelly acid in royal jelly. Chinese medicine science and Technology Press, Beijing, pp 109–113

Chapter 61
Characterization of Antifungal Chitinase from *Bacillus licheniformis* TCCC10016

Yu Zheng, Qingjuan Yang, Chaozheng Zhang, Jianmei Luo, Yanbing Shen and Min Wang

Abstract Fungal plant diseases are one of urgent problems to agricultural production. With an increased attention of environmental issue, biological control using microorganisms or their secretions exhibited an excellent performance for preventing plant diseases. Chitinase could inhibit the growth of pathogenic fungi by lysing the cell wall. In this work, a chitinase-producing strain, *Bacillus licheniformis* TCCC10016 was screened from 16 bacteria strains using chitin as the sole carbon source. Enzyme activity analysis showed that the expression of the extracellular chitinase was induced by the substance chitin. This chitinase showed an obviously inhibitory effect on pathogen, *Fusarium oxysporum*. Chitinase was purified by ammonium sulfate salt fractionation from the culture supernatant. The optimal pH and temperature of enzyme-catalyzed reaction were 7.0 and 60 °C, respectively. It exhibited a good stability in a broad pH range 5–8 or at the temperature of 37 °C and 60 °C. Additionally, the activity could be improved by Na^+ and Fe^{3+}, however, Zn^{2+} and Co^{2+} showed an inhibited effect.

Keywords *Bacillus licheniformis* · Biocontrol · Chitinase · Characterization

61.1 Introduction

One of the primary concerns to the agricultural production is the plant diseases caused by fungal pathogens. Conventionally, it was overcome by the chemical fungicides, however, this traditional treatment brings adverse environmental effects, such as pollution, health hazards to human and toxic effects on non-target

Y. Zheng · Q. Yang · C. Zhang · J. Luo · Y. Shen · M. Wang (✉)
Key Laboratory of Industrial Fermentation Microbiology, Tianjin Key Laboratory of Industrial Microbiology, Ministry of Education, College of Biotechnology, Tianjin University of Science and Technology, Tianjin 300457, People's Republic of China
e-mail: minw@tust.edu.cn

T.-C. Zhang et al. (eds.), *Proceedings of the 2012 International Conference on Applied Biotechnology (ICAB 2012)*, Lecture Notes in Electrical Engineering 249,
DOI: 10.1007/978-3-642-37916-1_61, © Springer-Verlag Berlin Heidelberg 2014

organisms including beneficial life forms, and fungicide-resistance of pathogens [1]. Besides, this approach is only effective for a short time in the growing season [2]. Hence, there are increasing concerns to biological control using microorganisms or their secretions to prevent plant pathogens and insect pests because it offers an environmentally friendly and realistic alternative strategy for the control of plant disease [3].

The general mechanism of biological control includes the competition for substrates and site exclusion, the production of antibiotic, induced systemic response and the parasitism, and production of extracellular enzymes. However, the widely used strategy for the biocontrol is searching appropriate strains which could produce extracellular substrates such as antimicrobial peptides, chitinolytic enzymes, proteases, and glucanases [4]. Among them, chitinases which occur in a wide range of organisms including viruses, bacteria, fungi, insects, higher plants, and animals can inhibit the growth of pathogenic fungi and cause cell lysis. It can disrupt the mature hyphae, conidia, chlamydospores, and sclerotia by depolymerizing the chitin which is the essential structural component of them ranging from 22–40 % [5]. Thus, chitinases play a critical role against fungal pathogens in biological control [6].

Bacteria secrete chitinase probably for digesting N-acetyl-D-glucosamine-containing macromolecules that is used as their carbon and nutrient sources [7]. Until now, some bacteria that can produce chitinase have been reported, including *Enterobacter* [8], *Aeromonas* [9], *Vibrio furnissii* [10], *Serratia marcescens* [11], *Bacillus thuringiensis* [12], *B. cereus* [13], *B. amyloliquefaciens* [14], *B. pumilus* [15], *B. licheniformis* [6], and other genera of bacteria. Here we have succeeded in screening a *B. licheniformis* which is able to produce chitinase. This study presents the concentration, characterization, and the biocontrol potential of chitinase from *B. licheniformis* TCCC10016.

61.2 Materials and Methods

61.2.1 Microorganism and Medium

B. subitlis, *B. licheniformis*, *B. cereus*, *B. polymyxa*, *B. amyloliquefaciens*, and *Fusarium oxysporum* were conserved in department of Biological Engineering, Tianjin University of Science and Technology, Tianjin, China.

Selection medium contains ($g \cdot L^{-1}$) diammonium citrate 0.625, NaCl 0.250, KH_2PO_4 0.375, $MgSO_4 \cdot 7H_2O$ 0.125, Na_2CO_3 0.375, 6.5 mL glycerol, and 2 % colloidal chitin, pH 7.0 [16].

LB medium was used for seed cultivation. For producing chitinase, colloidal chitin was added to the LB medium at the final concentration of 2 % as an inducer. The *F. oxysporum* was cultivated on potato dextrose agar (PDA).

61.2.2 Preparation of Colloidal Chitin

Colloidal chitin was prepared according to the method of Ramıreza and Avelizapa [17]. The definite means are as follows: 10 g of chitin powder from crab shells (Sigma) was added to 100 mL of 85 % phosphoric acid and kept in refrigerator (4 °C) for 24 h. Thereafter, 2 L tap water was added and the gelatinous white material formed was separated by filtration through filter paper. The retained cake was washed with tap water until the filtrate has a pH of 6.5. The colloidal chitin obtained had a soft, pasty consistency, with 90–95 % moisture.

61.2.3 Selection of Chitinase-Producing Bacteria

Bacteria capable of producing chitinase were selected from 16 strains, including *B. subitlis*, *B. licheniformis*, *B. Cereus*, *B. polymyxa*, and *B. amyloliquefaciens*. These strains were grown on selection medium at 37 °C for 3–4d with chitin as the sole carbon source. The chitinolytic ability was observed by the presence of clear haloes around the colonies.

61.2.4 Chitinase Activity Assay

As in enzymatic reaction substrate, colloidal chitin was dyed with Remazol Brilliant Blue R® (RBB). 25 g of colloidal chitin were homogeneously mixed with 100 mL of aqueous solution of RBB (Sigma) at 0.84 % ($m \cdot v^{-1}$). The resulting suspension was heated in a boiling water bath for 1 h with gentle stirring to fix the RBB color. The dyed colloidal material was obtained by filtration. The obtained material was suspended in 25 mL of aqueous solution of 1.5 % sodium dichromate and 1.5 % sodium potassium tartrate without any pH adjustment, followed by heating with gentle stirring in a boiling water bath for 10 min. The dyed material was then separated by filtration and washed with hot water until the filtrate was colorless. The gelatinous blue material (CC-RBB) obtained was sterilized by autoclaving and stored at 4 °C [18].

One mL of supernatant sample of fermentation broth and 1 mL of a 10 % ($w \cdot v^{-1}$) suspension of CC-RBB in 0.2 M sodium phosphate buffer (pH 7) were mixed and incubated at 50 °C for 1 h. After inactivation of the enzyme by heating in a boiling water bath for 5 min, the tubes were centrifuged at 4500 × g and the absorbance of the supernatant was read at 595 nm. One unit of chitinase activity was defined as the amount of enzyme that produced an increase of 0.01 in the absorbance.

61.2.5 Enzyme Production and Concentration

The seed culture was transferred into the fermentation medium (10 % inoculation volume) in a 250 mL flask and grown at 37 °C for 24 h in the shaker (180 rpm). The fermentation broth was centrifuged for 10 min at 10000 × g (4 °C) and the supernatant was used for enzyme purification. Ammonium sulfate was added to the supernatant at 30 % saturation. The solution was kept overnight at 4 °C. After centrifugation for 10 min at 10000 × g (4 °C), ammonium sulfate was added to the supernatant at 70 % saturation and the solution was kept overnight at 4 °C. The solution was centrifuged for 10 min at 11000 × g (4 °C), and then the precipitate was dissolved by 0.05 mol/L sodium phosphate buffer with pH 7.0 and dialyzed in the same buffer to obtain crude chitinase [19].

61.2.6 Antifungal Assays of Chitinase

Inhibition effect of the chitinases against *F. oxysporum* was determined by cylinder-plate method. To assay the effect of chitinases on spore germination of *F. oxysporum*, a spore suspension (10^5–10^6 spores·mL^{-1}) was prepared from *F. oxysporum* cultures. Spore suspensions (50 μL) supplemented with/without chitinases were added into oxford cup fixed on the PDA plate followed by incubation for 5–7d at 28 °C under moist conditions [20]. The inhibition activity was determined by the smallest inhibition diameter.

61.2.7 Effect of pH and Temperature on Chitinase Activity and Stability

To investigate the effect of temperature on schitinase activity, reaction mixtures were incubated at various temperatures ranged from 20 °C to 80 °C for 1 h in 50 mmol·L^{-1} sodium phosphate buffer at pH 7.0. The optimum pH of chitinase was determined at 50 °C but varying the pH value from 4.0 to 10.0 adjusted by using the following buffer, citrate-phosphate buffer (pH 3.0–5.0), NaH_2PO_4–Na_2HPO_4 buffer (pH 6.0–8.0), Glycine-NaOH buffer (pH 9.0–10.0) [21].

The temperature stability of chitinase was studied by incubating enzyme samples at different temperature. At certain time intervals, the residual activity was measured under standard assay condition. To determine the pH stability, enzyme samples were incubated at various buffer with pH range from 4–9 at 37 °C for 24 h, and the remained enzyme activity was measured under standard assay condition.

61.2.8 Effect of Various Metal Ions on Chitinase Activity

In order to study the effect of various metal ions on chitinase activity, enzyme samples were assayed with 10 % CC-RBB in the presence of various cations in final concentrations of 10 mM at 37 °C, 180 rpm for 30 min. The measured activities were compared with the activity of the samples without added under the same conditions.

61.3 Results and Discussion

61.3.1 Selection of Strain Producing Chitinase

Among 16 bacterial strains, 5 strains can grow on the plate with colloidal chitin as the sole carbon source. However, only *B. licheniformis* TCCC10016 exhibited a significant growth and formed the clear haloes around the colony when compared with the other strains (data not shown). Therefore, *B. licheniformis* TCCC10016 was chosen for the further research.

In order to investigate the inductivity of chitinase, *B. licheniformis* TCCC10016 was cultivated in LB medium containing/uncontaining chitin, respectively, and then the extracellular chitinase activities were analyzed. As demonstrated in Fig. 61.1, the highest chitinase activity (25.26 U/mL) was obtained after 20 h cultivation. However, little activity was detected when chitin was not present in medium, indicating that the expression of chitinase was induced by chitin.

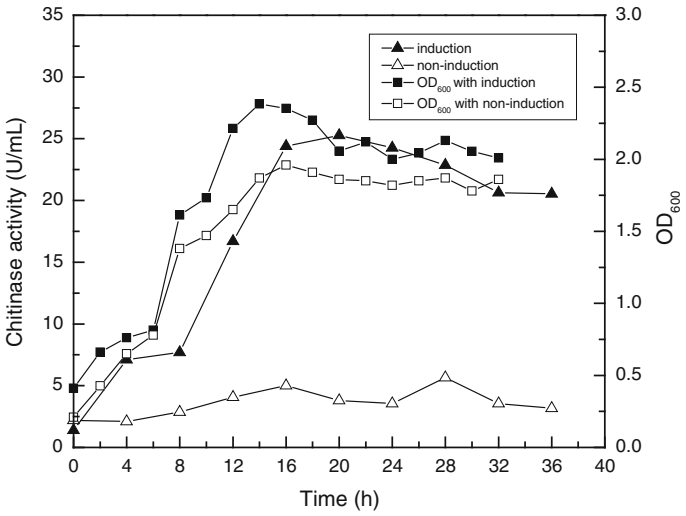

Fig. 61.1 Time course of cell growth and chitianse activity

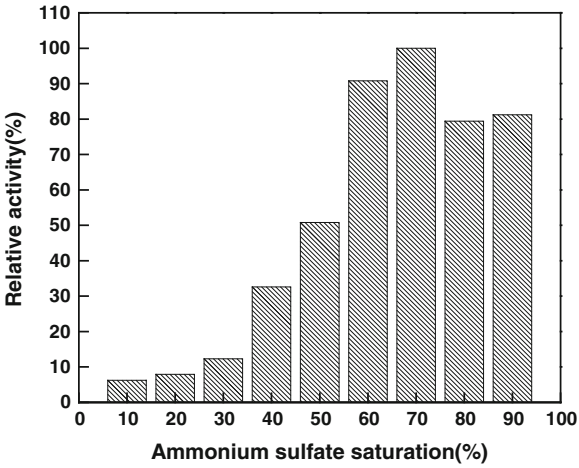

Fig. 61.2 Enzyme activity of ammonium sulfate salt fractionation

61.3.2 Concentration of Chitinase

Extracellular chitinase of *B. licheniformis* TCCC10016 was efficiently concentrated from fermentation broth by the salting-out method. The maximal activity was detected in the fractionation obtained with ammonium sulfate saturation of 70 % (Fig. 61.2).

61.3.3 The Antifungal Activity of Chitinase

The in vitro antifungal activity of chitinase was investigated using the method of cylinder-plate. Chitinase of *B. licheniformis* TCCC10016 show an obvious inhibition effect against phytopathogenis fungal *F. oxysporum* which caused plant damping off disease, as shown in Fig. 61.3a. Also, chitinase could effectively inhibit the germination of *F. oxysporum* spores (Fig. 61.3b). The inhibition ratio was 82.4 % when the concentration of chitinase was 55.11 U/mL. Therefore, chitinase from the strain *B. licheniformis* TCCC10016 could be potentially used for biocontrol against phytopathogenic fungi.

61.3.4 Effect of Temperature and pH on Chitinase Activity

The optimum temperature and pH for the chitinase of *B. licheniformis* TCCC10016 were 60 °C (Fig. 61.4) and 7.0 (Fig. 61.5), above which the relative activity sharply decreased, respectively, which were according with the other reports [22, 23].

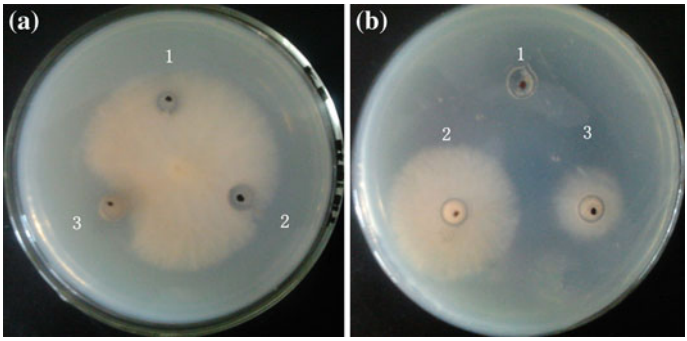

Fig. 61.3 Inhibitory activity of chitinase on *F. oxysporum,* **a** effect of chitinase on the growth of *F. oxysporum* (*1* sterile water; *2* phosphate buffer; *3* chitinase) **b**, effect of chitinase on spore germination of *F. oxysporum* (*1* phosphate buffer; *2* spore suspension; *3* spore suspension with chitinase)

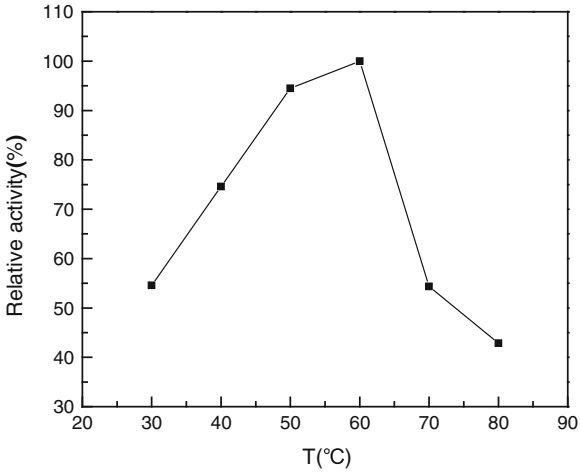

Fig. 61.4 Effect of temperature on the activity of chitinase from *B. licheniformis* TCCC10016

61.3.5 Effect of Temperature and pH on Chitinase Stability

As shown in Fig. 61.6, after 8 h of incubation at 37, 60, and 70 °C, the remained enzyme activity was 80, 60, and 15 %, respectively, indicating high temperature would accelerate the inactivity of chitinase. The relative activity remained more than 90 % after incubating for 30 min under pH 5–8 (Fig. 61.7). However, the chitinase from *B. licheniformis* DSM8785 is proved stable under pH4–11 [24].

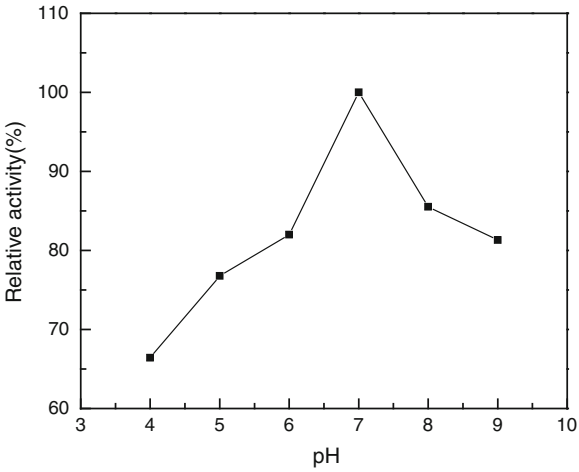

Fig. 61.5 Effect of pH on the activity of chitinase

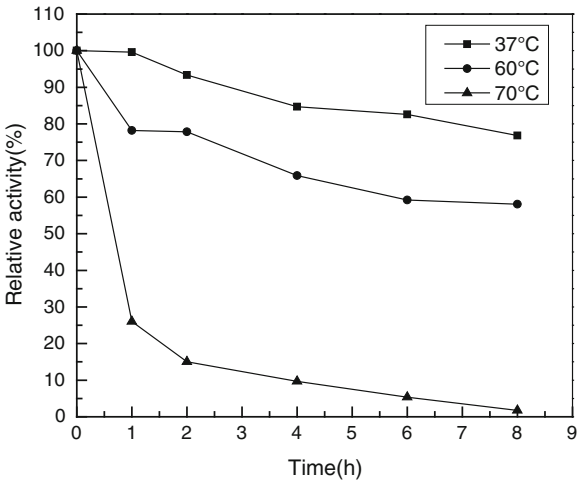

Fig. 61.6 Effect of temperature on the stability of chitinase

61.3.6 Effect of Metal Ions on Chitinase Activity

Certain metal ions could affect the activity of chitinase. As listed in Table 61.1, Na^+ and Fe^{3+} led to a slightly improved chitinase activity, while Zn^{2+} and Co^{2+} showed an inhibitory effect. Those results were consistent with the chitinase from *B. licheniformis* DMS13 and *Bacillus* sp. DAU101 [6, 25]. Generally, the chitinase activity influenced by metals depends on many factors, including the metal oxidation, masking the catalytically active subunits of the enzyme, degrading proteins, changing the conformation of the particles of the enzyme, and competing with cation activators connected with the formation of a substrate-enzyme complex [26].

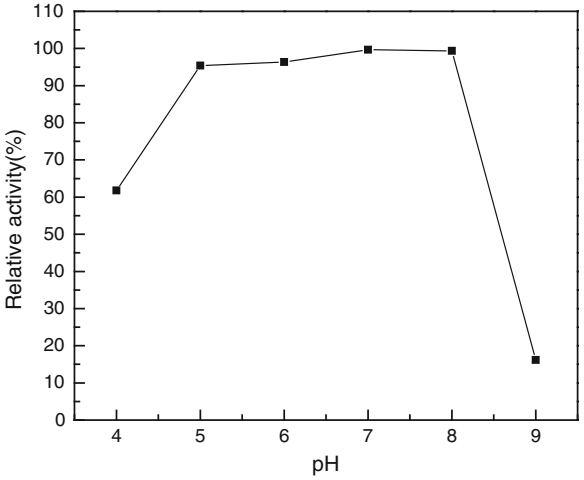

Fig. 61.7 Effect of pH on the stability of chitinase

Table 61.1 Effect of metal ions on the activity of chitinase

Metal ions	Relative activity (%)
Na^+	106.8 ± 0.5
K^+	98.6 ± 2
Zn^{2+}	62.2 ± 2
Fe^{2+}	87.2 ± 3
Mn^{2+}	92.4 ± 2
Mg^{2+}	99.9 ± 3
Cu^{2+}	90.3 ± 1
Ni^{2+}	88.6 ± 1
Co^{2+}	60.2 ± 1
Fe^{3+}	108.3 ± 0.3

61.4 Conclusion

Numerous microorganisms with biocontrol activity have been reported. Consequently, isolation and characterization of the specific fungicidal factors such as antibiotics, chitinolytic enzymes, and glucanases is primary objectives that biochemical researchers focused on. Many biocontrol bacterial can express chitinase to improve the plant resistance to disease by inhibiting the pathogens growth when plant was attacked by pathogenic fungi. Therefore, screening of microorganism producing chitinase known as one of the most potent enzymes for degrading fungal cell wall is important to study their biocontrol mechanism.

The strain *B. licheniformis* TCCC10016 selected in this report show a chitinolytic activity and can inhibit the growth of *F. oxysporum*. Furthermore, according to the results obtained from the characterization of chitinase, the expression of chitinase was induced by colloidal chitin or other substrate (not to study). The optimal temperature and pH for chitinolytic reaction is 60 °C and 7.0. Although

many questions remain to be solved before its application in the agricultural field, chitinase from *B. licheniformis* TCCC10016 shows a potential as a biocontrol agent toward plant pathogenic fungal, such as *F. oxysporum*.

Acknowledgments This work was supported by National High Technology Research and Development Program of China (2012AA022108, 2013AA102106), the Natural Science Foundation of Tianjin (09JCZDJC19100) and Foundation of Tianjin University of Science and Technology (20090403).

References

1. Dahiya N, Tewari R, Hoondal GS (2006) Biotechnological aspects of chitinolytic enzymes: a review. Appl Microbiol Biotechnol 71:773–782
2. Chen F, Wang M, Zheng Y et al (2010) Quantitative changes of plant defense enzymes and phytohormone in biocontrol of cucumber fusarium wilt by *Bacillus subtilis* B579.World J Microb Biot 26:675–684
3. Wang SL, Yen YH, Tsiao WJ et al (2002) Production of antimicrobial compounds by *Monascus purpureus* CCRC31499 using shrimp and crab shell powder as a carbon source. Enzyme Microb Tech 31:337–344
4. Gohel V, Singh A, Vimal M et al (2006) Bioprospecting and antifungal potential of chitinolytic microorganisms. Afr J Biot 5(2):54–72
5. Muzzarelli RAA (1977) Chitin. Pergamon Press Ltd, Oxford
6. Nguyen HA, Nguyen T, Nguyen TT et al (2012) Chitinase from *Bacillus licheniformis* DSM13: Expression in *Lactobacillus plantarum* WCFS1 and biochemical characterisation. Protein Expres Purif 81:166–174
7. Bhattacharya D, Nagpure A, Gupta RK (2007) Bacterial chitinases: properties and potential. Crit Rev Biotechnol 27:21–28
8. Chernin L, Ismailov Z, Haran S et al (1995) Chitinolytic enterobacter agglomerans antagonistic to fungal plant pathogens. Appl Environ Microb 61:1720–1726
9. Wu ML, Chuang YC, Chen JP et al (2001) Chang. Identification and characterization of the three chitin-binding domains with the multi-domain chitinase Chi92 from *Aeromonas hydrophila* JP101. Appl Environ Microb 67:5100–5106
10. Bassler BL, Yu C, Lee YC et al (1991) Chitin utilization by marine bacteria: degradation and catabolism of chitin oligosaccharides by *Vibrio furnissii*. J Biol Chem 266:24276–24286
11. Lysenko O (1976) Chitinase of *Serratia marcescens* and its toxicity in insects. J Invertebr Pathol 27:385–386
12. Swirnoff WA, Valero J (1977) Determination of the chitinolytic of nine subspecies of *Bacillus thuringiensis*. J Invertebr Pathol 30:265–266
13. Wang SY, Moyne AL, Thottappilly G et al (2001) Purification and characterization of *Bacillus cereus* exochitinase. Enzyme Microb Tech 28:492–498
14. Wang SL, Shi IL, Liang TW et al (2002) Purification and characterization of two antifungal chitinases extracellularly produced by *Bacillus amyloliquefaciens* V656 in a SCSP medium. J Agric Food Chem 50:2241–2248
15. Ahmadian G, Degrassi G, Venturi V et al (2007) *Bacillus pumilus* SG2 isolated from saline conditions produces and secretes two chitinases. J Appl Microb 103:1081–1089
16. Castaida-agull M (1956) Studies on the biosynthesis of extracellular proteases by bacteria. J Gen Physiol 89:369–373
17. Rojas-Ave lizapa LI, Cruz-Camarillo R, Guerrero MI et al (1999) Selection and characterization of a proteo-chitinolytic strain of *Bacillus thuringiensis*, able to grow in shrimp waste media. World J Microb Biot 15:299–308

18. Gomez Ramırez M, Rojas Avelizapa li, Rojas Avelizapa NG et al (2004) Colloidal chitin stained with remazol brilliant blue R, a useful substrate to select chitinolytic microorganisms and to evaluate chitinases. J Microb Meth 56:213–219
19. Park JK, Kim JD, Park YI et al (2012) Purification and characterization of a 1,3-β-D-glucanase from *Streptomyces torulosus* PCPOK-0324. Carbohyd Polym 87:1641–1648
20. Kamil Z, Rizk M, Saleh M et al (2007) Isolation and identification of rhizosphere soil chitinolytic bacteria and their potential in antifungal biocontrol. Global J Mol Sci 2(2):57–66
21. Liu Y, Tao J, Yan YJ et al (2011) Biocontrol efficiency of *Bacillus subtilis* SL-13 and characterization of an antifungal chitinase. Biotechol Bioeng 19(1):128–134
22. Waghmare SR, Ghosh JS (2010) Chitobiose production by using a novel thermostable chitinase from *Bacillus licheniformis* strain JS isolated from a mushroom bed. Carbohyd Res 345:2630–2635
23. Wang SL, Liu CP, Liang TW (2012) Fermented and enzymatic production of chitin/chitosan oligosaccharides by extracellular chitinases from *Bacillus cereus* TKU027. Carbohyd Polym 90:1305–1313
24. Songsiriritthigul C, Lapboonrueng S, Pechsrichuan P et al (2010) Expression and characterization of *Bacillus licheniformis* chitinase (ChiA), suitable for bioconversion of chitin waste. Bioresource Technol 101:4096–4103
25. Lee YS, Park IH, Yoo JS et al (2007) Cloning, purification, and characterization of chitinase from *Bacillus* sp. DAU101. Bioresource Technol 98:2734–2741
26. Donderski W, Brzezinska MS (2005) The influence of heavy metals on the activity of chitinases produced by planktonic, benthic and epiphytic bacteria. Polish J Environ Studies 14(6):851–859

Chapter 62
Ultrastructure of Starches in Two Canned-Bean Products Before and After Digestion In Vitro

Xiaohong Cao, Zhongkai Zhou, Jing Li, Fang Wang and Yumei Jiang

Abstract The changes in physical and chemical structure of starches in bean products pre- and post-digestion in vitro were examined. In comparison with the morphology of starch in food, resistant starch (RS) in digesta exhibits a narrow size distribution with most particles being from 4 to 7 μm. Fourier Transform Infrared Spectroscopy (FTIR) results showed that the absorbance band at 1022 cm^{-1}, which represents amorphous/disordered starch in food, is sensitive to amylolysis, whereas the absorbance band at 1047 cm^{-1}, which represents ordered starch was more pronounced in digesta. Scanning iodine spectrum results indicated that the average molecular weight of amylose in digesta was smaller than that in food. The molecular profile of RS showed a lack of higher molecular weight amylose. Study of SE-HPLC further proved that the amylopectin fraction is absent in RS molecular profile.

Keywords Starch · Resistant starch · Digestion · Amylose · Molecular structure

62.1 Introduction

Besides being a major plant metabolite, starch provides the principal energy source in the diet of most humans. Until about two decades ago, it was believed that starch was completely digested and absorbed in the small intestine. However, it is now realised that a variable fraction of ingested starch is resistant to digestion, passing through the small intestine and reaching the large bowel where it may be fermented by the colonic microflora [1]. This fraction, known as resistant starch (RS), is defined as the sum of starch and the products of starch degradation not

X. Cao · Z. Zhou (✉) · J. Li · F. Wang · Y. Jiang
Key Laboratory of Food Nutrition and Safety, Ministry of Education, Tianjin University of Science and Technology, Tianjin 300457, People's Republic of China
e-mail: zkzhou@tust.edu.cn

T.-C. Zhang et al. (eds.), *Proceedings of the 2012 International Conference on Applied Biotechnology (ICAB 2012)*, Lecture Notes in Electrical Engineering 249,
DOI: 10.1007/978-3-642-37916-1_62, © Springer-Verlag Berlin Heidelberg 2014

absorbed in the small intestine of healthy individuals [2]. RS can be subdivided into four major types according to the mechanism by which they resist digestion: RS1 refers to starch entrapped by botanical structures which render it inaccessible to digestive enzymes (e.g. in wholegrain foods); native, ungelatinized granules, such as those found in raw potatoes, under ripe bananas and high amylose maize starches, are resistant to amylolysis (RS2); retrograded starch (RS3), for example, that found in potato that has been cooked and allowed to cool; and starches that have undergone certain chemical modification, such as etherisation or esterification, that confers resistance to digestion processes (RS4) [3].

In recent years, an increasing number of studies have focused on the importance of RS as a substrate for stimulating colonic fermentation and promoting production of short-chain fatty acids, which are important for the health and normal functioning of the colon, in particular [1, 3]. It is clear that different resistant starches vary markedly in their effects on the composition and metabolic activity of the large bowel microflora, and thus their potential beneficial effects on intestinal health. There is also renewed interest in the possibility of improving management of diabetes, and reducing risk of type II diabetes and related chronic disorders, by altering postprandial glycemic impact through the strategic use of starches of low digestibility [4, 5].

Starch assimilation in the human gastrointestinal tract is a complex process. Susceptibility to hydrolysis by α-amylases is certainly influenced by the physicochemical properties of the starch itself; however, knowledge of the specific morphological and molecular properties which are responsible for resistance to enzymatic digestion is still very limited. Thus, the objective of present study is to define the differences in morphology and molecular characteristics of starches in canned beans before and after digestion in order to provide an insight into the molecular structure of digestible and resistant starches. The study foods were subjected to an in vitro process involving a dynamic multi-enzyme incubation system designed to simulate human digestion of starchy foods.

62.2 Materials and Methods

62.2.1 Materials

Industrially processed bean products (canned four-beans and red kidney bean:RKB) were obtained from supermarket. The former product contains a mixture of RKB, Baby Lima, Garbanzo and Great Northern beans. Alpha-amylase (from porcine pancreas), pepsin (from gastric porcine mucosa) and amyloglucosidase (from *Aspergillus niger*) were purchased from Sigma Chemical Co (NSW, Australia). Other chemicals and solvents used in this study were either analytical or high performance liquid chromatography (HPLC) grade.

62.2.2 Methods

62.2.2.1 Food Digestion In Vitro

The bean kernels were digested using an in vitro model of human starch digestion. Briefly, the beans were chopped using a manually operated domestic food processor and the macerated product containing 500 mg of carbohydrate were mixed with artificial saliva. The resulting mash was then subjected to a series of incubations at physiological pH and temperature and using a cocktail of enzymes of bacterial, fungal and mammalian origin, designed to mimic gastric and pancreatic digestion. Residual starch was isolated and used for the following analyses.

62.2.2.2 Amylose-Iodine Spectrum

Amylose-iodine complexing analysis was performed according to the procedure of Knutson [6]. Briefly, starch obtained as described above was dissolved at room temperature in a mixture of 90 % DMSO and 10 % water containing 6 mmol iodine. The solution was diluted to A_{max} of 1.0–1.1 using reverse osmosis (RO) water. Samples were allowed to stand in the dark at room temperature for 1 h under an aluminium foil cover to ensure maximum complex formation and colour development. Spectrophotometric measurements were made using a Varian (Model Cary 1E, U.S.A.) UV-Visible scanning spectrometer.

62.2.2.3 SE-HPLC for Analysis of Starch Molecular Size Distribution

A 10 ml aliquot of aqueous dimethylsulfoxide (90:10, DMSO/water, v/v) was added to 50 mg of freeze-dried food and digesta in separate 25 ml test tubes. Each tube was capped and placed in a boiling water bath for 60 min and then cooled to room temperature before centrifuging at 3,000 rpm for 15 min. The supernatant was collected into a separate 75 ml polypropylene centrifuge tube and the dissolved starch precipitated by adding 30 ml of 95 % ethanol. The tube was then centrifuged (3,000 rpm for 15 min), the supernatant was discarded and the starch precipitate was redissolved in 0.5 ml of 0.2 M sodium hydroxide solution and mixed vigorously for approximately 30 s. The solution was neutralised by addition of sodium acetate buffer (0.5 ml; 0.05 M, pH 4.0) before adding ion-exchange resin (0.25 g, BioRad AG® 501-X8, USA) and incubating at 40 °C for 2 h with occasional shaking. The resin was separated using centrifugation (10,000 rpm for 10 min) and the resultant supernatant removed and subjected to SE-HPLC for determining starch molecular size distribution. HPLC conditions have been described in our previous study [7].

62.2.2.4 Fourier Transform Infrared Spectroscopy

FTIR spectrum was recorded on a Varian spectrometer (Model: Excalibur 3100) equipped with a cooled deuterated triglycine sulphate (DTGS) detector. The measurement was performed on a MIRacle^{TM} attenuated total reflectance (ATR) crystal plate with Digital Readout High Pressure Clamp (Pike Technologies, USA). Freeze-dried bean products and digesta were directly loaded on the plate and scanned in the range of 3,600–600 cm^{-1} at a resolution of 4 cm^{-1}. Prior to recording, the spectra were transformed against an empty cell as background. Spectra were base-line-corrected at 1,060 and 980 cm^{-1}. Finally the spectra were ATR corrected and deconvoluted using Varian Resolutions Pro Software, and absorbance values at 1047, 1022 and 100–995 cm^{-1} were obtained from the spectra.

62.2.2.5 Morphologies of Starch and RS in Food and Digesta

An aliquot (20 ml) of aqueous ethanol (50:50, EtOH/water, v/v) was added to 100 mg of freeze-dried beans and digesta in separate 50 mL beakers. The mixture was allowed to stand at room temperature for 2 h with occasional gentle shaking before it was filtered using three layers of muslin cloth. The filtrate was allowed to stand for a further 60 min without shaking to allow fine particles to precipitate. Approximately, 200 μL of the mixture (filtrate and residue) was spread on a microscope slide and dried at room temperature. The slides were stained using diluted I_2-KI solution and air dried again before visualisation of the starch. An Olympus microscope (Model BX41, Japan) equipped with a reflected fluorescence system (Model: U-LH100HGAPO, Japan) with 6-position filter slide (Model: U-RSL6), was used to observe the microscopic features of starches in food and freeze-dried digesta.

62.3 Results and Discussion

62.3.1 Morphology of Starches in Bean Products Pre- and Post-digestion

Cell wall and cell wall-enclosed-gelatinized starch in the two bean products prior to digestion were visualised and presented in Fig. 62.1. During the food preparation, starch was gelatinized, which leads to an irreversible collapse (disruption) (Fig. 62.1) of its granules. The visualisation also suggested that the organised cell wall was the structural characterisation of bean products. In comparison with botanical structures present in cereal food (Fig not shown), bean products contain high amounts of dietary fibre in a form that gives cell walls a high degree of resistance to disintegration during cooking. The major cell walls were still generally intact after cooking (Fig. 62.1).

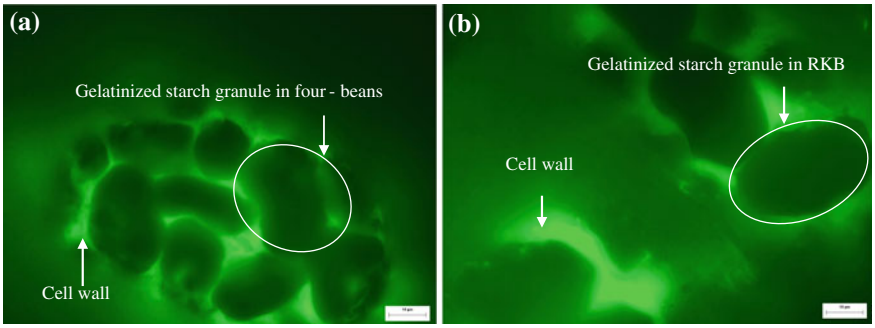

Fig. 62.1 Morphology of cell wall and cell wall-enclosed starches in four-beans and RKB. Bar = 10 μm

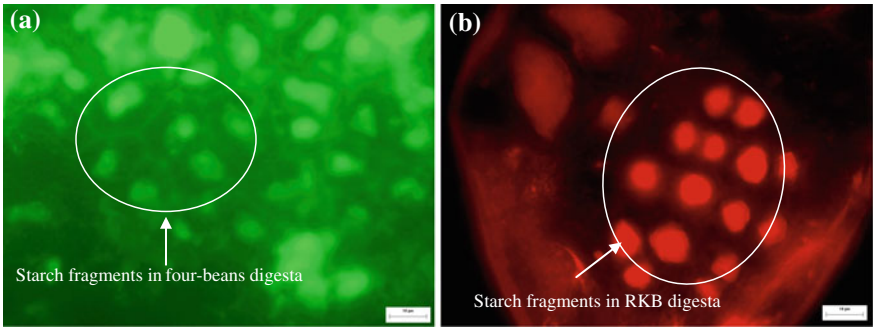

Fig. 62.2 Morphology of RS in digestion of four-beans (**a**) and RKB (**b**). Bar = 10 μm

The morphology of starch after digestion was presented in Fig. 62.2. It clearly demonstrates that the digestion process dramatically altered starch morphology. Unlike the starch present in the cooked beans (Fig. 62.1), starch fragments in digesta (i.e. RS) had a narrower size distribution (~4 to 7 μm) compared to the size of gelatinized starch granules in food (see Figs. 62.1 and 62.2). These fragments, which escape from digestion, were hypothesised to have an amylose-dominated structure.

62.3.2 FTIR Spectra of Starches in Bean Products Pre- and Post-digestion

The variation in IR spectrum as a function of digestion on starch polymorphs was measured and the absorbance characterisation in the range of 1,060–980 cm^{-1} is presented in Fig. 62.3. It is well known that bands at 1,047 and 1,022 cm^{-1} were

associated with the ordered and amorphous structures of starch, respectively, whereas the band at the 1,000–995 cm^{-1} region was found to be sensitive to water [8].

The band at 1,047 cm^{-1} was not sensitive to digestion (Fig. 62.3), suggesting the starch molecules corresponding to this band arrayed at an organised structure. It is clear that the band at 1,022 cm^{-1} was the most affected by digestion and it became less pronounced in digesta than in the food (Fig. 62.3), which indicated that the amorphous content of starch was eliminated by the digestion. Other study [9] indicated that the intensity of the band at 1,022 cm^{-1} increased from native to gelatinised starch (loss of ordered structures) and decreased from gelatinised starch to retrograded starch (reordering). The intensity of the band at 1,047 cm^{-1} was characterised by the opposite behaviour (i.e. decrease during gelatinisation, increase during retrogradation). Thus, the observation of the loss of the band at 1,022 cm^{-1} during the digestion allowed this band to be assigned to the amorphous fraction.

Furthermore, absorbance ratios 1047/1022 and 1022/995 cm^{-1} in Fig. 62.3 could be calculated to express the relative ordered structure of starch. A clear segregation existed in the digesta, defined by a higher ratio 1,047/1,022 cm^{-1} and a lower ratio 1,022/995 cm^{-1} compared to those in the food. Thus, this study suggested that, because of the removal of the less-organised region by amylolysis, the starch in digesta exhibited a higher level of organisation than that in the food. With such an organised structure (i.e. a higher ratio 1,047/1,022 and a lower ratio 1,022/995 cm^{-1}), the starch showed higher resistance to amylase hydrolysis compared to the starch with other structure, and this might be the major reason for the explanation of its escaping from the small intestine digestion.

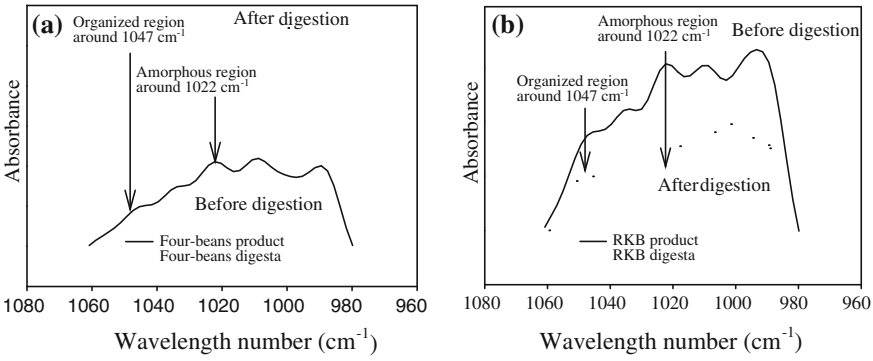

Fig. 62.3 FTIR spectra for four-beans (**a**) and RKB (**b**) before and after digestion

62.3.3 Molecular Characterisation of Starch in Bean Products and Digesta

62.3.3.1 Characteristics of Amylose-Iodine Spectrum

Amylose plays a major role in determining the physicochemical properties of starch, such as granule swelling, water absorption, molecule leaching, network formation, etc., during starch gelatinization, particularly in influencing the retrogradation process (i.e. the formation of RS3). Thus, the molecular size distribution of amylose in starches isolated from food and digesta was measured, using UV–Visible spectrophotometry, and the iodine spectra are shown in Fig. 62.4.

The amylose-iodine complexing spectra of starches isolated from the bean products were typical for high molecular weight amylose (Fig. 62.4). Five regions could be defined by their slopes, which were designated a, b, c, d and e [6]. The 'shoulder' region, represented by slopes 'a' and 'b' in Fig. 62.4, was the result of formation of complexing with the shorter chains of amylose molecules. After passing the point where colour formation occurs (degree of polymerisation-DP12 with a λ_{max} of 490 nm), the iodine colour changes from brown to blue when the chain length is up to DP 45 (with a λ_{max} of 570 nm). Thereafter, λ_{max} continues to rise with the increment of amylose chain length. After DP 400 ($\sim\lambda_{max}$ 645), λ_{max} is insensitive to amylose chain length. λ_{max} of amylopectin was similar to that of the lowest DP amylose (551 vs. 556 nm), but its absorptivity was much lower. Thus, the profile of amylose-iodine complexing spectrum could reflect the distribution of amylose with various molecular size (Fig. 62.4). Knutson [6] also suggested that as DP and absorptivity increased, the slope of the 'c' region increased rapidly; the slope of the 'd' region decreased, but less rapidly than the 'c' slope increase, resulting in a decrease in the d/c ratio with increase in molecular size.

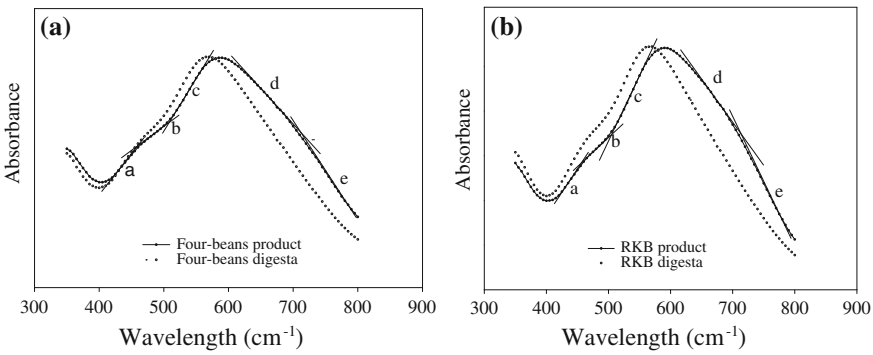

Fig. 62.4 UV spectra of starches isolated from four-beans (**a**) and RKB (**b**) before and after digestion

On the other hand, for the low molecular weight amylose, the slope of the 'd' region approached that of the 'e' region as the molecular weight decreased, until only one slope was detectable (Fig. 62.4).

62.3.3.2 Iodine Spectral Comparison of Starches Isolated from Food and Digesta

The differences between the two spectra of starches isolated from food and its digesta were presented in Fig. 62.4. For starch isolated from the food, the absorbance peak of its spectrum is not symmetrical around λ_{max}, which contributes to a decrease in the ratio of 'd' to 'c' (ratio d/c < 1). However, for the starch isolated from the digesta, the slope of the descending portion (above λ_{max}) decreased more rapidly (i.e. significantly more negative) than that of starch isolated from the food. The peak became symmetrical (ratio d/c ≈ 1), which indicates that the average molecular weight of amylose around the λ_{max} for digesta was smaller than that for the food. Another measurable significant variation ($P < 0.05$) between the two spectra (Fig. 62.4) is that the wavelength of maximum absorbance of starch isolated from digesta was lower compared to that of starch isolated from food, which further proved that the molecular size/chain length of amylose in the starch isolated from the digesta was shorter than that of amylose in the starch isolated from the food.

Furthermore, the variations between the two spectra appeared to indicate that the starch isolated from digesta had a narrower molecular size distribution of amylose than that of the starch isolated from the food (Fig. 62.4). More importantly, the slopes of the 'd' and 'e' regions disappeared after digestion. These spectrum characteristics suggest that high molecular weight fraction of amylose (i.e. around λ_{max} 715 nm) was absent in starch compositions of the digesta.

62.3.3.3 Molecular Weight Distribution of Starch in Food and Digesta (SE-HPLC)

The molecular size distribution of starches in food and its digesta was presented in Fig. 62.5. As shown in Fig. 62.4, the amylose-iodine spectrum provided detailed amylose size distribution in starches of food and digesta, while SE-HPLC chromatography reflected the molecular size distribution of both amylase and amylopectin molecules in food and digesta. The SE-HPLC results (Fig. 62.5) were consistent with the data obtained from amylose-iodine spectra, in which amylose molecular size of starch in digesta was lower than that of the starch in food. Most interestingly, the amylopectin fraction completely disappeared after digestion. The result of HPLC analysis together with those obtained from amylose-iodine spectral analysis provide a comprehensive insight into in changes occurring in starch structure with digestion. The marked difference in molecular size distribution between the starch present in food and that remaining in digesta indicate that the

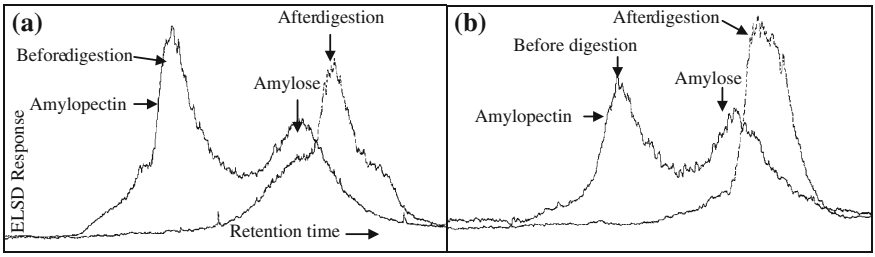

Fig. 62.5 Molecular profile of starch in four-beans of starches from four-beans (**a**) and RKB (**b**) before and after digestion

RS was mainly type 3 (re-associated starch molecules during retrogradation process).

While gelatinized starch is cooled to room temperature there is a strong driving force favouring crystallization. Particularly in the case of amylose, the driving force is strong, with an effective quench of at least 120 °C [10]. Thus, it has been proposed that, during the food preparation, gelatinization process differentiates starch molecular mobility because of different hydration behaviours between amylose and amylopectin, which would lead to uneven starch molecule distribution. During amylose gelation, the primary mechanism might attribute to a change from a random coil state to a phase-separated gel-like network with polymer-rich and polymer-deficient regions. Amylopectin forms shorter double helices and the re-associations of shorter double helices of branches of amylopectins would contribute to the region as imperfect regions during retrogradation. The high molecular size fraction of amylose also seems to belong to these types of regions. These regions were more readily digested, as is suggested by loss of amylose fraction with large molecular size as shown in UV-Visible spectra, and disappearance of amylopectin, as evidenced by SE-HPLC chromatography during digestion. Whereas amylose with smaller molecular size readily developed into more organised structure (i.e. formation of crystallites from amylose double helices) during retrogradation and contributed to the formation of RS.

62.4 Conclusions

The less organised regions of starch in food products were highly susceptible to enzymatic hydrolysis while the organised regions demonstrated resistance to enzymatic hydrolysis and escaped from digestion as RS. Molecular analysis indicated that the average molecular weight of amylose molecules in digesta was smaller than that present in the its food. The molecular profile of RS comprised exclusively high molecular weight amylose and amylopectin fractions. Because of the specific molecular structure of RS as studied by HPLC, the result suggested that the majority of RS, presenting in the digesta is type RS3.

References

1. Topping DL, Clifton PM (2001) Short-chain fatty acids and human colonic function: Roles of resistant starch and nonstarch polysaccharides. Physiol Rev 81:1031–1064
2. Asp NG, Van Amelsvoort JMM, Hautvast JGJ (1996) Nutritional implications of resistant starch. Nutr Res Rev 9:1–31
3. Bird AR, Brown IL, Topping DL (2000) Starches, resistant starches, the gut microflora and human health. Curr Issues Intest Microbiol 1:25–37
4. Jenkins DJA, Wolever TMS, Collier GR, Ocano A, Rao AV, Buckley G, Lam Y, Mayer A, Thompson LU (1987) Metabolic effect of a low glycemic-index diet. Am J Clin Nutr 46:968–975
5. Tovar J, Granfeldt Y, Björck IM (1992) Effect of processing on blood glucose and insulin response to starch in legumes. J Agr Food Chem 40:1846–1851
6. Knutson CA (1999) Evaluation of variations in amylose-iodine absorbance spectra. Carbohyd polym 42:65–72
7. Zhou ZK, Topping D, Morell M, Bird A (2010) Changes in starch physical characteristics following digestion of foods in the human small intestine. Brit J of Nutr 104:573–581
8. VanSoest JJG, Tournois H, deWit D, Vliegenthart JFG (1995) Short-range structure in (partially) crystalline potato starch determined with attenuated total reflectance Fourier-transform IR spectroscopy. Carbohyd Res 279:201–214
9. Liu Q, Charlet G, Yelle S, Arul J (2002) Phase transition in potato starch-water system. I. Starch gelatinization at high moisture level. Food Res Int 35:397–407
10. Parker R, Ring SG (2001) Aspects of the physical chemistry of starch. J Cereal Sci 34:1–17

Chapter 63
Research Progress on the Biosynthesis of Lycopene

Xin-Jia Wang, Xue-Gang Luo, Peng Wang, Guang Hu and Tong-Cun Zhang

Abstract Lycopene, as a red-colored intermediate of the β-carotene biosynthetic pathway, has attracted considerable attention due to its beneficial role in human health. And it is a potent antioxidant and of much bioactivity such as quenching singlet oxygen and scavenging free radicals, resulting in protection against oxidative DNA damage in vitro and in vivo. In this review we hope to concisely describe the nature of lycopene compounds, the scientific basis for its proposed anti cancer and cardiovascular protection properties and focus on discussion of such advances in microbial production of lycopene by fermentation.

Keywords Fermentation engineering · Genetic recombination · Lycopene · Microbial production

63.1 Introduction

Lycopene is a naturally occurring red carotenoid pigment found in grapefruit, watermelons, red palm oil, and papaya in addition to tomatoes [1]. It exists principally in the chromoplast of plant cells, and among them the content of tomato's is higher than the others, as much as 3–14 mg/100 g. Lycopene is also

X.-J. Wang · X.-G. Luo · P. Wang · T.-C. Zhang
Key Laboratory of Industrial Microbiology, Ministry of Education, College of Bioengineering, Tianjin University of Science and Technology, Tianjin, China
e-mail: tony@tust.edu.cn

X.-J. Wang · X.-G. Luo · P. Wang · G. Hu (✉) · T.-C. Zhang
Tianjin Key Laboratory of Industrial Microbiology, Tianjin, China
e-mail: oldmoonlake@gmail.com

G. Hu
Shaoxing Institute of Technology, College of Engineering, Peking University, Shaoxing, Zhejiang, China

T.-C. Zhang et al. (eds.), *Proceedings of the 2012 International Conference on Applied Biotechnology (ICAB 2012)*, Lecture Notes in Electrical Engineering 249,
DOI: 10.1007/978-3-642-37916-1_63, © Springer-Verlag Berlin Heidelberg 2014

synthesized by plants and microorganisms, but cannot be synthesized by animals and humans and can only be obtained via diet. Therefore, tomatoes and related tomato products are the major source of lycopene compounds, and are also considered as main food source of carotenoids in the human diet [2].

Lycopene is a highly polyunsaturated hydrocarbon that contains 11 conjugated and 2 unconjugated double bonds, whose structure is similar to that of β-carotene except for the β-ionone ring, and could be converted to β-carotene by cyclization. Lycopene, a noncyclic carotenoid having a chemical formula of $C_{40}H_{56}$ [3] and a molecular weight of 536.85 daltons, exists predominantly in an all-trans form of the most thermodynamically stable configuration. The double bonds in lycopene may isomerize from the all-trans-form to the mono or poly-cis form under the influence of light, heat, or certain chemical reactions.

As a member in carotenoid family, lycopene is one of the most potent antioxidants, with a singlet-oxygen-quenching capacity twice as high as that of β-carotene and 10 times higher than that of α-tocopherol. Its oxygen-quenching ability protects DNA against oxidative damage in vitro and in vivo and inhibits the spread or replication of cancer cell, thereby lycopene has been involved in prevention of cardiovascular disease (CVD) and even the aging process [4, 5] and enhancement of immune function [6]. It would be widely applied to food, medicine, cosmetic, and biotechnology industries with promising future.

63.2 Property of Lycopene

63.2.1 Physicochemical Property and Molecular Structure of Lycopene

Lycopene, also called ψ, ψ-carotene [4], takes the form of elongated, needle-like, and dark reddish-brown crystals with melting point of 172–175 °C when purified. Lycopene is more soluble in chloroform, benzene, and other organic solvents than in water and some strong polar solvents like ethanol, methanol, and so on. Being a polyene hydrocarbon, lycopene is an acyclic open-chain unsaturated carotenoid and is known to have 13 double bonds and 11 are conjugated double bonds arranged in a linear array. It is so instable and also very sensitive to light, heat, oxygen and acids [7], and some metallic ions such as Cu^{2+}, Fe^{3+} may catalyze its oxidation.

In addition, previous studies have suggested that the lycopene compounds in tomatoes or organic solvents could remain stable for up to 12 months of storage at ambient temperatures, whereas the isolated lycopene would be more likely to be oxidized (Fig. 63.1).

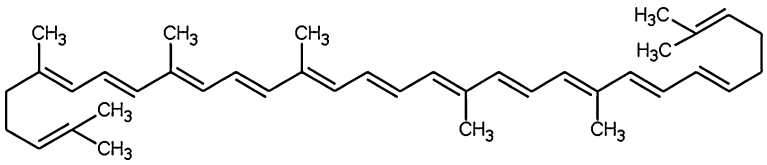

Fig. 63.1 The all-trans form of lycopene molecule

63.2.2 Physiological Functions of Lycopene

As the lycopene molecular has a high number of conjugated double bonds and thus has been found to be the most potent antioxidant in the group of carotenoids [8]. Lycopene has aroused considerable interest in recent years, due to its beneficial effect on human health, e.g., the functions include a scavenger of oxygen free radicals [9], an involvement in cancer prevention and an enhancer of immune responses [10].

(1) Cancer and tumor prevention. Evolving evidence suggests that lycopene may inhibit processes related to mutagenesis, carcinogenesis, and genetic expression of a cancer transfer proliferation factor called transforming growth factor alpha (TGF-α), and also facilitate synthesis of normal intercellular binding-protein which induces gap junctional communication between cells. Thus, it protects us from prostate cancer, pancreatic cancer, breast cancer, lymphatic tumors, etc., [11, 12].
(2) Cardiovascular protection. Generally speaking, the oxidative lipoprotein may play a role in the atherosclerosis development. The oxidation-protecting effect of lycopene on low-density lipoprotein (LDL) and cholesterol reduces the incidence and mortality rates of atherosclerosis and coronary heart disease (CHD) [13, 14].
(3) Osteoporosis alleviation and treatment [15]. Several epidemiological studies demonstrate that a direct correlation exists between oxidative stress and osteoporosis, which could be counterbalanced by some antioxidants like vitamin C, vitamin E, and β-carotene and thereby the risk of osteoporosis decreases. It has been proved that the antioxidative vitamins in women who are suffering from osteoporosis reduce. A recent American clinical research shows that the concentration of lycopene in plasma has been inversely associated with osteoporosis incidence in most of the case-control studies. It may therefore decrease the oxidative stress in vivo and reduce the risk of osteoporosis significantly with dietary lycopene supplementation.
(4) Diabetes prevention and treatment. Serum levels of lipid peroxide in the diabetics are higher than that in the healthy individuals, whereas the opposite is happening in the antioxidase activity of the two groups. As serum levels of lycopene increase, the glutathione peroxidase becomes more active and total antioxidant capacity gets improved accordingly. Some experiments have

indicated that lycopene could help lower fasting glucose levels in diabetic rats, and that when pretreatment with the lycopene compounds, hyperglycemia, and weight loss resulting from high blood sugar would be relieved to some extent as well.

63.2.3 Biosynthesis Pathway of Lycopene [16–18]

As a metabolic intermediate of carotenoids biosynthesis pathway, lycopene is synthesized either through the classical mevalonate (MVA) pathway in fungi and plants or the more recently discovered non-mevalonate pathway in eubacteria. All carotenoids are produced via a common precursor isopentenyl diphosphate (IPP), a mevalonic acid, which branches from glycolytic pathway intermediates of pyruvate and glyceraldehyde 3-phosphate (G3P) in *E. coli* and then is isomerized to dimethylallyl pyrophosphate (DMAPP) catalyzed by isopentenyl pyrophosphate isomerase (idi). And after series of condensation and desaturation reactions, lycopene is synthesized from IPP. The terminal isoprene of lycopene can be further cyclized to produce beta carotene. Figure 63.2 indicates the isoprenoid metabolism biosynthesis pathway of lycopene.

63.3 Production of Lycopene by Microbial Fermentation

Lycopene is produced from various microorganisms including some algae, fungi, yeasts, and engineered bacteria. So far, carotenogenic microbials contain gram-negative, epiphytic bacteria *Erwinia uredovora* [19] and *Erwinia herbicola*, mucor and aspergillus, e.g., *Blakeslea trispora*, Phycomyces, Choanephora, and engineered yeasts and bacteria [20]. While among the above species, *B. trispora* has been the most studied and the only one strain for industrialized production of carotene.

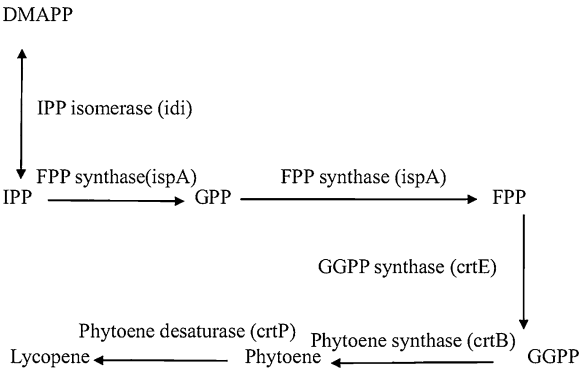

Fig. 63.2 Lycopene biosynthesis pathways in microorganisms. *FPP* farnesyl pyrophosphate, *GPP* geranyl pyrophosphate, *GGPP* geranylgeranyl pyrophosphate

63.3.1 Production of Lycopene in Engineered Bacteria

The basic protocols for genetically engineered bacteria to produce lycopene are as follows: First of all, a plasmid carrying the isolated lycopene biosynthesis gene clusters (*crtE*, *crtB*, *crtI*) is constructed. Subsequently, we transform the above plasmid to the host bacteria and then inoculate the transgenic strains under appropriate culture condition [21]. Finally, when fermentation ended, lycopene is extracted, purified, and crystalized after cell crush.

As early as 1990, when studying the function of carotenogenic genes in Erwinia uredovora, Misawa et al. found that *E. coli* JM109, if diverted the *crtE*, *crtI*, *crtB* genes carrying promoter and RBS of their own, could produce lycopene with yield up to 2.0 mg/g DCW [19]. At the same time, they noticed that recombinant *E. coli* with crtE deleted, could also produce carotenoids, nevertheless the production decreased to 2–4 % of the original, which indicates that the final carogenogenic precursor is GGPP other than FPP in *E. coli*. Thus, it has further been shown that the conversion from FPP to GGPP is a rate-limiting step for lycopene overexpression. Besides, Harker et al. found the overexpression of dxs encoding 1-deoxy-D-xylulose-5-phosphate synthase could enhance the lycopene accumulation [22]. And when dxs, appY, crl, or rpoS overexpressed through shot-gun method, all of them could increase the lycopene biosynthesis in *E. coli*. And then it has been observed that the accumulation level of lycopene by strains with dxs and the other three genes overexpressed together was higher than that of the control strain with only dxs overexpressed, of which the combination of dxs-appY is optimal [23].

However, most of the means for production of lycopene by recombinant *E. coli* is only used to "analyze," i.e., to overexpress, inhibit, or knockout the corresponding genes through molecular biological techniques and modify the target biochemical reactions for an increase in production. But little attention is paid upon "comprehensive" research, consequently we might utilize kinds of combinations to study the modified strains about their physiological state, gene expression, and metabolite flux, and then confirm the target of next gene modification to improve the lycopene production.

63.3.2 Production of Lycopene *in* B. trispora

Presently, *B. trispora* is the only one filamentous fungi producing β-carotene, which is just converted by lycopene cyclization. It is thereby that lycopene could be accumulated through improvement of strain, optimization of culture medium composition, and addition of cyclase inhibitor to block the last two cyclization reactions during β-carotene biosynthesis [24]. In addition, production of lycopene by *B. Trispora* is the most studied method for microbial production of the carotene. There have been successful cases for lycopene scale-up production in Western countries. And in China, Wang Yongsheng of Beijing University of Chemical

Technology studied the effect that the small molecule effector had on the lycopene production, i.e., added some blockers, and then the lycopene yield would be found to increase to a certain degree.

Although lycopene production in *B. trispora* is still in the stage of bench scale, considering the success of β-carotene industrial production in this strain, it will be the most prospective way for lycopene scale-up production.

63.3.3 Production of Lycopene in Yeast

Though the yeast cannot synthesize carotenoids in nature, they are found to be capable of accumulating large quantities of ergosterol in their membranes, whose biosynthetic pathway branches at FPP with carotenoids', as its principal isoprenoid compound during stationary phase. Hence, it may be feasible to divert the carbon flux for the ergosterol production partially to the pathway for carotenoid biosynthesis by means of the introduction of the carotenogenic genes starting with the Erwinia GGPP synthase gene (*crtE*). In the year of 1994, Shige-yuki Yamano et al. inserted carotenogenic genes (*crtE*, *crtB*, *crtI*, *crtY*) responsible for the biosynthesis of lycopene and β-carotene and their promoter into *Saccharomyces cerevisiae*, and then incubated in selected medium in 30 °C for 3 days. The final lycopene content extracted through acetone reached as much as 113 μg/g dry cell weight [25]. The edible yeast Candida utilis is another promising source of lycopene accumulation, and is usually used in large scale production of single-cell protein as well as several chemicals such as glutathione and RNA. Yutaka Miura et al. cultivated the recombinant Candida Utilis for the production of lycopene by diverting the carotenogenic genes of Erwinia, and ultimately 0.758 mg lycopene and 0.407 mg phytone per 1 g dry cell weight of Candida Utilis was yielded [26].

63.4 Conclusion

As having a variety of significant physiological functions, the demand, and market for lycopene have grown drastically. However, most of the study about microbial production of lycopene is confined to laboratory research, and we have seldom studied the control of the whole process of lycopene production by fermentation and that of microorganism metaboly, which would affect the production and productivity of lycopene and its scale-up experimentation.

Consequently, the following tasks should be further discussed: (1) The breeding of high-yielding strains of lycopene. (2) Modulation on the carotenogenic metabolite pathway. (3) Co-augmentation and integration of microbial fermentation. (4) Systematic biology research on the fermentation with multiple level.

Acknowledgments This study was financially supported by the Hi-tech research and development program of China (863 program) under contract NO. 2012AA022108 and the Program for Changjiang Scholars and Innovative Research Team in University of Ministry of Education of China (NO. IRT1166).

References

1. Story EN, Kopec RE, Schwartz SJ et al (2010) An update on the health effects of tomato lycopene. Annu Rev Food Sci T 1:189–210
2. Chalabi N, Le Corre L, Maurizis JC et al (2004) The effects of lycopene on the proliferation of human breast cells and *BRCA1* and *BRCA2* gene expression. Eur J Cancer 40:1768–1775
3. Nguyen ML (1999) Lycopene: chemical and biological properties. Food Technol 53:38–45
4. Gross MD, Snowdon DA (1996) Plasma antioxidant concentrations in a population of elderly women: findings from the nun study. Nutr Res 16:1881–1890
5. Snowdon DA, Gross MD, Butler SM (1996) Antioxidants and reduced functional capacity in the elderly: findings from the Nun Study. J Gerontol A Biol Sci Med Sci 51:M10–M16
6. Rao AV, Rao LG (2007) Carotenoids and human health. Pharmacol Res 55:207–216
7. Schierle J, Bretzel W, Buhler I et al (1997) Content and isomeric ratio of lycopene in food and human blood plasma. Food Chem 59:459–465
8. Di Mascio P, Kaiser S, Sies H (1989) Lycopene as the most efficient biological carotenoid singlet oxygen quencher. Arch Biochem Biophys 274:532–538
9. Sies H, Stahl W (1998) Lycopene: antioxidant and biological effects and its bioavailability in the human. Exp Biol Med 218:121–124
10. Watzl B, Bub A, Brandstetter BR et al (1999) Modulation of human T-lymphocyte functions by the consumption of carotenoid-rich vegetables. Br J Nutr 82:383–389
11. Wertz K, Siler U, Goralczyk R (2004) Lycopene: modes of action to promote prostate health. Arch Biochem Biophys 430:127–134
12. Giovannucci E (1999) Tomatoes, tomato-based products, lycopene, and cancer: review of the epidemiologic literature. J Natl Cancer Inst 91:317–331
13. Omoni AO, Aluko RE (2005) The anti-carcinogenic and anti-atherogenic effects of lycopene: a review. Trends Food Sci Technol 16:344–350
14. Rissanen T, Voutilainen S, Nyyssönen K et al (2002) Lycopene, atherosclerosis, and coronary Heart disease. Exp Biol Med 227:900–907
15. Rao LG, Mackinnon ES, Josse RG et al (2007) Lycopene consumption decreases oxidative stress and bone resorption markers in postmenopausal women. Osteoporosis Int 18:109–115
16. Rohmer M (1999) The discovery of a mevalonate-independent pathway for isoprenoid biosynthesis in bacteria, algae and higher plants. Nat Prod Rep 16:565–574
17. Lichtenthaler HK, Rohmer M, Schwender J (2006) Two independent biochemical pathways for isopentenyl diphosphate and isoprenoid biosynthesis in higher plants. Physiol Plant 101:643–652
18. Lichtenthaler HK (1999) The 1-deoxy-D-xylulose-5-phosphate pathway of isoprenoid biosynthesis in plants. Annu Rev Plant Biol 50:47–65
19. Misawa N, Nakagawa M, Kobayashi K et al (1990) Elucidation of the *Erwinia uredovora* carotenoid biosynthetic pathway by functional analysis of gene products expressed in *Escherichia coli*. J Bacteriol 172:6704–6712
20. Farmer WR, Liao JC (2000) Improving lycopene production in Escherichia coli by engineering metabolic control. Nat Biotechnol 18:533–537
21. Cunningham FX Jr, Chamovitz D, Misawa N et al (1993) Cloning and functional expression in *Escherichia coli* of a cyanobacterial gene for lycopene cyclase, the enzyme that catalyzes the biosynthesis of beta-carotene. FEBS Lett 328:130–138

22. Harker M, Bramley PM (1999) Expression of prokaryotic 1-deoxy-D-xylulose-5-phosphatases in *Escherichia coli* increases carotenoid and ubiquinone biosynthesis. FEBS Lett 448:115–119
23. Kang MJ, Lee YM, Yoon SH et al (2005) Identification of genes affecting lycopene accumulation in *Escherichia coli* using a shot-gun method. Biotechnol Bioeng 91:636–642
24. Sun Y, Yuan QP, Vriesekoop F (2007) Effect of two ergosterol biosynthesis inhibitors on lycopene production by Blakeslea trispora. Process Biochem 42:1460–1464
25. Yamano S, Ishii T, Nakagawa M et al (1994) Metabolic engineering for production of beta-carotene and lycopene in *Saccharomyces cerevisiae*. Biosci Biotechnol Biochem 58:1112–1114
26. Miura Y, Kondo K, Saito T et al (1998) Production of the carotenoids lycopene, beta-carotene, and astaxanthin in the food yeast Candida utilis. Appl Environ Microbiol 64:1226–1229

Chapter 64
Physicochemical Properties and In Vitro Digestion of Maize Starch and Tea Polyphenols Composites

Wentian Cai, Liming Zhang, Shuang Zhang, Jing Shan and Shaoling Cheng

Abstract Maize starch (MS) was blended with tea polyphenols (TP) during gelatinization to obtain composites, their physicochemical properties and in vitro digestibility was investigated. The interaction between TP and MS molecules was confirmed by the absorption band shifts of carbonyl and C=C aromatic ring according to the FT-IR spectra. X-ray diffraction results showed that the inhibitory effect of TP on recrystallization of starch occurred. The digestion rate was 86.6 % for the pregelatinized starch without TP after incubating 2 h, whereas the digestion rates were 66.5, 56.1, 47.5, 47.1, and 46.5 % for the composites with TP contents of 1.0, 2.5, 5.0, 7.5, and 10.0 %, respectively.

Keywords Digestibility · Physicochemical property · Maize starch · Tea polyphenols · Composite

64.1 Introduction

Starch is the most abundant component of cereal grains and an important structural constituent in cereal products. In China and other Asian countries, some starch-rich food and tea extracts are used together in food processing, not only as flavoring and coloring agents but also for health-promotion and food preservatives [1, 2]. Therefore, the nutritional impact of the interaction between starch and tea extracts has become a vital issue.

W. Cai · L. Zhang (✉) · S. Cheng
Key Laboratory of Industrial Fermentation Microbiology, Ministry of Education, Tianjin University of Science and Technology, Tianjin 300457, People's Republic of China
e-mail: zhlm@tust.edu.cn

S. Zhang · J. Shan
College of Bioengineering, Tianjin University of Science and Technology, Tianjin 300457, People's Republic of China

T.-C. Zhang et al. (eds.), *Proceedings of the 2012 International Conference on Applied Biotechnology (ICAB 2012)*, Lecture Notes in Electrical Engineering 249,
DOI: 10.1007/978-3-642-37916-1_64, © Springer-Verlag Berlin Heidelberg 2014

TP are the main compounds of green tea and there are a class of polyphenolic flavonoids known as catechins (the most abundant component), usually account for 30–42 wt.% of the dry weight of the solids in brewed green tea. Catechins are characterized by the di- or tri-hydroxyl group substitution of the B ring and the meta-5,7-dihydroxy substitutions of the A ring [3]. The potential application of TP in the food industry has attracted more interest. Apart from their splendid antibacterial and antioxidative activities [4, 5], TP are also shown to be inhibitors of α-amylase and α-glucosidase through forming various complexes [6–8]. It proved that TP were capable of binding and precipitating protein, suggesting a potential ability of TP to denature digestive enzymes [7]. The purpose of this study was to characterize the physicochemical properties of composites from MS with TP and their in vitro digestibility. The digestibility rate of these composites was examined by α-amylase hydrolysis.

64.2 Materials and Methods

64.2.1 Materials

Maize starch was purchased from Sigma Co. (Product of Switzerland, EC No. 2326864). TP were purchased from Wuxi century biopharmaceutical Co., Ltd. (Wuxi, China) with total polyphenols of 98 wt.%. Porcine pancreatin α-amylase (No. 7545) was obtained from Sigma-Aldrich Chemical Co. (St. Louis, MO). 3,5-dinitrosalicylic acid was purchased from Sinopharm Chemical Reagent Co., Ltd. All chemicals were of analytical grade.

64.2.2 Composites Preparation Method

The starch was blended with TP during gelatinization to prepare composites, and MS/TP mixing ratios were 5/0, 5/0.050, 5/0.125, 5/0.250, 5/0.375, and 5/0.500 (w/w) that equated with MS containing 0, 1.0, 2.5, 5.0, 7.5, and 10.0 % TP (based on MS weight), respectively. Firstly, starch (5.0 g) was placed into 250-mL tapered flask and 100 mL distilled water added. The mixture was pasted at the temperature 80 °C for 2 h with constant stirring at the speed of 200 rpm. Secondly, TP at the weight of 0, 0.050, 0.125, 0.250, 0.375, and 0.500 g was dissolved in 25 mL distilled water, dropped slowly into the flask in 10 min, respectively. Each of them was mechanically stirred at the temperature of 80 °C for 1 h. Lastly, the mixture was pouring into the plate (the thickness of sample was about 5 mm) and then cooled to the room temperature. The samples were freeze-dried by a freeze-dryer for about 24 h, the condenser temperature was approximately −50 °C. Each of the dried composites was milled and passed through a sieve (0.15 mm).

64.2.3 Fourier Transform Infrared (FT-IR) Spectroscopy

FT-IR spectra were obtained with a Bruker Vector 22 FT-IR spectrometer (Rheinstetten, Germany). The samples were equilibrated at 50 °C for 24 h prior to FT-IR analysis and were collected using the KBr pellet method. For each spectrum, 32 scans were recorded at room temperature at a resolution of 4 cm^{-1}. Spectra were baseline-corrected and then deconvoluted over the range of 4000 and 400 cm^{-1}.

64.2.4 X-ray Diffraction

The structures of the native starch and composites containing various ratios TP were carried out using wide-angle X-ray diffraction. They were recorded with a Rigaku D/max 2500 X-ray powder diffractometer (Rigaku, Tokyo, Japan). These power samples were scanned using Cu Kα radiation ($\lambda = 0.154056$ nm) at 40 kV and 150 mA. The scanning region of the angles (2θ) was from 3° to 50° at a scanning speed of 6°/min, a step size of 0.02°, a divergence slit width (DS) of 1°, a receiving slit width (RS) of 0.02 mm, and a scatter slit width (SS) of 1° [9]. The samples were equilibrated at 50 °C for 24 h prior to the analysis.

64.2.5 Experiments In Vitro Digestibility

The in vitro starch digestibility was measured according to the method described by Lee et al. [10] with slight modifications. The pancreatic α-amylase was dispersed in distilled water and centrifuged for 10 min at 2500 g, and the supernatant was collected. The solution was freshly prepared for the digestion analysis.

The sample (0.5000 g) was dispersed in 50 mL of 0.2 M phosphate buffer (pH 6.9) and 200 U/mL of pancreatic α-amylase was dissolved in 50 mL of the same buffer. Then, 0.5 mL of pancreatic α-amylase was added to the sample suspension which was incubated at 37 °C for up to 4 h. Invitro digestibility was determined as released maltose/g starch sample which was quantified by using a DNS (3,5-dinitrosalicylic acid) method. A standard curve was prepared using maltose. The starch digested rate (the proportion of starch degraded to maltose) was calculated as 100 times milligrams of maltose equivalents times 0.95 divided by milligrams of starch in sample.

64.3 Results and Discussion

64.3.1 Fourier Transform Infrared (FT-IR) Spectroscopy

FT-IR spectrum of TP is shown in Fig. 64.1. It can be seen that the broad band between 3500 and 3100 cm^{-1} is assigned to the stretch vibration absorption of O–H. The band at 1693 cm^{-1} is assigned to the stretching vibration absorption of carbonyl group. The bands at 1610, 1518, 1452 cm^{-1} are attributable to skeleton stretching vibration of aromatic rings. The band at 1316 cm^{-1} is related to the C–O bond stretching of hydroxybenzene. The characteristic absorption bands appeared at 1236, 1196 cm^{-1} assigned to anti-symmetry stretching vibration, and 1141, 1032 cm^{-1} for symmetry vibration of C–O–C groups [11].

FT-IR spectra of the control and composites containing various ratios are shown in Fig. 64.2 B1–B5. All the samples showed a broad band between 3600 and 3000 cm^{-1}, which are related to hydrogen-bonded hydroxyl groups of starch or hydroxyl groups of TP. The sharp band at 2933 cm^{-1} refers to the symmetrical stretching vibration of CH_2 existed in starch molecules. The band at 1645 cm^{-1} is attributed to the scissoring of two ŌH bonds of water molecules, while the band at 1418 cm^{-1} is due to the deformation vibration of CH_2 [12]. Compared to the control (Fig. 64.2 B1), the composites containing different TP contexts show that a broadened ŌH stretching and frequency redshifts of C̄ŌH bending was observed. The characteristic carbonyl absorption band shifted from 1693 to 1688 cm^{-1}, and the skeleton stretching vibration intensity of aromatic rings become weak, these overall results indicate the existence of possible interaction between TP and starch molecules. The interaction between TP and rice starch during gelatinization has

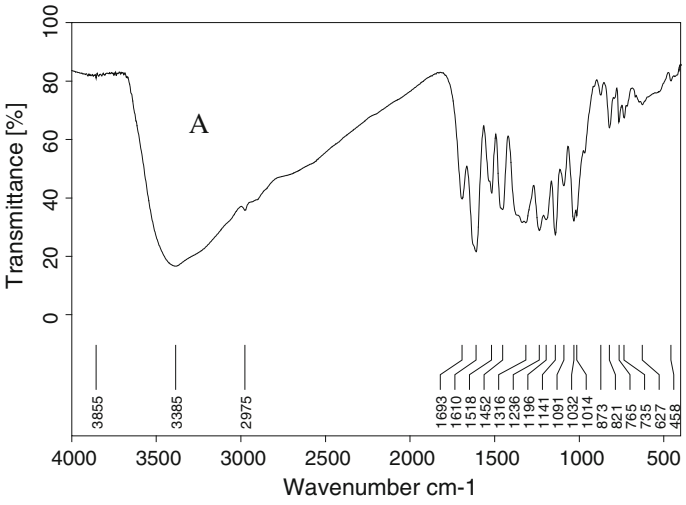

Fig. 64.1 FT-IR spectrum of tea polyphenols (TP)

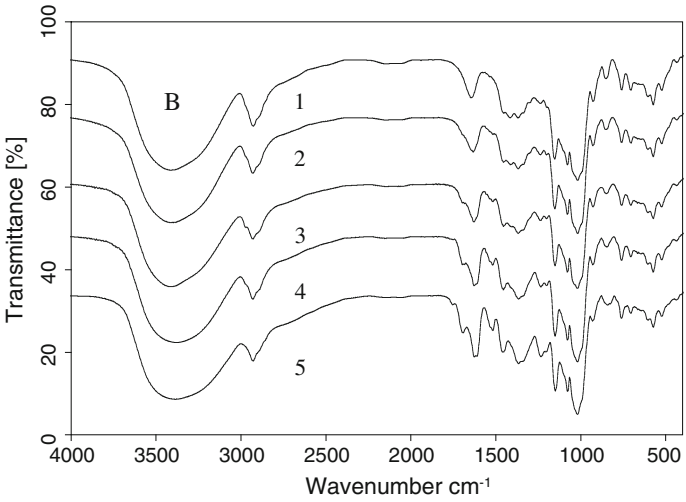

Fig. 64.2 FT-IR spectra of the control (*B*1) and composites containing various ratios TP (w/w): 2.5 % TP (*B*2), 5.0 % TP (*B*3), 7.5 % TP (*B*4), 10.0 % (*B*5)

also been reported by other researchers [13], their correlation analysis showed that samples A (the gelatinized sample of the blend of 16 % TP and rice starch) and B (the blend of 16 % TP and gelatinized rice starch) differed in H–H interaction and interaction strength of sample A may be stronger than that of sample B according to their ^{1}H-NMR measurements.

64.3.2 X-ray Diffraction (XRD)

X-ray diffractograms of TP, the control and composites containing various ratios TP are exhibited in Fig. 64.3. The pure TP shows a wide range diffraction peak at 23° (2θ), indicating that it is present as an amorphous form (Fig. 64.3g). Generally, native maize starch showed a typical A-type X-ray pattern having diffraction peaks at 15.3°, 17.0°, 18.0°, 20.0°, and 23.4° (2θ) [14, 15]. However, once native starch is gelatinized, it develops a B-type diffraction pattern during aging [16]. It can be seen from Fig. 64.3a that the control sample has a B-type diffraction pattern at 16.9° (2θ). The formation of this peak was the result of the crystallization of the amorphous starch melt, mainly of the amylopectin fraction that increased during storage [17, 18]. The intensity of a peak close to 17° (2θ) of composites containing various ratios TP (Fig. 64.3b–f) was nearly nonexistent in a representative X-ray diffractogram, indicating the disappearance of the typical B-pattern. There were no the diffraction peaks of TP at 23° of 2θ in the diffraction patterns of composites with different contents of TP. This implies that there are some interactions between TP and starch molecules.

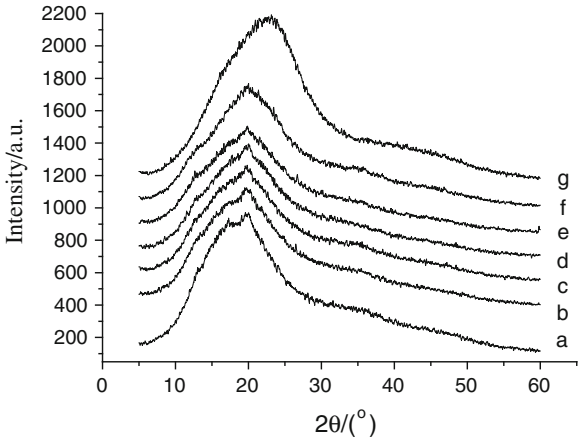

Fig. 64.3 X-ray diffraction patterns of the control (*a*) and composites containing various ratios TP (w/w): 1.0 % TP (*b*), 2.5 % TP (*c*), 5.0 % TP (*d*), 7.5 % TP (*e*), 10.0 %TP (*f*), TP (*g*)

64.3.3 In Vitro Starch Digestibility

The digestion rate of composites containing various ratios TP with porcine α-amylase is presented in Fig. 64.4. As shown in Fig. 64.4, the control is hydrolyzed rapidly and its susceptibility to α-amylase increases with the incubating time. There were obvious differences between the control and composites with different contents of TP in digestion rate. The digestion rate of the control is 73.1 % within 0.5 h, and reaches a plateau at 86.6 % after 2 h, whereas the digestion rate at 0.5 h for composites containing 1.0, 2.5, and 5.0 % TP is 57.9, 52.5, and 44.6 %, respectively. After incubating 2 h, the digestion rate was finally steady at about 66.5 % for the sample with 1.0 % TP, 56.1 % for the sample with 2.5 % TP, and about 47.5 % for the samples with TP of 5.0, 7.5, and 10.0 %. The reasonable content of TP was 5.0 %, as no significant difference is observed among the three

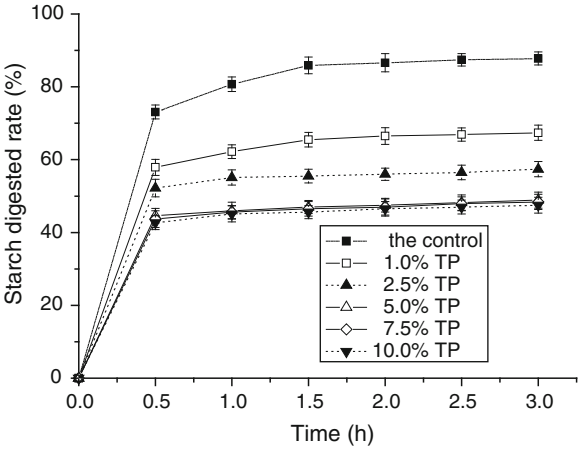

Fig. 64.4 Digestibility rate of the control and composites containing various ratios TP (w/w)

samples with TP contents of 5.0, 7.5, and 10.0 %. It proved that tea polyphenols were capable of binding and precipitating protein, suggesting a potential ability of TP to denature digestive enzymes [7]. According to the previous studies [6, 19], tea polyphenols are shown to be inhibitor of α-amylase. Consequently, when the composites with different contents of TP were formed, the TP would accompany with starch substrate and inhibit the activity of α-amylase. With the increase of amount of TP in the composites, the inhibition of α-amylase increased. On the other hand, the strong interaction between TP and starch during gelatinization [20] would also reduce the digestibility of starch. The composites with different contents of TP can become resistant to enzyme degradation, and the amount of residual starch was increased with the increase of the contents of TP [21, 22].

64.4 Conclusions

Starch was blended with TP during gelatinization, and composites containing various ratios TP were prepared. The TP obviously affected various properties of starch to different extents. FT-IR and XRD results showed that a possible interaction exists between TP and starch molecules, and the TP with amorphous form was dispersed in the starch molecules. XRD results of composites revealed that the marked inhibitory effect of TP on the recrystallization of MS had taken place. The digestion rate of composites incorporated with TP was significantly reduced and the amounts of starch residues were sharply increased in comparison with the control. Since these starches can benefit human health, this study may provide a scientific basis for controlling the digestion of starch.

Acknowledgments This work was financially supported by Technological Development Program of Tianjin Educational Commission (Grant No. 20090510).

References

1. Nakatani N (1994) Antioxidant and antimicrobial constituents of herbs and spices. In: Charalambous G (ed) Spices, herbs and edible fungi. Elsevier, New York
2. Shan B, Cai YZ, Brooks JD et al (2007) The in vitro antibacterial activity of dietary spice and medicinal herb extracts. Int J Food Microbiol 117:112–119
3. Khan N, Mukhtar H (2007) Tea polyphenols for health promotion. Life Sci 81:519–533
4. Cartriona MS, Cai Y, Russell M et al (1988) Polyphenol complexation-some thoughts and observations. Phytochem 27:2397–2409
5. Shi B, He XQ, Haslam E (1994) Polyphenol-gelatin interaction. J Am Leather Chem As 89(4):98–104
6. Hara Y, Honda M (1990) The inhibition of α-amylase by tea polyphenols. Agr Biol Chem 54:1939–1945
7. He Q, Lv Y, Yao K (2007) Effects of tea polyphenols on the activities of α-amylase, pepsin, trypsin and lipase. Food Chem 101:1178–1182

8. Matsui T, Tanaka T, Tamura S et al (2007) α-Glucosidase inhibitory profile of catechins and the aflavins. J Agr Food Chem 55:99–105
9. Wang SJ, Gao WY, Chen HX et al (2006) Studies on the morphological, thermal and crystalline properties of starches separated from medicinal plants. J Food Eng 76:420–426
10. Lee KY, Lee S, Lee HG (2010) Effect of the degree of enzymatic hydrolysis on the physicochemical properties and in vitro digestibility of rice starch. Food Sci Biotechnol 19:1333–1340
11. Wang XP, Zhou Z, Zhang JN (2002) Influence of microwave on extraction, structure and catechin composition of tea-polyphenol. Food Sci 23(1):37–39
12. Mano JF, Koniarova D, Reis RL (2003) Thermal properties of thermoplastic starch/synthetic polymer llends with potential biomedical applicability. J Mater Sci Mater Med 14(2):127–135
13. Wu Y, Chen ZX, Li XX et al (2009) Effect of tea polyphenols on the retrogradation of rice starch. Food Res Int 42:221–225
14. Arámbula VG, González H, Ordorica FCA (2001) Physicochemical, structural and textural properties of tortillas from extruded instant corn flour supplemented with various types of corn lipids. J Cereal Sci 33:245–252
15. Zobel HF (1988) Starch crystal transformations and their industrial importance. Starch/Stäke 40(1):1–7
16. Karim AA, Norziah MH, Seow CC (2000) Methods for the study of starch retrogradation. Food Chem 71:9–36
17. Osella CA, Sánchez HD, Carrara CR et al (2005) Water redistribution and structural changes of starch during storage of a gluten-free bread. Starch/Stäke 57(5):208–216
18. Thiré RMSM, Simáo RA, Andradeb CT (2003) High resolution imaging of the microstructure of maize starch films. Carbohyd Polym 54:149–158
19. Koh LW, Wong LL, Loo YY et al (2010) Evaluation of different teas against starch digestibility by mammalian glycosidases. J Agric Food Chem 58:148–154
20. Wu Y, Lin QL, Chen ZX et al (2011) The interaction between tea polyphenols and rice starch during gelatinization. Food Sci Technol Int 17:569–577
21. Yoon JH, Thompson L, Jenkins DJA (1983) The effect of phytic acid on in vitro rate of starch digestibility and blood glucose response. Am J Clin Nutr 38:835–842
22. Skrabanja V, Liljeberg HGM, Hedley CL et al (1999) Influence of genotype and processing on the in vitro rate of starch hydrolysis and resistant starch formation in peas. J. Agr Food Chem 47:2033–2039

Chapter 65
Screening, Characteristic and Culture Optimization of Acid-Tolerant Mutants of *Lentinula edodes* (Berk.) Pegler

Aijia Cao, Xinglin Li, Na Zhao, Yang Han and Xuefei Cao

Abstract A novel *Lentinula edodes* (Berk.) Pegler (*L. edodes*) mycelium mutant, Atm-02 (TCCC 59002) capable of producing exopolysaccharide (EPS) at pH 2.0 was screened through irradiating original mycelia of *L. edodes* by ultraviolet, performing antagonism assay and testing by selective medium. EPS production of Atm-02 in shake-flask culture was optimal at 26 °C and 180 rpm. Meanwhile, 4 % (w/v) sucrose and 0.7 % (w/v) beef extract resulted in maximum biomass production (0.335 ± 0.015 g/100 ml) and maximum EPS content (0.137 ± 0.009 g/100 ml). In conclusion, the acid-tolerance mutants might normally grow in open culture medium at pH 2.0, whereas the environmental microorganisms were inhibited. Furthermore, it was the first report on the method of screening of acid-tolerant mutants of *L. edodes*.

Keywords Acid-tolerant mutant · Exopolysaccharide · *Lentinula edodes* (Berk.) Pegler · Submerged mycelial culture

65.1 Introduction

The xylotrophic basidiomycete *Lentinula edodes* (Berk.) Pegler (*L. edodes*) is well-known for its nutritional value, medicinal value, and food industrial application throughout the world [1]. Polysaccharides extracted from *L. edodes* have been discovered to improve the human immune system and show anticancer, antioxidant activities, and antiviral activities. Up to now, as a highly functional biomacromolecule, the polysaccharides from *L. edodes* have been widely applied

A. Cao · X. Li (✉) · N. Zhao · Y. Han · X. Cao
College of Biotechnology, Tianjin University of Science and Technology, Tianjin 300457, People's Republic of China
e-mail: lxlszf@tust.edu.cn

T.-C. Zhang et al. (eds.), *Proceedings of the 2012 International Conference on Applied Biotechnology (ICAB 2012)*, Lecture Notes in Electrical Engineering 249,
DOI: 10.1007/978-3-642-37916-1_65, © Springer-Verlag Berlin Heidelberg 2014

to humans, animals and plants, because of the valuable biological activities and indispensable, nontoxic medicinal preparations.

Traditionally, mushrooms are cultivated on solid culture for the growth of fruiting body so as to extract bioactive substances [2]. However, the time for the formation of fruiting body is too long and its composition differs from batch to batch, and its product quality is hard to control when *L. edodes* is cultivated on solid culture [3]. As a result, more attention has been attracted to submerged culture. As submerged culture possesses considerable advantages, such as higher production of mycelia and exopolysaccharide (EPS) from the fermentation culture in a more compact space over a shorter time, with fewer chances of contamination [2, 4], and practicality of convenient control and simple downstream processing in comparison to the cultivation of fruiting body.

Culture pH, one of the most critical fermentation process parameters, has been known to significantly affect mycelium cell growth and biosynthesis of EPS in submerged cultures. However, the influence of pH on the mycelial growth and biosynthesis of EPS varies with different microorganisms, culturing conditions, and medium compositions. Fang and Zhong [5] reported that a low initial pH improved the production of EPS of *Ganoderma lucidum* in comparison to that of a previous study [6].

In order to explore a new pathway to produce EPS from *L. edodes* in open submerged culture with lower pH, in this paper, the authors tried to screen acid-tolerance mutants in the medium with low pH.

65.2 Materials and Methods

65.2.1 Preparation of Mycelium Mutants of L. edodes

Lentinula edodes was purchased from local market in Tianjin, China. The mycelium isolated from the fruiting body in laboratory, was maintained on potato dextrose agar (PDA, w/v, 20 % fresh potato, 2 % glucose, and 2 % agar) slants. The screened mutants were preserved in Tianjin Culture Collection of China (TCCC) at Tianjin University of Science and Technology, Tianjin, China.

The young mycelium was incubated on PDA medium in Petri dishes for 2 days at 25 °C, and then was irradiated by ultraviolet light.

65.2.2 Antagonistic Assay

Two blocks of mycelium were inoculated on PDA medium in a Petri dish, one was control mycelium and another was mutagenic mycelium, and then the growth potential, hyphae amount and antagonistic lines were estimated, respectively.

65.2.3 Culture Conditions

To prepare the inoculum, the mycelium was initially grown on PDA medium in Petri dishes at 25 °C for 6 days. Five mycelial agar disks (6 mm) were punched out by a puncher from the marginal culture and inoculated into 250 ml flasks containing 100 ml of liquid seed culture medium (20 % potato, 2 % glucose, 0.5 % yeast extract, 0.3 % KH_2PO_4, 0.15 % $MgSO_4$, and initial pH 6.0; all quantities: w/v.), and then incubated on a rotary shaker at 150 rpm and 25 °C for 6 days. The flask culture experiments were performed in 250 ml flasks containing 100 ml of basal fermentation medium (2 % glucose, 0.5 % yeast extract, 0.2 % KH_2PO_4, 0.1 % $MgSO_4$, and initial pH 2.5; all quantities, w/v.), which was inoculated with 10 % (v/v) of the seed culture on above rotary shaker at 25 °C for 12 days. All chemicals used in the study were of analytical grade.

The selective medium contained the same component as seed culture medium, which the initial pH was adjusted from 4.0 to 1.5, and the aseptic liquid medium was added to each Petri dish with 2 g aseptic perlite. Every Petri dish was inoculated with 100 μl of the inoculum (cultured for 6 days) in five different regions, and then acid-tolerant mycelia were obtained after several days.

65.2.4 Optimization of the Culture Condition and Medium

Only one factor was changed in each experiment, while keeping all others constant. The culture temperature, rotation speed, different carbon sources, nitrogen sources, and their different concentrations were initially studied at single factor test.

65.2.5 Estimation of Mycelial Biomass and EPS Production

Mycelial biomass and the crude EPS fraction were obtained from *L. edodes* as described by Leung et al. [7]. To determine mycelial growth curve and EPS production, the control (initial pH 6.0) and the mutants (initial pH 2.5) were cultured, respectively. The mycelial biomass and the crude EPS production were estimated as above, and the EPS content (the total carbohydrate content of EPS samples) was determined by the anthrone-sulphuric acid method using glucose as the standard with slight modification from the method of Leung et al. [7].

65.2.6 Environment Microorganism Assays in Open Culture at Different pH

In order to investigate the role of initial pH on the unnecessary microorganisms of lab environment in open culture, experiments were performed in flasks under the condition of standing open wide culture. The microorganism culture medium contained the same component as the liquid seed culture medium, but the pH value was modulated into 2.0, 3.0, 4.0, and 7.0, respectively.

65.2.7 Experimental Statistical Analysis

All assays and treatments were conducted with three replications to ensure reproducibility, and the results were represented by their mean ± standard deviation.

65.3 Results and Discussion

65.3.1 Environment Microorganism Assays in Open Culture at Different pH

The effects of culture pH on environment microorganism growth in open culture were shown in Fig. 65.1. In all cases, the growth of the microorganisms was affected significantly. When culture pH was 3.0 and 4.0, the lag phase time of the microorganism growth was delayed for about 30 h in contrast with pH 7.0; while culture pH was 2.0, it was delayed for above 70 h. Thus it could be seen that, in the medium with pH 2.0, the environment microorganism growth would be significantly inhibited, and the *L. edodes* mutants which can normally grow in acid conditions might be selected in advance for meeting open culture. The pH values were measured during this study, and the result (data not shown) indicates that they had no evident changes, thus the changes of pH in open flask culture were not taken into account.

65.3.2 Screening and Stability Test of the Acid-Tolerant Mutants of L. edodes

In primary screening, the *L. edodes* mutants, which were in well growth after irradiation for 0.5 to 1 min (Table 65.1), with distinct antagonistic lines (Fig. 65.2)

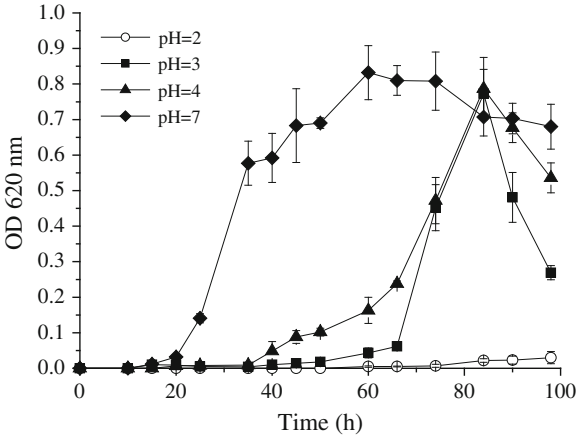

Fig. 65.1 The growth curves of the environmental microorganisms for open culture under acid conditions. The culture broth was taken at regular intervals and the absorbance of the sample was measured at 620 nm. Data points represent their means and standard deviations of three times trials. The test of pH 7.0 was acted as a control

might be selected first, and were assayed further by selective medium with pH 2.0 (Fig. 65.3).

Three replicates were included in each treatment group, and subsequently analyzed on physicochemical and microbiological properties after dark culture for 6 days.

Three kinds of mycelium mutants, termed Atm-01 (TCCC 59001), Atm-02 (TCCC 59002), and Atm-03 (TCCC 59003), respectively, were performed best in selective medium with the initial pH 2.0. The mycelium growth stabilities of Atm-01, Atm-02, and Atm-03 under different initial pH values ranging from 2.0 to 4.0 were shown in Fig. 65.4. After cultured for 12 days, the mycelial biomass and EPS production of them increased monotonically with the increasing pH. By contrast, Atm-01, Atm-02, and Atm-03 might have been fit for a lower culture pH and they also showed specific advantage over control group. Especially Atm-02, its

Table 65.1 Effect of ultraviolet irradiation on the growth of *Lentinula edodes* mycelium. The mycelium was irradiated for 0, 0.5, 1, 5, 10, 15, 20, 25 and 30 min with constant dose (90 μW/cm^2) in a special mutagenic box

Irradiation time (min)	Mycelial diameter cultured for 6 days (mm)	Hyphae amount	Growth potential
0 (CK)	65.0 ± 1.2	+ + + + +[a]	+ + + + +
0.5	46.0 ± 1.0	+ + + +	+ + + +
1	41.5 ± 1.1	+ + + +	+ + +
5	32.1 ± 0.7	+ + +	+ + +
10	28.8 ± 0.6	+ + +	+ + +
15	30.0 ± 0.5	+ + +	+ + +
20	26.3 ± 0.1	+ +	+ +
25	22.8 ± 0.2	+	+
30	24.5 ± 0.3	+	+

[a] More symbol "+" means better growth of the mycelium

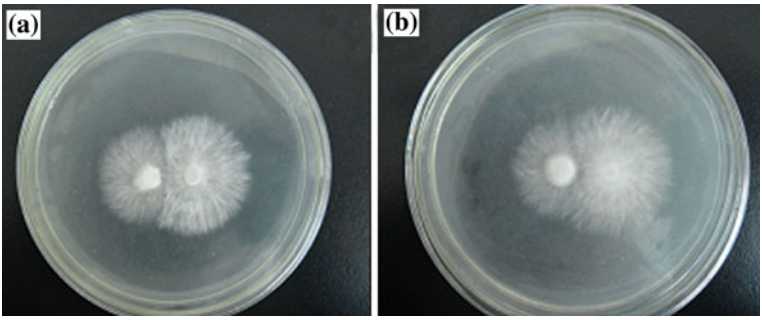

Fig. 65.2 The phenotype of intensive mycelial antagonism of a control and a mutant by ultraviolet irradiation (**a**), The phenotype of gentle mycelial antagonism of a control and a mutant (**b**)

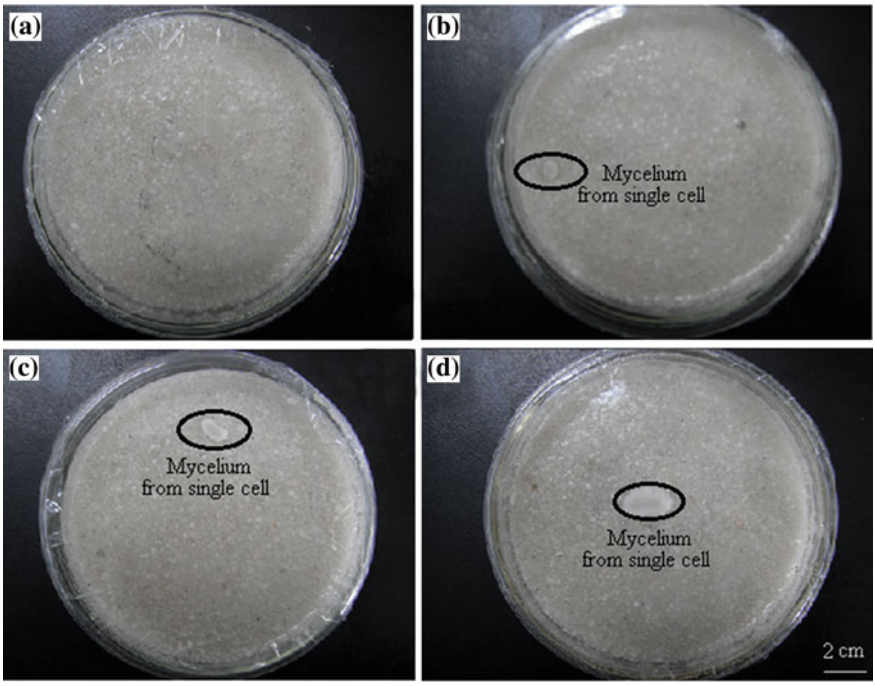

Fig. 65.3 The mycelia formations of the acid-tolerant mutants on selective medium with perlite. Three mutants were selected to grow into corresponding mycelia clones in selective medium with the initial pH 2.0 (**b**–**d**), respectively, whereas the cells without acid-tolerance characteristic did not exist in the medium (**a**)

mycelial biomass and EPS production were up to 0.002 ± 0.001 and 0.063 ± 0.003 g/100 ml at pH 2.0, 0.343 ± 0.014 and 0.111 ± 0.007 g/100 ml at pH 3.0, and 0.465 ± 0.013 and 0.149 ± 0.006 g/100 ml at pH 4.0, respectively. Ultimately, Atm-02, the optimal mutant was prepared for further study.

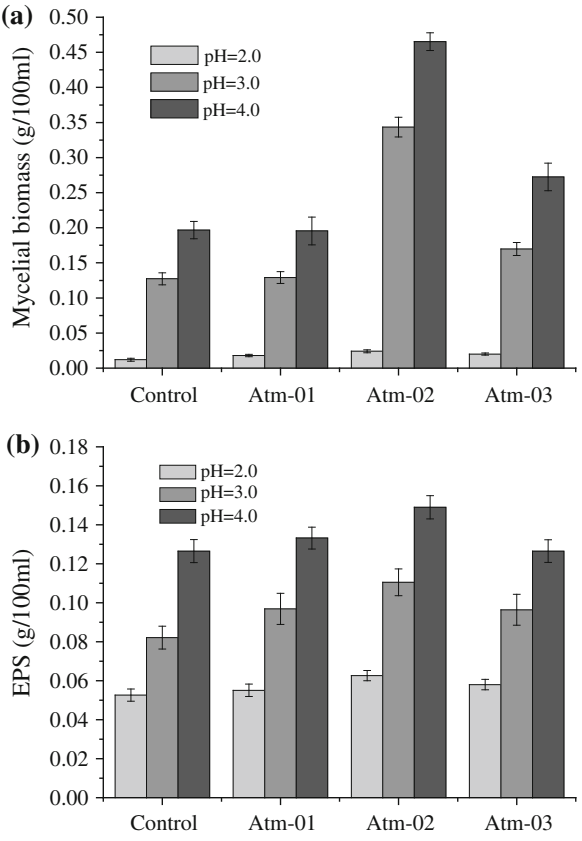

Fig. 65.4 The mycelial biomass (**a**, dry weight) and the EPS production (**b**, dry weight) of three acid-tolerant mutants in submerge culture. Control, Atm-01, Atm-02, and Atm-03 were cultured in the medium with initial pH ranging from 2.0 to 4.0, respectively. In order to show the differences between mycelial biomass at pH = 2.0, all of the values of the mycelial biomass at pH = 2.0 in the figure were expanded 10 times

65.3.3 Mycelial Biomass and EPS Content of Atm-02 in Open Culture

Figure 65.5 shows the typical curves of the mycelial growth and EPS production in the control mycelial culture with initial pH 6.0 and in Atm-02 mycelial culture with initial pH 2.5, respectively. For Atm-02, mycelial biomass attained a maximum concentration of 0.336 ± 0.010 g/100 ml after 12 days of cultivation, and EPS concentration reached its maximum value of 0.110 ± 0.010 g/100 ml after 12 days growth of Atm-02 in submerged culture. As shown in Fig. 65.5, the maximum EPS content of the control and Atm-02 were almost same, but fermentation period of Atm-02 was extended for 2 days by contrast with the control. Even that, this trial was favorable to keep shorter culture period (12 days) of mycelial fermentation for a more accumulation of EPS production than other high fungi under highly acidic condition. For example, the fermentation time of *Antrodia camphorate* was 13–14 days [8]; in most case, the culture period of *Mycoleptodonoides aitchisonii* in submerged culture was 14 days [9].

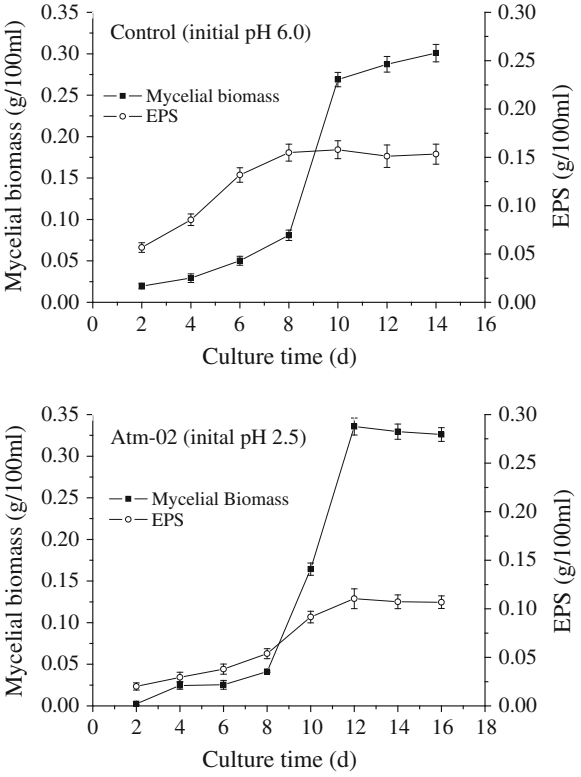

Fig. 65.5 The curves of the mycelial growth (dry wt.) and the EPS content (dry wt.) of the control (initial pH 6.0) and Atm-02 (initial pH 2.5)

65.3.4 Optimization of the Culture Condition and Medium of Atm-02

To investigate the effects of main fermentation factors on mycelial growth and EPS production of Atm-02, by single factor test, the factor temperature, rotation speed, and so on were assayed. The results shown in Table 65.2 indicates that, in terms of EPS production, the optimum levels of temperatures, rotation speed, carbon sources and its concentration, and nitrogen sources and its concentration were 26 °C, 180 rpm, 4 % (w/v) sucrose and 0.7 % (w/v) beef extract, respectively. Meanwhile, the maximum mycelial biomass was 0.335 ± 0.015 g/100 ml, and the maximum EPS content was 0.137 ± 0.009 g/100 ml. While maltose was the optimum carbon source for *Paecilomyces japonica* [10] and *Cordyceps jiangxiensis* [11]. Generally, disaccharides are better than monosaccharides for EPS production, and this may reflect their ease of polymerization [12]. For EPS formation, in contrast to other reports [13, 14], organic nitrogen gave a higher yield than inorganic nitrogen. The role of nitrogen sources on secondary metabolism should be determined by multifactors [15], and only beef extract was often used to meet necessary growth of cells in flask submerged culture. However, over high a

Table 65.2 Optimization of the culture condition and medium of Atm-02 on the mycelial biomass (dry wt.) and EPS production (dry wt.)

Factors	Ranges	Optimization levels		The final results		
		Mycelial biomass	EPS	Levels	Mycelial biomass (g/100 ml)	EPS (g/100 ml)
Temperature	18–28°C	26°C	26°C	26°C	0.170 ± 0.013	0.051 ± 0.005[a]
Rotation speed	80–200 rpm	180 rpm	180 rpm	180 rpm	0.188 ± 0.015	0.054 ± 0.005
Carbon source	Glucose; Sucrose; Maltose; Dextrin; Mannitol; Fructose	Sucrose	Sucrose	Sucrose	0.335 ± 0.015	0.097 ± 0.009
Sucrose concentration	1–5 %	3 %	4 %	4 %	0.316 ± 0.020	0.137 ± 0.009
Nitrogen source	Ammonium sulfate; Beef extract; Peptone; Yeast extract; Potassium nitrate; Ammonium nitrate	Beef extract	Beef extract	Beef extract	0.225 ± 0.007	0.095 ± 0.006
Beef extract concentration	0.1–1.1 %	0.9 %	0.7 %	0.7 %	0.248 ± 0.017	0.122 ± 0.009

[a] The values are the mean ± standard deviation of three replicates. The cultures were performed for 12 days

concentration of beef extract would decrease the accumulation of metabolites and the use of other carbon sources. The optimal temperature for mycelial growth and EPS production were both 26 °C, but their differences were slight in the temperature range 26–28 °C, and these were consistent with those of *Paecilomyces tenuipes* [16] and *Cordyceps jiangxiensis* [11]. Dissolved oxygen tension (DOT) had great effects on the formation of EPS, which was related to the rotating speed and medium capacity in flask culture. Under optimal medium capacity, higher speeds were supposed to imply better DOTs in the medium [17], and thus favorable for EPS production. As shown in Table 65.2, 180 rpm was optimal for EPS production.

Moreover, it was a fresh report on the submerged culture of acid-tolerant *L. edodes* mutants, until now, the metabolic mechanisms that mediate the production of polysaccharides are still not clearly understood, so it deserves a further study.

65.4 Conclusions

In conclusion, in the present study, screening new acid-tolerant mutants of *L. edodes* was important for mass production or industrialization in open culture. Under the optimal culture conditions, the acid-tolerant *L. edodes* mycelia in submerged culture were favorable for increasing production of mycelia and EPS. Furthermore, Atm-02 in open culture did not require strict aseptic culture condition referring to environment microorganism assays (Fig. 65.1), so it is possible that using acid-tolerant mutants would effectively reduce the cost of productive process. The improved production conditions described here will assist the development of EPS of *L. edodes* in the aspects of health foods, promising biofertilizer and drug discovery.

Acknowledgments The work was supported by "National Training Project of College Students' Innovative and Pioneering Work in Tianjin" and "Natural Science Funds of Tianjin University of Science and Technology (20100209)."

References

1. Hatvani N (2001) Antibacterial effect of the culture fluid of *Lentinus edodes* mycelium grown in submerged liquid culture. Int J Antimicrob Agents 17(1):71–74
2. Shih IL, Chou BW, Chen CC et al (2008) Study of mycelial growth and bioactive polysaccharide production in batch and fed-batch culture of *Grifola frondosa*. Bioresour Technol 99(4):785–793
3. Huang HC, Liu YC (2008) Enhancement of polysaccharide production by optimization of culture conditions in shake flask submerged cultivation of *Grifola umbellate*. J Chin Inst Chem Eng 39:307–311

4. Liu RS, Li DS, Li HM et al (2008) Response surface modeling the significance of nitrogen source on the cell growth and *Tuber* polysaccharides production by submerged cultivation of Chinese truffle *Tuber sinense*. Process Biochem 43:868–876
5. Fang QH, Zhong JJ (2002) Effect of initial pH on production of ganoderic acid and polysaccharide by submerged fermentation of *Ganoderma lucidum*. Process Biochem 37(7):769–774
6. Yang FC, Liau CB (1998) The influence of environmental conditions on polysaccharide formation by *Ganoderma lucidum* in submerged cultures. Process Biochem 33(5):547–553
7. Leung PH, Zhao SN, Ho KP et al (2009) Chemical properties and antioxidant activity of exopolysaccharides from mycelial culture of *Cordyceps sinensis* fungus Cs-HK1. Food Chem 114(4):1251–1256
8. Shu CH, Lung MY (2004) Effect of pH on the production and molecular weight distribution of exopolysaccharide by *Antrodia camphorata* in batch cultures. Process Biochem 39(8):931–937
9. Choi DB, Lee JH, Kim YS et al (2011) A study of mycelial growth and exopolysaccharide production from a submerged culture of *Mycoleptodonoides aitchisonii* in an air-lift bioreactor. Korean J Chem Eng 28:1427–1432
10. Bae JT, Park JP, Song CH et al (2001) Effect of carbon source on the mycelial growth and exo-biopolymer production by submerged culture of *Paecilomyces japonica*. J Biosci Bioeng 91:522–524
11. Xiao JH, Chen DX, Liu JW et al (2004) Optimization of submerged culture requirements for the production of mycelial growth and exopolysaccharide by *Cordyceps jiangxiensis* JXPJ 0109. J Appl Microbiol 96(5):1105–1116
12. Fan LF, Soccol AT, Pandey A et al (2007) Effect of nutritional and environmental conditions on the production of exo-polysaccharide of *Agaricus brasiliensis* by submerged fermentation and its antitumor activity. LWT-Food Sci Technol 40:30–35
13. Lim JM, Kim SW, Hwang HJ et al (2004) Optimization of medium by orthogonal matrix method for submerged mycelial culture and exopolysaccharide production in *Collybia maculata*. Appl Biochem Biotechnol 119(2):159–170
14. Kim SW, Hwang HJ, Xu CP et al (2003) Optimization of submerged culture process for the production of mycelial biomass and exo-polysaccharides by *Cordyceps militaris* C738. J Appl Microbiol 94(1):120–126
15. Xu F, Tao WY, Cheng L et al (2006) Strain improvement and optimization of the media of taxol-producing fungus *Fusarium maire*. Biochem Eng J 31(1):67–73
16. Xu CP, Kim SW, Hwang HJ et al (2003) Optimization of submerged culture conditions for mycelial growth and exo-polymer production by *Paecilomyces tenuipes* C240. Process Biochem 38(7):1025–1030
17. Yang FC, Huang HC, Yang MJ (2003) The influence of environmental conditions on the mycelial growth of *Antrodia cinnamomea* in submerged cultures. Enzyme Microb Technol 33:395–402